Appendix H

Scarborough Gas Development Hydrotest Discharge Modelling Study

Controlled Ref No: SA0006AF0000002   Revision: 5   DCP No: 1100144791

Uncontrolled when printed. Refer to electronic version for most up to date information.

WOODSIDE SCARBOROUGH PROJECT – HYDROTEST DISCHARGE MODELLING

Report

www.rpsgroup.com/mst

Document status

Version	Purpose of document	Authored by	Reviewed by	Approved by	Review date
Rev A	Internal review	B. Gómez J. Wynen-Gaugg M. Watt	D. Wright	D. Wright	08/03/2019
Rev 0	Client review	B. Gómez J. Wynen-Gaugg M. Watt	D. Wright	D. Wright	11/03/2019
Rev 1	Client review	B. Gómez J. Wynen-Gaugg M. Watt	D. Wright	D. Wright	22/03/2019
Rev 2	Client review	M. Watt	D. Wright	D. Wright	17/04/2019

Approval for issue

David Wright   17 April 2019

Prepared by: Prepared for:

RPS   ### Advisian

David Wright   Paul Nichols
Manager - Perth   Marine Sciences Manager (APAC)

Level 2, 27-31 Troode Street   600 Murray Street
West Perth WA 6005   West Perth WA 6005

Contents

Tables

Figures

EXECUTIVE SUMMARY

RPS was commissioned by Advisian Pty Ltd (Advisian), on behalf of Woodside Energy Ltd (Woodside), to undertake a marine dispersion modelling study of proposed hydrotest discharges from subsea infrastructure associated with the Scarborough Project's Floating Production Unit (FPU).

The Scarborough gas resource, located in Commonwealth waters approximately 375 km off the Burrup Peninsula, forms part of the Greater Scarborough gas fields, comprising the Scarborough, North Scarborough, Thebe and Jupiter gas fields.

As Operator of the Greater Scarborough gas fields, Woodside is proposing to develop the gas resource through new offshore facilities. These will be connected to the mainland through an approximately 430 km trunkline.

Once installation and hook-up of subsea infrastructure is complete, the infrastructure, including the SURF (subsea, umbilical, riser, flowline) and the trunkline, will be subject to pre-commissioning integrity tests. These may be conducted using hydrotest fluids, whereby the pipeline pressure will be monitored to detect leaks. Fluids will then be left in place to provide corrosion protection prior to the introduction of reservoir fluids, at which time they will be discharged at the offshore location (subject to regulatory requirements).

The principal aim of the study was to quantify the likely extents of the near-field and far-field mixing zones based on the required dilution levels for biocide in the hydrotest discharge. This will indicate whether concentrations of this contaminant are still likely to be above stated threshold levels at the limits of the mixing zones (i.e. are not predicted to be diluted below the relevant threshold).

To accurately determine the dilution of the hydrotest discharge and the total potential area of influence, the effect of near-field mixing needs to be considered first, followed by an investigation of the far-field mixing performance. Different modelling approaches are required for calculating near-field and far-field dilutions due to the differing hydrodynamic scales.

To assess the rate of mixing of the biocide in the hydrotest stream from the trunkline and SURF, dispersion modelling was carried out for flow rates of 795 m^3/hr and 220 m^3/hr at discharge depths of 930 m and 10 m below the water surface.

The potential area that may be influenced by the hydrotest discharge stream was assessed for three distinct seasons: (i) summer (December to February); (ii) the transitional periods (March and September to November); and (iii) winter (April to August). An annualised aggregation of outcomes was also assembled.

The main findings of the study are as follows:

Near-Field Modelling

- The results show that due to the momentum of the discharge a turbulent mixing zone is created in the immediate vicinity of the discharge point, which is 930 m (Cases 1 and 2) and 10 m (Case 3) below the water surface. The surface discharges are shown to increase the extent of the turbulent mixing zone. Following this initial mixing, the near neutrally-buoyant plumes are predicted to travel laterally in the water column.

- For Cases 1 and 2, the plumes are predicted to remain close to the seabed. For Case 3, the plume is predicted to plunge up to 19 m below the sea surface. For Cases 2 and 3, increased ambient current strengths are shown to increase the horizontal distance travelled by the plumes from the discharge point.

- The plume will reach a maximum horizontal distance of up to 152 m before reaching the trapping depth (at which the predictions of dispersion are halted due to the plume reaching equilibrium with the ambient receiving water).

- The maximum diameter of the plume at the end of the near-field zone was predicted as 23 m. Increases in current speed serve to restrict the diameter of the plume.

- For each discharge depth, the primary factor influencing dilution of the plume is the strength of the ambient current. Weak currents allow the plume to plunge further and reach the trapping depth closer to the discharge point, which slows the rate of dilution.

- For each combination of discharge flow rate and depth, the primary factor influencing dilution of the plume is the strength of the ambient current. Weak currents allow the plume to plunge further and reach the trapping depth closer to the discharge point, which slows the rate of dilution.

- The average dilution levels of the plume upon reaching the trapping depth under average current speeds are predicted to be 1:90 for Case 1, 1:465 for Case 2 and 1:482 for Case 3.

- The predictions of dilution rely on the persistence of current speed and direction over time and do not account for any build-up of plume concentrations due to slack currents or current reversals

- The results for the Case 1, 2 and 3 discharges indicate that the biocide constituent of the hydrotest discharge is not expected to reach the required levels of dilution in the near field mixing zone.

Far-Field Modelling

- For Case 1, dilution to reach threshold concentration is achieved for biocide within an area of influence extending up to 1,388 m at the 99th percentile. For Case 3, the maximum spatial extents of the relevant dilution contour are up to 124 m at the 99th percentile.

- For Case 1, the area of exposure defined by the relevant dilution contour is predicted to reach a maximum of 2.95 km^2 at the 99th percentile. For Case 3, the corresponding maximum area of exposure is up to 0.04 km^2 at the 99th percentile.

- Maximum depths reached by the discharges are predicted as 930 m (seabed) and 12 m for Cases 1 and 3, respectively.

Key Observations

- Due to the significant variations in magnitude of the hindcast currents between the surface and seabed, where potential discharges will occur, predicted outcomes are markedly different.

- The greater strength and variability in surface-layer currents will promote the highest levels of mixing and dilution, while transport patterns at the seabed will be dictated almost solely by tidal movements.

- Because the discharge will be initially neutrally-buoyant, it will travel laterally in the water column and even a surface discharge is unlikely to resurface in the vicinity of the discharge point prior to acclimation with ambient receiving water conditions.

- Outcomes show that below-threshold biocide concentrations are achieved closer to the discharge point for the surface discharge (220 m^3/hr over 20 hours) than for the seabed discharge (795 m^3/hr over 44 hours). This is partly attributable to the stronger currents at the surface, but primarily to the lower flow rate and much lower discharge duration in the surface-discharge case.

1   INTRODUCTION

1.1   Background

RPS was commissioned by Advisian Pty Ltd (Advisian), on behalf of Woodside Energy Ltd (Woodside), to undertake a marine dispersion modelling study of proposed hydrotest discharges from subsea infrastructure associated with the Scarborough Project's Floating Production Unit (FPU).

The Scarborough gas resource, located in Commonwealth waters approximately 375 km off the Burrup Peninsula, forms part of the Greater Scarborough gas fields, comprising the Scarborough, North Scarborough, Thebe and Jupiter gas fields.

As Operator of the Greater Scarborough gas fields, Woodside is proposing to develop the gas resource through new offshore facilities. These will be connected to the mainland through an approximately 430 km trunkline.

Once installation and hook-up of subsea infrastructure is complete, the infrastructure, including the SURF (subsea, umbilical, riser, flowline) and the trunkline, will be subject to pre-commissioning integrity tests. These may be conducted using hydrotest fluids, whereby the pipeline pressure will be monitored to detect leaks. Fluids will then be left in place to provide corrosion protection prior to the introduction of reservoir fluids, at which time they will be discharged at the offshore location (subject to regulatory requirements).

The principal aim of the study was to quantify the likely extents of the near-field and far-field mixing zones based on the required dilution levels for biocide in the hydrotest discharge. This will indicate whether concentrations of this contaminant are still likely to be above stated threshold levels at the limits of the mixing zones (i.e. are not predicted to be diluted below the relevant threshold).

To accurately determine the dilution of the hydrotest discharge and the total potential area of influence, the effect of near-field mixing needs to be considered first, followed by an investigation of the far-field mixing performance. Different modelling approaches are required for calculating near-field and far-field dilutions due to the differing hydrodynamic scales.

To assess the rate of mixing of the biocide in the hydrotest stream from the trunkline and SURF (location shown in Table 1.1), dispersion modelling was carried out for flow rates of 795 m^3/hr and 220 m^3/hr at discharge depths of 930 m and 10 m below the water surface.

The potential area that may be influenced by the hydrotest discharge stream was assessed for three distinct seasons: (i) summer (December to February); (ii) the transitional periods (March and September to November); and (iii) winter (April to August). An annualised aggregation of outcomes was also assembled.

All hydrotest discharge characteristics used as input to the modelling are specified in the Model Input Form for this study (Advisian, 2018).

Table 1.1   Location of the proposed FPU used as the release site for the hydrotest dispersion modelling assessment.

Release Site	Latitude (°S)	Longitude (°E)	Water Depth (m)
FPU	19° 53' 54.715"	113° 14' 19.561"	930
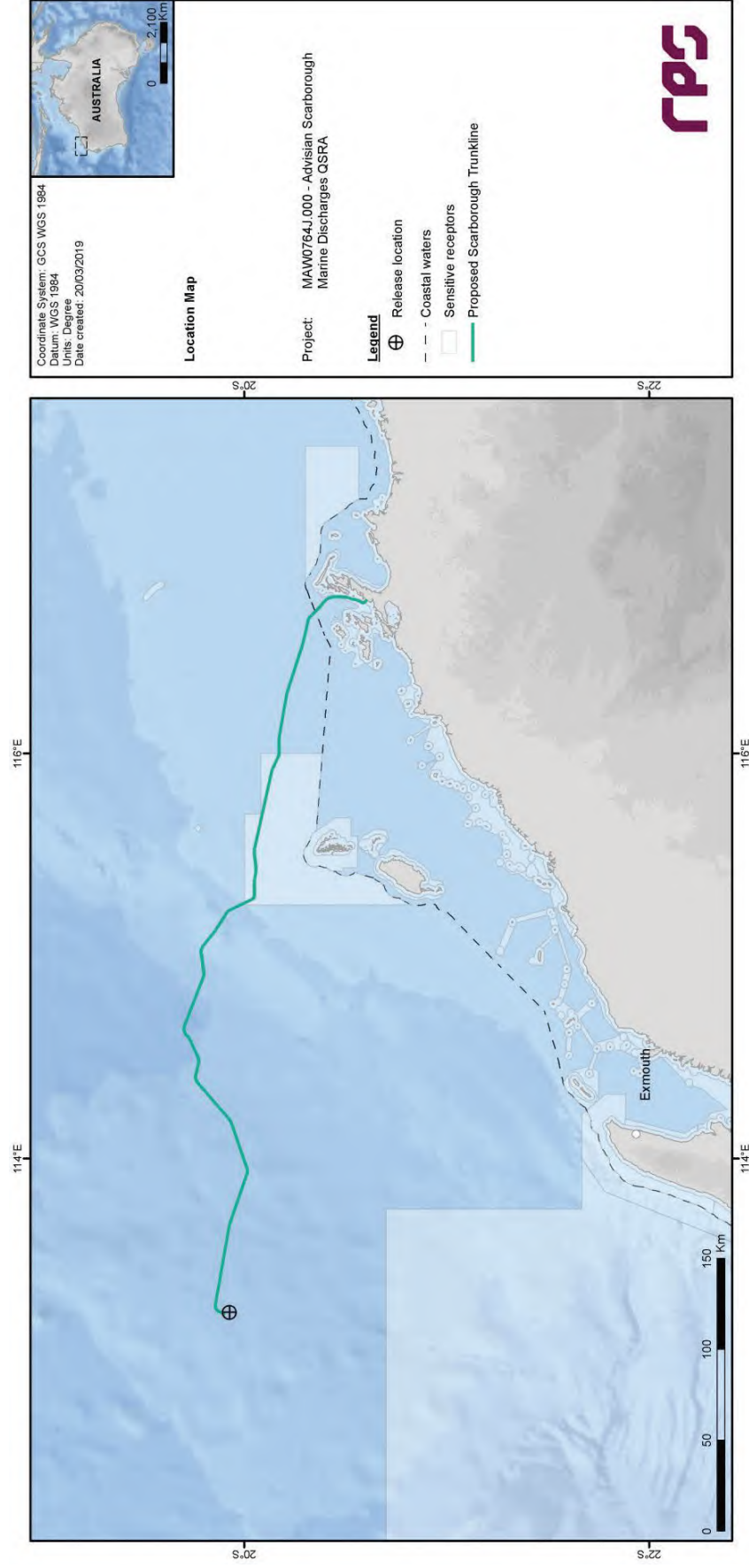
Figure 1.1   Location of the proposed Scarborough pipeline and FPU on the North West Shelf of Australia.

1.2   Modelling Scope

The physical mixing of the hydrotest plume was first investigated for the near-field mixing zone. The limits of the near-field mixing zone are defined by the area where the levels of mixing and dilution are controlled by the plume's initial jet momentum and the buoyancy flux, resulting from density differences between the plume and the receiving water. When the plume encounters a boundary such as the water surface, near-field mixing is complete. At this point, the plume is considered to enter the far-field mixing zone.

The scope of the modelling included the following components:

- Collation of a suitable three-dimensional, spatially-varying current data set surrounding the FPU location for a ten-year (2006-2015) hindcast period. The current data set included the combined influence of drift and tidal currents and was suitably long as to be indicative of interannual variability in ocean currents. The current data set was validated against metocean data collected in the Scarborough Project area.

- Derivation of statistical distributions for the current speed and directions for use in the near-field modelling. Analyses included percentile distributions and development of current roses. This analysis was important to ensure that current data samples applied in the dispersion model were statistically representative.

- Collation of seasonally-varying vertical water density profiles at the FPU location for use as input to the dispersion models.

- Near-field modelling conducted for each unique discharge to assess the initial mixing of the discharge due to turbulence and subsequent entrainment of ambient water. This modelling was conducted at high spatial and temporal resolution (scales of metres and seconds, respectively).

- Outcomes from the near-field modelling included estimates of the width, shape and orientation of the plumes, and resulting contaminant concentrations and dilutions, for each discharge at a range of incident current speeds.

- Establishment of a far-field dispersion model to repeatedly assess discharge scenarios under different sample conditions, with each sample represented by a unique time-sequence of current flow, chosen at random from the time series of current data.

- Analysis of the results of all simulations to quantify, by return frequency, the potential extent and shape of the mixing zone.

2 MODELLING METHODS

2.1 Near-Field Modelling

2.1.1 Overview

Numerical modelling was applied to quantify the area of influence of hydrotest water discharges, in terms of the distribution of the maximum contaminant concentrations that might occur with distance from the source given defined discharge configurations, source concentrations, and the distribution of the metocean conditions affecting the discharge location.

The dispersion of the hydrotest discharge will depend, initially, on the geometry and hydrodynamics of the discharges themselves, where the induced momentum and buoyancy effects dominate over background processes. This region is generally referred to as the near-field zone and is characterised by variations over short time and space scales. As the discharges mix with the ambient waters, the momentum and buoyancy signatures are eroded, and the background – or ambient – processes become dominant.

The shape and orientation of the discharged water plumes, and hence the distribution and dilution rate of the plume, will vary significantly with natural variation in prevailing water currents. Therefore, to best calculate the likely outcomes of the discharges, it is necessary to simulate discharge under a statistically representative range of current speeds representative of the FPU location.

2.1.2 Description of Near-Field Model: Updated Merge

The near-field mixing and dispersion of the water discharge was simulated using the Updated Merge (UM3) flow model. The UM3 model is a three-dimensional Lagrangian steady-state plume trajectory model designed for simulating single and multiple-port submerged discharges in a range of configurations, available within the Visual Plumes modelling package provided by the United States Environmental Protection Agency (Frick *et al.*, 2003). The UM3 model was selected because it has been extensively tested for various discharges and found to predict observed dilutions more accurately (Roberts & Tian, 2004) than other near-field models (i.e. RSB and CORMIX).

In the UM3 model, the equations for conservation of mass, momentum, and energy are solved at each time step, giving the dilution along the plume trajectory. To determine the change of each term, UM3 follows the shear (or Taylor) entrainment hypothesis and the projected-area-entrainment (PAE) hypothesis, which quantifies forced entrainment in the presence of a background ocean current. The flows begin as round buoyant jets and can merge to a plane buoyant jet (Carvalho *et al.*, 2002). Model output consists of plume characteristics including centreline dilution, rise-rate, width, centreline height and plume diameter. Dilution is reported as the "effective dilution", the ratio of the initial concentration to the concentration of the plume at a given point, following Baumgartner *et al.* (1994).

The near-field zone ends where the discharged plume reaches a physical boundary or assumes the same density as the ambient water.

Figure 2.1 shows a conceptual diagram of the dispersion and fates of a negatively buoyant discharge and the idealised representation of the discharge phases.
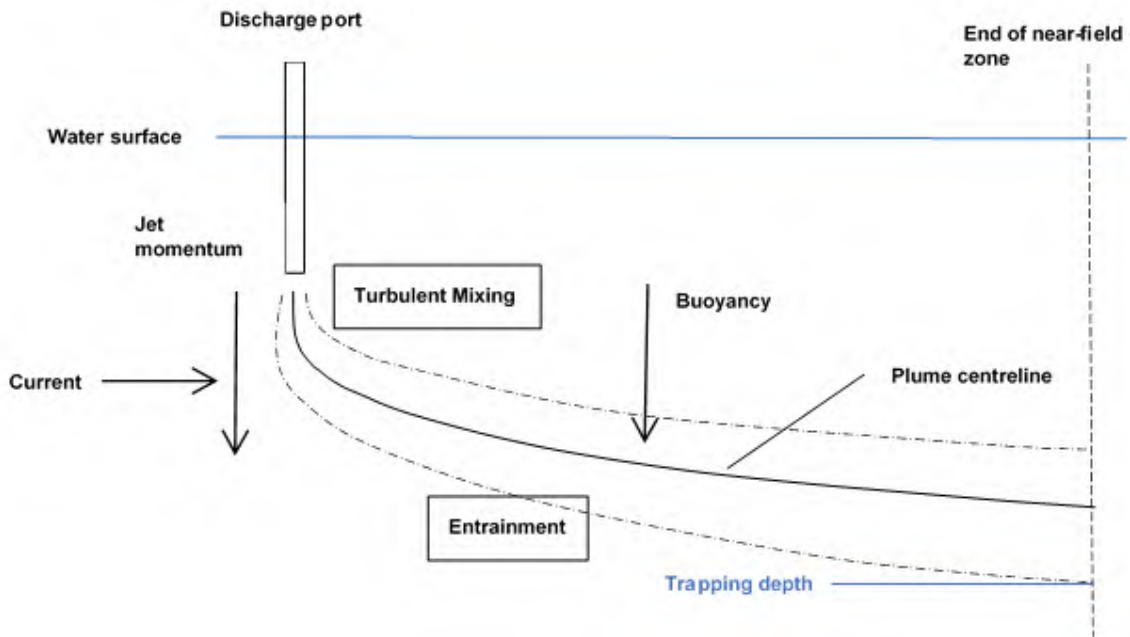
Figure 2.1   Conceptual diagram showing the general behaviour of negatively buoyant discharge.

2.1.3   Setup of Near-Field Model

2.1.3.1   Discharge Characteristics

The hydrotest discharge characteristics for cases 1 to 3 are summarised in Table 2.1.

Cases 1 and 2 were assumed to occur at a depth of 930 m below mean sea level (BMSL). The flow was assumed to occur through a single outlet of 0.1 m diameter at rates of 795 m^3/d and 220 m^3/d, respectively, and have a salinity of 35 parts per thousand (ppt) and temperature equivalent to ambient seabed conditions.

Case 3 was assumed to occur at a depth of 10 m below mean sea level (BMSL). The flow was assumed to occur through a single outlet of 0.1 m diameter at a rate of 220 m^3/d, and have a salinity of 35 parts per thousand (ppt) and temperature equivalent to ambient near-surface conditions.

The volume of hydrotest water for Case 1 was assumed as 232,800 m^3 while the volume for Cases 2 and 3 was assumed as 6,360 m^3, representing the full volumes of the trunkline and SURF equipment, respectively. Based on the engineering definitions available at the time of commissioning the dispersion modelling study, it is anticipated that the dewatering of the pipeline will take approximately 244 hours (Case 1) and 20 hours (Cases 2 and 3), based on average flow rates of 795 m^3/hr and 220 m^3/hr.

Concentrations of the constituent of interest (biocide) within the discharges are described in Table 2.2, along with the required dilution factor to reach the defined threshold concentration (Advisian, 2018).

Table 2.1   Summary of hydrotest discharge characteristics.

Parameter	Trunkline Hydrotest Discharge	SURF Hydrotest Discharge 1	SURF Hydrotest Discharge 2
Flow rate (m³/d)	795	220	
Discharge volume (m³)	232,800	6,360	
Discharge duration (hours)	244	20	
Outlet pipe internal diameter (m) [in]	0.1 [4]		
Outlet pipe orientation	Horizontal	Vertical (upwards)	Vertical (downwards)
Depth of pipe below sea surface (m)	930		10
Discharge salinity (ppt)	35		
Discharge temperature (°C)	Ambient (seabed)		Ambient (near-surface)

Table 2.2   Constituent of interest within the hydrotest discharges and criteria for analysis of exposure.

Constituent	Source Concentration (ppm)	Threshold Concentration (ppm)	Required Dilution Factor
Biocide	550	1	550

2.1.3.2 Ambient Environmental Conditions

Inputs of ambient environmental conditions to the UM3 model included a vertical profile of temperature and salinity, along with constant current speeds and general direction. The temperature and salinity profiles are required to accurately account for the buoyancy of the diluting plume, while the current speeds control the intensity of initial mixing and the deflection of the hydrotest plume. These inputs are described in the following sections.

2.1.3.2.1 Ambient Temperature and Salinity

Temperature and salinity data applied to the near-field modelling was sourced from the World Ocean Atlas 2013 (WOA13) database produced by the National Oceanographic Data Centre (National Oceanic and Atmospheric Administration, NOAA) and its co-located World Data Center for Oceanography (Levitus *et al.*, 2013).

Table 2.3 shows the average seasonal water temperature and salinity levels at varying depths from 0 m to 930 m. This data can be considered representative of seasonal conditions at the FPU location.

The seasonal temperature profiles exhibit a reasonably consistent reduction in temperature with increasing depth. Salinity levels are generally more consistent and exhibit a vertically well-mixed water body (34.6-35.5 practical salinity unit, PSU), irrespective of season or depth.

Table 2.3   Average temperature and salinity levels adjacent to the proposed FPU location.

Season	Depth (m)	Temperature (°C)	Salinity (PSU)
Summer	0	27.8	34.7
	20	27.3	34.8
	50	26.2	34.8
	200	18.4	35.4
	500	8.7	34.7
	1,000	5.1	34.6
Transitional	0	26.0	34.7
	20	25.7	34.7
	50	25.1	34.7
	200	18.6	35.5
	500	8.6	34.6
	1,000	5.1	34.6
Winter	0	26.4	34.7
	20	26.3	34.7
	50	26.2	34.7
	200	19.0	35.4
	500	8.9	34.6
	1,000	5.1	34.6
Annualised	0	26.6	34.7
	20	26.3	34.7
	50	25.8	34.7
	200	18.7	35.4
	500	8.7	34.6
	1,000	5.1	34.6

2.1.3.2.2 Ambient Current

Ocean current data was sourced from a 10-year hindcast data set of combined large-scale ocean (BRAN) and tidal currents. The data was statistically analysed to determine the 5th, 50th and 95th percentile current speeds. These statistical current speeds can be considered representative of seasonal conditions at the FPU location.

Table 2.4 presents the steady-state, unidirectional current speeds at varying depths used as input to the near-field model as forcing for each discharge case:

- 5th percentile current speed: weak currents, low dilution and slow advection.

- 50th percentile (median) current speed: average currents, moderate dilution and advection.

- 95th percentile current speed: strong currents, high dilution and rapid advection to nearby areas.

The 5th, 50th and 95th percentile values are referenced as weak, medium and strong current speeds, respectively.

Table 2.4   Adopted ambient current conditions adjacent to the proposed FPU location.

Season	Depth (m)	5th Percentile (Weak) Current Speed (m/s)	50th Percentile (Medium) Current Speed (m/s)	95th Percentile (Strong) Current Speed (m/s)
Summer	2.5	0.041	0.158	0.326
	22.7	0.049	0.154	0.312
	56.7	0.044	0.138	0.267
	205.2	0.035	0.120	0.237
	545.5	0.032	0.105	0.221
	995.5	0.013	0.050	0.106
Transitional	2.5	0.045	0.177	0.375
	22.7	0.045	0.173	0.369
	56.7	0.043	0.157	0.322
	205.2	0.043	0.140	0.287
	545.5	0.032	0.118	0.282
	995.5	0.016	0.056	0.116
Winter	2.5	0.044	0.172	0.395
	22.7	0.043	0.166	0.375
	56.7	0.039	0.156	0.341
	205.2	0.036	0.142	0.307
	545.5	0.035	0.116	0.278
	995.5	0.013	0.052	0.105
Annualised	2.5	0.043	0.170	0.374
	22.7	0.045	0.164	0.361
	56.7	0.042	0.151	0.320
	205.2	0.038	0.135	0.285
	545.5	0.033	0.114	0.267
	995.5	0.014	0.053	0.109

2.2   Far-Field Modelling

2.2.1   Overview

The far-field modelling expands on the near-field work by allowing the time-varying nature of currents to be included, and the potential for recirculation of the plume back to the discharge location to be assessed. In this case, concentrations near the discharge point can be increased due to the discharge plume mixing with the remnant plume from an earlier time. This may be a potential source of episodic increases in pollutant concentrations in the receiving waters.

2.2.2   Description of Far-Field Model: MUDMAP

The mixing and dispersion of the discharges was predicted using the three-dimensional discharge and plume behaviour model, MUDMAP (Koh & Chang, 1973; Khondaker, 2000).

The far-field calculation (passive dispersion stage) employs a particle-based, random walk procedure. Any chemicals/constituents within the discharge stream are represented by a sample of Lagrangian particles. These particles are moved in three dimensions over each subsequent time step according to the prevailing local current data as well as horizontal and vertical mixing coefficients.

MUDMAP treats the Lagrangian particles as conservative tracers (i.e. they are not removed over time to account for chemical interactions, decay or precipitation). Predicted concentrations will therefore be conservative overestimates where these processes actually do occur. Each particle represents a proportion of the discharge, by mass, and particles are released at a given rate to represent the rate of the discharge (mass per unit time). Concentrations of constituents are predicted over time by counting the number of particles that occur within a given depth level and grid square and converting this value to mass per unit volume.

The system has been extensively validated and applied for discharge operations in Australian waters (e.g. Burns *et al.*, 1999; King & McAllister, 1997, 1998).

2.2.3   Stochastic Modelling

A stochastic modelling procedure was applied in the far-field modelling to sample a representative set of conditions that could affect the distribution of constituents. This approach involves multiple (25) simulations of a given discharge scenario and season, with each simulation being carried out under a randomly-selected period of currents. This methodology ensures that the calculated movement and fate of each discharge is representative of the range of prevailing currents at the discharge location. Once the stochastic modelling is complete, all simulations are statistically analysed to develop the distribution of outcomes based on time and event.

2.2.4   Setup of Far-Field Model

2.2.4.1   Discharge Characteristics

The MUDMAP model simulated the discharge into a time-varying current field with the initial dilution set by the near-field results described in Section 2.1.

Two hydrotest discharge scenarios were modelled as a continuous discharge using 25 simulations for each season. Once the simulations were complete, they were reported on a seasonal basis: (i) summer

(December to February); (ii) transitional (March and September to November) and (iii) winter (April to August). The hydrotest discharge characteristics for the selected cases (Trunkline and SURF 2) are summarised in Table 2.5. These cases were chosen to cover the full range of proposed discharge flow rates and depths.

Table 2.5   Summary of far-field hydrotest discharge modelling assumptions.

Parameter	Trunkline Hydrotest Discharge	SURF Hydrotest Discharge 2
Hindcast modelling period	2006-2015	
Seasons	Summer (December to February) Transitional (March and September to November) Winter (April to August) Annual	
Flow rate (m³/d)	795	220
Discharge volume (m³)	232,800	6,360
Discharge duration (hours)	244	20
Discharge depth (m)	930	10
Discharge salinity (ppt)	35	
Discharge temperature (°C)	Ambient (seabed)	Ambient (near-surface)
Number of simulations	75 (25 per season)	
Simulated discharge type	One-off	
Simulated discharge period (days)	Discharge duration	

2.2.4.2 Mixing Parameters

The horizontal and vertical dispersion coefficients represent the mixing and diffusion caused by turbulence, both of which are sub-grid-scale processes. Both coefficients are expressed in units of rate of area change per second (m²/s). Increasing the horizontal dispersion coefficient will increase the horizontal spread of the discharge plume and decrease the centreline concentrations faster. Increasing the vertical dispersion coefficient spreads the discharge across the vertical layers (or depths) faster.

Spatially constant, conservative dispersion coefficients of 0.15 m²/s and 0.00005 m²/s were used to control the spreading of the hydrotest plume in the horizontal and vertical directions, respectively. Each of the mixing parameters was selected following extensive sensitivity testing to recreate the plume characteristics predicted by the near-field modelling. It would be expected that the in-situ mixing dynamics would be greater under average and high energy conditions by a factor of 10 (King & McAllister, 1997, 1998) and thus the far-field model results are designed to produce a worst-case result for concentration extents.

MUDMAP uses a three-dimensional grid to represent the geographic region under study (water depth and bathymetric profiles). Due to the rapid mixing and small-scale effect of the effluent discharge, it was necessary to use a fine grid with a resolution of 5 m x 5 m to track the movement and fate of the discharge plume. The extent of the grid region measured approximately 5 km (longitude or x-axis) by 5 km (latitude or y-axis), which was subdivided horizontally into 1,000 x 1,000 cells. The vertical resolution was set to 1 m.

2.2.5 Regional Ocean Currents

2.2.5.1 Background

The area of interest for this study is typified by strong tidal flows over the shallower regions, particularly along the inshore region of the North West Shelf and among the island groups stretching from the Dampier Archipelago to the North West Cape. However, the offshore regions with water depths exceeding 100-200 m experience significant large-scale drift currents. These drift currents can be relatively strong (1-2 knots) and complex, manifesting as a series of eddies, meandering currents and connecting flows. These offshore drift currents also tend to persist longer (days to weeks) than tidal current flows (hours between reversals) and thus will have greater influence upon the net trajectory of slicks over time scales exceeding a few hours.

Wind shear on the water surface also generates local-scale currents that can persist for extended periods (hours to days) and result in long trajectories. Hence, the current-induced transport of pollutants can be variably affected by combinations of tidal, wind-induced and density-induced drift currents. Depending on their local influence, it is critical to consider all these potential advective mechanisms to rigorously understand patterns of potential transport from a given discharge location.

To appropriately allow for temporal and spatial variation in the current field, dispersion modelling requires the current speed and direction over a spatial grid covering the potential migration of pollutants. As measured current data is not available for simultaneous periods over a network of locations covering the wide area of this study, the analysis relied upon hindcasts of the circulation generated by numerical modelling. Estimates of the net currents were derived by combining predictions of the drift currents, available from mesoscale ocean models, with estimates of the tidal currents generated by an RPS model set up for the study area.

2.2.5.2 Mesoscale Circulation Model

Representation of the drift currents that affect the area were available from the output of the BRAN (Bluelink ReANalysis; Oke *et al.*, 2008, 2009; Schiller *et al.*, 2008) ocean model, which is sponsored by the Australian Government through the Commonwealth Bureau of Meteorology (BoM), Royal Australian Navy, and Commonwealth Scientific and Industrial Research Organisation (CSIRO). BRAN is a data-assimilative, three-dimensional ocean model that has been run as a hindcast for many periods and is now used for ocean forecasting (Schiller *et al.*, 2008).

The BRAN predictions for drift currents are produced at a horizontal spatial resolution of approximately 0.1° over the region, at a frequency of once per day, averaged over the 24-hour period. Hence, the BRAN model data provides estimates of mesoscale circulation with horizontal resolution suitable to resolve eddies of a few tens of kilometres' diameter, as well as connecting stream currents of similar spatial scale. Drift currents that are represented over the inner shelf waters in the BRAN data are principally attributable to wind induced drift.

There are several versions of the BRAN database available. The latest BRAN simulation spans the period of January 1994 to August 2016. From this database, time series of current speed and direction were extracted for all points in the model domain for the years 2006-2015 (inclusive). The data was assumed to be a suitably representative sample of the current conditions over the study area for future years.

Figure 2.2 shows the seasonal distribution of current speeds and directions for the BRAN data point closest to the FPU location. Note that the convention for defining current direction is the direction towards which the current flows.

The data shows that current speeds and directions vary between seasons. In general, during transitional months (March and September to November) currents have the strongest average speed (0.22 m/s with a maximum of 0.56 m/s) and tend to flow south-east. During winter (April to August), current flow conditions are more variable, with lower average speed (0.21 m/s with a maximum of 0.53 m/s). During summer (December to February), the current flow occurs in a predominantly south/south-westerly direction with the lowest average speed (0.20 m/s with a maximum of 0.46 m/s).

Figure 2.2   **Seasonal current distribution (2006-2015, inclusive) derived from the BRAN database near to the proposed FPU location. The colour key shows the current magnitude, the compass direction provides the direction towards which the current is flowing, and the size of the wedge gives the percentage of the record.**

2.2.5.3 Tidal Circulation Model

As the BRAN model does not include tidal forcing, and because the data is only available at a daily frequency, a tidal model was developed for the study region using RPS' three-dimensional hydrodynamic model, HYDROMAP.

The model formulations and output (current speed, direction and sea level) of this model have been validated through field measurements around the world for more than 25 years (Isaji & Spaulding, 1984, 1986; Isaji *et al.*, 2001; Zigic *et al.*, 2003). HYDROMAP current data has also been widely used as input to

forecasts and hindcasts of oil spill migrations in Australian waters. This modelling system forms part of the National Marine Oil Spill Contingency Plan for the Australian Maritime Safety Authority (AMSA, 2002).

HYDROMAP simulates the flow of ocean currents within a model region due to forcing by astronomical tides, wind stress and bottom friction. The model employs a sophisticated dynamically nested-gridding strategy, supporting up to six levels of spatial resolution within a single domain. This allows for higher resolution of currents within areas of greater bathymetric and coastline complexity, or of particular interest to a study.

The numerical solution methodology of HYDROMAP follows that of Davies (1977a, 1977b) with further developments for model efficiency by Owen (1980) and Gordon (1982). A more detailed presentation of the model can be found in Isaji & Spaulding (1984).

A HYDROMAP model was established over a domain that extended approximately 3,300 km east-west by 3,100 km north-south over the eastern Indian Ocean. The grid extends beyond Eucla in the south and beyond Bathurst Island in the north (Figure 2.3).

Four layers of sub-gridding were applied to provide variable resolution throughout the domain. The resolution at the primary level was 15 km. The finer levels were defined by subdividing these cells into 4, 16 and 64 cells, resulting in resolutions of 7.5 km, 3.75 km and 1.88 km. The finer grids were allocated in a step-wise fashion to areas where higher resolution of circulation patterns was required to resolve flows through channels, around shorelines or over more complex bathymetry. Approximately 98,600 cells were used to define the region.

Bathymetric data used to define the three-dimensional shape of the study domain was extracted from the CMAP electronic chart database and supplemented where necessary with manual digitisation of chart data supplied by the Australian Hydrographic Office. Depths in the domain ranged from shallow intertidal areas through to approximately 7,200 m.

Ocean boundary data for the HYDROMAP model was obtained from the TOPEX/Poseidon global tidal database (TPXO7.2) of satellite-measured altimetry data, which provided estimates of tidal amplitudes and phases for the eight dominant tidal constituents (designated as K_2, S_2, M_2, N_2, K_1, P_1, O_1 and Q_1) at a horizontal scale of approximately 0.25°. Using the tidal data, sea surface heights are firstly calculated along the open boundaries at each time step in the model.

The TOPEX/Poseidon satellite data is produced, and quality controlled by the US National Atmospheric and Space Agency (NASA). The satellites, equipped with two highly accurate altimeters capable of taking sea level measurements accurate to less than ±5 cm, measured oceanic surface elevations (and the resultant tides) for over 13 years (1992-2005). In total, these satellites carried out more than 62,000 orbits of the planet. The TOPEX/Poseidon tidal data has been widely used amongst the oceanographic community, being the subject of more than 2,100 research publications (e.g. Andersen, 1995; Ludicone *et al.*, 1998; Matsumoto *et al.*, 2000; Kostianoy *et al.*, 2003; Yaremchuk & Tangdong, 2004; Qiu & Chen, 2010). As such, the TOPEX/Poseidon tidal data is considered suitably accurate for this study.

For the purpose of verification of the tidal predictions, the model output was compared against independent predictions of tides using the XTide database (Flater, 1998). The XTide database contains harmonic tidal constituents derived from measured water level data at locations around the world. Of more than 40 tidal stations within the HYDROMAP model domain, ten were used for comparison.

Water level time series for these locations are shown in Figure 2.4 for a one-month period (January 2005). All comparisons show that the model produces a very good match to the known tidal behaviour for a wide

range of tidal amplitudes and clearly represents the varying diurnal and semi-diurnal nature of the tidal signal.

The model skill was further evaluated through a comparison of the predicted and observed tidal constituents, derived from an analysis of model-predicted time-series at each location. A scatter plot of the observed and modelled amplitude (top) and phase (bottom) of the five dominant tidal constituents (S_2, M_2, N_2, K_1 and O_1) is presented in Figure 2.5. The red line on each plot shows the 1:1 line, which would indicate a perfect match between the modelled and observed data. Note that the data is generally closely aligned to the 1:1 line demonstrating the high quality of the model performance.

Figure 2.6 shows the seasonal distribution of current speeds and directions for the HYDROMAP data point closest to the FPU location. Note that the convention for defining current direction is the direction towards which the current flows.

The current data indicates cyclical tidal flow directions along a northeast-southwest axis, with maximum speeds of around 0.09 m/s.
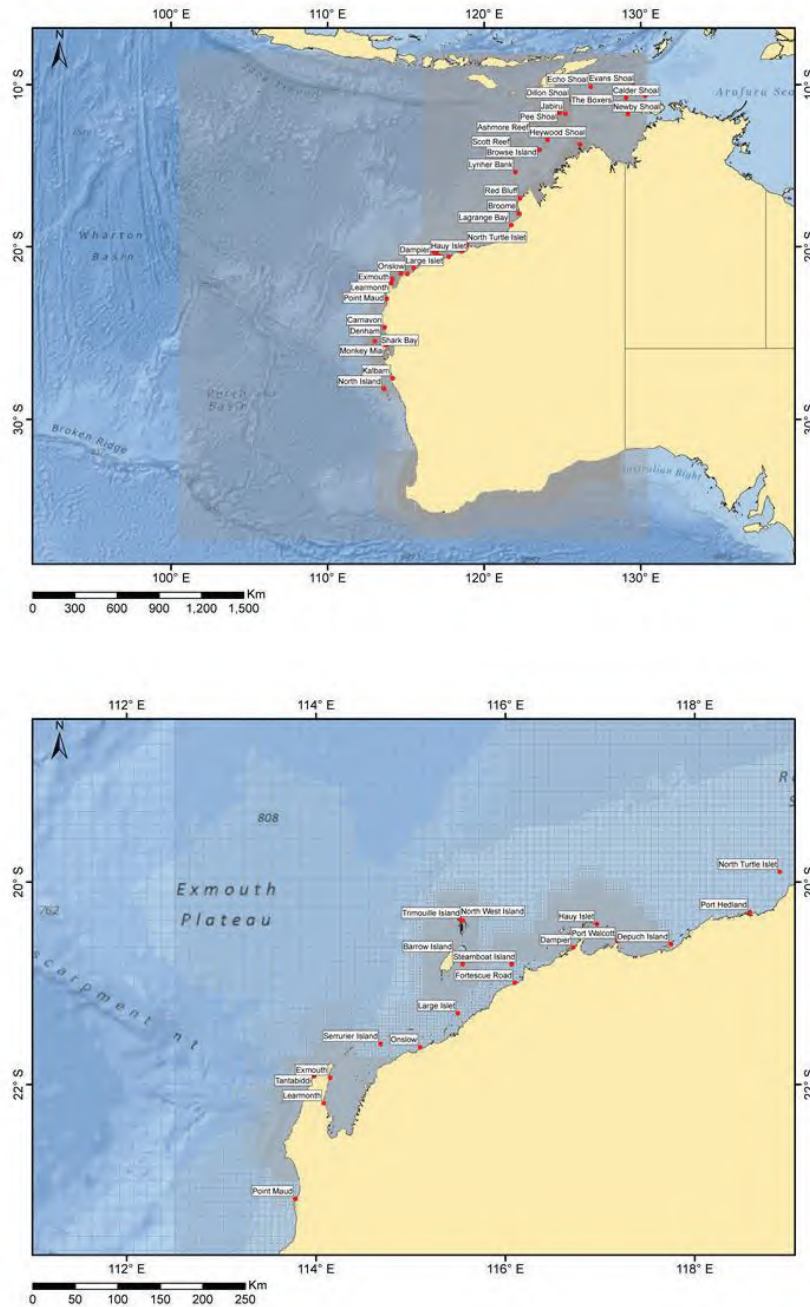
Figure 2.3   Hydrodynamic model grid (grey wire mesh) used to generate the tidal currents, showing locations available for tidal comparisons (red labelled dots). The top panel shows the full domain in context with the continental land mass, while the bottom panel shows a zoomed subset near the discharge locations. Higher-resolution areas are indicated by the denser mesh zones.
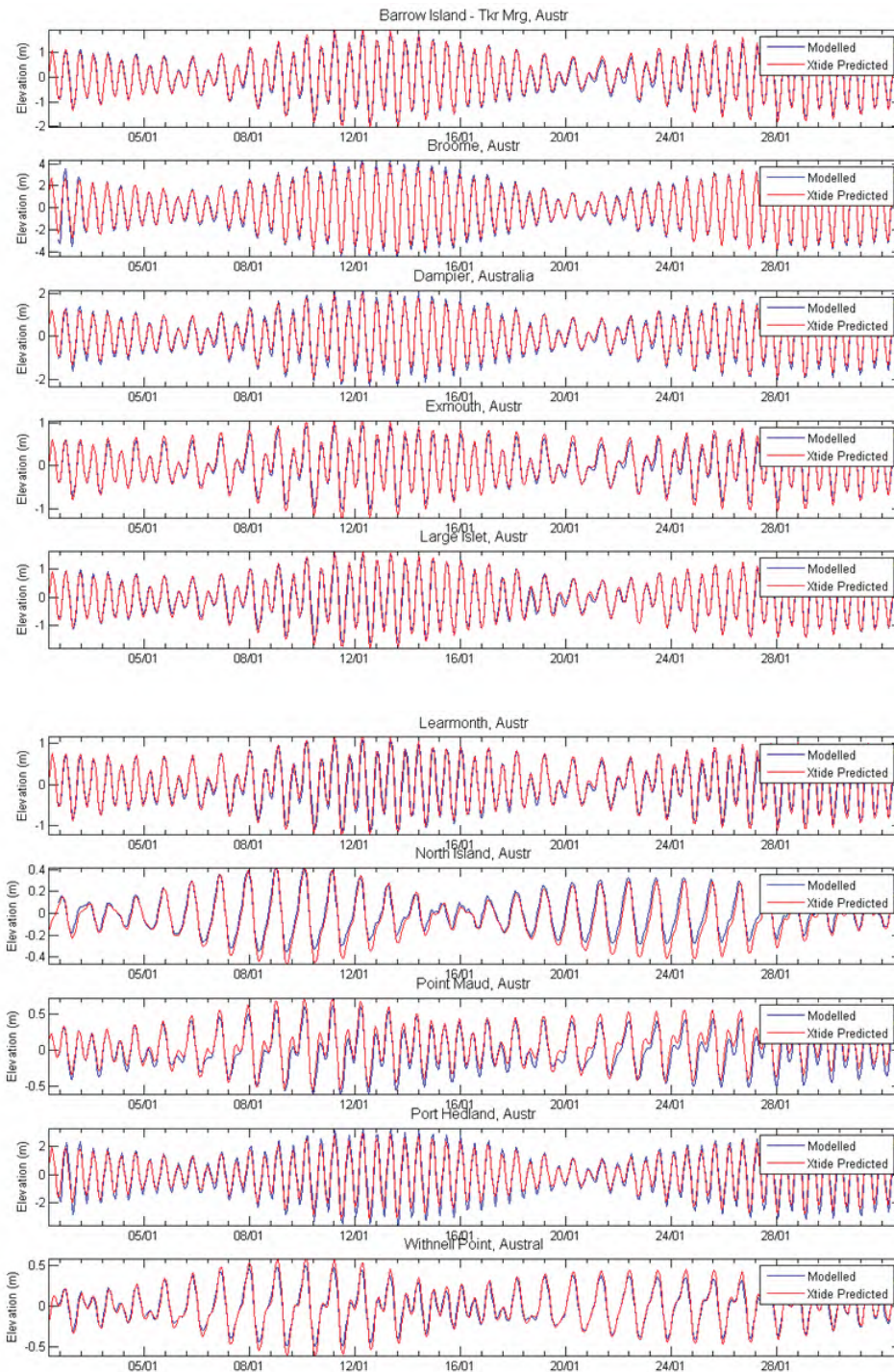
Figure 2.4 **Comparisons between the predicted (blue line) and observed (red line) surface elevation variations at ten locations in the tidal model domain for January 2005.**
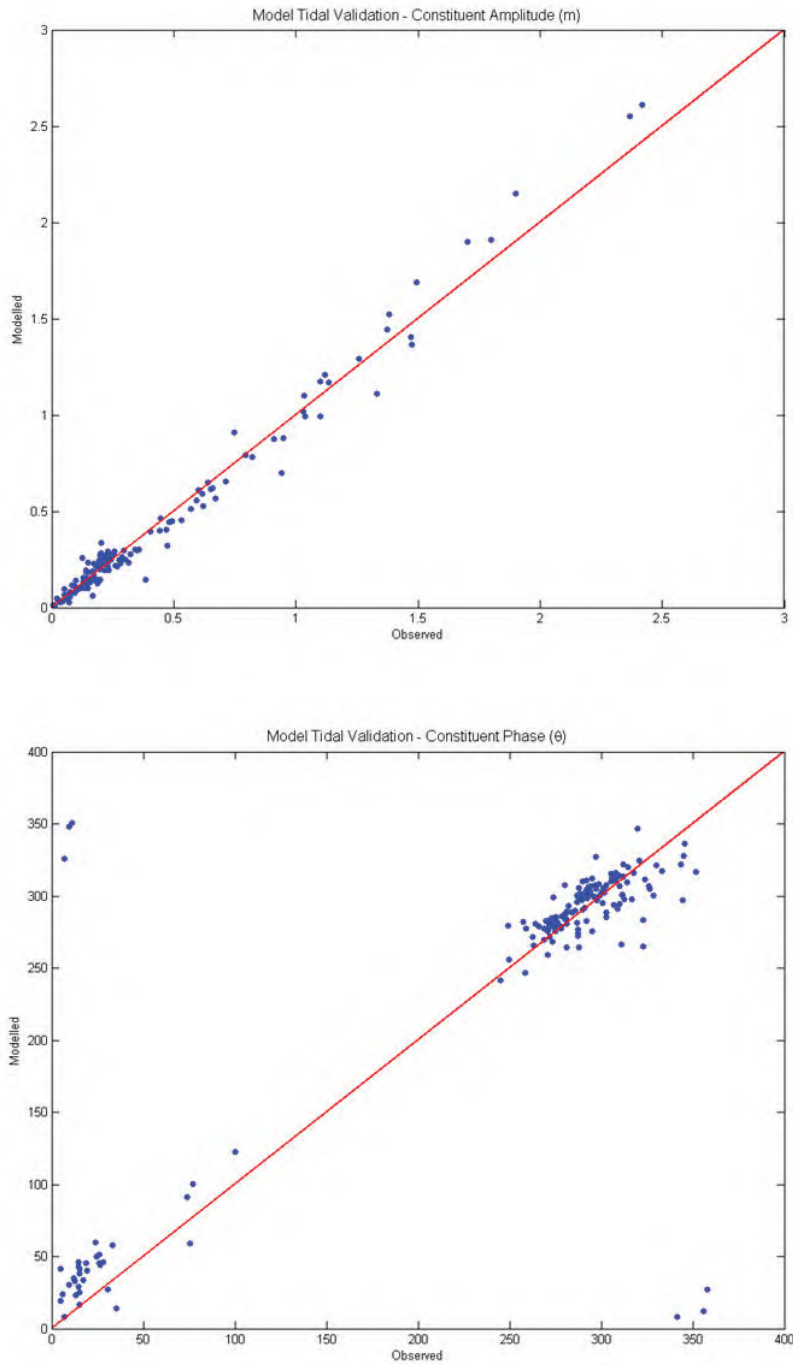
Figure 2.5   Comparisons between modelled and observed tidal constituent amplitudes (top) and phases (bottom) at all stations in the HYDROMAP model domain. The red line indicates a 1:1 correlation between the modelled and observed data.
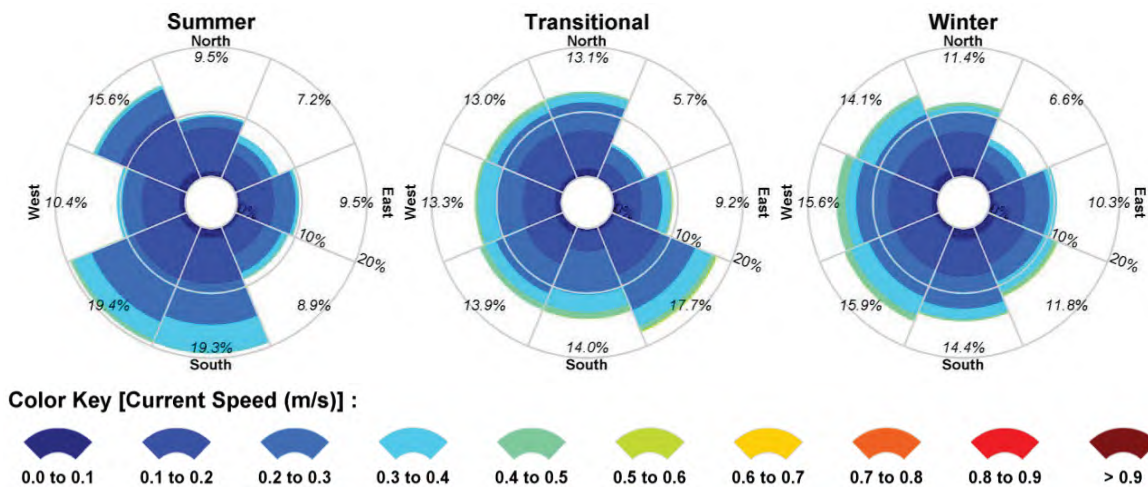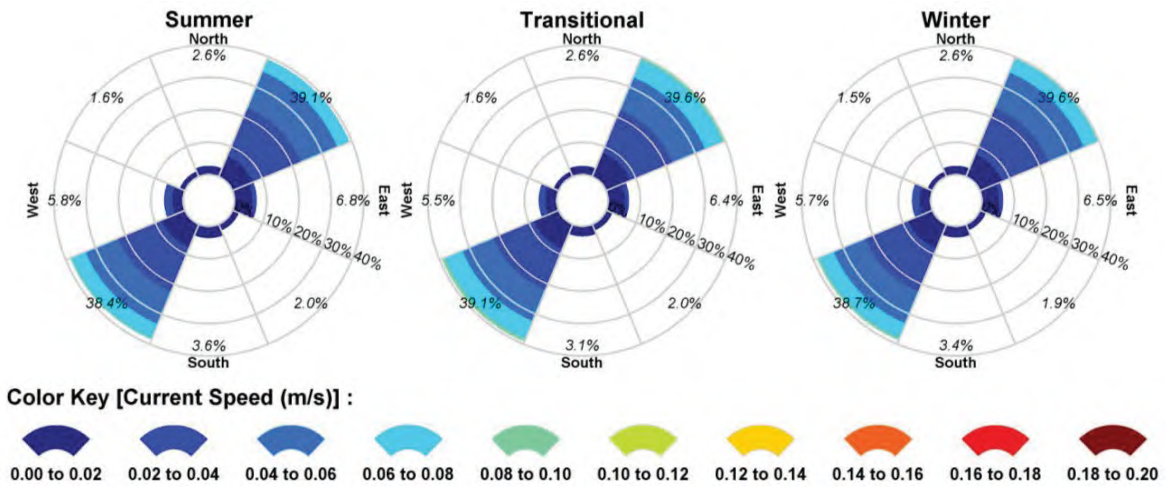
Figure 2.6 Seasonal current distribution (2006-2015, inclusive) derived from the HYDROMAP database near to the proposed FPU location. The colour key shows the current magnitude, the compass direction provides the direction towards which the current is flowing, and the size of the wedge gives the percentage of the record.

3   MODELLING RESULTS

3.1   Near-Field Modelling

3.1.1   Overview

In the following sections, information for each of the modelled discharge cases is presented first in a table summarising the predicted plume characteristics in the near-field mixing zone under varying current speeds, and then in further tables summarising the concentrations of biocide at the end of the near-field mixing zone, the concentration threshold, and the amount of dilution for each season and for the annual period. Any dilution rates indicated in red show that suitable dilution is not achieved during the near-field stage for at least one current-speed case.

Figure 3.1 to Figure 3.12 (note the differing x-axis and y-axis aspect ratios) show the change in average dilution and temperature of the plume under varying discharge rates (795 m^3/hr and 220 m^3/hr), depths (930 m and 10 m), seasonal conditions (summer, transitional, winter and annual) and current speeds (weak, medium and strong). The figures show the predicted horizontal distances travelled by the plume before the trapping depth is reached (i.e. before the plume becomes neutrally buoyant).

The results show that due to the momentum of the discharge a turbulent mixing zone is created in the immediate vicinity of the discharge point, which is 930 m (Cases 1 and 2) and 10 m (Case 3) below the water surface. The surface discharges are shown to increase the extent of the turbulent mixing zone. Following this initial mixing, the near neutrally-buoyant plumes are predicted to travel laterally in the water column. For Cases 1 and 2, the plumes are predicted to remain close to the seabed. For Case 3, the plume is predicted to plunge up to 19 m below the sea surface depending on season. For Cases 2 and 3, increased ambient current strengths are shown to increase the horizontal distance travelled by the plumes from the discharge point.

Table 3.1, Table 3.6 and Table 3.11 show the predicted plume characteristics for the varying discharge flow rates, depths, seasonal conditions and current speeds. The plume will reach a maximum horizontal distance of between 7 m and 152 m before reaching the trapping depth.

The diameter of the plume at the end of the near-field zone ranged from 10 m to 23 m. Increases in current speed serve to restrict the diameter of the plume.

For most combinations of season, flow rate and discharge depth, the primary factor influencing dilution of the plume is the strength of the ambient current. Weak currents allow the plume to plunge further and reach the trapping depth closer to the discharge point, which slows the rate of dilution (Table 3.1, Table 3.6 and Table 3.11). The average dilution levels of the plume upon reaching the trapping depth under medium and strong currents are predicted to be 1:90 and 1:81 for Case 1, 1:465 and 1:629 for Case 2, and 1:482 and 1:641 for Case 3, respectively. Note that predictions of dilution rely on the persistence of current speed and direction over time and do not account for any build-up of plume concentrations due to slack currents or current reversals.

The results for the Case 1 (Section 3.1.2.1; Table 3.2 to Table 3.5), Case 2 (Section 3.1.2.2; Table 3.7 to Table 3.10) and Case 3 (Section 3.1.2.3; Table 3.12 to Table 3.15) discharges indicate that the biocide constituent of the hydrotest discharge is not expected to reach the required levels of dilution in the near-field mixing zone.

3.1.2 Results – Tables and Figures

3.1.2.1 Discharge Case 1: Trunkline Hydrotest Discharge at 930 m Depth

Table 3.1 Predicted plume characteristics at the end of the near-field mixing zone for the trunkline hydrotest discharge for each season and current speed.

Season	Surface Current Speed (m/s)	Plume Diameter (m) at Depth [m]	Plume Temperature (°C)	Plume-Ambient Temperature Difference (°C)	Plume Dilution (1:x)		Maximum Horizontal Distance (m)
					Minimum	Average	
Summer	Weak (0.04)	10.0 [925.0]	5.74	0.00	52	97	23.8
	Medium (0.16)	10.0 [925.0]	5.74	0.00	52	90	21.1
	Strong (0.33)	10.0 [925.0]	5.74	0.00	55	81	18.1
Transitional	Weak (0.05)	10.0 [925.0]	5.71	0.00	52	97	23.7
	Medium (0.18)	10.0 [925.0]	5.71	0.00	53	90	21.0
	Strong (0.38)	10.0 [925.0]	5.71	0.00	54	78	17.2
Winter	Weak (0.04)	10.0 [925.0]	5.76	0.00	52	97	23.8
	Medium (0.17)	10.0 [925.0]	5.76	0.00	53	90	21.1
	Strong (0.40)	10.0 [925.0]	5.76	0.00	54	80	17.6
Annual	Weak (0.04)	10.0 [925.0]	5.73	0.00	52	97	23.8
	Medium (0.17)	10.0 [925.0]	5.73	0.00	53	90	21.0
	Strong (0.37)	10.0 [925.0]	5.73	0.00	55	80	17.6

Table 3.2 Concentration of biocide at the end of the near-field stage, and the required concentration threshold and number of dilutions for the summer season. Note from Table 3.1 that dilutions at the 5th, 50th and 95th percentile current speeds were 97, 90 and 81, respectively. Dilution rates highlighted in red indicate that suitable dilution is not achieved during the near-field stage.

Contaminant	Source Concentration (ppm)	End of Near-Field Concentration (ppm)			Threshold Concentration (ppm)	Required Dilution Factor
		5th %ile	50th %ile	95th %ile		
		97x Dilution	90x Dilution	81x Dilution		
Biocide	550	5.7	6.1	6.8	1	550

Table 3.3   Concentration of biocide at the end of the near-field stage, and the required concentration threshold and number of dilutions for the transitional season. Note from Table 3.1 that dilutions at the 5th, 50th and 95th percentile current speeds were 97, 90 and 78, respectively. Dilution rates highlighted in red indicate that suitable dilution is not achieved during the near-field stage.

Contaminant	Source Concentration (ppm)	End of Near-Field Concentration (ppm)			Threshold Concentration (ppm)	Required Dilution Factor
		5th %ile	50th %ile	95th %ile		
		97x Dilution	90x Dilution	78x Dilution		
Biocide	550	5.7	6.1	7.1	1	550

Table 3.4   Concentration of biocide at the end of the near-field stage, and the required concentration threshold and number of dilutions for the winter season. Note from Table 3.1 that dilutions at the 5th, 50th and 95th percentile current speeds were 97, 90 and 80, respectively. Dilution rates highlighted in red indicate that suitable dilution is not achieved during the near-field stage.

Contaminant	Source Concentration (ppm)	End of Near-Field Concentration (ppm)			Threshold Concentration (ppm)	Required Dilution Factor
		5th %ile	50th %ile	95th %ile		
		97x Dilution	90x Dilution	80x Dilution		
Biocide	550	5.7	6.1	6.9	1	550

Table 3.5   Concentration of biocide at the end of the near-field stage, and the required concentration threshold and number of dilutions for the annual period. Note from Table 3.1 that dilutions at the 5th, 50th and 95th percentile current speeds were 97, 90 and 80, respectively. Dilution rates highlighted in red indicate that suitable dilution is not achieved during the near-field stage.

Contaminant	Source Concentration (ppm)	End of Near-Field Concentration (ppm)			Threshold Concentration (ppm)	Required Dilution Factor
		5th %ile	50th %ile	95th %ile		
		97x Dilution	90x Dilution	80x Dilution		
Biocide	550	5.7	6.1	6.9	1	550

Figure 3.1 Near-field average dilution and temperature results for constant weak, medium and strong summer currents (930 m depth discharge at 795 m³/hr flow rate).

Figure 3.2   Near-field average dilution and temperature results for constant weak, medium and strong transitional currents (930 m depth discharge at 795 m³/hr flow rate).

Figure 3.3   Near-field average dilution and temperature results for constant weak, medium and strong winter currents (930 m depth discharge at 795 m³/hr flow rate).

Figure 3.4   Near-field average dilution and temperature results for constant weak, medium and strong annualised currents (930 m depth discharge at 795 m³/hr flow rate).

3.1.2.2 Discharge Case 2: SURF Hydrotest Discharge at 930 m Depth

Table 3.6   Predicted plume characteristics at the end of the near-field mixing zone for the SURF hydrotest discharge for each season and current speed.

Season	Surface Current Speed (m/s)	Plume Diameter (m) at Depth [m]	Plume Temperature (°C)	Plume-Ambient Temperature Difference (°C)	Plume Dilution (1:x)		Maximum Horizontal Distance (m)
					Minimum	Average	
Summer	Weak (0.04)	16.4 [910.9]	6.11	0.00	85	173	9.6
	Medium (0.16)	22.9 [914.2]	6.10	0.00	119	426	35.8
	Strong (0.33)	18.9 [914.2]	6.01	0.00	151	581	74.7
Transitional	Weak (0.05)	17.6 [910.3]	6.07	0.00	89	188	11.6
	Medium (0.18)	22.8 [910.8]	6.04	0.00	127	465	41.9
	Strong (0.38)	18.4 [914.7]	5.95	0.00	163	629	89.4
Winter	Weak (0.04)	16.8 [910.5]	6.11	0.00	87	178	10.2
	Medium (0.17)	22.8 [910.4]	6.10	0.00	122	443	38.7
	Strong (0.40)	18.8 [914.5]	6.01	0.00	159	613	83.0
Annual	Weak (0.04)	17.1 [910.9]	6.09	0.00	88	182	10.6
	Medium (0.17)	22.9 [910.6]	6.07	0.00	123	448	39.2
	Strong (0.37)	18.7 [914.6]	5.98	0.00	159	615	83.7

Table 3.7   Concentration of biocide at the end of the near-field stage, and the required concentration threshold and number of dilutions for the summer season. Note from Table 3.6 that dilutions at the 5th, 50th and 95th percentile current speeds were 173, 426 and 581, respectively. Dilution rates highlighted in red indicate that suitable dilution is not achieved during the near-field stage.

Contaminant	Source Concentration (ppm)	End of Near-Field Concentration (ppm)			Threshold Concentration (ppm)	Required Dilution Factor
		5th %ile	50th %ile	95th %ile		
		173x Dilution	426x Dilution	581x Dilution		
Biocide	550	3.2	1.3	0.9	1	550

Table 3.8 Concentration of biocide at the end of the near-field stage, and the required concentration threshold and number of dilutions for the transitional season. Note from Table 3.6 that dilutions at the 5th, 50th and 95th percentile current speeds were 188, 465 and 629, respectively. Dilution rates highlighted in red indicate that suitable dilution is not achieved during the near-field stage.

Contaminant	Source Concentration (ppm)	End of Near-Field Concentration (ppm)			Threshold Concentration (ppm)	Required Dilution Factor
		5th %ile	50th %ile	95th %ile		
		188x Dilution	465x Dilution	629x Dilution		
Biocide	550	2.9	1.2	0.9	1	550

Table 3.9 Concentration of biocide at the end of the near-field stage, and the required concentration threshold and number of dilutions for the winter season. Note from Table 3.6 that dilutions at the 5th, 50th and 95th percentile current speeds were 178, 443 and 613, respectively. Dilution rates highlighted in red indicate that suitable dilution is not achieved during the near-field stage.

Contaminant	Source Concentration (ppm)	End of Near-Field Concentration (ppm)			Threshold Concentration (ppm)	Required Dilution Factor
		5th %ile	50th %ile	95th %ile		
		178x Dilution	443x Dilution	613x Dilution		
Biocide	550	3.1	1.2	0.9	1	550

Table 3.10 Concentration of biocide at the end of the near-field stage, and the required concentration threshold and number of dilutions for the annual period. Note from Table 3.6 that dilutions at the 5th, 50th and 95th percentile current speeds were 182, 448 and 615, respectively. Dilution rates highlighted in red indicate that suitable dilution is not achieved during the near-field stage.

Contaminant	Source Concentration (ppm)	End of Near-Field Concentration (ppm)			Threshold Concentration (ppm)	Required Dilution Factor
		5th %ile	50th %ile	95th %ile		
		182x Dilution	448x Dilution	615x Dilution		
Biocide	550	3.0	1.2	0.9	1	550

Figure 3.5   Near-field average dilution and temperature results for constant weak, medium and strong summer currents (930 m depth discharge at 220 m³/hr flow rate).
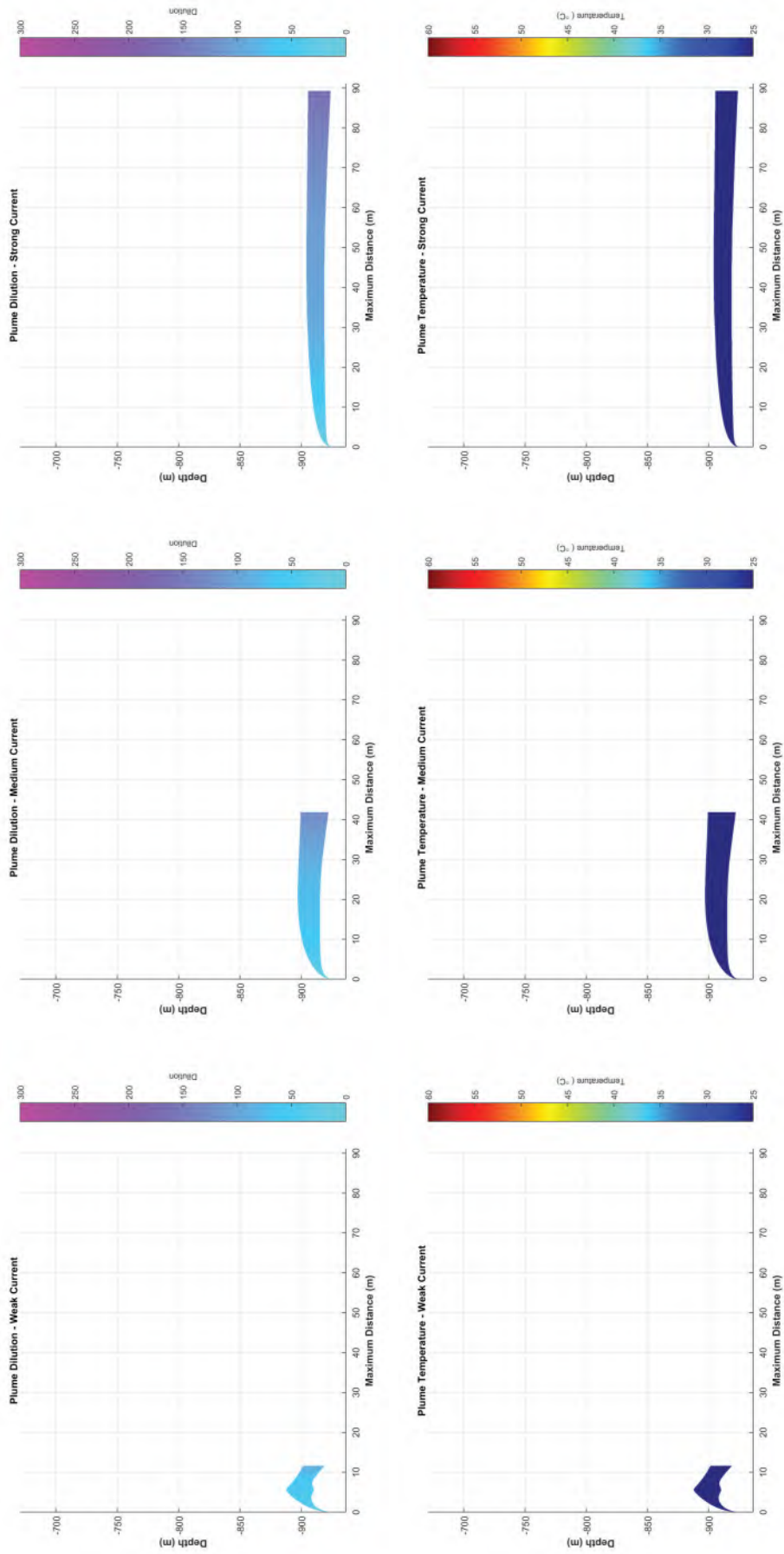
Figure 3.6   Near-field average dilution and temperature results for constant weak, medium and strong transitional currents (930 m depth discharge at 220 m³/hr flow rate).
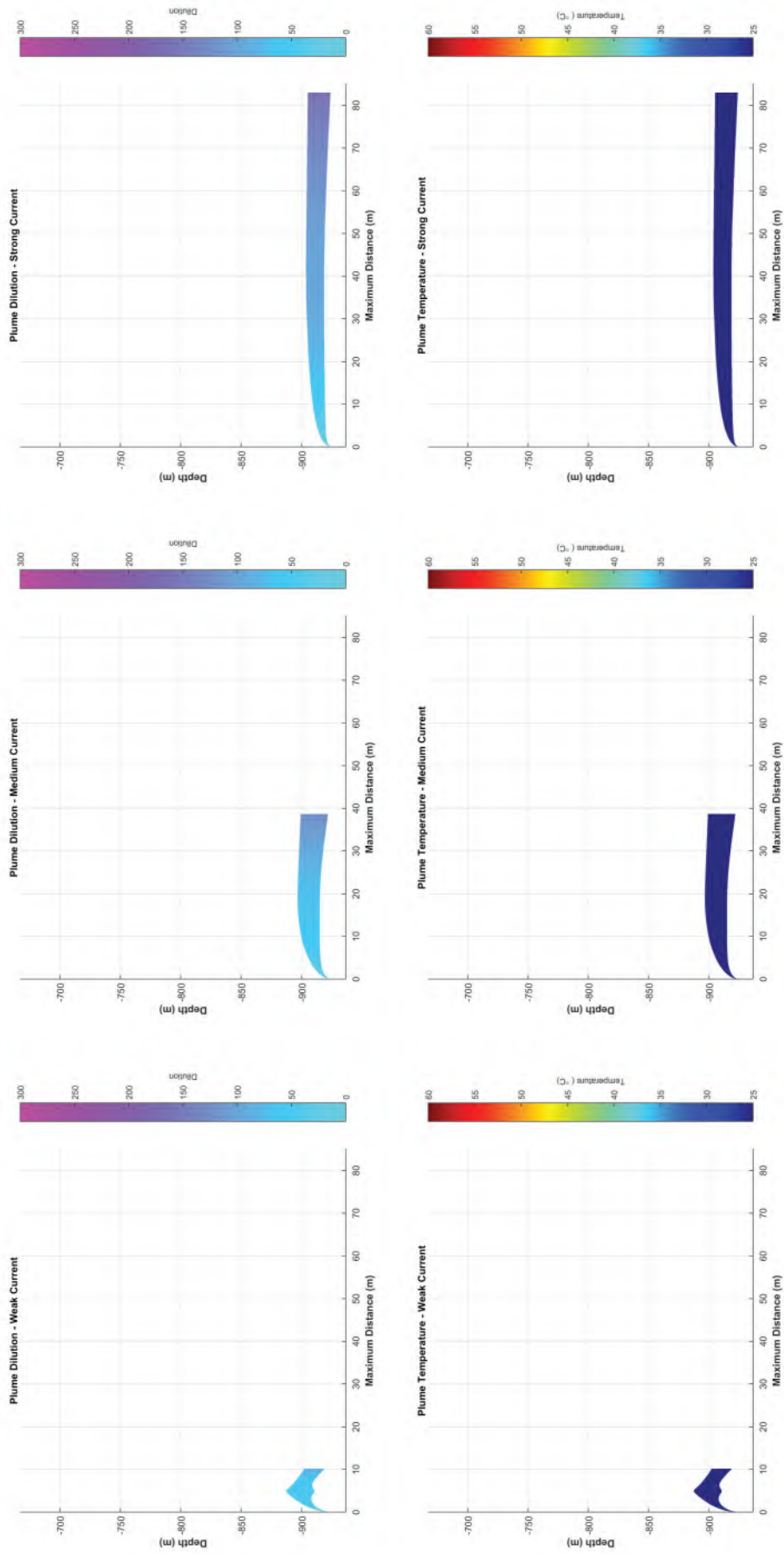
Figure 3.7   Near-field average dilution and temperature results for constant weak, medium and strong winter currents (930 m depth discharge at 220 m³/hr flow rate).
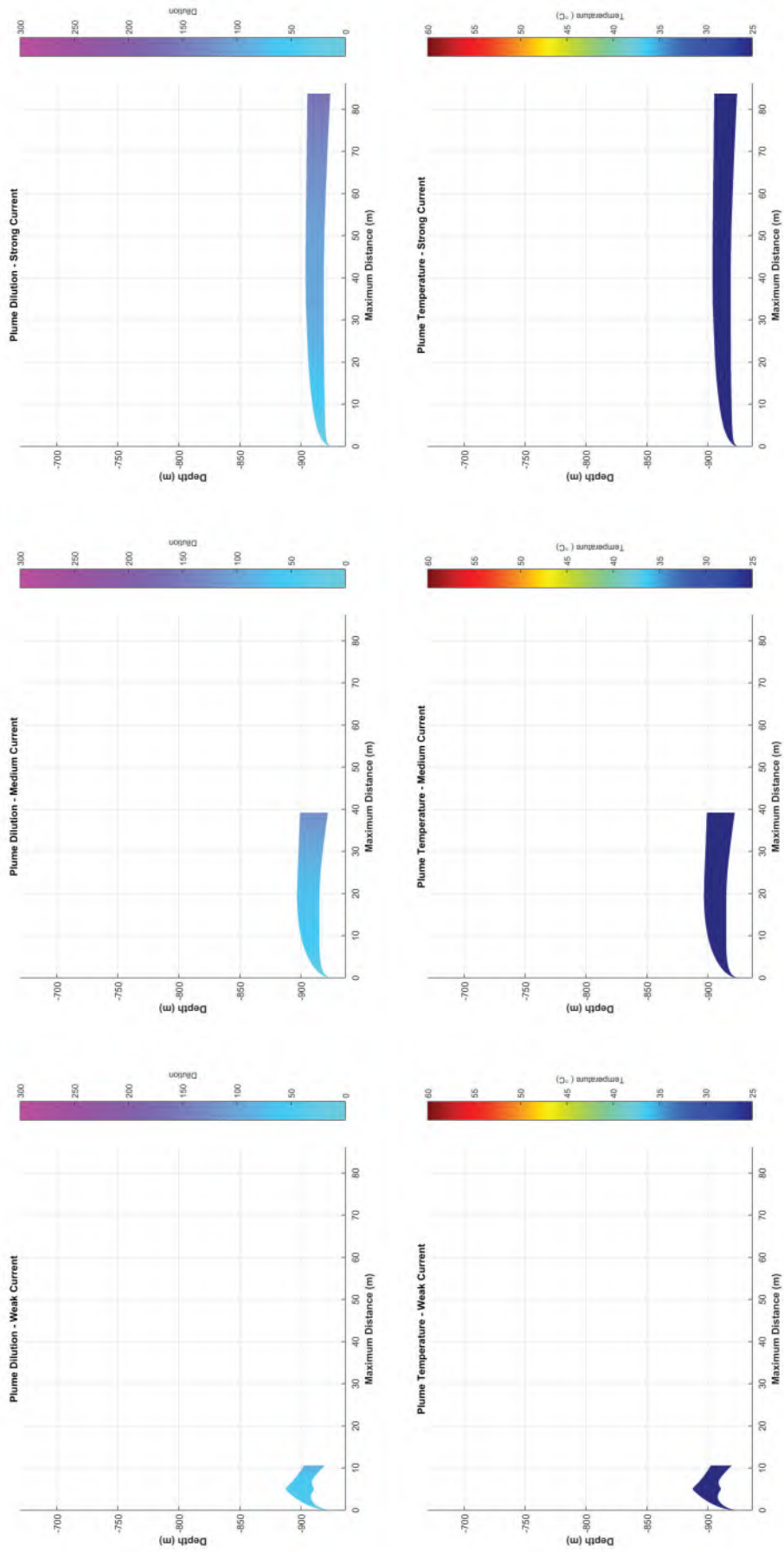
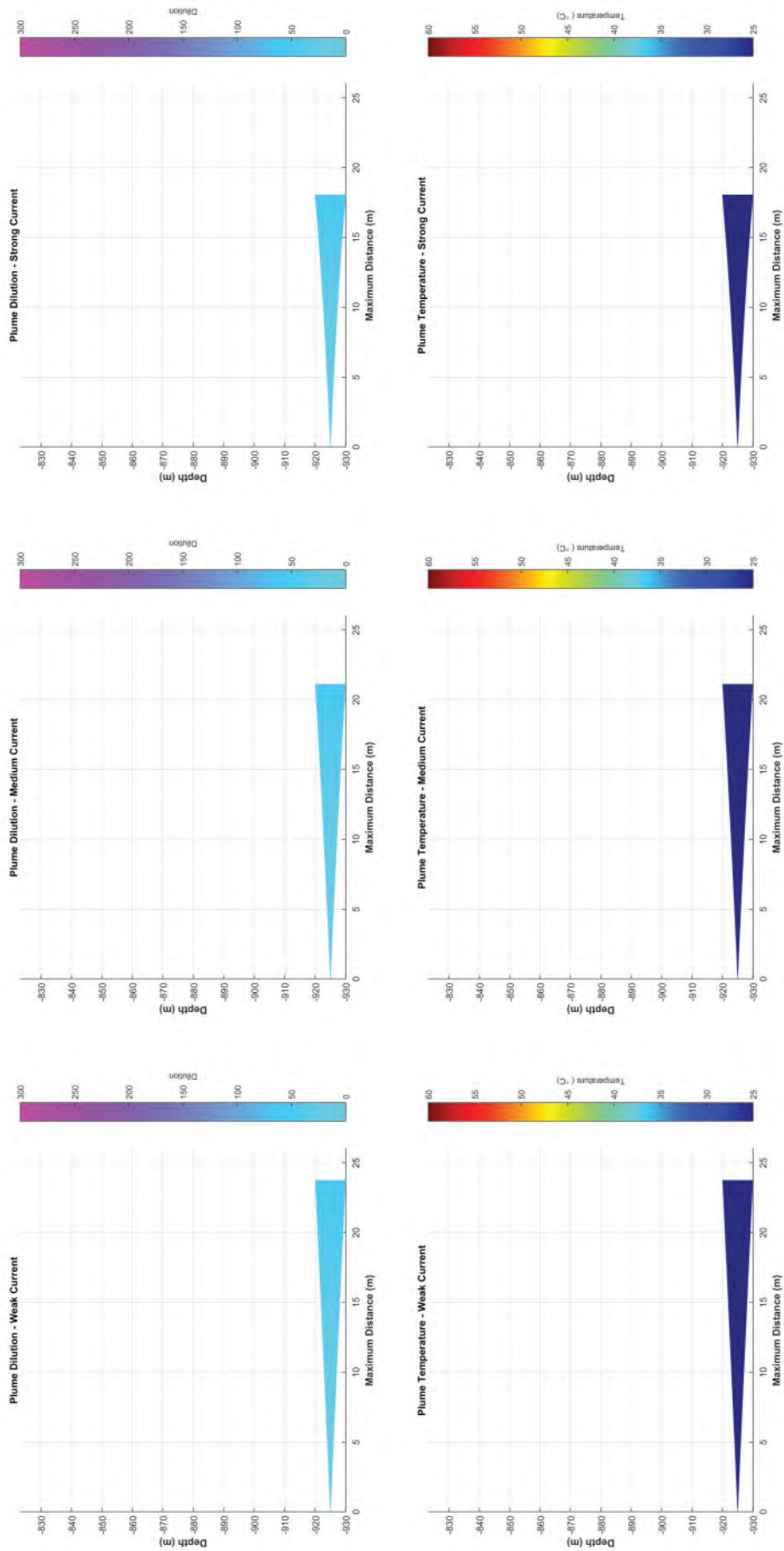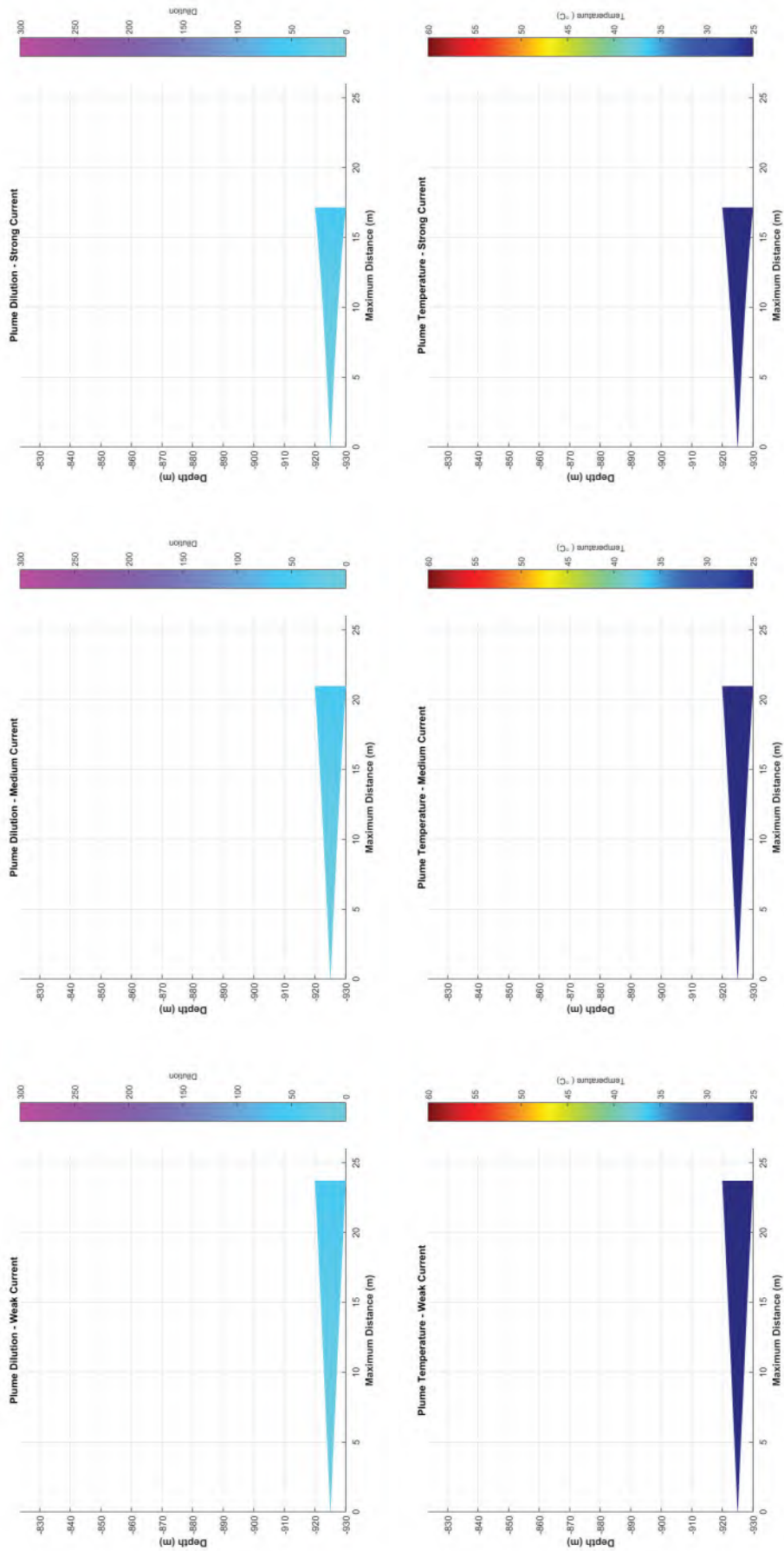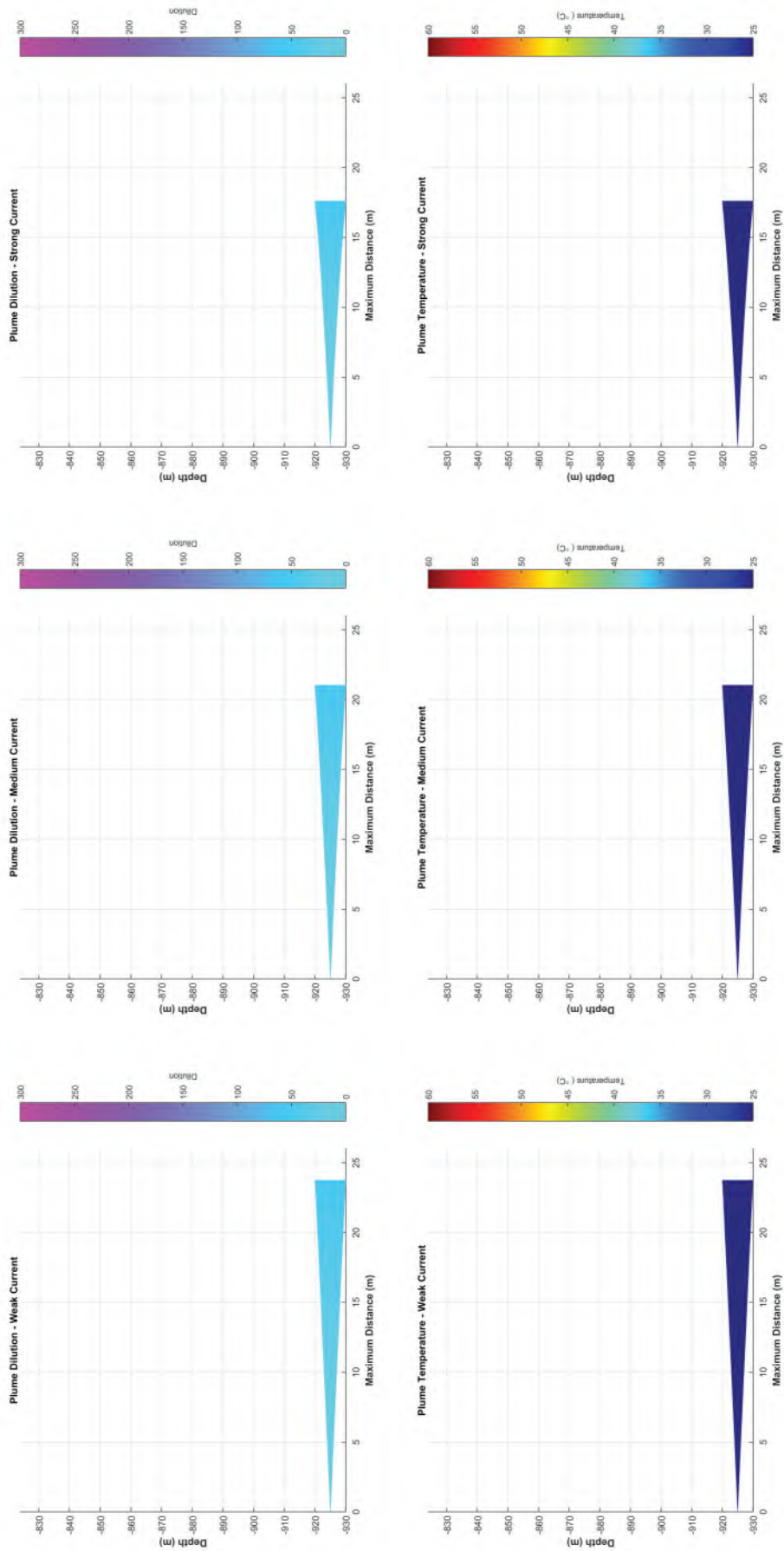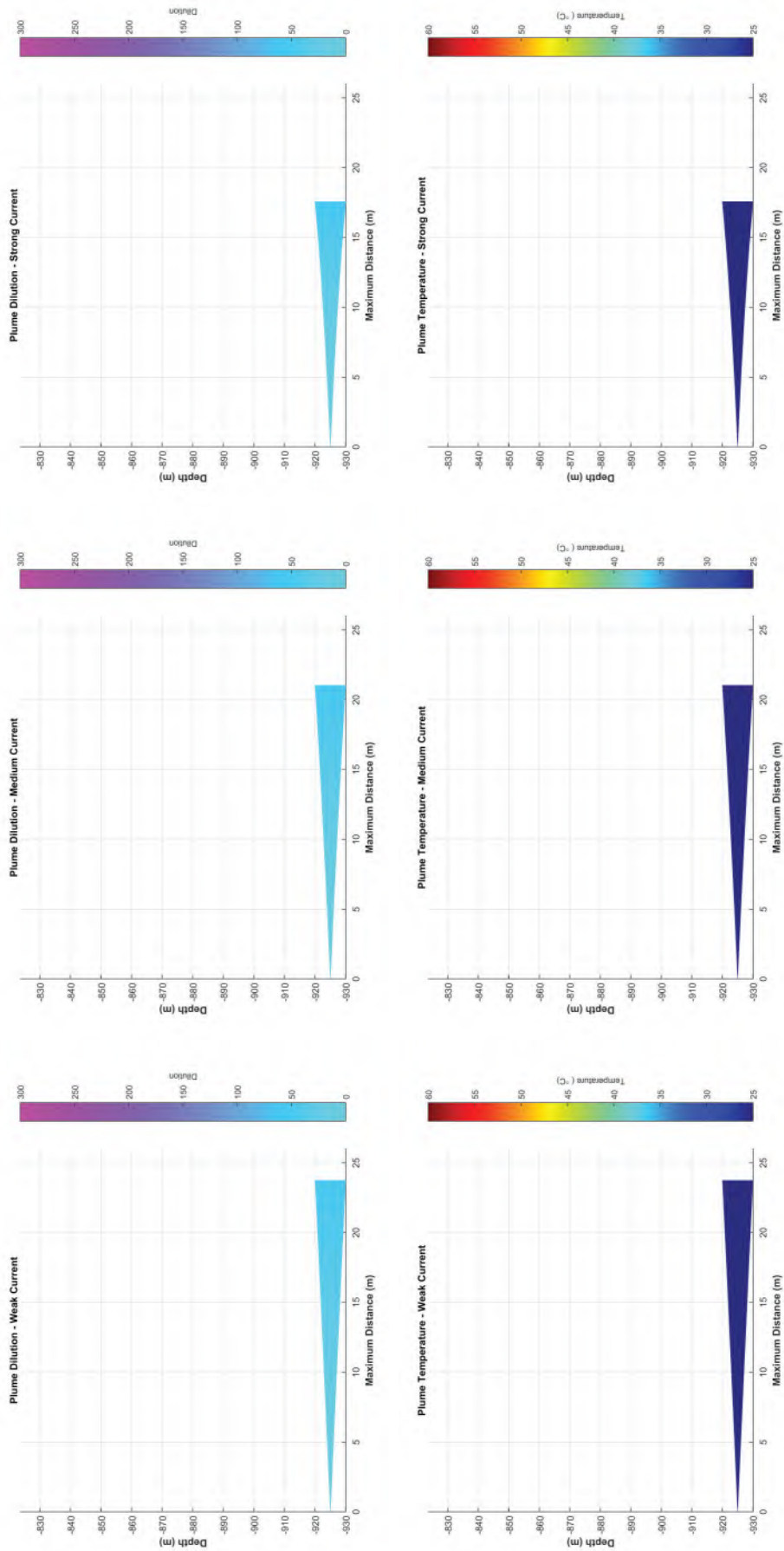**Figure 3.8   Near-field average dilution and temperature results for constant weak, medium and strong annualised currents (930 m depth discharge at 220 m³/hr flow rate).**

3.1.2.3 Discharge Case 3: SURF Hydrotest Discharge at 10 m Depth

Table 3.11 Predicted plume characteristics at the end of the near-field mixing zone for the SURF hydrotest discharge for each season and current speed.

Season	Surface Current Speed (m/s)	Plume Diameter (m) at Depth [m]	Plume Temperature (°C)	Plume-Ambient Temperature Difference (°C)	Plume Dilution (1:x)		Maximum Horizontal Distance (m)
					Minimum	Average	
Summer	Weak (0.04)	15.1 [28.9]	27.40	0.00	42	118	7.5
	Medium (0.16)	12.2 [21.4]	27.40	0.00	77	229	29.7
	Strong (0.33)	9.8 [18.2]	27.50	0.00	101	395	63.0
Transitional	Weak (0.05)	16.8 [21.8]	25.60	0.00	77	211	17.3
	Medium (0.18)	14.8 [17.9]	25.70	0.00	128	496	69.3
	Strong (0.38)	11.5 [15.6]	25.70	0.00	162	629	144.4
Winter	Weak (0.04)	16.7 [21.9]	26.00	0.00	77	207	16.8
	Medium (0.17)	14.8 [18.2]	26.00	0.00	125	482	65.8
	Strong (0.40)	11.3 [15.5]	26.10	0.00	165	641	151.7
Annual	Weak (0.04)	16.4 [22.1]	26.20	0.00	76	201	16.2
	Medium (0.17)	14.9 [18.3]	26.20	0.00	124	480	64.9
	Strong (0.37)	11.5 [15.6]	26.30	0.00	162	629	143.2

Table 3.12 Concentration of biocide at the end of the near-field stage, and the required concentration threshold and number of dilutions for the summer season. Note from Table 3.11 that dilutions at the 5th, 50th and 95th percentile current speeds were 118, 229 and 395, respectively. Dilution rates highlighted in red indicate that suitable dilution is not achieved during the near-field stage.

Contaminant	Source Concentration (ppm)	End of Near-Field Concentration (ppm)			Threshold Concentration (ppm)	Required Dilution Factor
		5th %ile	50th %ile	95th %ile		
		118x Dilution	229x Dilution	395x Dilution		
Biocide	550	4.7	2.4	1.4	1	550

Table 3.13 Concentration of biocide at the end of the near-field stage, and the required concentration threshold and number of dilutions for the transitional season. Note from Table 3.11 that dilutions at the 5th, 50th and 95th percentile current speeds were 211, 496 and 629, respectively. Dilution rates highlighted in red indicate that suitable dilution is not achieved during the near-field stage.

Contaminant	Source Concentration (ppm)	End of Near-Field Concentration (ppm)			Threshold Concentration (ppm)	Required Dilution Factor
		5th %ile	50th %ile	95th %ile		
		211x Dilution	496x Dilution	629x Dilution		
Biocide	550	2.6	1.1	0.9	1	550

Table 3.14 Concentration of biocide at the end of the near-field stage, and the required concentration threshold and number of dilutions for the winter season. Note from Table 3.11 that dilutions at the 5th, 50th and 95th percentile current speeds were 207, 482 and 641, respectively. Dilution rates highlighted in red indicate that suitable dilution is not achieved during the near-field stage.

Contaminant	Source Concentration (ppm)	End of Near-Field Concentration (ppm)			Threshold Concentration (ppm)	Required Dilution Factor
		5th %ile	50th %ile	95th %ile		
		207x Dilution	482x Dilution	641x Dilution		
Biocide	550	2.7	1.1	0.9	1	550

Table 3.15 Concentration of biocide at the end of the near-field stage, and the required concentration threshold and number of dilutions for the annual period. Note from Table 3.11 that dilutions at the 5th, 50th and 95th percentile current speeds were 201, 480 and 629, respectively. Dilution rates highlighted in red indicate that suitable dilution is not achieved during the near-field stage.

Contaminant	Source Concentration (ppm)	End of Near-Field Concentration (ppm)			Threshold Concentration (ppm)	Required Dilution Factor
		5th %ile	50th %ile	95th %ile		
		201x Dilution	480x Dilution	629x Dilution		
Biocide	550	2.7	1.1	0.9	1	550
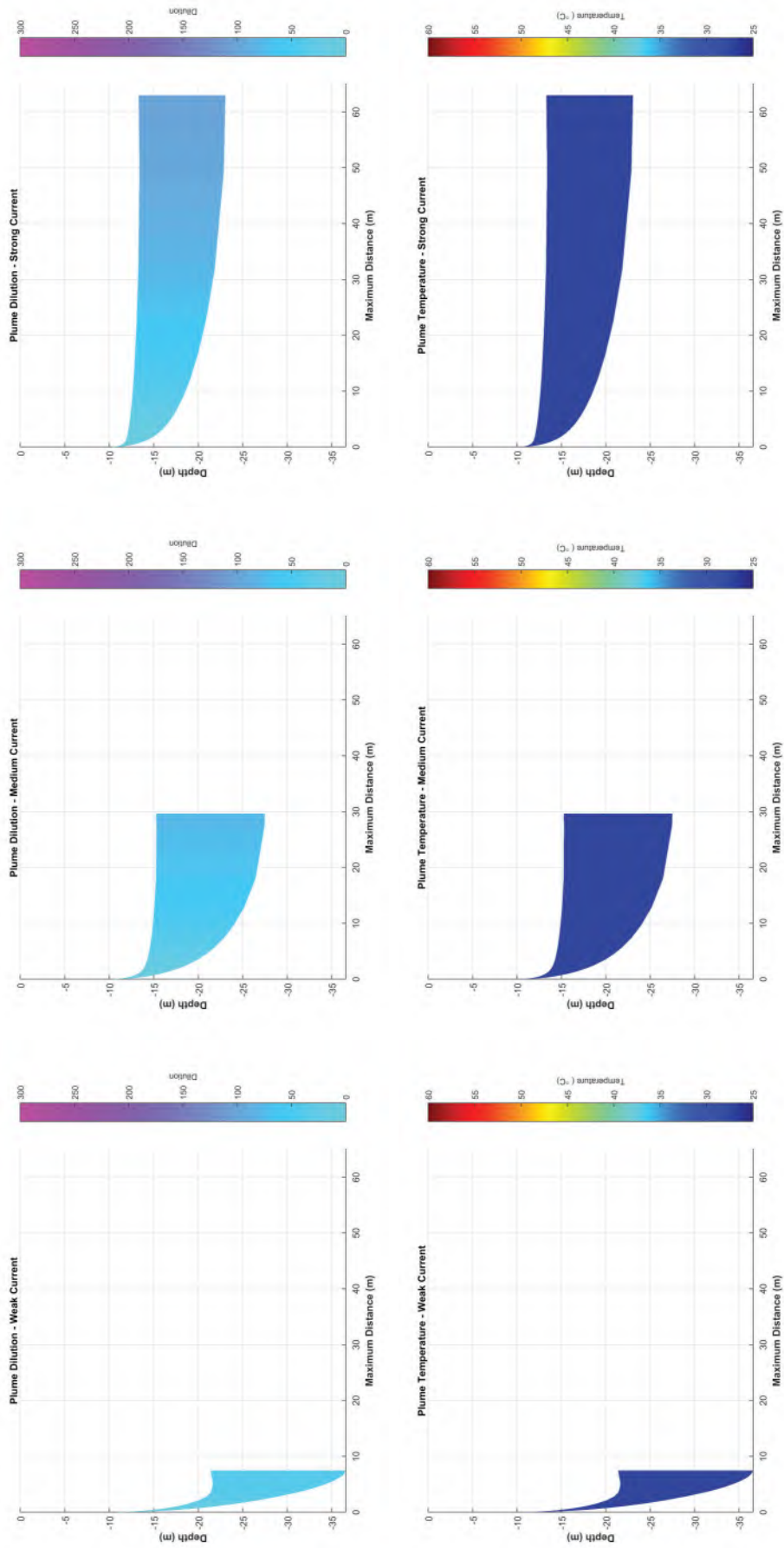
Figure 3.9 Near-field average dilution and temperature results for constant weak, medium and strong summer currents (10 m depth discharge at 220 m³/hr flow rate).
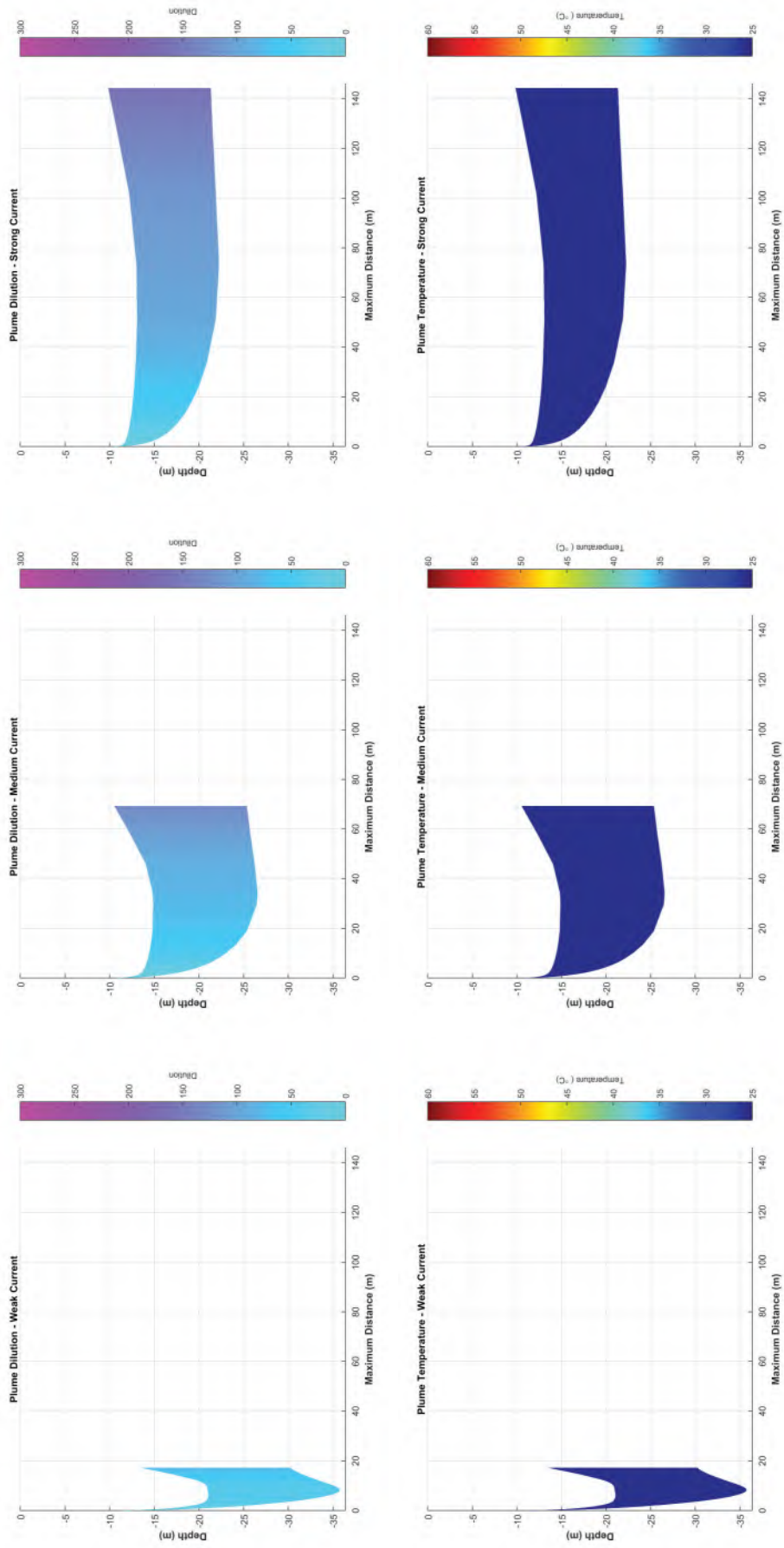
Figure 3.10 Near-field average dilution and temperature results for constant weak, medium and strong transitional currents (10 m depth discharge at 220 m³/hr flow rate).
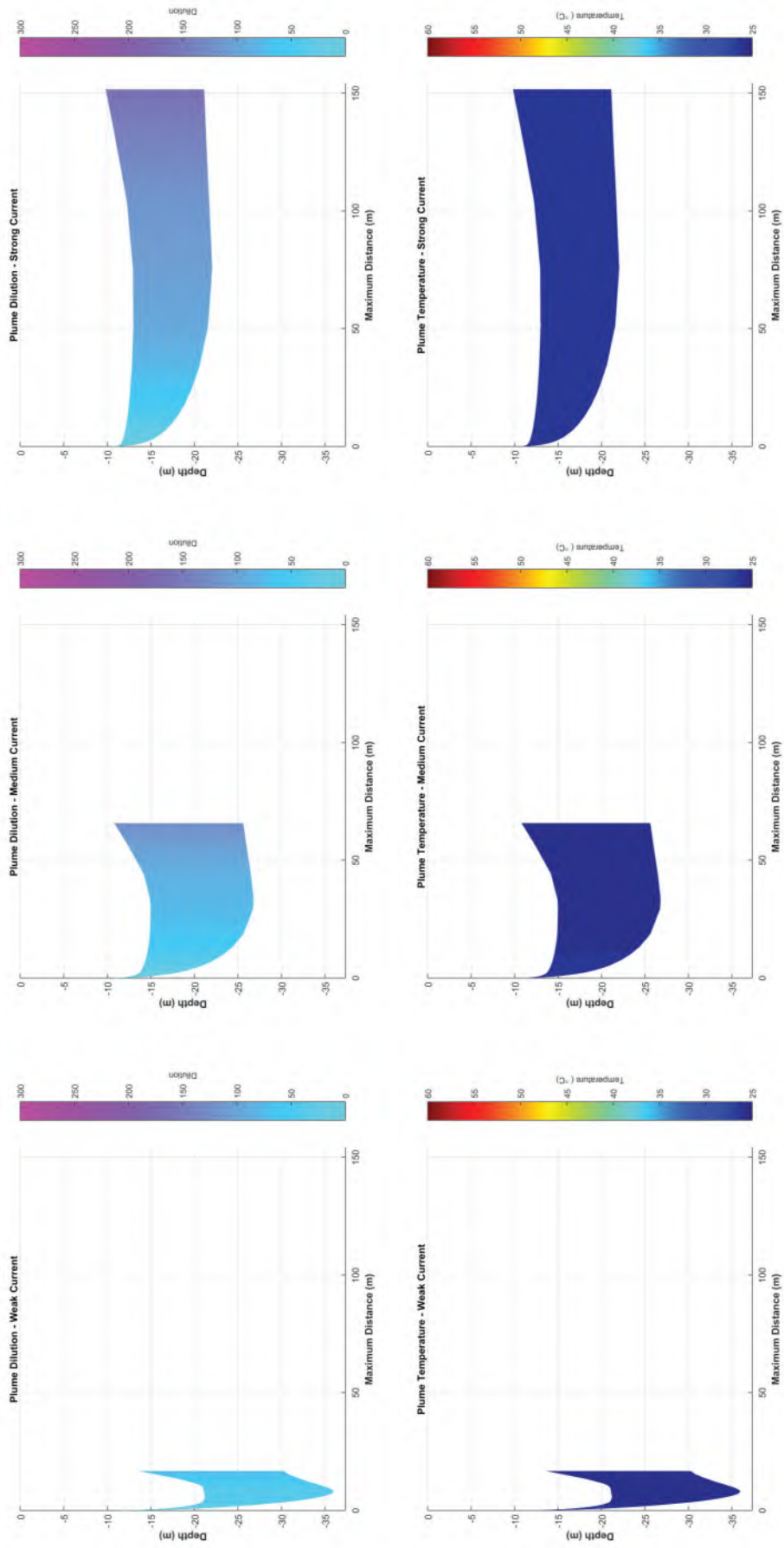
Figure 3.11 Near-field average dilution and temperature results for constant weak, medium and strong winter currents (10 m depth discharge at 220 m³/hr flow rate).
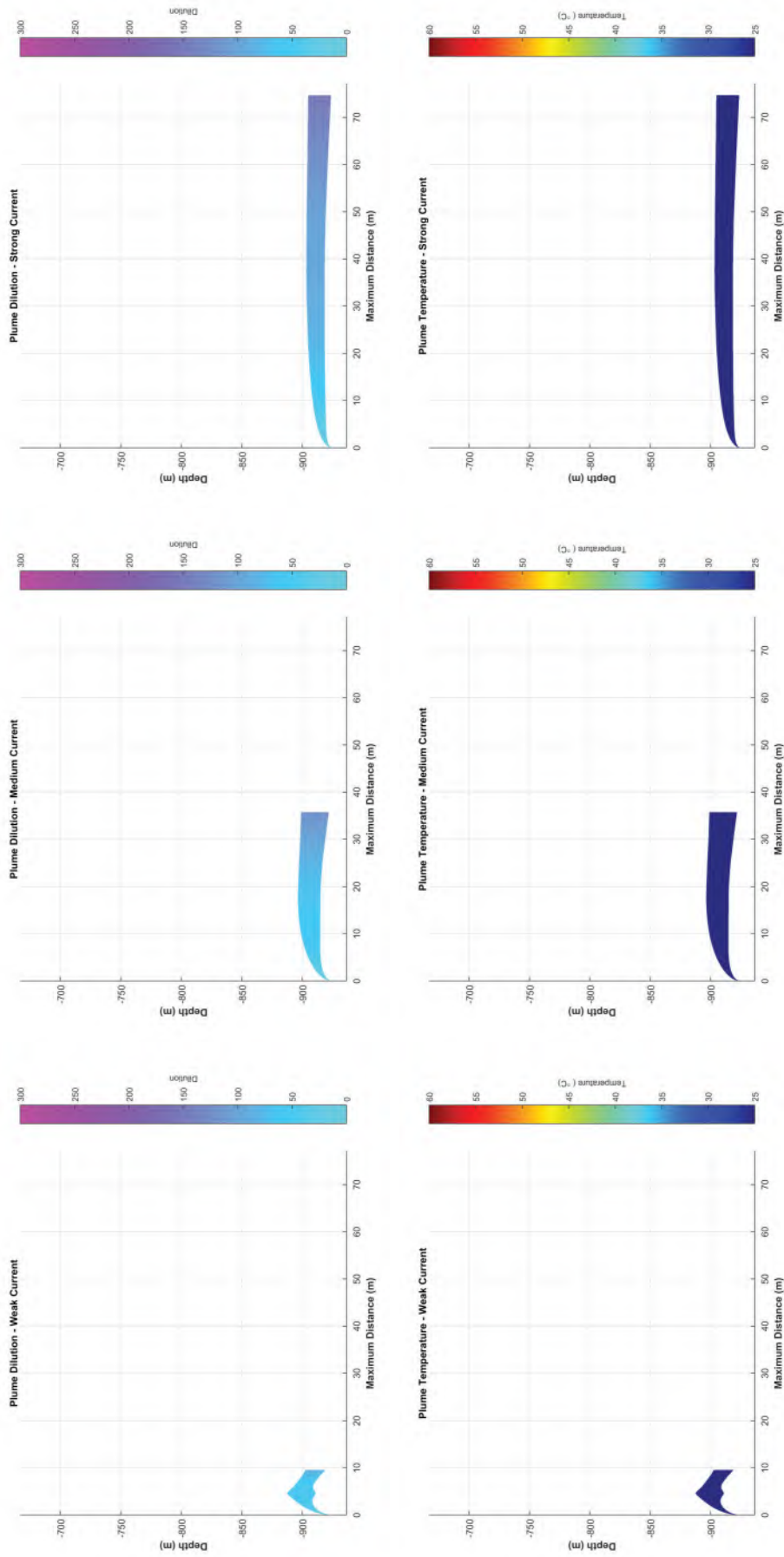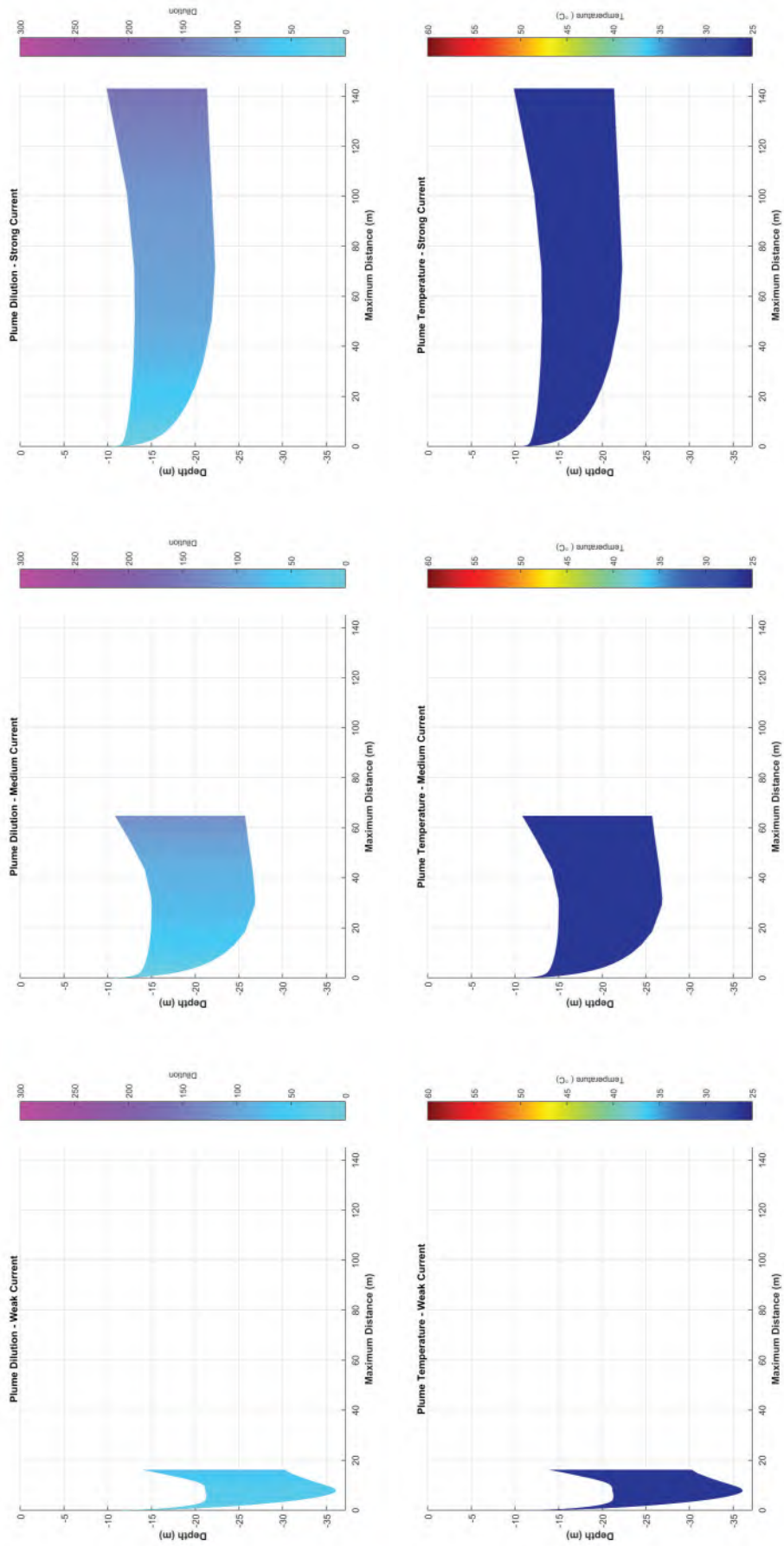
Figure 3.12 Near-field average dilution and temperature results for constant weak, medium and strong annualised currents (10 m depth discharge at 220 m³/hr flow rate).

3.2 Far-Field Modelling

3.2.1 Overview

It is important to note that near-field and far-field modelling are used to describe different processes and scales of effect, and therefore the far-field modelling results will not necessarily correspond to the outcomes at the end of the near-field mixing zone for any given discharge scenario. The far-field results included episodes of pooling of the discharge plume under weak currents, which caused lower dilutions (higher concentrations) further from the discharge location when the pooled plume was advected away. Episodes of recirculation – where the plume moved back under the discharge at some later time due to the oscillatory nature of the tide – were also observed, compounding the pooling effect and further lowering the dilution values.

3.2.2 Interpretation of Percentile Dilution Contours

For each of the modelled discharge cases, the results for all simulations were combined and a statistical analysis performed to produce percentile contours of dilution. In the following sections, outcomes based on 95th and 99th percentile dilution contours are presented.

Calculation of 95th and 99th percentile statistics is a common approach to assessing the impact of dispersing plumes and captures the variability in outcomes, for all but the most ephemeral of forcing conditions, in the data set under consideration. Impact assessment criteria for water quality are often defined using similar statistical indicators.

Note that the percentile figures do not represent the location of a plume at any point in time; they are a statistical and spatial summary of the percentage of time that particular dilution values occur across all replicate simulations and time steps. For example, if the 95th percentile minimum dilution at a particular location in the model domain is predicted as a value of 100, this means that for 95% of the time the dilution level will be higher than 100 and for only 5% of the time the dilution level will be lower than 100. A comparison of the plume extents shown in Figure 3.13 with those shown in Sections 3.2.4 and 3.2.5 demonstrates the significant difference between an instantaneous snapshot and a cumulative estimate of coverage over several days and many individual simulations.

Dilution contours are calculated from the ratios of dispersing contaminant concentrations in the receiving waters to the initial concentration of the contaminant in the discharge. Note that this assumes the background concentration of the constituent in the receiving waters is zero and there is no significant biodegradation of the discharged constituent over the short duration of the dispersion process.

Table 3.16 summarises the initial concentrations of biocide, as specified, and the equivalent dispersed concentrations required to yield particular dilution levels (1:100, 1:200 and 1:400). These concentrations may be useful to consider when interpreting the contour plots of percentile dilutions.

Table 3.16 Initial concentrations of biocide and equivalent concentrations at example dilution levels.

Biocide Parameter	Biocide Concentration (mg/L)
Initial concentration in discharge	550.0
Initial concentration in receiving waters	0.0
Concentration at 1:100 dilution	5.5
Concentration at 1:200 dilution	2.75
Concentration at 1:400 dilution	1.375

3.2.3　General Observations

Figure 3.13 shows example time series snapshots of predicted dilutions during a single simulation at 3-hour intervals from 04:00 to 19:00 on 4th February 2010. This simulation – selected merely to be representative of typical conditions – considers the Case 1 flow rate of 795 m^3/d at 930 m BMSL. The spatially-varying orientation of the plume with the currents and the rapidly-varying nature of the concentrations around the source can be observed. The snapshots also show the combined effect of the tide and the drift currents, with a clear tidal oscillation.

These snapshots illustrate that the dilutions (and in turn concentrations) become more variable over time because of changes in current speed and direction. Higher dilutions (lower concentrations) are predicted during periods of increased current speed, whereas patches of lower dilutions (higher concentrations) tend to accumulate during the turning of the tide or during periods of weak drift currents. During prolonged periods of lowered current speed, the plume has a more continuous appearance, with higher-concentration patches moving as a unified group. These findings agree with the research of King & McAllister (1997, 1998) who noted that concentrations within effluent plumes generated by an offshore platform were patchy and likely to peak around the reversal of the tides.
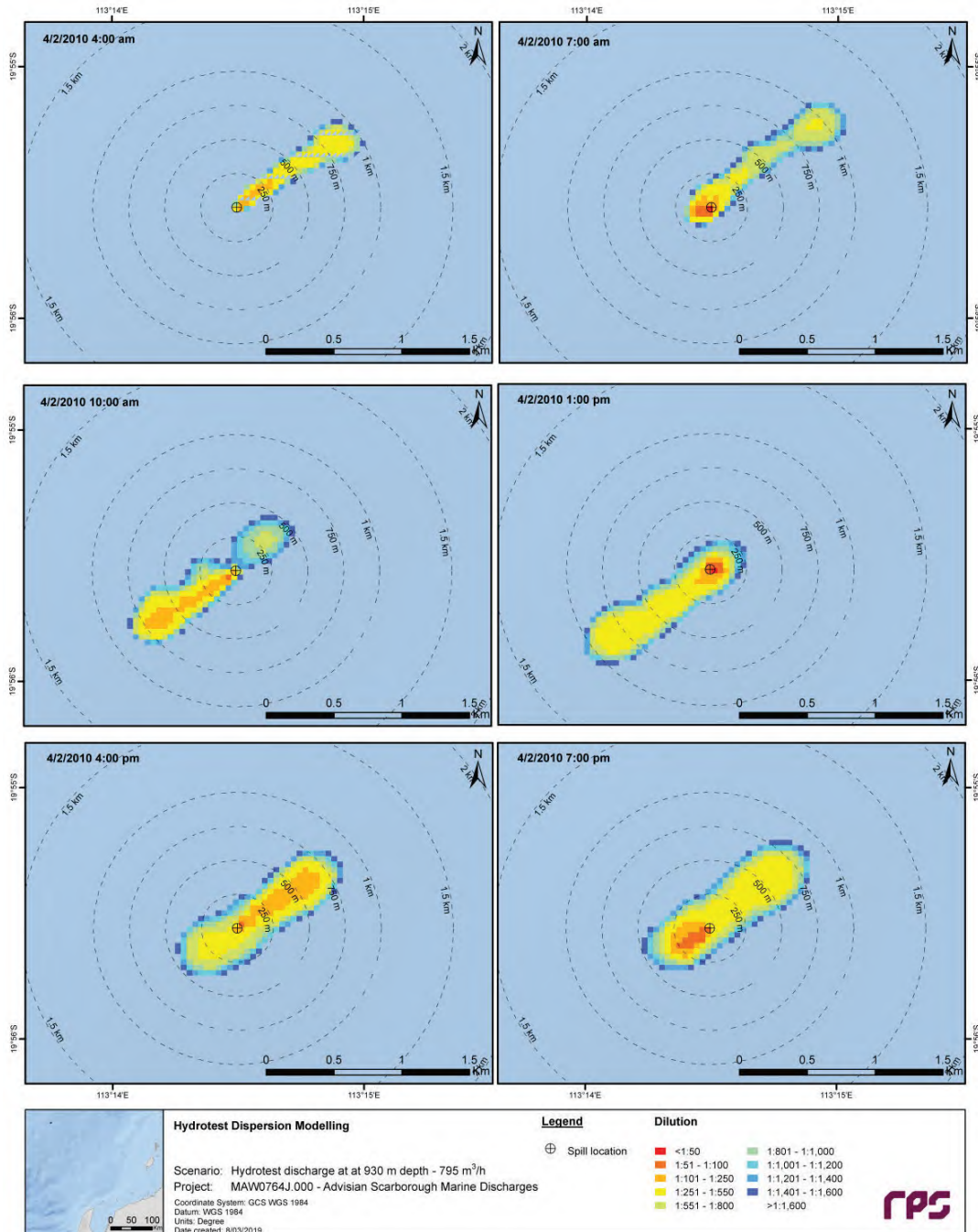
Figure 3.13 Snapshots of predicted dilution levels, at 3-hour intervals from 04:00 to 19:00 on 4th February 2010, for Case 1 (930 m depth discharge at 795 m³/hr flow rate).

3.2.4   Seasonal Analysis

The model outputs over the ten-year hindcast period (2006-2015) were combined and analysed on a seasonal basis (summer, transitional and winter). This approach assists with identifying the potential exposure to surrounding sensitive receptors whilst considering inter-annual variability in ocean current conditions.

Table 3.17 and Table 3.18 summarise, for Cases 1 and 3 respectively, the minimum dilution achieved at specific radial distances from the discharge location for each season and percentile.

Table 3.19 and Table 3.20 provide, for Cases 1 and 3 respectively, summaries of the maximum distances from the discharge location to achieve 1:550 dilution for each season and percentile. The results indicate that the release of effluent under all seasonal conditions results in rapid dispersion within the ambient environment. For Case 1, dilution to reach threshold concentration is achieved for biocide within an area of influence ranging from 1,173 m to 1,196 m at the 95th percentile across all seasons (Table 3.19). For Case 3, the maximum spatial extent of the relevant dilution contour is 18 m at the 95th percentile across all seasons (Table 3.20). The greatest spatial extents are observed in the transitional months.

Table 3.21 and Table 3.22 provide, for Cases 1 and 3 respectively, summaries of the total area of coverage for the 1:550 dilution contour for each season and percentile. For Case 1, the area of exposure defined by the relevant dilution contour is predicted to reach maximums of 2.21 km^2 to 2.30 km^2 at the 95th percentile (Table 3.21). For Case 3, the corresponding maximum area of exposure is <0.01 km^2 at the 95th percentile (Table 3.22).

Table 3.23 and Table 3.24 provide, for Cases 1 and 3 respectively, summaries of the maximum depths from the discharge location to achieve 1:550 dilution for each season and percentile. Maximum depths are predicted as 930 m (seabed; all seasons) and 12 m (all seasons) for Case 1 and Case 3, respectively.

For Cases 1 and 3, Figure 3.14 to Figure 3.25 show the aggregated spatial extents of the minimum dilutions for each season and percentile. Note that the contours represent the lowest predicted dilution (highest concentration) at any given time-step through the water column and do not consider frequency or duration.

The results presented assume that no processes other than dilution would reduce the source concentrations over time.

Table 3.17 Minimum dilution achieved at specific radial distances from the hydrotest discharge location in each season for Case 1 (930 m depth discharge at 795 m³/hr flow rate).

Percentile	Season	Minimum dilution (1:x) achieved at specific radial distances from discharge location															
		0.02 km	0.05 km	0.10 km	0.20 km	0.30 km	0.40 km	0.50 km	0.60 km	0.70 km	0.80 km	0.90 km	1.00 km	1.10 km	1.20 km	1.30 km	1.40 km	1.50 km
95th	Summer	1:21.7	1:31.0	1:36.8	1:52.0	1:63.9	1:74.5	1:81.9	1:90.5	1:104.3	1:117.2	1:153.8	1:208.9	1:314.0	1:453.5	1:666.7	1:952.8	1:1,444.3
	Transitional	1:20.7	1:30.1	1:35.1	1:49.6	1:62.9	1:73.9	1:84.0	1:93.4	1:105.0	1:114.0	1:138.9	1:181.4	1:273.4	1:400.2	1:603.2	1:869.8	1:1,386.1
	Winter	1:21.8	1:31.8	1:37.3	1:53.3	1:65.3	1:76.5	1:84.8	1:93.1	1:104.3	1:112.3	1:133.6	1:173.2	1:261.2	1:394.9	1:595.8	1:875.4	1:1,324.8
99th	Summer	1:18.5	1:24.6	1:30.5	1:41.4	1:51.0	1:59.1	1:65.9	1:73.4	1:83.1	1:90.6	1:103.9	1:120.1	1:168.1	1:243.5	1:382.9	1:557.4	1:825.5
	Transitional	1:17.6	1:24.2	1:28.1	1:39.9	1:50.6	1:59.7	1:68.4	1:75.6	1:83.3	1:90.0	1:99.4	1:106.8	1:126.3	1:174.2	1:275.8	1:428.9	1:632.9
	Winter	1:18.6	1:25.4	1:30.3	1:42.4	1:52.7	1:60.8	1:68.0	1:75.4	1:82.8	1:89.0	1:98.1	1:106.8	1:130.2	1:180.9	1:281.6	1:438.6	1:682.9

Table 3.18 Minimum dilution achieved at specific radial distances from the hydrotest discharge location in each season for Case 3 (10 m depth discharge at 220 m³/hr flow rate).

Percentile	Season	Minimum dilution (1:x) achieved at specific radial distances from discharge location															
		0.02 km	0.05 km	0.10 km	0.20 km	0.30 km	0.40 km	0.50 km	0.60 km	0.70 km	0.80 km	0.90 km	1.00 km	1.10 km	1.20 km	1.30 km	1.40 km	1.50 km
95th	Summer	1:501.3	1:930.5	1:1,243.6	>1:10,000	>1:10,000	>1:10,000	>1:10,000	>1:10,000	-	-	-	-	-	-	-	-	-
	Transitional	1:489.5	1:1,450.3	1:1,594.5	>1:10,000	>1:10,000	>1:10,000	>1:10,000	>1:10,000	-	-	-	-	-	-	-	-	-
	Winter	1:387.1	1:1,002.1	1:1,149.9	>1:10,000	>1:10,000	>1:10,000	-	-	-	-	-	-	-	-	-	-	-
99th	Summer	1:309.1	1:367.1	1:435.1	1:775.8	1:1,050.9	1:1,370.6	1:1,758.5	1:2,007.1	1:2,315.7	1:2,609.9	1:2,699.5	1:3,124.9	1:3,346.2	1:3,724.6	1:4,147.3	1:4,531.2	1:4,793.6
	Transitional	1:335.7	1:330.3	1:431.6	1:697.9	1:966.3	1:1,316.0	1:1,569.5	1:1,828.7	1:2,124.7	1:2,297.0	1:2,604.5	1:2,838.4	1:3,174.4	1:3,525.3	1:3,450.6	1:3,980.1	1:4,042.6
	Winter	1:160.9	1:279.8	1:320.5	1:600.5	1:779.8	1:1,129.1	1:1,364.3	1:1,609.3	1:1,881.9	1:2,202.9	1:2,595.3	1:2,937.8	1:3,472.2	1:3,580.6	1:3,938.0	1:4,743.0	1:5,882.2

Table 3.19 **Maximum distance from the hydrotest discharge location to achieve 1:550 dilution in each season for Case 1 (930 m depth discharge at 795 m³/hr flow rate).**

Percentile	Season	Maximum distance (m) from discharge location to achieve given dilution
95th	Summer	1,173
	Transitional	1,196
	Winter	1,196
99th	Summer	1,317
	Transitional	1,388
	Winter	1,373
100th	Summer	1,532
	Transitional	1,564
	Winter	1,551

Table 3.20 **Maximum distance from the hydrotest discharge location to achieve 1:550 dilution in each season for Case 3 (10 m depth discharge at 220 m³/hr flow rate).**

Percentile	Season	Maximum distance (m) from discharge location to achieve given dilution
95th	Summer	18
	Transitional	18
	Winter	18
99th	Summer	82
	Transitional	91
	Winter	124
100th	Summer	630
	Transitional	292
	Winter	1,147

Table 3.21   **Total area of coverage for 1:550 dilution in each season for Case 1 (930 m depth discharge at 795 m³/hr flow rate).**

Percentile	Season	Total area (km²) of coverage for given dilution
95th	Summer	2.213
	Transitional	2.266
	Winter	2.298
99th	Summer	2.751
	Transitional	2.902
	Winter	2.900
100th	Summer	3.531
	Transitional	3.699
	Winter	3.596

Table 3.22   **Total area of coverage for 1:550 dilution in each season for Case 3 (10 m depth discharge at 220 m³/hr flow rate).**

Percentile	Season	Total area (km²) of coverage for given dilution
95th	Summer	0.002
	Transitional	0.002
	Winter	0.002
99th	Summer	0.011
	Transitional	0.010
	Winter	0.029
100th	Summer	0.144
	Transitional	0.108
	Winter	0.495

Table 3.23   Maximum depth from the hydrotest discharge location to achieve 1:550 dilution in each season for Case 1 (930 m depth discharge at 795 m³/hr flow rate).

Season	Maximum depth (m) from discharge location to achieve given dilution
Summer	930 (seabed)
Transitional	930 (seabed)
Winter	930 (seabed)

Table 3.24   Maximum depth from the hydrotest discharge location to achieve 1:550 dilution in each season for Case 3 (10 m depth discharge at 220 m³/hr flow rate).

Season	Maximum depth (m) from discharge location to achieve given dilution
Summer	12
Transitional	12
Winter	12

Figure 3.14 Predicted minimum dilutions at the 95th percentile under summer conditions for Case 1 (930 m depth discharge at 795 m³/hr flow rate).

Figure 3.15 Predicted minimum dilutions at the 99th percentile under summer conditions for Case 1 (930 m depth discharge at 795 m³/hr flow rate).
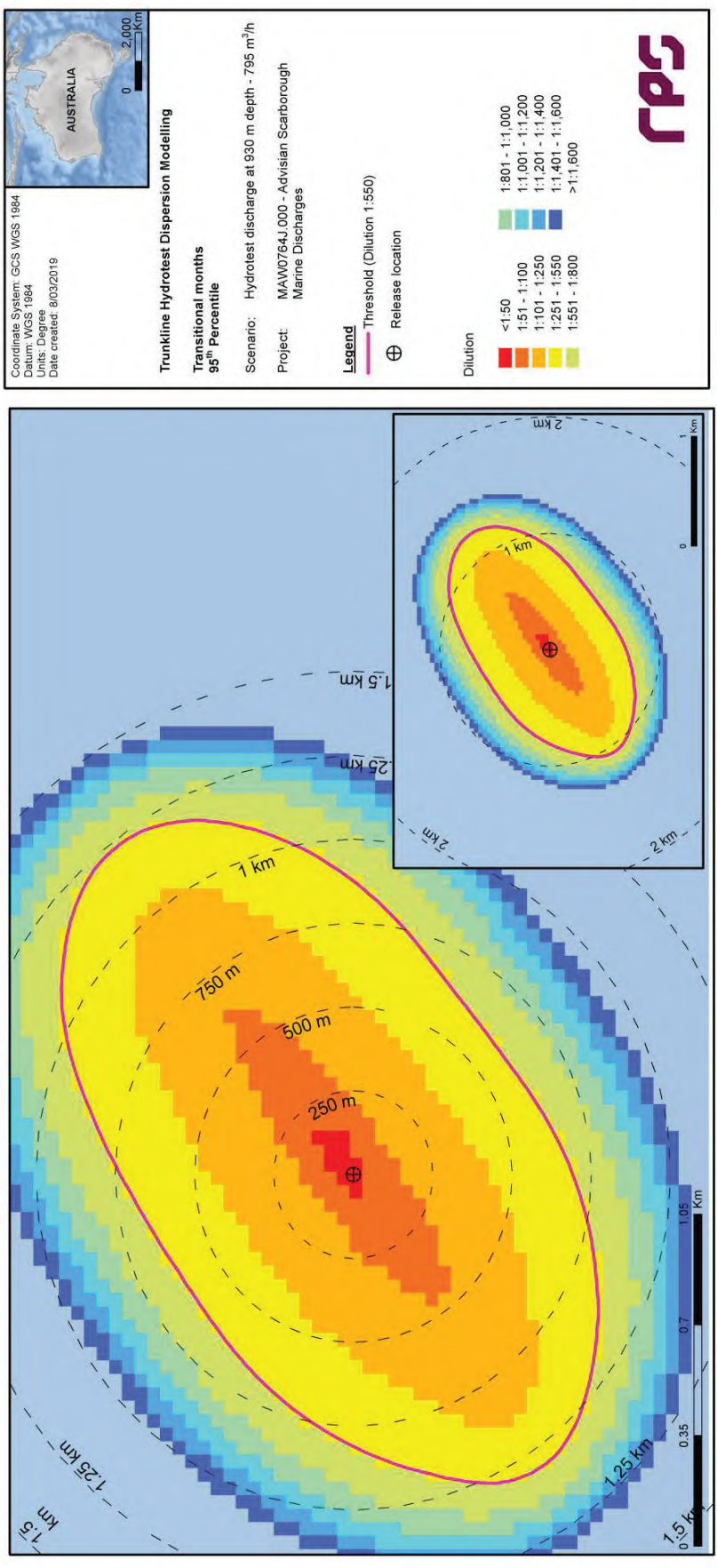
Figure 3.16 Predicted minimum dilutions at the 95th percentile under transitional conditions for Case 1 (930 m depth discharge at 795 m³/hr flow rate).
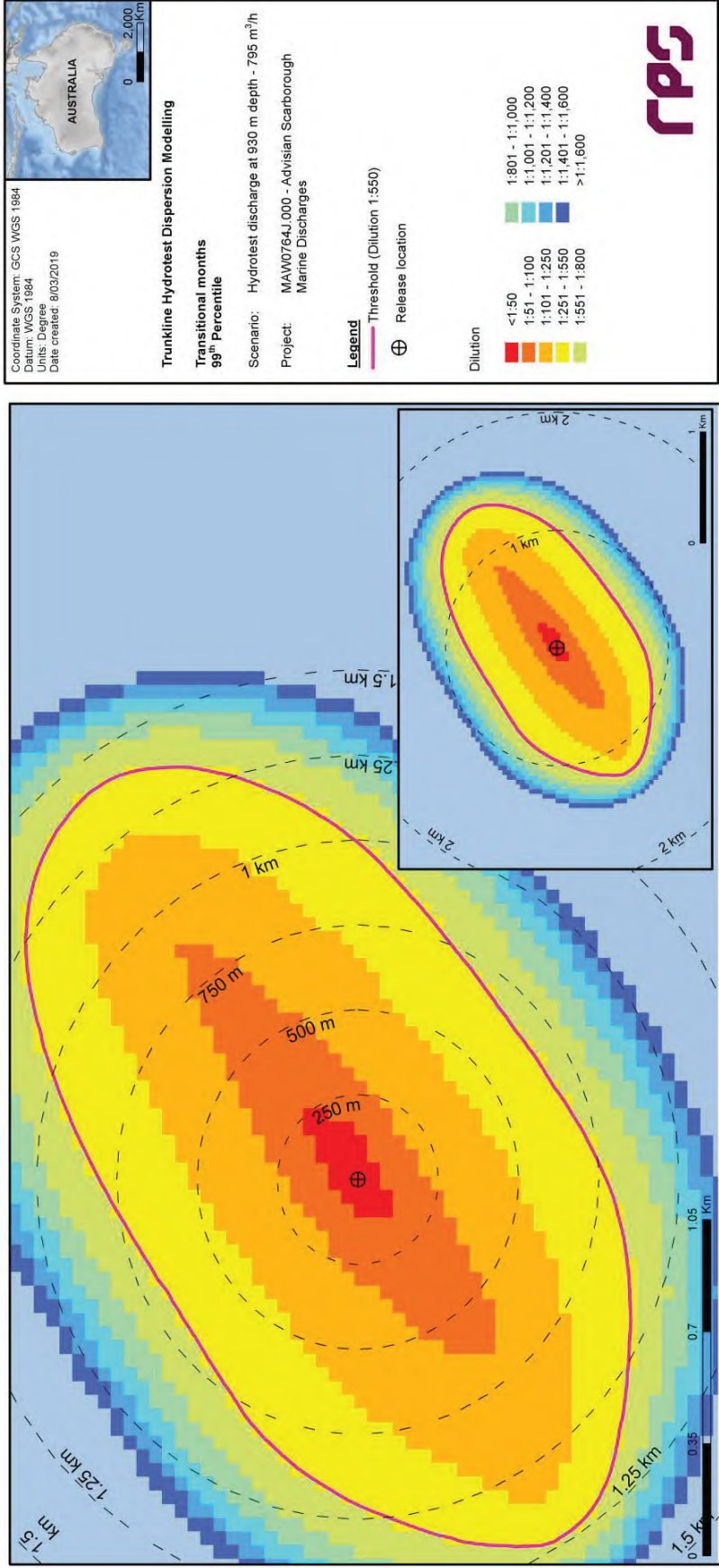
Figure 3.17 Predicted minimum dilutions at the 99th percentile under transitional conditions for Case 1 (930 m depth discharge at 795 m³/hr flow rate).
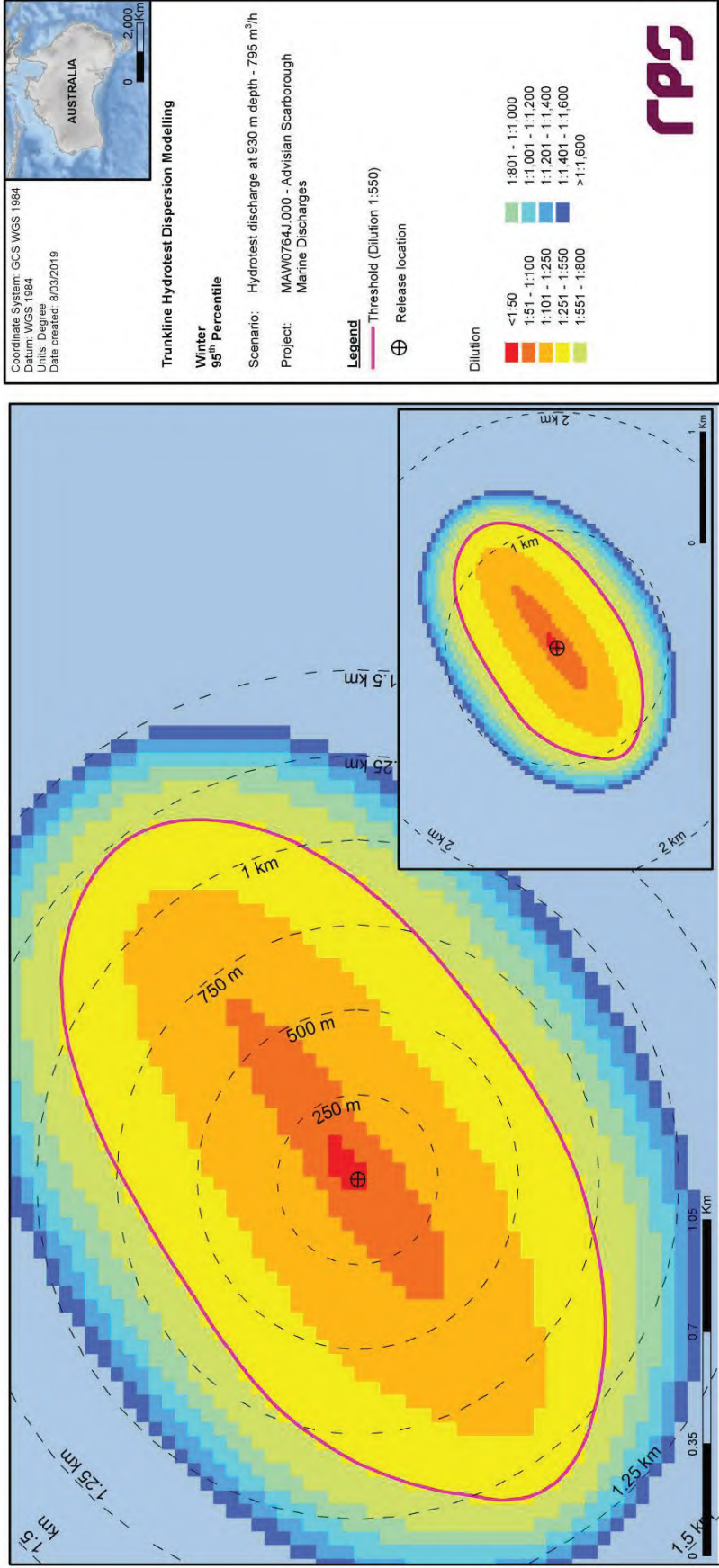
Figure 3.18 Predicted minimum dilutions at the 95th percentile under winter conditions for Case 1 (930 m depth discharge at 795 m³/hr flow rate).
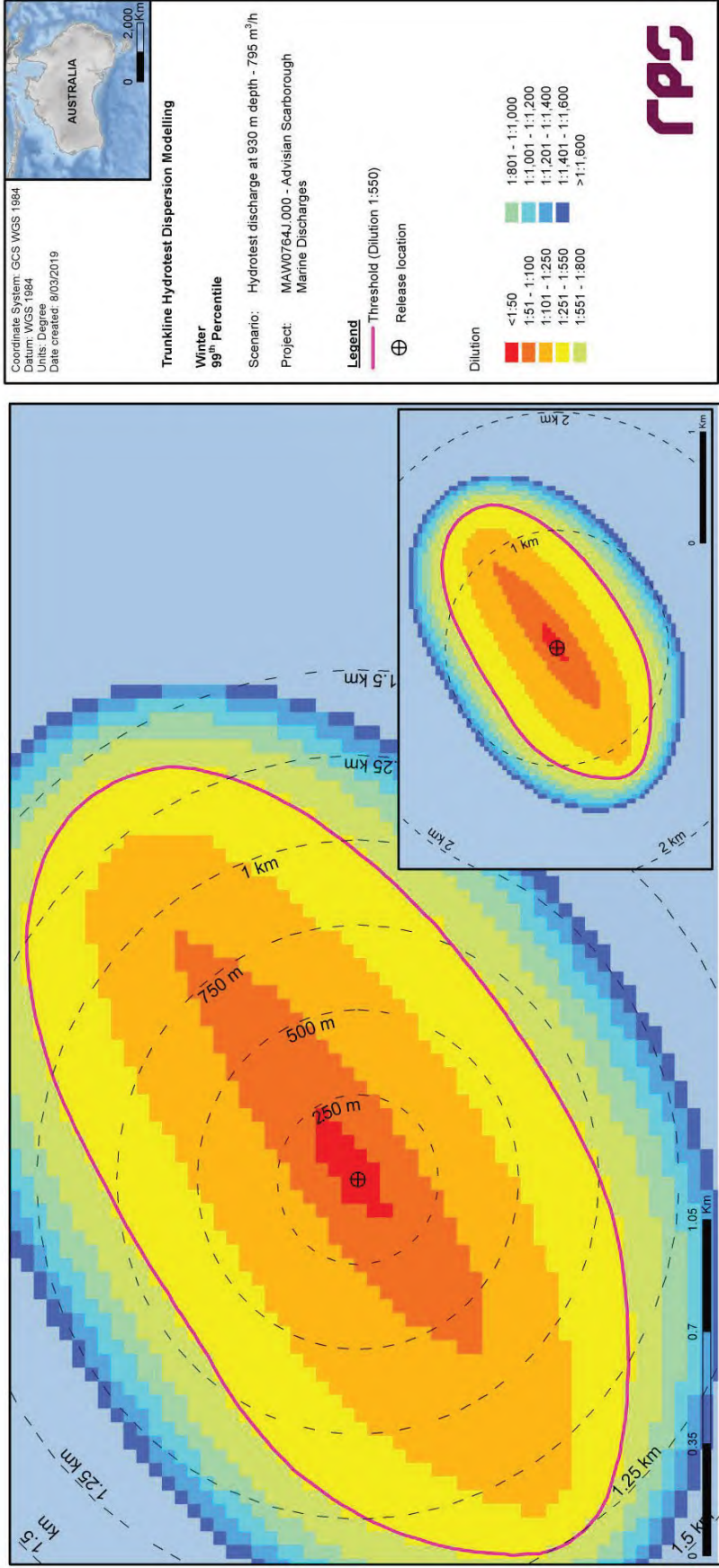
Figure 3.19 Predicted minimum dilutions at the 99th percentile under winter conditions for Case 1 (930 m depth discharge at 795 m³/hr flow rate).
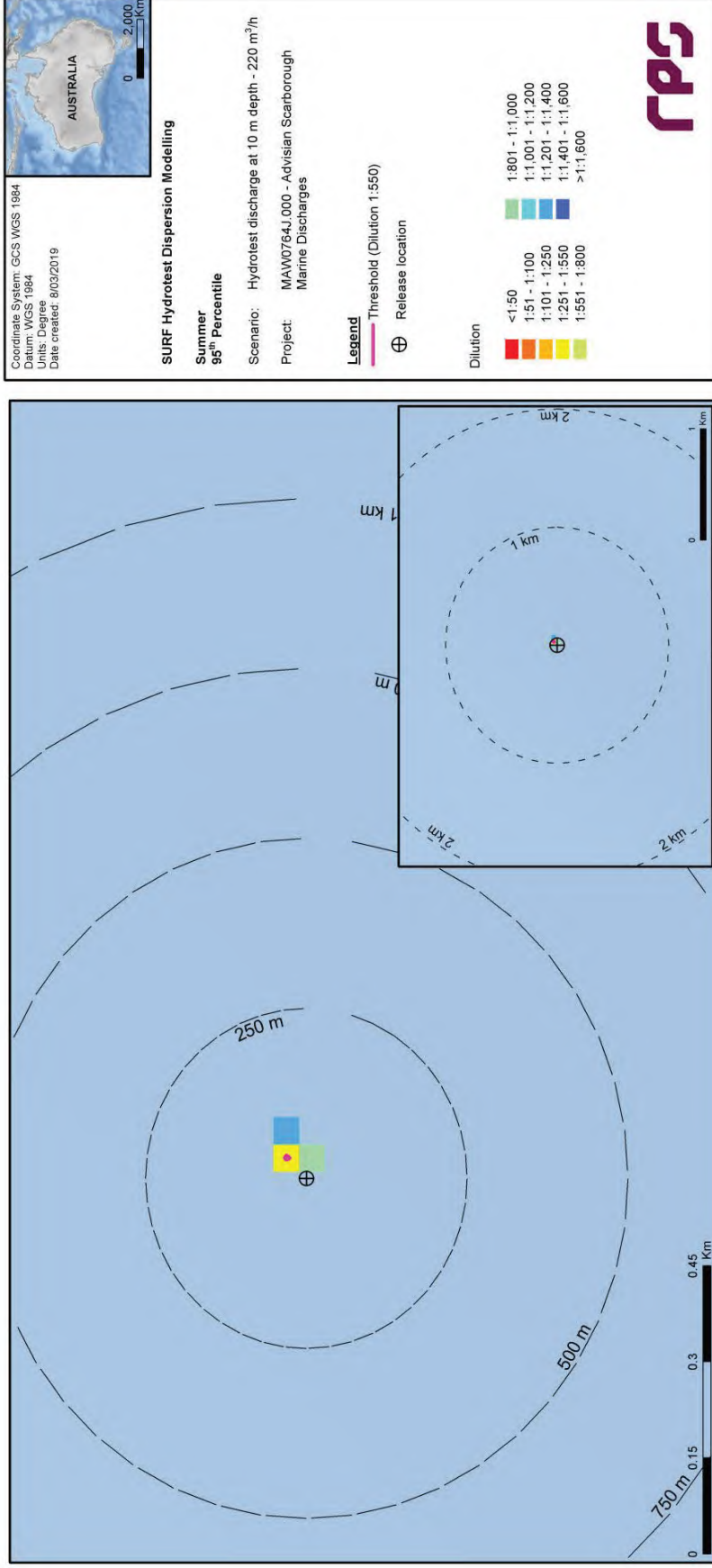
Figure 3.20 Predicted minimum dilutions at the 95th percentile under summer conditions for Case 3 (10 m depth discharge at 220 m³/hr flow rate).
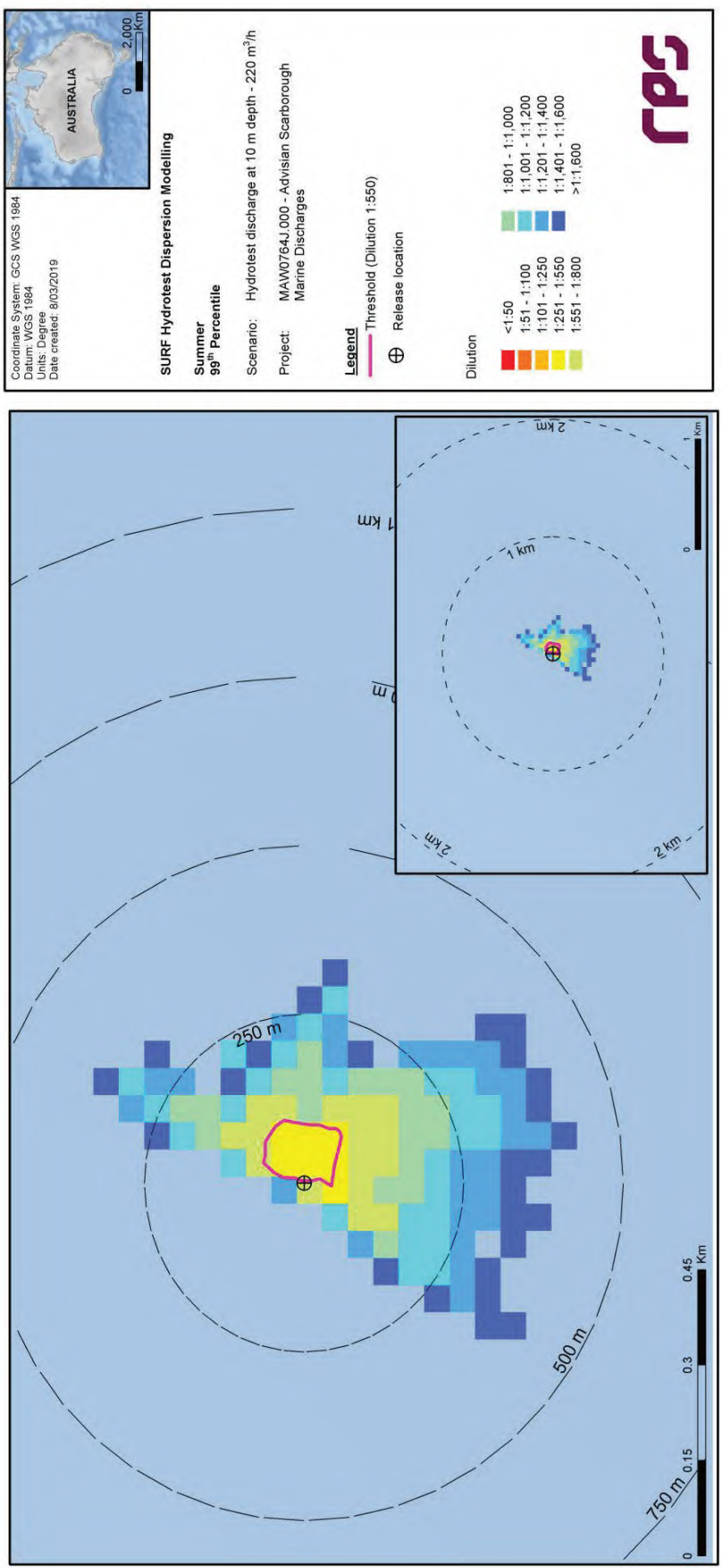
Figure 3.21 Predicted minimum dilutions at the 99th percentile under summer conditions for Case 3 (10 m depth discharge at 220 m³/hr flow rate).
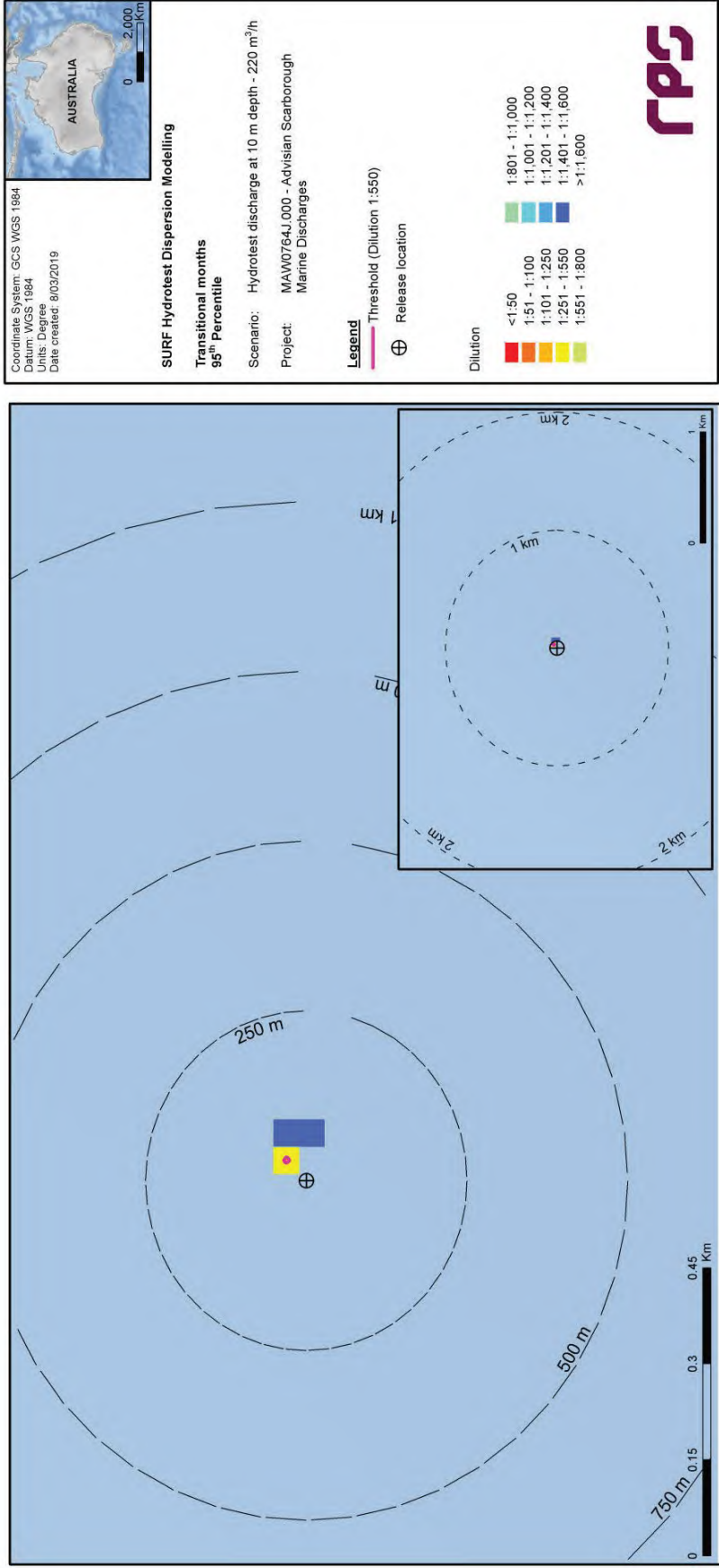
Figure 3.22 Predicted minimum dilutions at the 95th percentile under transitional conditions for Case 3 (10 m depth discharge at 220 m³/hr flow rate).
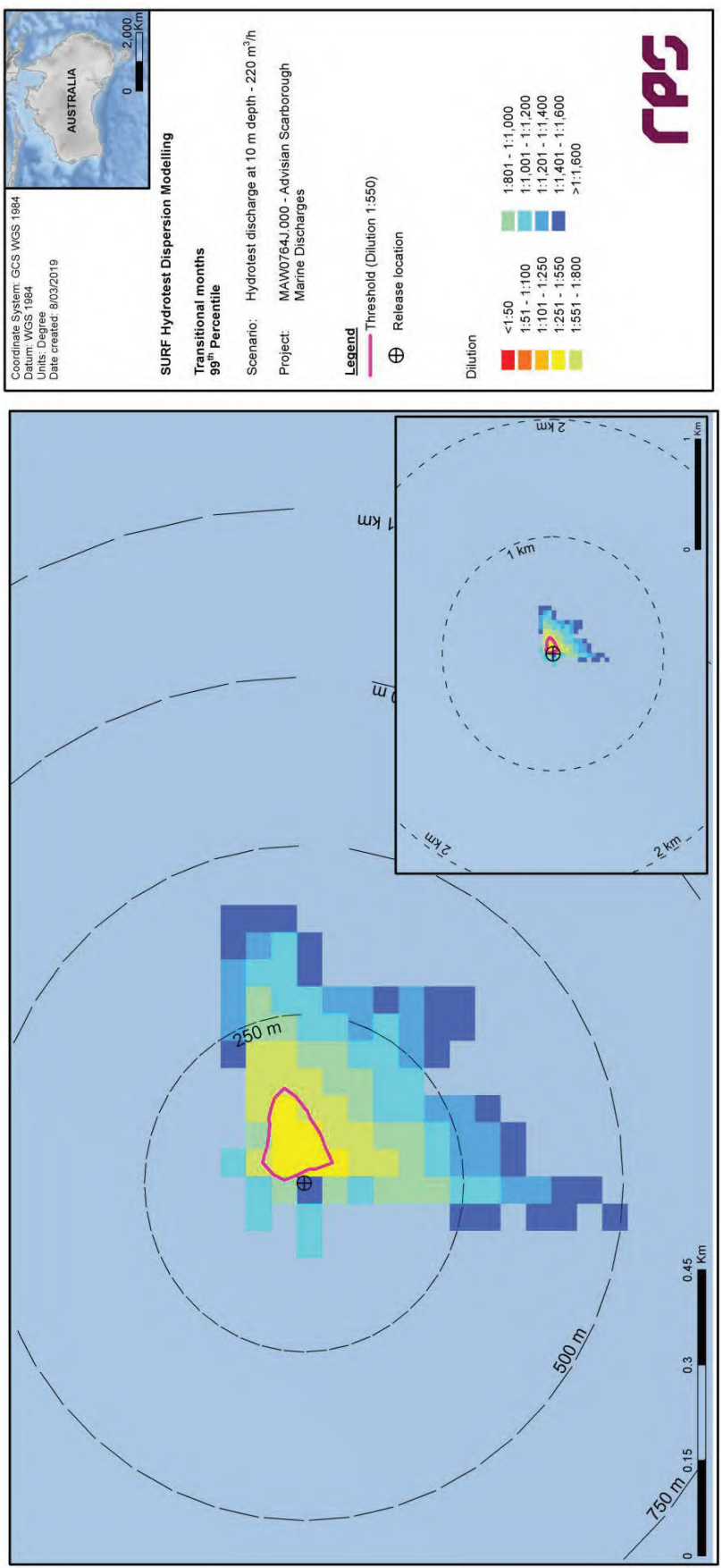
Figure 3.23 Predicted minimum dilutions at the 99th percentile under transitional conditions for Case 3 (10 m depth discharge at 220 m³/hr flow rate).
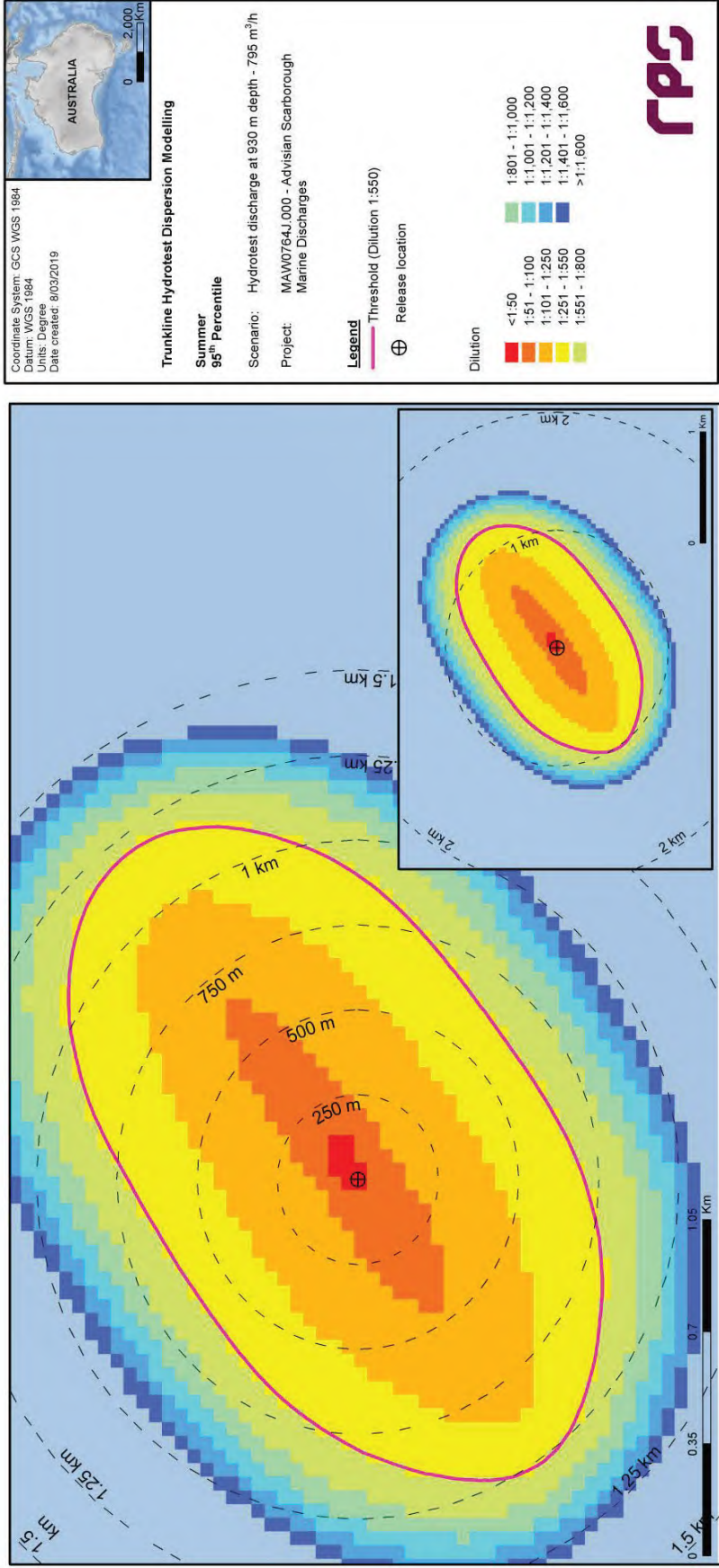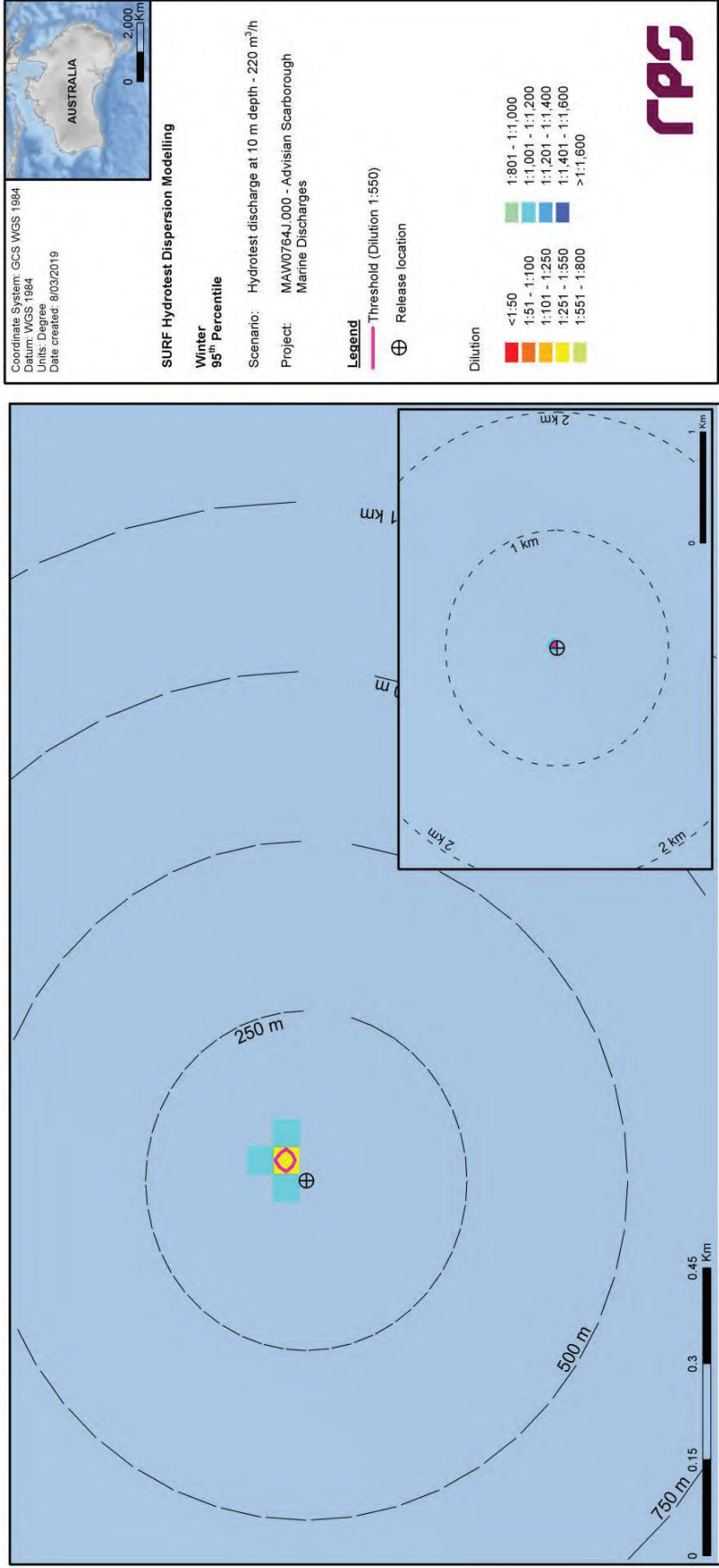
Figure 3.24 Predicted minimum dilutions at the 95th percentile under winter conditions for Case 3 (10 m depth discharge at 220 m³/hr flow rate).
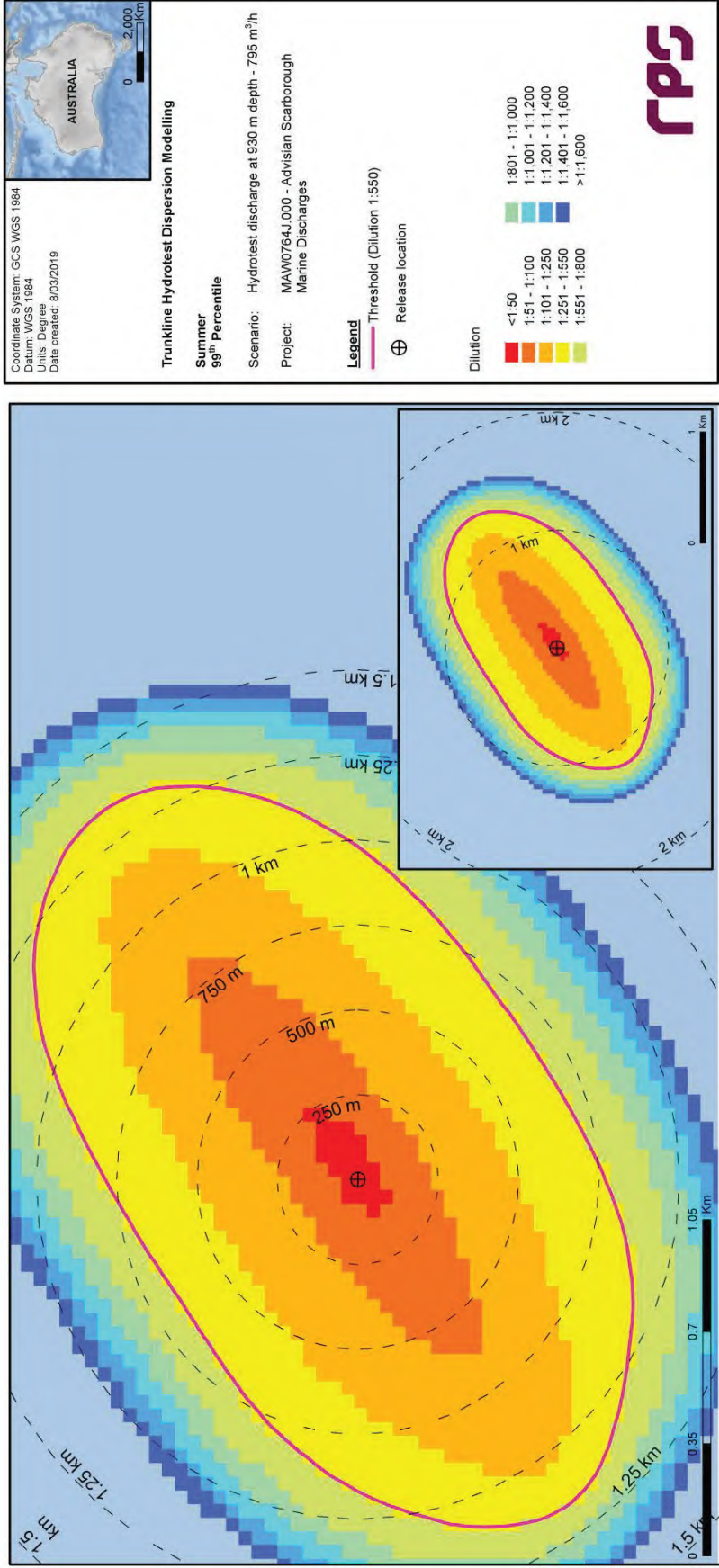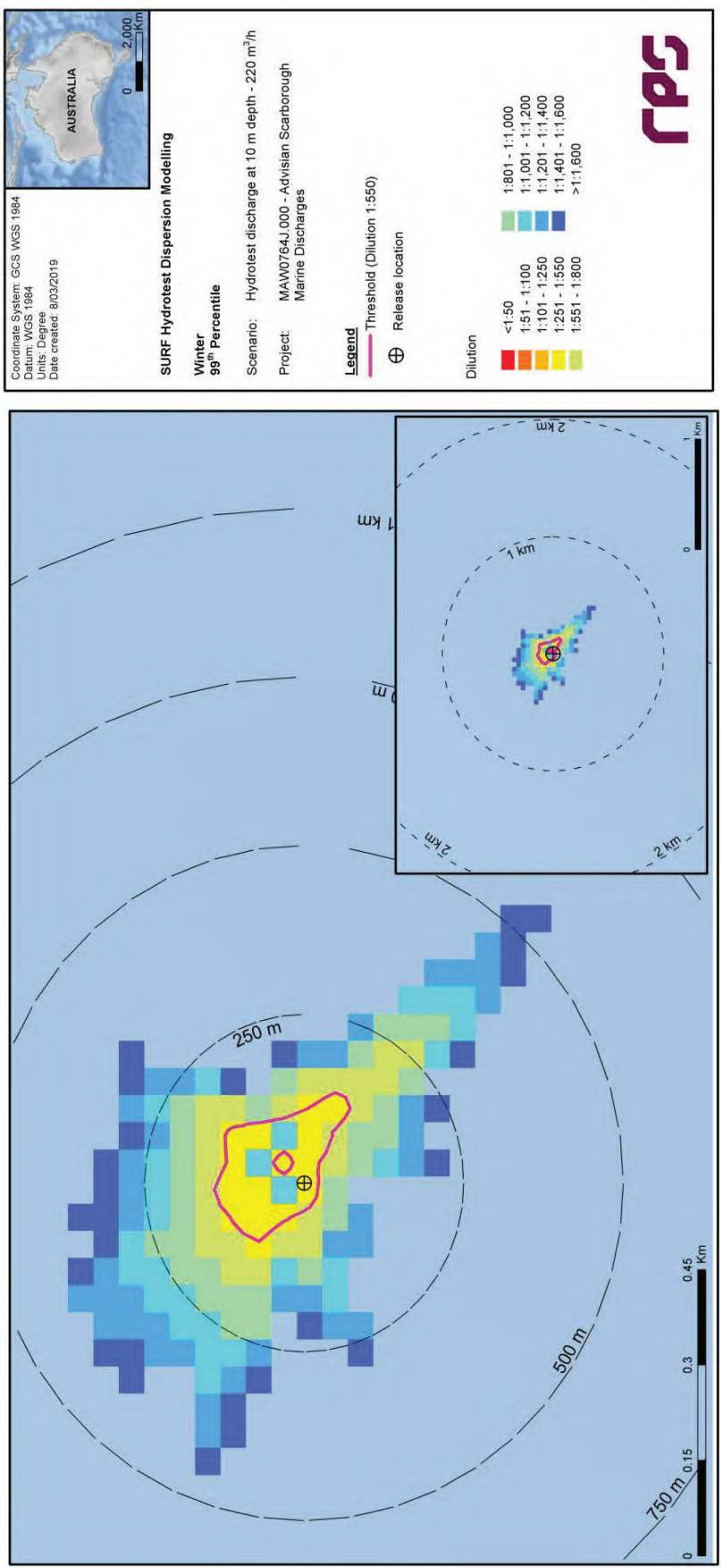
Figure 3.25 Predicted minimum dilutions at the 99th percentile under winter conditions for Case 3 (10 m depth discharge at 220 m³/hr flow rate).

3.2.5   Annualised Analysis

The model outputs for each season (summer, transitional and winter) over the ten-year hindcast period (2006-2015) were combined and analysed on an annualised basis.

Table 3.25 and Table 3.26 summarise, for Cases 1 and 3 respectively, the minimum dilution achieved at specific radial distances from the discharge location for each percentile over the annual period.

Table 3.27 and Table 3.28 provide, for Cases 1 and 3 respectively, summaries of the annualised maximum distances from the discharge location to achieve 1:550 dilution for each percentile. The results indicate that the release of effluent under all seasonal conditions results in rapid dispersion within the ambient environment. Dilution to reach threshold concentration is achieved for biocide within a maximum area of influence of 1,388 m (Case 1) and 124 m (Case 3) at the 99th percentile, this being the maximum spatial extent of the relevant dilution contour from the discharge location in any season.

Table 3.29 and Table 3.30 provide, for Cases 1 and 3 respectively, summaries of the total area of coverage for the 1:550 dilution contour for each percentile. The area of exposure defined by the relevant dilution contour is predicted to reach maximum values of 2.95 km^2 (Case 1) and 0.04 km^2 (Case 3) at the 99th percentile in any season.

For Cases 1 and 3, Figure 3.26 to Figure 3.29 show the aggregated spatial extents of the minimum dilutions for each percentile. Note that the contours represent the lowest predicted dilution (highest concentration) at any given time-step through the water column and do not consider frequency or duration.

The results presented assume that no processes other than dilution would reduce the source concentrations over time.

Table 3.25   Annualised minimum dilution achieved at specific radial distances from the hydrotest discharge location for Case 1 (930 m depth discharge at 795 m³/hr flow rate).

Percentile	Season	Minimum dilution (1:x) achieved at specific radial distances from discharge location																
		0.02 km	0.05 km	0.10 km	0.20 km	0.30 km	0.40 km	0.50 km	0.60 km	0.70 km	0.80 km	0.90 km	1.00 km	1.10 km	1.20 km	1.30 km	1.40 km	1.50 km
95th	Annual	1:20.7	1:30.1	1:35.1	1:49.6	1:62.9	1:73.9	1:81.9	1:90.5	1:104.3	1:112.3	1:133.6	1:173.2	1:261.2	1:394.9	1:595.8	1:869.8	1:1,324.8
99th		1:17.6	1:24.2	1:28.1	1:39.9	1:50.6	1:59.1	1:68.0	1:73.4	1:82.8	1:89.0	1:98.1	1:106.8	1:126.3	1:174.2	1:275.8	1:428.9	1:632.9

Table 3.26   Annualised minimum dilution achieved at specific radial distances from the hydrotest discharge location for Case 3 (10 m depth discharge at 220 m³/hr flow rate).

Percentile	Season	Minimum dilution (1:x) achieved at specific radial distances from discharge location																
		0.02 km	0.05 km	0.10 km	0.20 km	0.30 km	0.40 km	0.50 km	0.60 km	0.70 km	0.80 km	0.90 km	1.00 km	1.10 km	1.20 km	1.30 km	1.40 km	1.50 km
95th	Annual	1:387.1	1:930.5	1:1,149.9	>1:10,000	>1:10,000	>1:10,000	>1:10,000	>1:10,000	-	-	-	-	-	-	-	-	-
99th		1:160.9	1:279.8	1:320.5	1:600.5	1:779.8	1:1,129.1	1:1,364.3	1:1,609.3	1:1,881.9	1:2,202.9	1:2,595.3	1:2,838.4	1:3,174.4	1:3,525.3	1:3,450.6	1:3,980.1	1:4,042.6

Table 3.27 Annualised maximum distance from the hydrotest discharge location to achieve 1:550 dilution for Case 1 (930 m depth discharge at 795 m^3/hr flow rate).

Percentile	Season	Maximum distance (m) from discharge location to achieve given dilution
95th		1,196
99th	Annual	1,388
100th		1,564

Table 3.28 Annualised maximum distance from the hydrotest discharge location to achieve 1:550 dilution for Case 3 (10 m depth discharge at 220 m^3/hr flow rate).

Percentile	Season	Maximum distance (m) from discharge location to achieve given dilution
95th		18
99th	Annual	124
100th		1,147

Table 3.29 Annualised total area of coverage for 1:550 dilution for Case 1 (930 m depth discharge at 795 m^3/hr flow rate).

Percentile	Season	Total area (km^2) of coverage for given dilution
95th		2.325
99th	Annual	2.945
100th		3.730

Table 3.30 Annualised total area of coverage for 1:550 dilution for Case 3 (10 m depth discharge at 220 m^3/hr flow rate).

Percentile	Season	Total area (km^2) of coverage for given dilution
95th		0.002
99th	Annual	0.035
100th		0.522

Figure 3.26 Predicted annualised minimum dilutions at the 95th percentile for Case 1 (930 m depth discharge at 795 m³/hr flow rate).

Figure 3.27 Predicted annualised minimum dilutions at the 99th percentile for Case 1 (930 m depth discharge at 795 m³/hr flow rate).
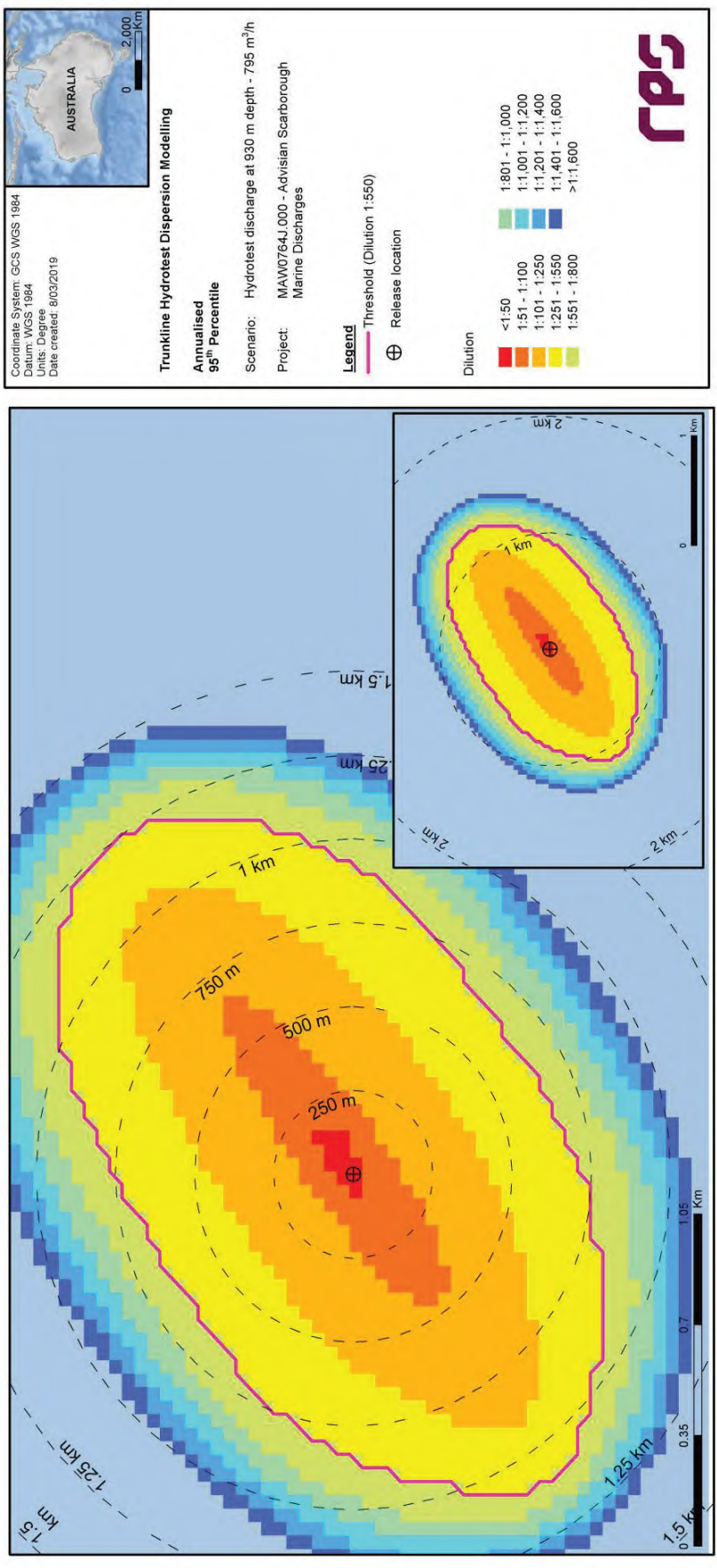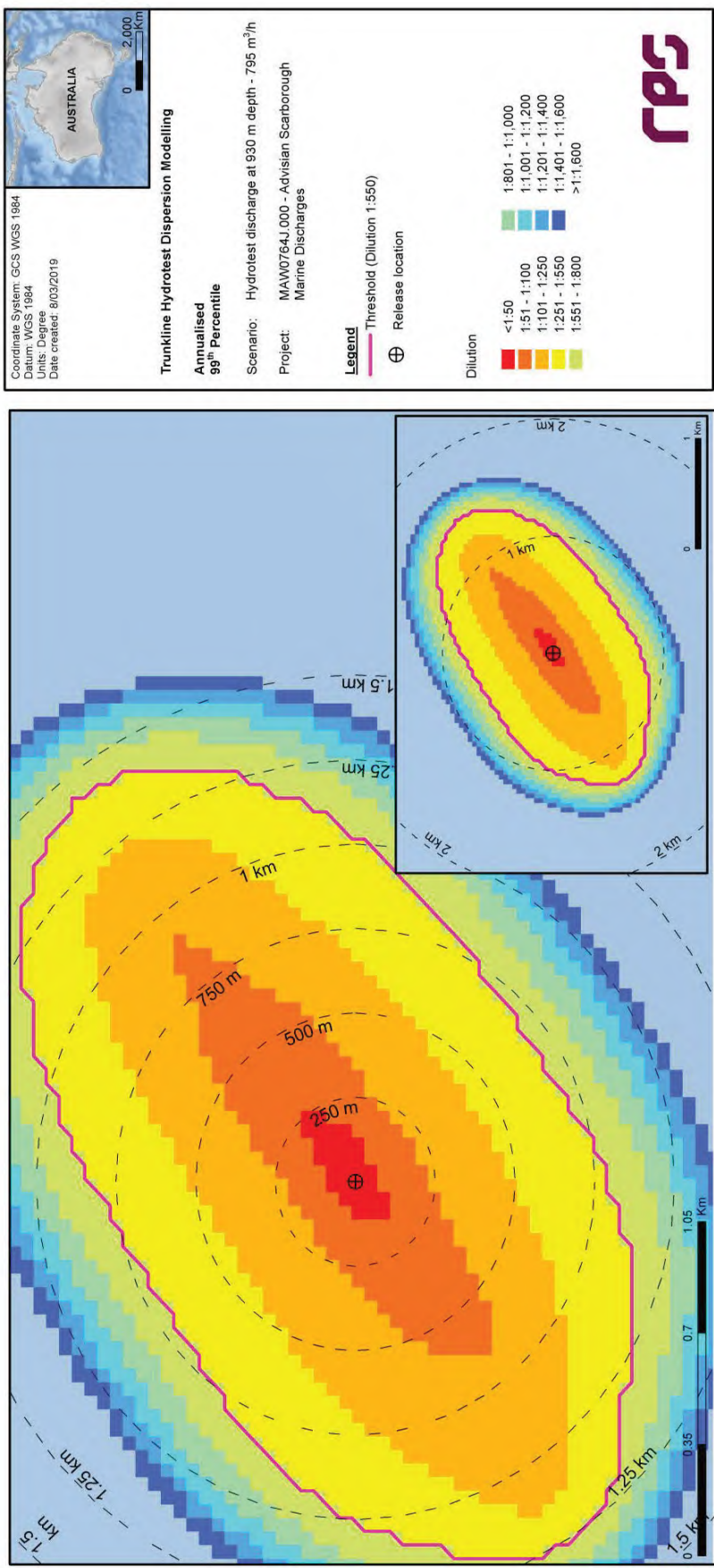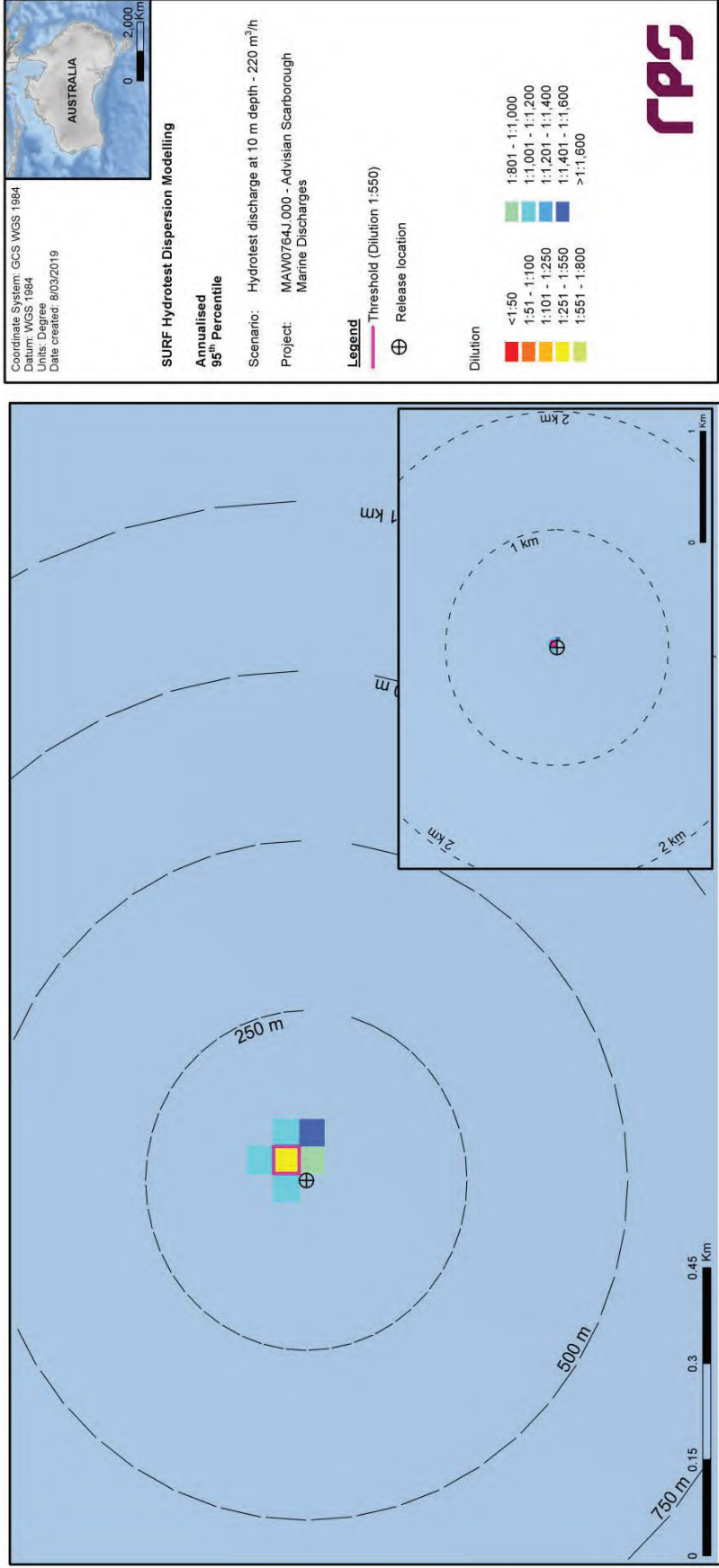
Figure 3.28 Predicted annualised minimum dilutions at the 95th percentile for Case 3 (10 m depth discharge at 220 m³/hr flow rate).
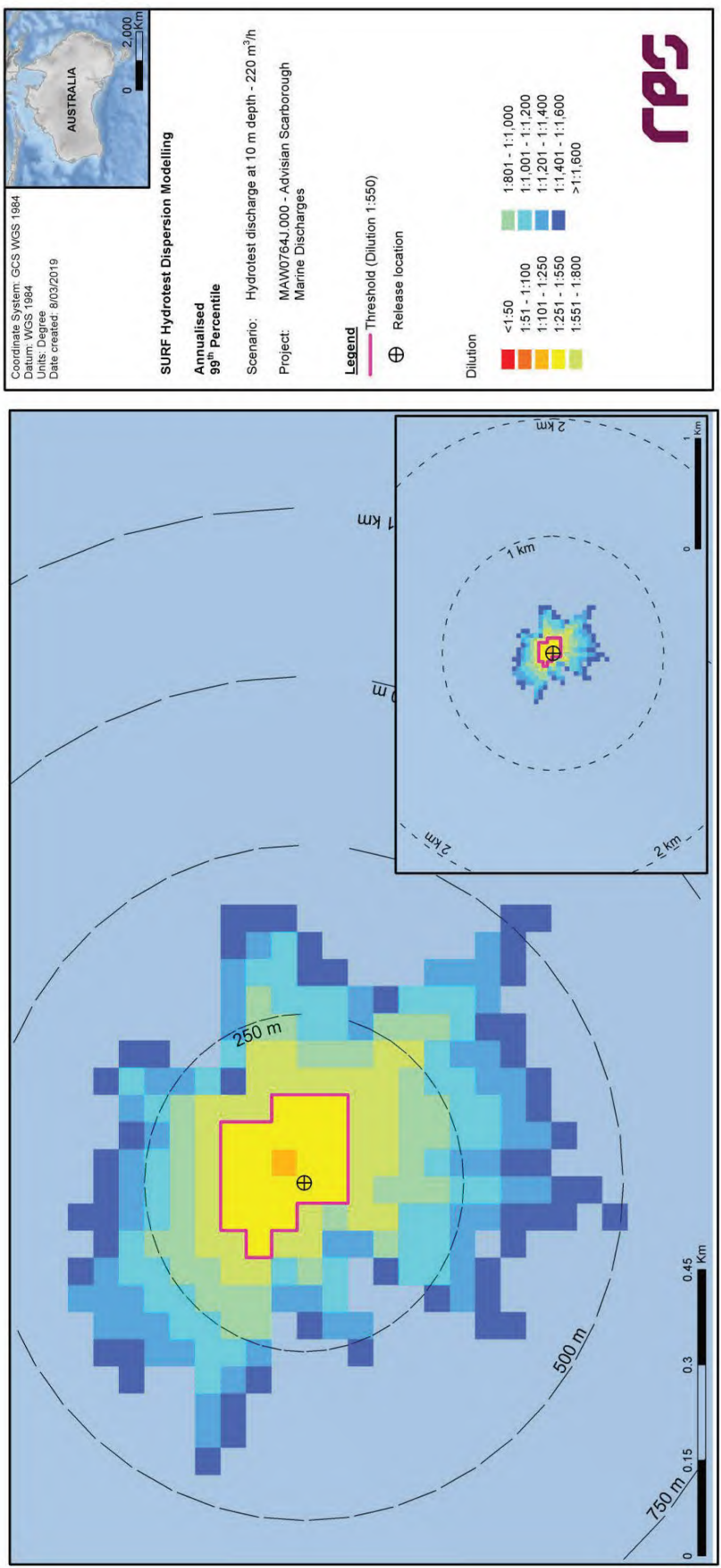
Figure 3.29 Predicted annualised minimum dilutions at the 99th percentile for Case 3 (10 m depth discharge at 220 m³/hr flow rate).

4   CONCLUSIONS

The main findings of the study are as follows:

Near-Field Modelling

- The results show that due to the momentum of the discharge a turbulent mixing zone is created in the immediate vicinity of the discharge point, which is 930 m (Cases 1 and 2) and 10 m (Case 3) below the water surface. The surface discharges are shown to increase the extent of the turbulent mixing zone. Following this initial mixing, the near neutrally-buoyant plumes are predicted to travel laterally in the water column.

- For Cases 1 and 2, the plumes are predicted to remain close to the seabed. For Case 3, the plume is predicted to plunge up to 19 m below the sea surface. For Cases 2 and 3, increased ambient current strengths are shown to increase the horizontal distance travelled by the plumes from the discharge point.

- The plume will reach a maximum horizontal distance of up to 152 m before reaching the trapping depth (at which the predictions of dispersion are halted due to the plume reaching equilibrium with the ambient receiving water).

- The maximum diameter of the plume at the end of the near-field zone was predicted as 23 m. Increases in current speed serve to restrict the diameter of the plume.

- For each discharge depth, the primary factor influencing dilution of the plume is the strength of the ambient current. Weak currents allow the plume to plunge further and reach the trapping depth closer to the discharge point, which slows the rate of dilution.

- For each combination of discharge flow rate and depth, the primary factor influencing dilution of the plume is the strength of the ambient current. Weak currents allow the plume to plunge further and reach the trapping depth closer to the discharge point, which slows the rate of dilution.

- The average dilution levels of the plume upon reaching the trapping depth under average current speeds are predicted to be 1:90 for Case 1, 1:465 for Case 2 and 1:482 for Case 3.

- The predictions of dilution rely on the persistence of current speed and direction over time and do not account for any build-up of plume concentrations due to slack currents or current reversals

- The results for the Case 1, 2 and 3 discharges indicate that the biocide constituent of the hydrotest discharge is not expected to reach the required levels of dilution in the near field mixing zone.

Far-Field Modelling

- For Case 1, dilution to reach threshold concentration is achieved for biocide within an area of influence extending up to 1,388 m at the 99th percentile. For Case 3, the maximum spatial extents of the relevant dilution contour are up to 124 m at the 99th percentile.

- For Case 1, the area of exposure defined by the relevant dilution contour is predicted to reach a maximum of 2.95 km^2 at the 99th percentile. For Case 3, the corresponding maximum area of exposure is up to 0.04 km^2 at the 99th percentile.

- Maximum depths reached by the discharges are predicted as 930 m (seabed) and 12 m for Cases 1 and 3, respectively.

Key Observations

- Due to the significant variations in magnitude of the hindcast currents between the surface and seabed, where potential discharges will occur, predicted outcomes are markedly different.

- The greater strength and variability in surface-layer currents will promote the highest levels of mixing and dilution, while transport patterns at the seabed will be dictated almost solely by tidal movements.

- Because the discharge will be initially neutrally-buoyant, it will travel laterally in the water column and even a surface discharge is unlikely to resurface in the vicinity of the discharge point prior to acclimation with ambient receiving water conditions.

- Outcomes show that below-threshold biocide concentrations are achieved closer to the discharge point for the surface discharge (220 m^3/hr over 20 hours) than for the seabed discharge (795 m^3/hr over 44 hours). This is partly attributable to the stronger currents at the surface, but primarily to the lower flow rate and much lower discharge duration in the surface-discharge case.

5 REFERENCES

Advisian 2018, *Hydrotest Discharge Modelling Data Requirements* [v2], provided to RPS by Advisian, West Perth, WA, Australia.

Andersen, OB 1995, 'Global ocean tides from ERS 1 and TOPEX/POSEIDON altimetry', *Journal of Geophysical Research: Oceans*, vol. 100, no. C12, pp. 25249-25259.

Australian Maritime Safety Authority (AMSA) 2002, *National marine oil spill contingency plan*, Australian Maritime Safety Authority, Canberra, ACT, Australia.

Baumgartner, D, Frick, WE & Roberts, P 1994, *Dilution Models for Effluent Discharges*, 3rd Edition, EPA/600/R-94/086, U.S. Environment Protection Agency, Pacific Ecosystems Branch, Newport, OR, USA.

Burns, K, Codi, S, Furnas, M, Heggie, D, Holdway, D, King, B & McAllister, F 1999, 'Dispersion and fate of produced formation water constituents in an Australian Northwest Shelf shallow water ecosystem', *Marine Pollution Bulletin*, vol. 38, pp. 593-603.

Carvalho, JLB, Roberts, PJW & Roldão, J 2002, 'Field observations of Ipanema Beach outfall', *Journal of Hydraulic Engineering*, vol. 128, no. 2, pp. 151-160.

Davies, AM 1977a, 'The numerical solutions of the three-dimensional hydrodynamic equations using a B-spline representation of the vertical current profile', in *Bottom Turbulence: Proceedings of the 8th Liege Colloquium on Ocean Hydrodynamics*, ed. Nihoul, JCJ, Elsevier.

Davies, AM 1977b, 'Three-dimensional model with depth-varying eddy viscosity', in *Bottom Turbulence: Proceedings of the 8th Liege Colloquium on Ocean Hydrodynamics*, ed. Nihoul, JCJ, Elsevier.

Flater, D 1998, *XTide: harmonic tide clock and tide predictor* (www.flaterco.com/xtide/).

Frick, WE, Roberts, PJW, Davis, LR, Keyes, J, Baumgartner, DJ & George, KP 2003, *Dilution Models for Effluent Discharges (Visual Plumes)*, 4th Edition, Ecosystems Research Division, NERL, ORD, US Environment Protection Agency, Pacific Ecosystems Branch, Newport, OR, USA.

Gordon, R 1982, *Wind driven circulation in Narragansett Bay*, PhD thesis, University of Rhode Island, Kingston, RI, USA.

Isaji, T & Spaulding, ML 1984, 'A model of the tidally induced residual circulation in the Gulf of Maine and Georges Bank', *Journal of Physical Oceanography*, vol. 14, no. 6, pp. 1119-1126.

Isaji, T & Spaulding, ML 1986, 'A numerical model of the M2 and K1 tide in the northwestern Gulf of Alaska', *Journal of Physical Oceanography*, vol. 17, no. 5, pp. 698-704.

Isaji, T, Howlett, E, Dalton, C & Anderson, E 2001, 'Stepwise-continuous-variable-rectangular-grid', in *Proceedings of the 24th Arctic and Marine Oil Spill Program Technical Seminar*, Edmonton, Alberta, Canada, pp. 597-610.

Khondaker, AN 2000, 'Modeling the fate of drilling waste in marine environment – an overview', *Journal of Computers and Geosciences*, vol. 26, pp. 531-540.

King, B & McAllister, FA 1997, 'The application of MUDMAP to investigate the dilution and mixing of the above water discharge at the Harriet A petroleum platform on the Northwest Shelf', in *Modelling the Dispersion of Produced Water Discharge in Australia*, Australian Institute of Marine Science, Canberra, ACT, Australia.

King, B & McAllister, FA 1998, 'Modelling the dispersion of produced water discharges', *APPEA Journal*, pp. 681-691.

Koh, RCY & Chang, YC 1973, *Mathematical model for barged ocean disposal of waste*, Environmental Protection Technology Series, EPA 660/2-73-029, U.S. Army Engineer Waterways Experiment Station, Vicksburg, MS, USA.

Kostianoy, AG, Ginzburg, AI, Lebedev, SA, Frankignoulle, M & Delille, B 2003, 'Fronts and mesoscale variability in the southern Indian Ocean as inferred from the TOPEX/POSEIDON and ERS-2 Altimetry data', *Oceanology*, vol. 43, no. 5, pp. 632-642.

Levitus, S, Antonov, JI, Baranova, OK, Boyer, TP, Coleman, CL, Garcia, HE, Grodsky, AI, Johnson, DR, Locarnini, RA, Mishonov, AV, Reagan, JR, Sazama, CL, Seidov, D, Smolyar, I, Yarosh, ES & Zweng, MM 2013, 'The world ocean database', *Data Science Journal*, vol. 12, pp. WDS229-WDS234.

Ludicone, D, Santoleri, R, Marullo, S & Gerosa, P 1998, 'Sea level variability and surface eddy statistics in the Mediterranean Sea from TOPEX/POSEIDON data', *Journal of Geophysical Research I,* vol. 103, no. C2, pp. 2995-3011.

Matsumoto, K, Takanezawa, T & Ooe, M 2000, 'Ocean tide models developed by assimilating TOPEX/POSEIDON altimeter data into hydrodynamical model: A global model and a regional model around Japan', *Journal of Oceanography*, vol. 56, no. 5, pp. 567-581.

Oke, PR, Brassington, GB, Griffin, DA & Schiller, A 2008, 'The Bluelink ocean data assimilation system (BODAS)', *Ocean Modeling*, vol. 21, no. 1-2, pp. 46-70.

Oke, PR, Brassington, GB, Griffin, DA & Schiller, A 2009, 'Data assimilation in the Australian Bluelink system', *Mercator Ocean Quarterly Newsletter*, no. 34, pp. 35-44.

Owen, A 1980, 'A three-dimensional model of the Bristol Channel', *Journal of Physical Oceanography*, vol. 10, no. 8, pp. 1290-1302.

Qiu, B & Chen, S 2010, 'Eddy-mean flow interaction in the decadally modulating Kuroshio Extension system', *Deep-Sea Research II*, vol. 57, no. 13, pp. 1098-1110.

Roberts, PJW & Tian, X 2004, 'New experimental techniques for validation of marine discharge models', *Environmental Modelling and Software*, vol. 19, no. 7-8, pp. 691-699.

Schiller, A, Oke, PR, Brassington, GB, Entel, M, Fiedler, R, Griffin, DA & Mansbridge, JV 2008, 'Eddy-resolving ocean circulation in the Asian-Australian region inferred from an ocean reanalysis effort', *Progress in Oceanography*, vol. 76, no. 3, pp. 334-365.

Yaremchuk, M & Tangdong, Q 2004, 'Seasonal variability of the large-scale currents near the coast of the Philippines', *Journal of Physical Oceanography*, vol. 34, no. 4, pp. 844-855.

Zigic, S, Zapata, M, Isaji, T, King, B & Lemckert, C 2003, 'Modelling of Moreton Bay using an ocean/coastal circulation model', in *Proceedings of the Coasts & Ports 2003 Australasian Conference*, Auckland, New Zealand, paper no. 170.

Appendix I

Scarborough Gas Development Quantitative Spill Risk Assessment Modelling Study

Controlled Ref No: SA0006AF0000002   Revision: 5   DCP No: 1100144791

Uncontrolled when printed. Refer to electronic version for most up to date information.

WOODSIDE SCARBOROUGH PROJECT – QUANTITATIVE SPILL RISK ASSESSMENT

Report

www.rpsgroup.com/mst

Document status

Version	Purpose of document	Authored by	Reviewed by	Approved by	Review date
Rev A	Internal review	M. Watt	D. Wright	D. Wright	28/02/2019
Rev 0	Client review	M. Watt	D. Wright	D. Wright	22/03/2019
Rev 1	Client review	M. Watt	D. Wright	D. Wright	17/04/2019

Approval for issue

David Wright	17 April 2019

Prepared by:	Prepared for:
RPS	**Advisian**
David Wright	Paul Nichols
Manager - Perth	Marine Sciences Manager (APAC)
Level 2, 27-31 Troode Street	600 Murray Street
West Perth WA 6005	West Perth WA 6005

Contents

Tables

Figures

EXECUTIVE SUMMARY

RPS was commissioned by Advisian Pty Ltd (Advisian), on behalf of Woodside Energy Ltd (Woodside), to undertake a quantitative spill risk assessment of three hydrocarbon spill scenarios related to the Scarborough Project.

The Scarborough gas resource, located in Commonwealth waters approximately 375 km off the Burrup Peninsula, forms part of the Greater Scarborough gas fields, comprising the Scarborough, North Scarborough, Thebe and Jupiter gas fields.

As Operator of the Greater Scarborough gas fields, Woodside is proposing to develop the gas resource through new offshore facilities. These will be connected to the mainland through an approximately 430 km trunkline.

The Scarborough gas field consists of gas which is classified as 'dry' with only trace levels of condensate, and as such a loss of well control event will not have a significant liquid component. As such, the exposure from an unplanned hydrocarbon release is based on a release of marine diesel oil (MDO) from a vessel.

The assessment focused on the risk of exposure to hydrocarbons for surrounding resources and sensitive receptors if defined spill scenarios were to occur. The main objectives of the study were to provide an assessment, through stochastic spill modelling, of the probabilities of oil contact (at greater than defined minimum concentrations), the potential concentrations that might be involved, and the minimum state of weathering of the oil in case of a release of hydrocarbons.

Woodside identified three hydrocarbon spill scenarios for investigation. Each scenario was modelled in a stochastic manner and assessed over an annual period in this study.

Oil spill modelling was undertaken using a three-dimensional oil spill trajectory and weathering model, SIMAP (Spill Impact Mapping and Analysis Program), which is designed to simulate the transport, spreading and weathering of specific oil types under the influence of changing meteorological and oceanographic forces.

The main findings of this study are as follows:

Metocean Influences

- Tidal flows will have a significant influence on the trajectory of any oil spilled at the modelled release sites, irrespective of the seasonal conditions.

- Large-scale drift currents will have a significant influence on the trajectory of any oil spilled at the modelled release sites, irrespective of the seasonal conditions. The prevailing drift currents will determine the trajectory of oil that is entrained beneath the water surface.

- Interactions with the prevailing wind will provide additional variation in the trajectory of spilled oil.

- Due to the location of the hypothetical spill site and the dominance of tidal flows, the coastal areas predicted to be most likely to be impacted by spilled oil are those bordering Mermaid Sound and its numerous passages.

Oil Characteristics and Weathering Behaviour

- Marine diesel is a mixture of volatile and persistent hydrocarbons with low percentages of highly volatile and residual components. If exposed to the atmosphere, around 41% of the mass would be expected to evaporate in around 24 hours, another 54% within a few days, and the remaining 5% would be expected

to persist in the marine environment until decayed. The influence of entrainment will regulate the degree of mass retention in the environment.

- During the surface release, floating oil will be susceptible to entrainment into the wave-mixed layer under typical wind conditions. Evaporation rates will be significant, given the moderate proportion of volatile compounds in the oil (41%). The low-volatility fraction of the oil (54%) will take longer durations of the order of days to evaporate, and the residual fraction of 5% is expected to persist in the environment until degradation processes occur. Considering the spill volume, there is a low potential for dissolution of soluble aromatic compounds.

Summary of Stochastic Assessment Results

Scenario 1: Short-Term (Instantaneous) Surface Release of Marine Diesel after a Vessel Collision outside Mermaid Sound

- Floating oil at concentrations equal to or greater than the 10 g/m^2, 50 g/m^2 and 100 g/m^2 thresholds could potentially be found up to 29 km, 21 km and 18 km from the spill site, respectively.

- The Dampier Archipelago shoreline receptor is predicted to be contacted by floating oil concentrations at the 10 g/m^2 threshold with a probability of 2% and a minimum time to contact of 27 hours.

- Potential for accumulation of oil on shorelines is predicted to be low, with a maximum accumulated volume and concentration of 3 m^3 and 156 g/m^2, respectively, forecast at the Dampier Archipelago.

- Entrained oil at concentrations equal to or greater than the 500 ppb threshold is predicted to be found up to around 163 km from the spill site.

- The Dampier MP and Dampier Archipelago receptors are predicted to receive entrained oil concentrations at the 500 ppb threshold with probabilities of 44% and 23%, respectively.

- The maximum entrained oil concentration forecast for any receptor is predicted as 10.9 ppm within the Dampier Archipelago.

- Dissolved aromatic hydrocarbons at concentrations equal to or greater than the 500 ppb threshold are predicted to be found up to around 34 km from the spill site.

- The Dampier MP is predicted to receive dissolved aromatic hydrocarbon concentrations at the 500 ppb threshold with a probability of 2%.

- The maximum dissolved aromatic hydrocarbon concentration forecast for any receptor is predicted as 635 ppb within the Dampier MP.

Scenario 2: Short-Term (Instantaneous) Surface Release of Marine Diesel after a Vessel Collision within Montebello Marine Park

- Floating oil at concentrations equal to or greater than the 10 g/m^2, 50 g/m^2 and 100 g/m^2 thresholds could potentially be found up to 39 km, 36 km and 33 km from the spill site, respectively.

- Given that the spill location lies within the Montebello MP receptor area, floating oil at concentrations equal to or greater than 100 g/m^2 are forecast with a probability of 100% and a minimum time to contact of less than 1 hour.

- Potential for accumulation of oil on shorelines is predicted to be low, with a maximum accumulated volume and concentration of $<1 \text{ m}^3$ and 1 g/m^2, respectively, forecast at Barrow Island.

- Entrained oil at concentrations equal to or greater than the 500 ppb threshold is predicted to be found up to around 308 km from the spill site.

- The Montebello MP and Muiron Islands MMA-WHA receptors are predicted to receive entrained oil concentrations at the 500 ppb threshold with probabilities of 70% and 7%, respectively.

- The maximum entrained oil concentration forecast for any receptor is predicted as 157.0 ppm within the Montebello MP.

- Dissolved aromatic hydrocarbons at concentrations equal to or greater than the 500 ppb threshold are predicted to be found up to around 85 km from the spill site.

- The Montebello MP is predicted to receive dissolved aromatic hydrocarbon concentrations at the 500 ppb threshold with a probability of 2%.

- The maximum dissolved aromatic hydrocarbon concentration forecast for any receptor is predicted as 2.0 ppm within the Montebello MP.

Scenario 3: Short-Term (Instantaneous) Surface Release of Marine Diesel after a Vessel Collision at the FPU Location

- Floating oil at concentrations equal to or greater than the 10 g/m^2, 50 g/m^2 and 100 g/m^2 thresholds could potentially be found up to 113 km, 60 km and 58 km from the spill site, respectively.

- No shoreline receptors are predicted to be contacted by floating oil concentrations at any of the assessed thresholds.

- No accumulation of oil on shorelines is predicted.

- Entrained oil at concentrations equal to or greater than the 500 ppb threshold is predicted to be found up to around 476 km from the spill site.

- The Gascoyne MP receptor is predicted to receive entrained oil concentrations at the 500 ppb threshold with a probability of 8%.

- The maximum entrained oil concentration forecast for any receptor is predicted as 7.2 ppm within the Gascoyne MP.

- Dissolved aromatic hydrocarbons at concentrations equal to or greater than the 500 ppb threshold are predicted to be found up to around 74 km from the spill site.

- No receptors are predicted to receive dissolved aromatic hydrocarbon concentrations at the 500 ppb threshold.

- The maximum dissolved aromatic hydrocarbon concentration forecast for any receptor is predicted as 462 ppb within the Gascoyne MP.

1   INTRODUCTION

1.1   Background

RPS was commissioned by Advisian Pty Ltd (Advisian), on behalf of Woodside Energy Ltd (Woodside), to undertake a quantitative spill risk assessment of three hydrocarbon spill scenarios related to the Scarborough Project.

The Scarborough gas resource, located in Commonwealth waters approximately 375 km off the Burrup Peninsula, forms part of the Greater Scarborough gas fields, comprising the Scarborough, North Scarborough, Thebe and Jupiter gas fields.

As Operator of the Greater Scarborough gas fields, Woodside is proposing to develop the gas resource through new offshore facilities. These will be connected to the mainland through an approximately 430 km trunkline.

The Scarborough gas field consists of gas which is classified as 'dry' with only trace levels of condensate, and as such a loss of well control event will not have a significant liquid component. As such, the exposure from an unplanned hydrocarbon release is based on a release of marine diesel oil (MDO) from a vessel.

The assessment focused on the risk of exposure to hydrocarbons for surrounding resources and sensitive receptors if defined spill scenarios were to occur. The main objectives of the study were to provide an assessment, through stochastic spill modelling, of the probabilities of oil contact (at greater than defined minimum concentrations), the potential concentrations that might be involved, and the minimum state of weathering of the oil in case of a release of hydrocarbons.

Woodside identified three hydrocarbon spill scenarios for investigation (Advisian, 2019). Each scenario was modelled in a stochastic manner and assessed over an annual period in this study.

The regional context of the spill location for each assessed scenario is shown in Figure 1.1.

The details of the scenarios assessed in this study are summarised in Table 1.1 and listed here:

- Scenario 1: A short-term (instantaneous) surface release of 2,000 m^3 of marine diesel, representing loss of vessel fuel tank integrity after a collision outside Mermaid Sound (20° 21' 3.28" S, 116° 42' 5.58" E).

- Scenario 2: A short-term (instantaneous) surface release of 2,000 m^3 of marine diesel, representing loss of vessel fuel tank integrity after a collision within Montebello Marine Park (MP) (20° 03' 1.44" S, 115° 31' 35.04" E).

- Scenario 3: A short-term (instantaneous) surface release of 2,000 m^3 of marine diesel, representing loss of vessel fuel tank integrity after a collision at the FPU location (19° 53' 54.72" S, 113° 14' 19.56" E).
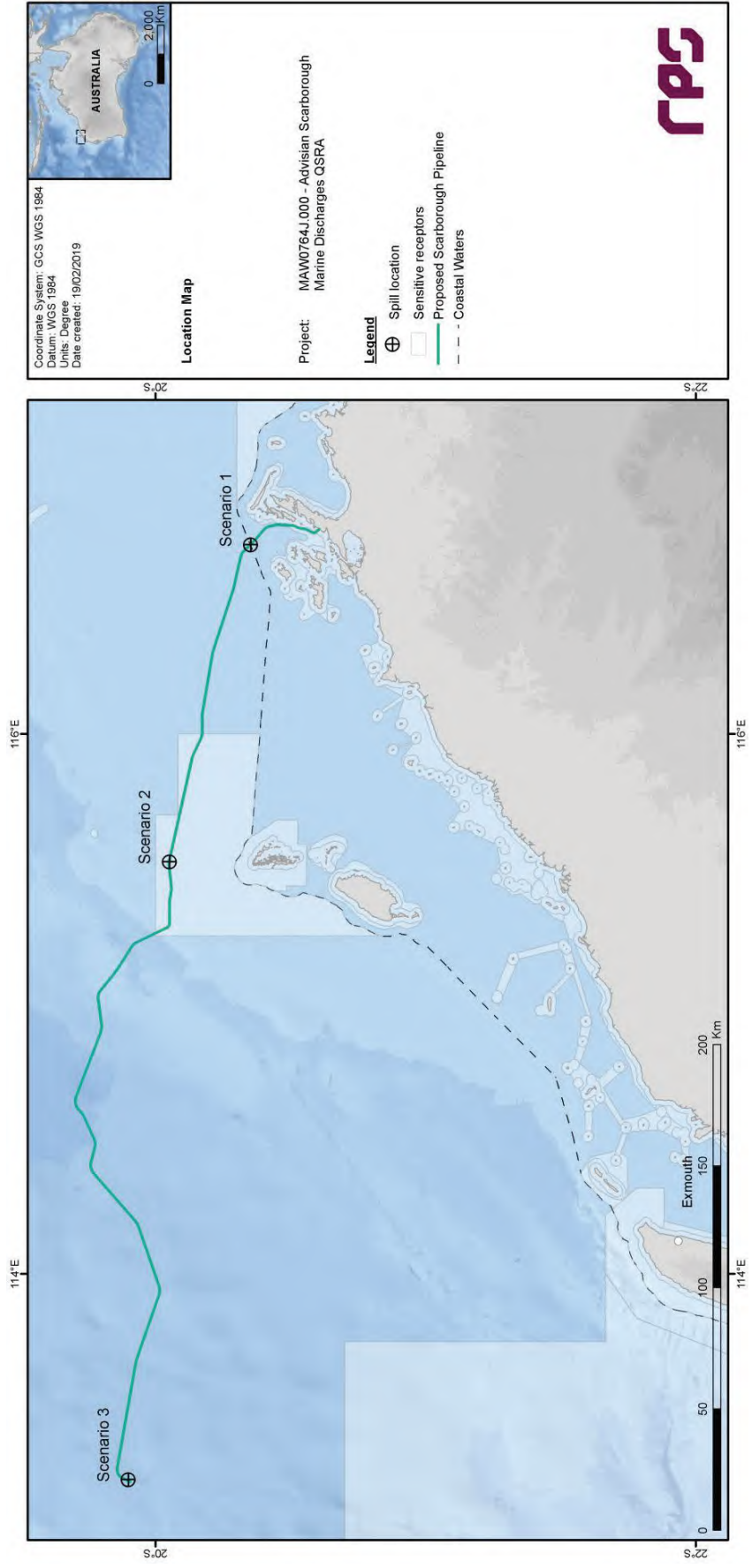
Figure 1.1   Locations of the modelled hydrocarbon spill scenario release sites.

1.2 Stochastic Modelling of Spill Scenarios

Oil spill modelling was undertaken using a three-dimensional oil spill trajectory and weathering model, SIMAP (Spill Impact Mapping and Analysis Program), which is designed to simulate the transport, spreading and weathering of specific oil types under the influence of changing meteorological and oceanographic forces.

The SIMAP model simulates both surface and subsurface releases and uses the unique physical and chemical properties of an oil type to calculate rates of evaporation and viscosity change, including the tendency to form oil-in-water emulsions. Moreover, the unique transport and dispersion of surface slicks and in-water components (entrained and dissolved) are modelled separately. Thus, the model can be used to understand the wider potential consequences of a spill, including direct contact to slick oil for surface features and exposure to entrained and dissolved oil for organisms in the water column.

To define trends and variations in the potential outcomes of a given scenario, a stochastic modelling scheme was followed in this study, whereby SIMAP was applied to repeatedly simulate the defined spill scenarios using different samples of current and wind data selected randomly from an historic time-series of wind and current data representative of the study area. Results of the replicate simulations were then statistically analysed and mapped to define contours of risk around the release point.

For this purpose, a long-term archive of spatially-variable wind and current data covering the North West Shelf of Australia and spanning 10 years (2006-2015, inclusive) was assembled. Current patterns accounted for temporal and spatial variations in large-scale drift currents over the outer shelf waters (typically >200 m depth) together with tidal and wind-driven currents. Modelling was carried out using current and wind data sampled from the data archive to quantify annualised risks of contact at surrounding locations.

Each simulation was run for the duration of the specified spill, plus a further period after the cessation of discharge to allow a sufficient time period for oil concentrations to decrease below the threshold concentrations applied in the analysis. It is expected that remnant floating oil, which may be present at low thresholds at the end of each simulation, would represent highly weathered and degraded products.

It is important to note that the modelling results presented in this document relate to the predicted outcomes once defined spill events have occurred. The probability of the spill scenarios occurring is not considered. The results should therefore be viewed as a guide to the likely outcomes should the spill scenarios occur. Furthermore, the results are presented in terms of statistical probability maps, based on many simulations under different conditions. Different locations within the potential zone of influence would be affected under each different time-series of environmental forces. Consequently, these contours for the potential zone of influence will cover a larger area than the area that is likely to be affected during any one single spill event. The contours should therefore be judged as contours of probability and not representations of the area swept by individual spill slicks.

Risk estimates were calculated from the multiple replicate simulations for each assessed scenario, including the probability of contact, the minimum time to contact, and the potential concentrations that might be involved.

The results of the stochastic modelling are presented in Section 3.

Table 1.1   Summary of the hydrocarbon spill scenarios assessed in a stochastic manner in this study.

Scenario	Description	Oil Type	Spilled Volume (m³)	Release Coordinates	Release Depth (m BMSL)	Spill Duration	Simulation Duration	Period
1	Loss of vessel fuel tank integrity after a collision outside Mermaid Sound	Marine Diesel	2,000	20° 21' 03.28" S 116° 42' 05.58" E	0	Instantaneous	42 days	Annual
2	Loss of vessel fuel tank integrity after a collision within Montebello Marine Park (MP)	Marine Diesel	2,000	20° 03' 01.44" S 115° 31' 35.04" E	0	Instantaneous	42 days	Annual
3	Loss of vessel fuel tank integrity after a collision at the FPU location	Marine Diesel	2,000	19° 53' 54.72" S 113° 14' 19.56" E	0	Instantaneous	42 days	Annual

1.3   Deterministic Analysis of Spill Scenarios

After assessing the stochastic modelling outcomes for all scenarios, Woodside determined there was a requirement for additional model outputs to be provided for selected replicate simulations of each scenario in order to contextualise the stochastic contours.

The results of the deterministic analysis are presented in Section 4.

1.4   Report Structure

The far-field computational models, risk assessment methodology, environmental data used as input to the models, environmental threshold trigger levels defined for the assessment and characteristics of the oil type used in the modelling of the defined scenarios are described in detail in Section 2.

Contour figures and tabulated results showing risk estimates for the receptors nominated by Woodside, produced for defined floating oil, entrained oil and dissolved aromatic hydrocarbon threshold concentrations, are presented in Section 3 to summarise the stochastic modelling outcomes.

Spatial figures for floating oil, entrained oil, dissolved aromatic hydrocarbons and shoreline oil are presented in Section 4 to summarise the outcomes of the deterministic analysis and modelling.

The overall findings of the study are summarised in Section 5.

2   MODELLING METHODOLOGY

2.1   Description of the SIMAP Model

The spill modelling was carried out using a purpose-developed oil spill trajectory and fates model, SIMAP (Spill Impact Mapping and Assessment Program). This model is designed to simulate the transport and weathering processes that affect the outcomes of hydrocarbon spills to the sea, accounting for the specific oil type, spill scenario, and prevailing wind and current patterns.

SIMAP is an evolution of the US EPA Natural Resource Damage Assessment model (French & Rines, 1997; French, 1998; French *et al.*, 1999) and is designed to simulate the fate and effects of spilled oils and fuels for both the surface slick and the three-dimensional plume that is generated in the water column. SIMAP includes algorithms to account for both physical transport and weathering processes. The latter are important for accounting for the partitioning of the spilled mass over time between the water surface (surface slick), water column (entrained oil and dissolved compounds), atmosphere (evaporated compounds) and land (stranded oil). The model also accounts for the interaction between weathering and transport processes.

The physical transport algorithms calculate transport and spreading by physical forces, including surface tension, gravity and wind and current forces for both surface slicks and oil within the water column. The fates algorithms calculate all of the weathering processes known to be important for oil spilled to marine waters. These include droplet and slick formation, entrainment by wave action, emulsification, dissolution of soluble components, sedimentation, evaporation, bacterial and photo-chemical decay and shoreline interactions. These algorithms account for the specific oil type being considered.

Evaporation rates vary over space and time dependent on the prevailing sea temperatures, wind and current speeds, the surface area of the slick and entrained droplets that are exposed to the atmosphere as well as the state of weathering of the oil. Evaporation rates will decrease over time, depending on the calculated rate of loss of the more volatile compounds. By this process, the model can differentiate between the fates of different oil types.

Entrainment, dissolution and emulsification rates are correlated to wave energy, which is accounted for by estimating wave heights from the sustained wind speed, direction and fetch (i.e. distance downwind from land barriers) at different locations in the domain. Dissolution rates are dependent upon the proportion of soluble, short-chained hydrocarbon compounds, and the surface area at the oil/water interface of slicks. Dissolution rates are also strongly affected by the level of turbulence. For example, dissolution rates will be relatively high at the site of the release for a deep-sea discharge at high pressure.

In contrast, the release of hydrocarbons onto the water surface will not generate high concentrations of soluble compounds. However, subsequent exposure of the surface slick to breaking waves will enhance entrainment of oil into the upper water column as oil droplets, which will enhance dissolution of the soluble components. Because the compounds that have high solubility also have high volatility, the processes of evaporation and dissolution will be in dynamic competition with the balance dictated by the nature of the release and the weather conditions that affect the oil after release. The SIMAP weathering algorithms include terms to represent these dynamic processes. Technical descriptions of the algorithms used in SIMAP and validations against real spill events are provided in French (1998), French *et al.* (1999) and French-McCay (2004).

Input specifications for oil types include the density, viscosity, pour-point, distillation curve (volume of oil distilled off versus temperature) and the aromatic/aliphatic component ratios within given boiling point ranges. The model calculates a distribution of the oil by mass into the following components:

- Surface-bound or floating oil.
- Entrained oil (non-dissolved oil droplets that are physically entrained by wave action).

- Dissolved hydrocarbons (principally the aromatic and short-chained aliphatic compounds).

- Evaporated hydrocarbons.

- Sedimented hydrocarbons.

- Decayed hydrocarbons.

2.2   Calculation of Exposure Risks

The stochastic model within SIMAP performs a large number of simulations for a given spill site, randomly varying the spill time for each simulation. The model uses the spill time to select samples of current and wind data from a long time-series of wind and current data for the area. Hence, the transport and weathering of each slick will be subject to a different sample of wind and current conditions.

This stochastic sampling approach provides an objective measure of the possible outcomes of a spill, because environmental conditions will be selected at a rate that is proportional to the frequency that these conditions occur over the study region. More simulations will tend to use the most commonly occurring conditions, while conditions that are more unusual will be represented less frequently.

During each simulation, the SIMAP model records the location (by latitude, longitude and depth) of each of the particles (representing a given mass of oil) on or in the water column, at regular time steps. For any particles that contact a shoreline, the model records the accumulation of oil mass that arrives on each section of shoreline over time, less any mass that is lost to evaporation and/or subsequent removal by current and wind forces.

The collective records from all simulations are then analysed by dividing the study region into a three-dimensional grid. For oil particles that are classified as being at the water surface (floating oil), the sum of the mass in all oil particles (including accounting for spreading and dispersion effects) located within a grid cell, divided by the area of the cell provides estimates of the concentration of oil in that grid cell, at each time step. For entrained and dissolved oil particles, concentrations are calculated at each time step by summing the mass of particles within a grid cell and dividing by the volume of the grid cell.

The concentrations of oil calculated for each grid cell, at each time step, are then analysed to determine whether concentration estimates exceed defined threshold concentrations over time.

Risks are then summarised as follows:

- The probability of exposure to a location is calculated by dividing the number of spill simulations where any instantaneous contact occurred above a specified threshold at that location by the total number of replicate spill simulations. For example, if contact occurred at a location (above a specified threshold) during 21 out of 100 simulations, a probability of exposure of 21% is indicated.

- The minimum potential time to a shoreline location is calculated by the shortest time over which oil at a concentration above a particular threshold was calculated to travel from the source to the location in any of the replicate simulations.

- The maximum potential concentration of oil predicted for each shoreline section is the greatest mass per m^2 of shoreline calculated to strand at any location within that section during any of the replicate simulations.

- The average of the maximum concentrations of oil predicted to potentially accumulate on each shoreline section is calculated by determining the greatest mass per m^2 of shoreline during each replicate simulation and calculating an average of these estimates across the simulations. Note that this statistic has been previously referred to as the "mean expected maximum" in earlier reports.

- Similar treatments are undertaken for entrained oil and dissolved aromatic hydrocarbons.

Thus, the minimum time to shoreline and the maximum potential concentration estimates indicate the worst potential outcome of the modelled spill scenario for each section of shoreline. However, the average over the replicates presents an average of the potential outcomes, in terms of oil that could strand.

Note also that results quoted for sections of shoreline or shoal are derived for any individual location within that section or shoal, as a conservative estimate. Locations will represent shoreline lengths of the order of ~1 km, while sections or regions will represent shorelines spanning tens to hundreds of kilometres and we do not imply that the maximum potential concentrations quoted will occur over the full extent of each section. We therefore warn against multiplying the maximum concentration estimates by the full area of the section because this will greatly overestimate the total volume expected on that section.

The maximum entrained hydrocarbon and maximum dissolved aromatic hydrocarbon concentration are calculated for water locations surrounding each defined shoreline (see Section 3.1). These zones are defined to provide a buffer area around shallow (<10 m) habitats to allow for spatial errors in model forecasts. The greatest calculated value at any time step during any replicate simulation is listed. These values therefore represent worst-case localised estimates (within a grid cell). The averages over all replicate values represent a central tendency of these simulated worst-case estimates.

2.3   Inputs to the Risk Assessment

2.3.1   Current Data

2.3.1.1 Background

The area of interest for this study is typified by strong tidal flows over the shallower regions, particularly along the inshore region of the North West Shelf and among the island groups stretching from the Dampier Archipelago to the North West Cape. However, the offshore regions with water depths exceeding 100-200 m experience significant large-scale drift currents. These drift currents can be relatively strong (1-2 knots) and complex, manifesting as a series of eddies, meandering currents and connecting flows. These offshore drift currents also tend to persist longer (days to weeks) than tidal current flows (hours between reversals) and thus will have greater influence upon the net trajectory of slicks over time scales exceeding a few hours.

Wind shear on the water surface also generates local-scale currents that can persist for extended periods (hours to days) and result in long trajectories. Hence, the current-induced transport of oil can be variably affected by combinations of tidal, wind-induced and density-induced drift currents. Depending on their local influence, it is critical to consider all these potential advective mechanisms to rigorously understand patterns of potential transport from a given spill location.

To appropriately allow for temporal and spatial variation in the current field, spill modelling requires the current speed and direction over a spatial grid covering the potential migration of oil. As measured current data is not available for simultaneous periods over a network of locations covering the wide area of this study, the analysis relied upon hindcasts of the circulation generated by numerical modelling. Estimates of the net currents were derived by combining predictions of the drift currents, available from mesoscale ocean models, with estimates of the tidal currents generated by an RPS model set up for the study area.

2.3.1.2 Mesoscale Circulation Model

Representation of the drift currents that affect the area were available from the output of the BRAN (Bluelink ReANalysis; Oke *et al.*, 2008, 2009; Schiller *et al.*, 2008) ocean model, which is sponsored by the Australian Government through the Commonwealth Bureau of Meteorology (BoM), Royal Australian Navy, and

Commonwealth Scientific and Industrial Research Organisation (CSIRO). BRAN is a data-assimilative, three-dimensional ocean model that has been run as a hindcast for many periods and is now used for ocean forecasting (Schiller *et al.*, 2008).

The BRAN predictions for drift currents are produced at a horizontal spatial resolution of approximately 0.1° over the region, at a frequency of once per day, averaged over the 24-hour period. Hence, the BRAN model data provides estimates of mesoscale circulation with horizontal resolution suitable to resolve eddies of a few tens of kilometres' diameter, as well as connecting stream currents of similar spatial scale. Drift currents that are represented over the inner shelf waters in the BRAN data are principally attributable to wind induced drift.

There are several versions of the BRAN database available. The latest BRAN simulation spans the period of January 1994 to August 2016. From this database, time series of current speed and direction were extracted for all points in the model domain for the years 2006-2015 (inclusive). The data was assumed to be a suitably representative sample of the current conditions over the study area for future years.

Figure 2.1 to Figure 2.3 show the monthly distribution of current speeds and directions for the BRAN data points closest to the spill locations for Scenarios 1 to 3. Note that the convention for defining current direction is the direction towards which the current flows.

The current data indicates higher average current speeds are characteristic of the May to September period, with the highest average speeds (0.26 m/s) occurring at the Scenario 3 spill site in September. Lower average current speeds at the release locations are more common during the February to April period, with lowest average speeds (0.04 m/s) occurring at the Scenario 1 spill site in April. Peak current speeds across all months and sites are approximately 0.7 m/s.

Throughout the year, westerly currents are dominant at the Scenario 2 spill site and westerly/south-westerly currents are dominant at the Scenario 3 spill site. Current directions at the Scenario 1 spill site are seasonal, with north-easterly currents dominant between September and March, and south-westerly currents dominant between April and August.

The extracted current data near the spill locations provides an insight into the expected initial behaviour of any released oil due to the drift currents alone. Oil moving beyond the release sites, particularly towards the coast, would be subject to considerable variation in the drift current regime.
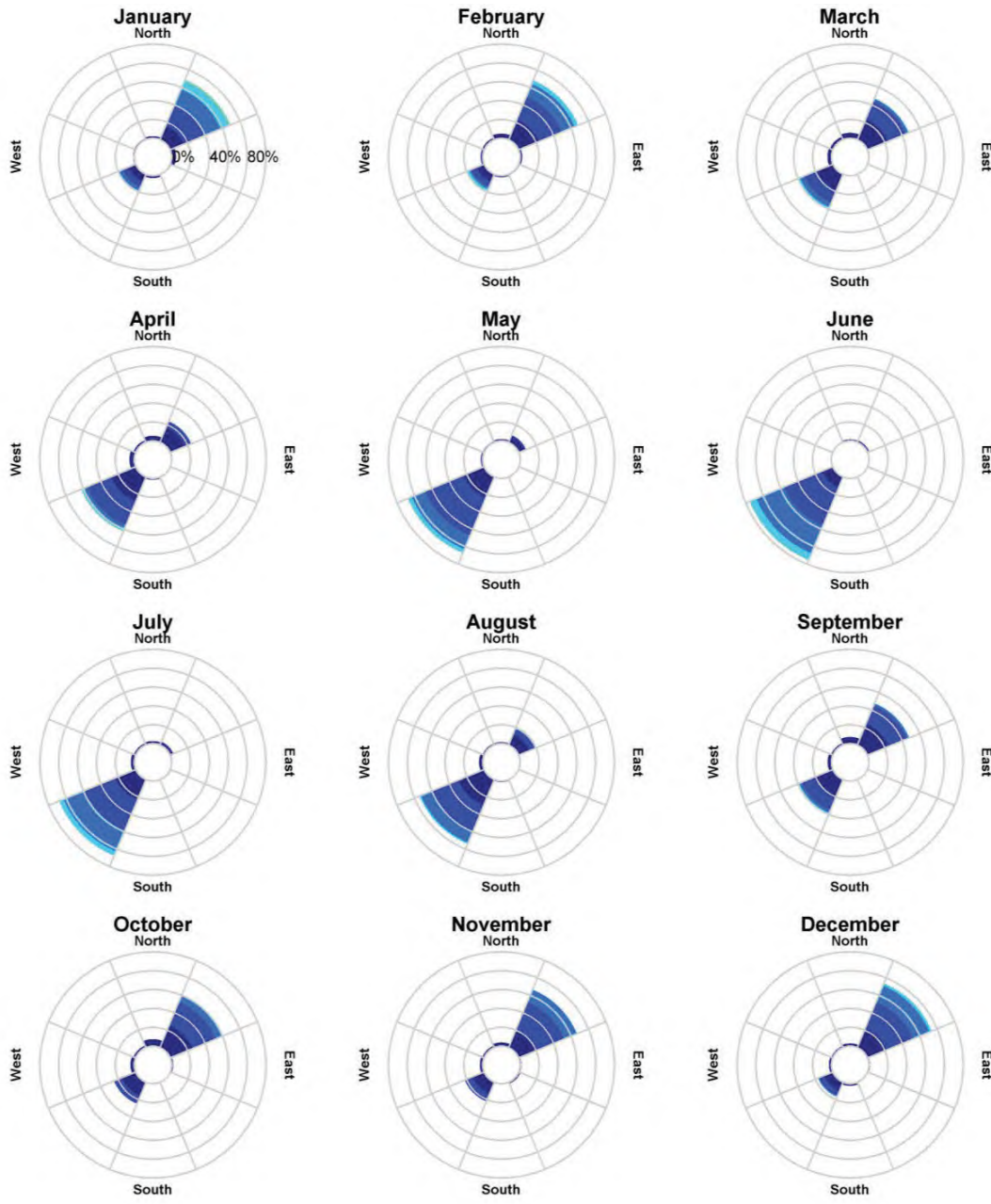
Figure 2.1 **Monthly current distribution (2006-2015, inclusive) derived from the BRAN database near to the Scenario 1 spill location. The colour key shows the current magnitude, the compass direction provides the direction towards which the current is flowing, and the size of the wedge gives the percentage of the record.**
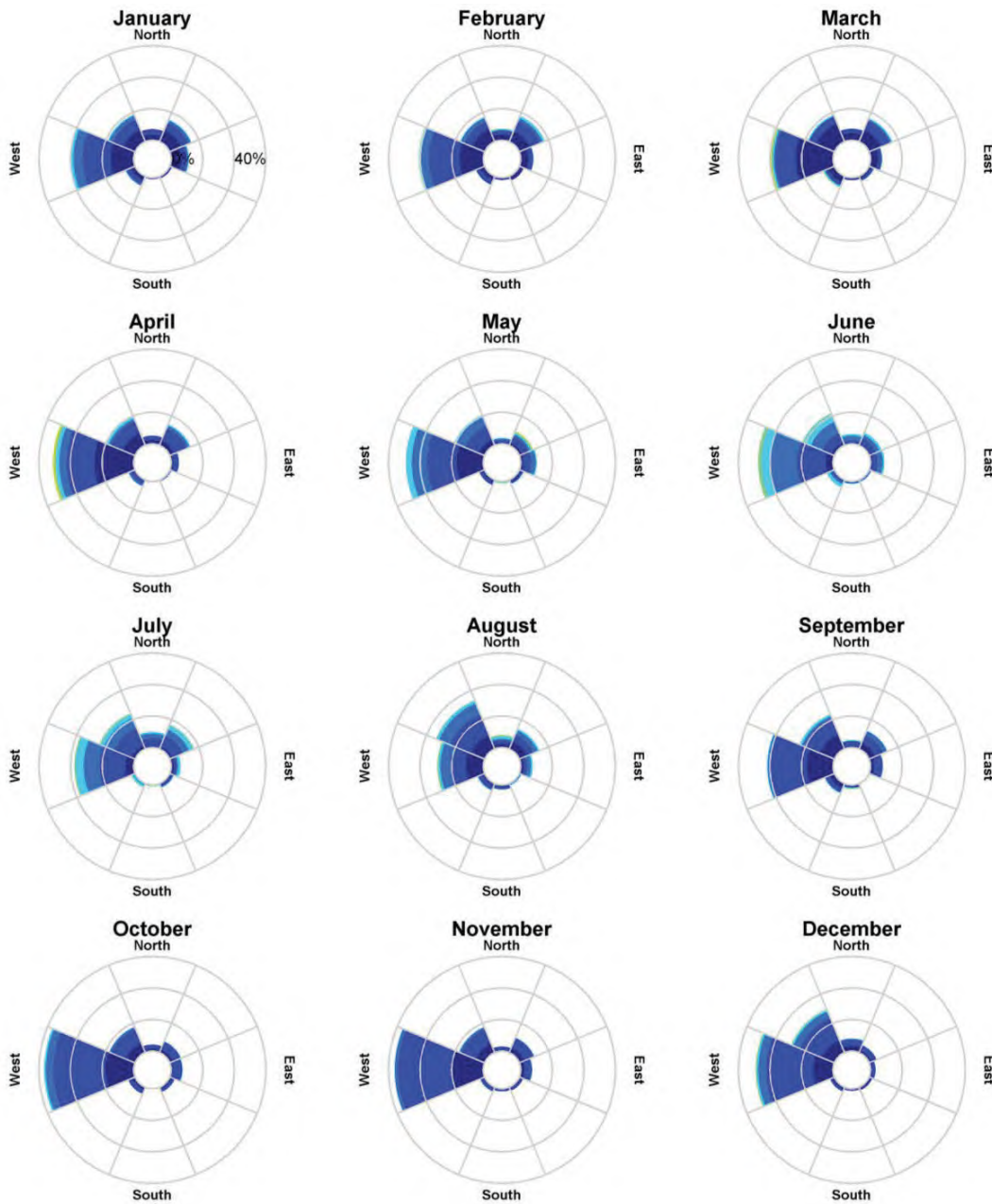
Figure 2.2 Monthly current distribution (2006-2015, inclusive) derived from the BRAN database near to the Scenario 2 spill location. The colour key shows the current magnitude, the compass direction provides the direction towards which the current is flowing, and the size of the wedge gives the percentage of the record.
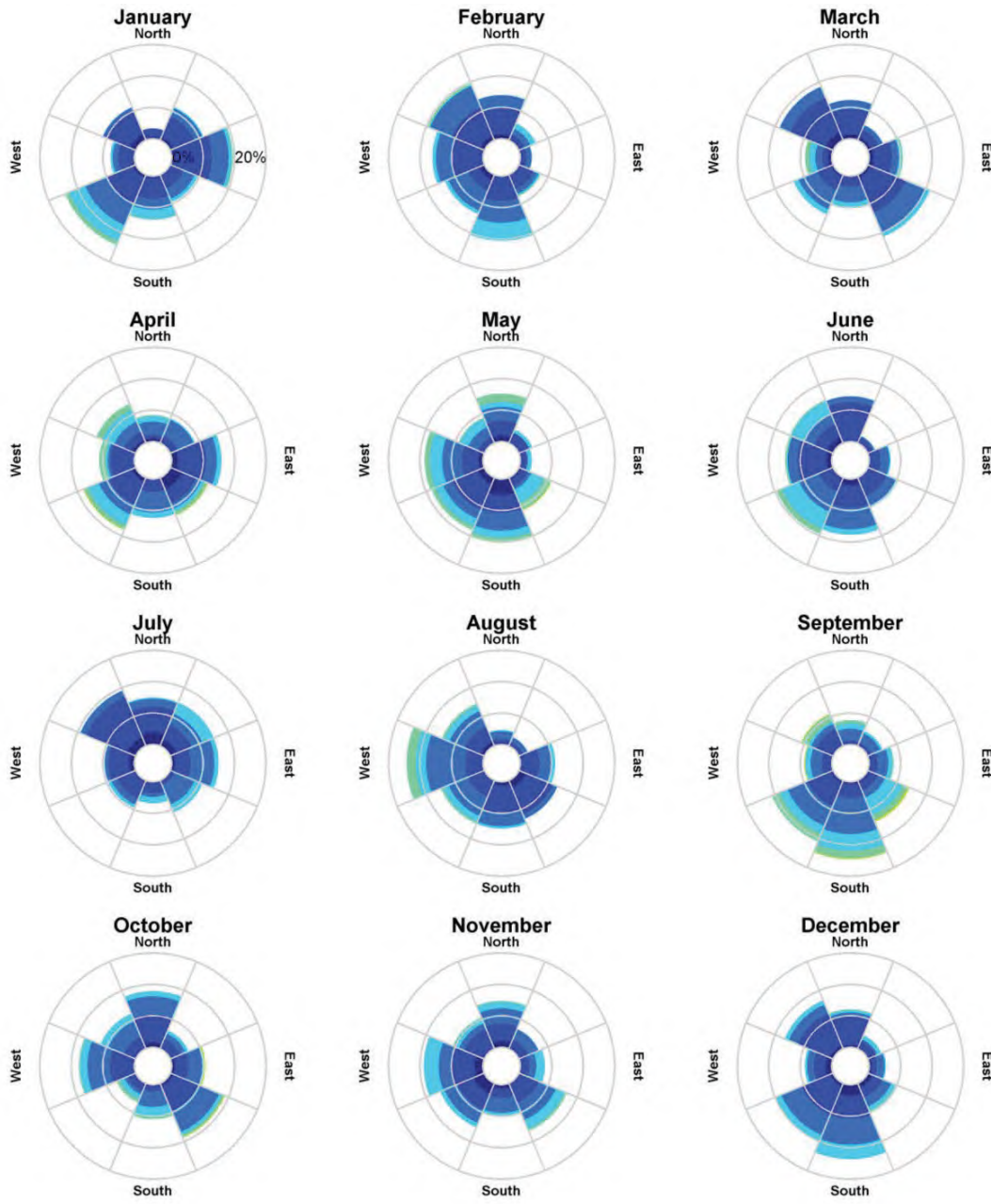
Figure 2.3 Monthly current distribution (2006-2015, inclusive) derived from the BRAN database near to the Scenario 3 spill location. The colour key shows the current magnitude, the compass direction provides the direction towards which the current is flowing, and the size of the wedge gives the percentage of the record.

2.3.1.3 Tidal Circulation Model

As the BRAN model does not include tidal forcing, and because the data is only available at a daily frequency, a tidal model was developed for the study region using RPS' three-dimensional hydrodynamic model, HYDROMAP.

The model formulations and output (current speed, direction and sea level) of this model have been validated through field measurements around the world for more than 25 years (Isaji & Spaulding, 1984, 1986; Isaji *et al.*, 2001; Zigic *et al.*, 2003). HYDROMAP current data has also been widely used as input to forecasts and hindcasts of oil spill migrations in Australian waters. This modelling system forms part of the National Marine Oil Spill Contingency Plan for the Australian Maritime Safety Authority (AMSA, 2002).

HYDROMAP simulates the flow of ocean currents within a model region due to forcing by astronomical tides, wind stress and bottom friction. The model employs a sophisticated dynamically nested-gridding strategy, supporting up to six levels of spatial resolution within a single domain. This allows for higher resolution of currents within areas of greater bathymetric and coastline complexity, or of particular interest to a study.

The numerical solution methodology of HYDROMAP follows that of Davies (1977a, 1977b) with further developments for model efficiency by Owen (1980) and Gordon (1982). A more detailed presentation of the model can be found in Isaji & Spaulding (1984).

A HYDROMAP model was established over a domain that extended approximately 3,300 km east-west by 3,100 km north-south over the eastern Indian Ocean. The grid extends beyond Eucla in the south and beyond Bathurst Island in the north (Figure 2.4).

Four layers of sub-gridding were applied to provide variable resolution throughout the domain. The resolution at the primary level was 15 km. The finer levels were defined by subdividing these cells into 4, 16 and 64 cells, resulting in resolutions of 7.5 km, 3.75 km and 1.88 km. The finer grids were allocated in a step-wise fashion to areas where higher resolution of circulation patterns was required to resolve flows through channels, around shorelines or over more complex bathymetry. Approximately 98,600 cells were used to define the region.

Bathymetric data used to define the three-dimensional shape of the study domain was extracted from the CMAP electronic chart database and supplemented where necessary with manual digitisation of chart data supplied by the Australian Hydrographic Office. Depths in the domain ranged from shallow intertidal areas through to approximately 7,200 m.

Ocean boundary data for the HYDROMAP model was obtained from the TOPEX/Poseidon global tidal database (TPXO7.2) of satellite-measured altimetry data, which provided estimates of tidal amplitudes and phases for the eight dominant tidal constituents (designated as K_2, S_2, M_2, N_2, K_1, P_1, O_1 and Q_1) at a horizontal scale of approximately 0.25°. Using the tidal data, sea surface heights are firstly calculated along the open boundaries at each time step in the model.

The TOPEX/Poseidon satellite data is produced, and quality controlled by the US National Atmospheric and Space Agency (NASA). The satellites, equipped with two highly accurate altimeters capable of taking sea level measurements accurate to less than ±5 cm, measured oceanic surface elevations (and the resultant tides) for over 13 years (1992-2005). In total, these satellites carried out more than 62,000 orbits of the planet. The TOPEX/Poseidon tidal data has been widely used amongst the oceanographic community, being the subject of more than 2,100 research publications (e.g. Andersen, 1995; Ludicone *et al.*, 1998; Matsumoto *et al.*, 2000; Kostianoy *et al.*, 2003; Yaremchuk & Tangdong, 2004; Qiu & Chen, 2010). As such, the TOPEX/Poseidon tidal data is considered suitably accurate for this study.

For the purpose of verification of the tidal predictions, the model output was compared against independent predictions of tides using the XTide database (Flater, 1998). The XTide database contains harmonic tidal

constituents derived from measured water level data at locations around the world. Of more than 40 tidal stations within the HYDROMAP model domain, ten were used for comparison.

Water level time series for these locations are shown in Figure 2.5 for a one-month period (January 2005). All comparisons show that the model produces a very good match to the known tidal behaviour for a wide range of tidal amplitudes and clearly represents the varying diurnal and semi-diurnal nature of the tidal signal.

The model skill was further evaluated through a comparison of the predicted and observed tidal constituents, derived from an analysis of model-predicted time-series at each location. A scatter plot of the observed and modelled amplitude (top) and phase (bottom) of the five dominant tidal constituents (S_2, M_2, N_2, K_1 and O_1) is presented in Figure 2.6. The red line on each plot shows the 1:1 line, which would indicate a perfect match between the modelled and observed data. Note that the data is generally closely aligned to the 1:1 line demonstrating the high quality of the model performance.

Figure 2.7 to Figure 2.9 show the monthly distribution of current speeds and directions for the HYDROMAP data points closest to the spill locations for Scenarios 1 to 3. Note that the convention for defining current direction is the direction towards which the current flows.

The current data indicates cyclical tidal flow directions along an east-west axis at the Scenario 1 site, an east-southeast/west-northwest axis at the Scenario 2 site, and a northeast-southwest axis at the Scenario 3 site. Maximum speeds at the Scenario 1 and 2 sites are in the range 0.5-0.6 m/s, with peak speeds at the Scenario 3 site being around 0.09 m/s.

The extracted current data near the spill locations provides an insight into the expected initial behaviour of any released oil due to the tidal currents alone. Oil moving beyond the release sites, particularly towards the coast, would be subject to considerable variation in the tidal current regime.
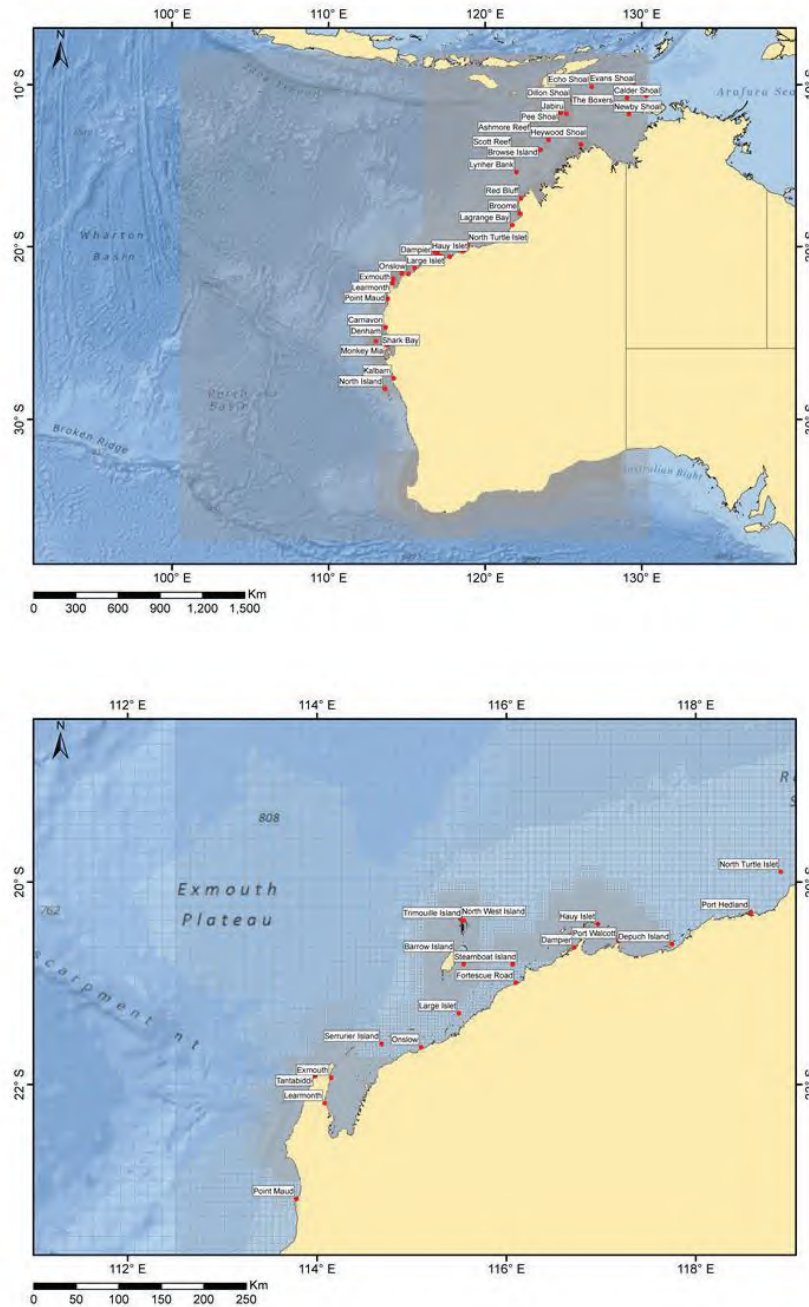
Figure 2.4   Hydrodynamic model grid (grey wire mesh) used to generate the tidal currents, showing locations available for tidal comparisons (red labelled dots). The top panel shows the full domain in context with the continental land mass, while the bottom panel shows a zoomed subset near the spill locations. Higher-resolution areas are indicated by the denser mesh zones.
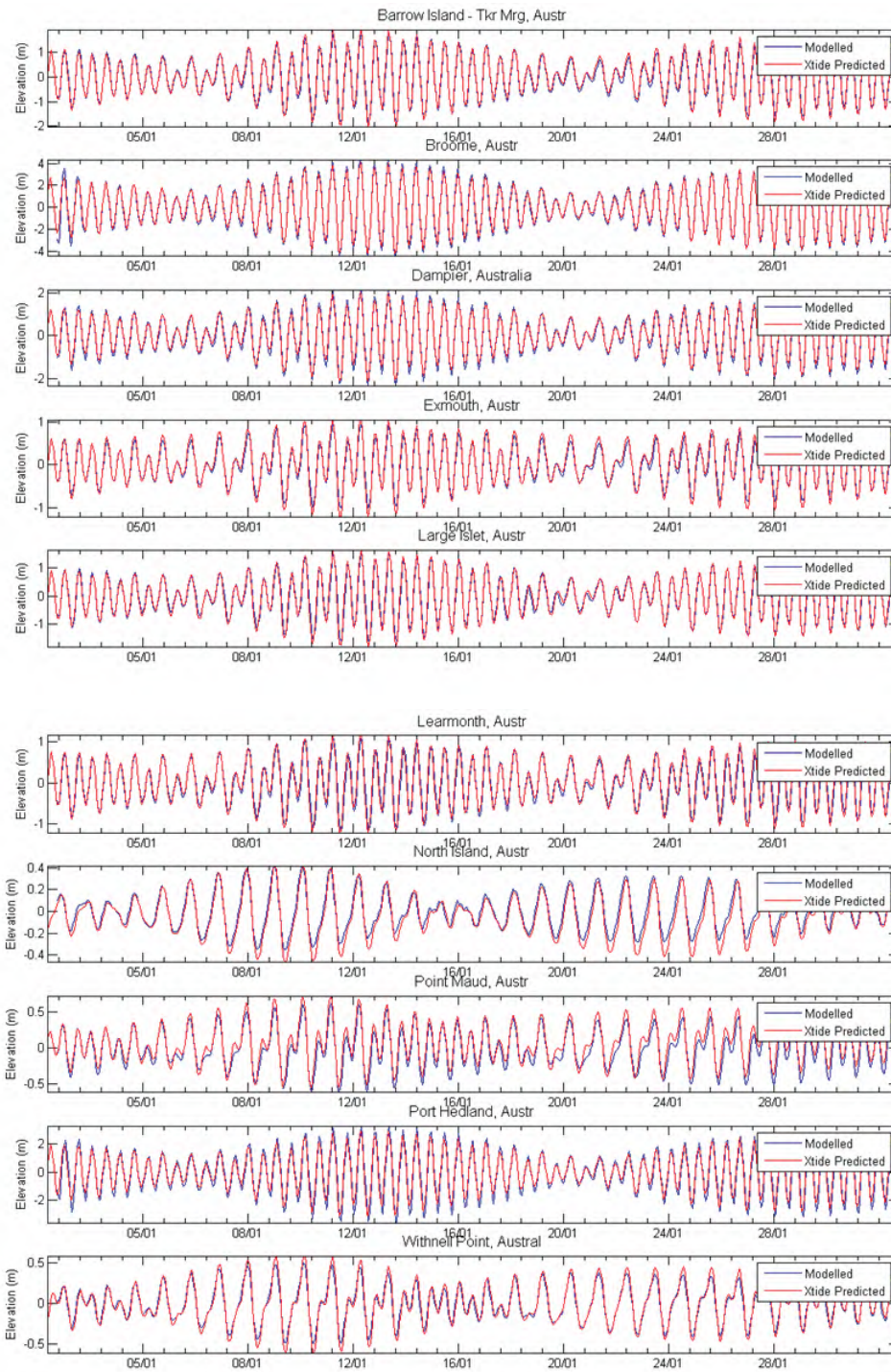
Figure 2.5   Comparisons between the predicted (blue line) and observed (red line) surface elevation variations at ten locations in the tidal model domain for January 2005.
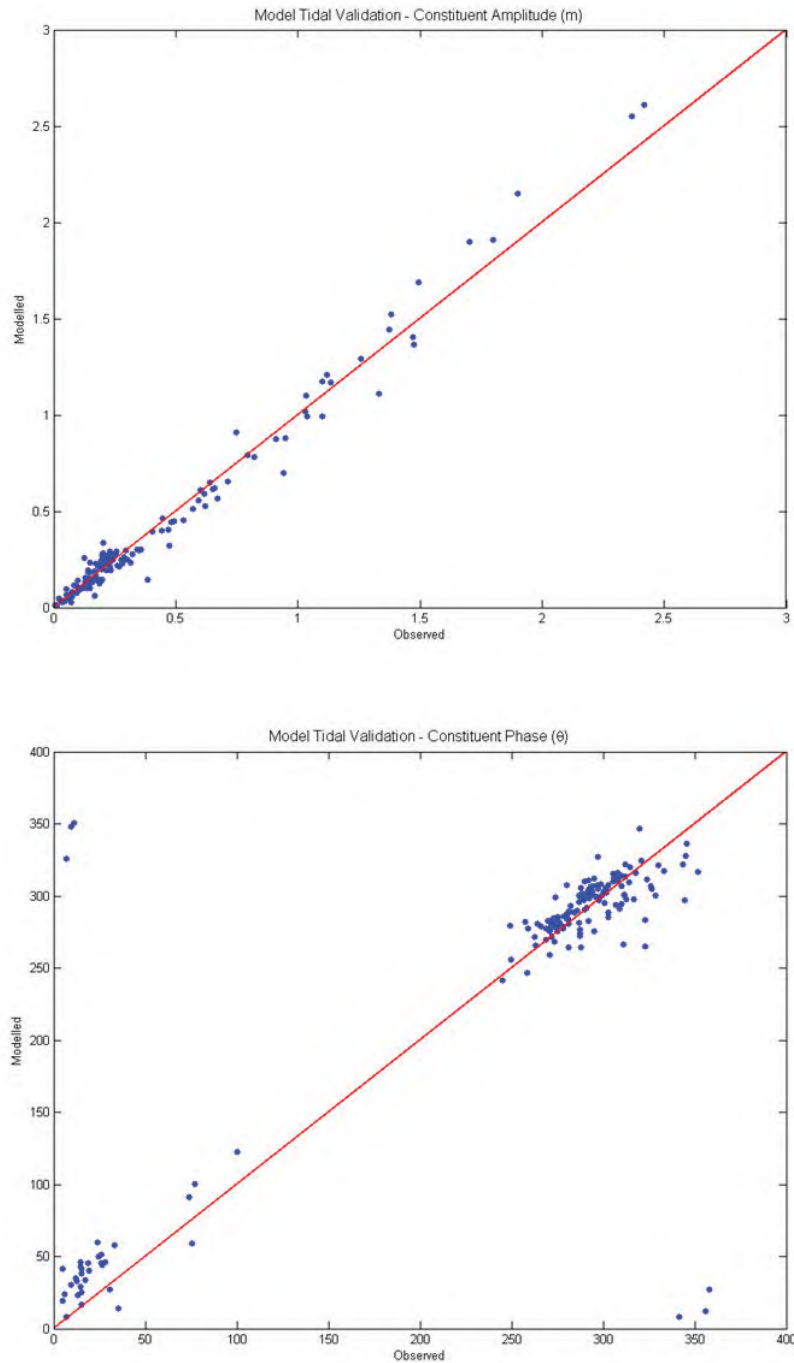
Figure 2.6   Comparisons between modelled and observed tidal constituent amplitudes (top) and phases (bottom) at all stations in the HYDROMAP model domain. The red line indicates a 1:1 correlation between the modelled and observed data.
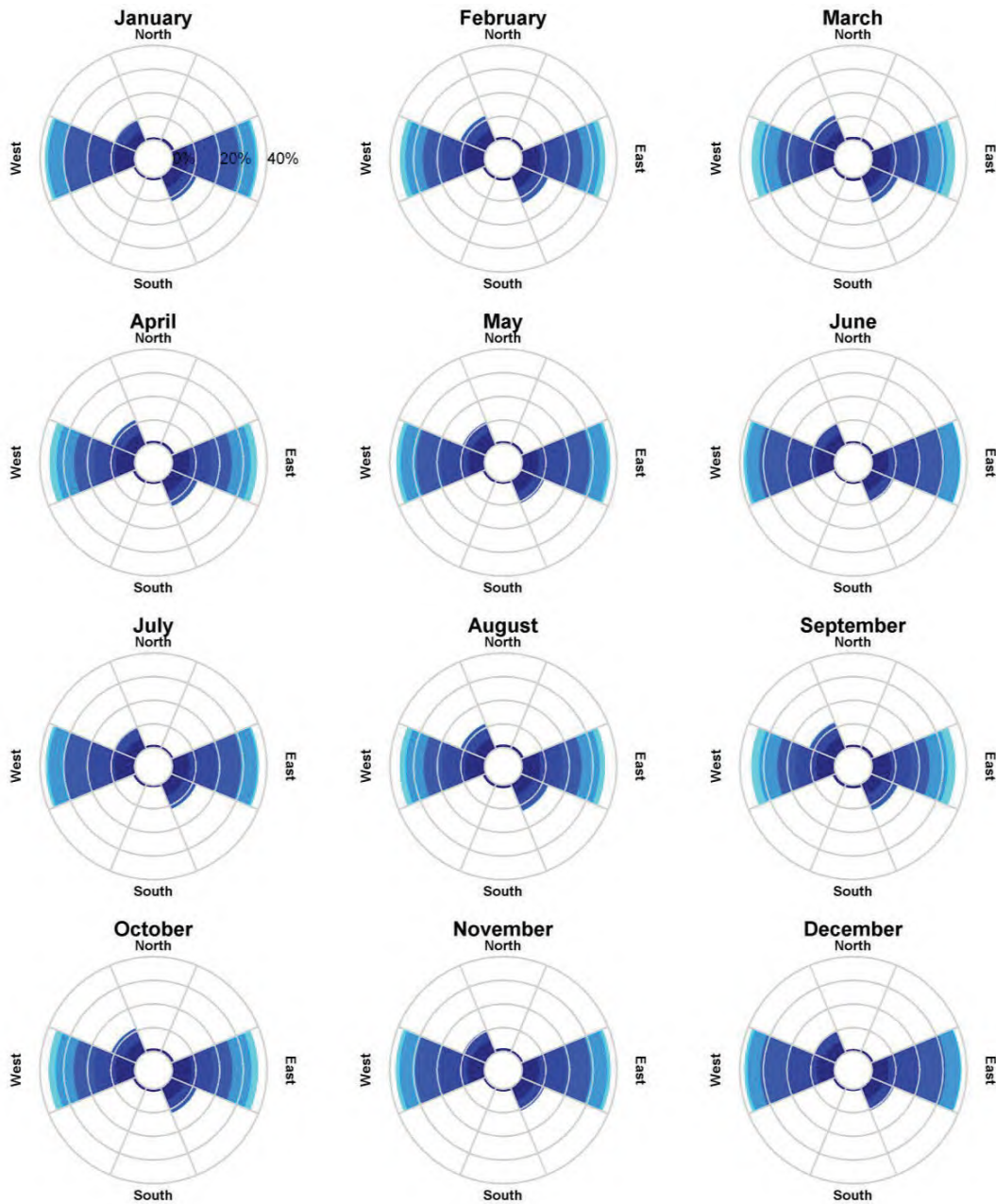
Figure 2.7 Monthly current distribution (2006-2015, inclusive) derived from the HYDROMAP database near to the Scenario 1 spill location. The colour key shows the current magnitude, the compass direction provides the direction towards which the current is flowing, and the size of the wedge gives the percentage of the record.
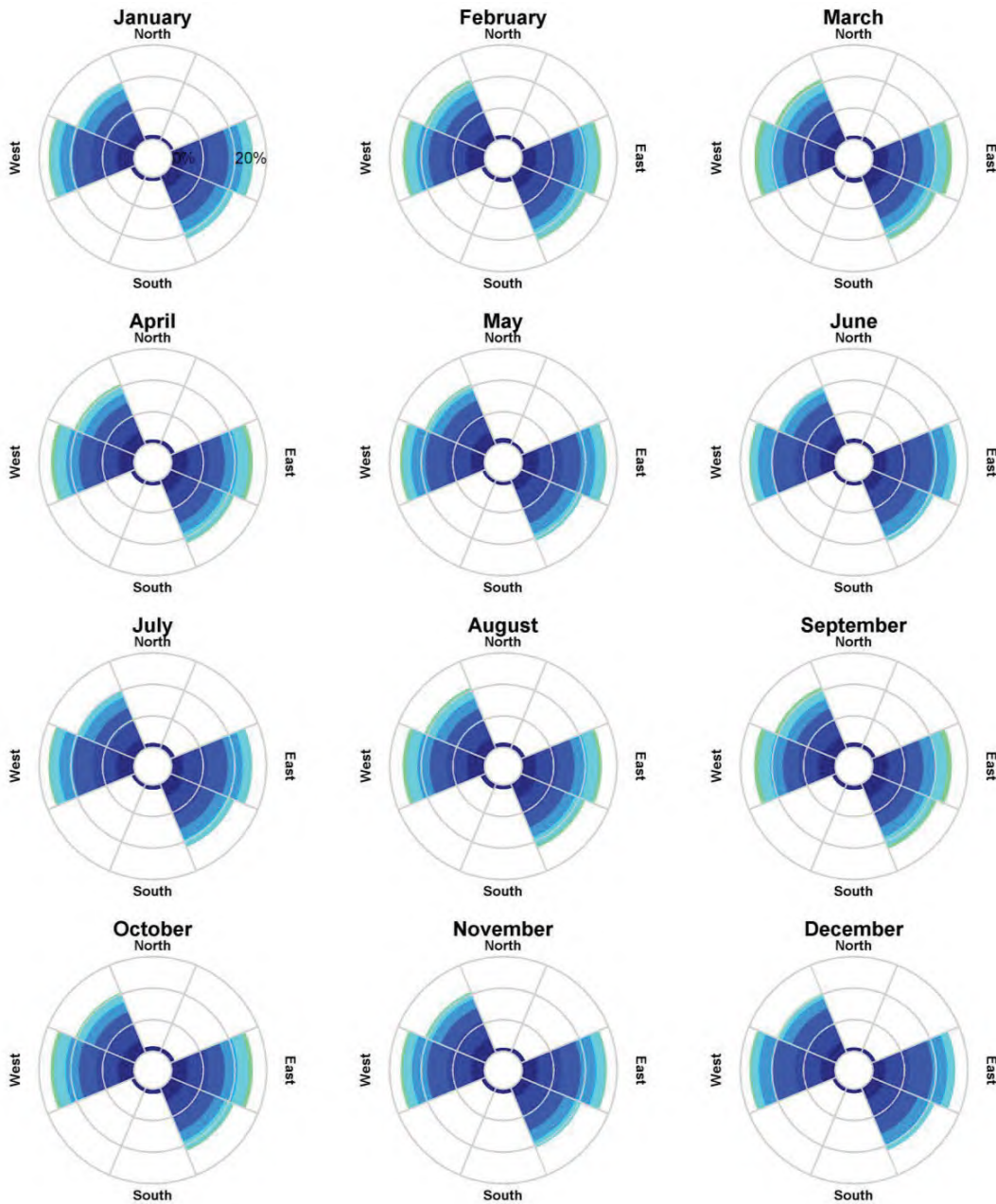
Figure 2.8 Monthly current distribution (2006-2015, inclusive) derived from the HYDROMAP database near to the Scenario 2 spill location. The colour key shows the current magnitude, the compass direction provides the direction towards which the current is flowing, and the size of the wedge gives the percentage of the record.
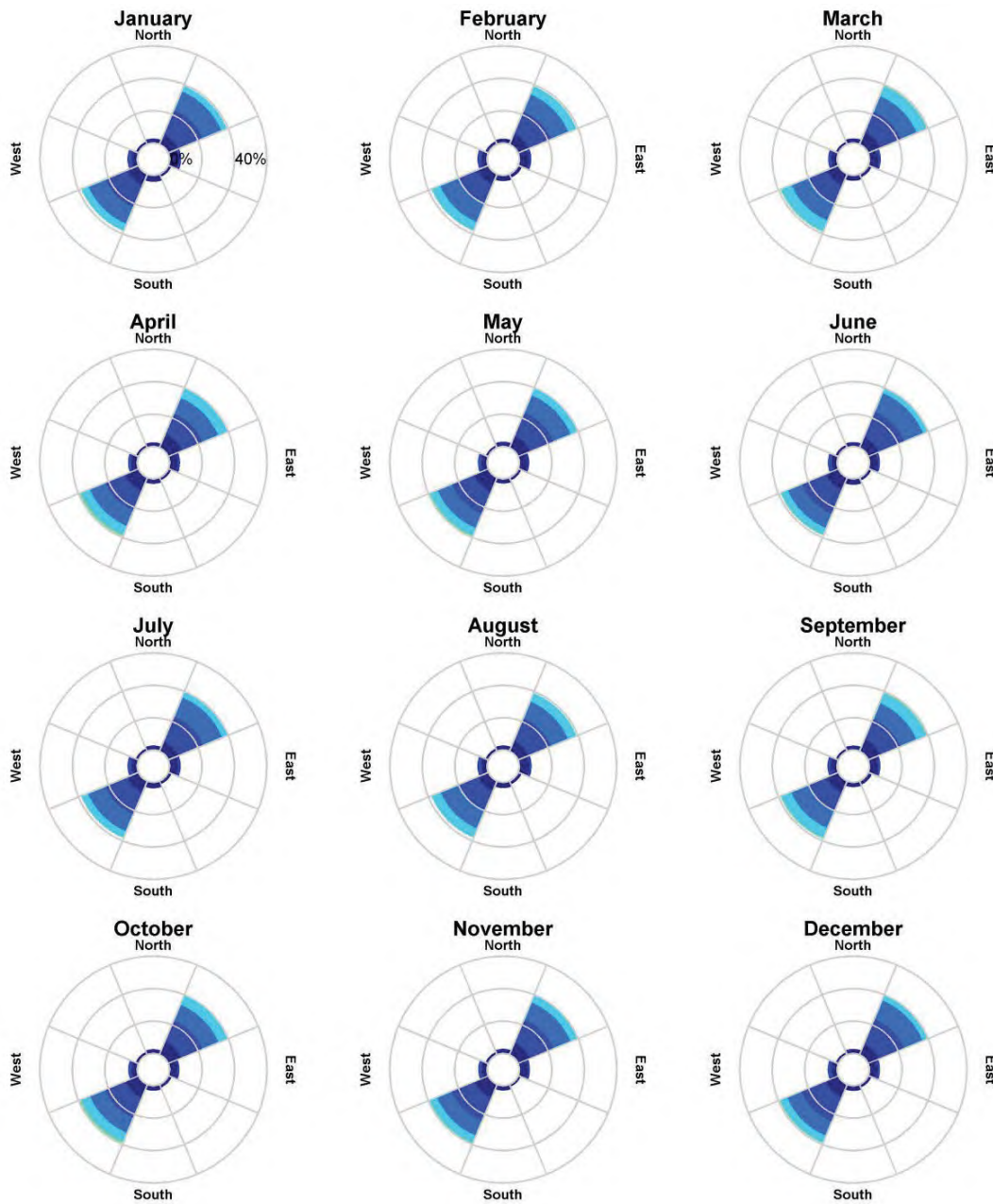
Figure 2.9 **Monthly current distribution (2006-2015, inclusive) derived from the HYDROMAP database near to the Scenario 3 spill location. The colour key shows the current magnitude, the compass direction provides the direction towards which the current is flowing, and the size of the wedge gives the percentage of the record.**

2.3.2 Wind Data

To account for the influence of the wind on surface-bound oil slicks, representation of the wind conditions was provided by spatial wind fields sourced from the National Center for Environmental Prediction (NCEP), via the National Oceanic and Atmospheric Administration (NOAA) and Cooperative Institute for Research in Environmental Sciences (CIRES) Climate Diagnostics Center (CDC). The NCEP Climate Forecast System Reanalysis (CFSR; Saha *et al.*, 2010) is a fully-coupled, data-assimilative hindcast model representing the interaction between the Earth's oceans, land and atmosphere. The gridded data output, including surface winds, is available at 0.25° resolution and 1-hourly time intervals.

Time series of wind speed and direction were extracted from the CFSR database for all nodes in the model domain for the same temporal coverage as the current data (2006-2015, inclusive). The data was assumed to be a suitably representative sample of the wind conditions over the study area for future years.

Figure 2.10 to Figure 2.12 show the monthly distribution of wind speed and direction for the CFSR data points closest to the spill locations for Scenarios 1 to 3. Note that the convention for defining wind direction is the direction from which the wind blows.

The wind data indicates similar trends in wind direction at the Scenario 1 and 2 spill locations, with predominantly easterly directions between May and July, and westerly/south-westerly directions dominating in the October to February period. At the Scenario 3 spill location, easterly/south-easterly directions are most common between April and August, with southerly directions most prominent between September and March. Average wind speeds across the year at the three spill locations vary in the range 5.9-6.5 m/s, with year-round maximum speeds of 25.5-29.4 m/s.

The extracted wind data near the spill location suggests possible initial trajectories due to the wind acting on surface slicks in the absence of any current effects. Note that the actual trajectories of surface slicks will be the net result of a combination of the prevailing wind and current vectors acting at a given time and location.
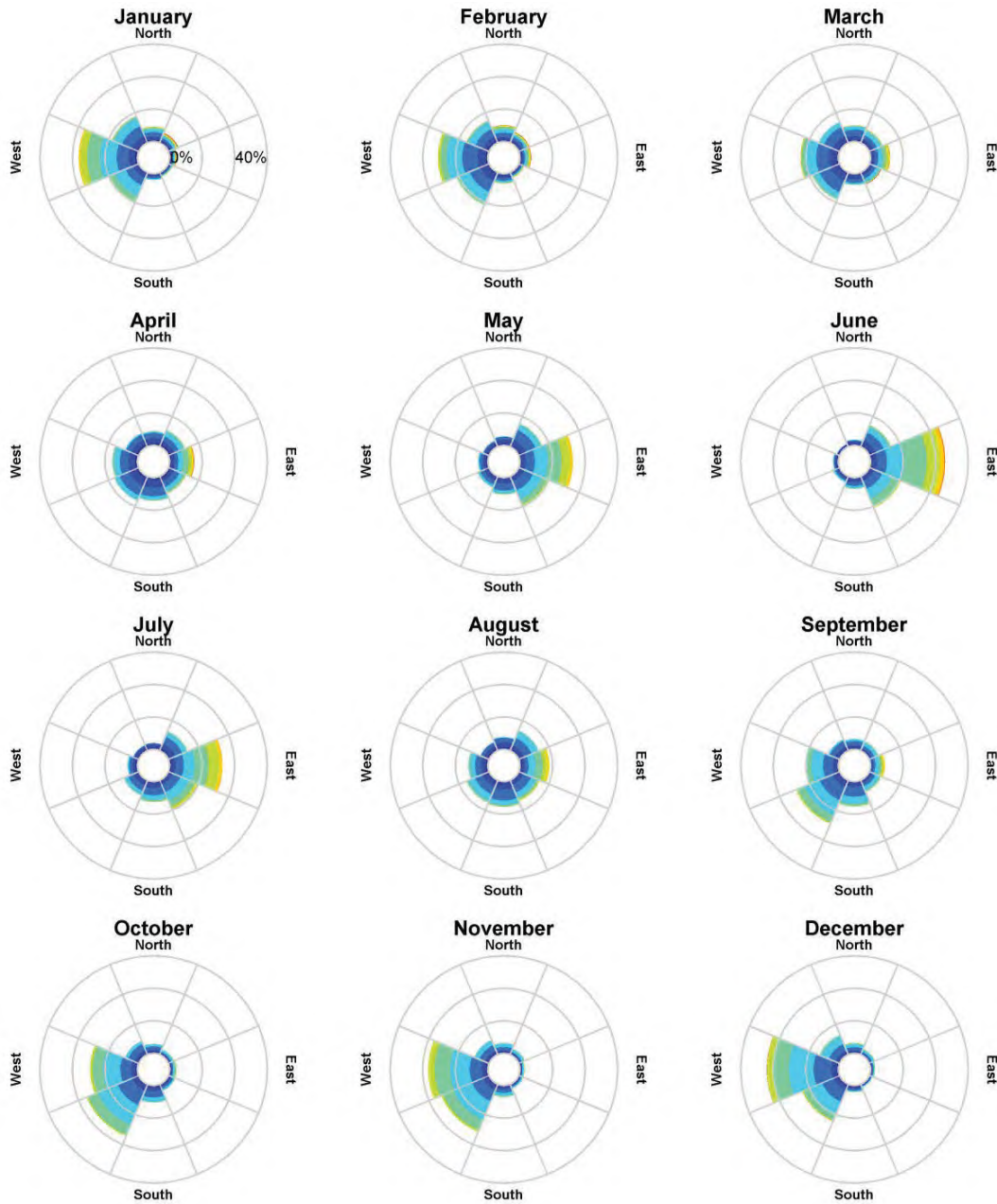
Figure 2.10 Monthly wind distribution (2006-2015, inclusive) derived from the CFSR database near to the Scenario 1 spill location. The colour key shows the wind magnitude, the compass direction provides the direction from which the wind is blowing, and the size of the wedge gives the percentage of the record.
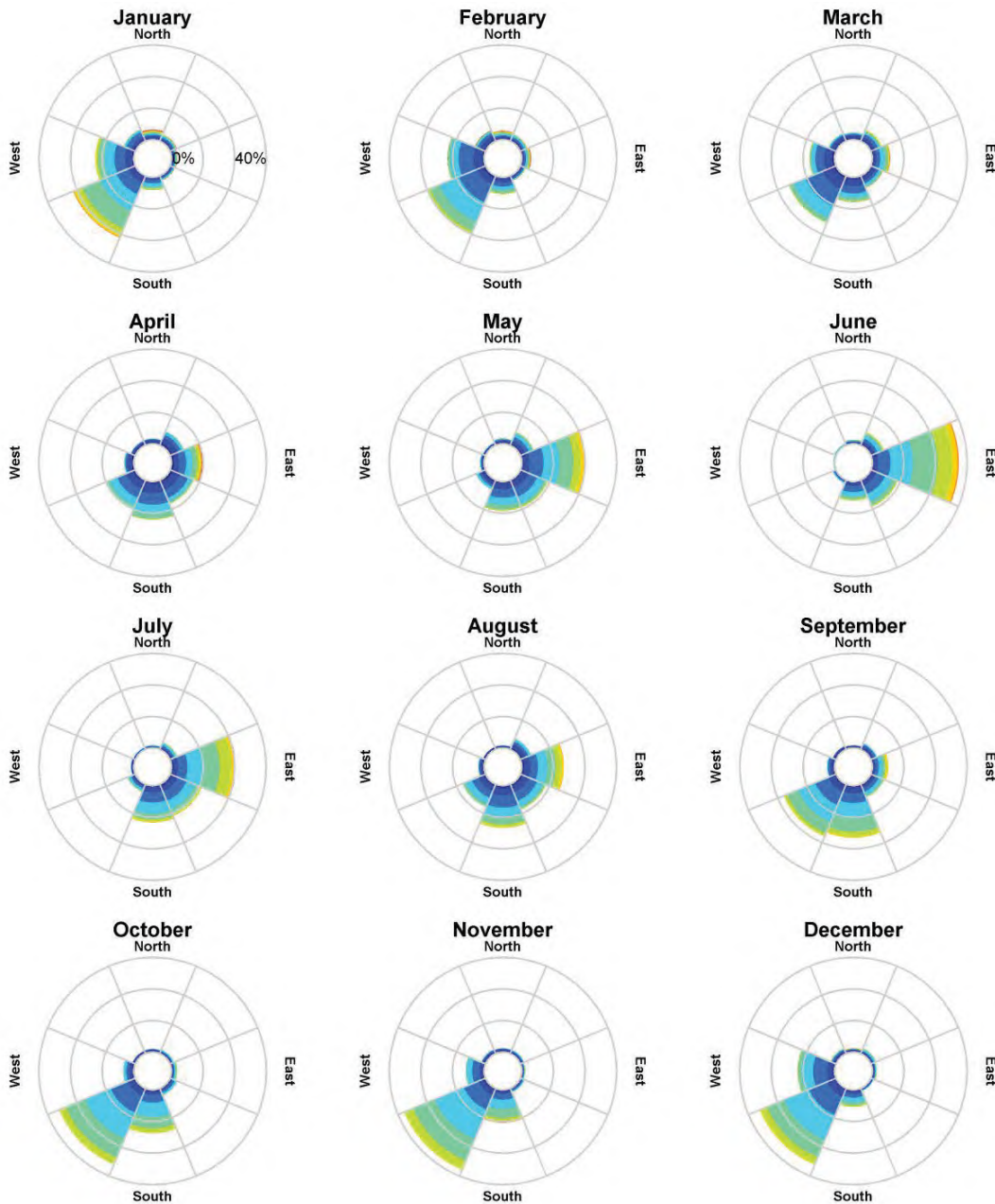
Figure 2.11   Monthly wind distribution (2006-2015, inclusive) derived from the CFSR database near to the Scenario 2 spill location. The colour key shows the wind magnitude, the compass direction provides the direction from which the wind is blowing, and the size of the wedge gives the percentage of the record.
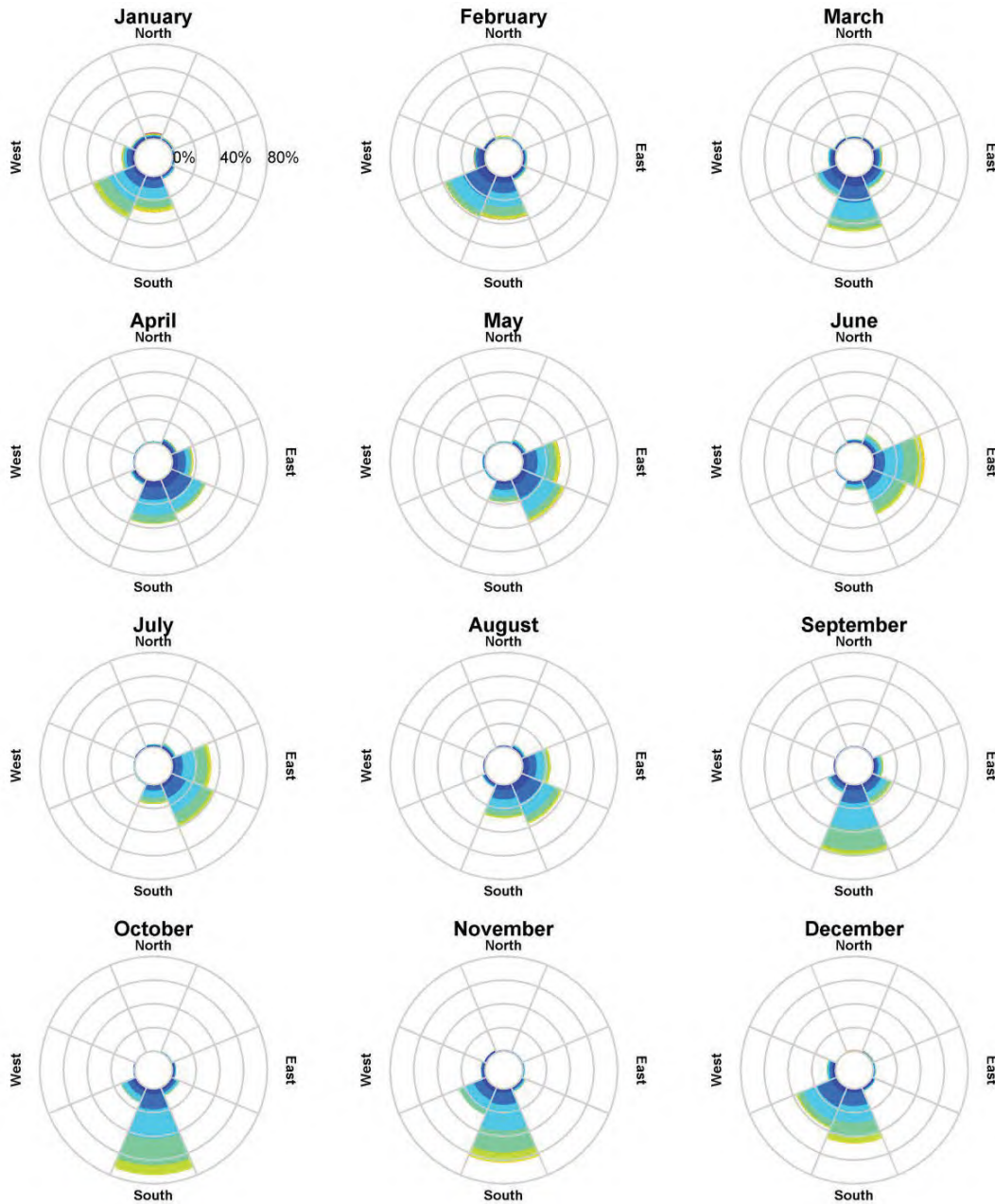
Figure 2.12 **Monthly wind distribution (2006-2015, inclusive) derived from the CFSR database near to the Scenario 3 spill location. The colour key shows the wind magnitude, the compass direction provides the direction from which the wind is blowing, and the size of the wedge gives the percentage of the record.**

2.3.3   Water Temperature and Salinity Data

The World Ocean Atlas 2013 (WOA13) is provided by NOAA and is a hindcast model of the climatological fields of in situ temperature, salinity, and a number of additional variables (NOAA, 2013a). WOA13 has a 0.25° resolution and has standard depth levels ranging from the water surface to 5,500 m (Locarnini *et al.*, 2013; Zweng *et al.*, 2013). Vertical profiles of sea temperature and salinity at the spill locations were retrieved from a data point in the WOA13 database near the Scarborough Project (19° 53' 54.60" S, 116° 14' 19.68" E), with monthly averages used as input to SIMAP.

Figure 2.13 shows the variation in water temperature and salinity both seasonally and over depth. During the period from May to September, surface mixing is evident over the upper 50-150 m of the water column (where the depth is approximately 1,000 m at this location). In contrast, during the period from October to April, the surface mixed layer is shallower, indicating stronger thermal stratification. The average temperature over the upper 200 m of the water column varies between approximately 15-29 °C across the year, while the average salinity over this depth range varies between approximately 34.6-35.8 PSU year-round.

2.3.4   Dispersion

A horizontal dispersion coefficient of 5 m^2/s was used to account for dispersive processes acting at the surface that are below the scale of resolution of the input current field, based on typical values for coastal waters (Okubo, 1971). Dispersion rates within the water column (applicable for entrained and dissolved plumes of hydrocarbons) were specified at 1 m^2/s, based on empirical data for the dispersion of hydrocarbon plumes over the North West Shelf (King & McAllister, 1998).

2.3.5   Replication

Multiple replicate simulations were completed for the defined scenarios to account for trends and variations in the trajectory and weathering of spilled oil, with an even number of replicates completed using samples of metocean data that commenced within each month. For Scenarios 1-3, a total of 100 replicate simulations were run over an annual period.
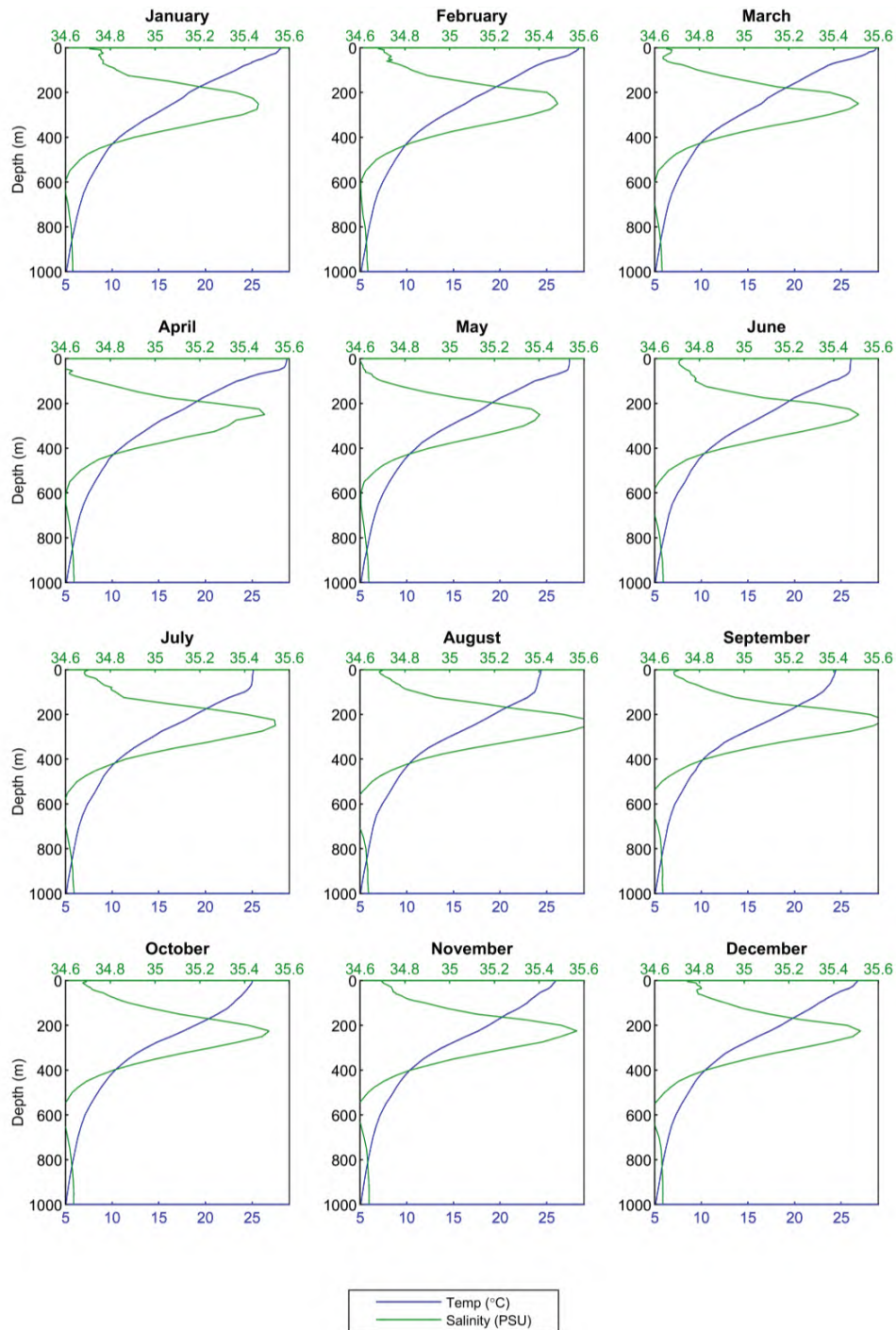
Figure 2.13 Temperature (blue line) and salinity (green line) profiles derived from the WOA13 database near the Scarborough Project (19° 53' 54.60" S, 113° 14' 19.68" E). Depth of 0 m is the water surface.

2.3.6   Contact Thresholds

2.3.6.1   Overview

The SIMAP model will track oil concentrations to very low levels. Hence, it is useful to define meaningful threshold concentrations for the recording of contact by oil components and determining the probability of exposure at a location (calculated from the number of replicate simulations in which this contact occurred).

The judgement of meaningful levels is complicated and will depend upon the mode of action, sensitivity of the biota contacted, the duration of the contact and the particular toxicity of the compounds that are represented in the oil. The latter factor is further complicated by the change in the composition of an oil type over time due to weathering processes. Without specific testing of the oil types, at different states of weathering against a wide range of the potential local receptors, such considerations are beyond the scope of this investigation.

For this case, thresholds for floating, entrained and dissolved aromatic hydrocarbons were specified by Woodside for use in defining the potential zone of influence of the spill event. These thresholds are summarised in Table 2.1 and discussed afterwards.

Table 2.1   Summary of the thresholds applied in this study.

Floating Oil Concentration (g/m^2)	Shoreline Oil Concentration (g/m^2)	Entrained Oil Concentration (ppb)	Dissolved Aromatic Hydrocarbon Concentration (ppb)
10	100	500	500
50			
100	250		

2.3.6.2   Floating Oil

Floating oil concentrations are relevant to describing the risks of oil coating emergent reefs, vegetation in the littoral zone and shoreline habitats, as well as the risk to wildlife found on the water surface, such as marine mammals, reptiles and birds. Floating oil is also visible at relatively low concentrations (> ~0.05 g/m^2). Hence, the area affected by visible oil, which might trigger social or economic impacts, will be larger than the area where biological impacts might be expected.

Estimates for the minimal thickness of floating oil that might result in harm to seabirds through ingestion from preening of contaminated feathers, or the loss of the thermal protection of their feathers, has been estimated by different researchers at approximately 10 g/m^2 (French-McCay, 2009) to 25 g/m^2 (Koops *et al.*, 2004). Hence, the 10 g/m^2 threshold is likely to be moderately conservative in terms of environmental harm for effects on seabirds, for example. The lower threshold of 1 g/m^2 is likely to be an indicator of where there is a visual presence of an oil slick that may trigger social and economic impacts but where there is little potential for environmental impact.

It is important to note that real spill events generate surface slicks that break up into multiple patches separated by areas of open water. Concentrations calculated and presented in this study represent necessary areal averaging over discrete model cells, and therefore indicate the potential for both higher and lower relative concentrations in the surrounding space.

2.3.6.3 Shoreline Oil

Shoreline oil concentrations are relevant to describing the risks of oil contact/stranding on shorelines and beaches. French *et al.* (1996) and French-McCay (2009) have defined an oil exposure threshold of 100 g/m² for shorebirds and wildlife (furbearing aquatic mammals and marine reptiles) on or along the shore, which is based on studies for sub-lethal and lethal impacts. The 100 g/m² threshold has been used in previous environmental risk assessment studies (French-McCay *et al.*, 2004, 2011, 2012; French-McCay, 2003; NOAA, 2013b). This threshold is also recommended in the Australian Maritime Safety Authority's foreshore assessment guide as the acceptable minimum thickness that does not inhibit the potential for recovery and is best remediated by natural coastal processes alone (AMSA, 2015). The 250 g/m² threshold is above the minimum thresholds observed to cause ecological impact and would therefore be considered high exposure.

2.3.6.4 Entrained Oil

Oil can be entrained into the water column from surface slicks due to wind and wave-induced turbulence, or be generated subsea by a pressurised discharge at depth. Entrained oil presents a number of possible mechanisms for exerting exposure. The entrained oil droplets may contain soluble compounds and hence have the potential to generate elevated concentrations of dissolved hydrocarbons (e.g. if mixed by breaking waves against a shoreline). Physical and chemical effects of the entrained oil droplets have also been demonstrated through direct contact with organisms; for example, through physical coating of gills and body surfaces, or accidental ingestion (NRC, 2005).

A review of the concentrations of physically entrained oil that has been demonstrated to have harmful effects in laboratory studies (NRC, 2005) showed wide variation depending on the test organisms and the initial oil mixture. For mortality of molluscs, reported LC_{50} values range from 500 ppb to 2,000 ppb with 96-hour exposure. Wider exposure sensitivities are displayed by species of crustaceans (100 ppb to 258,000 ppm) with 96-hour exposure, while marine fish larvae appear yet more sensitive with LC_{50} values as low as 45 ppb after 24-hour exposure.

As an indication of potential exposure, a threshold for concentrations of entrained oil was defined at 500 ppb. This threshold is particularly relevant for short duration (acute) exposure to organisms or fixed habitats affected by the dynamically-varying oil plume. A lower threshold, such as 10 ppb – which would be considered a conservative estimate of the lowest concentration that may be harmful to sensitive marine organisms over relatively long exposure times (tens of hours; French, 2000) – would be more meaningful for larvae and organisms that might be entrained (and therefore moving) within the oil plumes.

2.3.6.5 Dissolved Aromatic Hydrocarbons

The mode of action of soluble hydrocarbons is a narcotic effect resulting from uptake into the tissues of organisms. This effect is additive, increasing with exposure concentration or with time of exposure (French, 2000; NRC, 2005) For many oil mixtures, the concentration of aromatic hydrocarbons, and specifically the polyaromatic hydrocarbons (PAHs), in the water-soluble fraction is the best predictor of the toxicity of the oil.

As an indication of potential exposure, a threshold for concentrations of dissolved aromatic hydrocarbons was defined at 500 ppb. Because exposure times may be short (<1-2 hours) in the case of a slick passing over a fixed habitat (such as a reef), due to fluctuations in the plume location with changing environmental conditions, and because marine organisms can typically tolerate concentrations of toxic hydrocarbons that are two or more

orders of magnitude higher over such short durations (Pace *et al.*, 1995; French, 2000), the 500 ppb threshold is likely to be indicative of potentially harmful exposure to fixed habitats over short exposure durations.

2.3.7   Oil Characteristics

2.3.7.1 Overview

Characteristics of marine diesel are summarised in Table 2.2.

Table 2.2   Characteristics of the oil type used in the modelling of Scenarios 1-3.

Oil Type	Density (g/cm³)	Viscosity (cP)	Component	Volatile (%)	Semi-Volatile (%)	Low Volatility (%)	Residual (%)	Aromatics (%)
			Boiling point (°C)	<180 C4 to C10	180 - 265 C11 to C15	265 - 380 C16 to C20	>380 >C20	Of whole oil <380 BP
Marine Diesel	0.829 at 25 °C	4.000 at 25 °C	% of total	6.0	34.6	54.4	5.0	3.0
			% aromatics	1.8	1.0	0.2	-	-

The boiling points are dictated by the length of the carbon chains, with the longer and more complex compounds having a higher boiling point, and therefore lower volatility and evaporation rate.

The aromatic components within the volatile to low-volatility range are also soluble (with decreasing solubility following decreasing volatility) and will dissolve across the oil-water interface. The rate of dissolution will increase with increase in surface area. Hence, dissolution rates will be higher under discharge conditions that generate smaller oil droplets.

Atmospheric weathering will commence if and when oil droplets float to the water surface. Typical evaporation times once the hydrocarbons reach the surface and are exposed to the atmosphere are:

- Up to 12 hours for the C4 to C10 compounds (or less than 180 °C BP);

- Up to 24 hours for the C11 to C15 compounds (180-265 °C BP);

- Several days for the C16 to C20 compounds (265-380 °C BP); and

- Not applicable for the residual compounds (BP > 380 °C), which will resist evaporation, persist in the marine environment for longer periods, and be subject to relatively slow degradation.

The actual fate of released oil in the marine environment will depend greatly on the amount of oil that reaches the surface, either through the initial release or by rising after discharge in the water column.

2.3.7.2 Marine Diesel

Marine diesel is a mixture of volatile and persistent hydrocarbons with low proportions of highly volatile and residual components. In general, about 6% of the oil mass should evaporate within the first 12 hours (BP < 180 °C); a further 35% should evaporate within the first 24 hours (180 °C < BP < 265 °C); and a further 54% should evaporate over several days (265 °C < BP < 380 °C). Approximately 5% of the oil is shown to be persistent. The aromatic content of the oil is approximately 3%.

If released in the marine environment and in contact with the atmosphere (i.e. surface spill), approximately 41% by mass of this oil is predicted to evaporate over the first couple of days depending upon the prevailing

conditions, with further evaporation slowing over time. The heavier (low volatility) components of the oil have a tendency to entrain into the upper water column due to wind-generated waves, but can subsequently resurface if wind-waves abate. Therefore, the heavier components of this oil can remain entrained or on the sea surface for an extended period, with associated potential for dissolution of the soluble aromatic fraction.

2.3.8   Weathering Characteristics

2.3.8.1   Overview

A series of model weather tests were conducted to illustrate the potential behaviour of marine diesel when exposed to idealised and representative environmental conditions:

- Instantaneous release (1-hour discharge) onto the water surface at a discharge rate of 50 m³/hr under calm wind conditions (constant 5 knots), assuming low seasonal water temperature (27 °C) and average air temperature (25 °C). Slick also subject to ambient tidal and drift currents.

- Instantaneous release (1-hour discharge) onto the water surface at a discharge rate of 50 m³/hr under variable wind conditions (4-19 knots, drawn from representative data files), assuming low seasonal water temperature (27 °C) and average air temperature (25 °C). Slick also subject to ambient tidal and drift currents.

The first case is indicative of cumulative weathering rates under calm conditions that would not generate entrainment, while the second case may represent conditions that could cause a minor degree of entrainment. Both scenarios provide examples of potential behaviour during periods of a spill event, once the oil reaches the surface.

2.3.8.2   Marine Diesel

The mass balance forecast for the constant-wind case (Figure 2.14) for marine diesel shows that approximately 45% of the oil is predicted to evaporate within 24 hours. Under these calm conditions the majority of the remaining oil on the water surface will weather at a slower rate due to being comprised of the longer-chain compounds with higher boiling points. Evaporation of the residual compounds will slow significantly, and they will then be subject to more gradual decay through biological and photochemical processes.

Under the variable-wind case (Figure 2.15), where the winds are of greater strength, entrainment of marine diesel into the water column is indicated to be significant. Approximately 24 hours after the spill, around 45% of the oil mass is forecast to have entrained and a further 35% is forecast to have evaporated, leaving only a small proportion of the oil floating on the water surface (<1%). The residual compounds will tend to remain entrained beneath the surface under conditions that generate wind waves (approximately >6 m/s).

The increased level of entrainment in the variable-wind case will result in a higher percentage of biological and photochemical degradation, where the decay of the floating slicks and oil droplets in the water column occurs at an approximate rate of 1.8% per day with an accumulated total of ~13% after 7 days, in comparison to a rate of ~0.2% per day and an accumulated total of 1.5% after 7 days in the constant-wind case. Given the large proportion of entrained oil and the tendency for it to remain mixed in the water column, the remaining hydrocarbons will decay and/or evaporate over time scales of several weeks to a few months. This long weathering duration will extend the area of potential effect, requiring the break-up and dispersion of the slicks and droplets to reduce concentrations below the thresholds considered in this study.
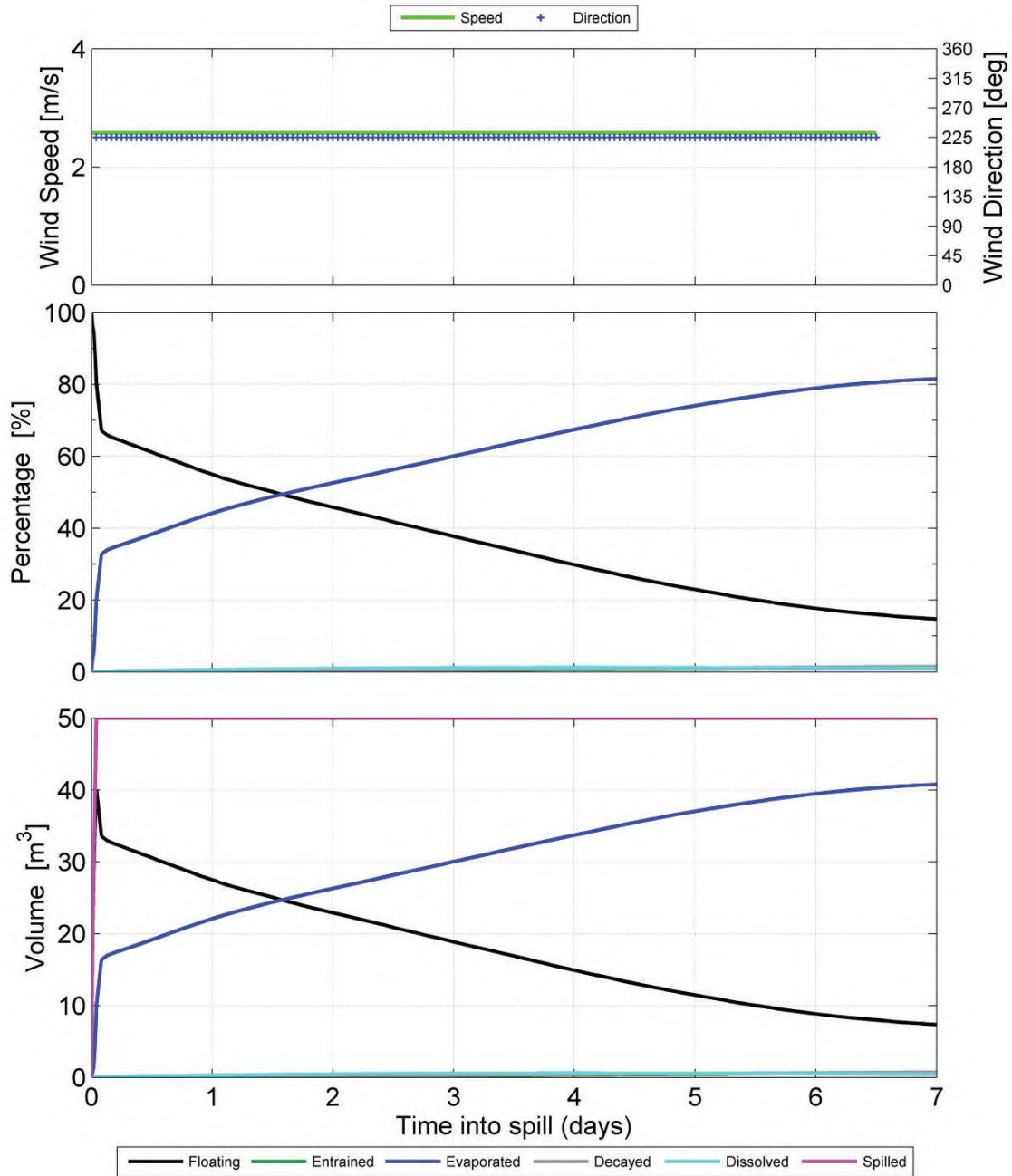
Figure 2.14 Mass balance plot representing, as proportion (middle panel) and volume (bottom panel), the weathering of marine diesel spilled onto the water surface as a one-off release (50 m³ over 1 hour) and subject to a constant 5 kn (2.6 m/s) wind at 27 °C water temperature and 25 °C air temperature.
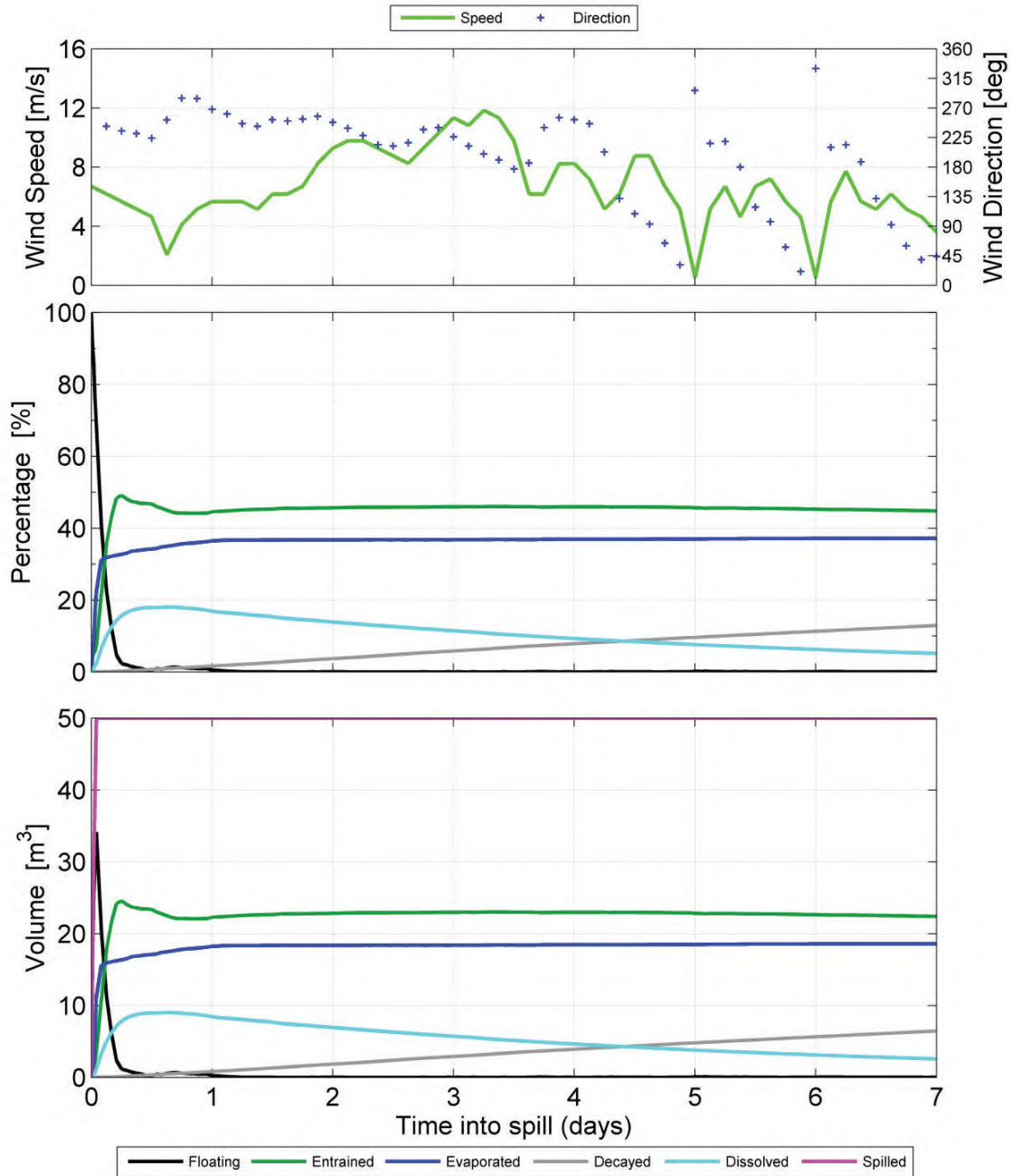
Figure 2.15 **Mass balance plot representing, as proportion (middle panel) and volume (bottom panel), the weathering of marine diesel spilled onto the water surface as a one-off release (50 m³ over 1 hour) and subject to variable wind at 27 °C water temperature and 25 °C air temperature.**

3 STOCHASTIC ASSESSMENT RESULTS

3.1 Overview

Predictions for the probability of contact and time to contact by oil concentrations equalling or exceeding defined thresholds for floating oil, entrained oil and dissolved aromatic hydrocarbons are provided in the following sections to summarise the results of the annualised stochastic modelling.

Contour maps present estimates for the annualised probability of contact by instantaneous concentrations of at least the defined minimum threshold concentrations (10 g/m^2, 50 g/m^2 and 100 g/m^2 for floating oil; 100 g/m^2 and 250 g/m^2 for shoreline oil; 500 ppb for entrained oil and dissolved aromatic hydrocarbons) for at least one time step. These contours summarise the outcomes for all replicate simulations commencing across the annual period – a total of 200 replicate simulations for each assessed scenario.

Readers should note that the contour maps presented in this report do not represent the predicted coverage of any one hydrocarbon spill or a depiction of a slick or plume at any particular instant in time. Rather, the contours are a composite of a large number of theoretical slick paths, integrated over the full duration of the simulations relevant to the assessed scenario. The contour maps should be treated as indications of the probability of exposure at defined concentrations, for individual locations, at some point in time after the defined spill commences, given the trends and variations in metocean conditions that occur around the study area.

Locations with higher probability ratings were exposed during a greater number of spill simulations, indicating that the combination of the prevailing wind and current conditions are more likely to result in contact to these locations if the spill scenario were to occur in the future. The areas outside of the lowest-percentage contour indicate that contact will be less likely under the range of prevailing conditions for this region than areas falling within higher probability contours. It is important to note that the probabilities are derived from the samples of data used in the modelling. Therefore, locations that are not calculated to receive exposure at threshold concentrations or greater in any of the replicate simulations might possibly be contacted if very unusual conditions were to occur. Hence, we do not attribute a probability of nil to areas beyond the lowest probability contour.

Tables are presented to summarise estimates of contact risk for locations within potentially sensitive receptors that were defined by Woodside. All sensitive receptors historically considered for Woodside spill risk assessments were included in the analysis, with those outlined here being the receptors shown to be at risk of contact for each assessed scenario.

The probability estimates for contact by floating oil that are presented in the tables summarise the probability that oil will arrive at shorelines as floating films at the specified threshold concentration or greater for at least one time step (1 hour).

The minimum time estimates shown in the tables present the shortest time for any oil to drift from the source to any part of the sensitive receptor, relative to the commencement of the spill. These times then indicate the minimum weathering time for oil that might make contact with the resource.

The mean and maximum shoreline concentrations indicate the concentrations forecast to potentially accumulate over time on any discrete part of a shoreline (calculated for individual portions of 0.8 km length). Accumulated concentrations are calculated by summing the mass of oil that arrives at any concentration (including < threshold) over time at a model cell and subtracting any mass lost through evaporation and washing off, where relevant.

The maximum local accumulated concentration in the worst replicate spill is the greatest accumulation predicted for any point on the shoreline during any replicate simulation, and thus represents an extreme

estimate. The maximum local accumulated concentration averaged over all replicate spills is the greatest concentration calculated for any point on the shoreline after averaging over all replicate simulations.

Note that it is possible that oil films arriving at concentrations that are less than the threshold may accumulate over the course of a spill event to result in concentrations that apparently exceed the threshold. Hence, the mean expected and maximum concentrations of accumulated oil can exceed the threshold applied to the probability calculations for the arrival of floating oil even where no instantaneous exceedances above threshold are predicted. It is important to understand that the two parameters (floating concentration and shoreline concentration) are quite distinct, calculated in different ways and representative of alternative outcomes. The floating probability estimates and the shoreline accumulative estimates should therefore be treated as independent estimators of different exposure outcomes, and not directly compared.

For the entrained and dissolved components, the tabulated results summarise interrogations of cells representing the water surrounding the sensitive receptor shorelines (or submerged features), with individual buffer zones. Buffer zones were defined with consideration of the bathymetry bordering each receptor, natural boundaries, or sensible legislative boundaries.

The modelling for each assessed scenario assumed no mitigation efforts are undertaken to collect or otherwise affect the natural transport and weathering of the oil.

The predicted outcomes based on the modelling results are discussed in the following sections in terms of floating, entrained and dissolved aromatic hydrocarbons. Discussion is based around the outcomes of stochastic risk contours. Plots of the Zones of Consequence (ZoCs) and minimum time to exceedance of concentration thresholds are presented for the assessed thresholds.

Figure 3.1 shows transect lines intersecting at the release locations along which maximum entrained oil and dissolved aromatic hydrocarbon concentrations in the water column were extracted for each assessed scenario.
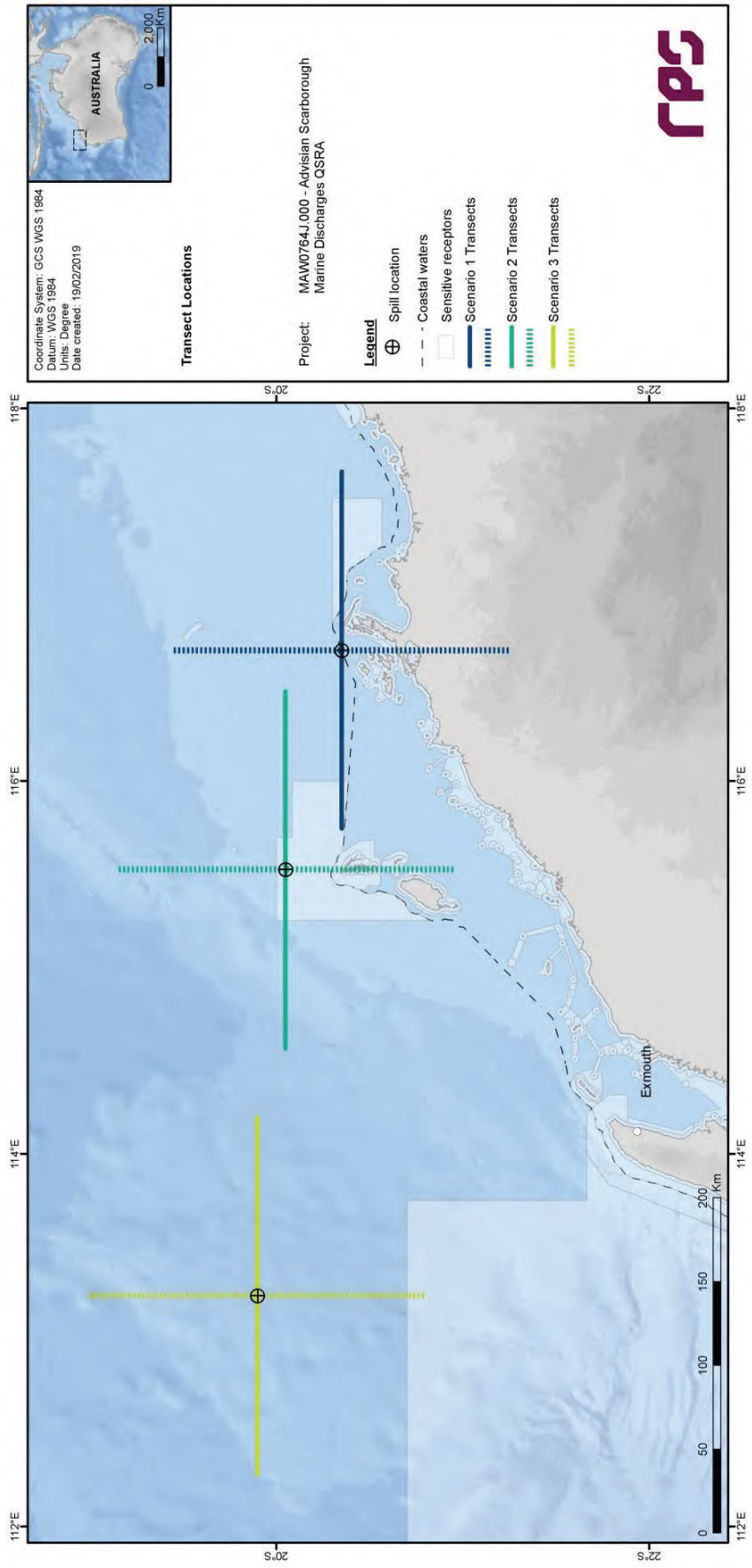
Figure 3.1 Locations of cross-sections, over a varying latitude (dashed line) and longitude (solid line), along which the distributions of maximum entrained oil and dissolved aromatic hydrocarbon concentrations were extracted for each spill scenario in this study.

3.2 Scenario 1: Short-Term (Instantaneous) Surface Release of Marine Diesel after a Vessel Collision outside Mermaid Sound

3.2.1 Discussion of Results

3.2.1.1 Overview

This scenario investigated the probability of exposure to surrounding regions by oil resulting from a short-term (instantaneous) surface release of 2,000 m^3 of marine diesel outside Mermaid Sound during operations at any time of year, with no mitigation measures applied.

Considering the discharge characteristics, the properties of the oil and its expected weathering behaviour, floating oil will be susceptible to entrainment into the wave-mixed layer under typical wind conditions. Evaporation rates will be significant, given the moderate proportion of volatile compounds in the oil (41%). The low-volatility fraction of the oil (54%) will take longer durations of the order of days to evaporate, and the residual fraction of 5% is expected to persist in the environment until degradation processes occur. Considering the spill volume, there is a low potential for dissolution of soluble aromatic compounds.

3.2.1.2 Floating and Shoreline Oil

The probability contour figures for floating oil indicate that concentrations equal to or greater than the 10 g/m^2, 50 g/m^2 and 100 g/m^2 thresholds could potentially be found, in the form of slicks, up to 29 km, 21 km and 18 km from the spill site, respectively (Figure 3.2, Figure 3.3 and Figure 3.4).

The Dampier Archipelago shoreline receptor is predicted to be contacted by floating oil concentrations at the 10 g/m^2 threshold with a probability of 2% and a minimum time to contact of 27 hours (Table 3.1). Probabilities of floating oil contact at the 50 g/m^2 and 100 g/m^2 thresholds are forecast to be equal to or less than 1% for other shoreline receptors.

Potential for accumulation of oil on shorelines is predicted to be low, with a maximum accumulated volume of 3 m^3 and a maximum local accumulated concentration on shorelines of 156 g/m^2 forecast at the Dampier Archipelago (Table 3.1).

The forecast annualised minimum times to contact, ZoC and smoothed ZoC for floating oil at or above the 10 g/m^2, 50 g/m^2 and 100 g/m^2 threshold concentrations are depicted in Figure 3.5 to Figure 3.7, Figure 3.8 to Figure 3.10 and Figure 3.11 to Figure 3.13, respectively.

3.2.1.3 Entrained Oil

Entrained oil at concentrations equal to or greater than the 500 ppb threshold is predicted to be found up to around 163 km from the spill site (Figure 3.15).

The Dampier MP and Dampier Archipelago receptors are predicted to receive entrained oil concentrations at the 500 ppb threshold with probabilities of 44% and 23%, respectively (Table 3.2). The maximum entrained oil concentration is forecast as 10.9 ppm within the Dampier Archipelago.

The forecast annualised minimum times to contact, ZoC and smoothed ZoC for entrained oil at or above the 500 ppb threshold concentration are depicted in Figure 3.16, Figure 3.17 and Figure 3.18, respectively.

The cross-sectional transects of maximum entrained oil concentrations in the vicinity of the release site show that concentrations above 25,000 ppb are expected to extend from the sea surface to depths of around 20 m (Figure 3.19).

3.2.1.4 Dissolved Aromatic Hydrocarbons

Dissolved aromatic hydrocarbons at concentrations equal to or greater than the 500 ppb threshold are predicted to be found up to around 34 km from the spill site (Figure 3.20).

The Dampier MP receptor is predicted to receive dissolved aromatic hydrocarbon concentrations at the 500 ppb threshold with a probability of 2% (Table 3.3). The maximum dissolved aromatic hydrocarbon concentration is forecast as 635 ppb within the Dampier MP.

The forecast annualised minimum times to contact, ZoC and smoothed ZoC for dissolved aromatic hydrocarbons at or above the 500 ppb threshold concentration are depicted in Figure 3.21, Figure 3.22 and Figure 3.23, respectively.

The cross-sectional transects of maximum dissolved aromatic hydrocarbon concentrations in the vicinity of the release site show that concentrations above 1,000 ppb are expected to extend from the sea surface to depths of around 20 m (Figure 3.24).

3.2.2 Results Tables and Figures

3.2.2.1 Floating and Shoreline Oil

Table 3.1 Expected annualised floating and shoreline oil outcomes at sensitive receptors resulting from an instantaneous surface release of marine diesel after a vessel collision outside Mermaid Sound.

Receptor	Probability (%) of floating oil concentration ≥10 g/m²	Probability (%) of floating oil concentration ≥50 g/m²	Probability (%) of floating oil concentration ≥100 g/m²	Minimum time to receptor (hours) for floating oil at ≥10 g/m²	Minimum time to receptor (hours) for floating oil at ≥50 g/m²	Minimum time to receptor (hours) for floating oil at ≥100 g/m²	Probability (%) of shoreline oil concentration ≥100 g/m²	Probability (%) of shoreline oil concentration ≥250 g/m²	Minimum time to receptor (hours) for shoreline oil at ≥100 g/m²	Minimum time to receptor (hours) for shoreline oil at ≥250 g/m²	Maximum local accumulated concentration (g/m²) averaged over all replicate simulations	Maximum local accumulated concentration (g/m²) in the worst replicate simulation	Maximum accumulated volume (m³) along this shoreline, averaged over all replicate simulations	Maximum accumulated volume (m³) along this shoreline, in the worst replicate simulation
Barrow Island	<1	<1	<1	NC	NC	NC	<1	<1	NC	NC	<0.1	4.6	<1	<1
Dampier Archipelago	2	1	<1	27	42	NC	1	<1	53	NC	2.8	156	<1	3
Glomar Shoals*	<1	<1	<1	NC	NC	NC	NA	NA	NA	NA	NA	NA	NA	NA
Montebello Islands	<1	<1	<1	NC	NC	NC	<1	<1	NC	NC	<0.1	4.2	<1	<1
Muiron Islands MMA-WHA	<1	<1	<1	NC	NC	NC	<1	<1	NC	NC	<0.1	3.4	<1	<1
Ningaloo Coast North WHA	<1	<1	<1	NC	NC	NC	<1	<1	NC	NC	<0.1	1.5	<1	<1
Ningaloo RUZ*	<1	<1	<1	NC	NC	NC	NA	NA	NA	NA	NA	NA	NA	NA
Pilbara - Middle Pilbara - Islands & Shoreline	<1	<1	<1	NC	NC	NC	<1	<1	NC	NC	<0.1	4.3	<1	<1
Pilbara - Northern Pilbara - Islands & Shoreline	<1	<1	<1	NC	NC	NC	<1	<1	NC	NC	NC	NC	<1	<1
Pilbara Islands - Southern Island Group	<1	<1	<1	NC	NC	NC	<1	<1	NC	NC	0.3	7	<1	<1
Rankin Bank*	<1	<1	<1	NC	NC	NC	NA	NA	NA	NA	NA	NA	NA	NA
Lowendal Islands	<1	<1	<1	NC	NC	NC	<1	<1	NC	NC	<0.1	2	<1	<1
Montebello MP*	<1	<1	<1	NC	NC	NC	NA	NA	NA	NA	NA	NA	NA	NA
Montebello State Marine Park	<1	<1	<1	NC	NC	NC	<1	<1	NC	NC	<0.1	4.2	<1	<1
Muiron Islands	<1	<1	<1	NC	NC	NC	<1	<1	NC	NC	<0.1	3.4	<1	<1
Dampier MP*	2	<1	<1	37	NC	NC	NA	NA	NA	NA	NA	NA	NA	NA
Eighty Mile Beach MP*	<1	<1	<1	NC	NC	NC	NA	NA	NA	NA	NA	NA	NA	NA
Gascoyne MP*	<1	<1	<1	NC	NC	NC	NA	NA	NA	NA	NA	NA	NA	NA
WA Coastline	3	1	<1	26	43	NC	1	<1	53	NC	2.8	156	<1	3

NC: No contact to receptor predicted for specified threshold. NA: Not applicable.

* Floating oil will not accumulate on submerged features and at open ocean locations.
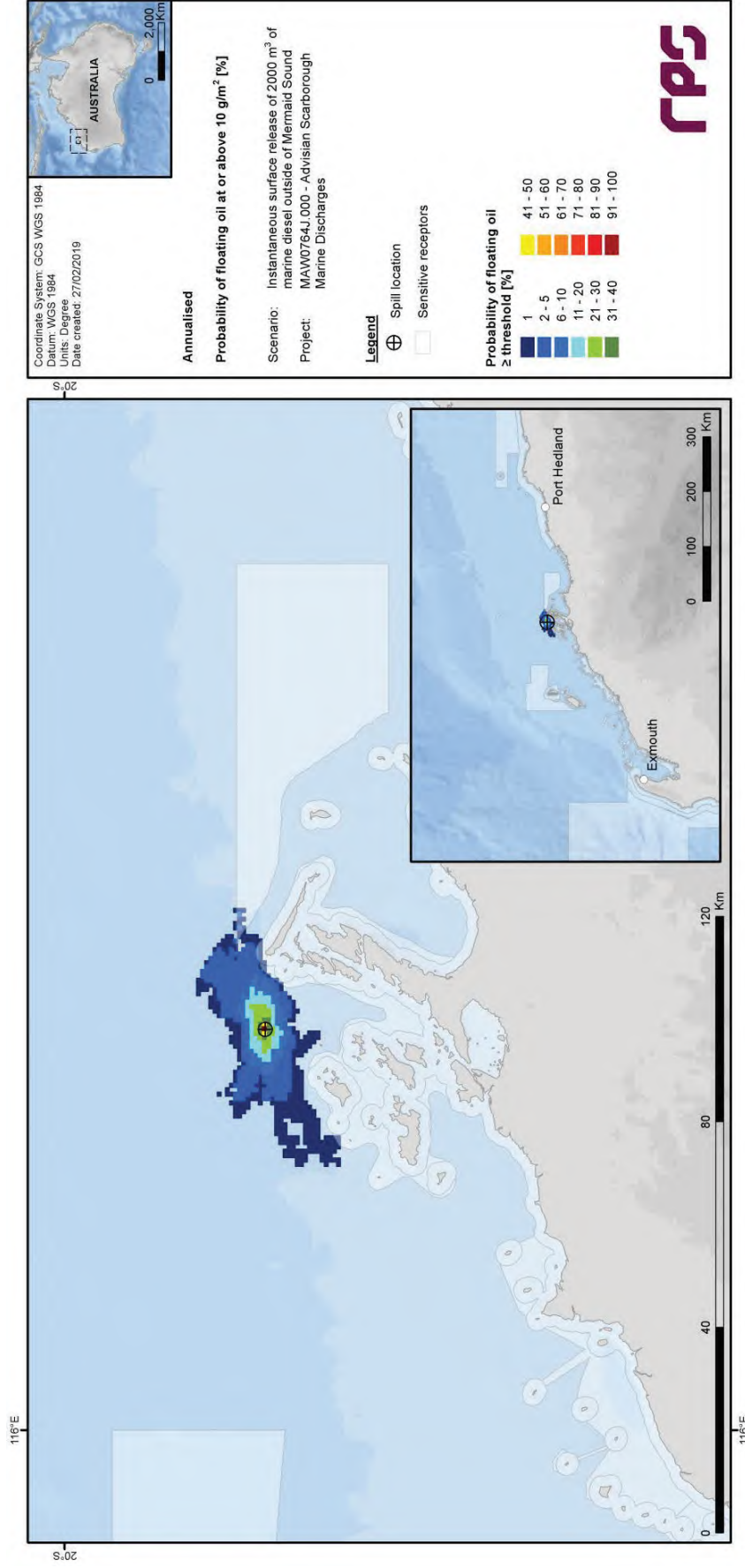
Figure 3.2 Predicted annualised probability of floating oil concentrations at or above 10 g/m² resulting from an instantaneous surface release of marine diesel after a vessel collision outside Mermaid Sound.

Figure 3.3 **Predicted annualised probability of floating oil concentrations at or above 50 g/m² resulting from an instantaneous surface release of marine diesel after a vessel collision outside Mermaid Sound.**

Figure 3.4   Predicted annualised probability of floating oil concentrations at or above 100 g/m² resulting from an instantaneous surface release of marine diesel after a vessel collision outside Mermaid Sound.

Figure 3.5 **Predicted annualised minimum times to contact by floating oil concentrations at or above 10 g/m² resulting from an instantaneous surface release of marine diesel after a vessel collision outside Mermaid Sound.**

Figure 3.6 **Predicted annualised minimum times to contact by floating oil concentrations at or above 50 g/m² resulting from an instantaneous surface release of marine diesel after a vessel collision outside Mermaid Sound.**
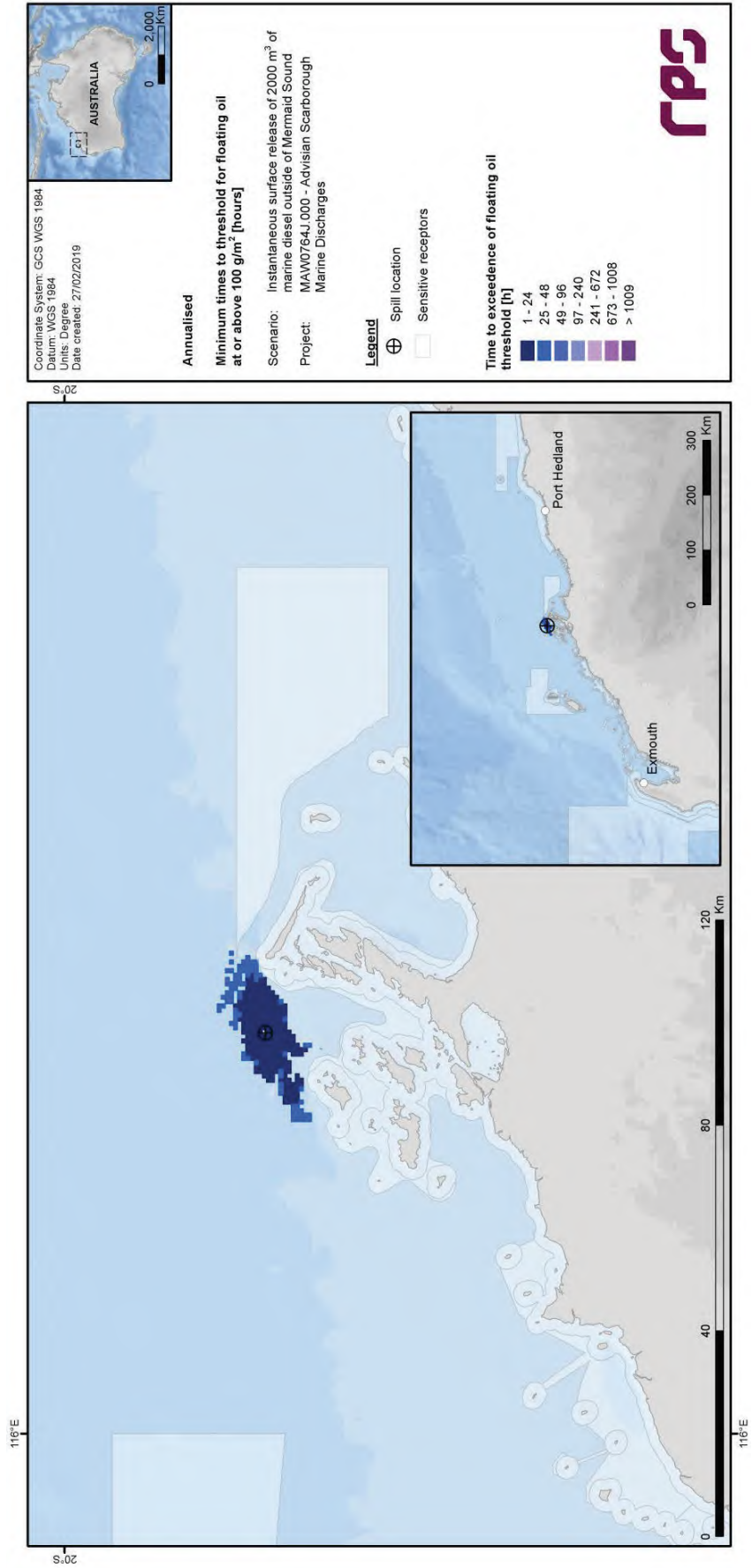
Figure 3.7   Predicted annualised minimum times to contact by floating oil concentrations at or above 100 g/m² resulting from an instantaneous surface release of marine diesel after a vessel collision outside Mermaid Sound.
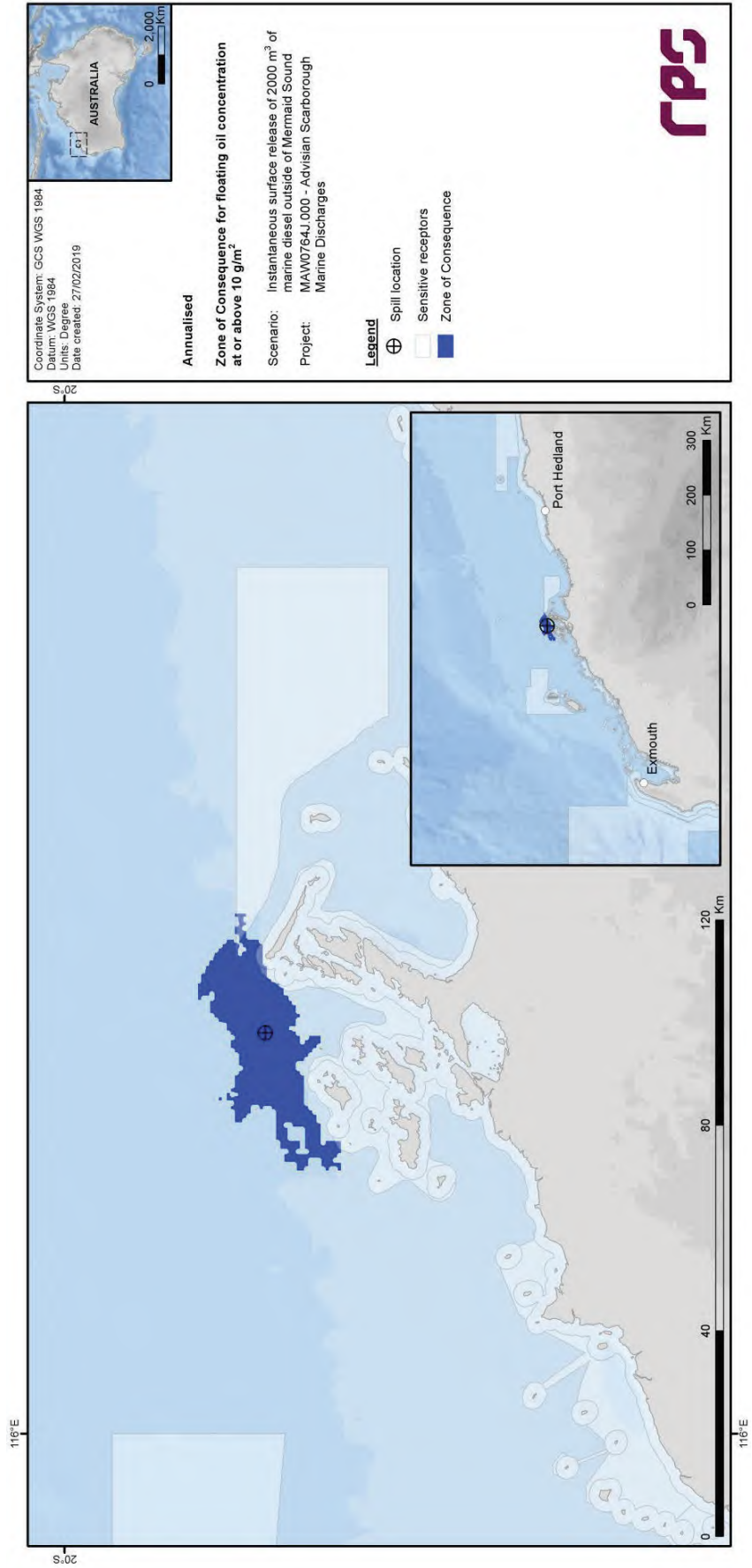
Figure 3.8   Predicted annualised Zone of Consequence of floating oil concentrations at or above 10 g/m² resulting from an instantaneous surface release of marine diesel after a vessel collision outside Mermaid Sound.
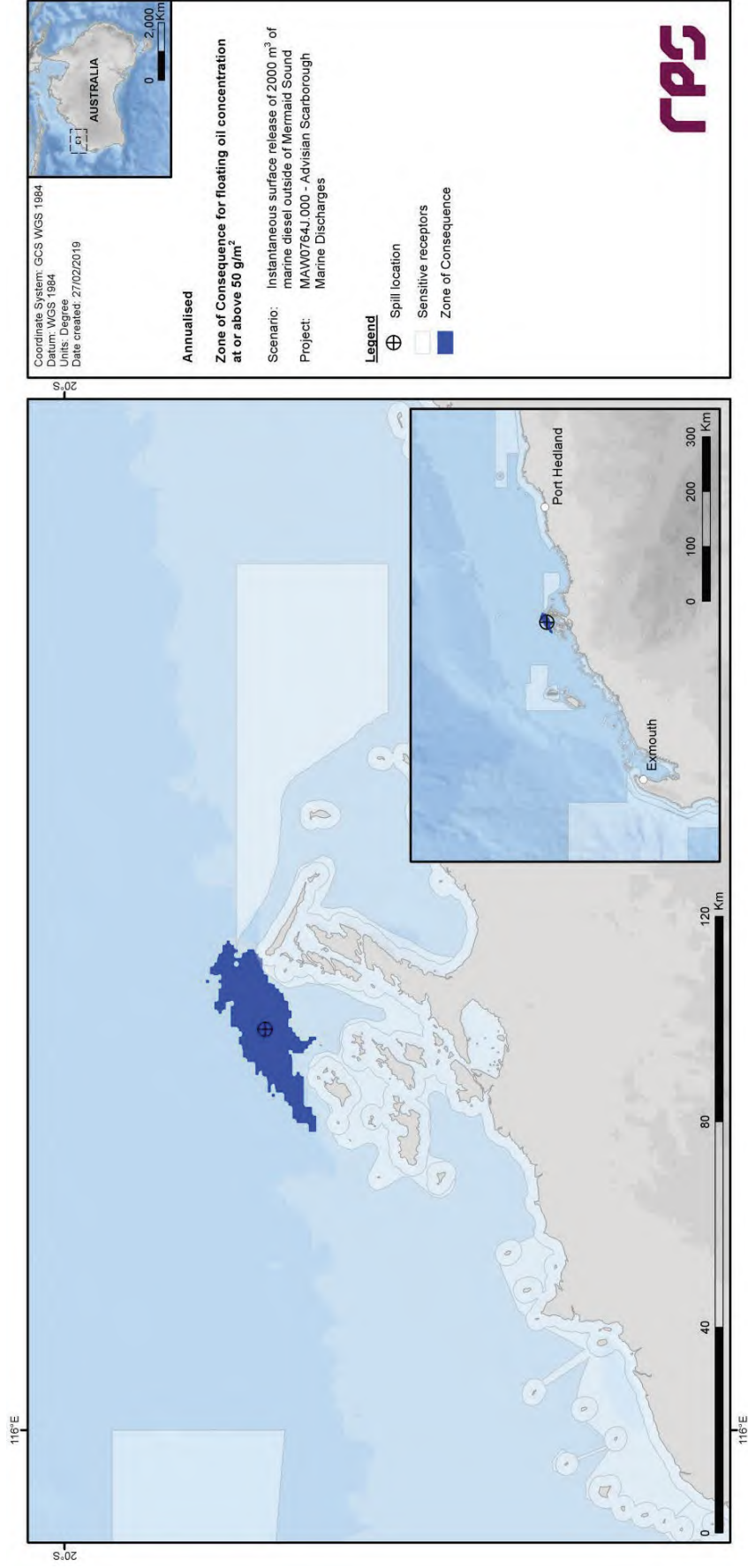
Figure 3.9 Predicted annualised Zone of Consequence of floating oil concentrations at or above 50 g/m² resulting from an instantaneous surface release of marine diesel after a vessel collision outside Mermaid Sound.
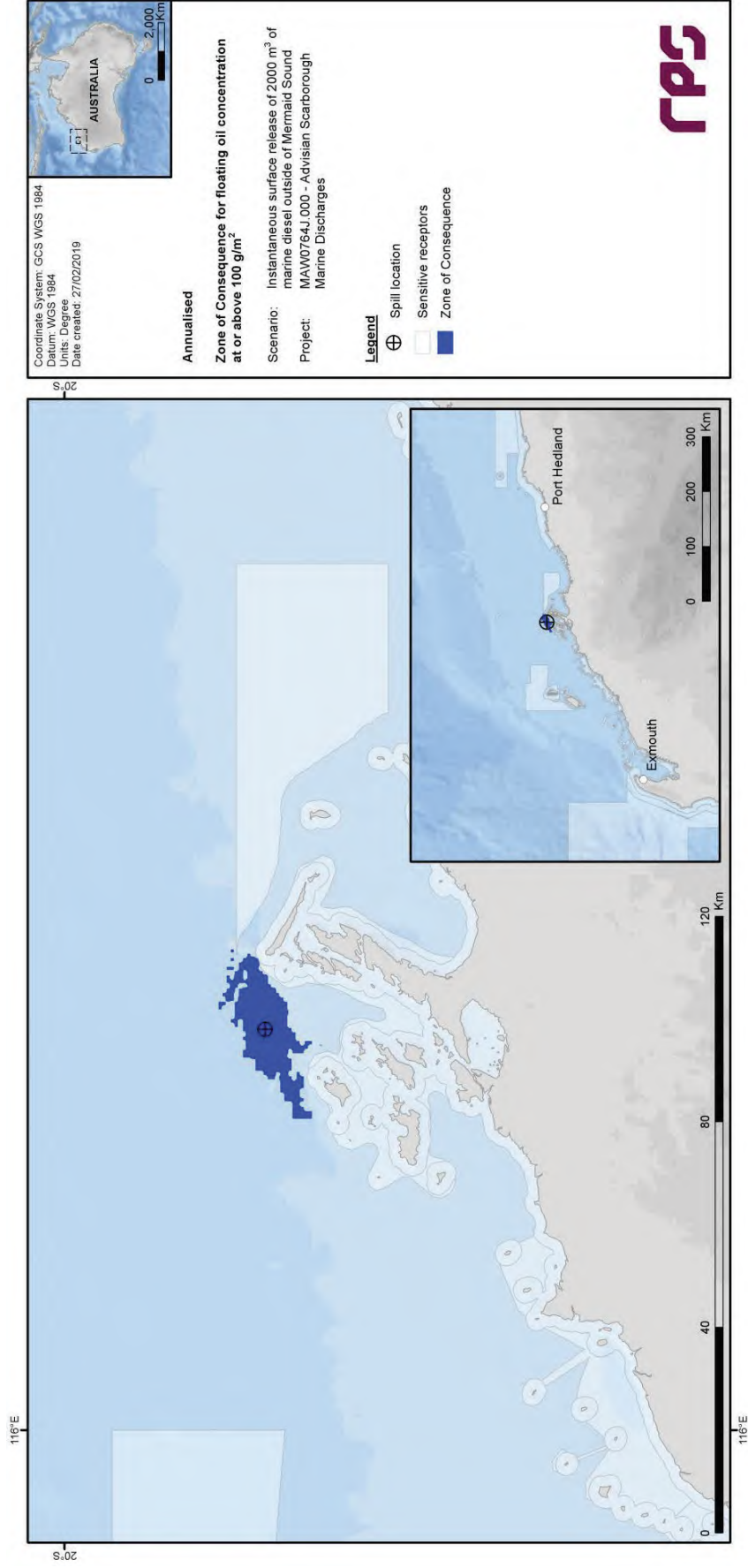
Figure 3.10 Predicted annualised Zone of Consequence of floating oil concentrations at or above 100 g/m² resulting from an instantaneous surface release of marine diesel after a vessel collision outside Mermaid Sound.
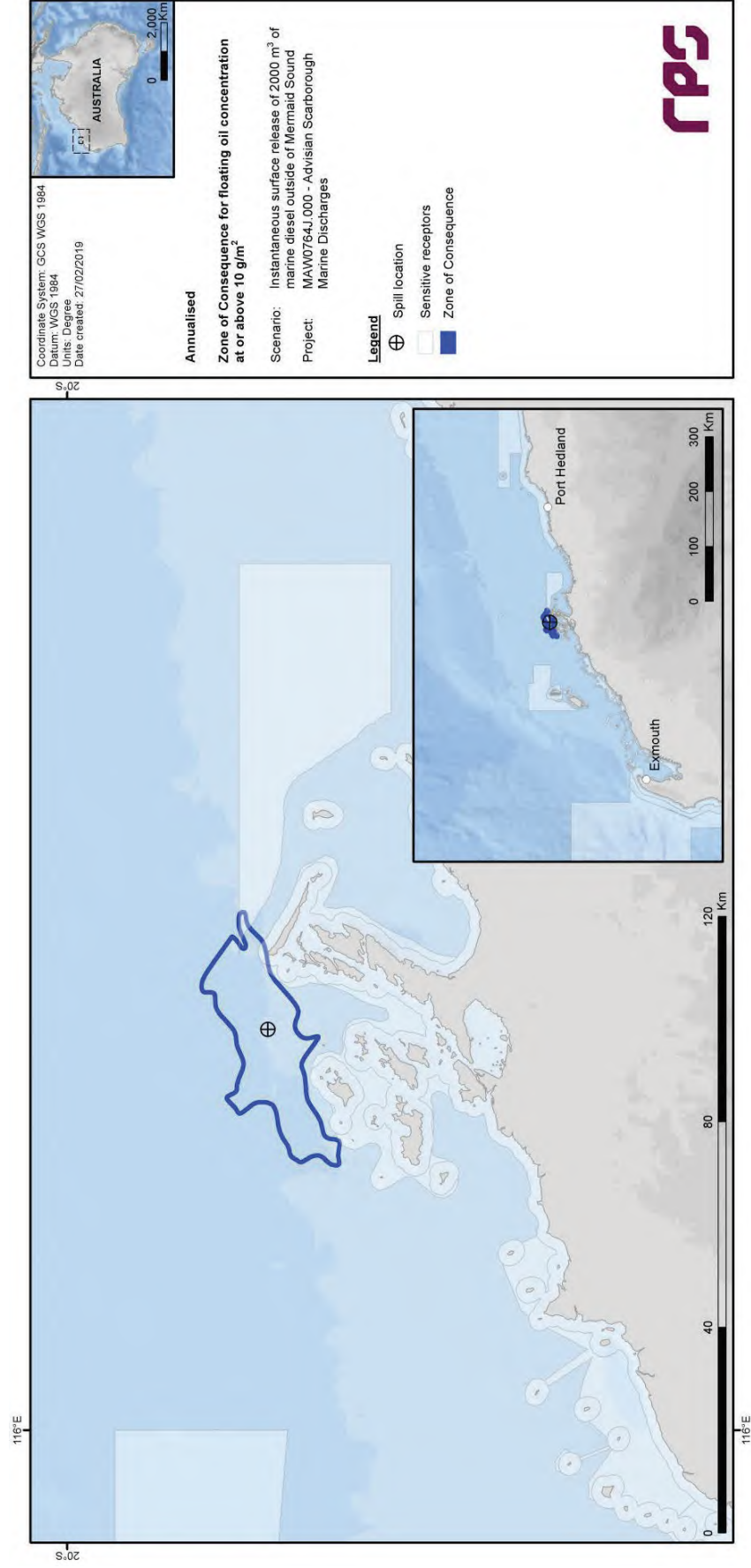
Figure 3.11 Predicted annualised smoothed Zone of Consequence of floating oil concentrations at or above 10 g/m² resulting from an instantaneous surface release of marine diesel after a vessel collision outside Mermaid Sound.
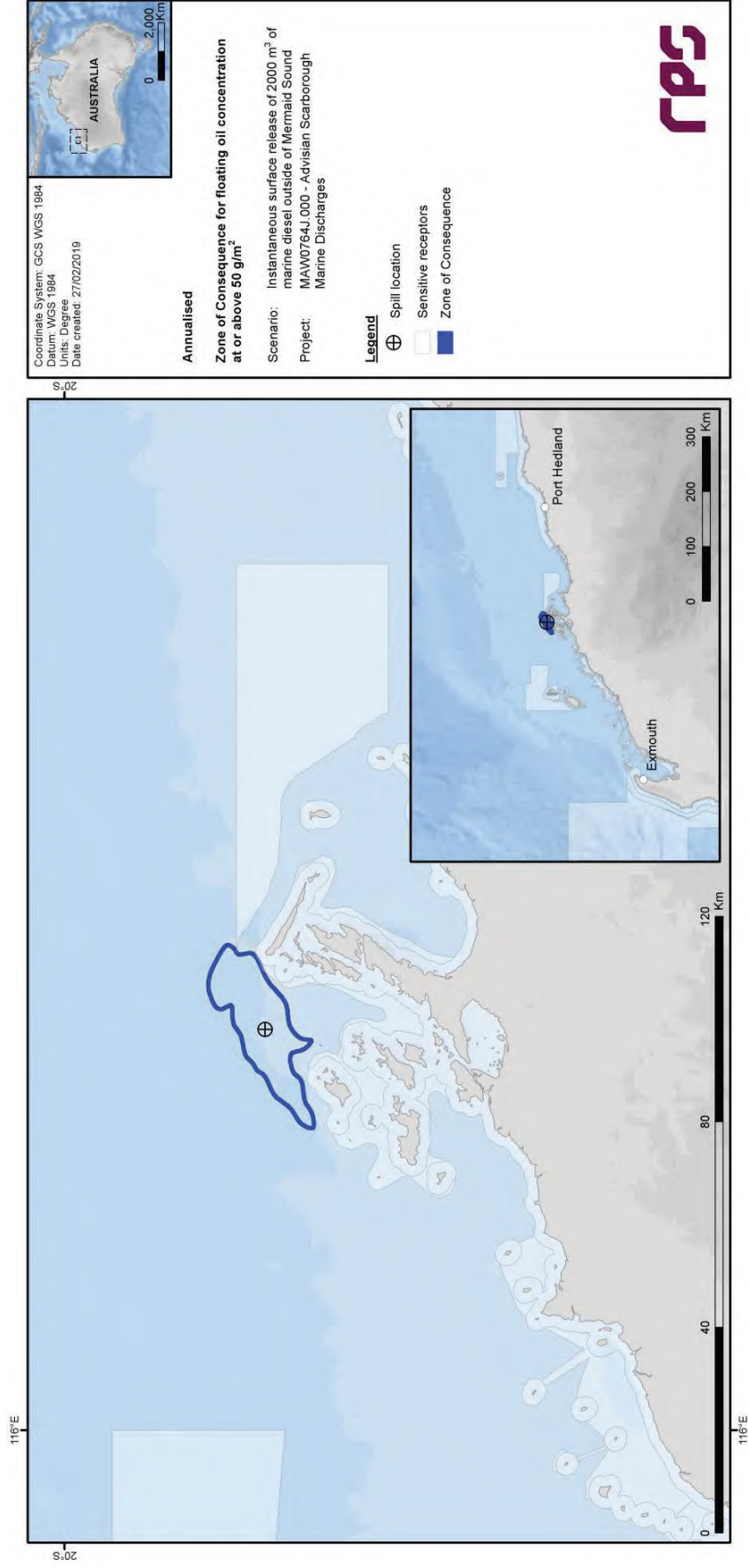
Figure 3.12 Predicted annualised smoothed Zone of Consequence of floating oil concentrations at or above 50 g/m² resulting from an instantaneous surface release of marine diesel after a vessel collision outside Mermaid Sound.

Figure 3.13 Predicted annualised smoothed Zone of Consequence of floating oil concentrations at or above 100 g/m² resulting from an instantaneous surface release of marine diesel after a vessel collision outside Mermaid Sound.

Figure 3.14 Predicted annualised probability of shoreline oil concentrations at or above 100 g/m² resulting from an instantaneous surface release of marine diesel after a vessel collision outside Mermaid Sound.

3.2.2.2 Entrained Oil

Table 3.2 Expected annualised entrained oil outcomes at sensitive receptors resulting from an instantaneous surface release of marine diesel after a vessel collision outside Mermaid Sound.

Receptor	Probability (%) of entrained oil concentration ≥500 ppb	Minimum time to receptor (hours) for entrained oil at ≥500 ppb	Maximum entrained oil concentration (ppb) averaged over all replicate simulations	Maximum entrained oil concentration (ppb), at any depth, in the worst replicate simulation
Barrow Island	<1	NC	6	72
Dampier Archipelago	23	15	583	10,911
Glomar Shoals*	<1	NC	3	3
Montebello Islands	<1	NC	15	235
Muiron Islands MMA-WHA	<1	NC	9	185
Ningaloo Coast North WHA	<1	NC	4	70
Ningaloo RUZ	<1	NC	4	70
Pilbara - Middle Pilbara - Islands & Shoreline	<1	NC	14	150
Pilbara - Northern Pilbara - Islands & Shoreline	<1	NC	3	79
Pilbara Islands - Southern Island Group	<1	NC	15	192
Rankin Bank*	<1	NC	<1	13
Lowendal Islands	<1	NC	4	66
Montebello MP	1	433	30	822
Montebello State Marine Park	<1	NC	16	263
Muiron Islands	<1	NC	9	172
Dampier MP	44	20	1,215	10,407
Eighty Mile Beach MP	<1	NC	6	161
Gascoyne MP	<1	NC	4	222
WA Coastline	23	15	583	6,832

NC: No contact to receptor predicted for specified threshold.

* Probabilities and maximum concentrations calculated at depth of submerged feature.

Figure 3.15 Predicted annualised probability of entrained oil concentrations at or above 500 ppb resulting from an instantaneous surface release of marine diesel after a vessel collision outside Mermaid Sound.

Annualised

Minimum times to threshold for entrained oil at or above 500 ppb [hours]

Scenario: Instantaneous surface release of 2000 m³ of marine diesel outside of Mermaid Sound

Project: MAW0764J.000 - Advisian Scarborough Marine Discharges

Coordinate System: GCS WGS 1984
Datum: WGS 1984
Units: Degree
Date created: 27/02/2019

Legend

⊕ Spill location

☐ Sensitive receptors

Time to exceedence of entrained oil threshold [h]

1 - 24
25 - 48
49 - 96
97 - 240
241 - 672
673 - 1008
> 1009

Figure 3.16 Predicted annualised minimum times to contact by entrained oil concentrations at or above 500 ppb resulting from an instantaneous surface release of marine diesel after a vessel collision outside Mermaid Sound.

Figure 3.17 Predicted annualised Zone of Consequence of entrained oil concentrations at or above 500 ppb resulting from an instantaneous surface release of marine diesel after a vessel collision outside Mermaid Sound.

Figure 3.18   Predicted annualised smoothed Zone of Consequence of entrained oil concentrations at or above 500 ppb resulting from an instantaneous surface release of marine diesel after a vessel collision outside Mermaid Sound.

Figure 3.19 Cross-section transects of predicted annualised maximum entrained oil concentrations for an instantaneous surface release of marine diesel after a vessel collision outside Mermaid Sound. Transect locations are shown in Figure 3.1.

3.2.2.3 Dissolved Aromatic Hydrocarbons

Table 3.3   Expected annualised dissolved aromatic hydrocarbon outcomes at sensitive receptors resulting from an instantaneous surface release of marine diesel after a vessel collision outside Mermaid Sound.

Receptor	Probability (%) of dissolved aromatic hydrocarbon concentration ≥500 ppb	Maximum dissolved aromatic hydrocarbon concentration (ppb) averaged over all replicate simulations	Maximum dissolved aromatic hydrocarbon concentration (ppb), at any depth, in the worst replicate simulation
Barrow Island	<1	<1	<1
Dampier Archipelago	<1	27	366
Glomar Shoals*	<1	NC	NC
Montebello Islands	<1	<1	<1
Muiron Islands MMA-WHA	<1	NC	NC
Ningaloo Coast North WHA	<1	NC	NC
Ningaloo RUZ	<1	NC	NC
Pilbara - Middle Pilbara - Islands & Shoreline	<1	<1	<1
Pilbara - Northern Pilbara - Islands & Shoreline	<1	<1	<1
Pilbara Islands - Southern Island Group	<1	NC	NC
Rankin Bank*	<1	<1	NC
Lowendal Islands	<1	<1	<1
Montebello MP	<1	<1	7
Montebello State Marine Park	<1	<1	<1
Muiron Islands	<1	NC	NC
Dampier MP	2	41	635
Eighty Mile Beach MP	<1	NC	NC
Gascoyne MP	<1	NC	NC
WA Coastline	<1	27	366

NC: No contact to receptor predicted for specified threshold.

* Probabilities and maximum concentrations calculated at depth of submerged feature.
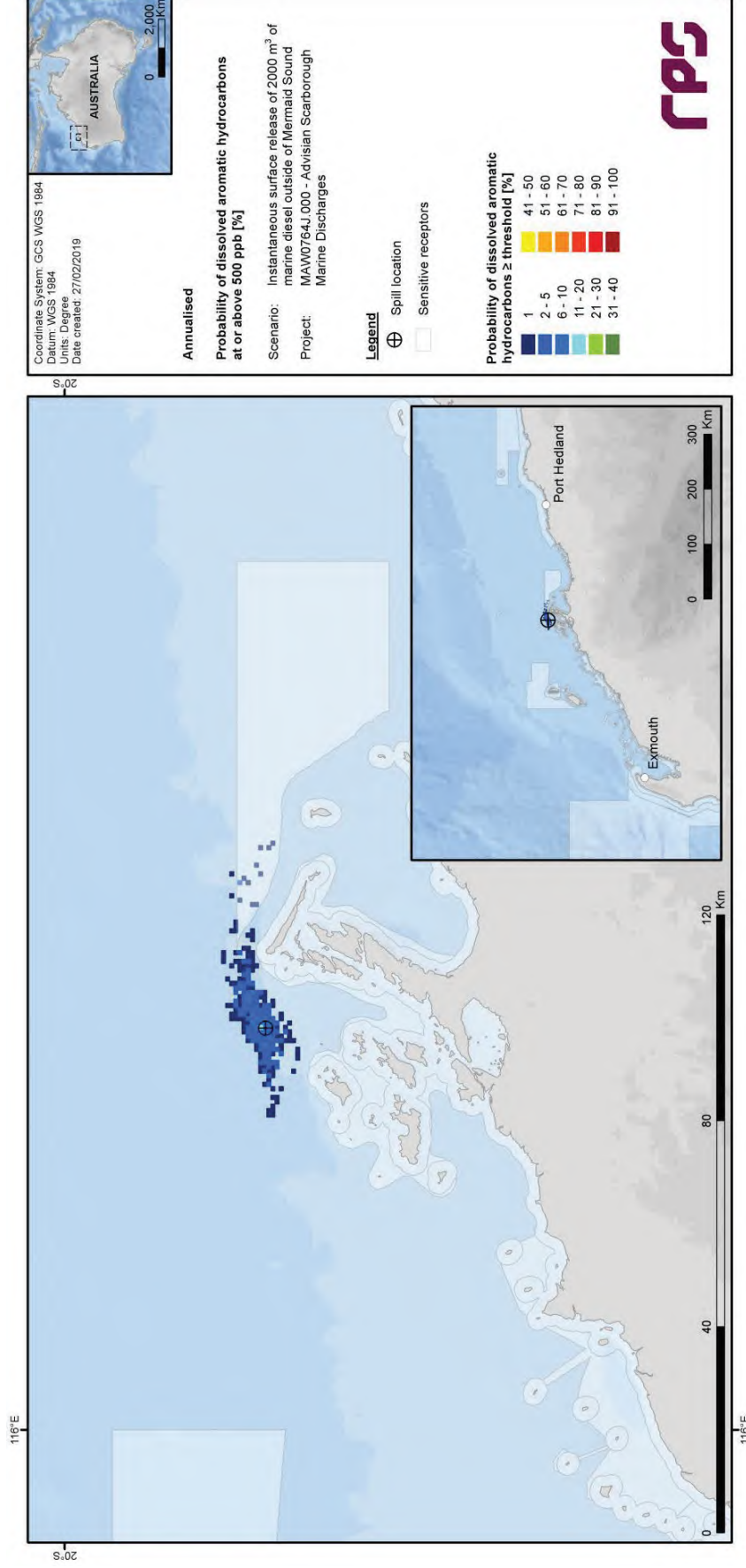
Figure 3.20 **Predicted annualised probability of dissolved aromatic hydrocarbon concentrations at or above 500 ppb resulting from an instantaneous surface release of marine diesel after a vessel collision outside Mermaid Sound.**
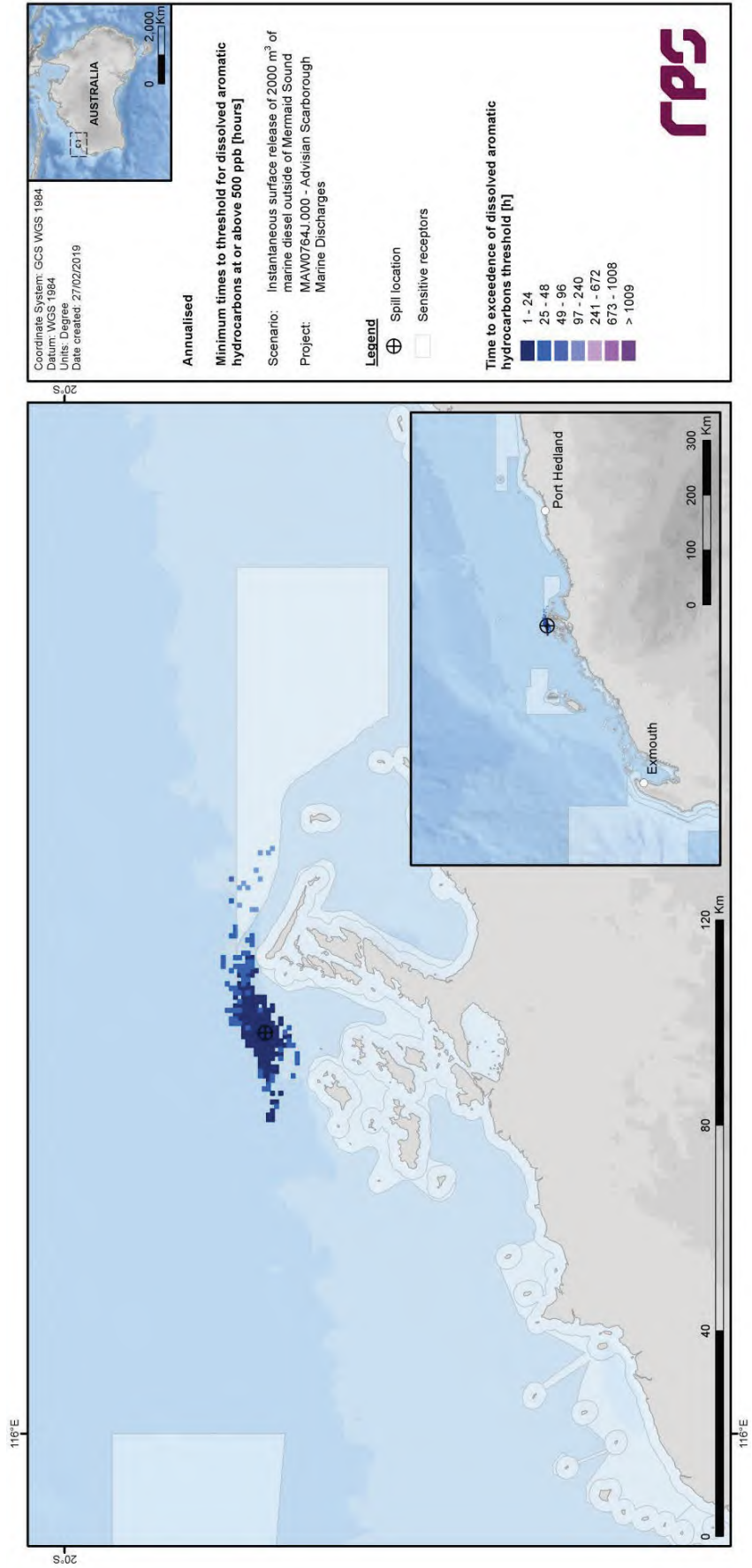
Figure 3.21 Predicted annualised minimum times to contact by dissolved aromatic hydrocarbon concentrations at or above 500 ppb resulting from an instantaneous surface release of marine diesel after a vessel collision outside Mermaid Sound.
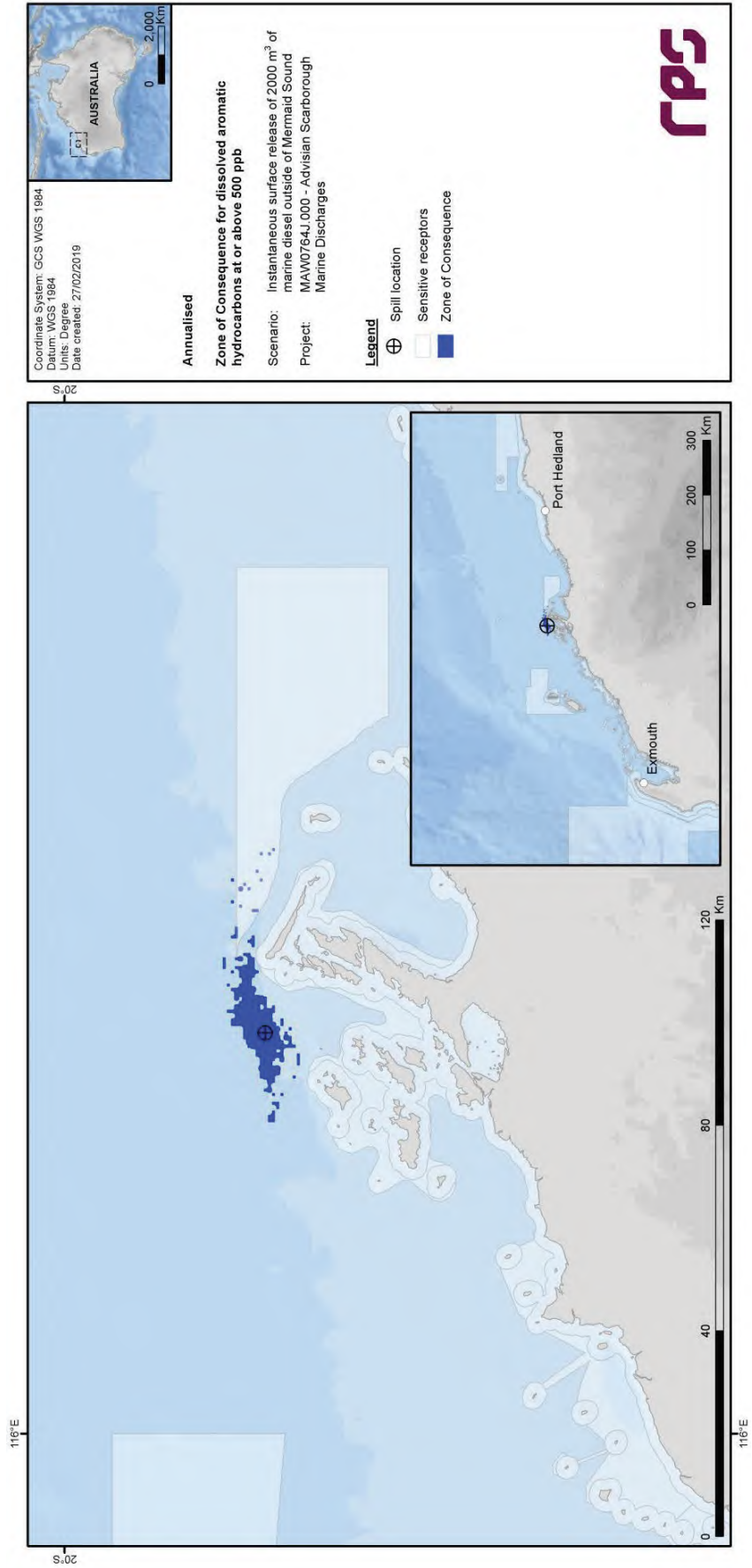
Figure 3.22 Predicted annualised Zone of Consequence of dissolved aromatic hydrocarbon concentrations at or above 500 ppb resulting from an instantaneous surface release of marine diesel after a vessel collision outside Mermaid Sound.
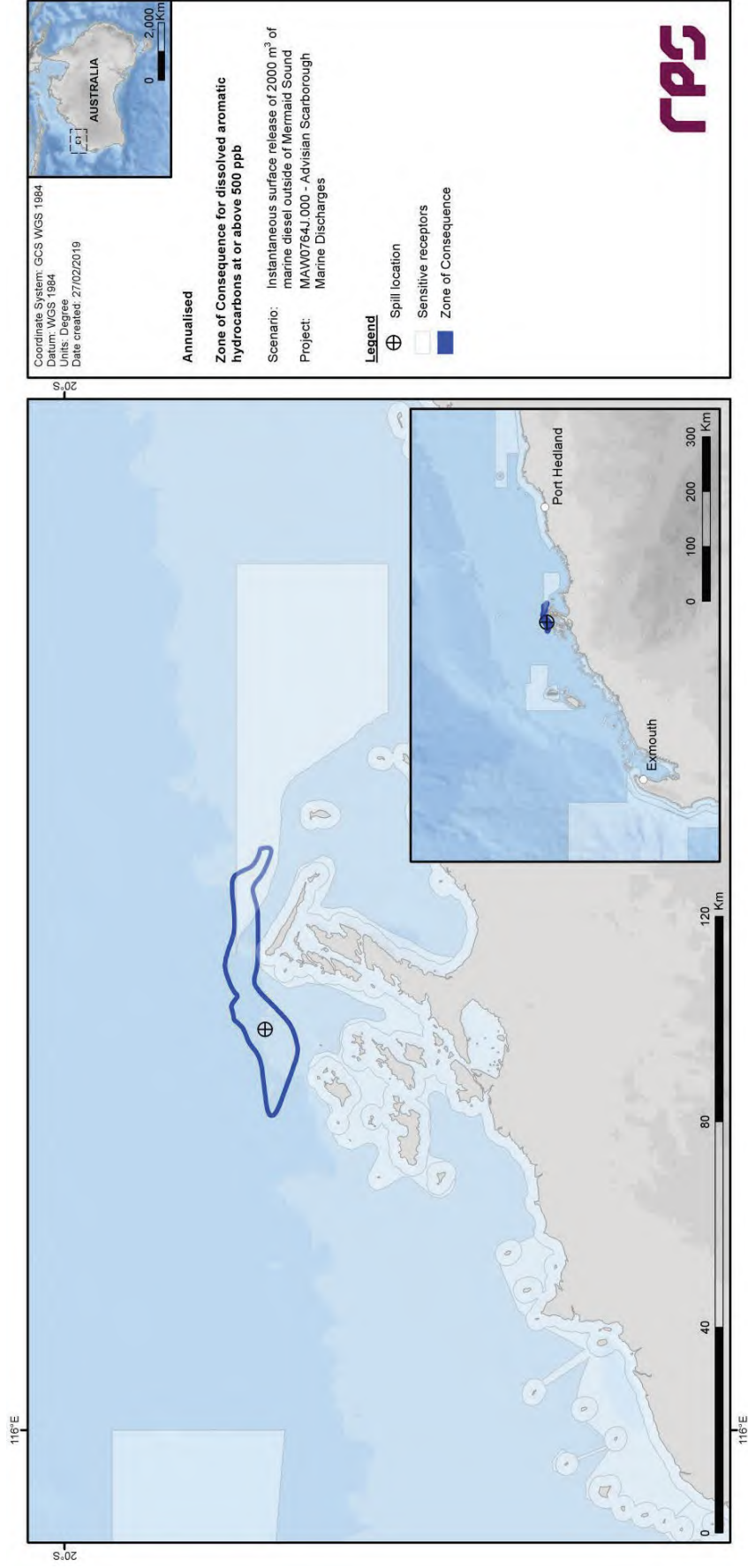
Figure 3.23 Predicted annualised smoothed Zone of Consequence of dissolved aromatic hydrocarbon concentrations at or above 500 ppb resulting from an instantaneous surface release of marine diesel after a vessel collision outside Mermaid Sound.

Figure 3.24 Cross-section transects of predicted annualised maximum dissolved aromatic hydrocarbon concentrations for an instantaneous surface release of marine diesel after a vessel collision outside Mermaid Sound. Transect locations are shown in Figure 3.1.

3.3 Scenario 2: Short-Term (Instantaneous) Surface Release of Marine Diesel after a Vessel Collision within Montebello Marine Park

3.3.1 Discussion of Results

3.3.1.1 Overview

This scenario investigated the probability of exposure to surrounding regions by oil resulting from a short-term (instantaneous) surface release of 2,000 m³ of marine diesel within the Montebello Marine Park during operations at any time of year, with no mitigation measures applied.

Considering the discharge characteristics, the properties of the oil and its expected weathering behaviour, floating oil will be susceptible to entrainment into the wave-mixed layer under typical wind conditions. Evaporation rates will be significant, given the moderate proportion of volatile compounds in the oil (41%). The low-volatility fraction of the oil (54%) will take longer durations of the order of days to evaporate, and the residual fraction of 5% is expected to persist in the environment until degradation processes occur. Considering the spill volume, there is a low potential for dissolution of soluble aromatic compounds.

3.3.1.2 Floating and Shoreline Oil

The probability contour figures for floating oil indicate that concentrations equal to or greater than the 10 g/m², 50 g/m² and 100 g/m² thresholds could potentially be found, in the form of slicks, up to 39 km, 36 km and 33 km from the spill site, respectively (Figure 3.25, Figure 3.26 and Figure 3.27).

Given that the spill location lies within the Montebello MP receptor area, floating oil at concentrations equal to or greater than 100 g/m² are forecast with a probability of 100% and a minimum time to contact of less than 1 hour (Table 3.4). Probabilities of floating oil contact at the 10 g/m² threshold are forecast to be less than 1% for all other shoreline receptors.

Potential for accumulation of oil on shorelines is predicted to be low, with a maximum accumulated volume of <1 m³ and a maximum local accumulated concentration on shorelines of 11 g/m² forecast at Barrow Island (Table 3.4).

The forecast annualised minimum times to contact, ZoC and smoothed ZoC for floating oil at or above the 10 g/m², 50 g/m² and 100 g/m² threshold concentrations are depicted in Figure 3.28 to Figure 3.30, Figure 3.31 to Figure 3.33 and Figure 3.34 to Figure 3.36, respectively.

3.3.1.3 Entrained Oil

Entrained oil at concentrations equal to or greater than the 500 ppb threshold is predicted to be found up to around 308 km from the spill site (Figure 3.37).

The Montebello MP and Muiron Islands MMA-WHA receptors are predicted to receive entrained oil concentrations at the 500 ppb threshold with probabilities of 70% and 7%, respectively (Table 3.5). The maximum entrained oil concentration is forecast as 157.0 ppm within the Montebello MP.

The forecast annualised minimum times to contact, ZoC and smoothed ZoC for entrained oil at or above the 500 ppb threshold concentration are depicted in Figure 3.38, Figure 3.39 and Figure 3.40, respectively.

The cross-sectional transects of maximum entrained oil concentrations in the vicinity of the release site show that concentrations above 25,000 ppb are expected to extend from the sea surface to depths of around 15 m (Figure 3.41).

3.3.1.4 Dissolved Aromatic Hydrocarbons

Dissolved aromatic hydrocarbons at concentrations equal to or greater than the 500 ppb threshold are predicted to be found up to around 85 km from the spill site (Figure 3.42).

The Montebello MP receptor is predicted to receive dissolved aromatic hydrocarbon concentrations at the 500 ppb threshold with a probability of 9% (Table 3.6). The maximum dissolved aromatic hydrocarbon concentration is forecast as 2.0 ppm within the Montebello MP.

The forecast annualised minimum times to contact, ZoC and smoothed ZoC for dissolved aromatic hydrocarbons at or above the 500 ppb threshold concentration are depicted in Figure 3.43, Figure 3.44 and Figure 3.45, respectively.

The cross-sectional transects of maximum dissolved aromatic hydrocarbon concentrations in the vicinity of the release site show that concentrations above 1,000 ppb are expected to extend from the sea surface to depths of around 15 m (Figure 3.46).

3.3.2 Results Tables and Figures

3.3.2.1 Floating and Shoreline Oil

Table 3.4   Expected annualised floating and shoreline oil outcomes at sensitive receptors resulting from an instantaneous surface release of marine diesel after a vessel collision within Montebello Marine Park.

Receptor	Probability (%) of floating oil concentration ≥10 g/m²	Probability (%) of floating oil concentration ≥50 g/m²	Probability (%) of floating oil concentration ≥100 g/m²	Minimum time to receptor (hours) for floating oil at ≥10 g/m²	Minimum time to receptor (hours) for floating oil at ≥50 g/m²	Minimum time to receptor (hours) for floating oil at ≥100 g/m²	Probability (%) of shoreline oil concentration ≥100 g/m²	Probability (%) of shoreline oil concentration ≥250 g/m²	Minimum time to receptor (hours) for shoreline oil at ≥100 g/m²	Minimum time to receptor (hours) for shoreline oil at ≥250 g/m²	Maximum local accumulated concentration (g/m²) averaged over all replicate simulations	Maximum local accumulated concentration (g/m²) in the worst replicate simulation	Maximum accumulated volume (m³) along this shoreline, averaged over all replicate simulations	Maximum accumulated volume (m³) along this shoreline, in the worst replicate simulation
Argo-Rowley Terrace MP*	<1	<1	<1	NC	NC	NC	NA	NA	NA	NA	NA	NA	NA	NA
Barrow Island	<1	<1	<1	NC	NC	NC	<1	<1	NC	NC	0.1	11	<1	<1
Glomar Shoals*	<1	<1	<1	NC	NC	NC	NA	NA	NA	NA	NA	NA	NA	NA
Montebello Islands	<1	<1	<1	NC	NC	NC	<1	<1	NC	NC	<0.1	4.1	<1	<1
Muiron Islands MMA-WHA	<1	<1	<1	NC	NC	NC	<1	<1	NC	NC	<0.1	7.1	<1	<1
Ningaloo Coast Middle	<1	<1	<1	NC	NC	NC	<1	<1	NC	NC	NC	NC	NC	NC
Ningaloo Coast Middle WHA	<1	<1	<1	NC	NC	NC	<1	<1	NC	NC	NC	NC	NC	NC
Ningaloo Coast North	<1	<1	<1	NC	NC	NC	<1	<1	NC	NC	<0.1	7	<1	<1
Ningaloo Coast North WHA	<1	<1	<1	NC	NC	NC	<1	<1	NC	NC	<0.1	7	<1	<1
Ningaloo Coast South WHA	<1	<1	<1	NC	NC	NC	<1	<1	NC	NC	NC	NC	NC	NC
Ningaloo RUZ*	<1	<1	<1	NC	NC	NC	NA	NA	NA	NA	NA	NA	NA	NA
Pilbara Islands - Southern Island Group	<1	<1	<1	NC	NC	NC	<1	<1	NC	NC	<0.1	1.7	<1	<1
Rankin Bank*	<1	<1	<1	NC	NC	NC	NA	NA	NA	NA	NA	NA	NA	NA
Shark Bay Open Ocean Coast	<1	<1	<1	NC	NC	NC	<1	<1	NC	NC	NC	NC	NC	NC
Shark Bay WHA	<1	<1	<1	NC	NC	NC	<1	<1	NC	NC	NC	NC	NC	NC
Bernier & Dorre Islands	<1	<1	<1	NC	NC	NC	<1	<1	NC	NC	NC	NC	NC	NC
Lowendal Islands	<1	<1	<1	NC	NC	NC	<1	<1	NC	NC	NC	NC	NC	NC
Montebello MP*	100	100	100	1	1	1	NA	NA	NA	NA	NA	NA	NA	NA
Montebello State Marine Park	<1	<1	<1	NC	NC	NC	<1	<1	NC	NC	<0.1	4.1	<1	<1
Muiron Islands	<1	<1	<1	NC	NC	NC	<1	<1	NC	NC	<0.1	7.1	<1	<1
Gascoyne MP*	<1	<1	<1	NC	NC	NC	NA	NA	NA	NA	NA	NA	NA	NA
WA Coastline	<1	<1	<1	NC	NC	NC	<1	<1	NC	NC	0.1	11	<1	<1

NC: No contact to receptor predicted for specified threshold. NA: Not applicable.

* Floating oil will not accumulate on submerged features and at open ocean locations.

Figure 3.25   Predicted annualised probability of floating oil concentrations at or above 10 g/m² resulting from an instantaneous surface release of marine diesel after a vessel collision within Montebello Marine Park.

Figure 3.26   Predicted annualised probability of floating oil concentrations at or above 50 g/m² resulting from an instantaneous surface release of marine diesel after a vessel collision within Montebello Marine Park.

Figure 3.27 Predicted annualised probability of floating oil concentrations at or above 100 g/m² resulting from an instantaneous surface release of marine diesel after a vessel collision within Montebello Marine Park.

Figure 3.28 Predicted annualised minimum times to contact by floating oil concentrations at or above 10 g/m² resulting from an instantaneous surface release of marine diesel after a vessel collision within Montebello Marine Park.

Annualised

Minimum times to threshold for floating oil at or above 50 g/m² [hours]

Scenario: Instantaneous surface release of 2000 m³ of marine diesel within the Montebello MP

Project: MAW0764J.000 - Advisian Scarborough Marine Discharges

Legend

⊕ Spill location

☐ Sensitive receptors

Time to exceedence of floating oil threshold [h]

- 1 - 24
- 25 - 48
- 49 - 96
- 97 - 240
- 241 - 672
- 673 - 1008
- > 1009

Figure 3.29 Predicted annualised minimum times to contact by floating oil concentrations at or above 50 g/m² resulting from an instantaneous surface release of marine diesel after a vessel collision within Montebello Marine Park.

Figure 3.30 Predicted annualised minimum times to contact by floating oil concentrations at or above 100 g/m² resulting from an instantaneous surface release of marine diesel after a vessel collision within Montebello Marine Park.

Figure 3.31 Predicted annualised Zone of Consequence of floating oil concentrations at or above 10 g/m² resulting from an instantaneous surface release of marine diesel after a vessel collision within Montebello Marine Park.
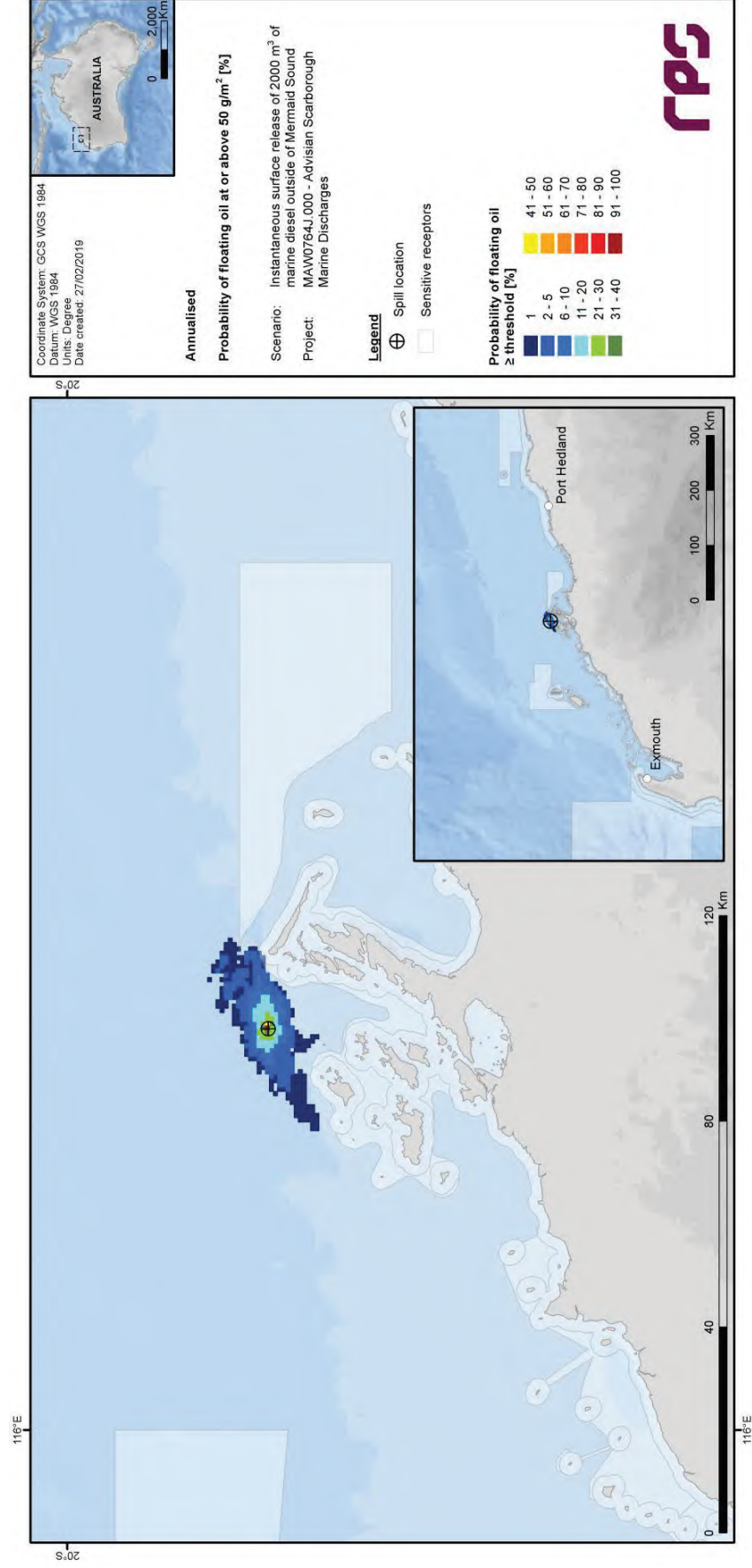
Figure 3.32   Predicted annualised Zone of Consequence of floating oil concentrations at or above 50 g/m² resulting from an instantaneous surface release of marine diesel after a vessel collision within Montebello Marine Park.
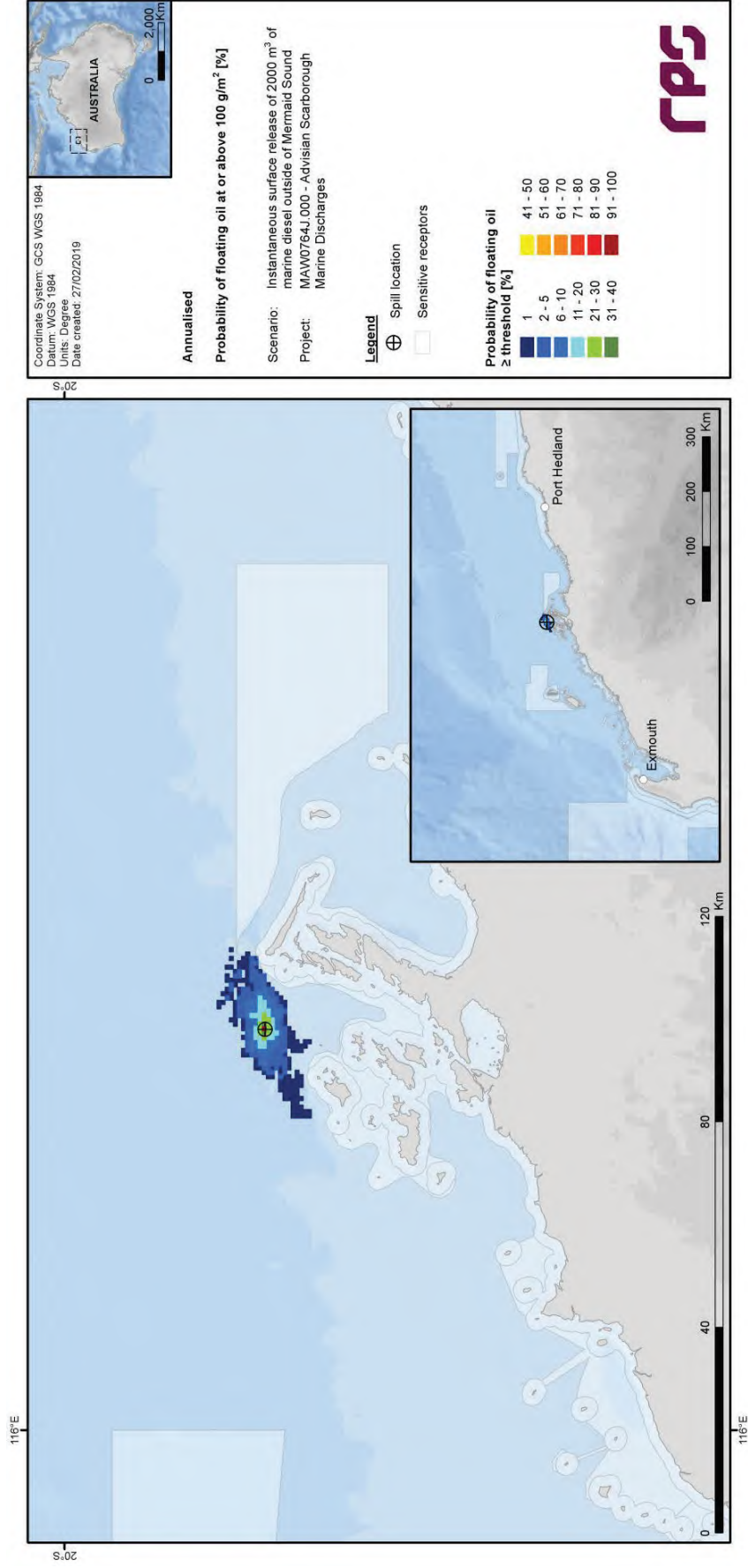
Figure 3.33 Predicted annualised Zone of Consequence of floating oil concentrations at or above 100 g/m² resulting from an instantaneous surface release of marine diesel after a vessel collision within Montebello Marine Park.

Figure 3.34 **Predicted annualised smoothed Zone of Consequence of floating oil concentrations at or above 10 g/m² resulting from an instantaneous surface release of marine diesel after a vessel collision within Montebello Marine Park.**
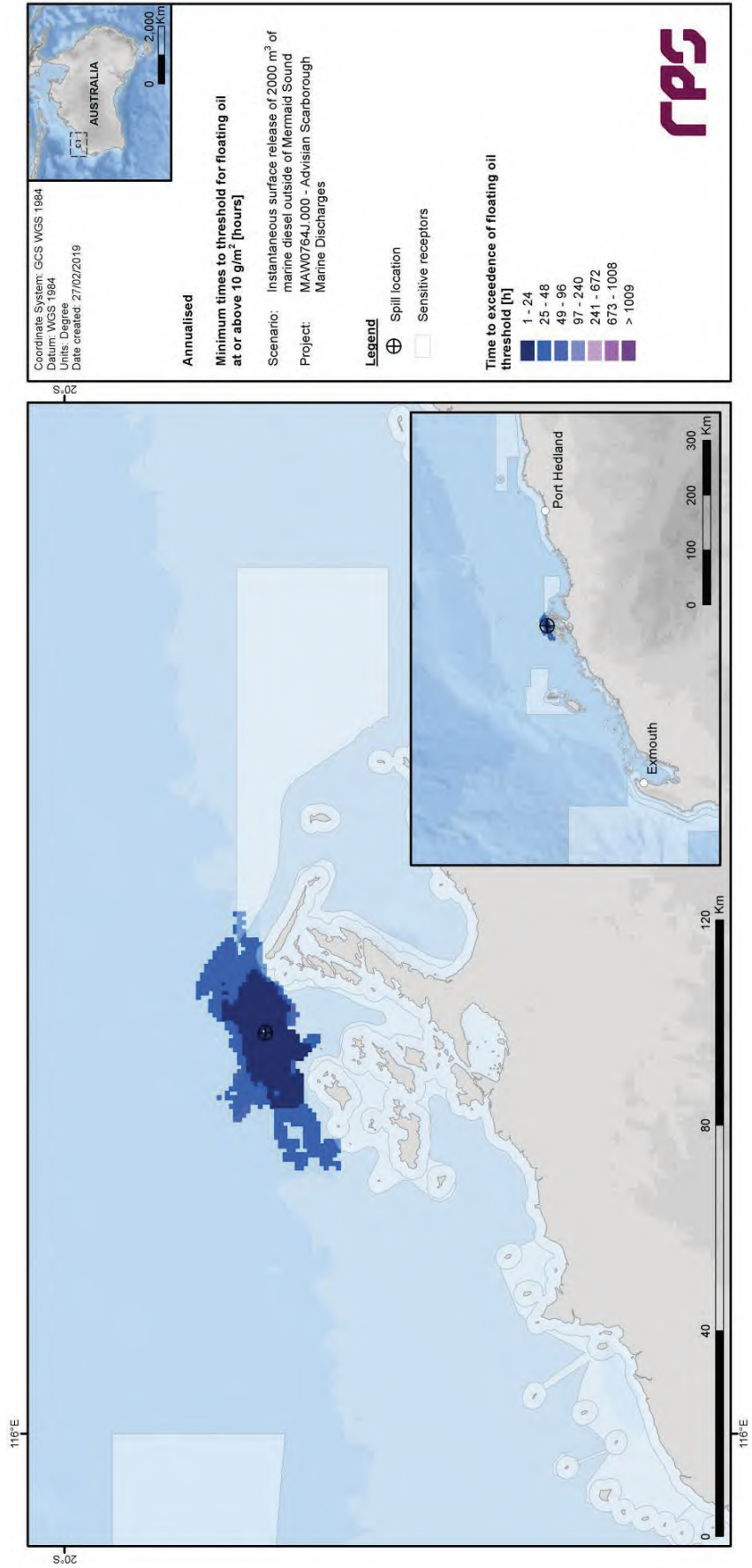
Figure 3.35 Predicted annualised smoothed Zone of Consequence of floating oil concentrations at or above 50 g/m² resulting from an instantaneous surface release of marine diesel after a vessel collision within Montebello Marine Park.
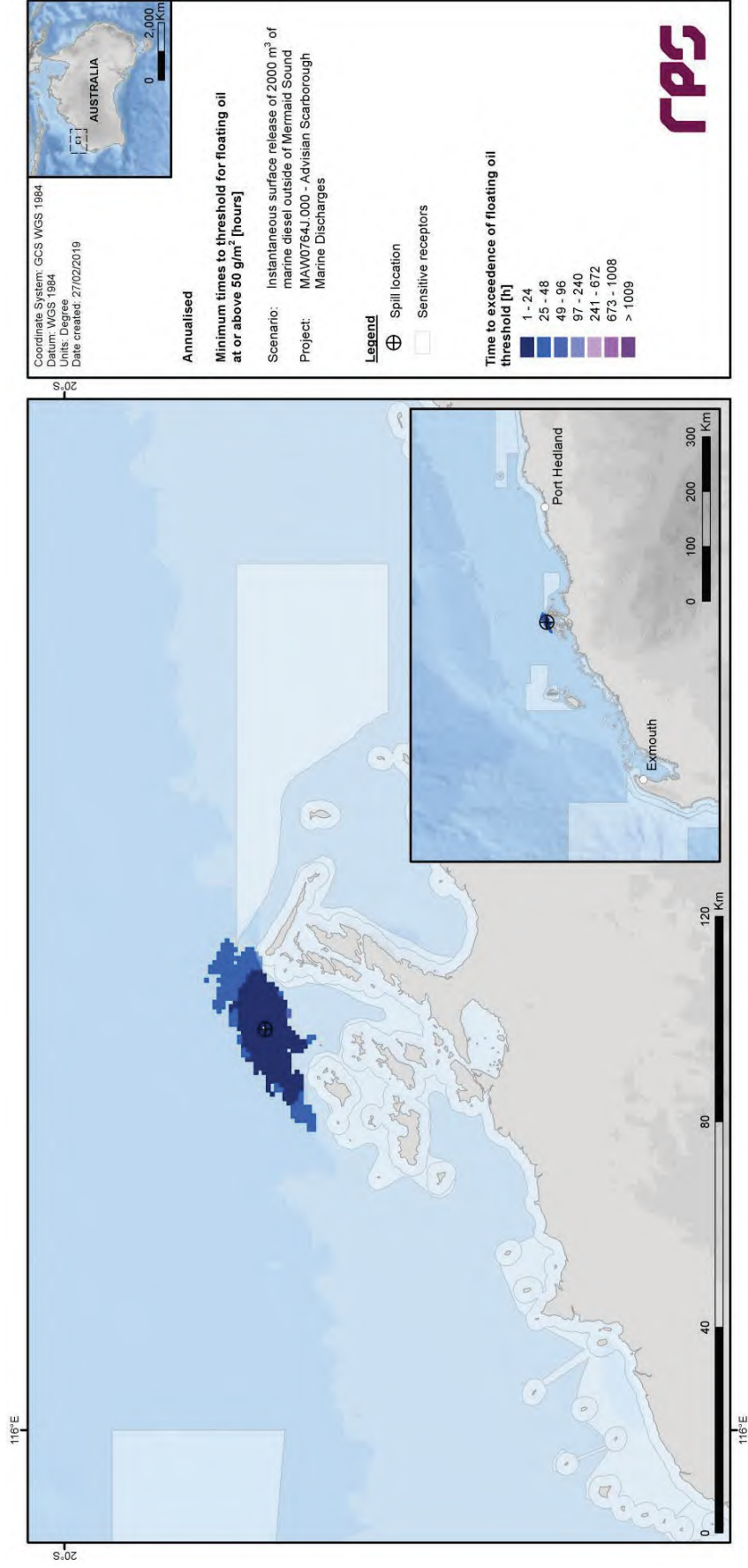
Figure 3.36 Predicted annualised smoothed Zone of Consequence of floating oil concentrations at or above 100 g/m² resulting from an instantaneous surface release of marine diesel after a vessel collision within Montebello Marine Park.

3.3.2.2 Entrained Oil

Table 3.5 Expected annualised entrained oil outcomes at sensitive receptors resulting from an instantaneous surface release of marine diesel after a vessel collision within Montebello Marine Park.

Receptor	Probability (%) of entrained oil concentration ≥500 ppb	Minimum time to receptor (hours) for entrained oil at ≥500 ppb	Maximum entrained oil concentration (ppb) averaged over all replicate simulations	Maximum entrained oil concentration (ppb), at any depth, in the worst replicate simulation
Argo-Rowley Terrace MP	<1	NC	2	109
Barrow Island	1	88	55	4,225
Glomar Shoals*	<1	389	9	8
Montebello Islands	2	212	28	963
Muiron Islands MMA-WHA	7	183	100	2,392
Ningaloo Coast Middle	<1	NC	3	228
Ningaloo Coast Middle WHA	<1	NC	7	472
Ningaloo Coast North	1	314	24	690
Ningaloo Coast North WHA	4	223	66	2,438
Ningaloo Coast South WHA	<1	NC	<1	51
Ningaloo RUZ	4	223	66	2,438
Pilbara Islands - Southern Island Group	2	171	45	2,536
Rankin Bank*	<1	101	78	193
Shark Bay Open Ocean Coast	<1	NC	2	153
Shark Bay WHA	<1	NC	2	153
Bernier & Dorre Islands	<1	NC	2	156
Lowendal Islands	1	164	8	639
Montebello MP	70	1	14,381	156,954
Montebello State Marine Park	4	85	95	4,577
Muiron Islands	5	185	78	1,676
Gascoyne MP	2	339	36	836
WA Coastline	5	93	71	3,381

NC: No contact to receptor predicted for specified threshold.

* Probabilities and maximum concentrations calculated at depth of submerged feature.
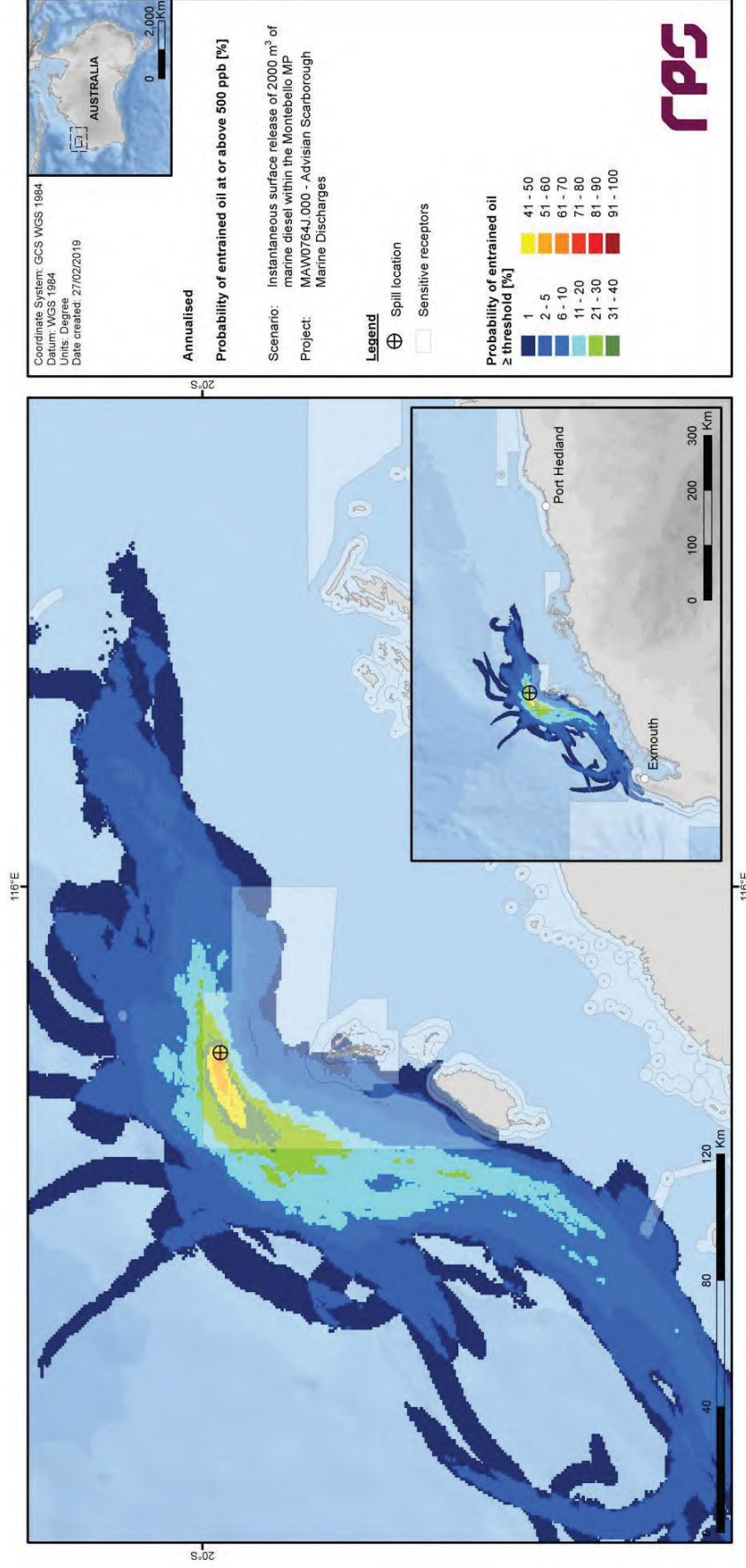
Figure 3.37 Predicted annualised probability of entrained oil concentrations at or above 500 ppb resulting from an instantaneous surface release of marine diesel after a vessel collision within Montebello Marine Park.
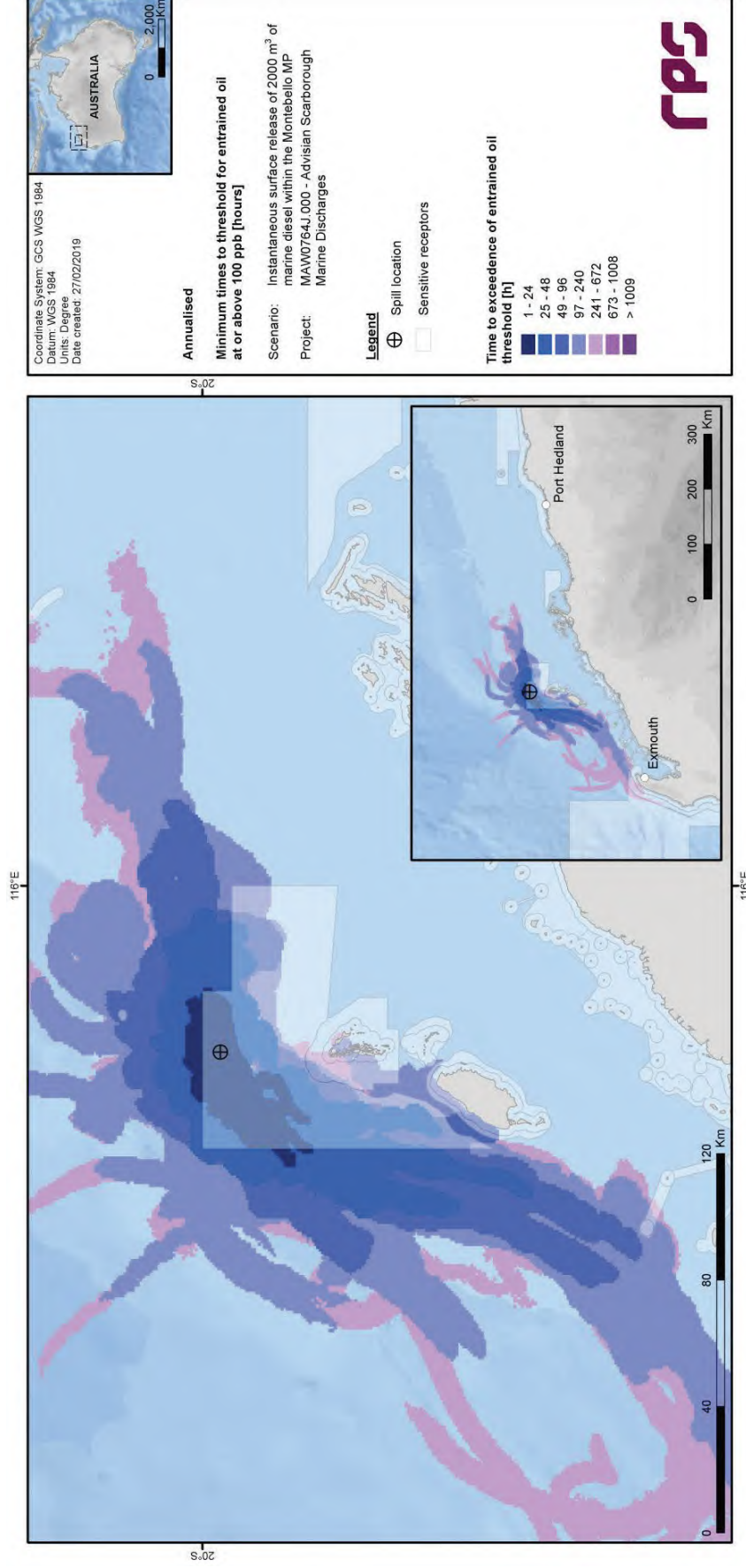
Figure 3.38 Predicted annualised minimum times to contact by entrained oil concentrations at or above 500 ppb resulting from an instantaneous surface release of marine diesel after a vessel collision within Montebello Marine Park.
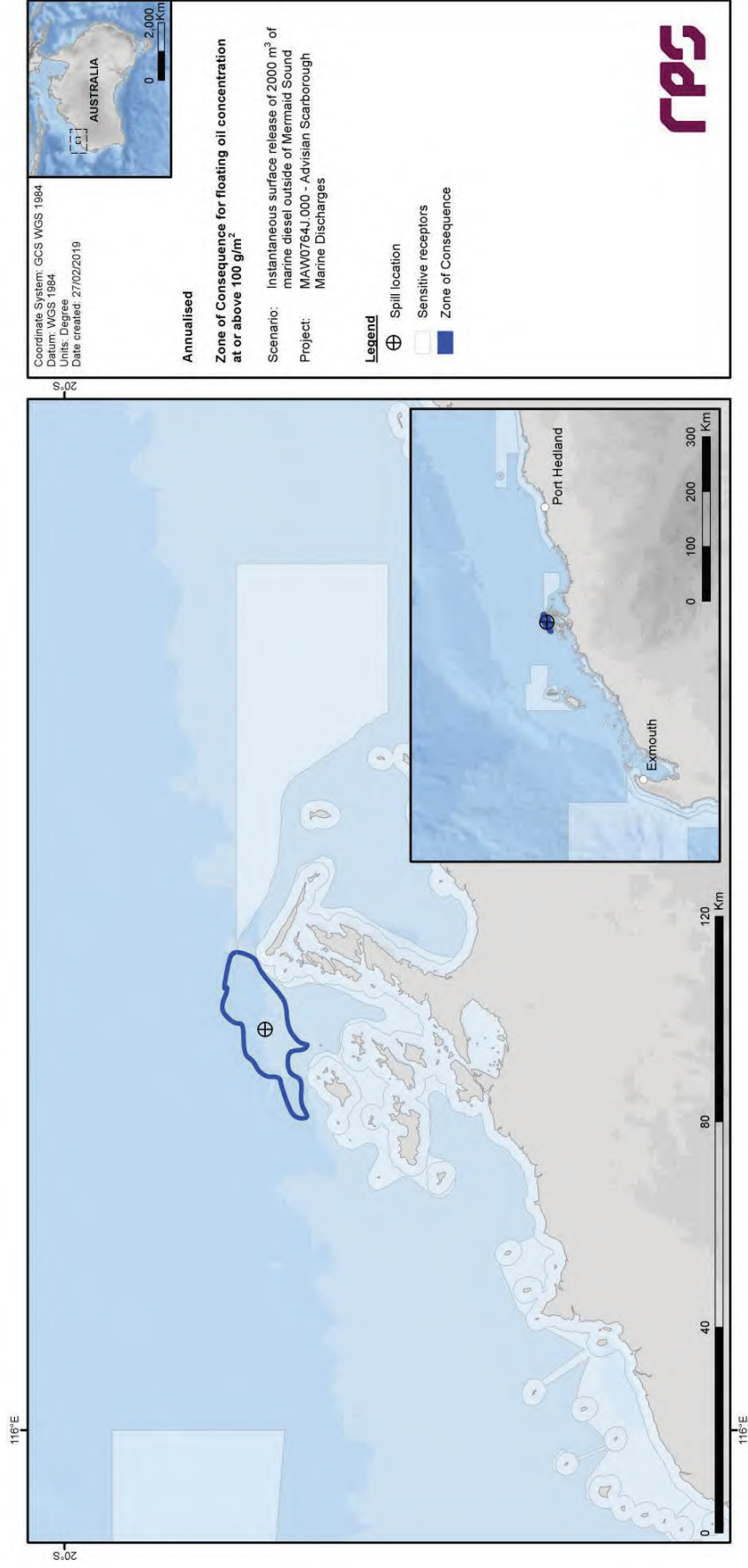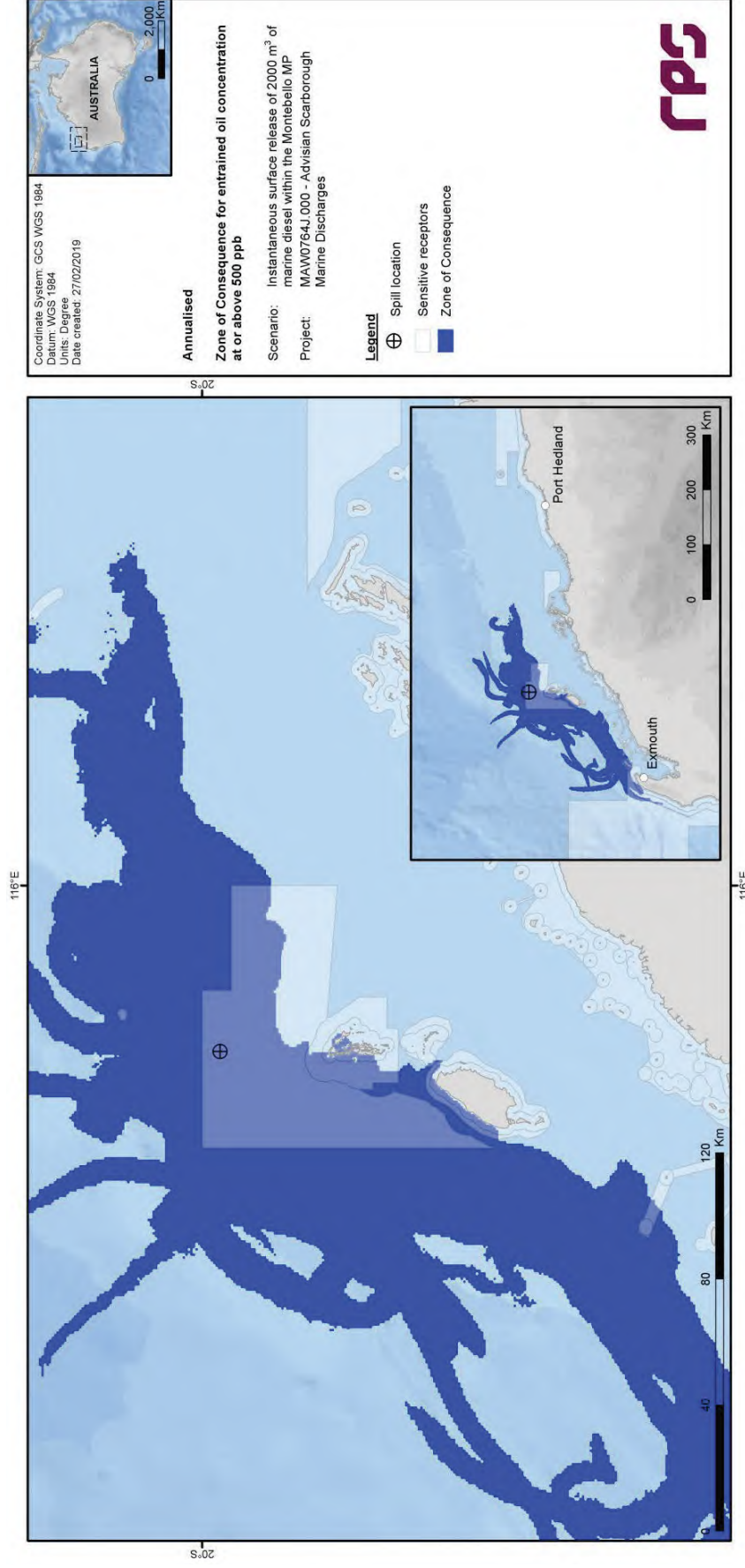
Figure 3.39 Predicted annualised Zone of Consequence of entrained oil concentrations at or above 500 ppb resulting from an instantaneous surface release of marine diesel after a vessel collision within Montebello Marine Park.
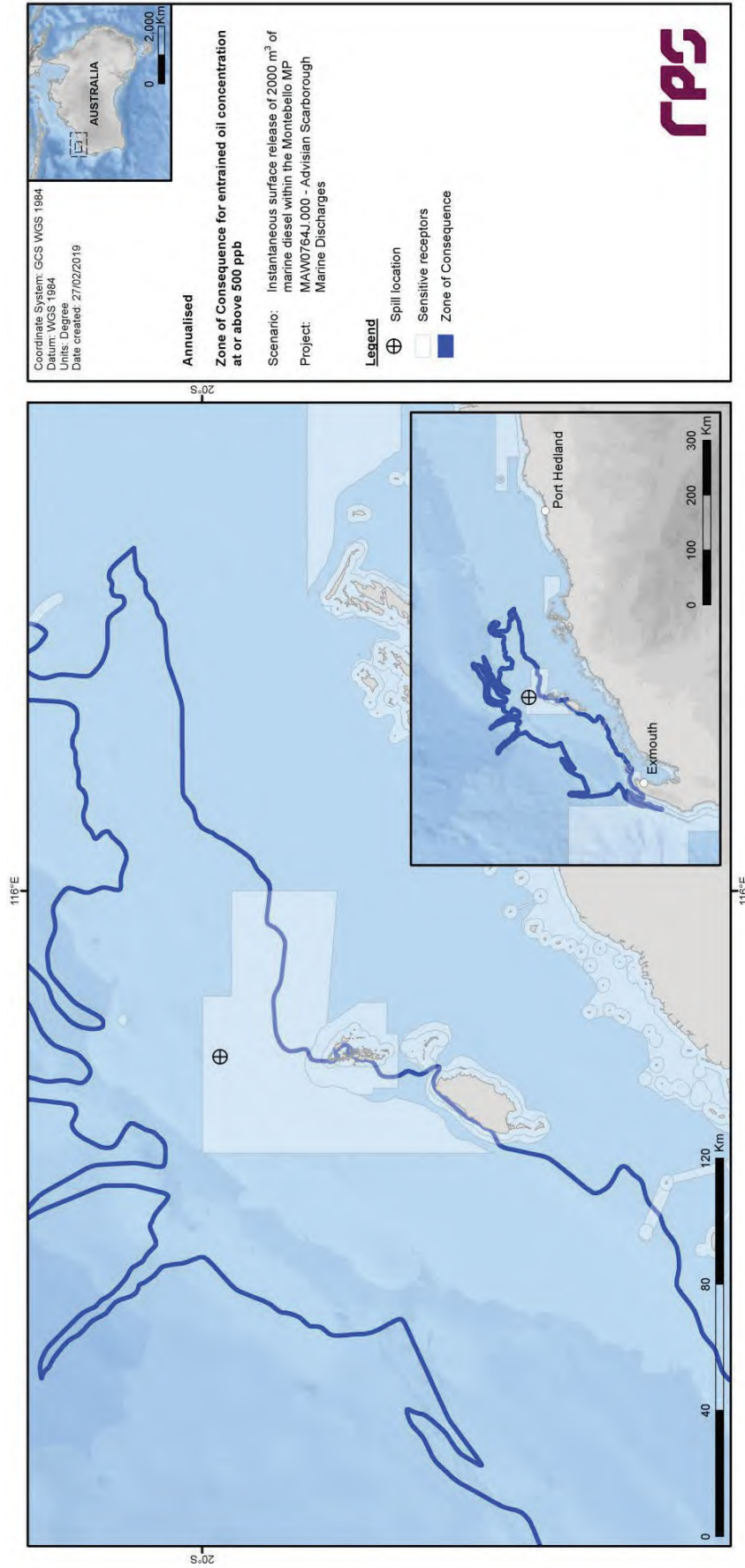
Figure 3.40 Predicted annualised smoothed Zone of Consequence of entrained oil concentrations at or above 500 ppb resulting from an instantaneous surface release of marine diesel after a vessel collision within Montebello Marine Park.
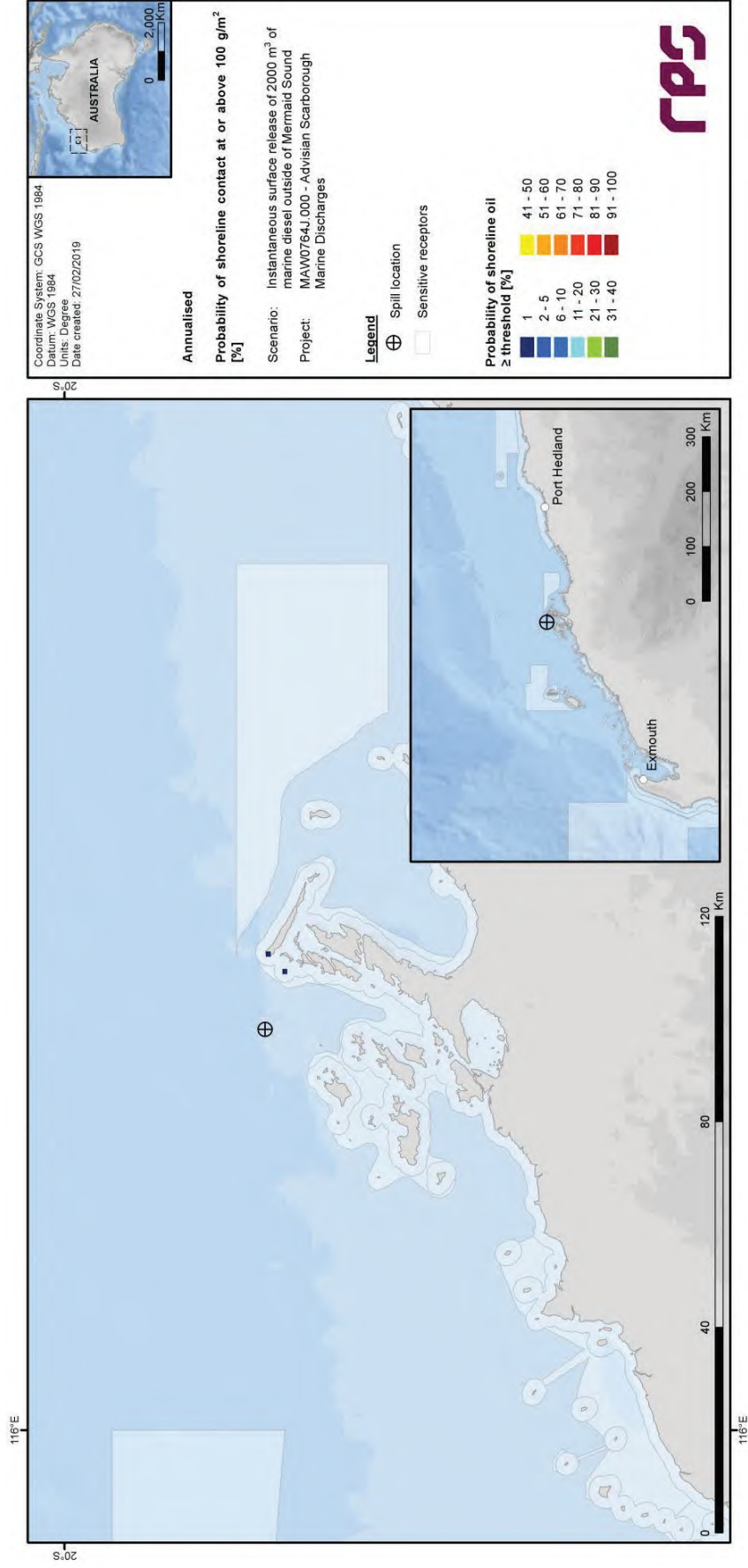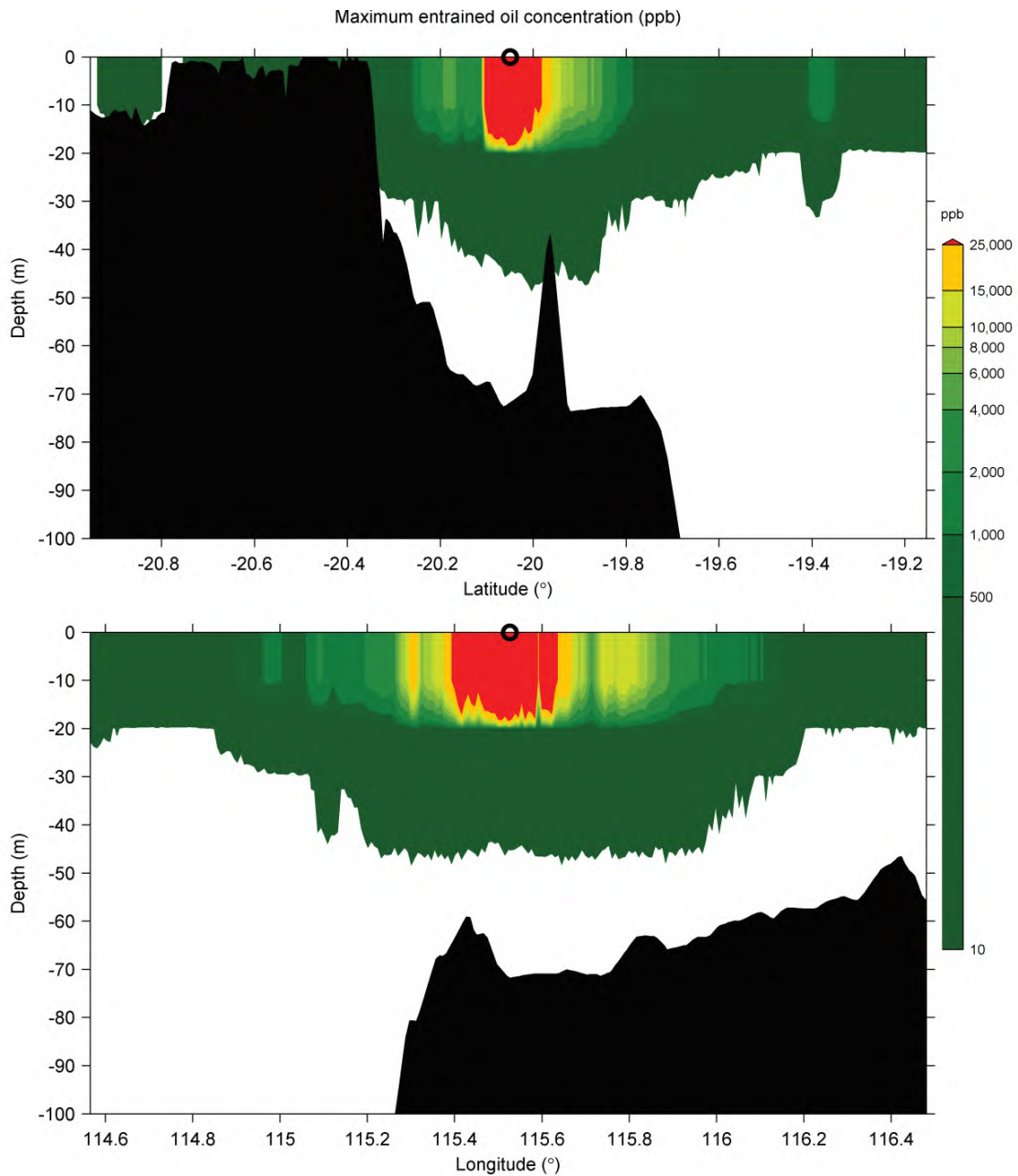
Figure 3.41 Cross-section transects of predicted annualised maximum entrained oil concentrations for an instantaneous surface release of marine diesel after a vessel collision within Montebello Marine Park. Transect locations are shown in Figure 3.1.

3.3.2.3 Dissolved Aromatic Hydrocarbons

Table 3.6   Expected annualised dissolved aromatic hydrocarbon outcomes at sensitive receptors resulting from an instantaneous surface release of marine diesel after a vessel collision within Montebello Marine Park.

Receptor	Probability (%) of dissolved aromatic hydrocarbon concentration ≥500 ppb	Maximum dissolved aromatic hydrocarbon concentration (ppb) averaged over all replicate simulations	Maximum dissolved aromatic hydrocarbon concentration (ppb), at any depth, in the worst replicate simulation
Argo-Rowley Terrace MP	<1	NC	NC
Barrow Island	<1	3	200
Glomar Shoals*	<1	<1	<1
Montebello Islands	<1	<1	56
Muiron Islands MMA-WHA	<1	<1	29
Ningaloo Coast Middle	<1	<1	2
Ningaloo Coast Middle WHA	<1	<1	2
Ningaloo Coast North	<1	<1	10
Ningaloo Coast North WHA	<1	<1	47
Ningaloo Coast South WHA	<1	<1	<1
Ningaloo RUZ	<1	<1	47
Pilbara Islands - Southern Island Group	<1	<1	25
Rankin Bank*	<1	2	69
Shark Bay Open Ocean Coast	<1	NC	NC
Shark Bay WHA	<1	NC	NC
Bernier & Dorre Islands	<1	NC	NC
Lowendal Islands	<1	<1	3
Montebello MP	9	154	1,990
Montebello State Marine Park	<1	2	108
Muiron Islands	<1	<1	26
Gascoyne MP	<1	<1	23
WA Coastline	<1	<1	97

NC: No contact to receptor predicted for specified threshold.

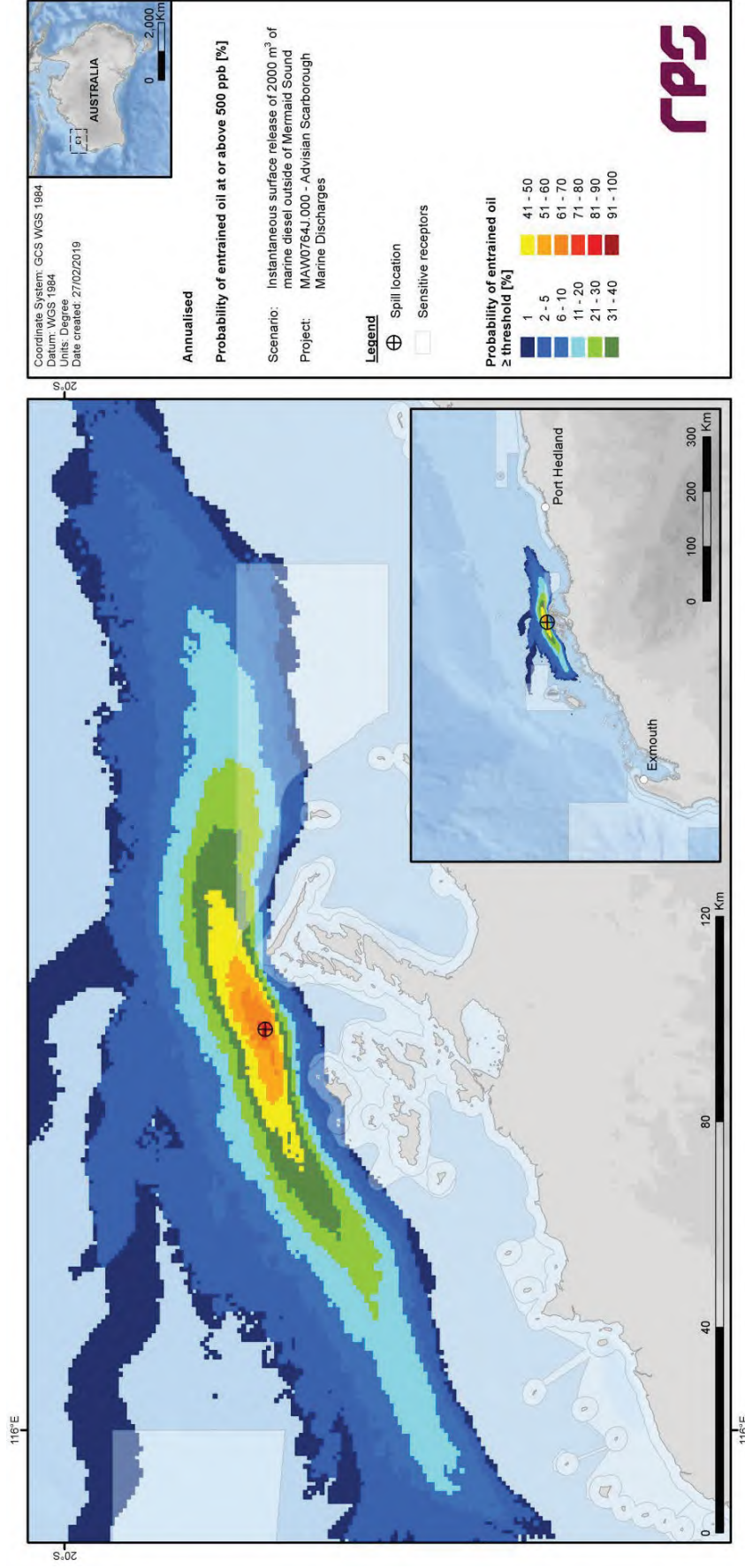* Probabilities and maximum concentrations calculated at depth of submerged feature.
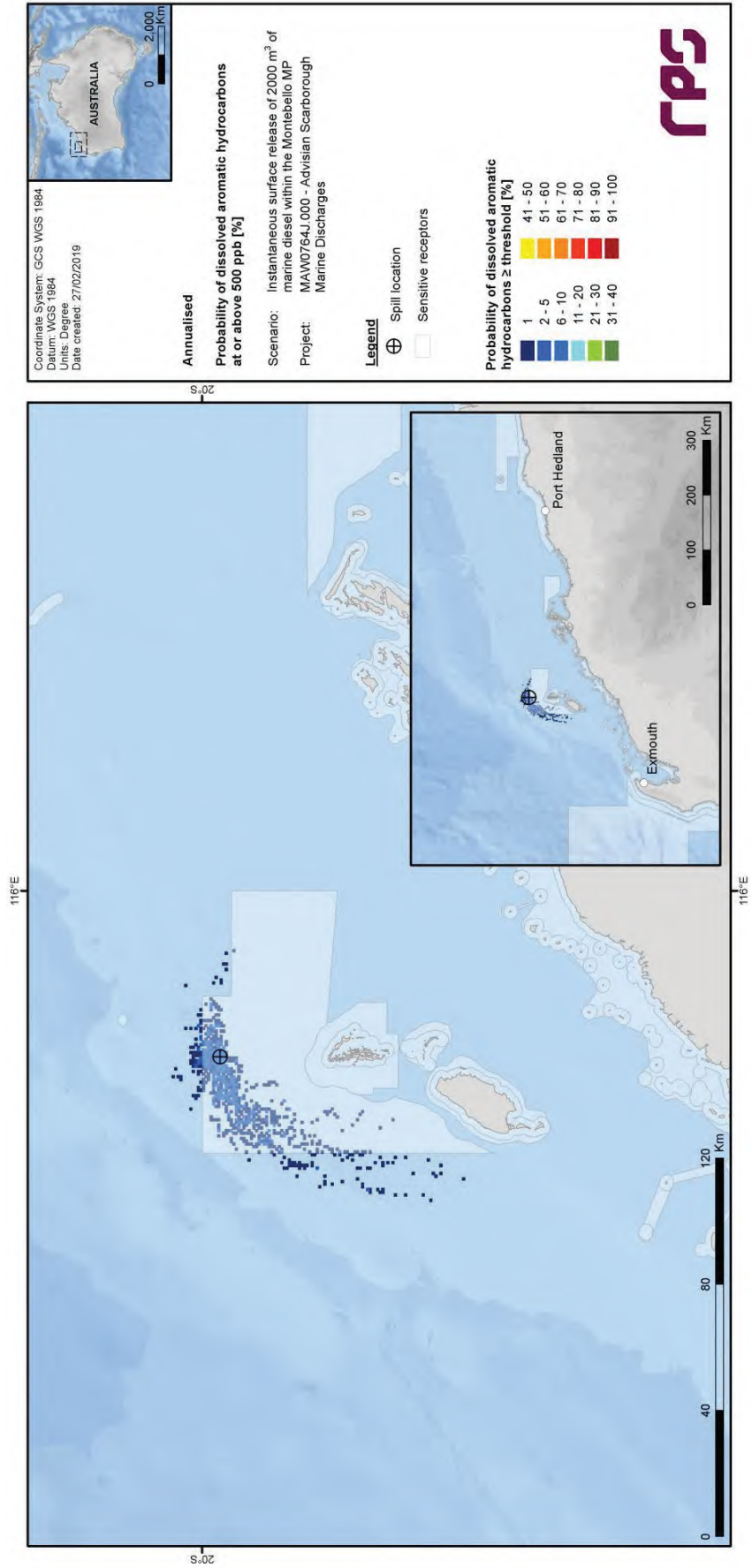
Figure 3.42 Predicted annualised probability of dissolved aromatic hydrocarbon concentrations at or above 500 ppb resulting from an instantaneous surface release of marine diesel after a vessel collision within Montebello Marine Park.
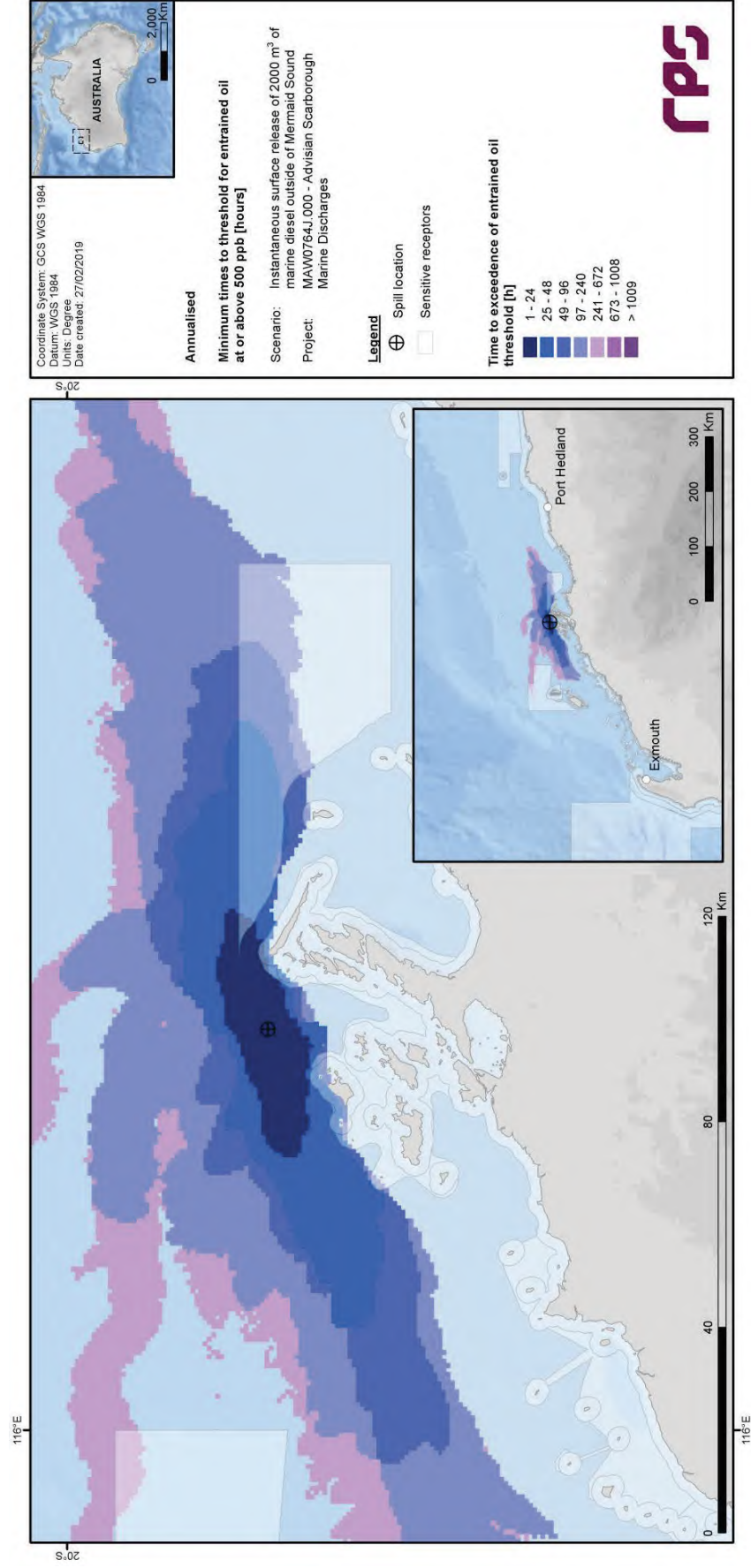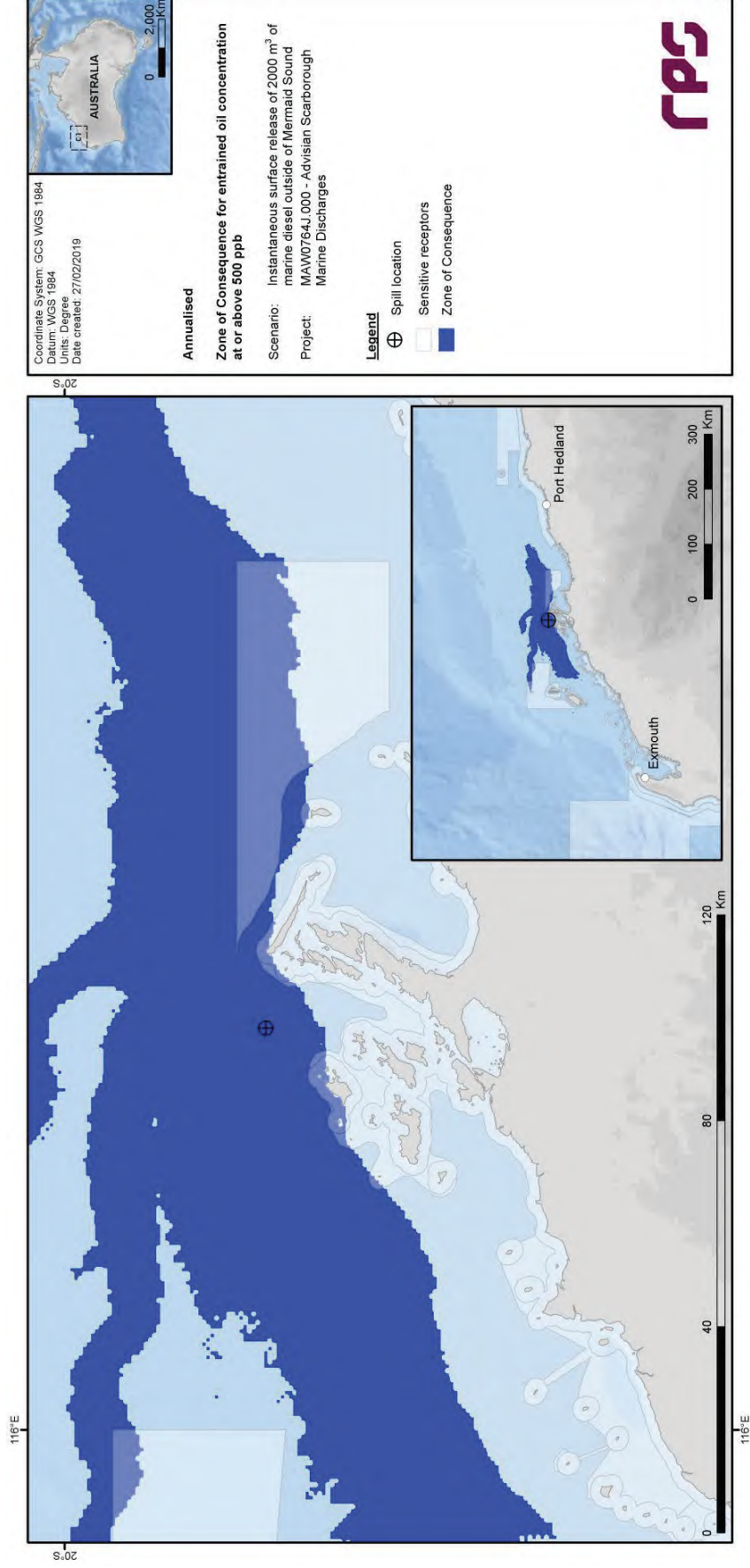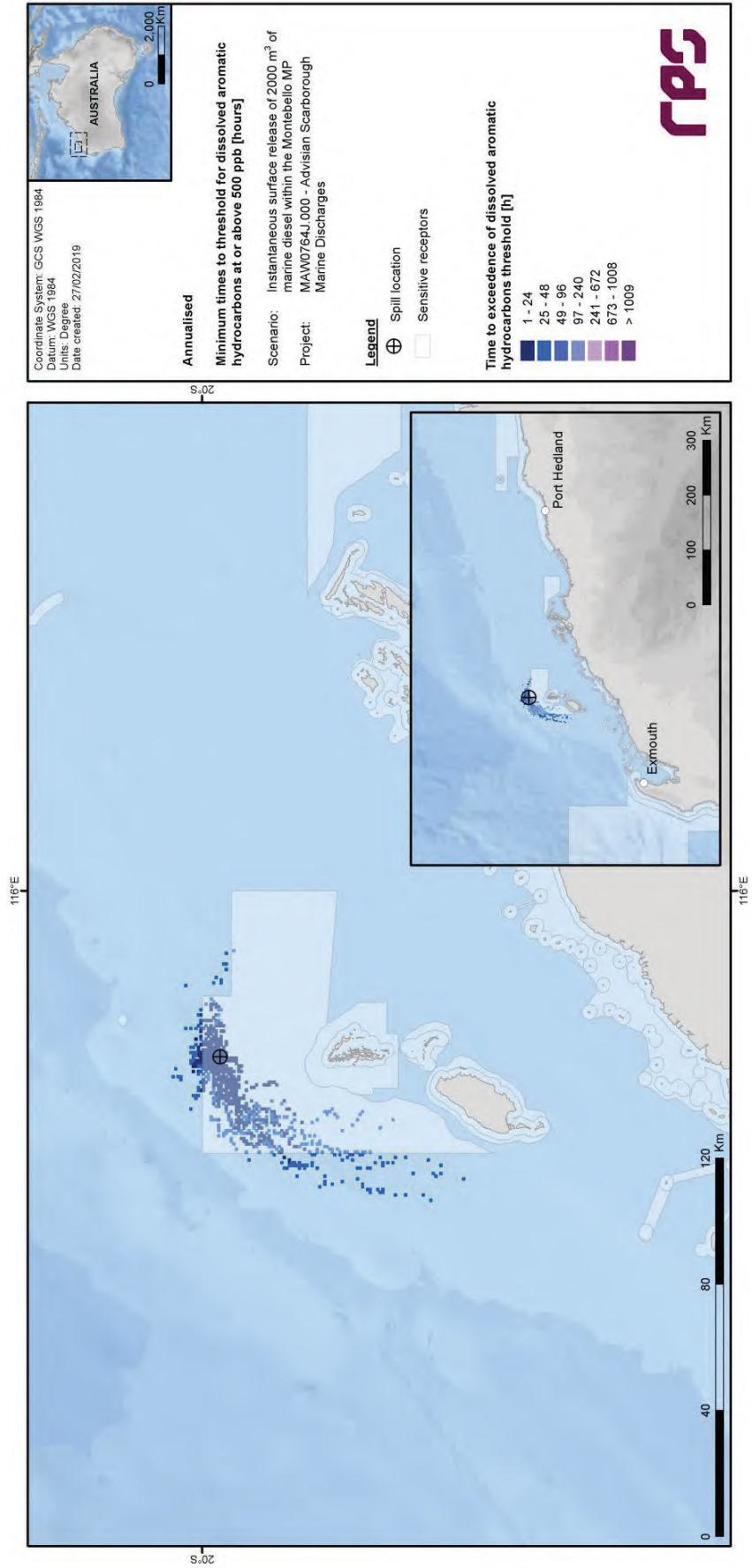
Figure 3.43 Predicted annualised minimum times to contact by dissolved aromatic hydrocarbon concentrations at or above 500 ppb resulting from an instantaneous surface release of marine diesel after a vessel collision within Montebello Marine Park.
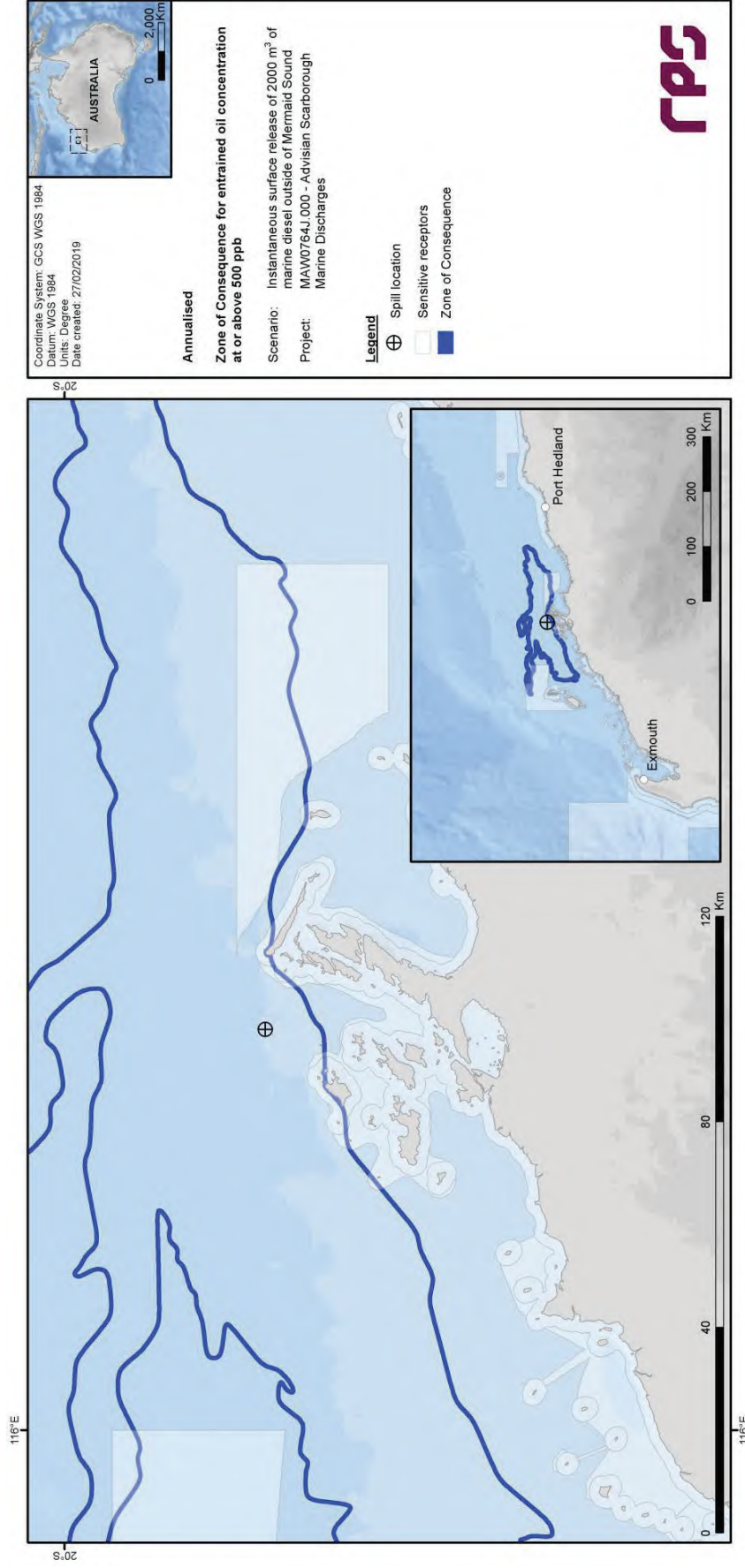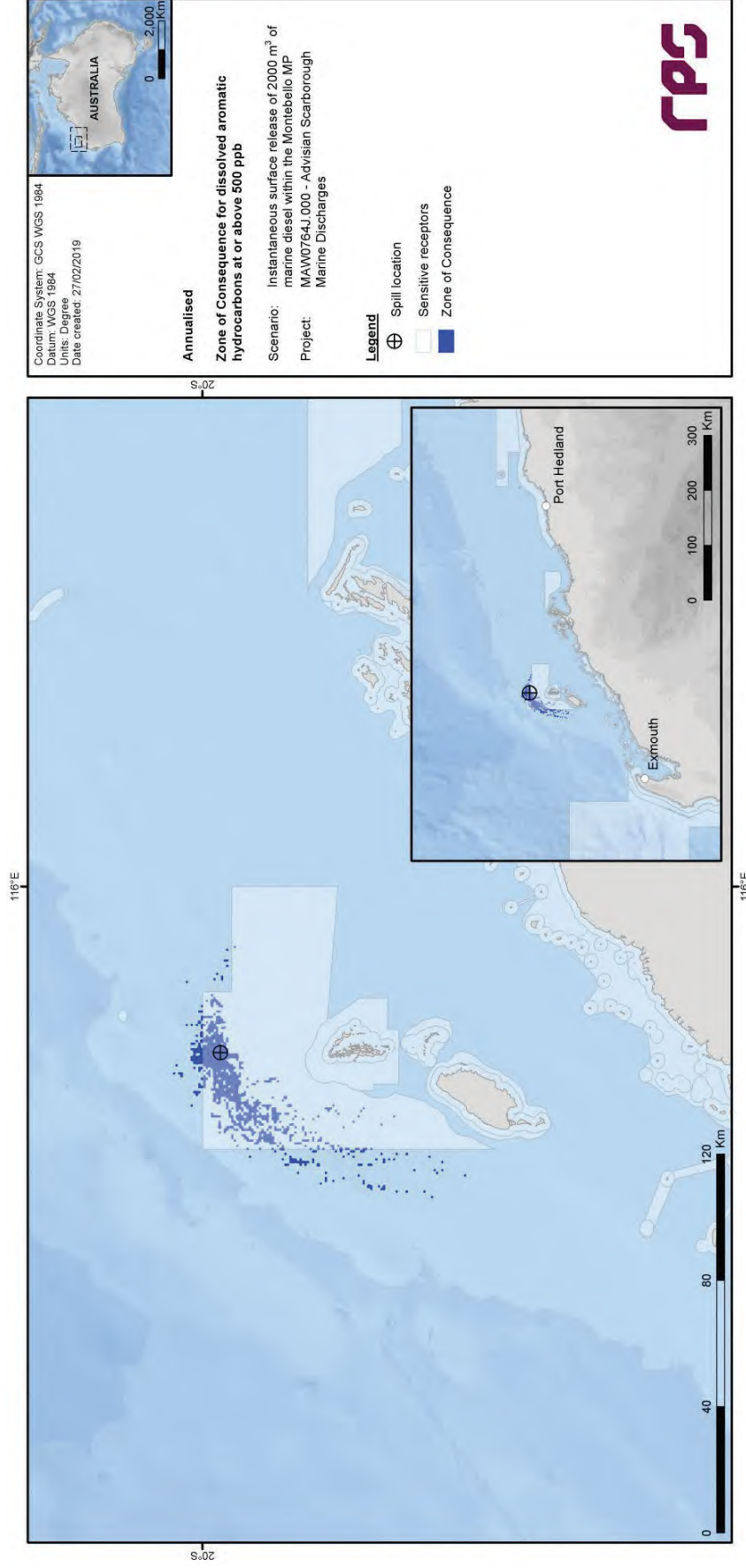
Figure 3.44 Predicted annualised Zone of Consequence of dissolved aromatic hydrocarbon concentrations at or above 500 ppb resulting from an instantaneous surface release of marine diesel after a vessel collision within Montebello Marine Park.
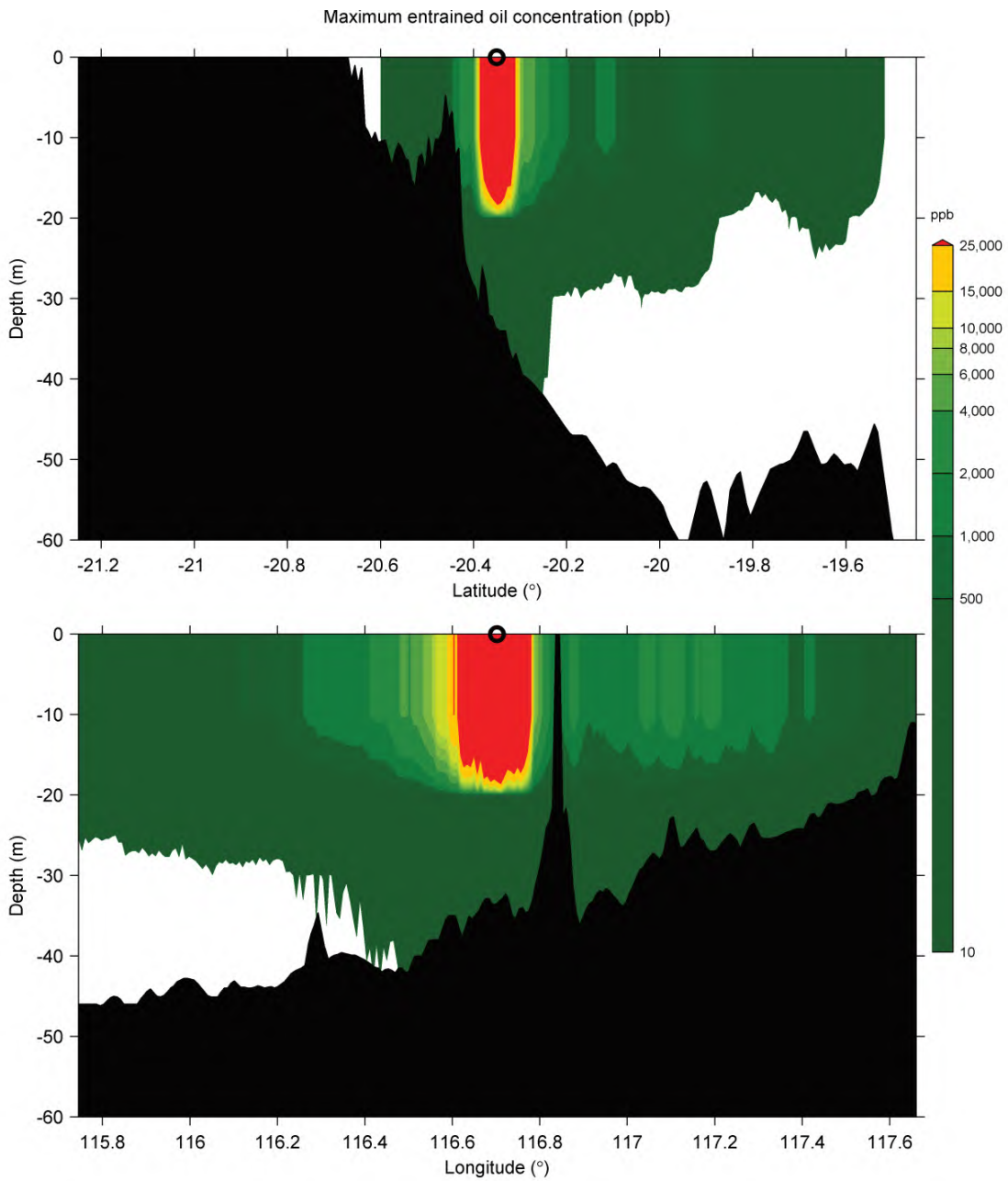
Annualised

Zone of Consequence for dissolved aromatic hydrocarbons at or above 500 ppb

Scenario: Instantaneous surface release of 2000 m³ of marine diesel within the Montebello MP

Project: MAW0764J.000 - Advisian Scarborough Marine Discharges

Legend

⊕ Spill location

Sensitive receptors

Zone of Consequence

Coordinate System: GCS WGS 1984
Datum: WGS 1984
Units: Degree
Date created: 27/02/2019

Figure 3.45 Predicted annualised smoothed Zone of Consequence of dissolved aromatic hydrocarbon concentrations at or above 500 ppb resulting from an instantaneous surface release of marine diesel after a vessel collision within Montebello Marine Park.

Maximum dissolved aromatic hydrocarbon concentration (ppb)
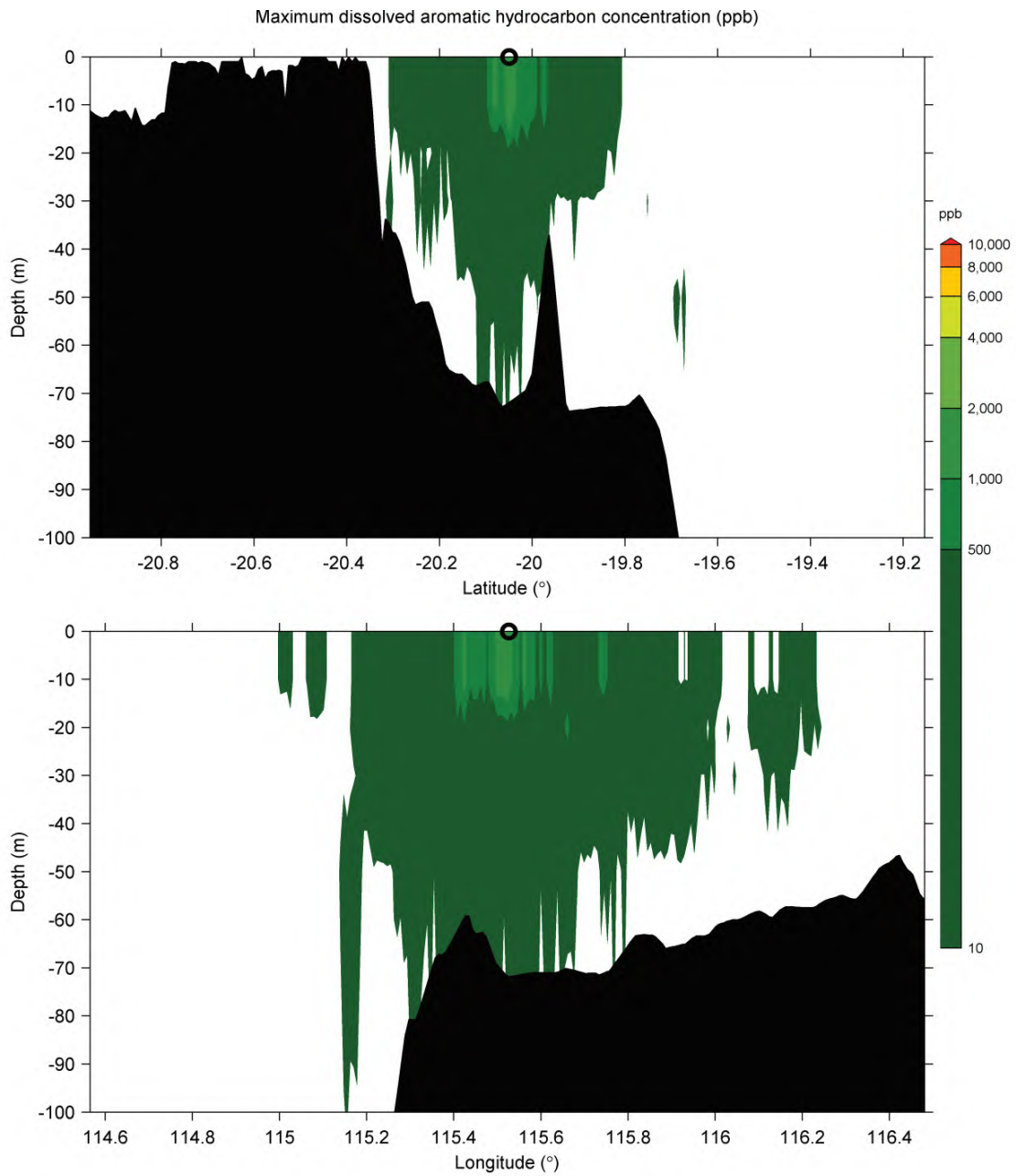
Figure 3.46 Cross-section transects of predicted annualised maximum dissolved aromatic hydrocarbon concentrations for an instantaneous surface 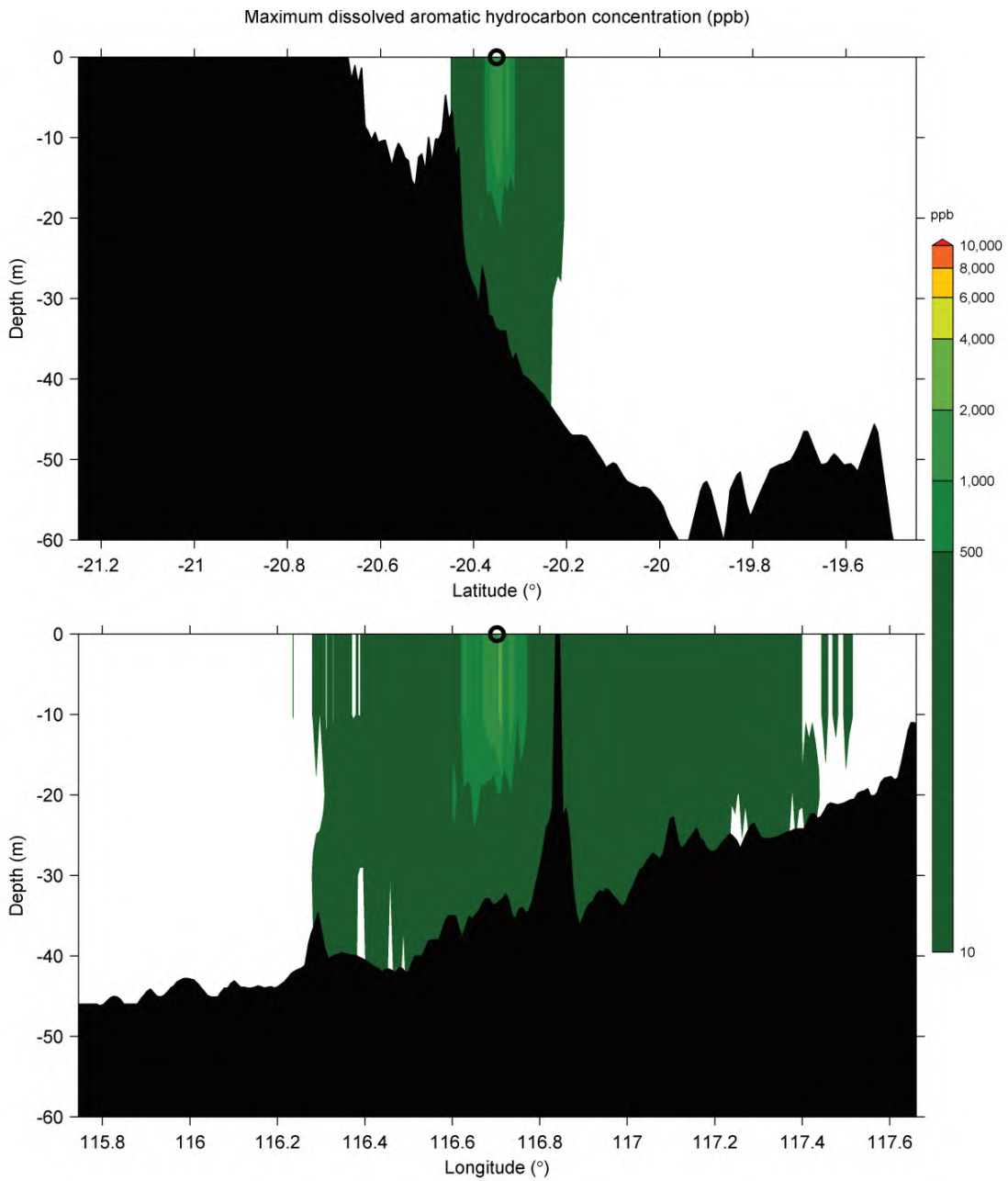release of marine diesel after a vessel collision within Montebello Marine Park. Transect locations are shown in Figure 3.1.

3.4 Scenario 3: Short-Term (Instantaneous) Surface Release of Marine Diesel after a Vessel Collision at the FPU Location

3.4.1 Discussion of Results

3.4.1.1 Overview

This scenario investigated the probability of exposure to surrounding regions by oil resulting from a short-term (instantaneous) surface release of 2,000 m^3 of marine diesel at the FPU location during operations at any time of year, with no mitigation measures applied.

Considering the discharge characteristics, the properties of the oil and its expected weathering behaviour, floating oil will be susceptible to entrainment into the wave-mixed layer under typical wind conditions. Evaporation rates will be significant, given the moderate proportion of volatile compounds in the oil (41%). The low-volatility fraction of the oil (54%) will take longer durations of the order of days to evaporate, and the residual fraction of 5% is expected to persist in the environment until degradation processes occur. Considering the spill volume, there is a low potential for dissolution of soluble aromatic compounds.

3.4.1.2 Floating and Shoreline Oil

The probability contour figures for floating oil indicate that concentrations equal to or greater than the 10 g/m^2, 50 g/m^2 and 100 g/m^2 thresholds could potentially be found, in the form of slicks, up to 113 km, 60 km and 58 km from the spill site, respectively (Figure 3.47, Figure 3.48 and Figure 3.49).

No shoreline receptors are predicted to be contacted by floating oil concentrations at any of the assessed thresholds (Table 3.7). Floating oil at the 10 g/m^2 threshold is predicted to arrive at the surface waters of the Gascoyne MP receptor with a probability of 1% after 64 hours.

No accumulation of oil on shorelines is predicted (Table 3.7).

The forecast annualised minimum times to contact, ZoC and smoothed ZoC for floating oil at or above the 10 g/m^2, 50 g/m^2 and 100 g/m^2 threshold concentrations are depicted in Figure 3.50 to Figure 3.52, Figure 3.53 to Figure 3.55 and Figure 3.56 to Figure 3.58, respectively.

3.4.1.3 Entrained Oil

Entrained oil at concentrations equal to or greater than the 500 ppb threshold is predicted to be found up to around 476 km from the spill site (Figure 3.59).

The Gascoyne MP is predicted to receive entrained oil concentrations at the 500 ppb threshold with a probability of 8% (Table 3.8). The maximum entrained oil concentration is forecast as 7.2 ppm within the Gascoyne MP.

The forecast annualised minimum times to contact, ZoC and smoothed ZoC for entrained oil at or above the 500 ppb threshold concentration are depicted in Figure 3.60, Figure 3.61 and Figure 3.62, respectively.

The cross-sectional transects of maximum entrained oil concentrations in the vicinity of the release site show that concentrations above 25,000 ppb are expected to extend from the sea surface to depths of around 15 m (Figure 3.63).

3.4.1.4 Dissolved Aromatic Hydrocarbons

Dissolved aromatic hydrocarbons at concentrations equal to or greater than the 500 ppb threshold are predicted to be found up to around 74 km from the spill site (Figure 3.64).

No receptors are predicted to receive dissolved aromatic hydrocarbon concentrations at the 500 ppb threshold (Table 3.9). The maximum dissolved aromatic hydrocarbon concentration is forecast as 462 ppb within the Gascoyne MP.

The forecast annualised minimum times to contact, ZoC and smoothed ZoC for dissolved aromatic hydrocarbons at or above the 500 ppb threshold concentration are depicted in Figure 3.65, Figure 3.66 and Figure 3.67, respectively.

The cross-sectional transects of maximum dissolved aromatic hydrocarbon concentrations in the vicinity of the release site show that concentrations above 1,000 ppb are expected to extend from the sea surface to depths of around 15 m (Figure 3.68).

3.4.2 Results Tables and Figures

3.4.2.1 Floating and Shoreline Oil

Table 3.7 Expected annualised floating and shoreline oil outcomes at sensitive receptors resulting from an instantaneous surface release of marine diesel after a vessel collision at the FPU location.

Receptor	Probability (%) of floating oil concentration ≥10 g/m²	Probability (%) of floating oil concentration ≥50 g/m²	Probability (%) of floating oil concentration ≥100 g/m²	Minimum time to receptor (hours) for floating oil at ≥10 g/m²	Minimum time to receptor (hours) for floating oil at ≥50 g/m²	Minimum time to receptor (hours) for floating oil at ≥100 g/m²	Probability (%) of shoreline oil concentration ≥100 g/m²	Probability (%) of shoreline oil concentration ≥250 g/m²	Minimum time to receptor (hours) for shoreline oil at ≥100 g/m²	Minimum time to receptor (hours) for shoreline oil at ≥250 g/m²	Maximum local accumulated concentration (g/m²) averaged over all replicate simulations	Maximum local accumulated concentration (g/m²) in the worst replicate simulation	Maximum accumulated volume (m³) along this shoreline, averaged over all replicate simulations	Maximum accumulated volume (m³) along this shoreline, in the worst replicate simulation
Ningaloo Coast North WHA	<1	<1	<1	NC	NC	NC	<1	<1	NC	NC	NC	NC	NC	NC
Ningaloo RUZ*	<1	<1	<1	NC	NC	NC	NA	NA	NA	NA	NA	NA	NA	NA
Abrolhos Islands MP*	<1	<1	<1	NC	NC	NC	NA	NA	NA	NA	NA	NA	NA	NA
Camarvon Canyon MP*	<1	<1	<1	NC	NC	NC	NA	NA	NA	NA	NA	NA	NA	NA
Gascoyne MP*	1	<1	<1	64	NC	NC	NA	NA	NA	NA	NA	NA	NA	NA

NC: No contact to receptor predicted for specified threshold. NA: Not applicable.

* Floating oil will not accumulate on submerged features and at open ocean locations.
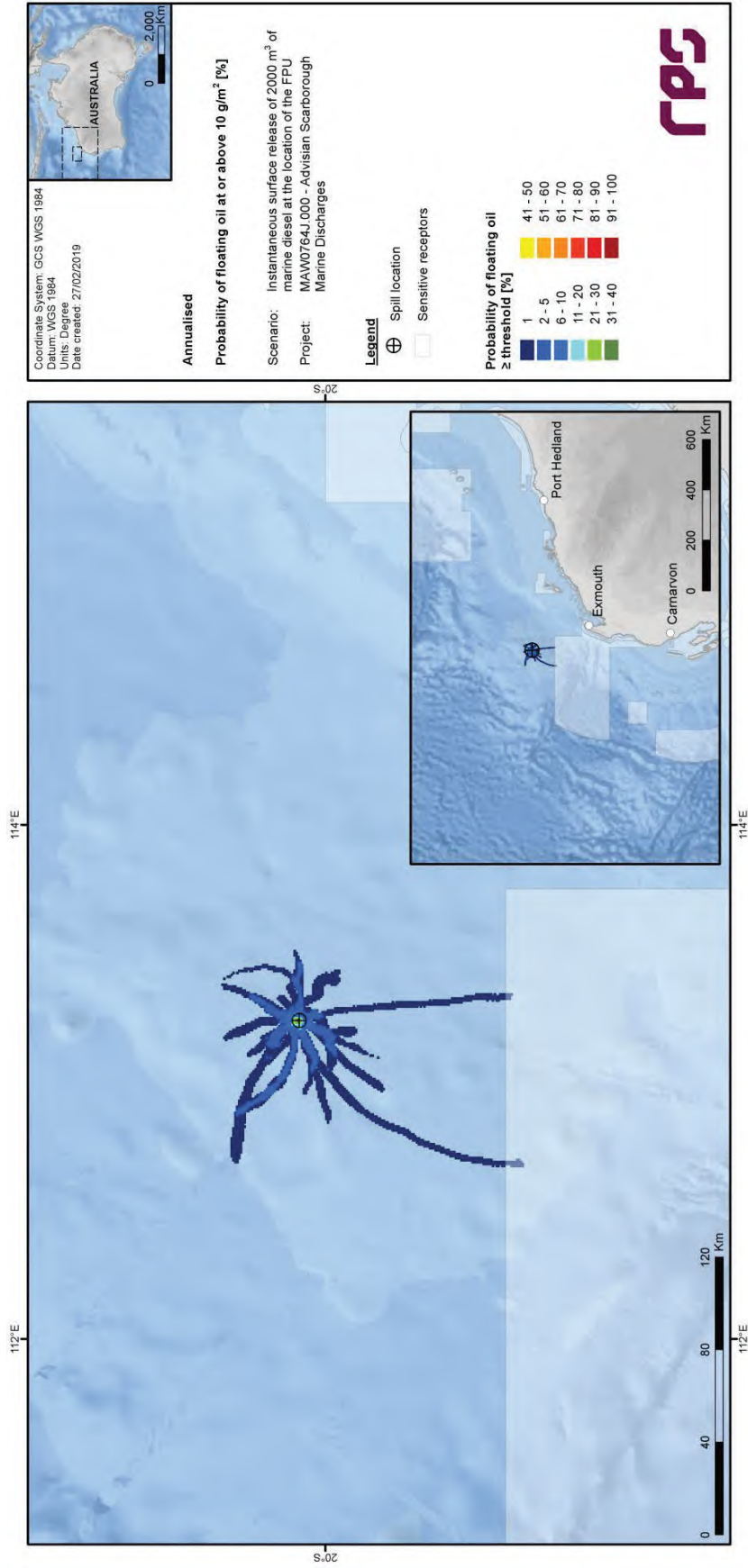
Figure 3.47 Predicted annualised probability of floating oil concentrations at or above 10 g/m² resulting from an instantaneous surface release of marine diesel after a vessel collision at the FPU location.
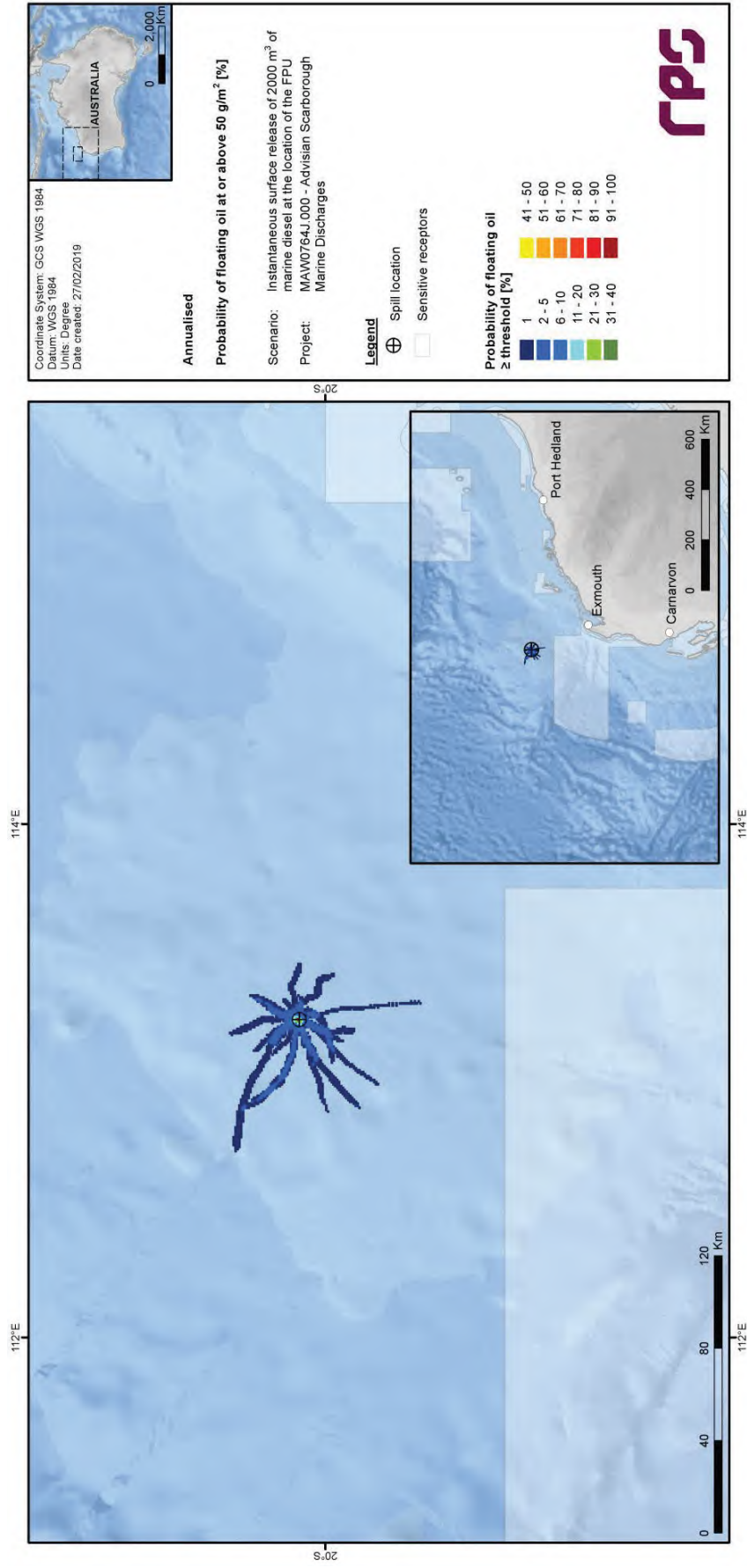
Figure 3.48 Predicted annualised probability of floating oil concentrations at or above 50 g/m² resulting from an instantaneous surface release of marine diesel after a vessel collision at the FPU location.
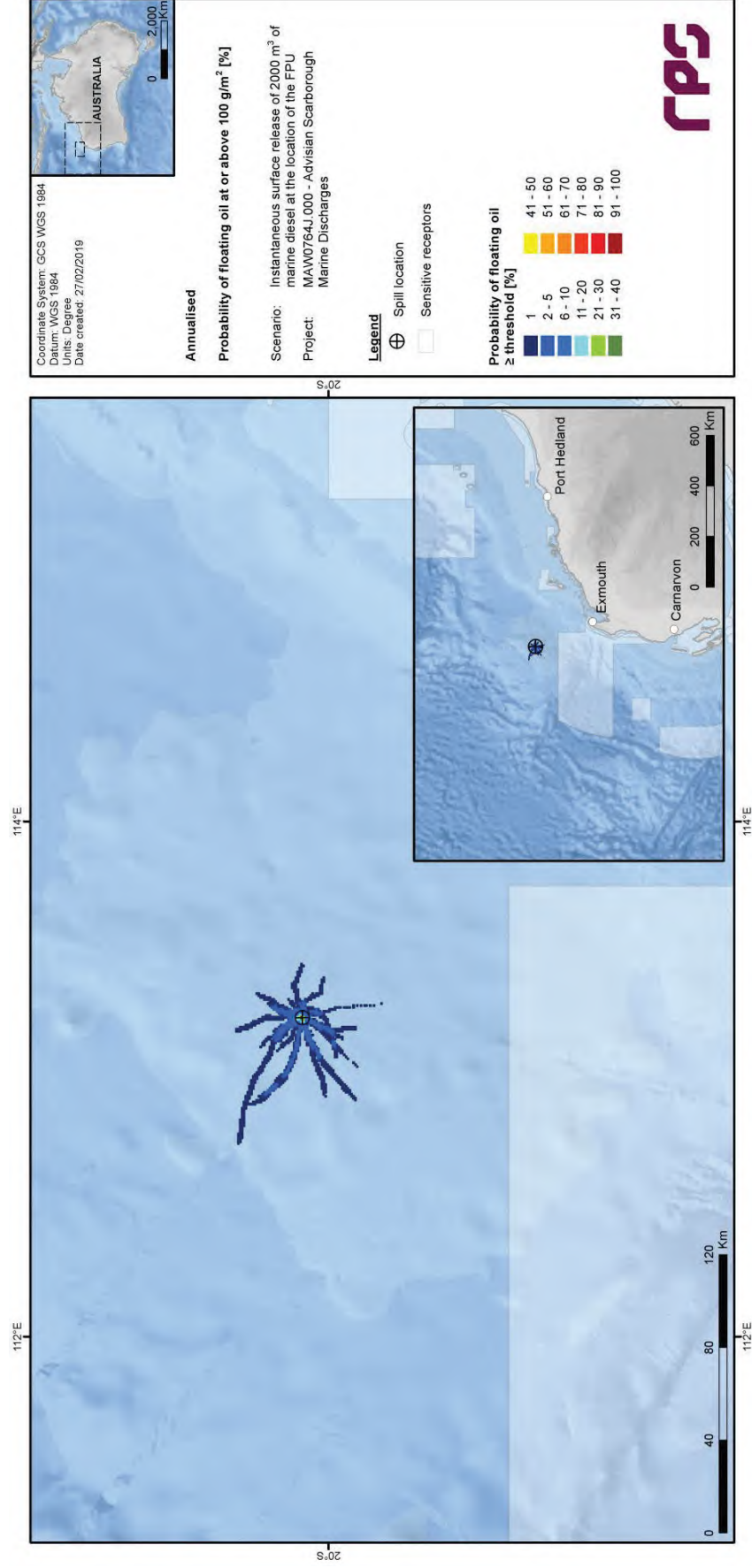
Figure 3.49 Predicted annualised probability of floating oil concentrations at or above 100 g/m² resulting from an instantaneous surface release of marine diesel after a vessel collision at the FPU location.

Annualised

Minimum times to threshold for floating oil at or above 10 g/m² [hours]

Scenario: Instantaneous surface release of 2000 m³ of marine diesel at the location of the FPU

Project: MAW0764J.000 - Advisian Scarborough Marine Discharges

Legend

⊕ Spill location

☐ Sensitive receptors

Time to exceedence of floating oil threshold [h]

1 - 24
25 - 48
49 - 96
97 - 240
241 - 672
673 - 1008
> 1009
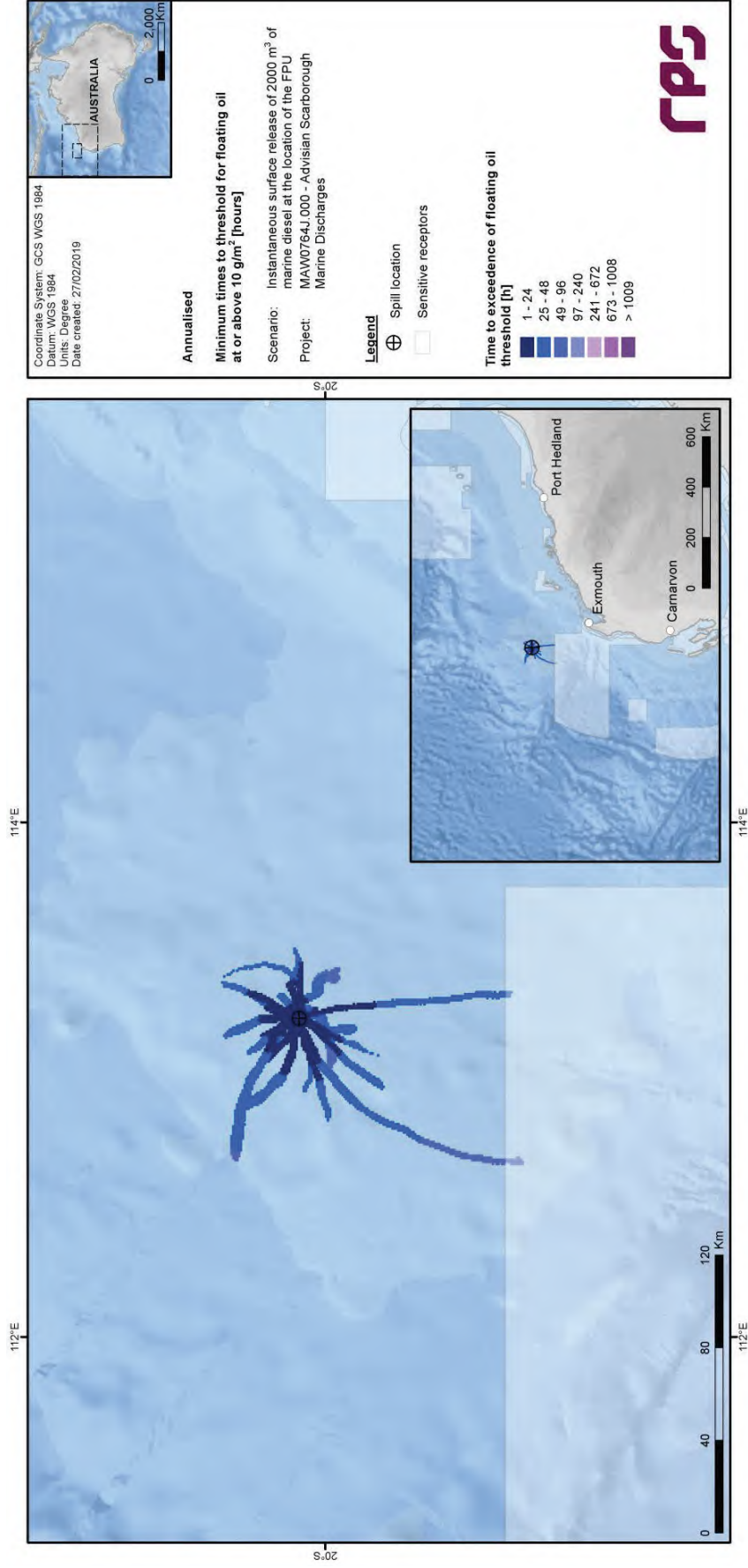
Figure 3.50 Predicted annualised minimum times to contact by floating oil concentrations at or above 10 g/m² resulting from an instantaneous surface release of marine diesel after a vessel collision at the FPU location.
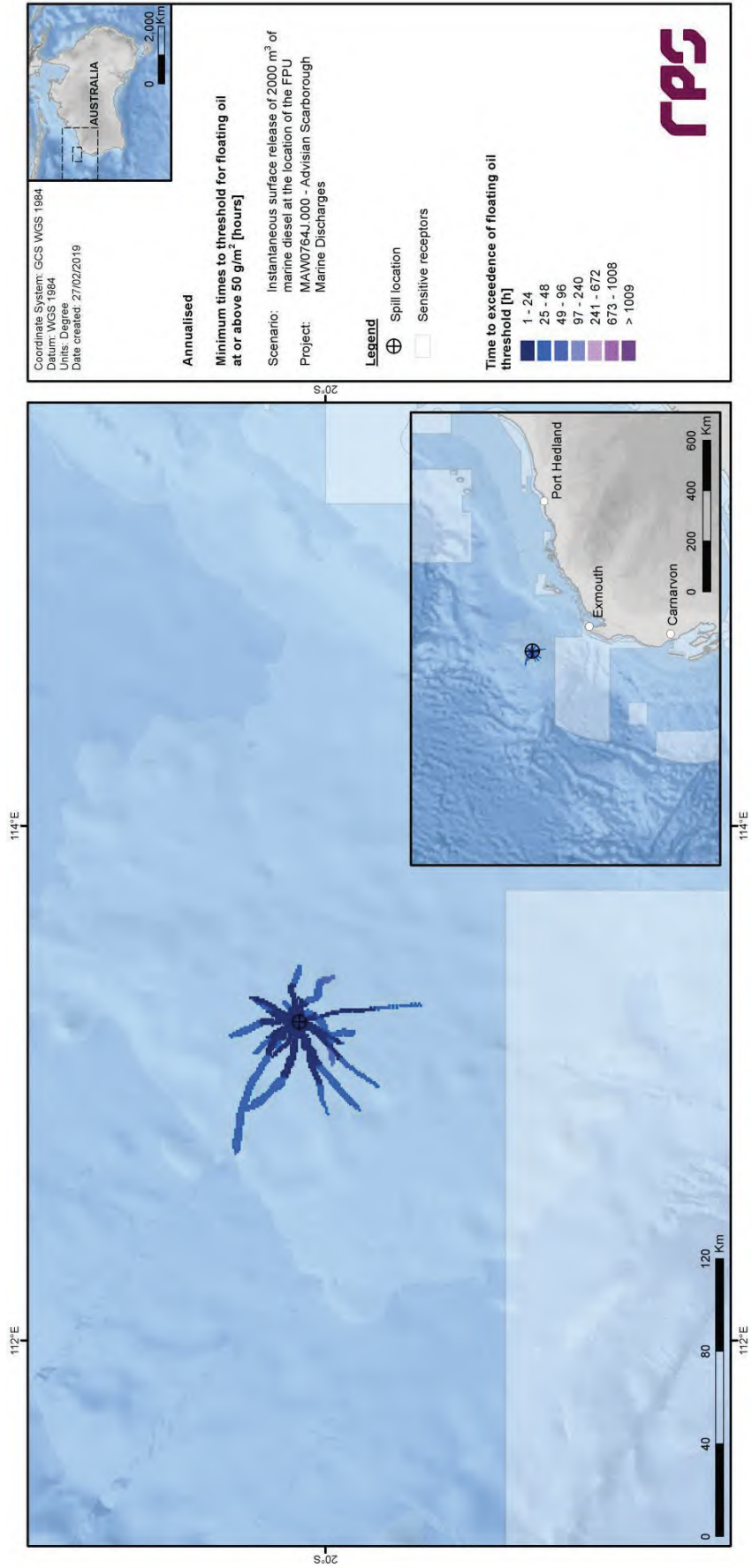
Figure 3.51 Predicted annualised minimum times to contact by floating oil concentrations at or above 50 g/m² resulting from an instantaneous surface release of marine diesel after a vessel collision at the FPU location.
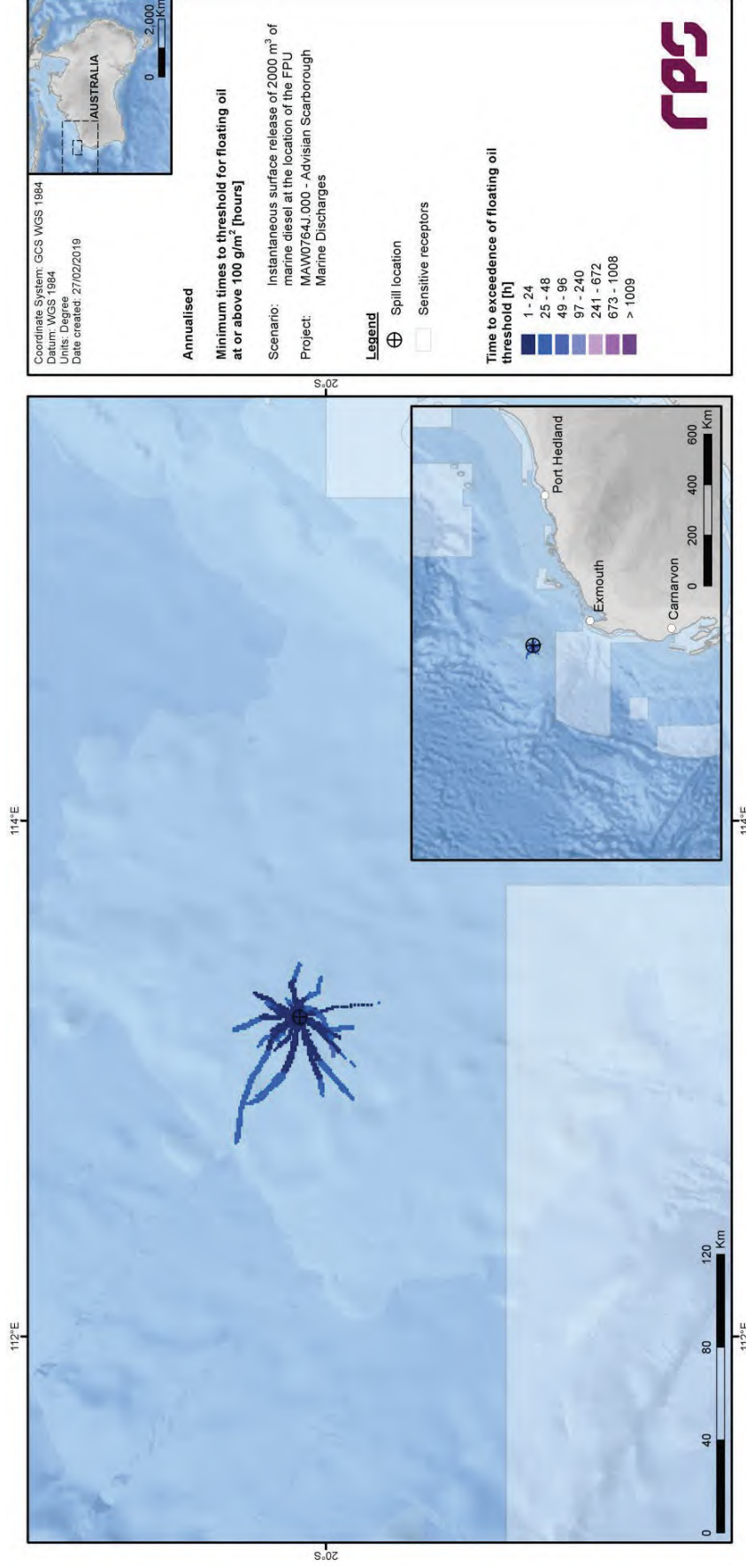
Figure 3.52 Predicted annualised minimum times to contact by floating oil concentrations at or above 100 g/m² resulting from an instantaneous surface release of marine diesel after a vessel collision at the FPU location.
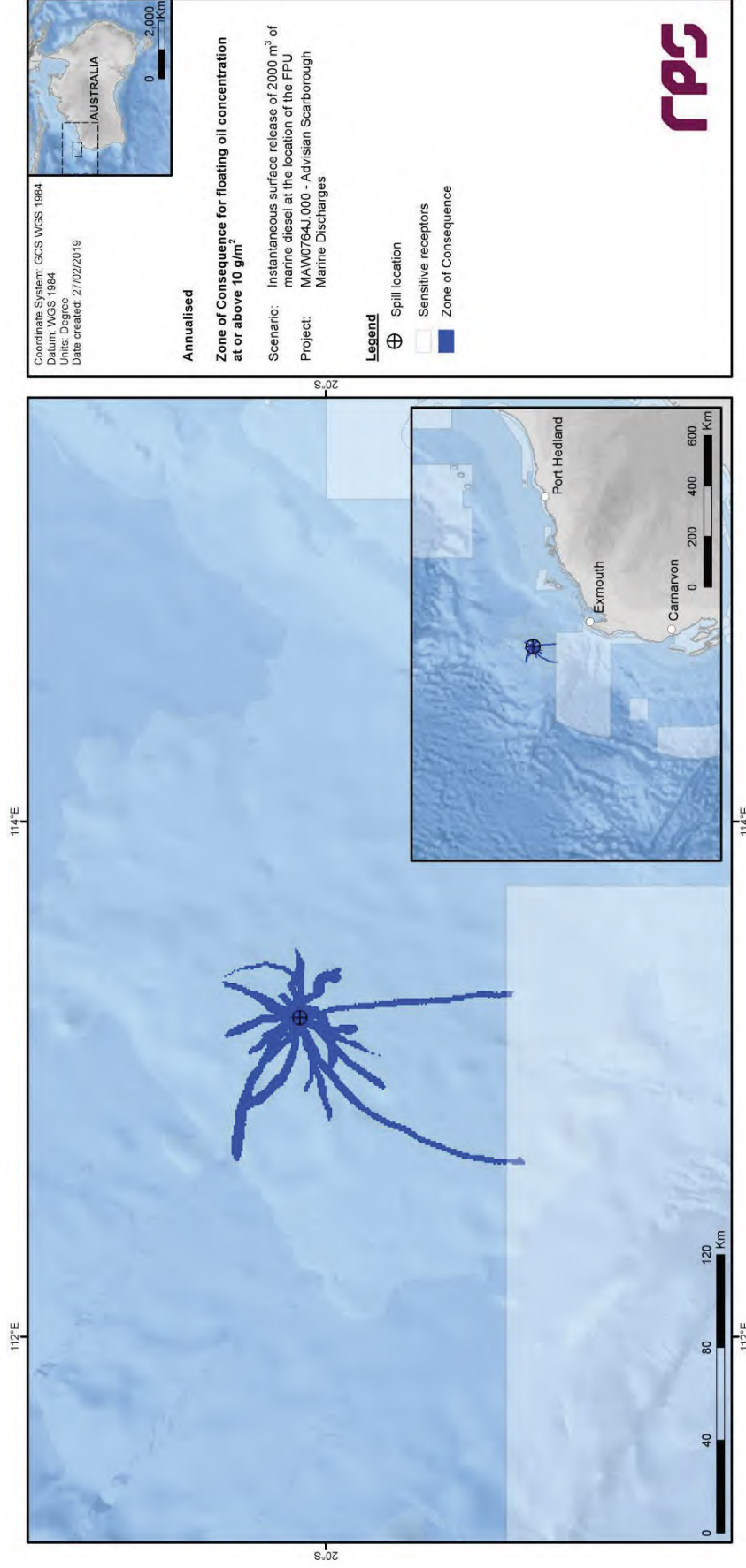
Figure 3.53 Predicted annualised Zone of Consequence of floating oil concentrations at or above 10 g/m² resulting from an instantaneous surface release of marine diesel after a vessel collision at the FPU location.
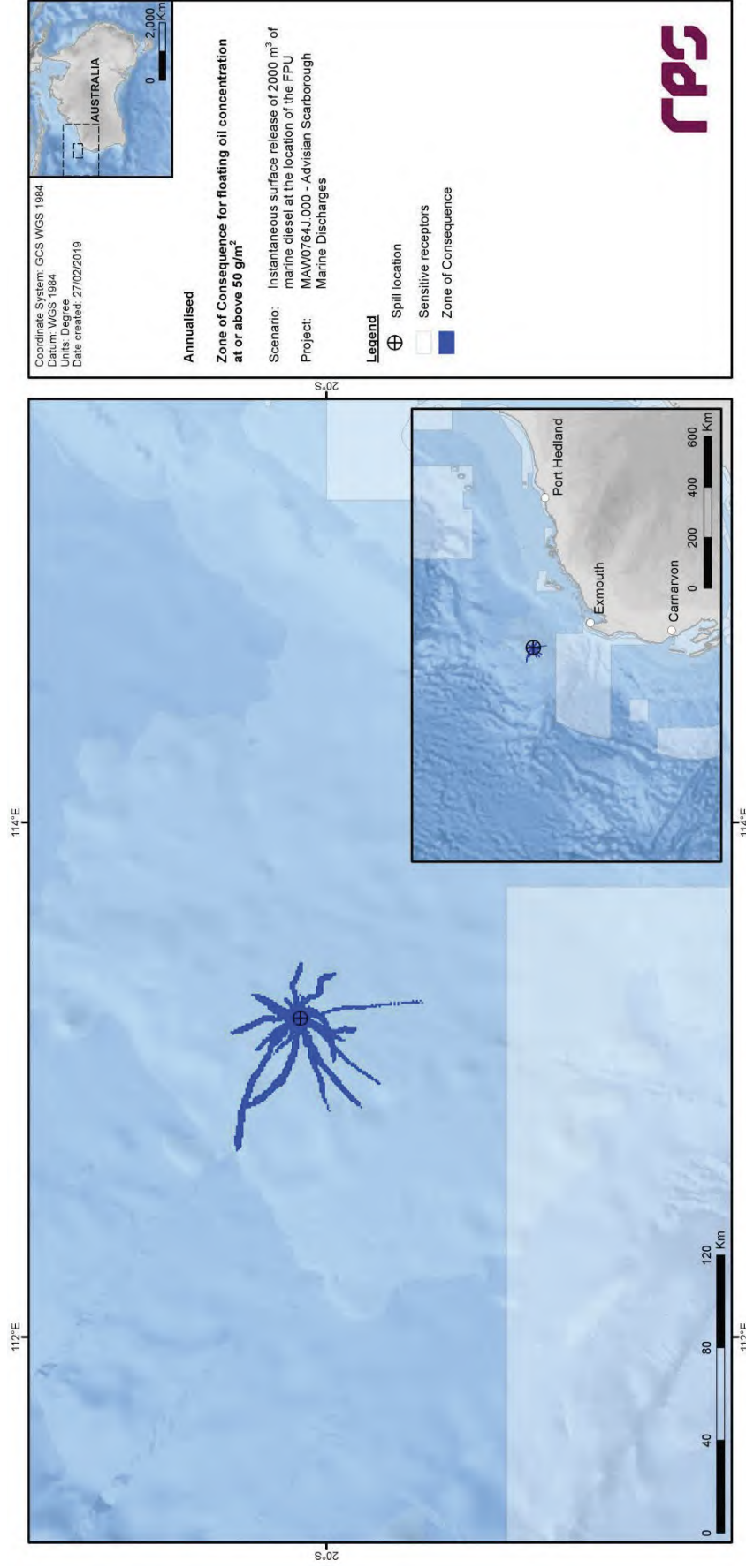
Figure 3.54 Predicted annualised Zone of Consequence of floating oil concentrations at or above 50 g/m² resulting from an instantaneous surface release of marine diesel after a vessel collision at the FPU location.
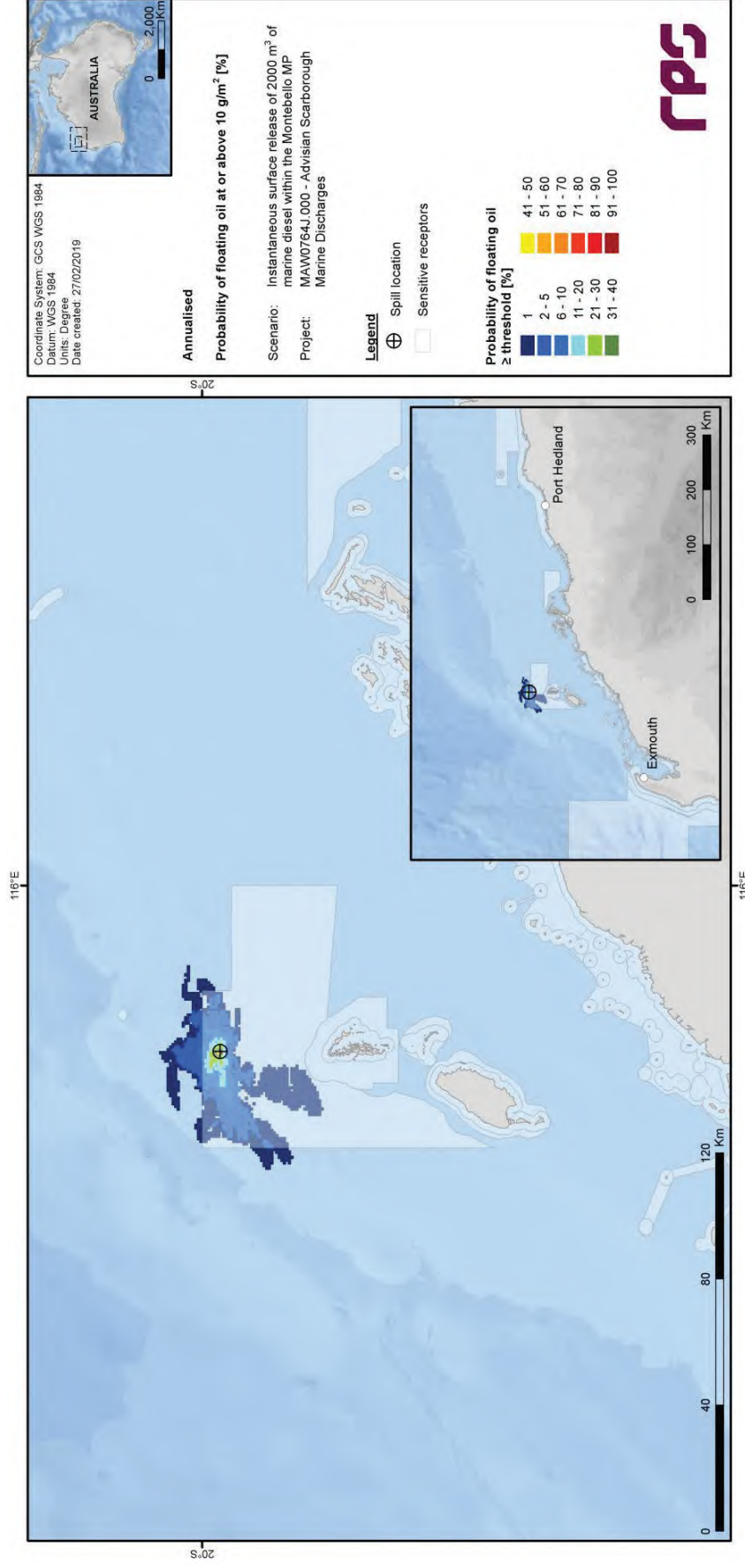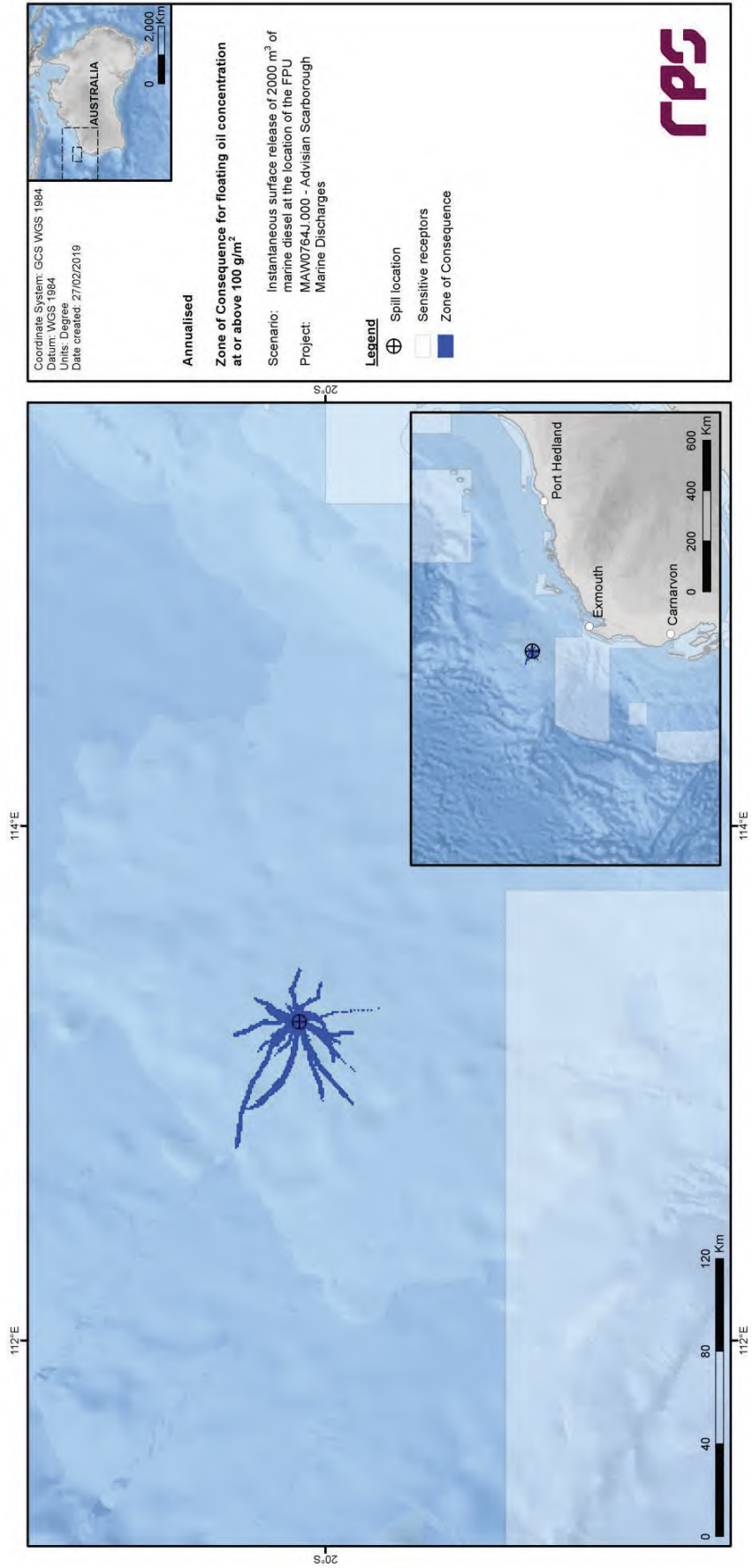
Figure 3.55 **Predicted annualised Zone of Consequence of floating oil concentrations at or above 100 g/m² resulting from an instantaneous surface release of marine diesel after a vessel collision at the FPU location.**
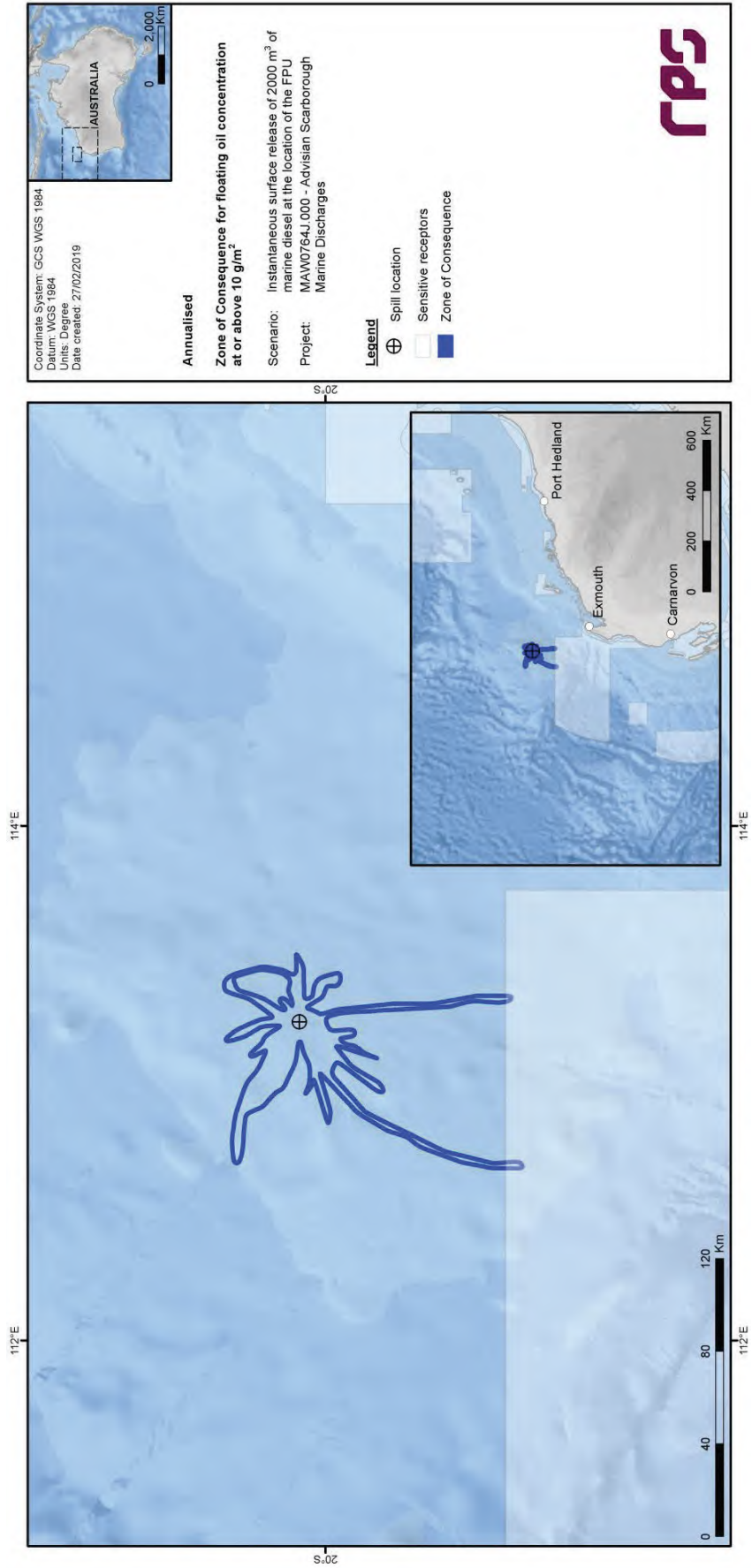
Figure 3.56 Predicted annualised smoothed Zone of Consequence of floating oil concentrations at or above 10 g/m² resulting from an instantaneous surface release of marine diesel after a vessel collision at the FPU location.

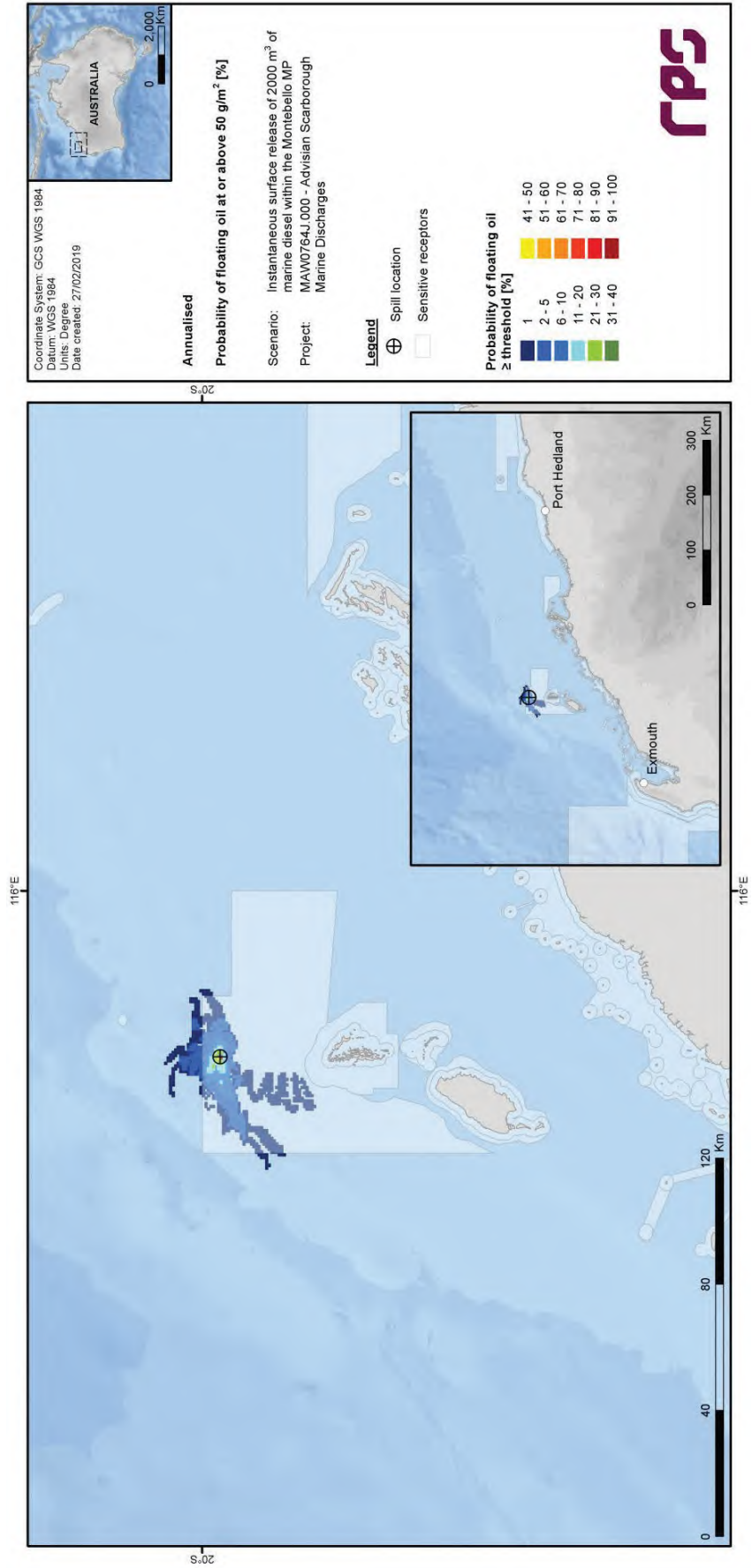**Annualised**

Zone of Consequence for floating oil concentration at or above 50 g/m²

Scenario: Instantaneous surface release of 2000 m³ of marine diesel at the location of the FPU

Project: MAW0764J.000 - Advisian Scarborough Marine Discharges

Legend

⊕ Spill location

▢ Sensitive receptors

▮ Zone of Consequence
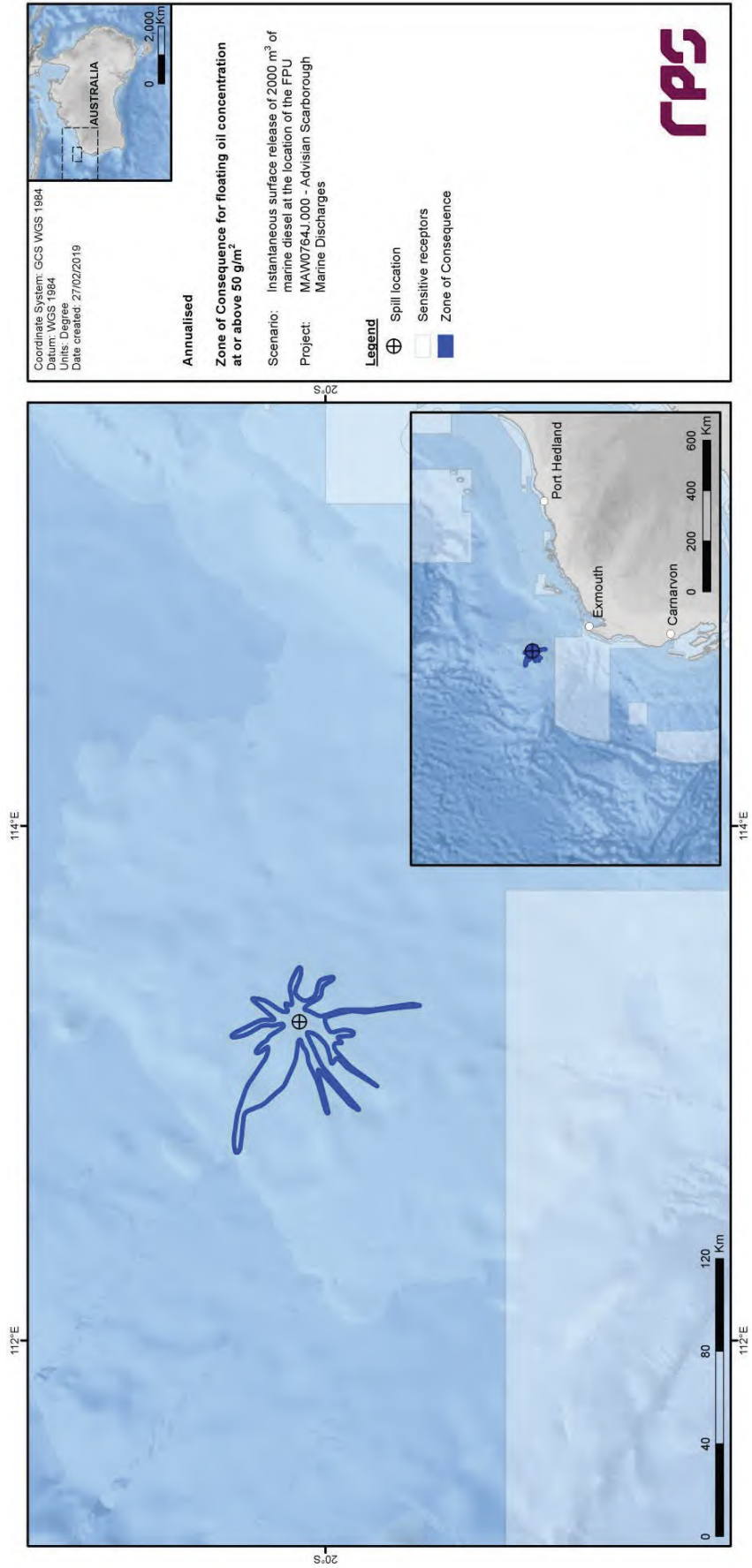
Figure 3.57 Predicted annualised smoothed Zone of Consequence of floating oil concentrations at or above 50 g/m² resulting from an instantaneous surface release of marine diesel after a vessel collision at the FPU location.
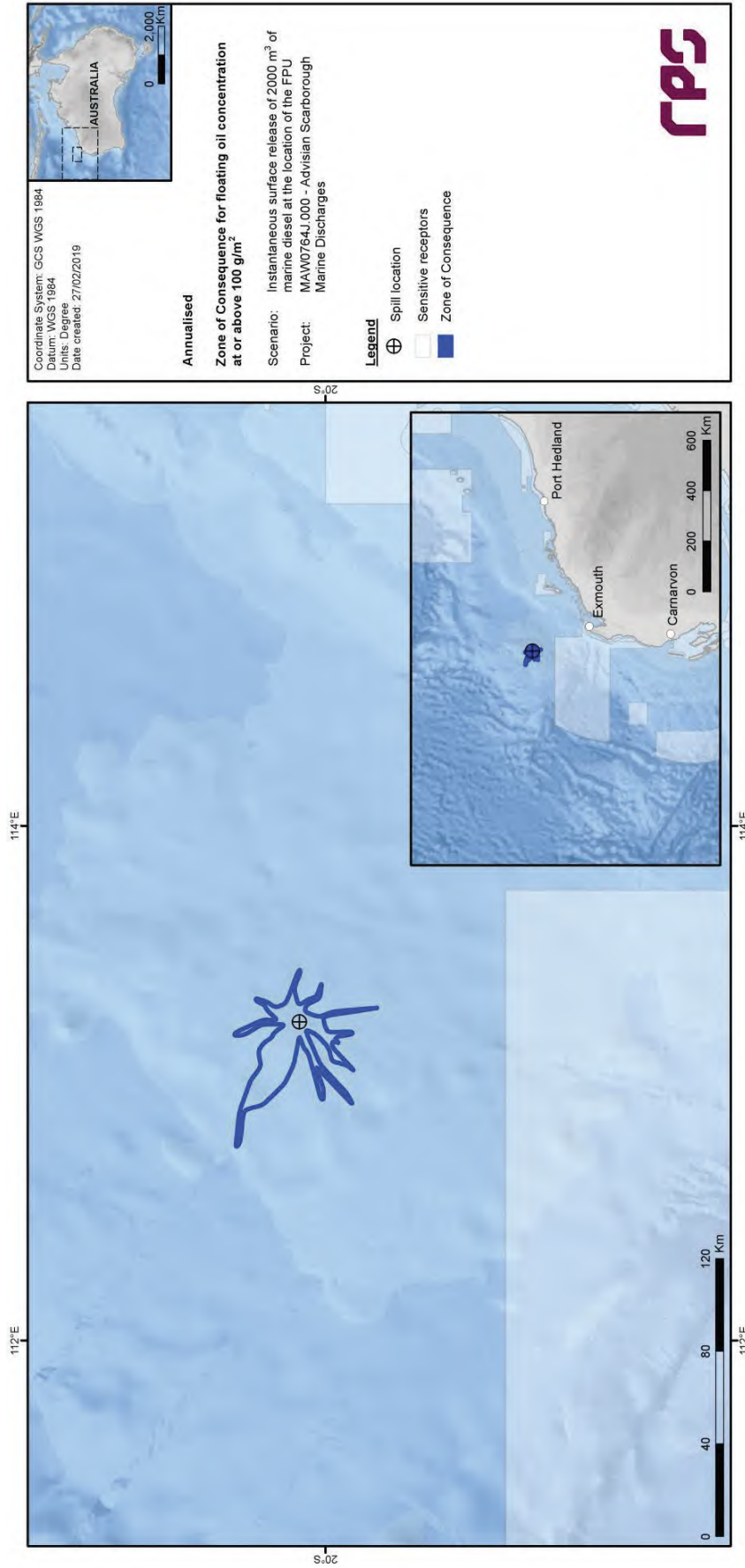
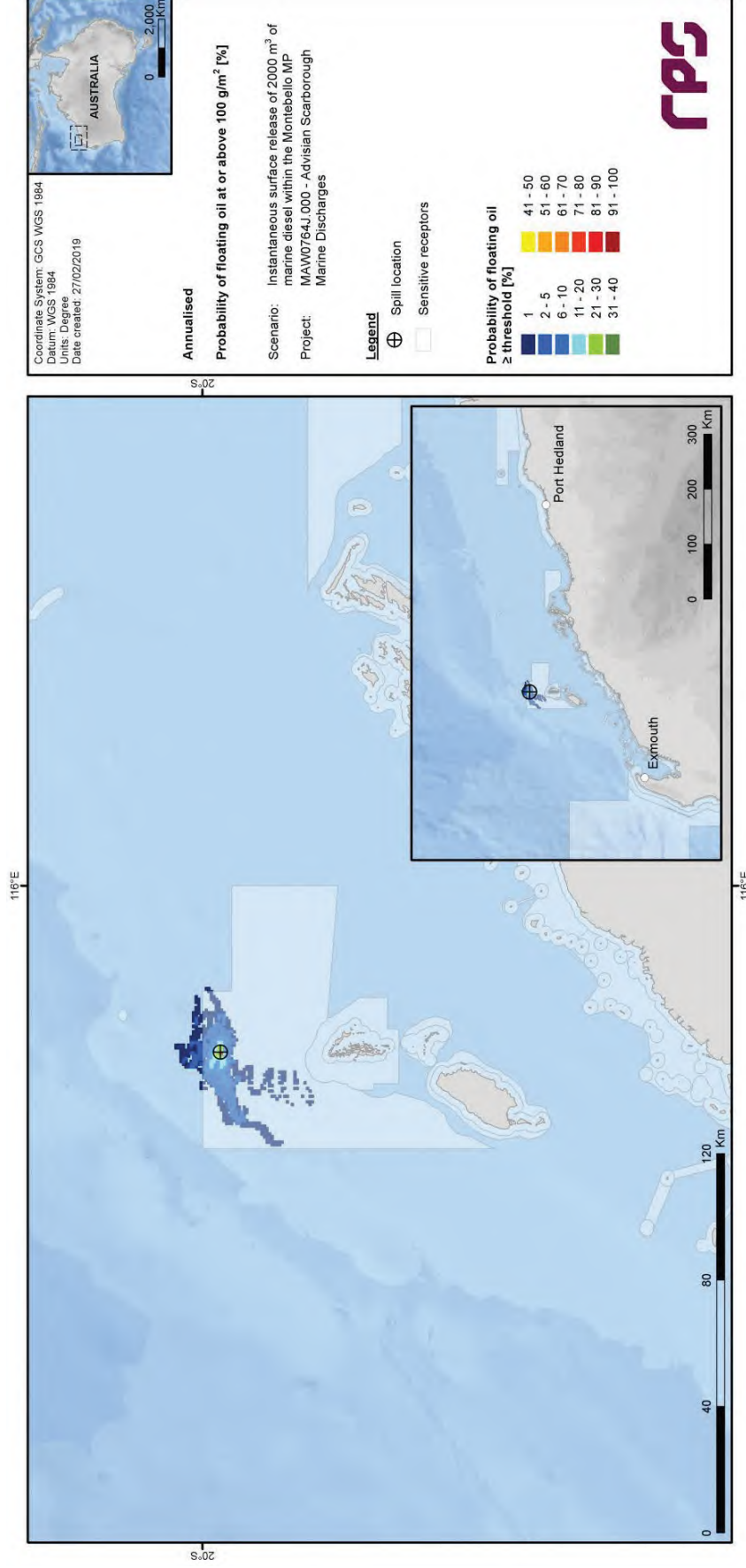**Figure 3.58 Predicted annualised smoothed Zone of Consequence of floating oil concentrations at or above 100 g/m² resulting from an instantaneous surface release of marine diesel after a vessel collision at the FPU location.**
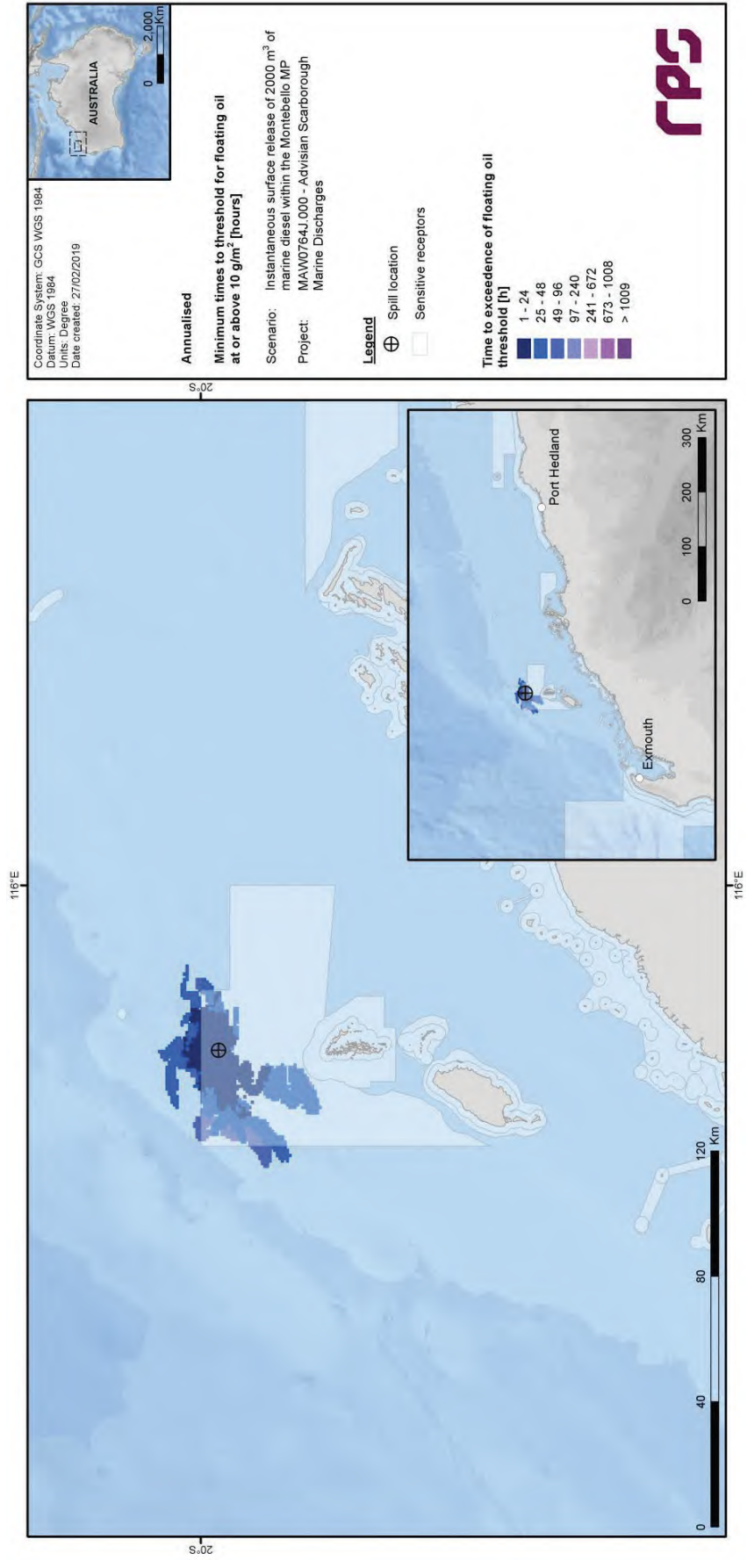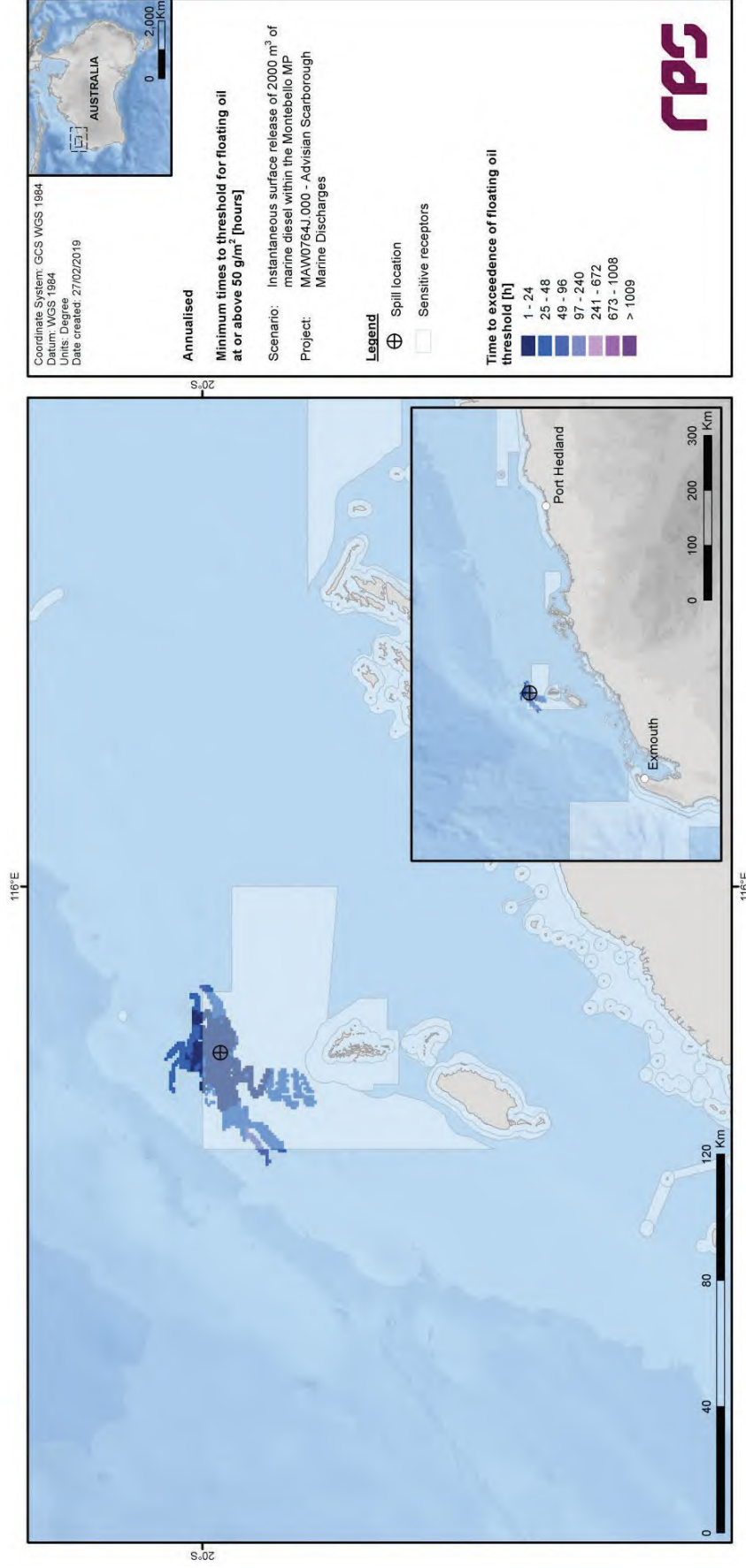
Legend

⊕ Spill location

Sensitive receptors

Zone of Consequence

Annualised

Zone of Consequence for floating oil concentration at or above 100 g/m²

Scenario: Instantaneous surface release of 2000 m³ of marine diesel at the location of the FPU

Project: MAW0764J.000 - Advisian Scarborough Marine Discharges

Coordinate System: GCS WGS 1984
Datum: WGS 1984
Units: Degree
Date created: 27/02/2019

3.4.2.2 Entrained Oil

Table 3.8 **Expected annualised entrained oil outcomes at sensitive receptors resulting from an instantaneous surface release of marine diesel after a vessel collision at the FPU location.**

Receptor	Probability (%) of entrained oil concentration ≥500 ppb	Minimum time to receptor (hours) for entrained oil at ≥500 ppb	Maximum entrained oil concentration (ppb) averaged over all replicate simulations	Maximum entrained oil concentration (ppb), at any depth, in the worst replicate simulation
Ningaloo Coast North WHA	<1	NC	<1	52
Ningaloo RUZ	<1	NC	<1	52
Abrolhos Islands MP	<1	NC	2	167
Carnarvon Canyon MP	<1	NC	3	196
Gascoyne MP	8	62	185	7,236

NC: No contact to receptor predicted for specified threshold.

* Probabilities and maximum concentrations calculated at depth of submerged feature.
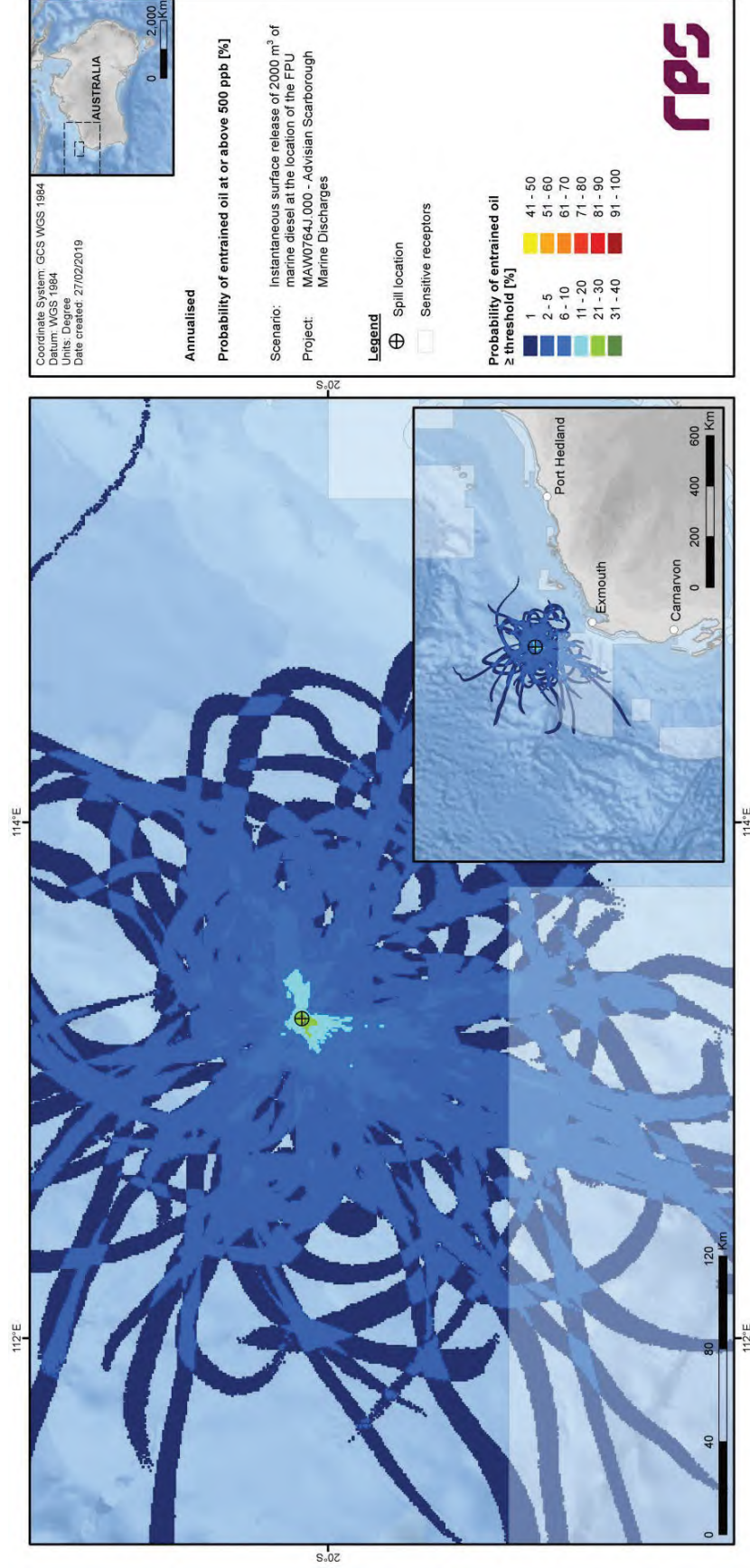
Figure 3.59 Predicted annualised probability of entrained oil concentrations at or above 500 ppb resulting from an instantaneous surface release of marine diesel after a vessel collision at the FPU location.
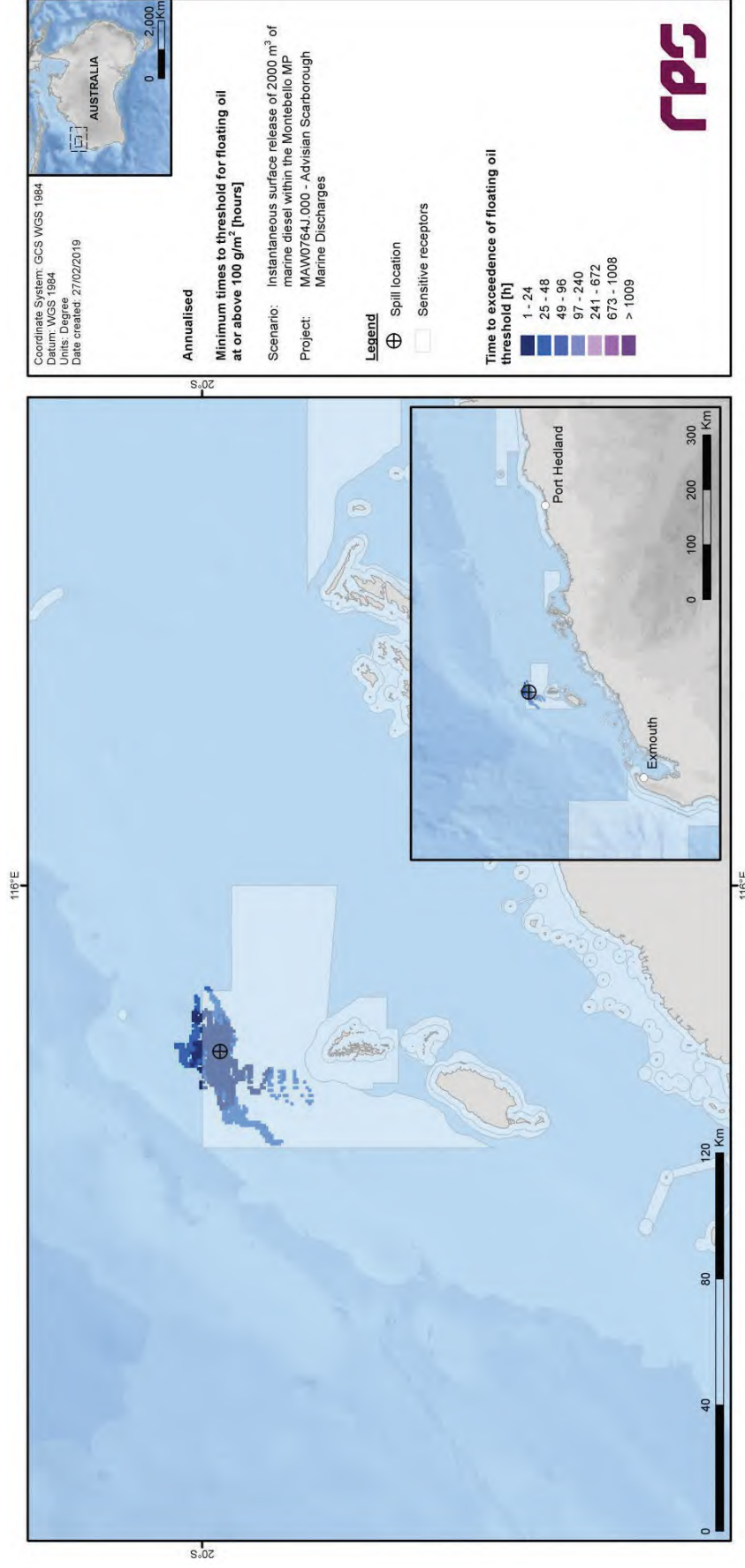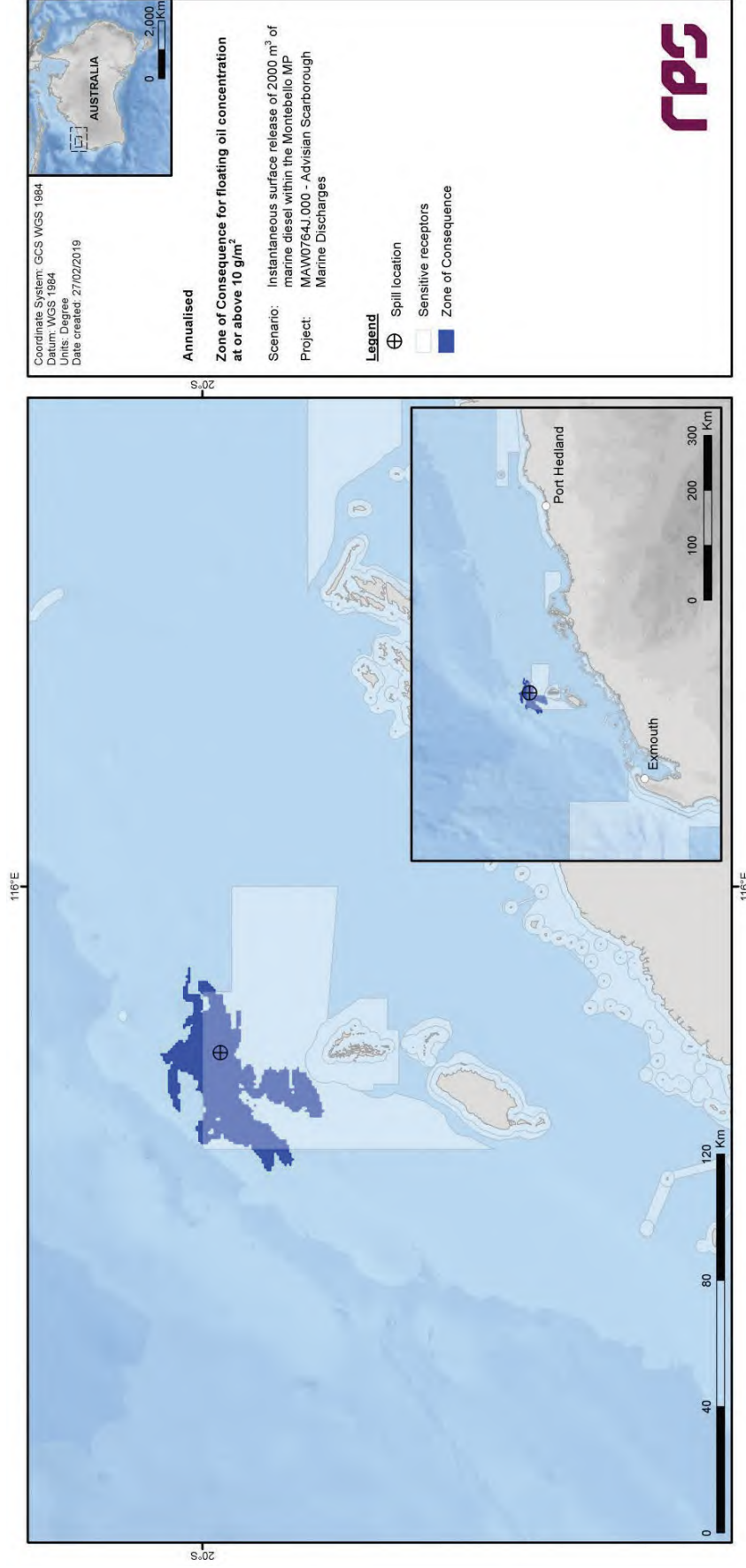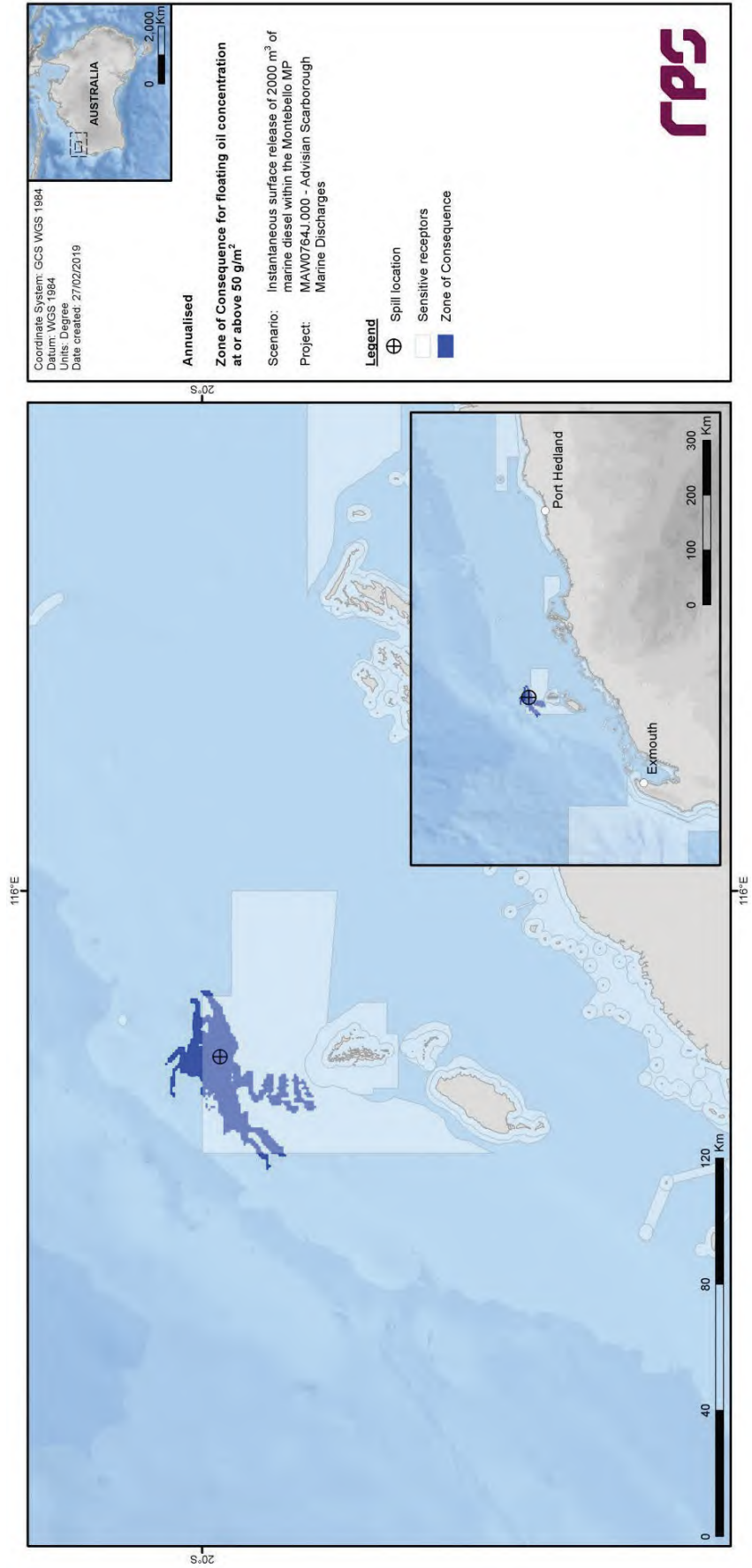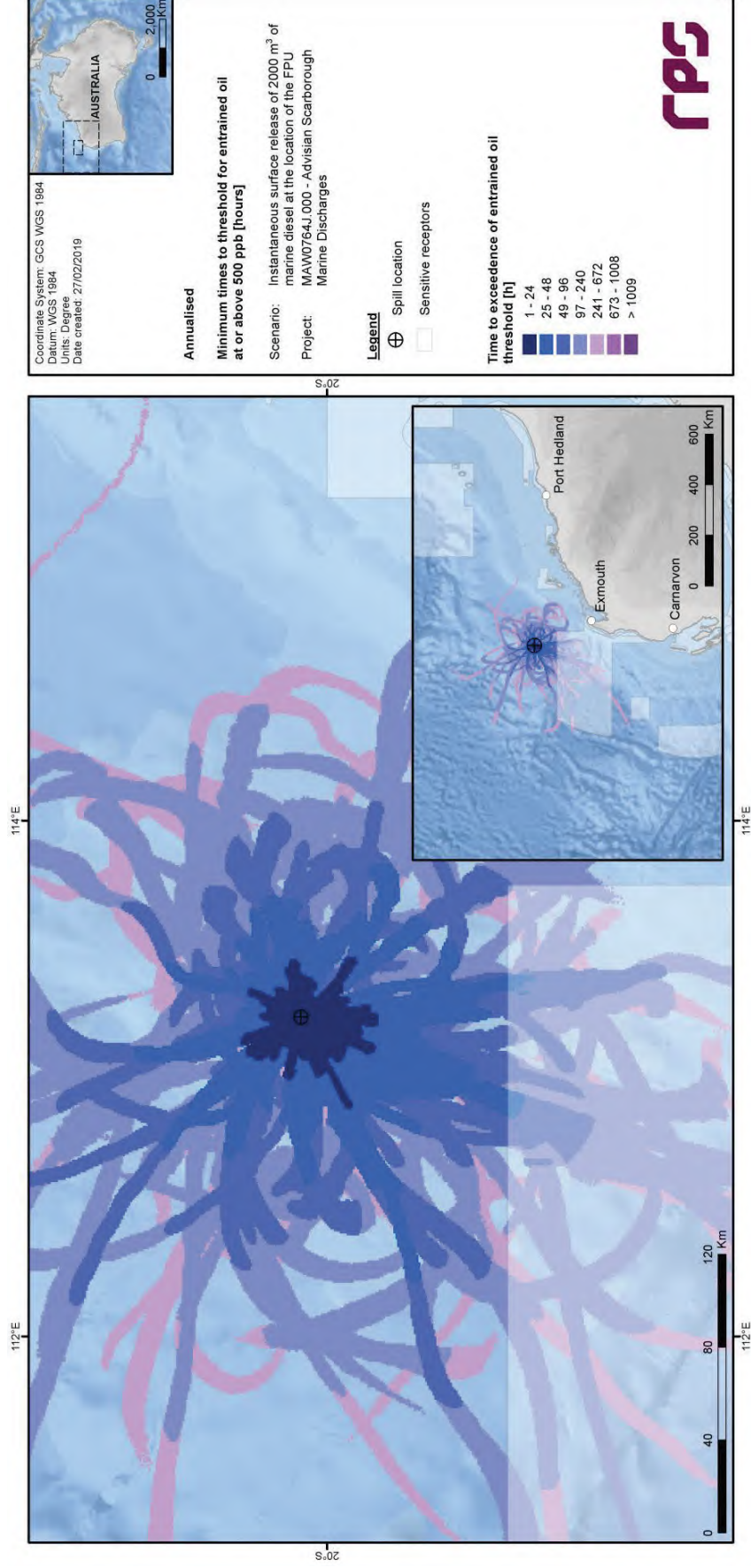
Figure 3.60 **Predicted annualised minimum times to contact by entrained oil concentrations at or above 500 ppb resulting from an instantaneous surface release of marine diesel after a vessel collision at the FPU location.**
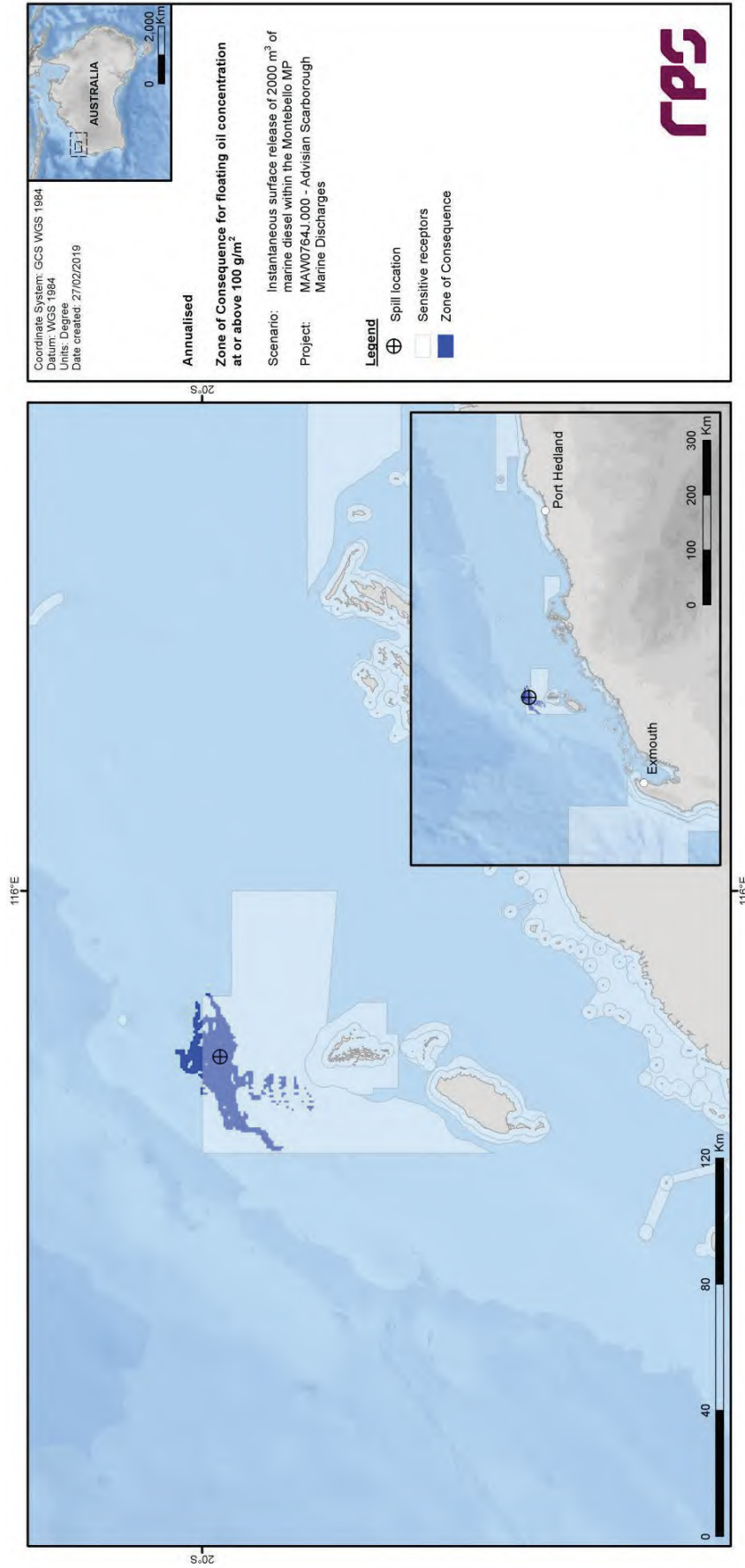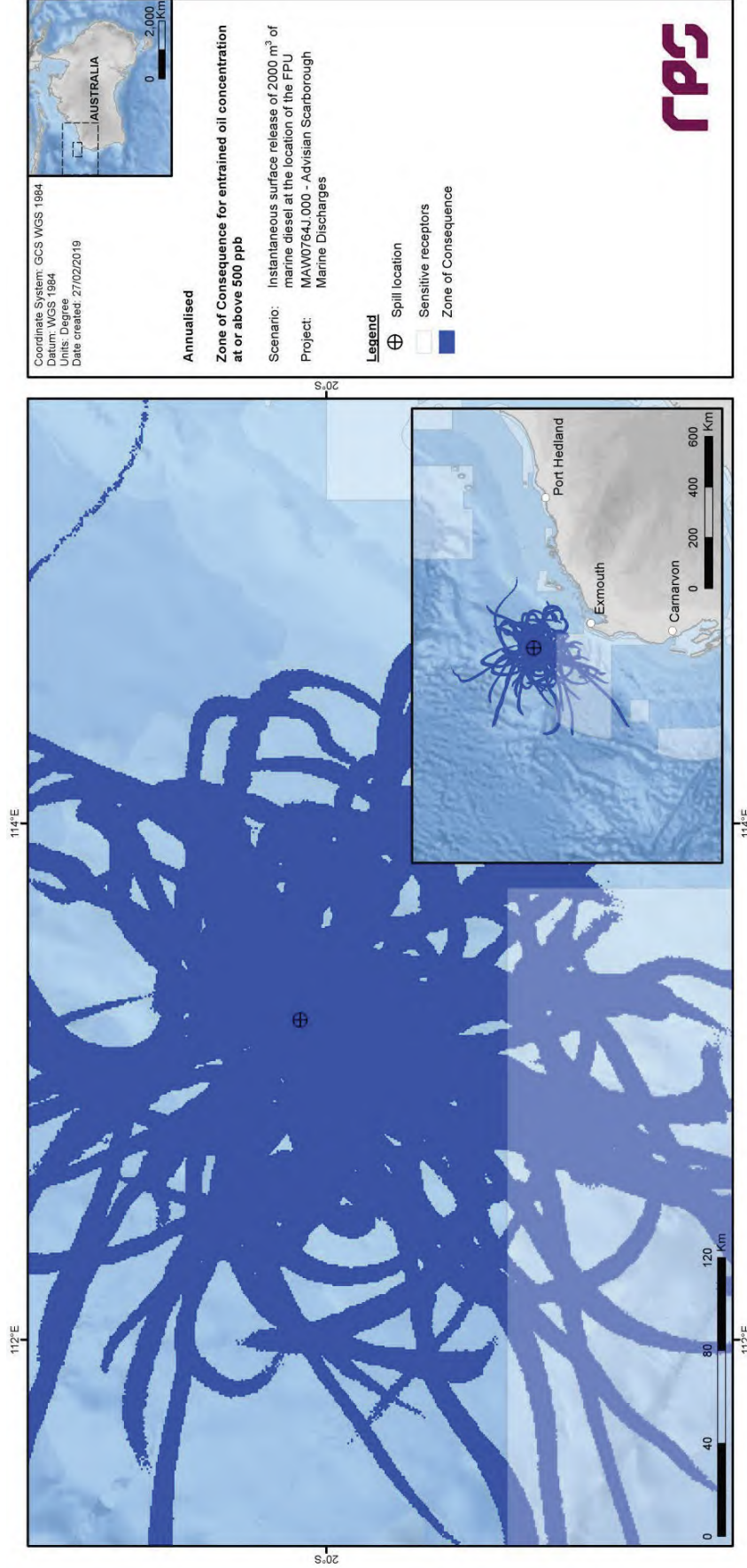
Figure 3.61 Predicted annualised Zone of Consequence of entrained oil concentrations at or above 500 ppb resulting from an instantaneous surface release of marine diesel after a vessel collision at the FPU location.
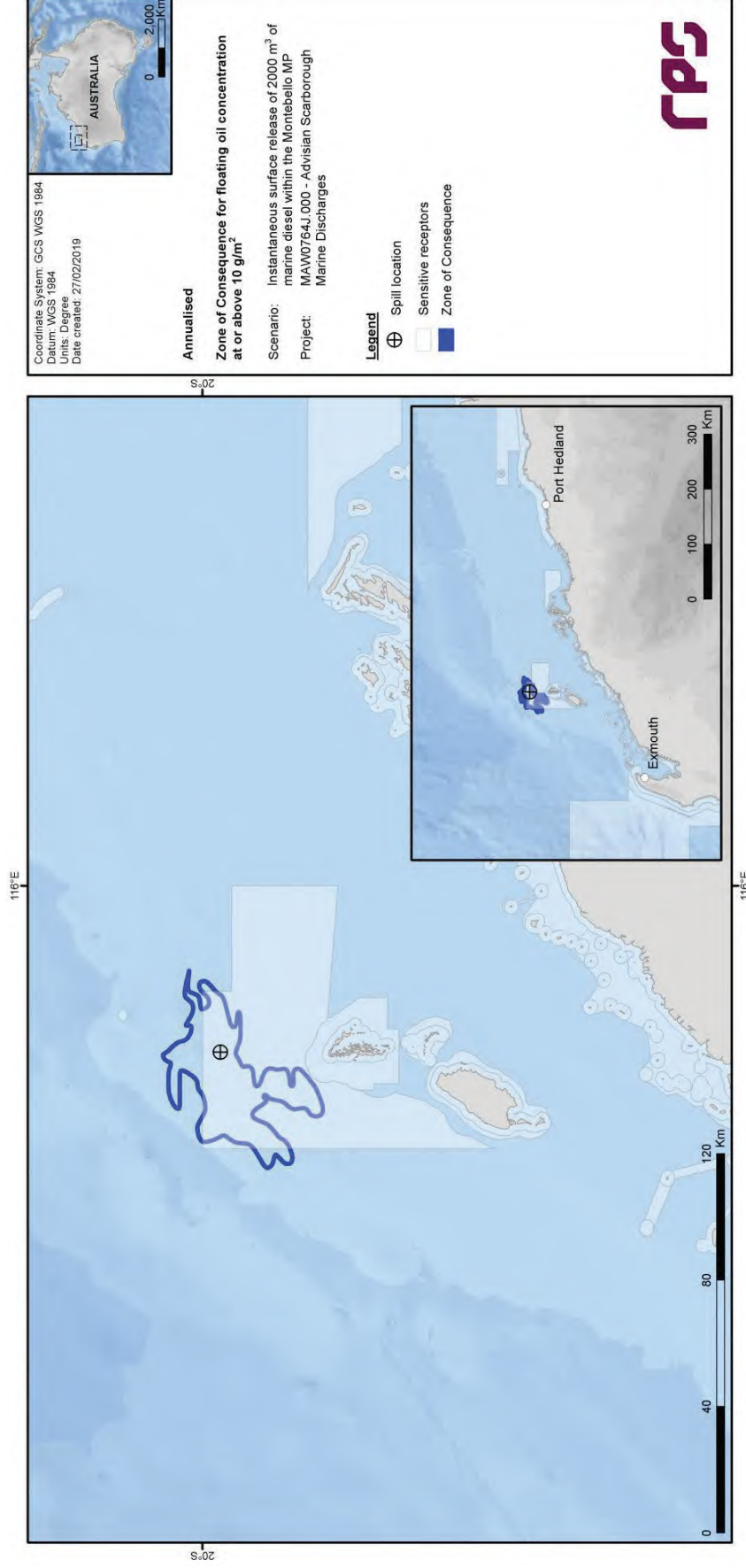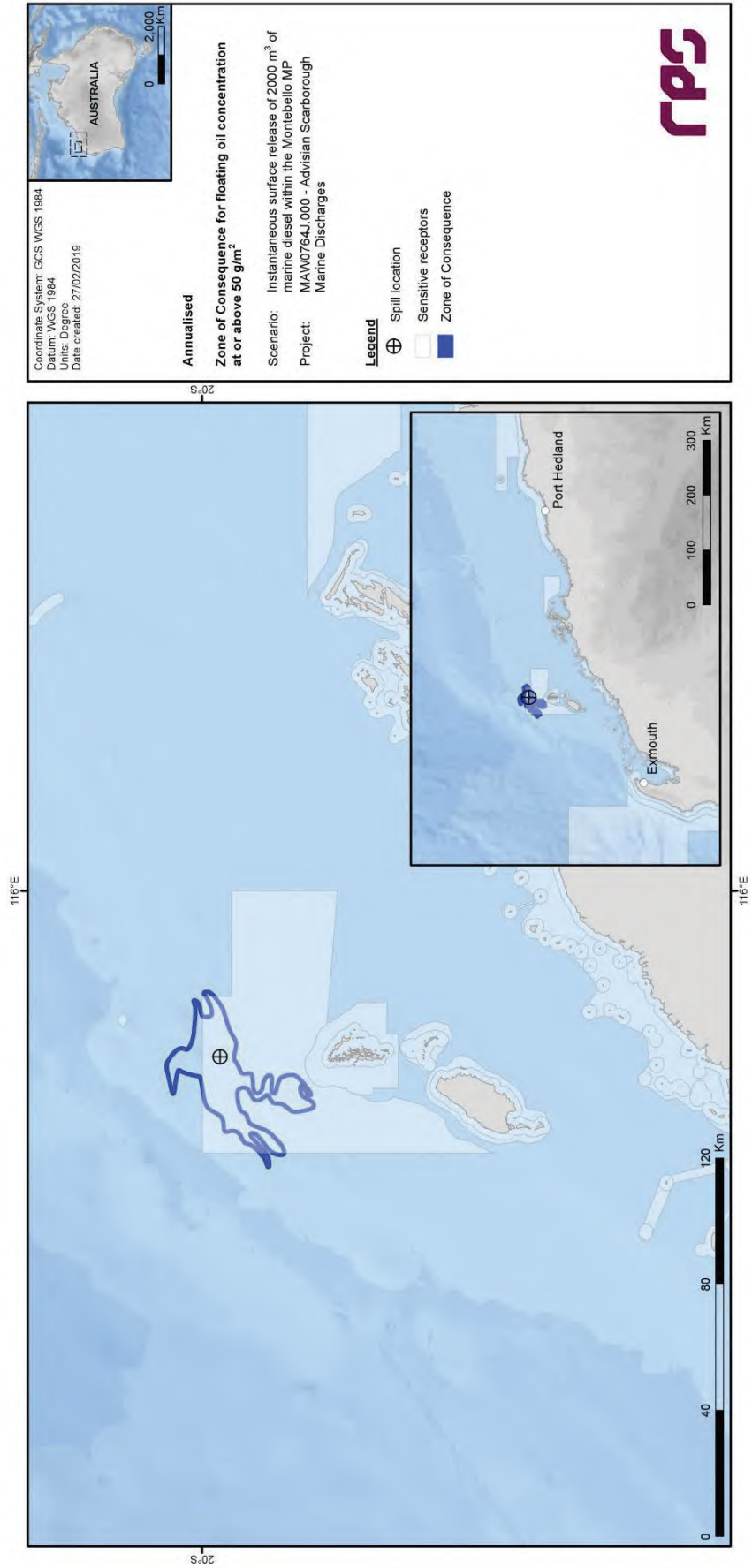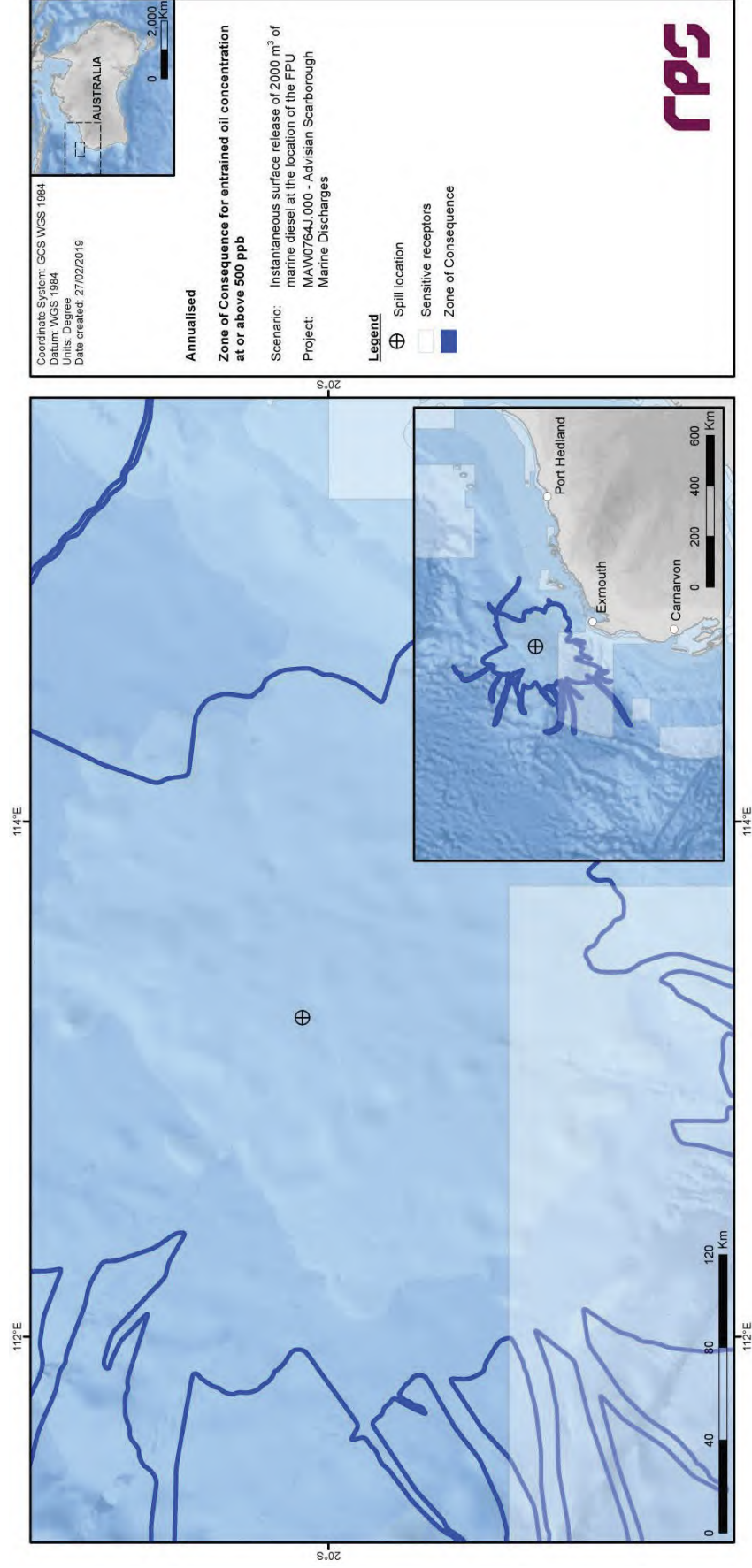
Figure 3.62 Predicted annualised smoothed Zone of Consequence of entrained oil concentrations at or above 500 ppb resulting from an instantaneous surface release of marine diesel after a vessel collision at the FPU location.

Maximum entrained oil concentration (ppb)
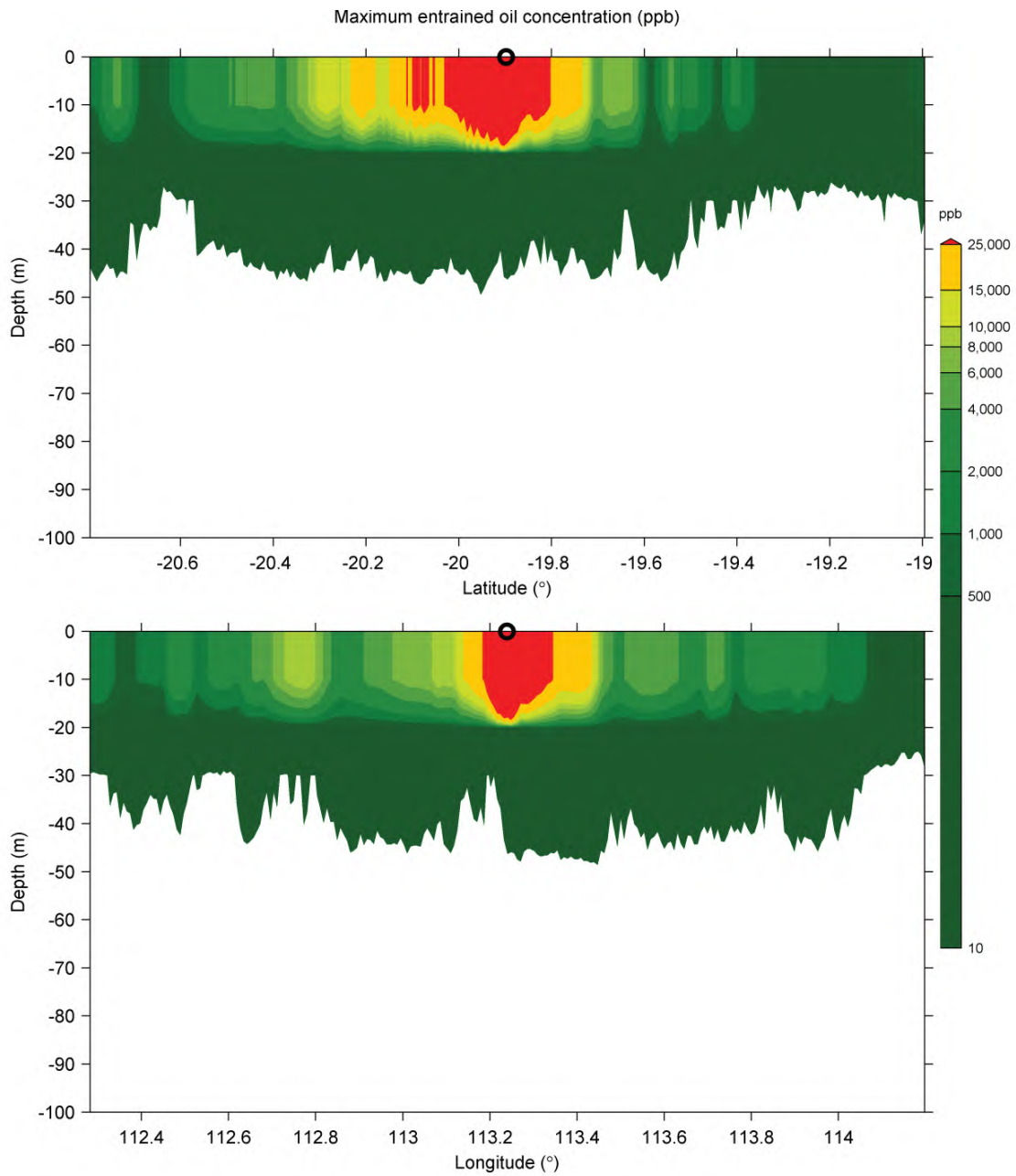
Figure 3.63 Cross-section transects of predicted annualised maximum entrained oil concentrations for an instantaneous surface release of marine diesel after a vessel collision at the FPU location. Transect locations are shown in Figure 3.1.

3.4.2.3 Dissolved Aromatic Hydrocarbons

Table 3.9 **Expected annualised dissolved aromatic hydrocarbon outcomes at sensitive receptors resulting from an instantaneous surface release of marine diesel after a vessel collision at the FPU location.**

Receptor	Probability (%) of dissolved aromatic hydrocarbon concentration ≥500 ppb	Maximum dissolved aromatic hydrocarbon concentration (ppb) averaged over all replicate simulations	Maximum dissolved aromatic hydrocarbon concentration (ppb), at any depth, in the worst replicate simulation
Ningaloo Coast North WHA	<1	<1	2
Ningaloo RUZ	<1	<1	3
Abrolhos Islands MP	<1	<1	<1
Carnarvon Canyon MP	<1	<1	6
Gascoyne MP	<1	6	462

NC: No contact to receptor predicted for specified threshold.

* Probabilities and maximum concentrations calculated at depth of submerged feature.
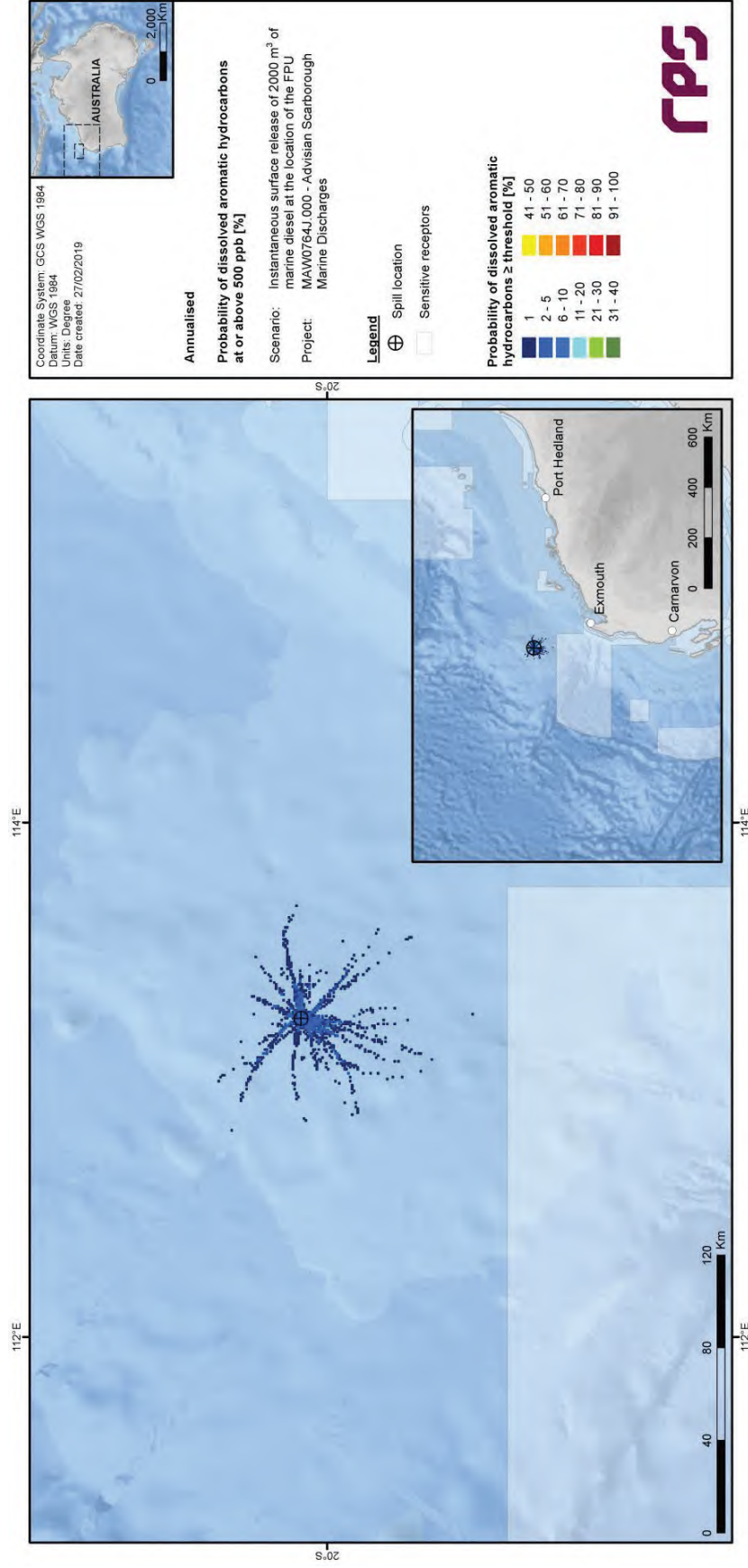
Figure 3.64 Predicted annualised probability of dissolved aromatic hydrocarbon concentrations at or above 500 ppb resulting from an instantaneous surface release of marine diesel after a vessel collision at the FPU location.
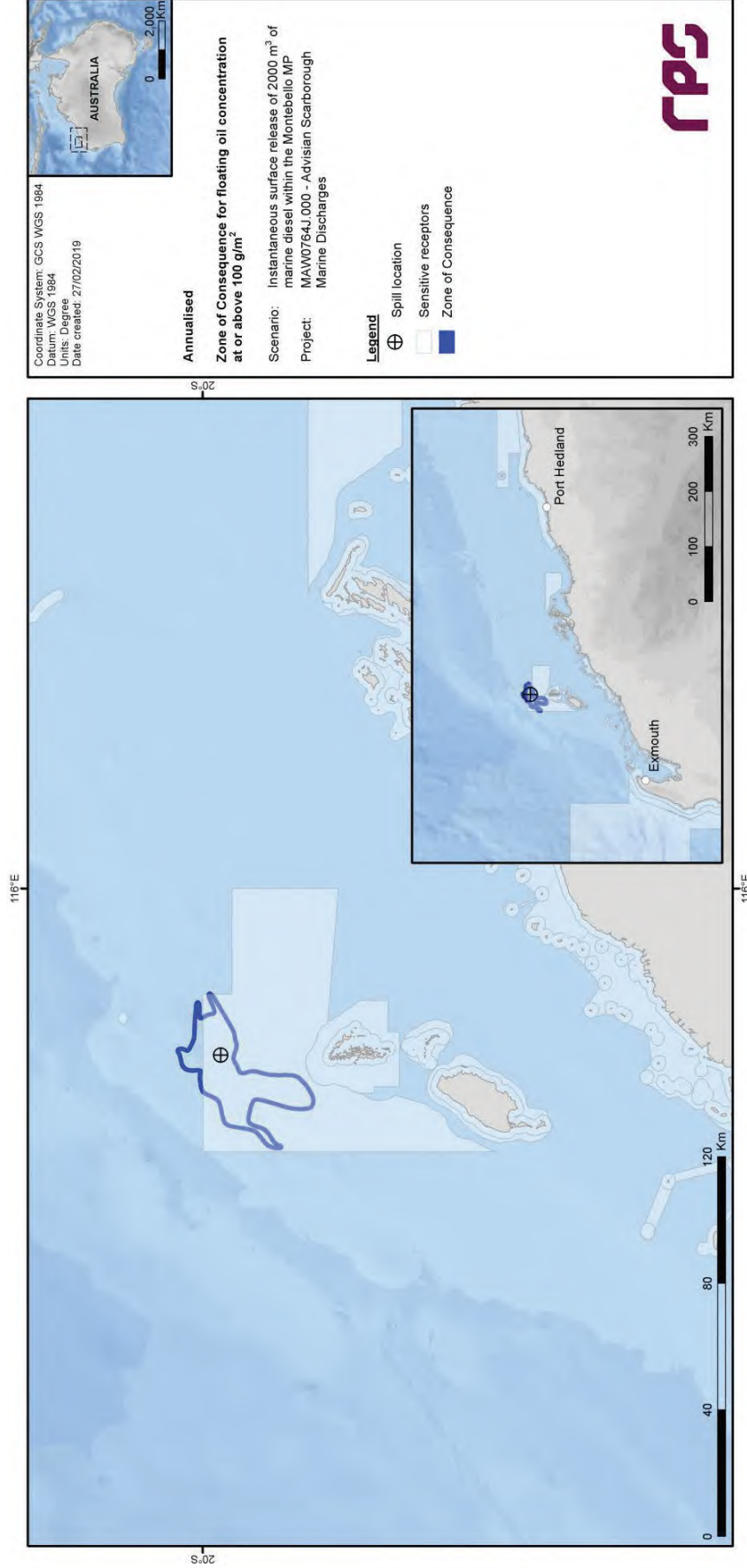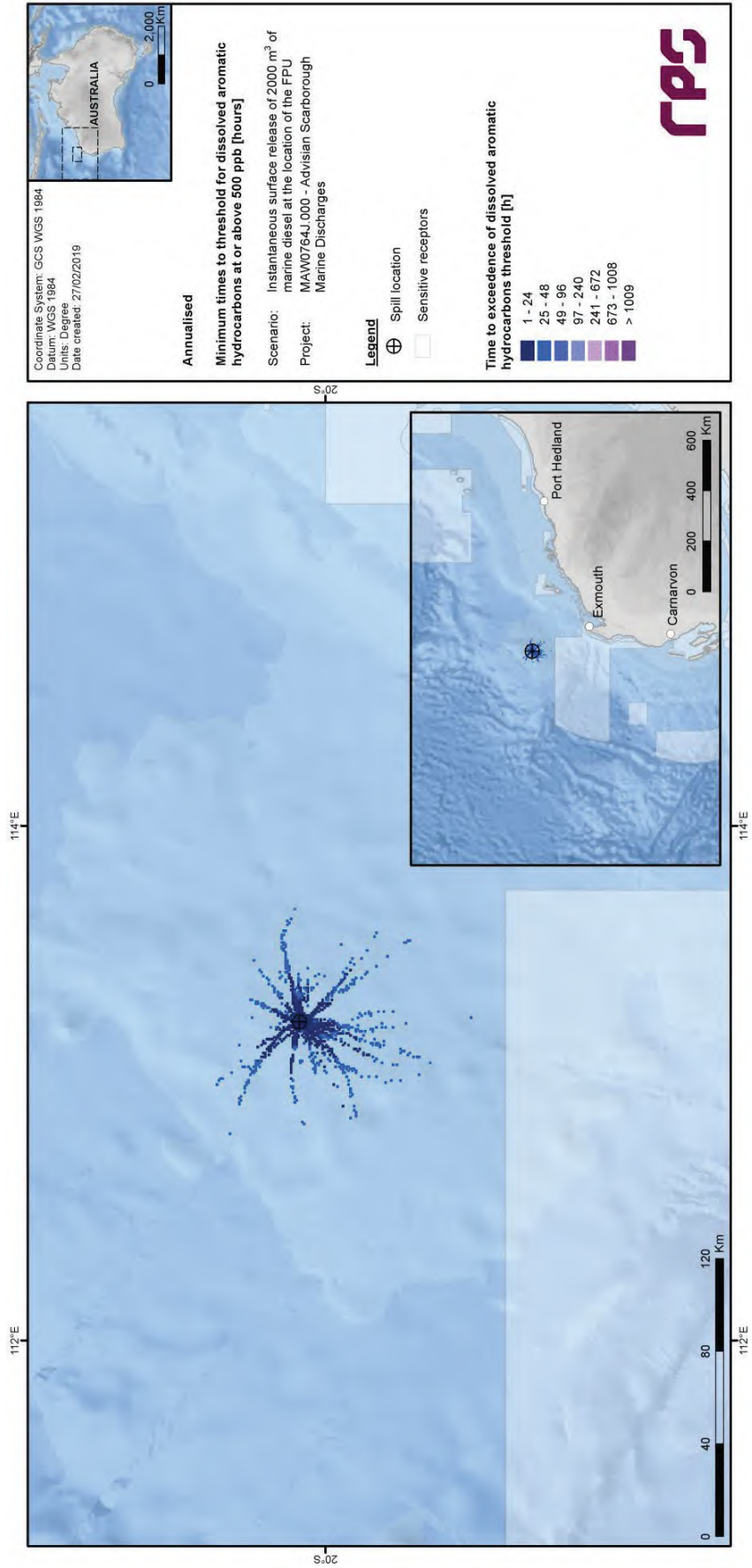
Figure 3.65 Predicted annualised minimum times to contact by dissolved aromatic hydrocarbon concentrations at or above 500 ppb resulting from an instantaneous surface release of marine diesel after a vessel collision at the FPU location.
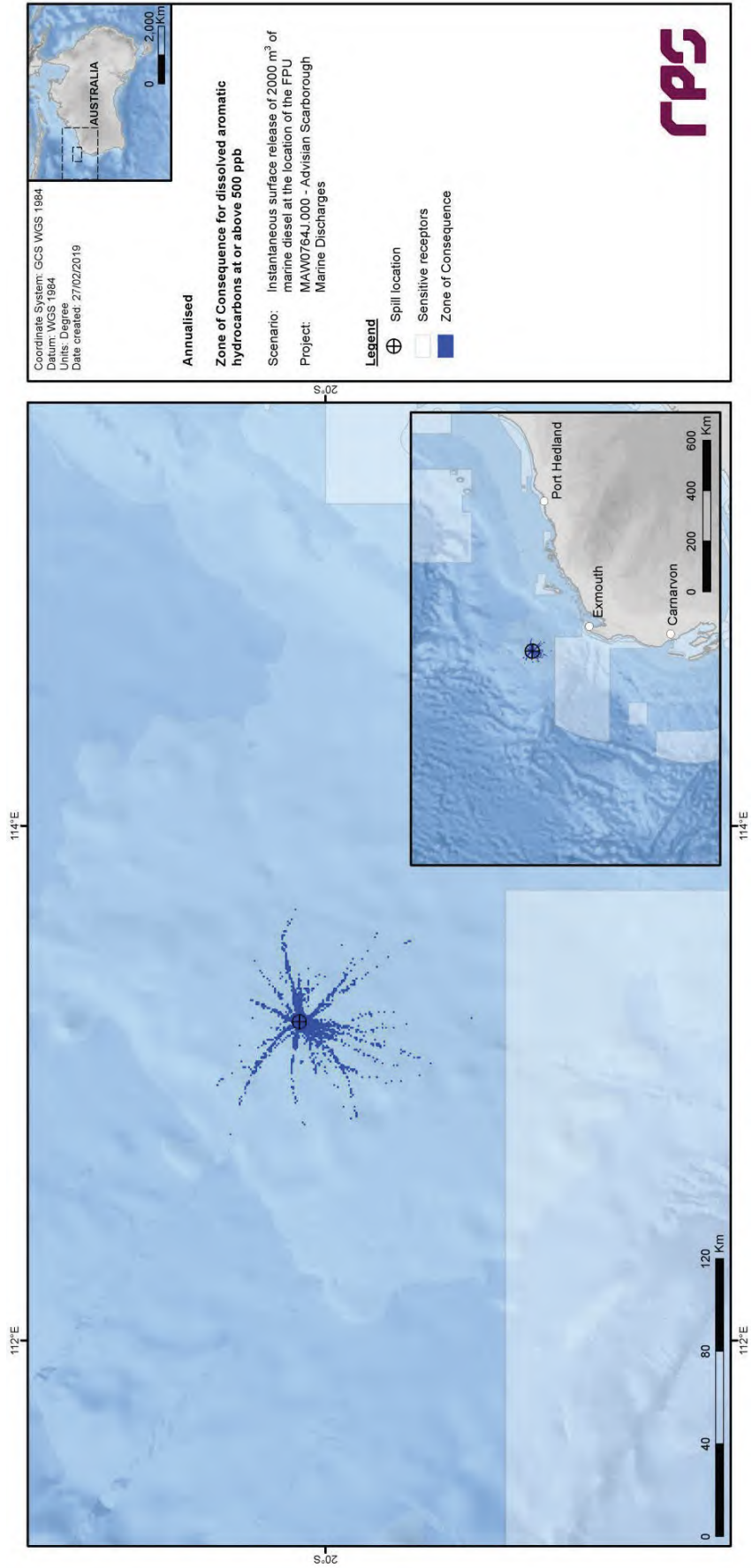
Figure 3.66 Predicted annualised Zone of Consequence of dissolved aromatic hydrocarbon concentrations at or above 500 ppb resulting from an instantaneous surface release of marine diesel after a vessel collision at the FPU location.
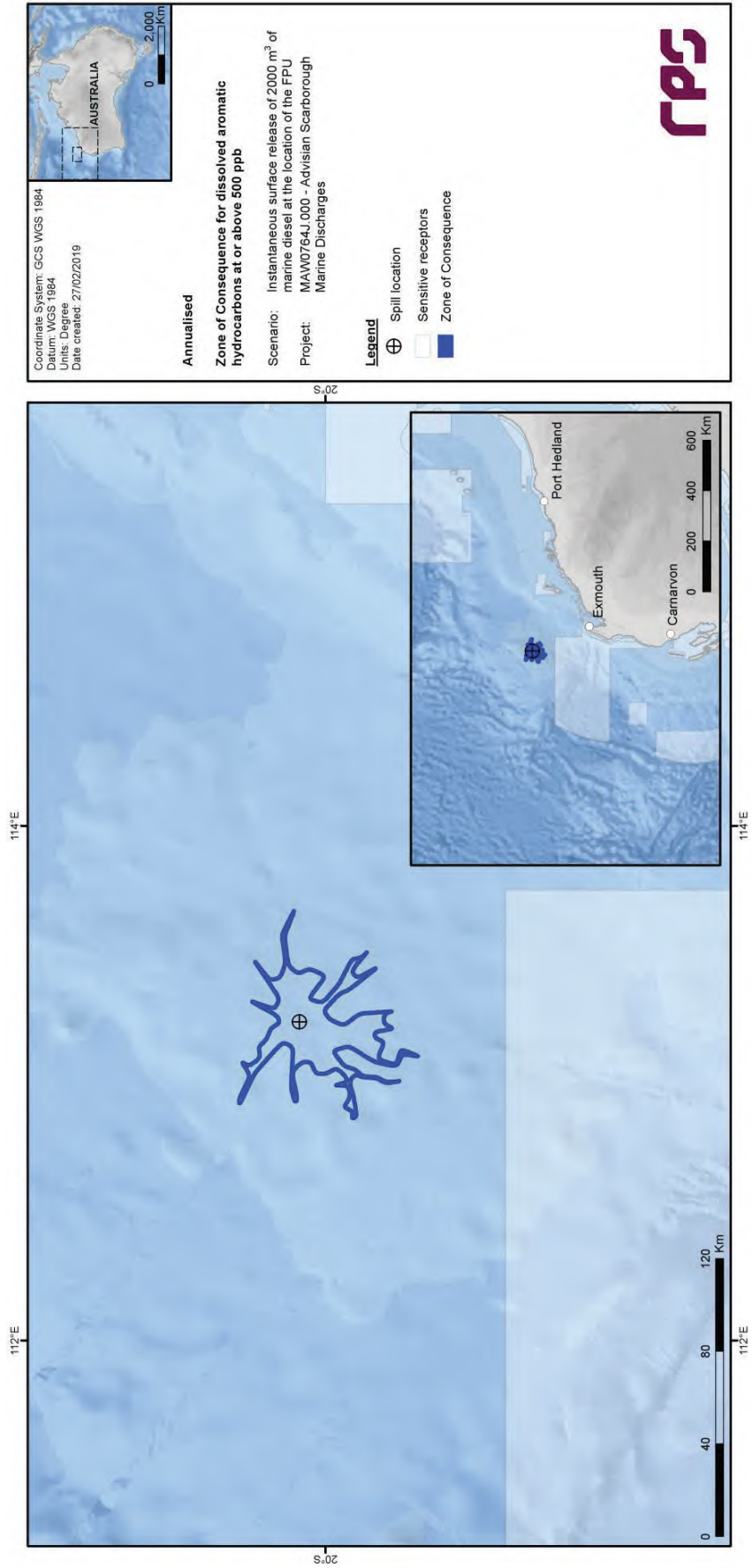
Figure 3.67 Predicted annualised smoothed Zone of Consequence of dissolved aromatic hydrocarbon concentrations at or above 500 ppb resulting from an instantaneous surface release of marine diesel after a vessel collision at the FPU location.

Maximum dissolved aromatic hydrocarbon concentration (ppb)
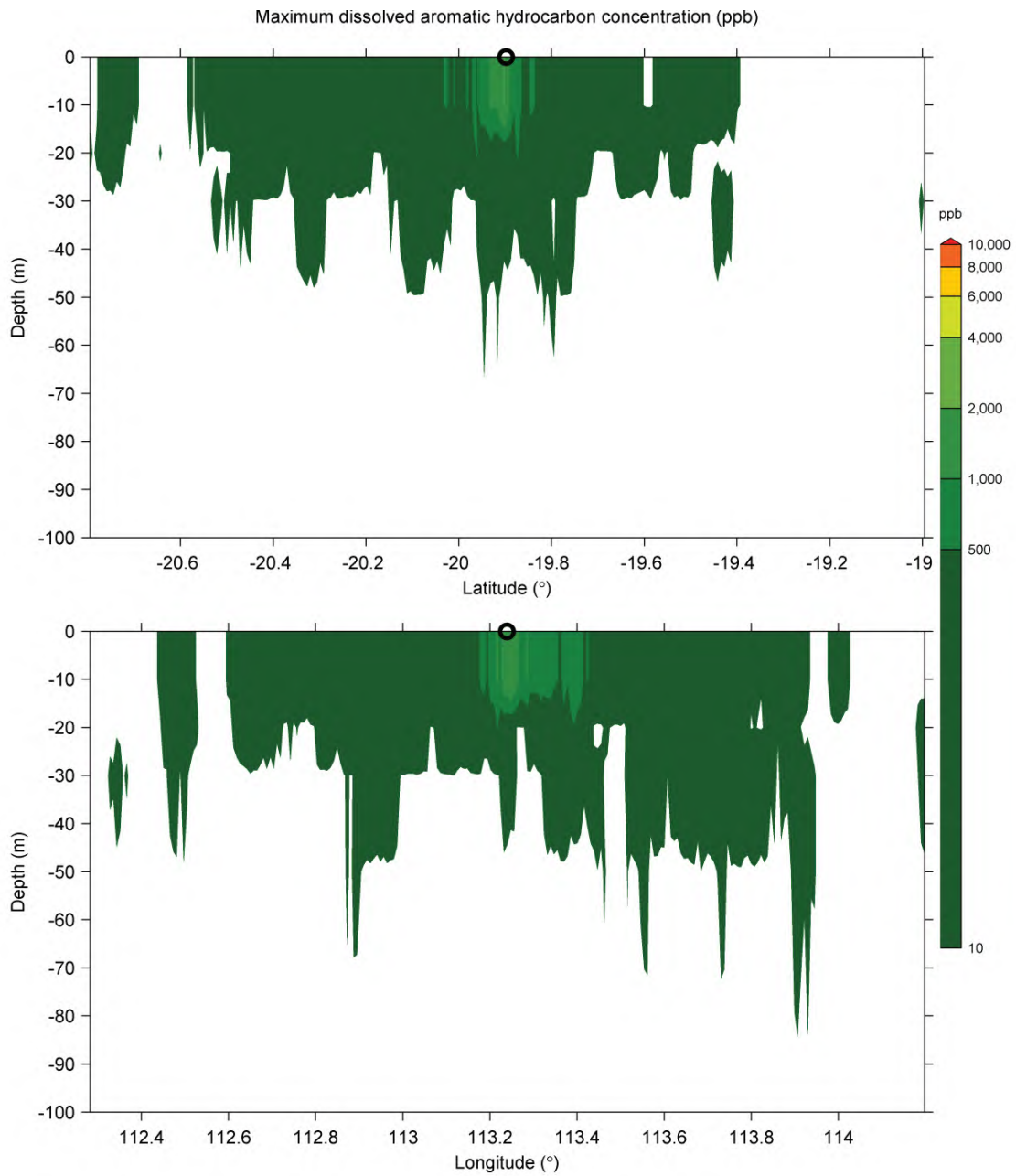
Figure 3.68 Cross-section transects of predicted annualised maximum dissolved aromatic hydrocarbon concentrations for an instantaneous surface release of marine diesel after a vessel collision at the FPU location. Transect locations are shown in Figure 3.1.

4 DETERMINISTIC ASSESSMENT RESULTS

4.1 Overview

For each scenario, deterministic model runs of interest were selected from the stochastic set of replicate simulations according to the following criteria:

- Maximum distance in a south-westerly direction from the release site reached by entrained oil (at a threshold of 500 ppb);

- Maximum total area covered by entrained oil (at a threshold of 500 ppb) over the course of a simulation.

A time series compilation of figures from each deterministic replicate simulation (i.e. a single spill event) for each scenario is presented in the following sections. Each of the figure compilations includes areal exposure at discrete time intervals during the simulation.

4.2 Scenario 1: Short-Term (Instantaneous) Surface Release of Marine Diesel after a Vessel Collision outside Mermaid Sound

4.2.1 Simulation with Maximal South-Westerly Extent of Entrained Oil at the 500 ppb Threshold
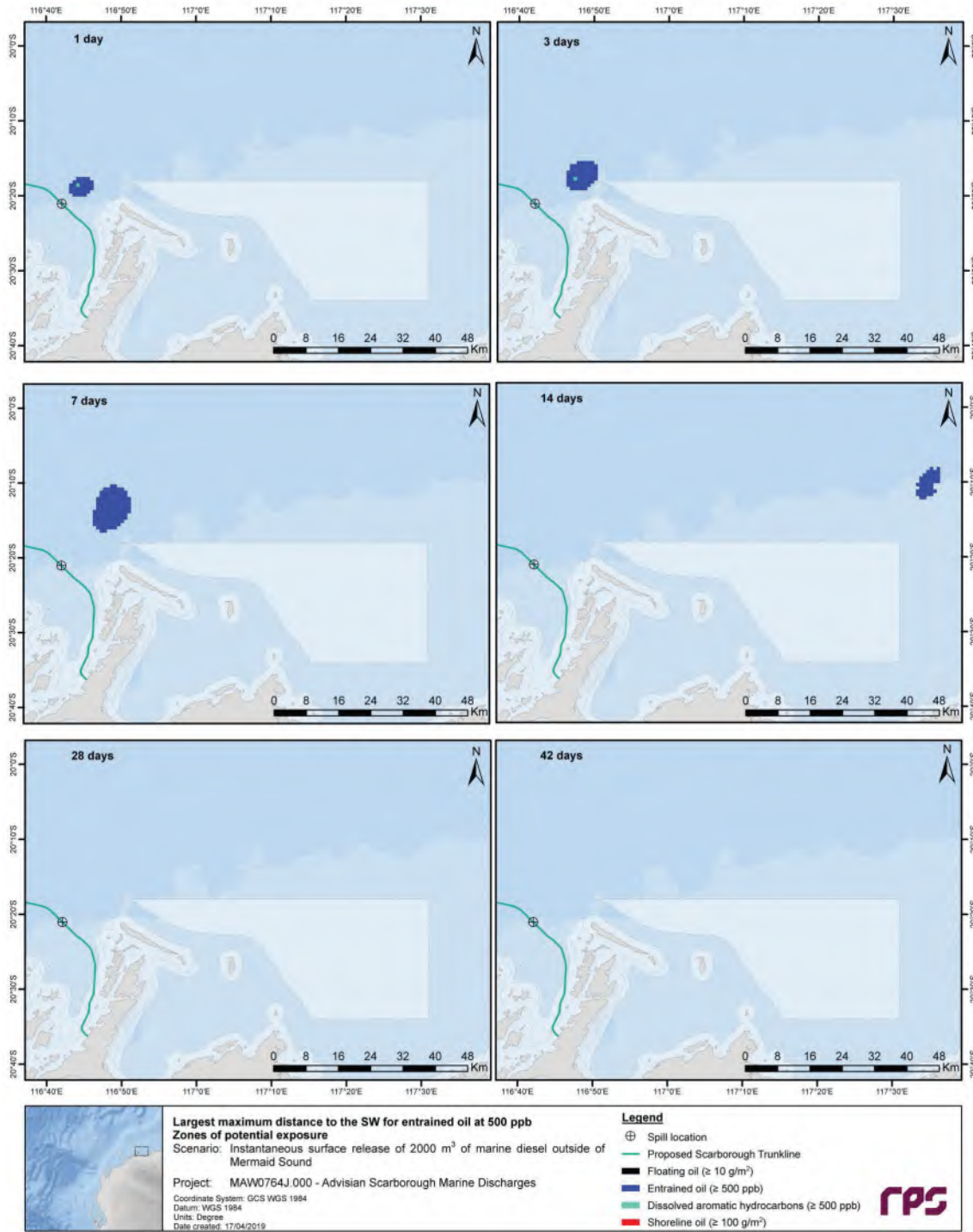
Figure 4.1 Time-varying areal extent of potential exposure at defined floating oil, entrained oil, dissolved aromatic hydrocarbon and shoreline oil threshold concentrations, resulting from an instantaneous surface release of marine diesel after a vessel collision outside Mermaid Sound, for the replicate simulation where entrained oil at the 500 ppb threshold is forecast to reach the greatest distance in a south-westerly direction from the release site.

4.2.2 Simulation with Maximal Overall Swept Area of Entrained Oil at the 500 ppb Threshold
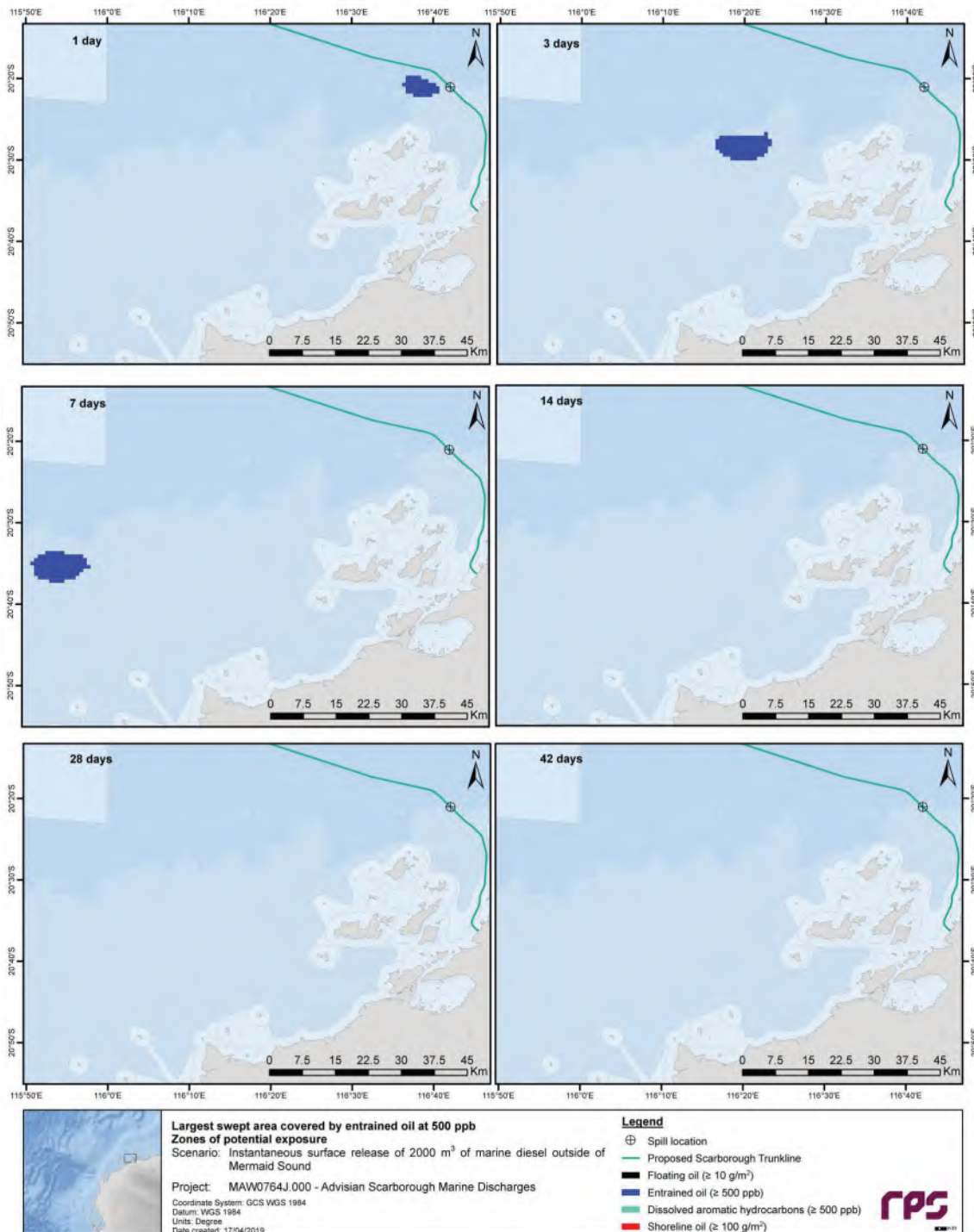
Figure 4.2 **Time-varying areal extent of potential exposure at defined floating oil, entrained oil, dissolved aromatic hydrocarbon and shoreline oil threshold concentrations, resulting from an instantaneous surface release of marine diesel after a vessel collision outside Mermaid Sound, for the replicate simulation where entrained oil at the 500 ppb threshold is forecast to cover the greatest total area over the course of a simulation.**

4.3 Scenario 2: Short-Term (Instantaneous) Surface Release of Marine Diesel after a Vessel Collision within Montebello Marine Park

4.3.1 Simulation with Maximal South-Westerly Extent of Entrained Oil at the 500 ppb Threshold
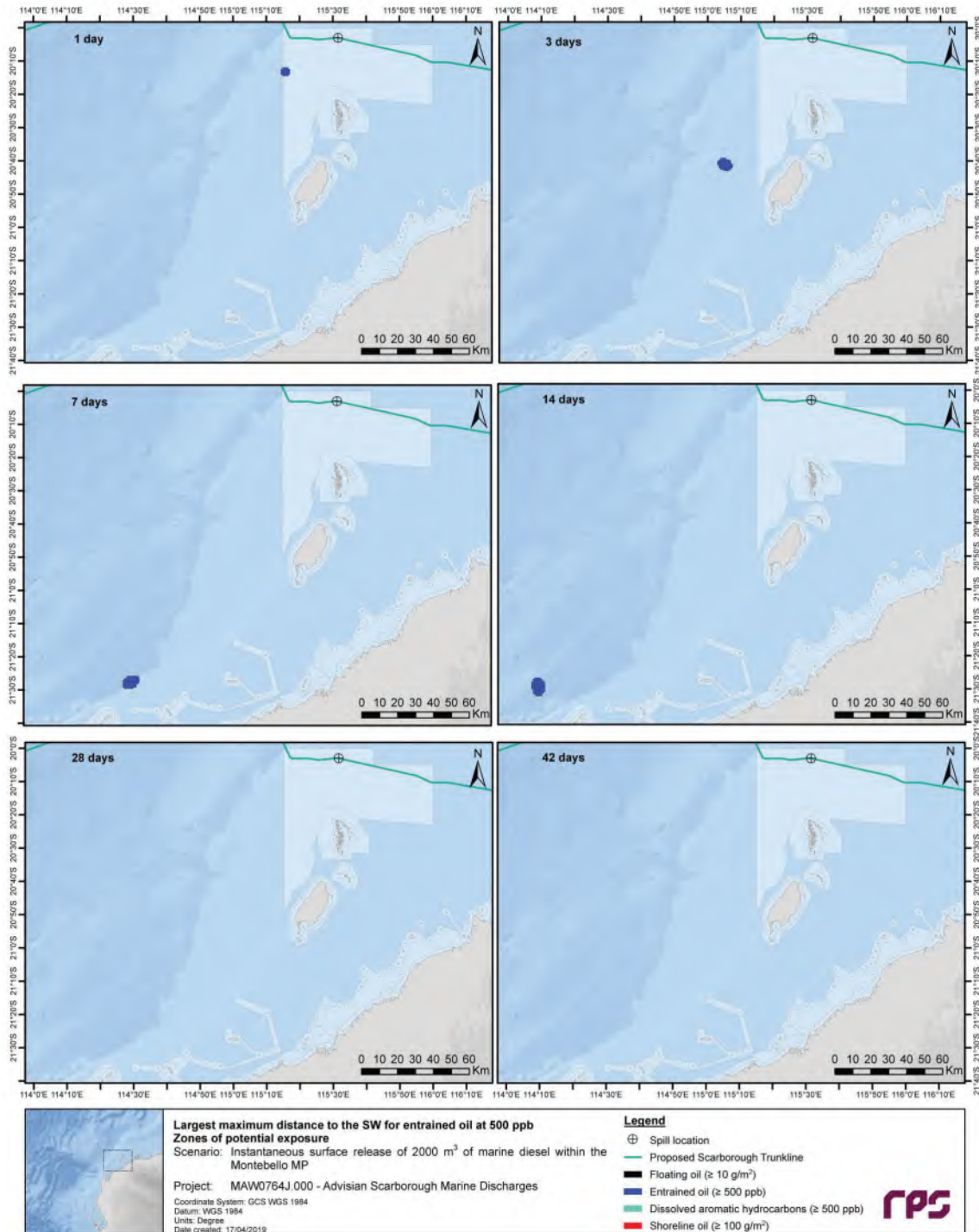
Figure 4.3 **Time-varying areal extent of potential exposure at defined floating oil, entrained oil, dissolved aromatic hydrocarbon and shoreline oil threshold concentrations, resulting from an instantaneous surface release of marine diesel after a vessel collision within Montebello Marine Park, for the replicate simulation where entrained oil at the 500 ppb threshold is forecast to reach the greatest distance in a south-westerly direction from the release site.**

4.3.2 Simulation with Maximal Overall Swept Area of Entrained Oil at the 500 ppb Threshold
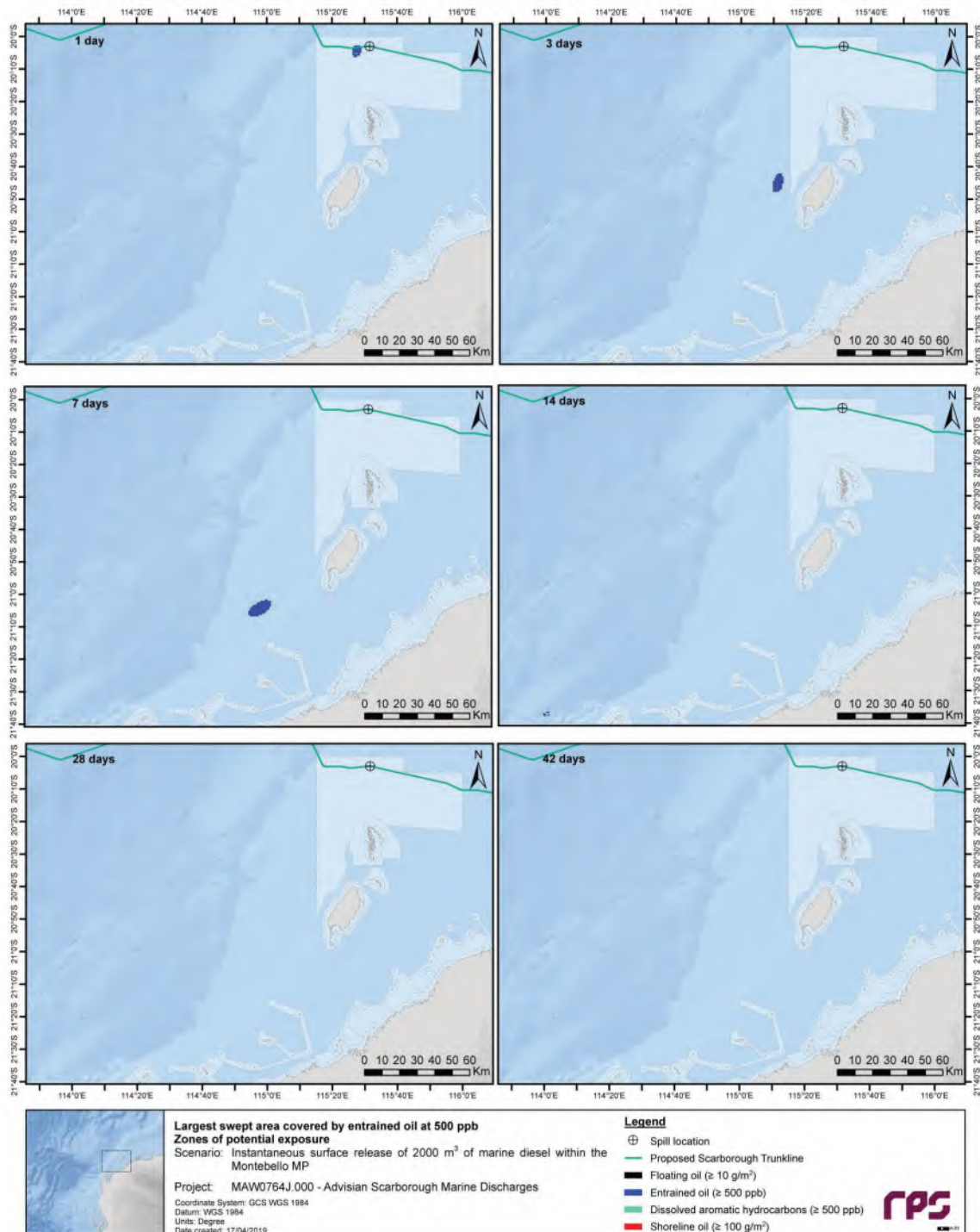
Figure 4.4 **Time-varying areal extent of potential exposure at defined floating oil, entrained oil, dissolved aromatic hydrocarbon and shoreline oil threshold concentrations, resulting from an instantaneous surface release of marine diesel after a vessel collision within Montebello Marine Park, for the replicate 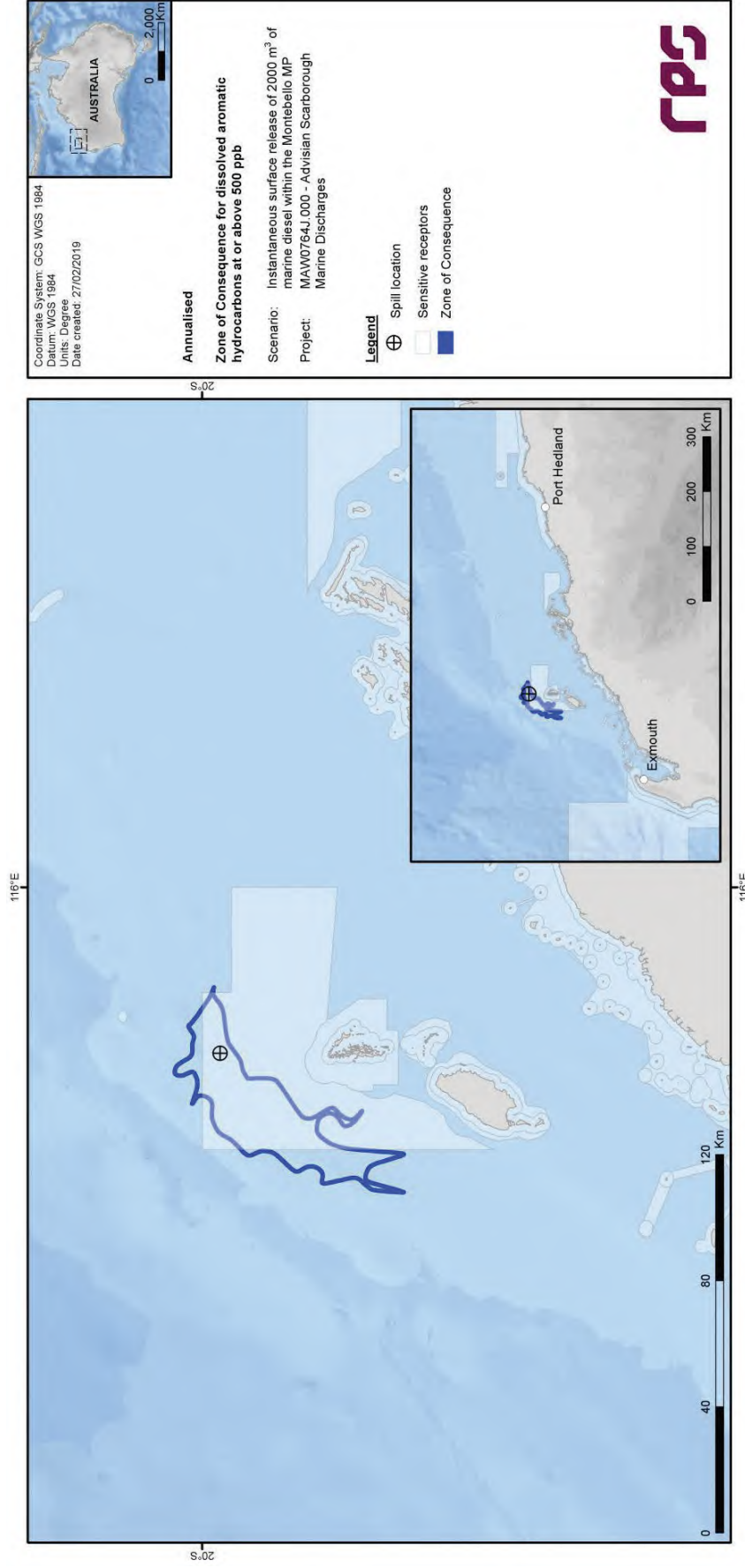simulation where entrained oil at the 500 ppb threshold is forecast to cover the greatest total area over the course of a simulation.**

4.4 Scenario 3: Short-Term (Instantaneous) Surface Release of Marine Diesel after a Vessel Collision at the FPU Location

4.4.1 Simulation with Maximal South-Westerly Extent of Entrained Oil at the 500 ppb Threshold
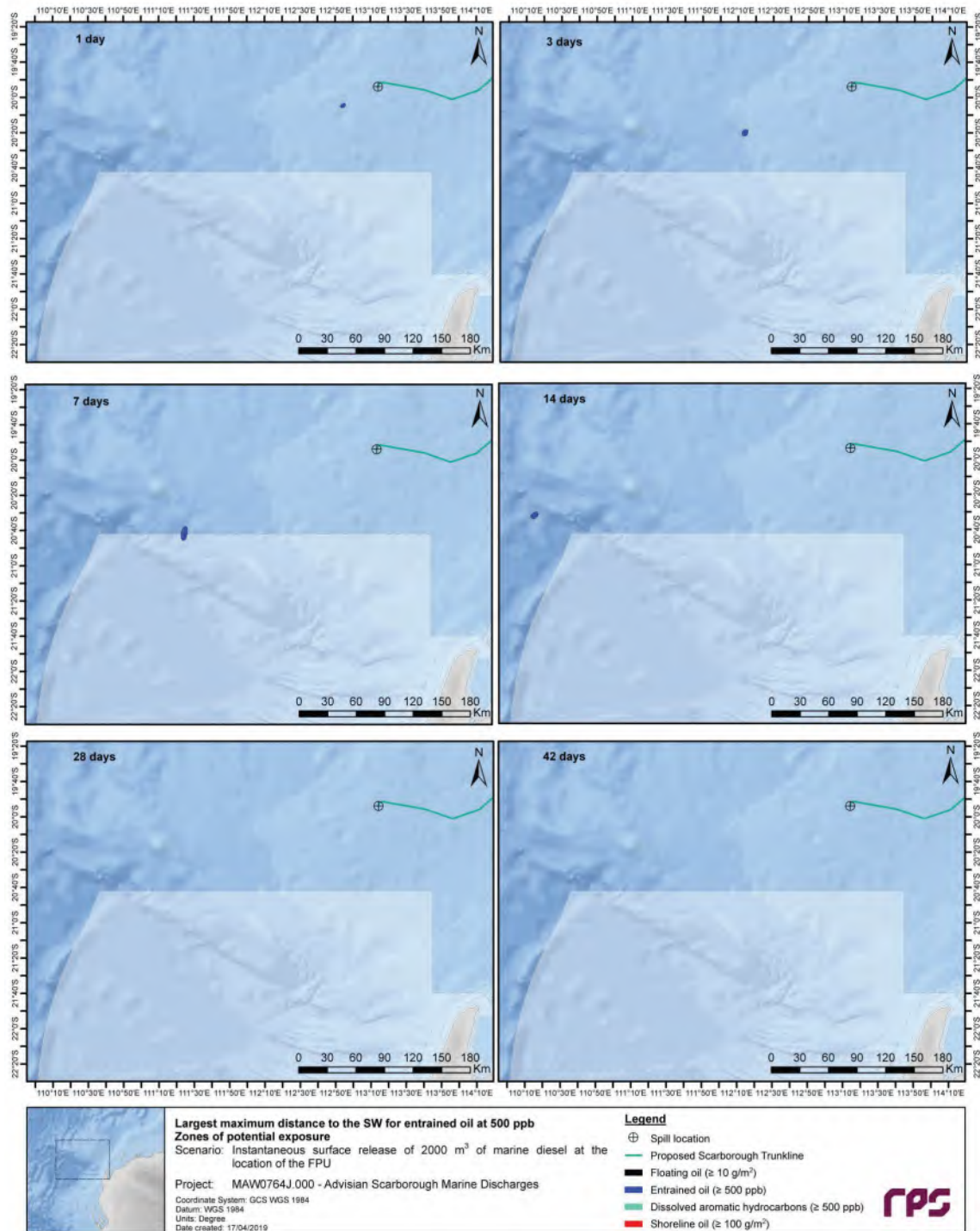
Figure 4.5 **Time-varying areal extent of potential exposure at defined floating oil, entrained oil, dissolved aromatic hydrocarbon and shoreline oil threshold concentrations, resulting from an instantaneous surface release of marine diesel after a vessel collision at the FPU location, for the replicate simulation where entrained oil at the 500 ppb threshold is forecast to reach the greatest distance in a south-westerly direction from the release site.**

4.4.2   Simulation with Maximal Overall Swept Area of Entrained Oil at the 500 ppb Threshold
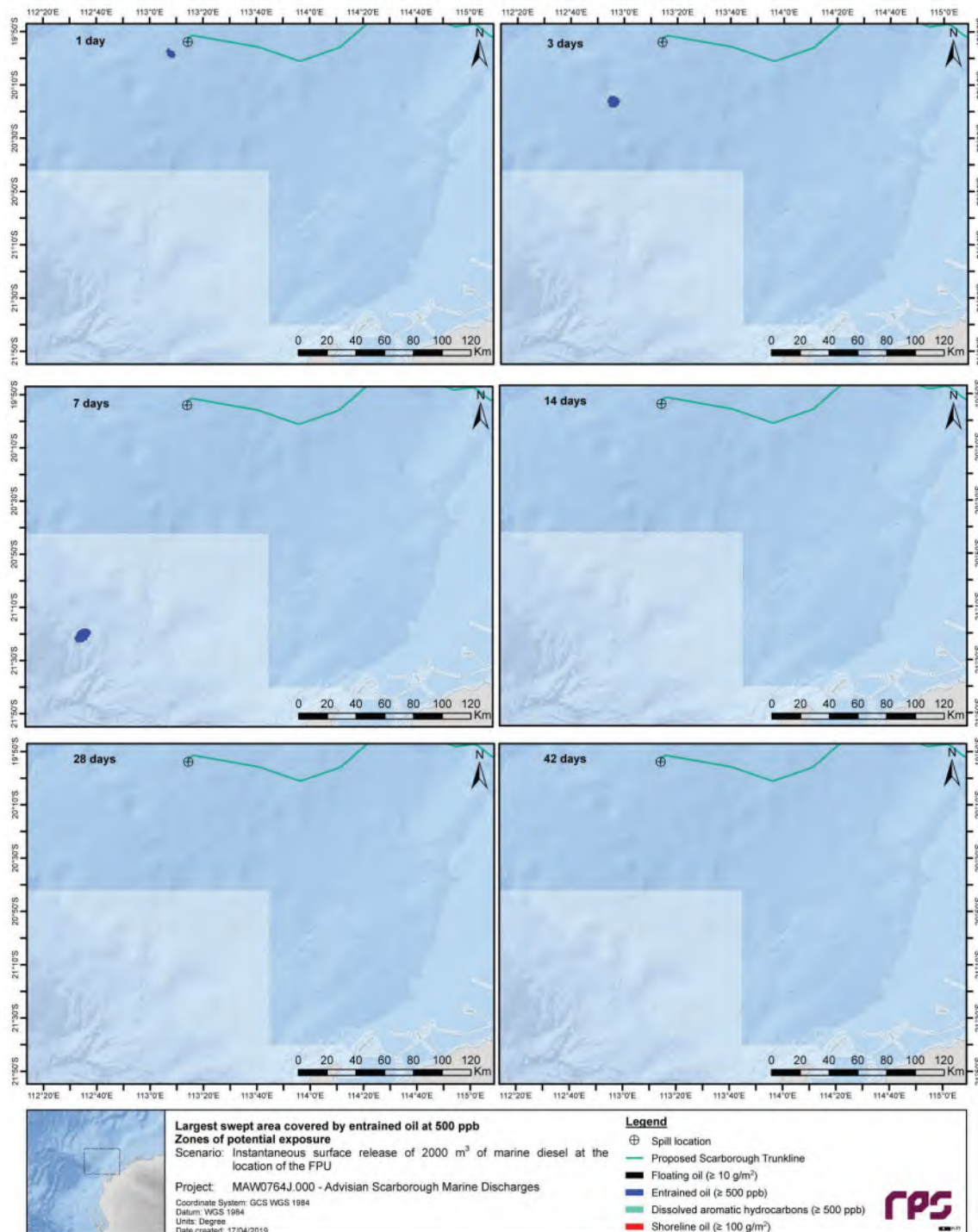
Figure 4.6   Time-varying areal extent of potential exposure at defined floating oil, entrained oil, dissolved aromatic hydrocarbon and shoreline oil threshold concentrations, resulting from an instantaneous surface release of marine diesel after a vessel collision at the FPU location, for the replicate simulation where entrained oil at the 500 ppb threshold is forecast to cover the greatest total area over the course of a simulation.

5 CONCLUSIONS

The main findings of this study are as follows:

Metocean Influences

- Tidal flows will have a significant influence on the trajectory of any oil spilled at the modelled release sites, irrespective of the seasonal conditions.

- Large-scale drift currents will have a significant influence on the trajectory of any oil spilled at the modelled release sites, irrespective of the seasonal conditions. The prevailing drift currents will determine the trajectory of oil that is entrained beneath the water surface.

- Interactions with the prevailing wind will provide additional variation in the trajectory of spilled oil.

- Due to the location of the hypothetical spill site and the dominance of tidal flows, the coastal areas predicted to be most likely to be impacted by spilled oil are those bordering Mermaid Sound and its numerous passages.

Oil Characteristics and Weathering Behaviour

- Marine diesel is a mixture of volatile and persistent hydrocarbons with low percentages of highly volatile and residual components. If exposed to the atmosphere, around 41% of the mass would be expected to evaporate in around 24 hours, another 54% within a few days, and the remaining 5% would be expected to persist in the marine environment until decayed. The influence of entrainment will regulate the degree of mass retention in the environment.

- During the surface release, floating oil will be susceptible to entrainment into the wave-mixed layer under typical wind conditions. Evaporation rates will be significant, given the moderate proportion of volatile compounds in the oil (41%). The low-volatility fraction of the oil (54%) will take longer durations of the order of days to evaporate, and the residual fraction of 5% is expected to persist in the environment until degradation processes occur. Considering the spill volume, there is a low potential for dissolution of soluble aromatic compounds.

Summary of Stochastic Assessment Results

Scenario 1: Short-Term (Instantaneous) Surface Release of Marine Diesel after a Vessel Collision outside Mermaid Sound

- Floating oil at concentrations equal to or greater than the 10 g/m^2, 50 g/m^2 and 100 g/m^2 thresholds could potentially be found up to 29 km, 21 km and 18 km from the spill site, respectively.

- The Dampier Archipelago shoreline receptor is predicted to be contacted by floating oil concentrations at the 10 g/m^2 threshold with a probability of 2% and a minimum time to contact of 27 hours.

- Potential for accumulation of oil on shorelines is predicted to be low, with a maximum accumulated volume and concentration of 3 m^3 and 156 g/m^2, respectively, forecast at the Dampier Archipelago.

- Entrained oil at concentrations equal to or greater than the 500 ppb threshold is predicted to be found up to around 163 km from the spill site.

- The Dampier MP and Dampier Archipelago receptors are predicted to receive entrained oil concentrations at the 500 ppb threshold with probabilities of 44% and 23%, respectively.

- The maximum entrained oil concentration forecast for any receptor is predicted as 10.9 ppm within the Dampier Archipelago.

- Dissolved aromatic hydrocarbons at concentrations equal to or greater than the 500 ppb threshold are predicted to be found up to around 34 km from the spill site.

- The Dampier MP is predicted to receive dissolved aromatic hydrocarbon concentrations at the 500 ppb threshold with a probability of 2%.

- The maximum dissolved aromatic hydrocarbon concentration forecast for any receptor is predicted as 635 ppb within the Dampier MP.

Scenario 2: Short-Term (Instantaneous) Surface Release of Marine Diesel after a Vessel Collision within Montebello Marine Park

- Floating oil at concentrations equal to or greater than the 10 g/m^2, 50 g/m^2 and 100 g/m^2 thresholds could potentially be found up to 39 km, 36 km and 33 km from the spill site, respectively.

- Given that the spill location lies within the Montebello MP receptor area, floating oil at concentrations equal to or greater than 100 g/m^2 are forecast with a probability of 100% and a minimum time to contact of less than 1 hour.

- Potential for accumulation of oil on shorelines is predicted to be low, with a maximum accumulated volume and concentration of <1 m^3 and 1 g/m^2, respectively, forecast at Barrow Island.

- Entrained oil at concentrations equal to or greater than the 500 ppb threshold is predicted to be found up to around 308 km from the spill site.

- The Montebello MP and Muiron Islands MMA-WHA receptors are predicted to receive entrained oil concentrations at the 500 ppb threshold with probabilities of 70% and 7%, respectively.

- The maximum entrained oil concentration forecast for any receptor is predicted as 157.0 ppm within the Montebello MP.

- Dissolved aromatic hydrocarbons at concentrations equal to or greater than the 500 ppb threshold are predicted to be found up to around 85 km from the spill site.

- The Montebello MP is predicted to receive dissolved aromatic hydrocarbon concentrations at the 500 ppb threshold with a probability of 2%.

- The maximum dissolved aromatic hydrocarbon concentration forecast for any receptor is predicted as 2.0 ppm within the Montebello MP.

Scenario 3: Short-Term (Instantaneous) Surface Release of Marine Diesel after a Vessel Collision at the FPU Location

- Floating oil at concentrations equal to or greater than the 10 g/m^2, 50 g/m^2 and 100 g/m^2 thresholds could potentially be found up to 113 km, 60 km and 58 km from the spill site, respectively.

- No shoreline receptors are predicted to be contacted by floating oil concentrations at any of the assessed thresholds.

- No accumulation of oil on shorelines is predicted.

- Entrained oil at concentrations equal to or greater than the 500 ppb threshold is predicted to be found up to around 476 km from the spill site.

- The Gascoyne MP receptor is predicted to receive entrained oil concentrations at the 500 ppb threshold with a probability of 8%.

- The maximum entrained oil concentration forecast for any receptor is predicted as 7.2 ppm within the Gascoyne MP.

- Dissolved aromatic hydrocarbons at concentrations equal to or greater than the 500 ppb threshold are predicted to be found up to around 74 km from the spill site.

- No receptors are predicted to receive dissolved aromatic hydrocarbon concentrations at the 500 ppb threshold.

- The maximum dissolved aromatic hydrocarbon concentration forecast for any receptor is predicted as 462 ppb within the Gascoyne MP.

6   REFERENCES

Advisian 2019, *Oil Spill Modelling Data Requirements* [v2], provided to RPS by Advisian, West Perth, WA, Australia.

Andersen, OB 1995, 'Global ocean tides from ERS 1 and TOPEX/POSEIDON altimetry', *Journal of Geophysical Research: Oceans*, vol. 100, no. C12, pp. 25249-25259.

Australian Maritime Safety Authority (AMSA) 2002, *National marine oil spill contingency plan*, Australian Maritime Safety Authority, Canberra, ACT, Australia.

Australian Maritime Safety Authority (AMSA) 2015, *National plan guidance on: Response, assessment and termination of cleaning for oil contaminated foreshores*, NP-GUI-025, Australian Maritime Safety Authority, Canberra, ACT, Australia.

Davies, AM 1977a, 'The numerical solutions of the three-dimensional hydrodynamic equations using a B-spline representation of the vertical current profile', in *Bottom Turbulence: Proceedings of the 8th Liege Colloquium on Ocean Hydrodynamics*, ed. Nihoul, JCJ, Elsevier.

Davies, AM 1977b, 'Three-dimensional model with depth-varying eddy viscosity', in *Bottom Turbulence: Proceedings of the 8th Liege Colloquium on Ocean Hydrodynamics*, ed. Nihoul, JCJ, Elsevier.

Flater, D 1998, *XTide: harmonic tide clock and tide predictor* (www.flaterco.com/xtide/).

French, D, Reed, M, Jayko, K, Feng, S, Rines, H, Pavignano, S, Isaji, T, Puckett, S, Keller, A, French III, FW, Gifford, D, McCue, J, Brown, G, MacDonald, E, Quirk, J, Natzke, S, Bishop, R, Welsh, M, Phillips, M & Ingram, BS 1996 'Final Report, The CERCLA Type A Natural Resource Damage Assessment Model for Coastal and Marine Environments (NRDAM/CME)', *Technical Documentation, Vol. I – V*, Submitted to the Office of Environmental Policy and Compliance, U.S. Department of the Interior, Washington, DC, USA.

French, DP & Rines, HM 1997, 'Validation and use of spill impact modelling for impact assessment', in *Proceedings of the 1997 International Oil Spill Conference*, Fort Lauderdale, FL, USA, pp. 829-834.

French, DP 1998, 'Modelling the impacts of the North Cape oil spill', in *Proceedings of the 21st Arctic and Marine Oilspill Program (AMOP) Technical Seminar*, Edmonton, AB, Canada, pp. 387-430.

French, DP, Schuttenberg, H & Isaji, T 1999, 'Probabilities of oil exceeding thresholds of concern: Examples from an evaluation for Florida Power and Light', in *Proceedings of the 22nd Arctic and Marine Oilspill Program (AMOP) Technical Seminar*, Calgary, AB, Canada, pp. 243-270.

French, DP 2000, 'Estimation of oil toxicity using an additive toxicity model', in *Proceedings of the 23rd Arctic and Marine Oil Spill Program Technical Seminar*, Vancouver, British Columbia, Canada, pp. 561-600.

French-McCay, DP 2003, 'Development and application of damage assessment modelling: Example assessment for the North Cape oil spill', *Marine Pollution Bulletin,* vol. 47, no. 9-12, pp. 341-359.

French-McCay, DP 2004, 'Oil spill impact modelling: development and validation', *Environmental Toxicology and Chemistry*, vol. 23, no. 10, pp. 2441-2456.

French McCay, D, Whittier, N, Sankaranarayanan, S, Jennings, J & Etkin, DS 2004, 'Estimation of potential impacts and natural resource damages of oil', *Journal of Hazardous Materials*, vol. 107, no. 1-2, pp. 11-25.

French-McCay, DP 2009, 'State-of-the-art and research needs for oil spill impact assessment modelling', in *Proceedings of the 32nd Arctic and Marine Oilspill Program (AMOP) Technical Seminar on Environmental Contamination and Response*, Vancouver, BC, Canada, pp. 601-654.

French-McCay, D, Reich, D, Rowe, J, Schroeder, M & Graham, E 2011, 'Oil spill modeling input to the offshore environmental cost model (OECM) for US-BOEMRE's spill risk and costs evaluations', in *Proceedings of the 34th Arctic and Marine Oilspill Program (AMOP) Technical Seminar on Environmental Contamination and Response*, Banff, AB, Canada, pp. 146-168.

French-McCay, D, Reich, D, Michel, J, Etkin, DS, Symons, L, Helton, D & Wagner J 2012, 'Oil spill consequence analysis of potentially-polluting shipwrecks', in *Proceedings of the 35th Arctic and Marine Oilspill Program (AMOP) Technical Seminar on Environmental Contamination and Response*, Environment Canada, Ottawa, ON, Canada.

Gordon, R 1982, *Wind driven circulation in Narragansett Bay*, PhD thesis, University of Rhode Island, Kingston, RI, USA.

Isaji, T & Spaulding, ML 1984, 'A model of the tidally induced residual circulation in the Gulf of Maine and Georges Bank', *Journal of Physical Oceanography*, vol. 14, no. 6, pp. 1119-1126.

Isaji, T & Spaulding, ML 1986, 'A numerical model of the M2 and K1 tide in the northwestern Gulf of Alaska', *Journal of Physical Oceanography*, vol. 17, no. 5, pp. 698-704.

Isaji, T, Howlett, E, Dalton, C & Anderson, E 2001, 'Stepwise-continuous-variable-rectangular grid hydrodynamics model', in *Proceedings of the 24th Arctic and Marine Oilspill Program (AMOP) Technical Seminar*, Edmonton, AB, Canada, pp. 597-610.

King, B & McAllister, FA 1998, 'Modelling the dispersion of produced water discharges', *APPEA Journal*, pp. 681-691.

Koops, W, Jak, RG & van der Veen, DPC 2004, 'Use of dispersants in oil spill response to minimize environmental damage to birds and aquatic organisms', in *Proceedings of Interspill 2004*, Trondheim, Norway, paper no. 429.

Kostianoy, AG, Ginzburg, AI, Lebedev, SA, Frankignoulle, M & Delille, B 2003, 'Fronts and mesoscale variability in the southern Indian Ocean as inferred from the TOPEX/POSEIDON and ERS-2 Altimetry data', *Oceanology*, vol. 43, no. 5, pp. 632-642.

Locarnini, RA, Mishonov, AV, Antonov, JI, Boyer, TP, Garcia, HE, Baranova, OK, Zweng, MM, Paver, CR, Reagan, JR, Johnson, DR, Hamilton, M & Seidov, D 2013, *World Ocean Atlas 2013, Volume 1: Temperature.* S. Levitus, Ed., A. Mishonov, Technical Ed., NOAA Atlas NESDIS 73, Silver Spring, MD, USA, 40 pp.

Ludicone, D, Santoleri, R, Marullo, S & Gerosa, P 1998, 'Sea level variability and surface eddy statistics in the Mediterranean Sea from TOPEX/POSEIDON data', *Journal of Geophysical Research I,* vol. 103, no. C2, pp. 2995-3011.

Matsumoto, K, Takanezawa, T & Ooe, M 2000, 'Ocean tide models developed by assimilating TOPEX/POSEIDON altimeter data into hydrodynamical model: A global model and a regional model around Japan', *Journal of Oceanography*, vol. 56, no. 5, pp. 567-581.

National Oceanic and Atmospheric Administration (NOAA) 2013a, *World Ocean Atlas 2013*, National Oceanic and Atmospheric Administration, Silver Spring, MD, USA (www.nodc.noaa.gov/OC5/WOA13/).

National Oceanic and Atmospheric Administration (NOAA) 2013b, *Screening Level Risk Assessment Package: Manzanillo*, National Oceanic and Atmospheric Administration, Washington, DC, USA.

National Research Council (NRC) 2005, *Oil Spill Dispersants: Efficacy and Effects*, National Research Council of the National Academies, The National Academies Press, Washington, DC, USA.

Oke, PR, Brassington, GB, Griffin, DA & Schiller, A 2008, 'The Bluelink ocean data assimilation system (BODAS)', *Ocean Modeling*, vol. 21, no. 1-2, pp. 46-70.

Oke, PR, Brassington, GB, Griffin, DA & Schiller, A 2009, 'Data assimilation in the Australian Bluelink system', *Mercator Ocean Quarterly Newsletter*, no. 34, pp. 35-44.

Okubo, A 1971, 'Oceanic diffusion diagrams', *Deep Sea Research and Oceanographic Abstracts*, vol. 18, no. 8, pp. 789-802.

Owen, A 1980, 'A three-dimensional model of the Bristol Channel', *Journal of Physical Oceanography*, vol. 10, no. 8, pp. 1290-1302.

Pace, CB, Clark, JR & Bragin, GE 1995, 'Comparing crude oil toxicity under standard and environmentally realistic exposures', in *Proceedings of the 1995 International Oil Spill Conference*, Long Beach, CA, USA, paper no. 327.

Qiu, B & Chen, S 2010, 'Eddy-mean flow interaction in the decadally modulating Kuroshio Extension system', *Deep-Sea Research II*, vol. 57, no. 13, pp. 1098-1110.

Saha, S, Moorthi, S, Pan, HL, Wu, X, Wang, J, Nadiga, S 2010, 'The NCEP climate forecast system reanalysis', *Bulletin of the American Meteorological Society*, vol. 91, pp. 1015-1057.

Schiller, A, Oke, PR, Brassington, GB, Entel, M, Fiedler, R, Griffin, DA & Mansbridge, JV 2008, 'Eddy-resolving ocean circulation in the Asian-Australian region inferred from an ocean reanalysis effort', *Progress in Oceanography*, vol. 76, no. 3, pp. 334-365.

Yaremchuk, M & Tangdong, Q 2004, 'Seasonal variability of the large-scale currents near the coast of the Philippines', *Journal of Physical Oceanography*, vol. 34, no. 4, pp. 844-855.

Zigic, S, Zapata, M, Isaji, T, King, B & Lemckert, C 2003, 'Modelling of Moreton Bay using an ocean/coastal circulation model', in *Proceedings of the Coasts & Ports 2003 Australasian Conference*, Auckland, New Zealand, paper no. 170.

Zweng, MM, Reagan, JR, Antonov, JI, Locarnini, RA, Mishonov, AV, Boyer, TP, Garcia, HE, Baranova, OK, Johnson, DR, Seidov, D & Biddle MM 2013, *World Ocean Atlas 2013, Volume 2: Salinity*. S. Levitus, Ed., A. Mishonov, Technical Ed., NOAA Atlas NESDIS 74, Silver Spring, MD, USA, 39 pp.

Appendix J

Scarborough Development Dredged Sediment Dispersion Modelling

SCARBOROUGH DEVELOPMENT DREDGED SEDIMENT DISPERSION MODELLING

Report

Document status

Version	Purpose of document	Authored by	Reviewed by	Approved by	Review date
Rev A	Internal review	N. Page R. Alexander	D. Wright	D. Wright	14/03/2019
Rev 0	Client review	N. Page R. Alexander	D. Wright	D. Wright	21/03/2019
Rev 1	Client review	N. Page R. Alexander	D. Wright	D. Wright	10/05/2019
Rev 2	Client review	R. Alexander	D. Wright	D. Wright	24/05/2019
Rev 3	Client review	R. Alexander	D. Wright	D. Wright	30/05/2019
Rev 4	Client review	R. Alexander	D. Wright	D. Wright	07/06/2019

Approval for issue

David Wright   7 June 2019

Prepared by:

RPS

David Wright
Manager - Perth

Level 2, 27-31 Troode Street
West Perth WA 6005

Prepared for:

Advisian

Paul Nichols
Marine Sciences Manager (APAC)

Level 4, Signet House
600 Murray Street
West Perth WA 6005

Contents

Tables

Figures

1 INTRODUCTION

1.1 Background

RPS was commissioned by Advisian Pty Ltd (Advisian), on behalf of Woodside Energy Ltd (Woodside), to undertake sediment dispersion modelling of dredging, disposal and backfill operations associated with the development of Scarborough, in support of the State and Commonwealth referrals and an Offshore Project Proposal to NOPSEMA. The Scarborough gas field is located within offshore permit WA-1-R.

Dredging, disposal and backfill operations along the Scarborough pipeline route, from the mainland of the Burrup Peninsula outwards to a chainage of KP50, are proposed as part of the project (Figure 1.1).

RPS has conducted sediment dispersion modelling to quantify the potential magnitude, intensity and spatial distribution of suspended sediment concentrations (SSC) and sedimentation that would be expected for the dredging, disposal and backfill operations proposed for the development of Scarborough. The predicted outcomes are to be used to inform the assessment of the potential for influence or impact upon water quality and benthic habitats in the region.

This technical report contains a summary of the sediment fate model inputs, methodologies and assumptions, and the model outcomes following analysis of specified threshold criteria.
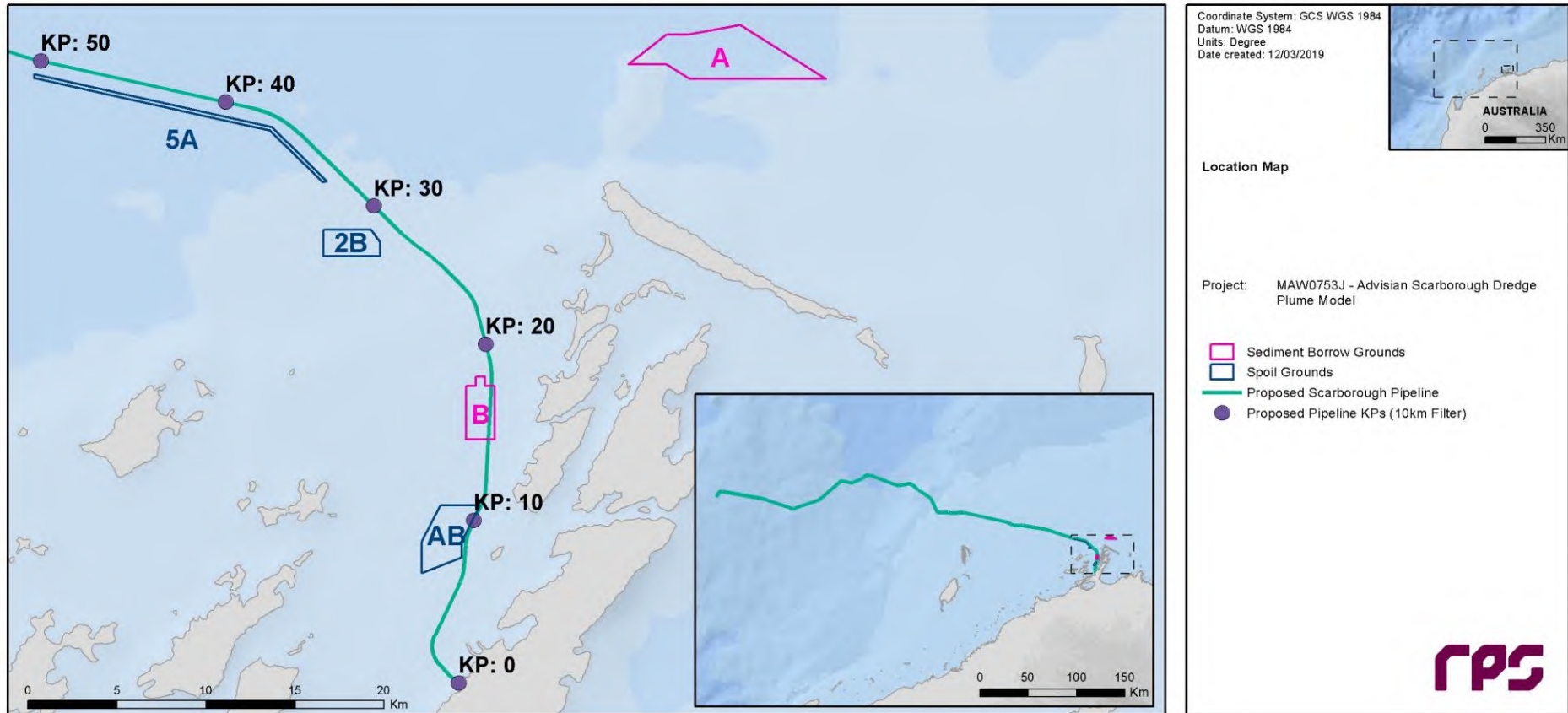
Figure 1.1   Route of the inner sections (KP0 to KP50) of the proposed Scarborough pipeline on the North West Shelf of Australia, and locations of the existing spoil grounds (AB, 2B and 5A) and sediment borrow grounds (A and B) that will be utilised during disposal and backfill activities.

1.2 Modelling Scope

RPS was commissioned to conduct sediment dispersion modelling for the following activities:

- Dredging of sediment along the pipeline route and disposal of dredged sediment at three nominated spoil grounds;

- Dredging of the borrow ground and backfill and stabilisation of the pipeline.

The scope of work required to complete the sediment dispersion modelling included:

1. Hydrodynamic Modelling.

    a. An initial assessment of the existing D-FLOW hydrodynamic model framework in the Mermaid Sound region determined that refinements were necessary to suit the requirements of this scope of work. Reconfiguration of the model was conducted, followed by re-validation of the model predictions against available measurements of water levels and currents for the same validation period as utilised previously.

    b. Two years (2016-2017) of hydrodynamic simulation data was produced for use as input to the sediment dispersion model.

2. Wave Modelling.

    a. An initial assessment of the existing D-WAVE wave model framework in the Mermaid Sound region determined that refinements were necessary to suit the requirements of this scope of work. Reconfiguration of the model was conducted, followed by re-validation of the model predictions against available predictions from an operational RPS model for the same validation period as utilised previously.

    b. Two years (2016-2017) of wave simulation data was produced for use as input to the sediment dispersion model.

3. Sediment Dispersion Modelling.

    a. Inputs for the dredging program were prepared for the DREDGEMAP model, accounting for all potential concurrent sources of sediment characterised by location, intensity, particle size distribution, vertical distribution in the water column, and levels of cohesivity.

    b. Four dredging, disposal and backfill scenarios were simulated: (i) dredging commencing in winter including an offshore borrow ground; (ii) dredging commencing in winter including an inshore borrow ground; (iii) dredging commencing in summer including an offshore borrow ground; (iv) dredging commencing in summer including an inshore borrow ground.

    c. Simulation outputs from each separate dredging, disposal and backfill activity were post-processed, combined and analysed to determine outcomes including zones of impact and influence for each scenario based on specified threshold criteria.

    d. Key model outcomes were provided as spatial datasets in GIS shapefile format.

4. Reporting. A technical report detailing the sediment fate model inputs, methodologies, assumptions and model outcomes following analysis of specified threshold criteria was provided.

1.3   Definitions of Relevant Terms and Abbreviations

BHD:

Backhoe Dredge. A pontoon equipped with a hydraulic excavator. The pontoon is stabilised and secured by three spuds. The excavator uses a large arm fitted with a bucket to excavate material from the seabed and discharge it into (typically) a split hopper barge moored alongside. BHDs are mainly used for dredging or breaking up the sedimentary rock below a layer of unconsolidated sediments, or for dredging in areas inaccessible to larger self-propelled vessels.

Dewatering:

Draining of excess water from a split hopper barge using its drainage system.

Overflow:

Excess water and suspended solids that leave a TSHD hopper and are discharged to the water column via a weir and discharge pipe located at the base of the vessel.

Resuspension:

Removal of deposited material from the seabed to the water column as a result of natural or artificial agitation.

Sedimentation rate:

Rate of sediment accumulation on the seabed following deposition of SSC from the water column.

Side-dump vessel:

Self-propelled vessel that is capable of transporting and installing a variety of different sizes of rock. Large cranes of fall pipes are used to dump rocks from the vessels to the seabed.

Split hopper barge:

Vessel with a large open hold used to load and transport dredged material. The unloading is performed by splitting the two halves of the hull to release the material towards the seabed.

SSC:

Suspended Solids Concentration (or Suspended Sediment Concentration). The concentration of sediment material in the water column following natural or artificial resuspension from the seabed.

TSHD:

Trailer Suction Hopper Dredge. A self-propelled vessel with one or two suction tubes/arms, equipped with drag-heads that are lowered to the seabed and trailed over the bottom. The vessel has a powerful pump system that sucks up a mixture of sediment and water and discharges it in the hopper (hold) of the vessel. TSHDs are mainly used for dredging loose and soft soils such as sand, gravel, silt or clay.

2 HYDRODYNAMIC AND WAVE MODELLING

2.1 Overview

Modelling of the potential sediment dispersion from the dredging, disposal and backfill activities associated with the development of Scarborough required temporal and spatial representation of the hydrodynamic and wave conditions within the project area. A hydrodynamic and wave model framework for the Mermaid Sound area was constructed, calibrated and validated for a past marine modelling study of dredge spoil stability and navigation for Woodside (RPS, 2016). This model framework has been refined for the Scarborough scope of work and is described in the following sections.

The hydrodynamic and wave modelling for the project was conducted using the Delft3D suite of software. The Delft3D suite is a fully integrated computer software package composed of several modules (e.g. flow, waves, sediment, water quality, and ecology) grouped around a common interface. This software suite has been developed to carry out studies with a multi-disciplinary approach and multi-dimensional calculations (e.g. 2-D and 3-D) for a range of systems, such as oceanic, coastal, estuarine and river environments. It can simulate the interaction of flows, waves, sediment transport, morphological developments, water quality and aquatic ecology. Specific modules of the Delft3D suite are referenced in this report, following the convention of the software developers, with the suffix D- (e.g. D-FLOW for the Delft3D Hydrodynamics module and D-WAVE for the Delft3D Spectral Wave module).

The Delft3D suite has been developed by Deltares, an independent institute for applied research on water with over 30 years of experience in modelling aquatic systems (http://www.deltares.nl/en). The Delft3D suite of models adheres to the International Association for Hydro-Environment Engineering and Research guidelines for documenting the validity of computational modelling software, closely replicating an array of analytical, laboratory, schematic and real-world data.

The configuration of the current and wave models is in line with recommendations of best practice for sediment dispersion modelling in Western Australia as outlined by WAMSI Dredging Science Node guidance (Sun *et al.*, 2016). Inclusion of mesoscale ocean currents is recommended, as these currents have a significant influence on the net drift of suspended material over the time scales of dredging operations (days to weeks) and are therefore important to predictions of sediment transport. The use of three-dimensional current modelling with a series of interconnected grids of progressively finer resolution is also recommended, as are coupling of the current and wave models and validation of current predictions against measured data.

2.2 Hydrodynamic Model (D-FLOW)

2.2.1 Model Description

To simulate the hydrodynamics within Mermaid Sound and the surrounding area, a three-dimensional model with accurate representations of the bathymetry, bottom roughness and spatially-varying wind stress was utilised for the region. The model framework was developed through the combination of a large-scale regional model with smaller refined regions, or sub-domains.

The D-FLOW model is ideally suited to represent the hydrodynamics of complex coastal waters, including regions where the tidal range creates large intertidal zones and where buoyancy processes are important. RPS has applied the model for numerous studies in the region.

D-FLOW is a multi-dimensional (2-D or 3-D) hydrodynamic (and transport) simulation program which calculates non-steady flow and transport phenomena that result from tidal, meteorological and baroclinic forcing on a rectilinear or a curvilinear, boundary-fitted grid. In three-dimensional simulations, the vertical grid

can be defined following the sigma-coordinate approach, where the local water depth is divided into a series of layers with thickness at a set proportion of the depth.

D-FLOW allows for the establishment of a series of interconnected (two-way, dynamically-nested) curvilinear grids of varying resolution; a technique referred to as "domain decomposition". This allows for the generation of a series of grids with progressively increasing spatial resolution, down to an appropriate scale for accurate resolution of the hydrodynamics associated with features such as dredged channels. The main advantage of domain decomposition over traditional one-way, or static, nesting systems is that the model domains interact seamlessly, allowing transport and feedback between the regions of different scales. The ability to dynamically couple multiple model domains offers a flexible framework for hydrodynamic model development. This modelling method was applied in this study.

Inputs to the model, as discussed in the following sections, included:

- Bathymetry of the study area, including shipping channels, islands, and adjacent features. The wetting and drying of the intertidal zones was simulated in applicable areas.

- Boundary elevation forcing data.

- Spatially-varying surface wind and pressure data.

2.2.2   Bathymetry and Domain Definition

The hydrodynamic model was established over the domain shown in Figure 2.1. Accurate bathymetry is a significant factor in development of a model framework required to resolve highly variable wave and current conditions. The bathymetry was developed using data provided by Woodside and supplemented with data from Geoscience Australia and the C-MAP electronic chart database where relevant and required.

The composite bathymetric data was interpolated onto the D-FLOW Cartesian grid. The resultant bathymetry is shown in Figure 2.2. The extent and shape of the model coastline will change as water levels rise and fall with tidal movements due to the inclusion of wetting and drying within the model system.

The vertical grid of the model comprised five layers of varying thickness, depending on location, throughout the domain. Five layers was found to be enough to resolve the circulation and provide suitable bed level currents, without overly compromising model performance. As the model was set up as a proportional sigma-grid in the vertical dimension, these layers therefore represented a terrain-following arrangement with a layer thickness of 20% of the total local water depth.

To offset the computational effort required for a large, multi-layered model domain, and to achieve adequate horizontal and temporal resolution, a multiple-grid (domain-decomposition) strategy was applied using three sub-domains of varying horizontal grid cell size (Figure 2.1 and Figure 2.2). Horizontal resolutions within each sub-domain were 250 m for the Mermaid Sound region from Enderby Island to Legendre Island (sub-grid 2), 500 m for the intermediate region (sub-grid 1) and 2 km for the outer domain (sub-grid 0).

Each sub-domain is an individual hydrodynamic model simulated in parallel with the others, with dynamic coupling at the shared boundaries between sub-domains. The outermost sub-domain captured large-scale oceanographic phenomena which progressively fed into the finer-resolution domains representing the area of interest. The resolution of the innermost sub-domain was specified after assessment of the requirement to adequately resolve the variation in current fields, and in turn the sediment dynamics.
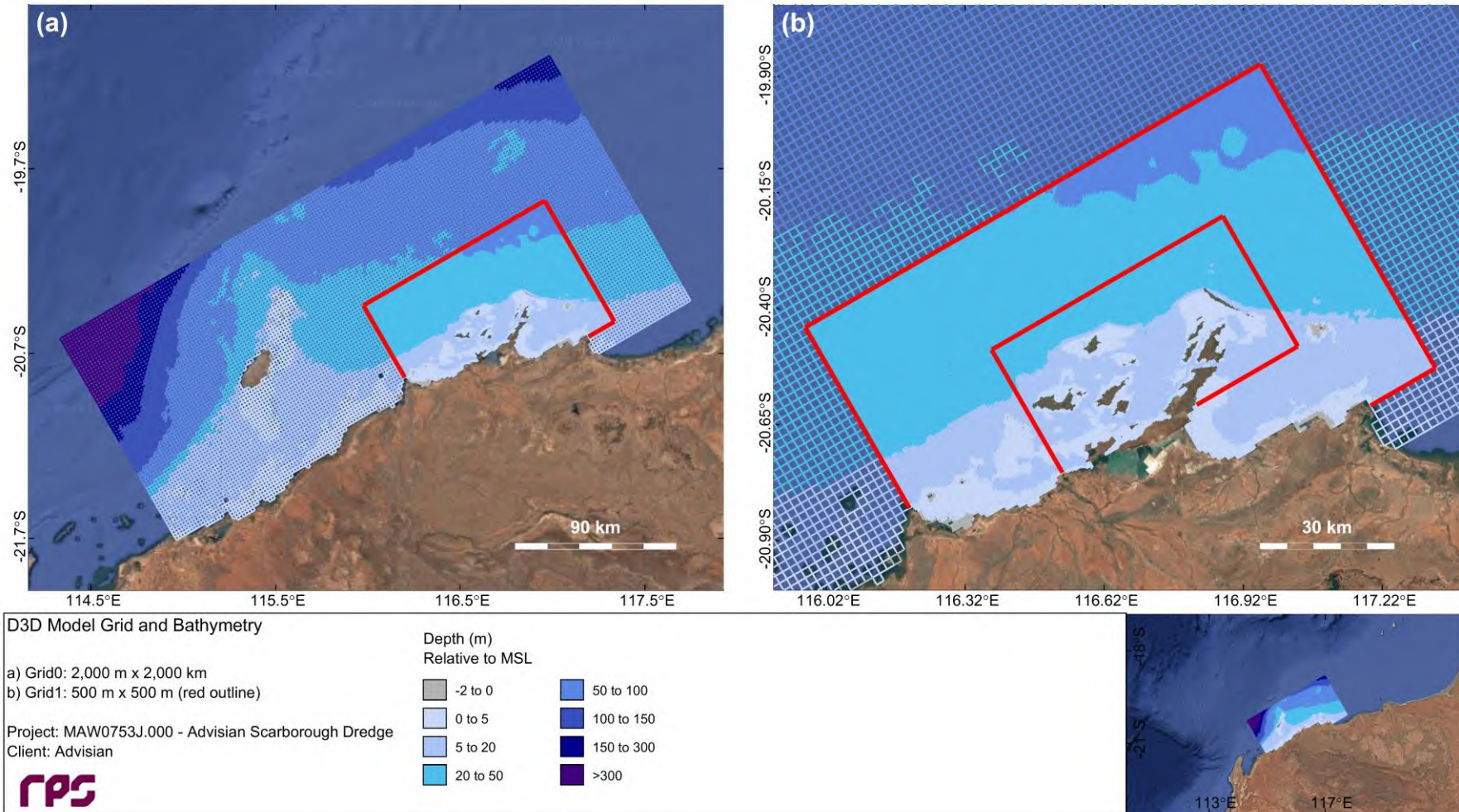
Figure 2.1   Model grid setup showing the domain-decomposition scheme applied, highlighting the two outermost grids.
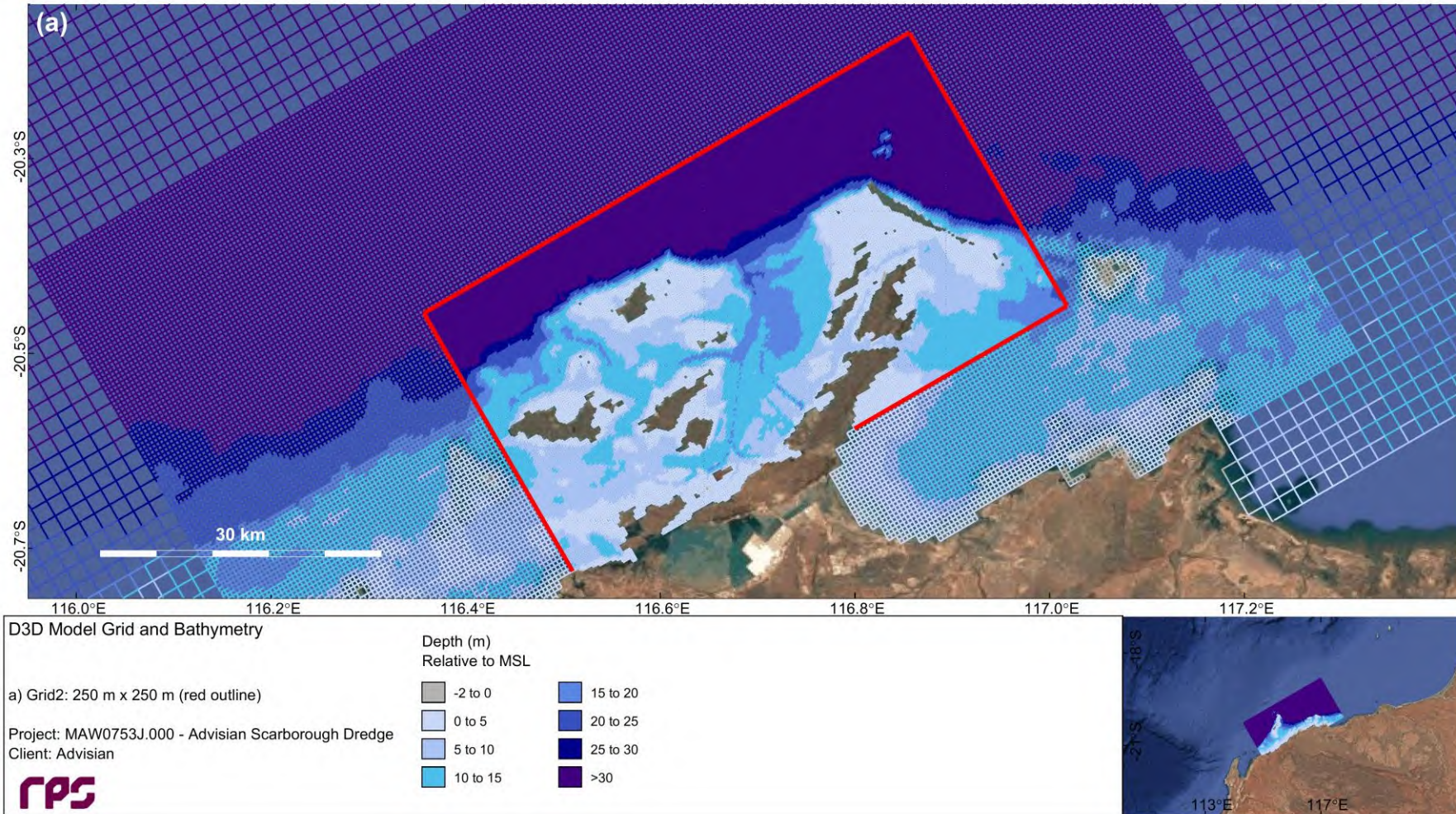
Figure 2.2   Model grid setup showing the domain-decomposition scheme applied, highlighting the innermost grid.

2.2.3   Boundary and Initial Conditions

2.2.3.1 Overview

As the hydrodynamics in the study area are controlled primarily by tidal flows and wind forcing, these processes were explicitly included in the developed model.

The model was forced on the open boundaries of the outer sub-domain with time series of water elevation obtained for the chosen simulation period. Spatially-varying wind speed and wind direction data was used to force the model across the entire domain.

2.2.3.2 Water Elevation

Water elevations at hourly intervals were obtained from the TPXO8.0 database, which is the most recent iteration of a global model of ocean tides derived from measurements of sea-surface topography by the TOPEX/Poseidon satellite-borne radar altimeters. Tides are provided as complex amplitudes of earth-relative sea-surface elevation for eight primary (M_2, S_2, N_2, K_2, K_1, O_1, P_1, Q_1), two long-period (M_f, M_m) and three non-linear (M_4, MS_4, MN_4) harmonic constituents at a spatial resolution of 0.25°.

The tidal sea level data was augmented with non-tidal sea level elevation data from the global Hybrid Coordinate Ocean Model (HYCOM; Bleck, 2002; Chassignet *et al.*, 2003; Halliwell, 2004), created by the USA's National Ocean Partnership Program (NOPP) as part of the Global Ocean Data Assimilation Experiment (GODAE). The HYCOM model is a three-dimensional model that assimilates observations of sea surface temperature, sea surface salinity and surface height, obtained by satellite instrumentation, along with atmospheric forcing conditions from atmospheric models to predict drift currents generated by such forces as wind shear, density, sea height variations and the rotation of the Earth.

The HYCOM model is configured to combine the three vertical coordinate types currently in use in ocean models: depth (z-levels), density (isopycnal layers), and terrain-following (σ-levels). HYCOM uses isopycnal layers in the open, stratified ocean, but uses the layered continuity equation to make a dynamically smooth transition to a terrain-following coordinate in shallow coastal regions, and to z-level coordinates in the mixed layer and/or unstratified seas. Thus, this hybrid coordinate system allows for the extension of the geographic range of applicability to shallow coastal seas and unstratified parts of the world ocean. It maintains the significant advantages of an isopycnal model in stratified regions while allowing more vertical resolution near the surface and in shallow coastal areas, hence providing a better representation of the upper ocean physics than non-hybrid models. The model has global coverage with a horizontal resolution of 1/12th of a degree (~7 km at mid-latitudes) and a temporal resolution of 24 hours.

2.2.3.3 Wind Forcing

Spatially-variable wind data was sourced from the Global Data Assimilation System (GDAS), which is used by the National Centers for Environmental Prediction (NCEP) Global Forecast System (GFS) model to place observations into a gridded model space for the purpose of starting, or initializing, weather forecasts with observed data. The GFS Forecasts model variant used has a horizontal resolution of 1/12th of a degree and a temporal resolution of 6 hours (NCEP, 2016).

2.2.4   Model Validation

2.2.4.1 Comparison of Modelled and Measured Water Elevation

Validation of the water level changes predicted by the D-FLOW hydrodynamic model configuration was provided through comparisons to independent predictions from the XTide tidal constituent database (Flater,

1998). Comparison of model tidal amplitudes with the XTide database showed strong agreement (Figure 2.3), with slight overprediction of tidal amplitudes at some stations. Time series comparisons for two tide stations situated at locations that are relevant to this study also showed good agreement (Figure 2.4).

In general, a consistent match is observed between water elevations calculated by the D-FLOW model and those predicted by XTide (Figure 2.4). Both the amplitude and phase of the semidiurnal tidal signal are clearly reproduced at each station, as is the timing of the spring-neap cycle. The D-FLOW model slightly overpredicts high tides and underpredicts low tides, which indicates there was a small difference between the datums used to compare these different data sets rather than actual amplitude differences.
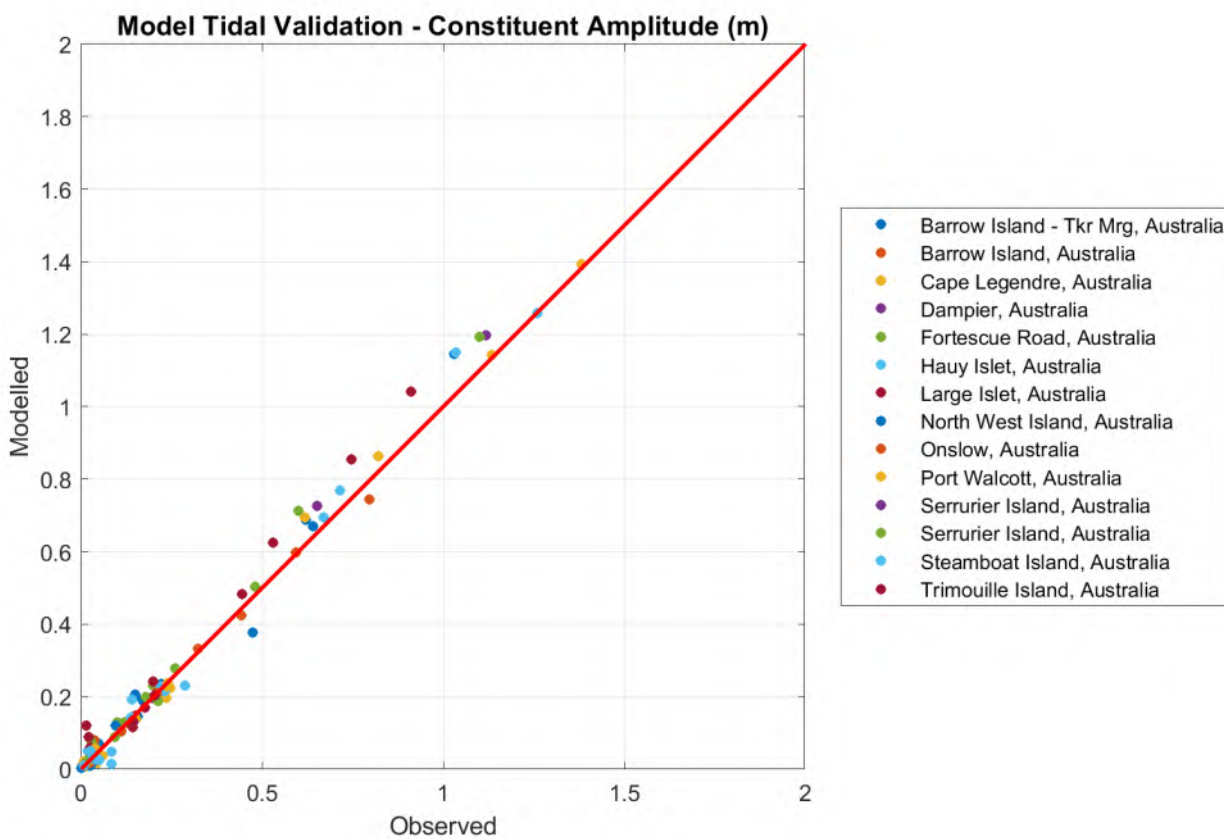
Figure 2.3   Comparison of tidal amplitudes from the D-FLOW hydrodynamic model (y-axis) with those from the XTide database (x-axis) at 14 stations located within the model domain.
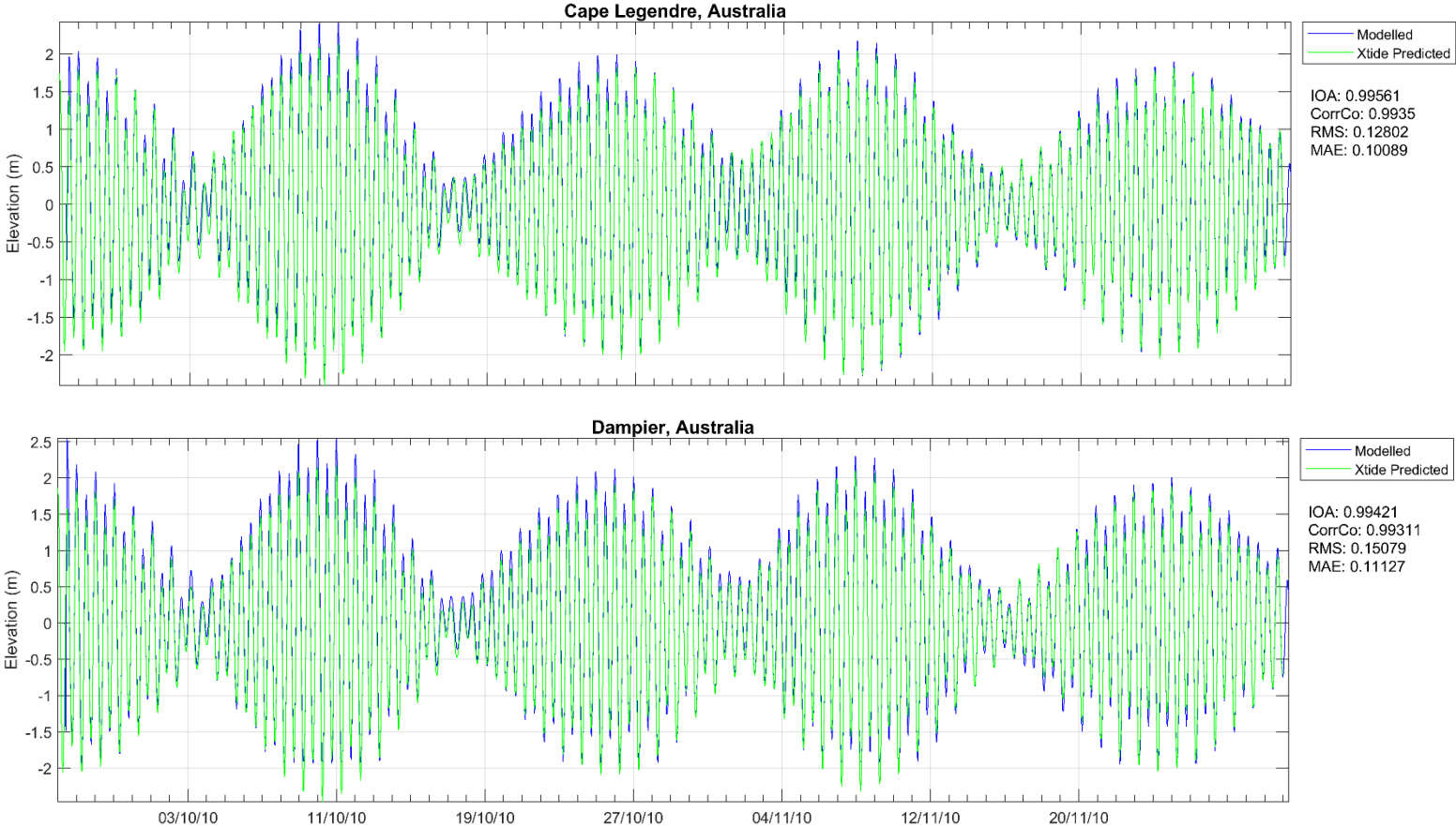
Figure 2.4   Comparisons of water elevations predicted by the D-FLOW hydrodynamic model (blue line) with those predicted by the XTide database (green line) over the validation period of October-November 2010 at two selected station locations.

2.2.4.2 Comparison of Modelled and Measured Currents

Validation of the model-predicted currents was conducted for a spring/neap tide period during October and November 2010 by comparing the model results to measured data from the Woodside LNG Channel AWAC that was located within Mermaid Sound (116.738° E, 20.561° S) in water depth of approximately 12 m. Comparisons of current speed and direction at a depth interval representative of the mid-water column are provided in Figure 2.5.

Overall, the comparison indicates that the model provides a good prediction of tidal currents at the comparison site. There was a minor mismatch in the phase of the tidal oscillations, with a slight lag apparent in the modelled data. However, this lag was not evident in the XTide water level comparisons (Figure 2.4).

The amplitudes of the modelled and measured current fluctuations were generally well-matched, but there were some spikes in the measured data that were not reproduced. These spikes in the measured data, assuming they were not instrument errors, may have been caused by local-scale events related to wind-driven currents. These events are difficult to reproduce in the model because the horizontal grid scale of the model in this region is 250 m. The GFS wind driving the model can be less accurate close to the coast when sea breeze effects are dominant. The inability of the model to reproduce some spikes observed in the measured data might be explained by inaccuracies in the NCEP wind data near to the Woodside LNG Channel AWAC location.
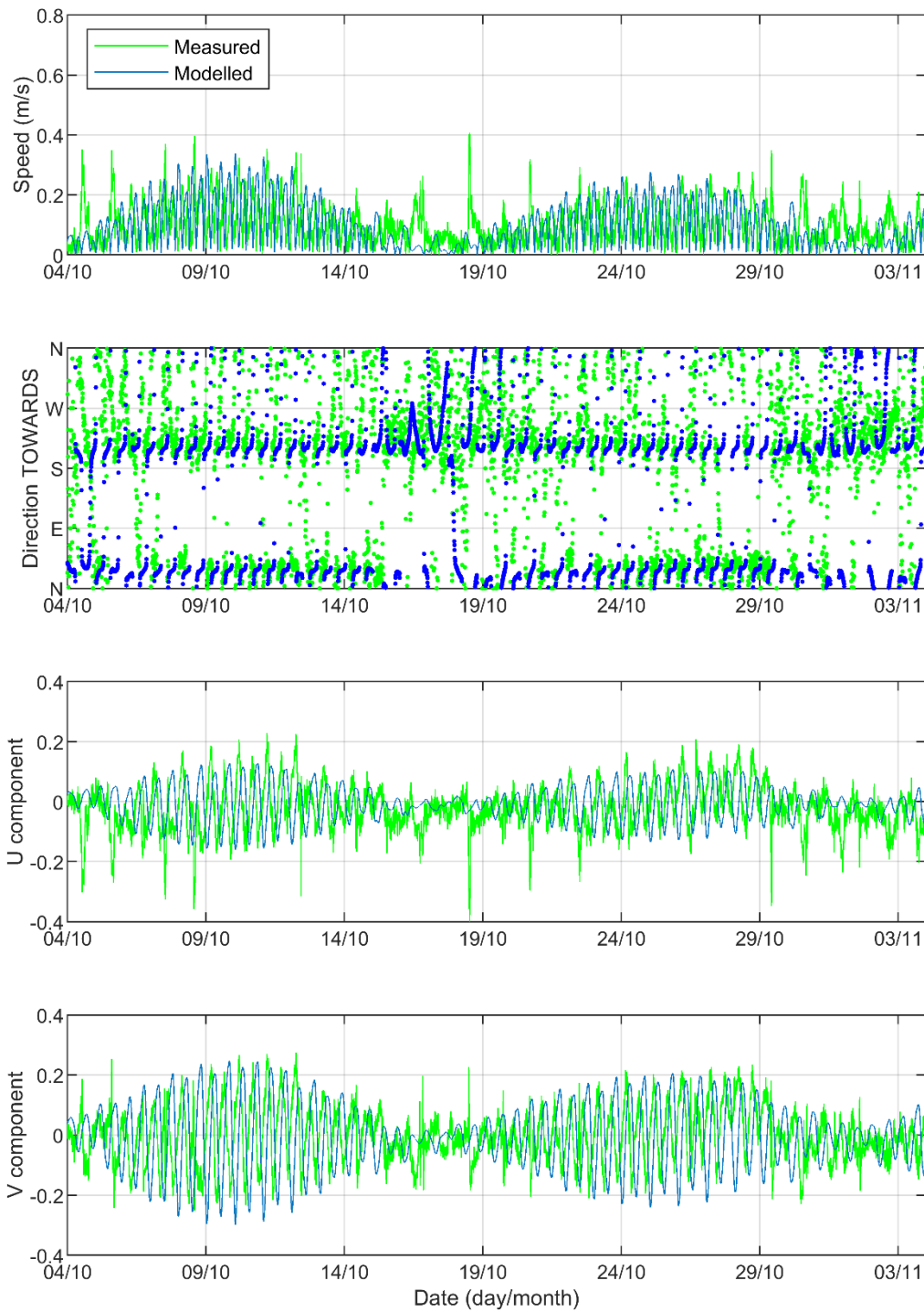
Figure 2.5   Comparisons of modelled (blue line) and measured (green line) currents for a mid-water column depth interval at the Woodside LNG Channel AWAC location during the 2010 validation period.

2.3 Wave Model (D-WAVE)

2.3.1 Model Description

Reliable forecasting for the fate of fine sediments in the study location, which is a wave-exposed coastal region, required the input of wave spectra information to calculate the shear-stress and orbital velocities imposed by waves which will affect the settlement and re-suspension of fine material that is initially suspended by dredging and related operations. D-WAVE is a variant of the well-known SWAN wave model that has been customised for compatibility with the Delft3D software suite.

The D-WAVE model is a spectral phase-averaging wave model originally developed by the Delft University of Technology. D-WAVE, a third-generation model based on the energy balance equation, is a numerical model for simulating realistic estimates of wave parameters in coastal areas for given wind, bottom and current conditions.

D-WAVE includes algorithms for the following wave propagation processes: propagation through geographic space; refraction and shoaling due to bottom and current variations; blocking and reflections by opposing currents; and transmission through or blockage by obstacles. The model also accounts for dissipation effects due to white-capping, bottom friction and wave breaking as well as non-linear wave-wave interactions. D-WAVE is fully spectral (in all directions and frequencies) and computes the evolution of wind waves in coastal regions with shallow water depths and ambient currents.

RPS has successfully applied D-WAVE in many studies in the region, including ambient condition modelling in Mermaid Sound and dredging fate projects in the wider Pilbara region.

2.3.2 Model Implementation

The D-WAVE model was developed to cover the same grid regions defined by the hydrodynamic model (Figure 2.1 and Figure 2.2). The bathymetry and wind data input to the wave model was the same as used for the hydrodynamic model. Time-varying water level information for each grid node in the wave model was provided by the output of the hydrodynamic model. The boundary data to represent swells imposed from a distance was sourced from the WAVEWATCH III 0.5° model, operated by the National Oceanic and Atmospheric Administration (NOAA) (NOAA, 2018).

The wave model was run in a coupled mode with the hydrodynamic model for the years of 2016 and 2017. The model results were independently validated by comparison to other modelled wave data for the Mermaid Sound region that is held internally by RPS.

3 SEDIMENT FATE MODELLING

3.1 General Approach

Estimates for the three-dimensional distribution of sediments suspended by dredging, disposal and backfill operations have been derived for the full duration of the pipeline dredging and backfill program using numerical modelling. The approach of modelling dredging operations in full and in three dimensions is in line with best practice for sediment dispersion modelling in Western Australia as outlined by WAMSI Dredging Science Node guidance (Sun *et al.*, 2016).

This modelling relied upon specification of sediment discharges over time for each of the expected sources of sediment suspension, and predicted the evolution of the combined sediment plumes via current transport, dispersion, sinking and sedimentation. The model allowed for the subsequent resuspension of settling sediments due to the erosive effects of currents and waves. Thus, the fate of sediments was assessed beyond their initial settling.

Forcing was provided using predictions of three-dimensional current fields and two-dimensional wave fields for the study area, which are described in Section 2.

3.2 Model Description

Modelling of the dispersion of suspended sediment resulting from the various dredging, disposal and backfill operations was undertaken using an advanced sediment fate model, Suspended Sediment FATE (SSFATE), operating within the RPS DREDGEMAP model framework. This model computes the advection, dispersion, differential sinking, settlement and resuspension of sediment particles. The model can be used to represent inputs from a wide range of suspension sources, producing predictions of sediment fate both over the short-term (minutes to days following a discharge source) and longer term (days to years following a discharge source).

SSFATE allows the three-dimensional predictions of SSC and seabed sedimentation to be assessed against allowable exposure thresholds. Sedimentation thresholds often relate to burial depths or rates, while SSC thresholds are usually more complicated, involving tiered exposure duration and intensities. As a result, assessing the project-generated sediment distributions against these thresholds in both three-dimensional space and time is a computationally intensive task. A variety of SSC threshold formulations have recently been applied in Western Australian coastal waters and at present there are no general guidelines.

SSFATE is a computer model originally developed jointly by the US Army Corps of Engineers (USACE) Engineer Research and Development Center (ERDC) and RPS to estimate SSC generated in the water column and deposition patterns generated due to dredging operations in a current-dominated environment, such as a river (Johnson *et al.*, 2000; Swanson *et al.*, 2000, 2004). RPS has significantly enhanced the capability of SSFATE to allow the prediction of sediment fate in marine and coastal environments where wave forcing becomes important for reworking the distribution of sediments (Swanson *et al.*, 2007).

SSFATE is formulated to simulate far-field effects (~25 m or larger scale) in which the mean transport and turbulence associated with ambient currents are dominant over the initial turbulence generated at the discharge point. A five-class particle-based model predicts the transport and dispersion of the suspended material. The classes include the 0-130 μm range of sediment grain sizes that typically result in plumes. Heavier sediments tend to settle very rapidly, remain more stable over time and are not relevant over the longer durations (>1 hour) and larger spatial scales (>25 m) of interest here. Table 3.1 shows the standard material classes used in SSFATE for suspended sediment.

Table 3.1   Material size classes used in SSFATE.

Material Class Description	Particle Size Range (µm)
Clay	<7
Fine Silt	8-34
Coarse Silt	35-74
Fine Sand	75-130
Coarse Sand	>130

Particle advection is calculated using three-dimensional current fields, obtained from hydrodynamic modelling, thus the model can account for vertical changes in the currents within the water column. For example, as particles sink towards the seabed they will tend to be moved at slower speeds due to the slowing of currents by friction at the seabed. Particle diffusion is assumed to follow a random walk process using a Lagrangian approach of calculating transport, which uses a grid-less space to remove limitations of grid resolution, artefacts due to grid boundaries, and also maintain a high degree of mass conservation.

Following release into the model space, the sediment cloud evolves according to the following processes:

- Advection due to the three-dimensional current field.

- Diffusion by a random walk model with the mass diffusion rate specified, ideally, from measurements at the site. As particles represent an ensemble of real particles, each particle in the model has an associated Gaussian distribution governed by particle age and the mass diffusion properties of the surrounding water.

- Settlement or sinking of the sediment due to buoyancy forces. Settlement rates are determined from the particle class sizes and include allowance for flocculation and other concentration-dependent behaviour, following the model of Teeter (2000).

- Potential deposition to the seabed determined using a model that couples the deposition across particle classes (Teeter, 2000). The likelihood and rate of deposition depends on the shear stress at the seabed. High shear inhibits deposition, and in some cases excludes it altogether with sediment remaining in suspension. The model allows for partial deposition of individual particles according to a practical deposition rate, thereby allowing the bulk sediment mass to be represented by fewer particles.

- Potential resuspension from the seabed, if previously deposited, at a rate governed by exceedance of a shear stress threshold at the seabed due to the combined action of waves and currents. Different thresholds are applied for resuspension depending upon the size of the particle and the duration of sedimentation, based on empirical studies that have demonstrated that newly-settled sediments will have higher water content and are more easily resuspended by lower shear stresses (Swanson *et al.*, 2007). The resuspension flux calculation also accounts for armouring of fine particles within the interstitial spaces of larger particles. Thus, the model can indicate whether deposits will stabilise or continue to erode over time given the shear forces that occur at the site. Resuspended material is released back into the water column to be affected by the processes defined above.

SSFATE formulations and proof of performance have been documented in a series of USACE Dredging Operations and Environmental Research (DOER) Program technical notes (Johnson *et al.*, 2000; Swanson *et al.*, 2000), and published in the peer-reviewed literature (Andersen *et al.*, 2001; Swanson *et al.*, 2004; Swanson *et al.*, 2007). SSFATE has been applied and validated by RPS against observations of sedimentation and suspended sediments at multiple locations in Australia, notably Cockburn Sound for Fremantle Ports and Mermaid Sound for the LNG Foundation Project dredging program.

3.3   Model Limitations

There are inherent limitations to the accuracy of numerical models. The possible sources of uncertainty within the modelling conducted for the sediment fate assessment of the Scarborough development include:

- *The equations and algorithms applied in the model*. The formulations included in the model, as discussed in Section 3.2, were selected to achieve the best possible representation of the relevant processes and have been proven to be valid over a range of projects.

- *The accuracy of the physical (current and wave) inputs to the model*. Current and wave forcing inputs were provided from validated three-dimensional hydrodynamic and wave models created and customised for the study area. The accuracy of these models is suitable, as good correlations with field measurements and independent model predictions have been achieved, with the uncertainties minimised and quantifiable. The hydrodynamic and wave models are described in Section 2. It should be noted that the model inputs are a hindcast of past metocean conditions; the overall trends reflected in this data will be broadly reflected in future conditions, but conditions on any given day during the actual dredging operations may be quite different.

- *The accuracy of dredge methodology inputs to the model*. Specification of the proposed dredge and disposal methodologies was provided by Woodside after consultation with the dredging contractors that may be engaged to perform the work. Any assumptions made to achieve a realistic representation of the dredging and disposal activities are outlined in Section 3.5 and were based on extensive past project experience.

- *The accuracy of the material properties input to the model*. Geotechnical information obtained during previous site investigations for the LNG Foundation Project was provided by Woodside (Woodside, 2018b) and is discussed in Section 3.6. From this data, the properties of the in situ material to be dredged are reasonably well-known. However, it is not possible to determine how the material properties will be changed by the action of the dredge and the mixing of the material with seawater in the process of pumping it to the hopper. Therefore, assumptions were made in the model with regard to the material that is released into the water column from dredging and the material properties of the sediments that are to be placed at the spoil grounds.

- *The accuracy of the dredging and disposal sediment source terms input to the model*. The source definition in the model is flexible and can be applied to any sediment source by specifying the time-varying flux rate, particle size distribution (PSD) and vertical profile in the water column. This information will be specific to the equipment used and the material encountered at the site, and therefore can only be determined with confidence from a pilot study at the site or field measurements during dredging. In the absence of such data, assumptions were made with regard to these parameters. The assumptions are outlined in Section 3.7 and were based on literature review, including the recent WAMSI Dredging Science Node reports, and extensive past project experience.

The major sources of uncertainty for the sediment fate modelling are the modelled dredging methodology and sediment source inputs to the model. The assumptions made were based on literature review and experience, and aimed to give a good representation of the sources of suspended sediment that will result from the proposed dredging, disposal and backfill activities. However, as there were uncertainties in the inputs to the model, the results should be considered as indicative of the expected ranges in magnitude and distribution of suspended sediments and sedimentation, rather than an exact prediction.

3.4   Model Domain and Bathymetry

The DREDGEMAP model domain established for the Scarborough dredging works extended approximately 95 km north-south by 115 km east-west (Figure 3.1). The model grid covers the section of the Western Australian coastline from Regnard Bay, south of West Intercourse Island, to Point Samson in the east. The offshore boundaries of the domain were imposed at a reasonable distance from the proposed dredging areas, to allow potential sediment drift patterns in offshore directions to be adequately captured.

This region lies within the model domain of the Delft3D hydrodynamic and wave models that provide the current and wave inputs to DREDGEMAP (see Section 2). A grid resolution of 100 m by 100 m was selected to ensure that existing features in the domain, including the many bays, islands and passages of the Dampier Archipelago, were adequately defined.
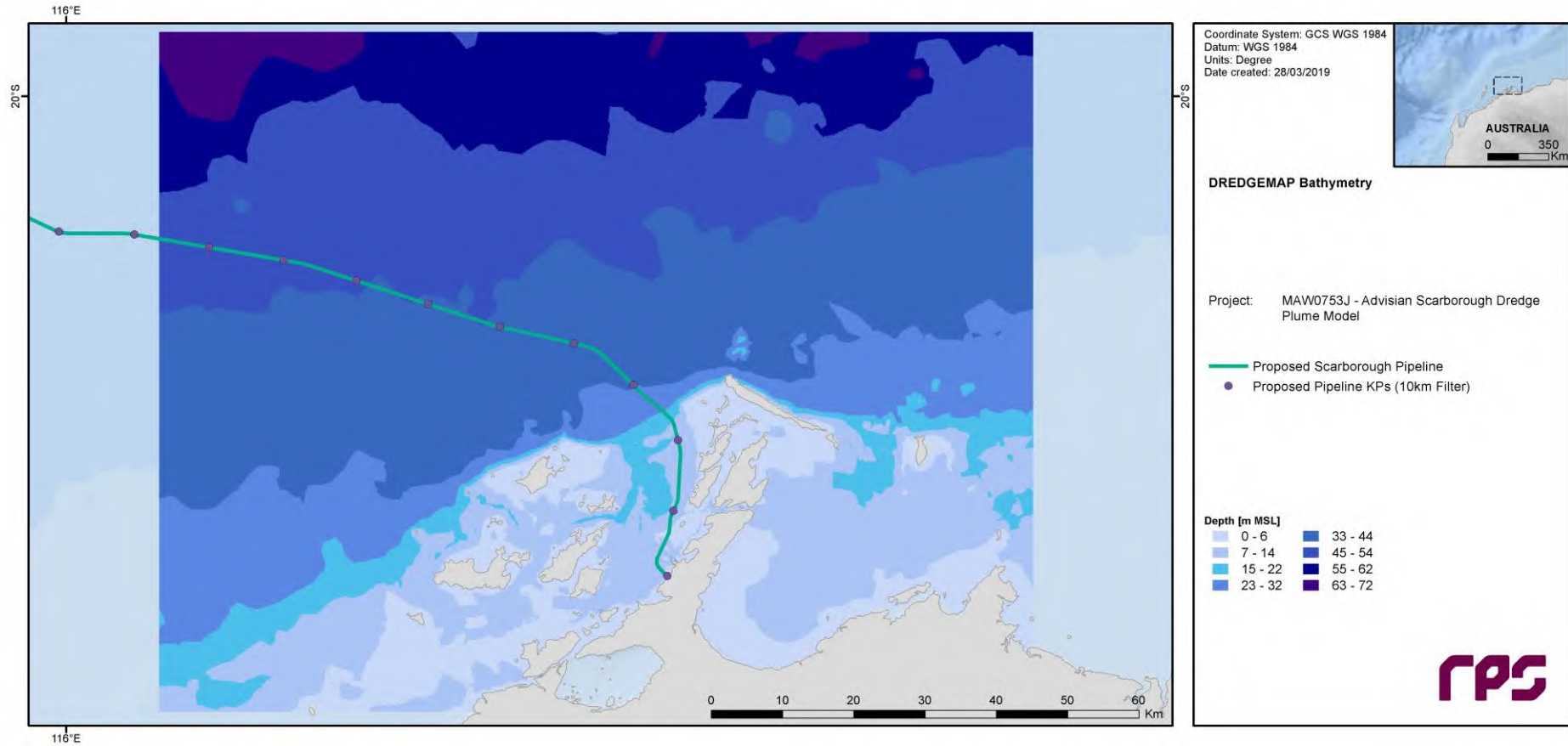
Figure 3.1   DREDGEMAP model domain and bathymetry (m MSL).

3.5 Dredging Project Description and Model Operational Assumptions

3.5.1 Overview

Information outlining the proposed dredging, disposal and backfill operations for the development of Scarborough has been drawn from the Scope of Work document (Advisian, 2018), subsequent email discussions, and input data provided by Woodside and its potential dredging contractors. At the time of commencement of modelling, the collated information represented the best available data with regard to geotechnical properties of the project areas, the dredging and construction methodologies expected to be used within these areas, and the typical characteristics of vessels that may be engaged for the work.

The operations modelled have been broken into two phases with four main activities:

- Phase 1 (Dredging):

    – Dredging of sediment along the pipeline route;

    – Disposal of dredged sediment at three nominated spoil grounds.

- Phase 2 (Backfilling):

    – Dredging of the borrow ground;

    – Backfill and stabilisation of the pipeline.

The pipeline route, spoil grounds and borrow grounds will cover State and Commonwealth Waters (Figure 1.1).

The following sections outline the details of the operations for each of these activities and highlight any assumptions that were made.

3.5.2 Methods and Equipment

3.5.2.1 Pipeline Route Dredging

The material to be dredged from the pipeline route will consist mainly of marine sediments (approximately 3.8 Mm^3) and marine sediment/coarse material mix (approximately 0.2 Mm^3).

The dredging operations for the pipeline route have been divided into ten sections as outlined in Table 3.2, with seven of these sections requiring dredging. The dredging in each of the seven sections was assumed to be completed with either a backhoe dredge (BHD) or a trailing suction hopper dredge (TSHD). Typically, a TSHD will dredge unconsolidated sediments and a BHD will dredge sedimentary rock, and the quantities of each material type assumed in this case are detailed in Section 3.5.3. The assumed BHD bucket size was in the range of 20 m^3 (rock) to 30 m^3 (general purpose), while the TSHD hopper size was assumed to be 12,000 m^3 (filled 98% to capacity). It has been specified that overflow of fines from the TSHD hopper and dewatering of the split hopper barges that accompany the BHD will be permitted.

The estimated cycle times for dredging within each pipeline section where the BHD will operate are presented in Table 3.3, and those for each pipeline section where the TSHD will operate are presented in Table 3.4 (Woodside, 2018a).

The potential for sediment mobilisation by TSHD propeller-wash effects has been considered along all relevant pipeline sections. This has been done using supplied data on vessel characteristics, and local depth and

seabed composition. For the purposes of the modelling assessment, the relevant specifications were as follows:

- Vessel draft: 10.0 m loaded and 6.0 m empty.

- Number of propellers: 2 (ducted).

- Diameter of propellers: 4.0 m.

- Thrust power: 5,800 kW per propeller.

Table 3.2   Provisional outline of proposed pipeline dredging and disposal activities.

Pipeline Zone	Pipeline Location	Vessel	Task Description	Disposal Location
PRE1	KP0.1 – KP0.6	BHD & barges	Dredging of a 3.5 m deep trench. Dredging of pre-treated sediment if required.	AB
PRE2	KP0.6 – KP3.6	BHD & barges and TSHD	Dredging of a 3.5-4.0 m deep trench.	AB
PRE3	KP3.6 – KP4.6	TSHD	Clearing out of a pre-excavated trench across the NWS Shipping Channel.	AB
PRE4	KP4.6 – KP6.2	BHD & barges and TSHD	Dredging of a 3.0 m deep trench.	AB
PRE5	KP6.2 – KP11.0	N/A	No dredging.	N/A
PRE6	KP11.0 – KP18.4	TSHD	Dredging of a 2.0-3.0 m deep trench.	2B
PRE7	KP18.4 – KP19.3	N/A	No dredging.	N/A
PRE8	KP19.3 – KP21.3	TSHD	Dredging of a 2.5-3.0 m deep trench.	2B
PRE9	KP21.3 – KP24.4	N/A	No dredging.	N/A
PRE10	KP24.4 – KP50.0	TSHD	Dredging of a 2.5-3.5 m trench along sections with unconsolidated sediment.	5A

Table 3.3   Estimated cycle times for each pipeline section where the BHD will be operating.

Pipeline Zone	Non-Dewatering Time (min)	Dewatering Time (min)	Disposal Time (min)	Sailing Time (min)	Total Cycle Time (min)
PRE1	90	360	20	84	464
PRE2	160	640	20	72	732
PRE4	160	640	20	48	708

Table 3.4   Estimated cycle times for each pipeline section where the TSHD will be operating.

Pipeline Zone	Non-Overflow Time (min)	Overflow Time (min)	Disposal Time (min)	Sailing Time (min)	Total Cycle Time (min)
PRE2	45	210	20	77	352
PRE3	45	210	20	64	339
PRE4	45	210	20	58	333
PRE6	45	210	20	102	377
PRE8	45	210	20	83	358
PRE10	45	210	20	40	315

3.5.2.2 Spoil Ground Disposal

As outlined in Table 3.2, it was assumed that all material dredged by the BHD will be placed into a waiting split hopper barge and transported to the offshore disposal areas, while all material dredged by the TSHD will be transported directly to the offshore disposal areas.

It was assumed that the BHD will be accompanied by two split hopper barges, assumed to be approximately 3,800 m³ in capacity, to be used for disposal of dredged material. Material discharges from the split hopper barges were assumed to occur between depths of 5.8 m and 1.5 m below mean sea level.

The TSHD hopper doors, from which discharge will occur, were assumed to be opened at a depth of 12.75 m below sea level. The modelled vessel draft will be reduced as spoil is discharged to a minimum depth of 8.75 m below sea level when empty.

The split hopper barges will be pushed or towed by a harbour tug. The potential for sediment mobilisation by tug propeller-wash effects has been considered along all relevant pipeline sections. This has been done using supplied data on vessel characteristics, and local depth and seabed composition. For the purposes of the modelling assessment, the relevant specifications were as follows:

- Vessel draft: 4.5 m (tug).

- Number of propellers: 2 (ducted).

- Diameter of propellers: 2.5 m.

- Thrust power: 1,850 kW per propeller.

The allocations of dredge spoil from each pipeline section to each spoil ground are shown in Table 3.5. It was assumed that the broad aim of the spoil disposal patterns will be to evenly distribute the total volume of allocated material across the entire spoil ground area by the conclusion of all activities, so the spacing of individual disposal operations (which are restricted to a comparatively small area within the spoil ground) was designed to achieve this.

Table 3.5   Anticipated spoil ground allocations of dredge volumes from each pipeline section.

Spoil Ground	Pipeline Zone	Spoil Volume (m³)	Spoil Ground Area (m²)	Theoretical Thickness (m)
AB	PRE1-4	501,832	4,000,000	0.13
2B	PRE6 & 8	424,677	2,600,000	0.16
5A	PRE10	943,032	3,200,000	0.29

3.5.2.3 Borrow Ground Dredging

Dredging of backfill material from the borrow ground locations will consist of the removal of approximately 2 Mm³ of sandy sediments with a low proportion of fines.

It was assumed that dredging of the borrow grounds will be conducted using a TSHD, with two options modelled. For Option A all material will be dredged from borrow ground A, and for Option B all material will be dredged from borrow ground B (Figure 1.1). The TSHD hopper size was assumed to be 9,700 m³ (filled at a rate of approximately 90 m³/min). It has been specified that overflow of fines from the TSHD hopper will be permitted.

The estimated cycle times for TSHD dredging within the borrow grounds and placement of material within each pipeline section are presented in Table 3.6 (Woodside, 2018a).

The pipeline route runs through the eastern edge of borrow ground B. Although the dredging and backfill activities are obviously not coincident in time, it has been assumed that dredging of backfill material will be restricted to approximately the western three-quarters of the borrow ground to avoid disturbing the previously-dredged pipeline route.

The potential for sediment mobilisation by TSHD propeller-wash effects has been considered in both borrow grounds. This has been done using supplied data on vessel characteristics, and local depth and seabed composition. For the purposes of the modelling assessment, the relevant specifications were as follows:

- Vessel draft: 10.0 m loaded and 6.0 m empty.
- Number of propellers: 2 (ducted).
- Diameter of propellers: 4.0 m.
- Thrust power: 5,800 kW per propeller.

Table 3.6   Estimated cycle times for each pipeline section where the TSHD will be placing material dredged from the borrow grounds.

Pipeline Zone	Non-Overflow Time (min)	Overflow Time (min)	Placement Time (min)	Sailing Time (min)	Total Cycle Time (min)
POST2	30	74	107	46	257
POST4	30	74	107	46	257
POST6	30	74	107	53	264
POST8	30	74	107	53	264
POST10	30	74	107	58	269

3.5.2.4 Pipeline Route Backfill

The backfill operations for the pipeline route have been divided into ten sections as outlined in Table 3.7. It was assumed that rock backfill will be placed by a side-dump vessel and sand backfill will be placed by a TSHD.

The side-dump vessel was assumed to have a capacity of 4,500 tonnes with an average installation rate of approximately 2,250 tonnes/hr, with rock dumped from a fixed height at the sea surface. The TSHD hopper size was assumed to be 9,700 m^3 (emptied at a rate of approximately 90 m^3/min), with sand discharged through the suction pipe at an elevation of approximately 5 m above the pipeline.

The potential for sediment mobilisation by TSHD and side-dump vessel propeller-wash effects has been considered along the relevant pipeline sections. This has been done using supplied data on vessel characteristics, and local depth and seabed composition. For the purposes of the modelling assessment, the relevant specifications were as follows:

- Vessel draft:
    - 10.0 m loaded and 6.0 m empty (TSHD).
    - 4.8 m loaded (side-dump vessel).
- Number of propellers:
    - 2 (ducted; TSHD).
    - 2+2 (ducted; side-dump vessel).
- Diameter of propellers:
    - 4.0 m (TSHD).
    - 2.5 m (side-dump vessel).
- Thrust power:
    - 5,800 kW per propeller (TSHD).
    - 2 x 1,250 kW and 2 x 1,000 kW (side-dump vessel).

Table 3.7   Provisional outline of proposed pipeline backfill and stabilisation activities.

Pipeline Zone	Pipeline Location	Vessel	Task Description	Borrow Location
POST1	KP0.1 – KP0.6	Side-dump vessel	Rock backfill (1.2-2.0 m cover over top of pipe).	Rock from the Nickol Bay Quarry.
POST2	KP0.6 – KP3.6	TSHD	Sand backfill (≥3.0 m cover over top of pipe).	Sand from the borrow grounds indicated in Figure 1.1.
POST3	KP3.6 – KP4.6	Side-dump vessel	Rock backfill (2.0 m cover over top of pipe).	Rock from the Nickol Bay Quarry.
POST4	KP4.6 – KP6.2	TSHD	Sand backfill (1.7-2.5 m cover over top of pipe).	Sand from the borrow grounds indicated in Figure 1.1.
POST5	KP6.2 – KP11.0	Side-dump vessel	No cover rock berm (flush to top of pipe).	Rock from the Nickol Bay Quarry.
POST6	KP11.0 – KP18.4	TSHD	Sand backfill (0.8-1.7 m cover over top of pipe).	Sand from the borrow grounds indicated in Figure 1.1.
POST7	KP18.4 – KP19.3	Side-dump vessel	No cover rock berm (flush to top of pipe).	Rock from the Nickol Bay Quarry.
POST8	KP19.3 – KP21.3	TSHD	Sand backfill (1.2-1.7 m cover over top of pipe).	Sand from the borrow grounds indicated in Figure 1.1.
POST9	KP21.3 – KP24.4	Side-dump vessel	No cover rock berm (flush to top of pipe).	Rock from the Nickol Bay Quarry.
POST10	KP24.4 – KP50.0	TSHD	Sand backfill (0.7-1.7 m cover over top of pipe).	Sand from the borrow grounds indicated in Figure 1.1.

3.5.3   Quantities and Production Rates

For dredging of each section along the pipeline route, the proposed dredge depths, quantities for each material type, and production rates for each material type were specified for input to the modelling (Table 3.8). The table has two material categories, defined as "soft" (unconsolidated sediments) and "moderate" (calcareous sedimentary rock). It is understood that no "hard" material (andesite igneous rock) will be present due to its removal during capital dredging activities for the LNG Foundation Project (Woodside, 2018b).

For sand backfill of each relevant section along the pipeline route, which involves dredging of one of the two potential borrow grounds, the proposed quantities and production rates for each material type were specified for input to the modelling (Table 3.9). The sole material category within the borrow grounds was assumed to be unconsolidated sediments ("soft" material). It was also assumed that production rates for dredging at each potential borrow ground were identical.

For rock backfill section where rock is to be placed, quantities for each material category were specified (Table 3.10).

It is understood that:

- The estimated material quantities were based on the latest surveyed bathymetry and a geotechnical model incorporating existing geotechnical data;
- The estimated production rates were based on the material type and equipment that may be used for dredging;
- The estimated production rates were average values inclusive of expected downtime estimates.

Table 3.8   Modelled dredge depths, quantities of material type, and production rates by material type for dredging of each pipeline section.

Pipeline Zone	Dredge Depth (m CD)	Dredged Quantities (m³)			Production Rates (m³/week)	
	Target	Soft Material	Moderate Material	Total	Soft Material	Moderate Material
PRE1	+4.3 / -5.5	13,811	10,131	23,942	40-60,000	15-20,000
PRE2	-13.1 / -11.1	216,995	21,256	238,251	175-225,000	15-20,000
PRE3	-10.7 / -18.6	131,992	-	131,992	175-225,000	-
PRE4	-9.7 / -11.3	87,890	19,760	107,650	175-225,000	15-20,000
PRE6	-13.0 / -16.0	349,334	-	349,334	175-225,000	-
PRE8	-14.4 / -17.7	75,343	-	75,343	175-225,000	-
PRE10	-24.0 / -44.9	943,032	-	943,032	175-225,000	-
	Totals	**1,818,397**	**51,147**	**1,869,544**	-	-

Table 3.9   Modelled quantities of material type and production rates by material type for dredging of sand backfill material for each pipeline section from the borrow grounds.

Pipeline Zone	Dredged/Backfill Quantities (m³)	Production Rates (m³/week)
	Soft Material	Soft Material
POST2	159,992	325,000
POST4	80,394	325,000
POST6	349,334	325,000
POST8	75,343	325,000
POST10	943,032	325,000
Totals	**1,608,095**	-

Table 3.10 Modelled quantities of material type for placement of rock backfill material within each pipeline section.

Pipeline Zone	Backfill Quantities (m³)		
	Material Category 1	Material Category 2	Total
POST1	4,577	5,399	9,976
POST3	8,395	21,979	30,374
POST5	6,384	10,032	16,416
POST7	2,170	3,410	5,580
POST9	4,270	6,710	10,980
Totals	25,896	47,530	73,426

3.5.4 Schedules

For dredging of each section along the pipeline route, the proposed duration and sequencing of operations has been specified for input to the modelling (Table 3.11). The table has two material categories, as described in Section 3.5.3.

The sequence of dredging has been assumed to start in zone PRE1 and proceed consecutively to zone PRE10. Modelling of each section involves a series of dredging and related disposal activities. Allocations of spoil material from each pipeline section to each of the three spoil grounds are outlined in Table 3.2.

For backfill of each section along the pipeline route, the proposed duration and sequencing of operations has been specified for input to the modelling (Table 3.12). The table has two material categories, as described in Section 3.5.3.

The sequence of backfilling has been assumed to involve completing all sand backfill tasks (proceeding consecutively from zone POST2 to zone POST10) and then completing all rock backfill tasks (proceeding consecutively from zone POST1 to zone POST9). Modelling of each section involves a series of dredging and related backfill activities. For the pipeline sections where rock backfill will be placed, no associated borrow ground dredging will occur.

Table 3.11 Modelled durations of dredging and disposal operations by material type for each pipeline section.

Pipeline Zone	Duration of Operations (weeks)		
	Material Category 1	Material Category 2	Total
PRE1	0.3	0.6	0.9
PRE2	0.9	1.2	2.1
PRE3	0.5	-	0.5
PRE4	0.4	1.1	1.5
PRE6	1.4	-	1.4
PRE8	0.3	-	0.3
PRE10	3.8	-	3.8
Totals	7.6	2.9	10.5

Table 3.12   Modelled durations of dredging and backfill operations by material type for each pipeline section.

Pipeline Zone	Duration of Operations (weeks)		
	Material Category 1	Material Category 2	Total
POST1	0.2	0.2	0.4
POST2	1.0	0.0	1.0
POST3	0.3	0.9	1.2
POST4	0.5	0.0	0.5
POST5	0.3	0.4	0.7
POST6	2.0	0.0	2.0
POST7	0.1	0.1	0.2
POST8	0.5	0.0	0.5
POST9	0.2	0.3	0.5
POST10	6.0	0.0	6.0
Totals	**11.1**	**1.9**	**13.0**

3.5.5   Scenario Summary

The provisional schedule for the dredging works indicates a July 2021 start for dredging of the pipeline route followed by a December 2021 start for backfill and stabilisation works. Analysis of wind data in the region from 1993-2017 has shown that the period of 2016-2017 is likely to be representative of typical conditions. The dredge modelling simulations were conducted using hydrodynamic and wave data drawn from this period, with nominal start dates for model simulation purposes being chosen as 1st July 2016 (winter) and 1st January 2017 (summer).

A summary of the scenarios that were modelled is as follows:

- Dredging works to commence on 1st July 2016 (winter start):

  – Option A: dredging of backfill material from borrow ground A (Scenario 1A).

    ○ TSHD dredging and disposal operations were programmed to occur between 1st July 2016 and 21st August 2016.

    ○ BHD dredging and disposal operations were programmed to occur between 21st August 2016 and 10th September 2016.

    ○ A simulation run-on period was assumed to occur between 10th September 2016 and 1st December 2016. Sediments suspended in the water column during previous operations were subject to settlement and progressively-reducing levels of resuspension during this time.

    ○ TSHD dredging and sand backfill operations were programmed to occur between 1st December 2016 and 9th February 2017.

    ○ Side-dump vessel rock backfill operations were programmed to occur between 9th February 2017 and 2nd March 2017.

- A further simulation run-on period was assumed to occur between 2nd March 2017 and 30th April 2017. Sediments suspended in the water column during previous operations were subject to settlement and progressively-reducing levels of resuspension during this time.

  – Option B: dredging of backfill material from borrow ground B (Scenario 1B).

  - Sequence of operations as per Option A, but with the use of the alternate borrow ground.

- Dredging works to commence on 1st January 2017 (summer start):

  – Option A: dredging of backfill material from borrow ground A (Scenario 2A).

  - TSHD dredging and disposal operations were programmed to occur between 1st January 2017 and 21st February 2017.

  - BHD dredging and disposal operations were programmed to occur between 21st February 2017 and 13th March 2017.

  - A simulation run-on period was assumed to occur between 13th March 2017 and 1st June 2017. Sediments suspended in the water column during previous operations were subject to settlement and progressively-reducing levels of resuspension during this time.

  - TSHD dredging and sand backfill operations were programmed to occur between 1st June 2017 and 10th August 2017.

  - Side-dump vessel rock backfill operations were programmed to occur between 10th August 2017 and 31st August 2017.

  - A further simulation run-on period was assumed to occur between 31st August 2017 and 31st October 2017. Sediments suspended in the water column during previous operations were subject to settlement and progressively-reducing levels of resuspension during this time.

  – Option B: dredging of backfill material from borrow ground B (Scenario 2B).

  - Sequence of operations as per Option A, but with the use of the alternate borrow ground.

The outcomes of the summer-start and winter-start scenarios have been analysed and presented separately, for comparison, in Section 5. The outcomes of each borrow ground dredging option have also been analysed and presented separately for each of the two seasonal scenarios.

3.6   Geotechnical Information

The dredged material from the pipeline route will consist mainly of marine sediments (approximately 3.8 Mm^3) and marine sediment/coarse material mix (approximately 0.2 Mm^3). The backfill material to be dredged from the borrow ground locations will consist of the removal of 2 Mm^3 of sandy sediments with a low proportion of fines.

The critical geotechnical information required as input to the modelling is PSD data for the sediments to be dredged along the pipeline route, for the sediments to be dredged from the borrow grounds and for the quarry-rock material.

This data has been specified (Woodside, 2018b) for the dredging and sand backfill operations relating to each pipeline section. The resultant PSDs for each pipeline section have been redistributed to match the material size classes used in the DREDGEMAP model, as shown in Table 3.13, Table 3.14 and Table 3.15.

For the rock backfill operations, in the absence of grading information it has been conservatively assumed that the fraction of material within the quarry rubble classified as "fines" in this context (diameters less than 100 mm)

will be 5% of the total volume. From experience, this is a typical upper limit for the "fines" fraction of well-graded limestone rubble, with the breakdown of this figure into smaller size classes usually unknown. Although the most conservative approach would be to further assume that all of the "fines" material is potentially available for resuspension into the water column, the assumed PSD has been heavily slanted towards the least-mobile coarse sand (>130 μm) category to account for the typically minimal proportion of the finest material categories. The chosen PSD is shown in Table 3.16.

The PSD data for borrow ground A can be characterised mainly as coarse sand with a low fines fraction, with coarseness and layer thickness increasing towards the eastern part of the borrow ground. For modelling purposes, PSDs measured close to the proposed trunkline route between KP30 and KP50 have been used. These PSDs consider a medium sand with higher fines content and are thus considered conservative.

The PSD data for borrow ground B is aligned with measured PSDs close to the proposed trunkline route between KP14 and KP19. For backfill purposes, a material with a PSD curve showing a $d_{10} > 100$ μm and a $d_{50} > 300$ μm is required to ensure the long-term stability of the pipeline. Borrow ground B is expected to have a substantially lower yield of acceptable material for trench backfill use.

In addition to PSD information, data and assumptions relating to the dry bulk density of the material to be dredged from the pipeline route and borrow grounds, and of the quarry-rock material, was used as input to the modelling. A typical average dry bulk density value of 2,150 kg/m³ was assumed.

Table 3.13 **In situ PSDs broken down into DREDGEMAP material classes for each pipeline section to be dredged, derived from available geotechnical information.**

Sediment Grain Size Class	Size Range (μm)	Zone PRE1 (%)	Zone PRE2 (%)	Zone PRE3 (%)	Zone PRE4 (%)	Zone PRE6 (%)	Zone PRE8 (%)	Zone PRE10 (%)
Clay	<7	10.0	10.0	10.0	10.0	10.0 (<KP16.5) 1.0 (>KP16.5)	1.0	8.0 (<KP30) 2.5 (>KP30)
Fine Silt	8-34	14.0	14.0	14.0	14.0	14.0 (<KP16.5) 1.0 (>KP16.5)	1.0	12.0 (<KP30) 2.5 (>KP30)
Coarse Silt	35-74	16.0	16.0	16.0	16.0	16.0 (<KP16.5) 4.0 (>KP16.5)	4.0	14.0 (<KP30) 10.0 (>KP30)
Fine Sand	75-130	20.0	20.0	20.0	20.0	20.0 (<KP16.5) 2.0 (>KP16.5)	2.0	14.0 (<KP30) 15.0 (>KP30)
Coarse Sand	>130	40.0	40.0	40.0	40.0	40.0 (<KP16.5) 92.0 (>KP16.5)	92.0	52.0 (<KP30) 70.0 (>KP30)

Table 3.14 **In situ PSDs broken down into DREDGEMAP material classes for the sand backfill material of each pipeline section if it were dredged from borrow ground <u>A</u>, derived from available geotechnical information.**

Sediment Grain Size Class	Size Range (μm)	Zone POST2 (%)	Zone POST4 (%)	Zone POST6 (%)	Zone POST8 (%)	Zone POST10 (%)
Clay	<7	2.5	2.5	2.5	2.5	2.5
Fine Silt	8-34	2.5	2.5	2.5	2.5	2.5
Coarse Silt	35-74	10.0	10.0	10.0	10.0	10.0
Fine Sand	75-130	15.0	15.0	15.0	15.0	15.0
Coarse Sand	>130	70.0	70.0	70.0	70.0	70.0

Table 3.15 **In situ PSDs broken down into DREDGEMAP material classes for the sand backfill material of each pipeline section if it were dredged from borrow ground <u>B</u>, derived from available geotechnical information.**

Sediment Grain Size Class	Size Range (μm)	Zone POST2 (%)	Zone POST4 (%)	Zone POST6 (%)	Zone POST8 (%)	Zone POST10 (%)
Clay	<7	1.0	1.0	1.0	1.0	1.0
Fine Silt	8-34	1.0	1.0	1.0	1.0	1.0
Coarse Silt	35-74	4.0	4.0	4.0	4.0	4.0
Fine Sand	75-130	2.0	2.0	2.0	2.0	2.0
Coarse Sand	>130	92.0	92.0	92.0	92.0	92.0

Table 3.16 **In situ PSDs broken down into DREDGEMAP material classes for the rock backfill material of each pipeline section, assumed as typical values for well-graded limestone rubble.**

Sediment Grain Size Class	Size Range (μm)	Zone POST1 (%)	Zone POST3 (%)	Zone POST5 (%)	Zone POST7 (%)	Zone POST9 (%)
Clay	<7	0.5	0.5	0.5	0.5	0.5
Fine Silt	8-34	0.5	0.5	0.5	0.5	0.5
Coarse Silt	35-74	0.5	0.5	0.5	0.5	0.5
Fine Sand	75-130	0.5	0.5	0.5	0.5	0.5
Coarse Sand	>130	98.0	98.0	98.0	98.0	98.0

3.7 Model Sediment Sources

3.7.1 Overview

To accurately represent the pipeline dredging, disposal and backfill operations in DREDGEMAP, a range of information was defined for the proposed operations, including dredge, disposal and backfill methodology, production rates, sediment/rock types and quantities (see Section 3.5). It is evident that there will be seven different sources of suspended sediment plumes during dredging, disposal and backfill operations, which can be broadly defined as:

- Direct suspension of material from the BHD bucket, from grabbing and lifting unconsolidated sediments and sedimentary rock through the water column, accounting for periods of no-dewatering and dewatering from the split hopper barge;

- Disposal of sediment and rock excavated by the BHD from split hopper barges to the nominated spoil grounds;

- Direct suspension of material by the TSHD during dredging of unconsolidated sediments, accounting for no-overflow and overflow periods;

- Disposal of sediment dredged by the TSHD to the nominated spoil grounds;

- Indirect suspension of material due to the propeller wash of the BHD barge tug and TSHD while dredging;

- Suspension of material during backfill activities, via TSHD, using sediments dredged from the borrow ground;

- Suspension of material during backfill activities, via side-dump vessel, using rock from onshore quarries.

Each of these sources of suspended sediment plumes will vary in strength and persistence depending on the nature of the operations. In the DREDGEMAP model, each source is defined by specifying the time-varying flux rate, PSD and vertical profile in the water column. The following sections outline how the information provided has been used to represent the dredging operations in the model and explain any assumptions that have been made to supplement the available information.

3.7.2 Representation of BHD Dredging

A BHD will be used to excavate all unconsolidated sediments and sedimentary rock material from zone PRE1, and all sedimentary rock material from zones PRE2 and PRE4 (following TSHD dredging of unconsolidated sediments in these zones). The BHD will use a large excavator arm fitted with an open bucket of (nominally) 20-30 m^3 capacity. The excavator will lift material in the bucket and deliver it to one of two waiting split hopper barges – assumed for the purposes of modelling to be 3,800 m^3 in capacity – for transport to spoil ground AB for disposal.

Sources of sediment suspension from this type of operation include:

- Disturbance of the seabed sediments by the excavator bucket;

- Dewatering of the split hopper barge, resulting in the discharge of water and entrained sediments.

Past observations have shown that material is suspended due to the initial grab at the seabed. Further suspension is generated as sediment spills from the bucket as it is lifted through the water column. Spillage of water and sediment also occurs as the bucket breaks free of the water surface and drains freely. Only sediments <130 μm in diameter are considered "lost" (i.e. suspended into the water column), because the coarser material spilled from the bucket while being lifted to the surface will fall immediately to the bottom

where it will be re-dredged during subsequent grabs. As such, the distribution of material suspended by the bucket spillage is assumed to be distributed across the four smaller sediment size classes in the model.

For the dredging of the unconsolidated sediments during periods with no dewatering from the barge, the PSD used in the model is based on PSDs from nearby boreholes (see Section 3.6), with the proportion >130 µm removed and the remaining distribution normalised to 100% by scaling up the proportions in the four remaining size classes (Table 3.17). The same PSD is used for the sedimentary rock component, assuming that due to the excavation action of the BHD the rock will break down into similar proportions of fines. Because the dredging action of the excavator involves no cutting or hydraulic pumping, this is a conservative assumption. During dewatering periods, an increase in the rate of release of fine sediments, and hence initial turbidity, is observed (Anchor Environmental, 2003). The water released during dewatering of the barge contains a high proportion of fines because the coarse material settles rapidly in the barge while the fine material remains in suspension. After the barge begins dewatering, a PSD heavily weighted towards finer particles has been assumed based on previous field measurements of hopper barge dewatering at Geraldton Port (OPR, 2010), with the proportion >75 µm removed and the remaining distribution normalised to 100% by scaling up the proportions in the three remaining size classes (Table 3.18).

Table 3.19 shows the assumed vertical distribution of the suspended material during the BHD operations while the barge is not dewatering. The distribution is higher at the seabed and water surface, to represent the larger loss rate of material during the initial grab and as the bucket breaks free of the water column. After the barge begins dewatering, a uniform distribution of sediments throughout the water column, between the hull depth and the seabed, has been assumed to represent a continuous stream of material being discharged from the barge (Table 3.20).

Table 3.17   **Assumed PSDs of sediments initially suspended into the water column during BHD dredging operations along the pipeline route while the barge <u>is not</u> dewatering.**

Sediment Grain Size Class	Size Range (µm)	PSD (%) for Sediment and Sedimentary Rock Removal – Zone PRE1	PSD (%) for Sedimentary Rock Removal – Zone PRE2	PSD (%) for Sedimentary Rock Removal – Zone PRE4
Clay	<7	16.7	16.7	16.7
Fine Silt	8-34	23.3	23.3	23.3
Coarse Silt	35-74	26.7	26.7	26.7
Fine Sand	75-130	33.3	33.3	33.3
Coarse Sand	>130	0.0	0.0	0.0

Table 3.18   Assumed PSDs of sediments initially suspended into the water column during BHD dredging operations along the pipeline route while the barge is dewatering.

Sediment Grain Size Class	Size Range (µm)	PSD (%) for Sediment and Sedimentary Rock Removal – Zone PRE1	PSD (%) for Sedimentary Rock Removal – Zone PRE2	PSD (%) for Sedimentary Rock Removal – Zone PRE4
Clay	<7	43.0	43.0	43.0
Fine Silt	8-34	30.2	30.2	30.2
Coarse Silt	35-74	26.8	26.8	26.8
Fine Sand	75-130	0.0	0.0	0.0
Coarse Sand	>130	0.0	0.0	0.0

Table 3.19   Assumed vertical distribution of sediments initially suspended into the water column during BHD dredging operations along the pipeline route while the barge is not dewatering.

Elevation	Example Elevation (m ASB) – 10 m Water Depth	Vertical Distribution (%) of Sediments
Surface/water depth	10.0	23.0
0.8 x water depth	8.0	16.0
0.5 x water depth	5.0	14.0
0.3 x water depth	3.0	19.0
0.1 x water depth	1.0	28.0

Table 3.20   Assumed vertical distribution of sediments initially suspended into the water column during BHD dredging operations along the pipeline route while the barge is dewatering.

Elevation	Example Elevation (m ASB) – 10 m Water Depth and 5.8 m Hull Depth	Vertical Distribution (%) of Sediments
Hopper hull elevation	4.2	20.0
0.75 x hull elevation	3.2	20.0
0.50 x hull elevation	2.1	20.0
0.25 x hull elevation	1.0	20.0
0.50 m (ASB)	0.5	20.0

Loss rates from similar operations are known to vary based on such factors as the size and type of bucket (i.e. open or closed), nature of the seabed material, presence of debris, current speed and depth of water, as well as the care of the operator (Hayes & Wu, 2001; Anchor Environmental, 2003). Reported rates compared by Anchor Environmental (2003) varied from 0.1% to 10%, with a mean of 2.1%. In the absence of measurements for the specific situation and equipment, the mean of 2.1% of production rate is assumed for all BHD operations during periods with no dewatering, and a rate of 2.4% of production rate is assumed for all BHD operations

3.7.3 Representation of Disposal of BHD-Dredged Material

All material dredged by the BHD will be placed into one of two waiting 3,800 m³ split hopper barges and transported (by harbour tug) to spoil ground AB for disposal. This material will include all unconsolidated sediments and sedimentary rock material from zone PRE1, and all sedimentary rock material from zones PRE2 and PRE4.

For the disposal of the unconsolidated sediments dredged by BHD, the PSD used in the model is based on PSDs from nearby boreholes (see Section 3.6). The same PSD is used for the sedimentary rock component, assuming that due to the excavation action of the BHD the rock will break down into similar proportions of fines. Because the dredging action of the excavator involves no cutting or hydraulic pumping, this is a conservative assumption. This PSD is adjusted by removal of the component treated as suspended during dredging (see Section 3.7.2), but as this represents only 2.1% of the mass for the minor components, the modified PSD is not significantly different to the in situ PSD (Table 3.21).

Once at the AB spoil ground, the split hopper barge will open to release the sediments from the bottom of the hull at a depth of approximately 5.8 m below sea level. Previous observations of sediment dumping from hopper vessels (e.g. CSMW, 2005) have shown that there is an initial rapid descent of solids, with the heavy particles tending to entrain lighter particles, followed by a billowing of lighter components back into the water column after contact with the seabed (Figure 3.2). A proportion of the lighter components will also remain suspended and may be trapped by density layers, if present.

Because simulations in this study focused on the far-field fate of sediment particles due to transport and sinking after the initial dump phase, simulations were run with the initial vertical distribution specified to represent the post-collision phase for a case where a high proportion of the sediments are resuspended after collision with the seabed. To represent this, an assumed vertical distribution for the sediments (Table 3.22) has been specified following published information from previous hopper disposal operations (CSMW, 2005; NEPA, 2001). This vertical distribution, with the majority of the material input near the seabed and only 7% of the material released in the upper half of the water column, is in line with values quoted in the recent literature review by Mills & Kemps (2016), which found that sediment resuspension from individual dredged material disposal events was generally less than 10% of the disposed material load.

It is estimated that 95-99% of the bulk load deposits directly onto the seabed in a typical case, with the remainder released into the water column (CSMW, 2005, NEPA, 2001). It is difficult to find other definitive source values in the literature, but a value of 5% of each load agrees well with past experience and appears to be a conservative estimate based on the values quoted above. Accordingly, 5% of each hopper load was placed in suspension in the water column in the sediment fate model.

In addition to the proportion of material immediately suspended in the water column, disposal from the barge will result in the stockpiling of sediment as a mound on the seabed that will be subject to resuspension by tidal and wave forces. Because fine sediments in the deposited mass may be subject to ongoing resuspension and dispersion over time, it was necessary to specify the deposits as a further source of sediment potentially subject to resuspension. For this purpose, it was assumed that 5% of the deposited mass – representing the upper surface layer – would be subject to resuspension. It should be noted that the model maintains a mass balance estimate of the remaining sediment of each size class within each grid cell to derive an estimate of the median particle size in the surface-layer sediments. In turn, the potential for ongoing resuspension of fines is calculated. In this way, the model represents the increased armouring of sediments as the average particle size increases.

The disposal time for the barge material within each dredge cycle was assumed to be 20 minutes (Table 3.3). The disposal location within spoil ground AB was varied for each dredge cycle in a randomised manner, with the ultimate aim of ensuring an even distribution of dredged material within the spoil ground by the conclusion of all activities.

Table 3.21   Assumed PSDs of sediments initially suspended into the water column during split hopper barge disposal operations at spoil ground AB.

Sediment Grain Size Class	Size Range (μm)	PSD (%) for Sediment and Sedimentary Rock Disposal – Zone PRE1	PSD (%) for Sedimentary Rock Disposal – Zone PRE2	PSD (%) for Sedimentary Rock Disposal – Zone PRE4
Clay	<7	9.7	9.7	9.7
Fine Silt	8-34	13.5	13.5	13.5
Coarse Silt	35-74	15.4	15.4	15.4
Fine Sand	75-130	19.3	19.3	19.3
Coarse Sand	>130	42.1	42.1	42.1

Table 3.22   Assumed vertical distribution of sediments initially suspended into the water column during split hopper barge disposal operations at spoil ground AB.

Elevation	Example Elevation (m ASB) – 10 m Water Depth	Vertical Distribution (%) of Sediments
Surface/water depth	10.0	2.0
0.6 x water depth	6.0	5.0
0.4 x water depth	4.0	15.0
0.15 x water depth	1.5	35.0
0.1 x water depth	1.0	43.0
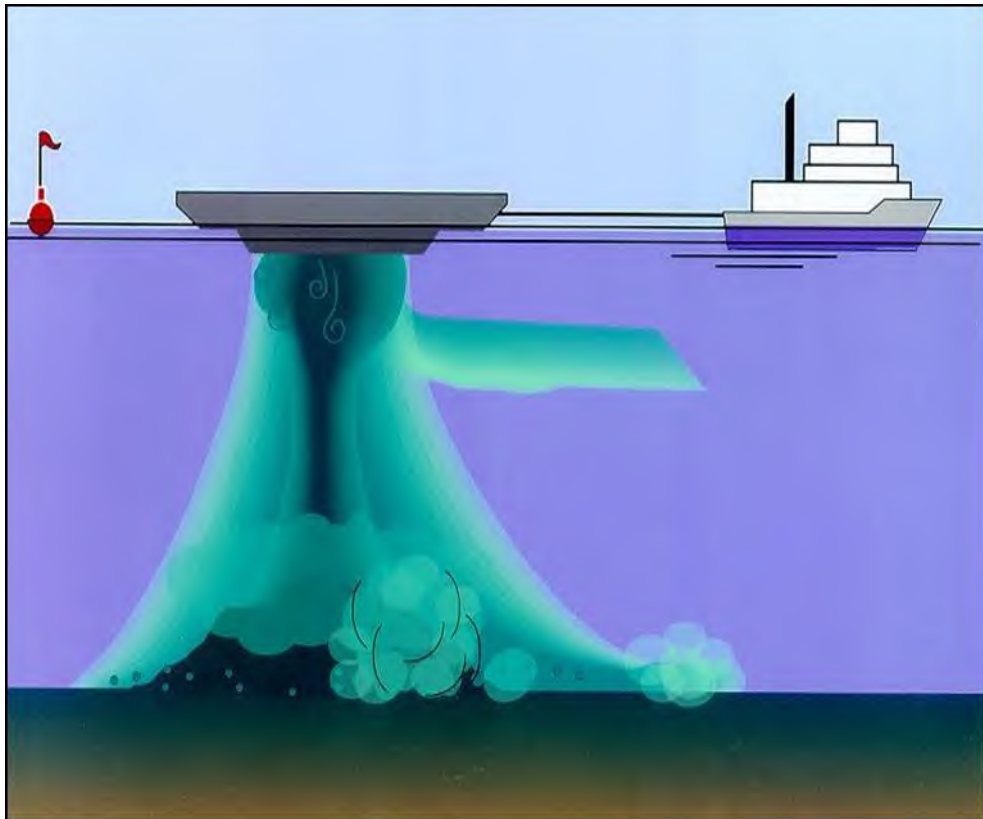
Figure 3.2 **Conceptual diagram showing the general behaviour of sediments dumped from a split hopper barge and the vertical distribution of material set up by entrainment and billowing (source: ASA, 2004).**

3.7.4 Representation of TSHD Dredging

A TSHD will be used to excavate all unconsolidated sediments from zones PRE2, PRE3 and PRE4 with disposal at spoil ground AB, zones PRE6 and PRE8 with disposal at spoil ground 2B, and zone PRE10 with disposal at spoil ground 5A. A smaller TSHD will be used to dredge backfill material from the borrow grounds, with disposal along the pipeline route. For the purposes of modelling, the capacities of the TSHDs to be used for dredging of the pipeline route and borrow grounds were assumed as 12,000 m³ and 9,700 m³, respectively.

TSHD vessels remove sediments by dragging a large drag-head over the seabed and drawing up the disturbed sediment by hydraulic suction. Sources of sediment suspension from this type of operation include:

• Hydraulic disturbance of the seabed sediments by the trailing arm;

• Propeller-wash generated as the vessel manoeuvres;

• Overflow of the on-board hoppers, resulting in the discharge of water and entrained sediments.

The characteristics of each of these sources vary greatly due to a wide range of factors (USACE, 2008) making the generalisation of source terms difficult. It appears however, that the overflow source term is dominant, being typically an order of magnitude greater than the drag-head and propeller-wash terms.

For the dredging of the unconsolidated sediments during periods with no overflow, the PSDs used in the model are based on PSDs from nearby boreholes (see Section 3.6). The PSDs applied to dredging along the pipeline

route and within the borrow grounds are shown in Table 3.23 and Table 3.25, respectively. During overflow periods, an increase in the rate of release of fine sediments, and hence initial turbidity, is observed (Anchor Environmental, 2003). The overflow water contains a high proportion of fines because the coarse material settles rapidly in the hopper while the fine material remains in suspension. After the hopper begins overflowing, PSDs heavily weighted towards finer particles has been assumed based on previous field measurements of hopper barge overflow at Geraldton Port (OPR, 2010), with the proportion >75 μm removed and the remaining distribution normalised to 100% by scaling up the proportions in the three remaining size classes. The PSDs applied to dredging along the pipeline route and within the borrow grounds are shown in Table 3.24 and Table 3.26, respectively.

Table 3.27 shows the assumed vertical distribution of the suspended material during the TSHD operations while the hopper is not overflowing. The distribution is concentrated near the seabed and decreases in intensity towards the surface, to represent the disturbance of seabed material by the drag-head and propeller-wash effects (HR Wallingford, 2003). After the hopper begins overflowing, a uniform distribution of sediments throughout the water column, between the hull depth and the seabed, has been assumed to represent a continuous stream of material being discharged from the hopper (Table 3.28). This is consistent with measured ADCP profiles presented by Hitchcock & Bell (2004), which show a reasonably even distribution of sediment through the water column during hopper overflow.

Table 3.23   Assumed PSDs of sediments initially suspended into the water column during TSHD dredging operations along the pipeline route while the hopper <u>is not</u> overflowing.

Sediment Grain Size Class	Size Range (μm)	PSD (%) for Sediment Removal – Zone PRE2	PSD (%) for Sediment Removal – Zone PRE3	PSD (%) for Sediment Removal – Zone PRE4	PSD (%) for Sediment Removal – Zone PRE6	PSD (%) for Sediment Removal – Zone PRE8	PSD (%) for Sediment Removal – Zone PRE10
Clay	<7	10.0	10.0	10.0	10.0 (<KP16.5) 1.0 (>KP16.5)	1.0	8.0 (<KP30) 2.5 (>KP30)
Fine Silt	8-34	14.0	14.0	14.0	14.0 (<KP16.5) 1.0 (>KP16.5)	1.0	12.0 (<KP30) 2.5 (>KP30)
Coarse Silt	35-74	16.0	16.0	16.0	16.0 (<KP16.5) 4.0 (>KP16.5)	4.0	14.0 (<KP30) 10.0 (>KP30)
Fine Sand	75-130	20.0	20.0	20.0	20.0 (<KP16.5) 2.0 (>KP16.5)	2.0	14.0 (<KP30) 15.0 (>KP30)
Coarse Sand	>130	40.0	40.0	40.0	40.0 (<KP16.5) 92.0 (>KP16.5)	92.0	52.0 (<KP30) 70.0 (>KP30)

Table 3.24 Assumed PSDs of sediments initially suspended into the water column during TSHD dredging operations along the pipeline route while the hopper <u>is</u> overflowing.

Sediment Grain Size Class	Size Range (µm)	PSD (%) for Sediment Removal – Zone PRE2	PSD (%) for Sediment Removal – Zone PRE3	PSD (%) for Sediment Removal – Zone PRE4	PSD (%) for Sediment Removal – Zone PRE6	PSD (%) for Sediment Removal – Zone PRE8	PSD (%) for Sediment Removal – Zone PRE10
Clay	<7	43.0	43.0	43.0	43.0 (<KP16.5) 52.7 (>KP16.5)	52.7	52.7 (<KP30) 44.3 (>KP30)
Fine Silt	8-34	30.2	30.2	30.2	30.2 (<KP16.5) 26.4 (>KP16.5)	26.4	26.4 (<KP30) 29.8 (>KP30)
Coarse Silt	35-74	26.8	26.8	26.8	26.8 (<KP16.5) 20.9 (>KP16.5)	20.9	20.9 (<KP30) 25.9 (>KP30)
Fine Sand	75-130	0.0	0.0	0.0	0.0	0.0	0.0
Coarse Sand	>130	0.0	0.0	0.0	0.0	0.0	0.0

Table 3.25 Assumed PSDs of sediments initially suspended into the water column during TSHD dredging operations at borrow grounds A and B while the hopper <u>is not</u> overflowing.

Sediment Grain Size Class	Size Range (µm)	PSD (%) for Sediment Removal – Borrow Ground A	PSD (%) for Sediment Removal – Borrow Ground B
Clay	<7	2.5	1.0
Fine Silt	7-34	2.5	1.0
Coarse Silt	35-74	10.0	4.0
Fine Sand	75-130	15.0	2.0
Coarse Sand	>130	70.0	92.0

Table 3.26 Assumed PSDs of sediments initially suspended into the water column during TSHD dredging operations at borrow grounds A and B while the hopper <u>is</u> overflowing.

Sediment Grain Size Class	Size Range (µm)	PSD (%) for Sediment Removal – Borrow Ground A	PSD (%) for Sediment Removal – Borrow Ground B
Clay	<7	49.2	52.7
Fine Silt	7-34	25.5	26.4
Coarse Silt	35-74	25.3	20.9
Fine Sand	75-130	0.0	0.0
Coarse Sand	>130	0.0	0.0

Table 3.27   Assumed vertical distribution of sediments initially suspended into the water column during TSHD dredging operations along the pipeline route and at borrow grounds A and B while the hopper is not overflowing.

Elevation	Example Elevation (m ASB) – 30 m Water Depth	Vertical Distribution (%) of Sediments
10.0 m (ASB)	10.0	5.0
7.0 m (ASB)	7.0	15.0
3.0 m (ASB)	3.0	20.0
2.0 m (ASB)	2.0	40.0
1.0 m (ASB)	1.0	20.0

Table 3.28   Assumed vertical distribution of sediments initially suspended into the water column during TSHD dredging operations along the pipeline route and at borrow grounds A and B while the hopper is overflowing.

Elevation	Example Elevation (m ASB) – 30 m Water Depth and 10 m Hull Depth	Vertical Distribution (%) of Sediments
Hopper hull elevation	20.0	20.0
0.75 x hull elevation	15.0	20.0
0.50 x hull elevation	10.0	20.0
0.25 x hull elevation	5.0	20.0
0.50 m (ASB)	0.5	20.0

The resuspension of sediment when the TSHD hopper is not overflowing was estimated by combining the drag-head and propeller-wash terms. The propeller-wash component typically dominates the drag-head component, but both sources were assessed. Propeller wash generation was estimated by applying a model of the bed-induced shear stress from the larger of the TSHD vessels (12,000 m³ capacity) over the range of under-keel clearances expected during the dredging operations.

Field measurements of drag-head-induced sediment suspension was reported by Coastline Surveys Ltd (CSL, 1999). The inferred production rate was less than 1 kg/s and it was concluded that, generally, drag-head production is small in comparison to the quantity of sediment released via overflow. Given the above, a loss rate of 0.6% of the gross production rate, representing a combined sediment flux due to losses from the drag-head and propeller-wash, was assumed when the TSHD is not overflowing. This rate is within the range of values (less than 1%) summarised in a review of contemporary practice conducted as part of the WAMSI Dredging Science Node by Kemps & Masini (2017).

The resuspension of sediment when the TSHD hopper is overflowing was estimated based on measurements taken of the concentrations within overflowing waters, which are generally less than 10,000 mg/L adjacent to the hopper (Hitchcock & Bell, 2004). Typical values appear to be in the 5,000-6,000 mg/L range, which correlate well with data drawn from other Western Australian projects that cannot be cited here for reasons of confidentiality. A conservative hopper overflow concentration of 10,000 mg/L was assumed for this study, which – when balanced with the expected pumping and loading rates of the dredge – resulted in a source estimate of 2.4% of the gross production rate. This flux rate is a conservative rate compared to the range of

published measurements from TSHD operations (0.1-5.0%; Hayes & Wu, 2001) and is within the range of values used in modelling studies (0.3-9.8%) outlined in a review of contemporary practice by Kemps & Masini (2017).

3.7.5   Representation of Disposal of TSHD-Dredged Material

All material dredged by the TSHD along the pipeline route will be transported to spoil ground AB, 2B or 5A (as appropriate) for disposal. This material will include all unconsolidated sediments from zones PRE2, PRE3, PRE4, PRE6, PRE8 and PRE10.

For the disposal of the unconsolidated sediments dredged by TSHD, the PSDs used in the model are based on PSDs from nearby boreholes (see Section 3.6). These PSDs are adjusted by removal of the component treated as suspended during dredging along the pipeline route (see Section 3.7.4), but as this represents only between 0.6% and 2.4% (averaged value depending on the relative contributions of overflow and non-overflow periods to the overall mass flux) of the mass for the minor components, the modified PSDs are not significantly different to the in situ PSDs (Table 3.29).

Once at the appropriate spoil ground, the hopper will open to release the sediments from the bottom of the hull at a depth of approximately 12.75 m below sea level. Previous observations of sediment dumping from hopper vessels (e.g. CSMW, 2005) have shown that there is an initial rapid descent of solids, with the heavy particles tending to entrain lighter particles, followed by a billowing of lighter components back into the water column after contact with the seabed (Figure 3.3). A proportion of the lighter components will also remain suspended and may be trapped by density layers, if present.

Because simulations in this study focused on the far-field fate of sediment particles due to transport and sinking after the initial dump phase, simulations were run with the initial vertical distribution specified to represent the post-collision phase for a case where a high proportion of the sediments are resuspended after collision with the seabed. To represent this, an assumed vertical distribution for the sediments (Table 3.30) has been specified following published information from previous hopper disposal operations (CSMW, 2005; NEPA, 2001). This vertical distribution, with the majority of the material input near the seabed and only 15% of the material released at hull depth or above, is in line with values quoted in the recent literature review by Mills & Kemps (2016), which found that sediment resuspension from individual dredged material disposal events was generally less than 10% of the disposed material load.

It is estimated that 95-99% of the bulk load deposits directly onto the seabed in a typical case, with the remainder released into the water column (CSMW, 2005, NEPA, 2001). It is difficult to find other definitive source values in the literature, but a value of 5% of each load agrees well with past experience and appears to be a conservative estimate based on the values quoted above. Accordingly, 5% of each hopper load was placed in suspension in the water column in the sediment fate model.

In addition to the proportion of material immediately suspended in the water column, disposal from the hopper will result in the stockpiling of sediment as a mound on the seabed that will be subject to resuspension by tidal and wave forces. Because fine sediments in the deposited mass may be subject to ongoing resuspension and dispersion over time, it was necessary to specify the deposits as a further source of sediment potentially subject to resuspension. For this purpose, it was assumed that 5% of the deposited mass – representing the upper surface layer – would be subject to resuspension. It should be noted that the model maintains a mass balance estimate of the remaining sediment of each size class within each grid cell to derive an estimate of the median particle size in the surface-layer sediments. In turn, the potential for ongoing resuspension of fines is calculated. In this way, the model represents the increased armouring of sediments as the average particle size increases.

The disposal time for the hopper material within each dredge cycle was assumed to be 20 minutes (Table 3.4). The disposal location within the relevant spoil ground was varied for each dredge cycle in a randomised manner, with the ultimate aim of ensuring an even distribution of dredged material within each spoil ground by the conclusion of all activities (Table 3.5).

Table 3.29 **Assumed PSDs of sediments initially suspended into the water column during TSHD hopper disposal operations at spoil grounds AB, 2B and 5A.**

Sediment Grain Size Class	Size Range (µm)	PSD (%) for Sediment Disposal – Zone PRE2	PSD (%) for Sediment Disposal – Zone PRE3	PSD (%) for Sediment Disposal – Zone PRE4	PSD (%) for Sediment Disposal – Zone PRE6	PSD (%) for Sediment Disposal – Zone PRE8	PSD (%) for Sediment Disposal – Zone PRE10
Clay	<7	9.0	9.0	9.0	9.0 (<KP16.5) 0.0 (>KP16.5)	0.0	0.0 (<KP30) 6.9 (>KP30)
Fine Silt	8-34	13.3	13.3	13.3	13.3 (<KP16.5) 0.1 (>KP16.5)	0.1	0.1 (<KP30) 11.3 (>KP30)
Coarse Silt	35-74	15.3	15.3	15.3	15.3 (<KP16.5) 3.5 (>KP16.5)	3.5	3.5 (<KP30) 13.4 (>KP30)
Fine Sand	75-130	20.0	20.0	20.0	20.0 (<KP16.5) 2.0 (>KP16.5)	2.0	2.0 (<KP30) 14.0 (>KP30)
Coarse Sand	>130	42.4	42.4	42.4	42.4 (<KP16.5) 94.4 (>KP16.5)	94.4	94.4 (<KP30) 54.4 (>KP30)

Table 3.30 **Assumed vertical distribution of sediments initially suspended into the water column during TSHD hopper disposal operations at spoil grounds AB, 2B and 5A.**

Elevation	Example Elevation (m ASB) – 20 m Water Depth and 12.75 m Hull Depth	Vertical Distribution (%) of Sediments
Surface/water depth	20.0	5.0
Hopper hull elevation	7.5	10.0
0.75 x hull elevation	5.6	20.0
0.50 x hull elevation	3.8	30.0
0.25 x hull elevation	1.9	35.0

3.7.6 Representation of BHD Barge Tug/TSHD Propeller Wash

Modelling of sediment suspended by propeller-induced motion at the seabed was conducted to estimate likely sediment concentrations generated by the TSHD and harbour tug propellers while manoeuvring during dredging operations. A specialised numerical model developed by RPS, named PROPMAP, was used to estimate a time- and space-varying rate of sediment flux from the seabed due to the thrust imposed by each vessel's propellers at the seabed level behind the moving vessel. The model uses characteristics of the vessel of interest to estimate the three-dimensional thrust-field generated by the propellers. This thrust-field is then combined with the grain size and degree of cohesion of the seabed sediments, and the varying under-keel clearance along the typical vessel paths, to calculate variations in the suspended sediment flux from the seabed in time and space.

The following details were used as input to PROPMAP to calculate variable rates of sediment flux from the seabed due to propeller-wash effects:

- Vessel tracks and speeds;

- Vessel draft, engine power and propeller size;

- Bathymetry along the vessel tracks;

- Grain size distributions of the sediment, defining the proportions of clay and silt along the vessel tracks.

The calculation steps applied by PROPMAP at discrete intervals along each vessel path were as follows:

- Based on the vessel's engine power and propeller size, determine the propeller-induced velocity profile;

- Based on the vessel's draft and the local bathymetry, determine the intersection of the thrust-field with the seabed and find the thrust imposed on it;

- Based on the velocity of water flow at the seabed, calculate the shear stress acting on it;

- Based on the calculated shear stress, and the sediment grain size and cohesiveness, calculate a theoretical erosion flux (mass per unit time) for seabed sediment.

Propeller-induced velocity profiles were calculated using empirical expressions from Blaauw & van de Kaa (1978). Thrust at the seabed will depend upon the level of the bed, which will intersect as a plane (Figure 3.3). For an under-keel clearance of 1 m, a velocity field exceeding 5 m/s would intersect the bed in this example, while at a clearance of 4 m the bed velocity would be reduced to <2 m/s. The influence of this thrust will vary with the sediment grain size. Consequently, outcomes will be sensitive to the magnitude of the thrust, the under-keel clearance and the PSD of the bed.

Sediment erosion flux was estimated from the derived velocity field using the empirical formulations of van Rijn (1989). The sediment flux component attributable to propeller wash was found to be depth-limited for areas where the under-keel clearance was less than 3 m, assuming a fully-loaded vessel (maximum draft). Simulations over deeper areas, including the areas where vessels would transit to the spoil grounds, indicated that flux would be minimal (compared to other sources) and representative of short-lived suspension of the surface-layer sediments followed by rapid settlement. This settlement time was estimated to be shorter than the simulation output time-step. Propeller-wash was found to be more significant in the shallow areas and would be greater over sediments previously suspended by dredging.

These findings were used to inform the definition of the sediment flux rates during TSHD dredging operations (see Section 3.7.4).
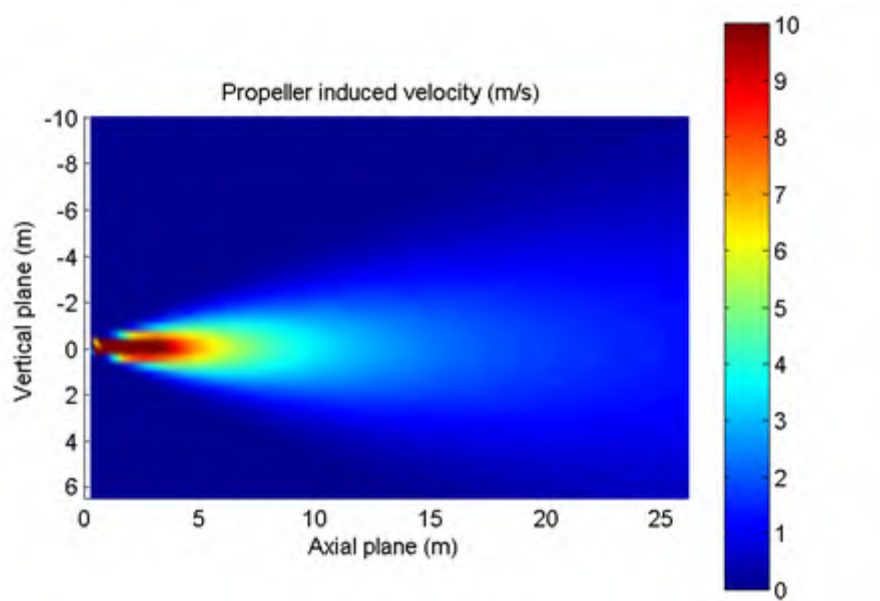
Figure 3.3   Two-dimensional view of a propeller-induced velocity profile.

In summary, propeller-wash effects were considered: (i) along each pipeline section during dredging; (ii) between each pipeline section and the spoil grounds during dredging; and (iii) between borrow ground B and each pipeline section during backfilling. For borrow ground A, and the waters between it and the pipeline, propeller-wash effects are not relevant due to the greater water depths.

In the absence of definitive information relating to the seabed composition of the areas traversed by the barge tug or TSHD between the pipeline and the spoil grounds (or traversed by the TSHD between borrow ground B and the pipeline), for simplicity the seabed composition was assumed to be described by the PSD of the area from which the vessel began its journey.

3.7.7   Representation of TSHD Backfill

All material dredged by the TSHD within the borrow grounds will be transported to sections POST2, POST4, POST6, POST8 and POST10 of the pipeline route for placement.

For the backfill of the pipeline using unconsolidated sediments dredged by TSHD, the PSDs used in the model are based on PSDs from nearby boreholes (see Section 3.6). These PSDs are adjusted by removal of the component treated as suspended during dredging within the borrow grounds (see Section 3.7.4), but as this represents only between 0.6% and 2.4% (averaged value depending on the relative contributions of overflow and non-overflow periods to the overall mass flux) of the mass for the minor components, the modified PSDs are not significantly different to the in situ PSDs (Table 3.31). It has been assumed, conservatively, that all sediment dredged from the borrow grounds is available for use as backfill material.

Once at the appropriate location, the TSHD suction pipe will discharge material at an elevation of approximately 5 m above the pipeline. Sediment release from the suction pipe will occur as a jet of slurry that will have an initial rapid descent of solids followed by a billowing of lighter components back into the water column after contact with the seabed/pipeline (Swanson *et al.*, 2004). The plume that results from disposal of a jet of slurry from a pipe is typically concentrated near the seabed, with most of the material within 3 m of the

bottom, and lower concentrations extend up towards the surface (Figure 3.4). Table 3.32 shows the assumed vertical distribution of the suspended material for the TSHD backfill source.

It is estimated that 95-99% of the bulk load deposits directly onto the seabed in a typical case, with the remainder released into the water column (CSMW, 2005, NEPA, 2001). It is difficult to find other definitive source values in the literature, and no site-specific sampling has been conducted for TSHD backfill placement operations, but a value of 5% of each load agrees well with past experience and appears to be a conservative estimate based on the values quoted above. Accordingly, 5% of each hopper load was placed in suspension in the water column in the sediment fate model.

The placement time for the hopper material within each dredge cycle was assumed to be 107 minutes (Table 3.6).

Table 3.31   Assumed PSDs of sediments initially suspended into the water column during TSHD backfill operations using material dredged at borrow grounds A and B.

Sediment Grain Size Class	Size Range (µm)	PSD (%) for Sediment Backfill – Borrow Ground A	PSD (%) for Sediment Backfill – Borrow Ground B
Clay	<7	1.3	0.0
Fine Silt	7-34	1.9	0.1
Coarse Silt	35-74	9.4	3.5
Fine Sand	75-130	15.0	2.0
Coarse Sand	>130	72.4	94.4

Table 3.32   Assumed vertical distribution of sediments initially suspended into the water column during TSHD backfill operations using material dredged at borrow grounds A and B.

Elevation	Example Elevation (m ASB) – 20 m Water Depth and 5 m Pipe Elevation	Vertical Distribution (%) of Sediments
Surface/water depth	20.0	5.0
Suction pipe elevation	5.0	10.0
0.75 x pipe elevation	3.8	15.0
0.50 x pipe elevation	2.5	20.0
0.25 x pipe elevation	1.3	50.0
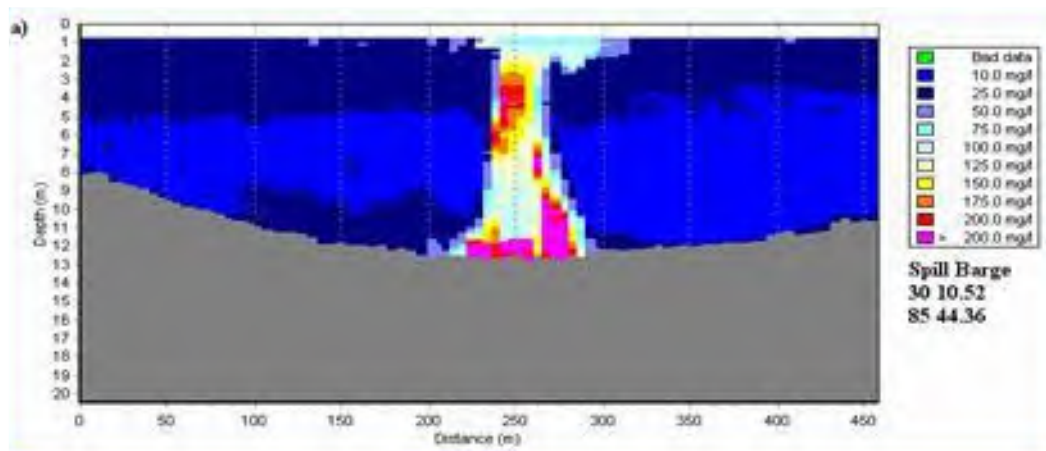
Figure 3.4   **Example of a vertical cross-section through a typical open-water discharge plume from a spreader barge pipe (source: Swanson *et al.*, 2004).**

3.7.8   Representation of Side-Dump Vessel Backfill

Rock material from an onshore quarry source will be transported by a side-dump vessel to sections POST1, POST3, POST5, POST7 and POST9 of the pipeline route for placement.

Based on previous project experience, quarry rock used for breakwater core construction or pipeline armouring typically contains around 5% material with diameters less than 100 mm. Therefore, a conservative loss rate of 5% of the total volume of dumped rock material was applied in the modelling. Based on material testing from previous projects, the volume of quarried core/rock material less than 130 µm in size is typically even lower, in the order of 2%. Table 3.33 (equivalent to Table 3.16) presents the PSD that was applied in the modelling of the rock backfill source. The composition of the material is dominated by coarse sand and larger particles, with the 2% of finer material assumed to be evenly spread over the four smaller material classes. Although coarse sand material will be initially suspended in the water column, it will not be available for resuspension once it settles.

Because the rock backfill material will be dumped from the deck of the vessel, it will move through the whole water column as it falls to the seabed. Therefore, a uniform vertical distribution of suspended material in the water column has been assumed (Table 3.34).

The placement time for the rock material within each cycle was assumed to be 120 minutes (Woodside, 2018a). Other than an increased placement time, the operational cycle is assumed to be equivalent to that for TSHD backfill operations outlined in Table 3.6.

Table 3.33   **Assumed PSDs of sediments initially suspended into the water column during side-dump vessel backfill operations using material from an onshore quarry.**

Sediment Grain Size Class	Size Range (µm)	PSD (%) for Rock Backfill
Clay	<7	0.5
Fine Silt	7-34	0.5
Coarse Silt	35-74	0.5
Fine Sand	75-130	0.5
Coarse Sand	>130	98.0

Table 3.34   **Assumed vertical distribution of sediments initially suspended into the water column during side-dump vessel backfill operations using material from an onshore quarry.**

Elevation	Example Elevation (m ASB) – 10 m Water Depth	Vertical Distribution (%) of Sediments
Surface/water depth	10.0	20.0
0.8 x water depth	8.0	20.0
0.6 x water depth	6.0	20.0
0.4 x water depth	4.0	20.0
0.2 x water depth	2.0	20.0

3.7.9   Summary of Source Rates and Volumes

For each source of suspended sediment plumes during dredging, disposal and backfill operations, as described in the preceding sections, Table 3.35 summaries the associated loss rates and approximate volumes of suspended sediment expected. The volumes assigned to the respective non-overflow and overflow periods for TSHD dredging, and non-dewatering and dewatering periods for BHD dredging, are based on the modelled cycle times detailed in Table 3.3, Table 3.4 and Table 3.6.

A total of approximately 246,230 m^3 of sediment is expected to be initially suspended in the water column over the course of the modelled program. This volume represents approximately 6.9% of the in situ dredged (and quarry) volume. If all deposited material assumed to be available for potential resuspension following spoil ground disposal operations is actually resuspended, a total of 339,076 m^3 of sediment will be suspended in the water column over the program duration; this will represent approximately 9.5% of the in situ dredged (and quarry) volume.

Table 3.35   Summary of sediment sources applied in the model.

Phase	Operation	Source Rate (% Production Rate)	Dredged Volume (m³)	Suspended Volume (m³)
Pipeline dredging	BHD excavator bucket	2.1	51,147	215
	BHD excavator bucket + dewatering from barge	2.4		982
	Disposal from hopper barge	5 (water column) 5 (seabed; *potential*)		2,557 *2,557*
	TSHD drag-head + propeller-wash	0.6	1,818,397	1,925
	TSHD drag-head + propeller-wash + overflow	2.4		35,940
	Disposal from TSHD	5 (water column) 5 (seabed; *potential*)		90,920 *90,920*
Pipeline backfilling	TSHD drag-head + propeller-wash	0.6	1,608,095	2,783
	TSHD drag-head + propeller-wash + overflow	2.4		27,461
	Placement from TSHD	5		80,405
	Placement from side-dump vessel	5	73,426	3,671
	Totals		**3,551,065**	**246,229** *339,076*

4 ENVIRONMENTAL THRESHOLD ANALYSIS

4.1 Overview

Predictions of SSC for each scenario were assessed against a series of water quality thresholds to categorise the modelled outcomes into management zones of influence and impact, defined with regard to environmental sensitivities in the study region. These thresholds, and the technical justification which followed guidance from the WAMSI Dredging Science Node, were supplied to RPS by Advisian (MScience, 2019). Thresholds were selected for benthic habitats on the basis of past and present mapping of communities in the project area.

Thresholds for three management zones – a Zone of Influence (ZoI), a Zone of Moderate Impact (ZoMI) and a Zone of High Impact (ZoHI) – were defined. The criteria associated with each management zone also varied across three ecological zones, which were broadly defined based on past studies of these areas. The ecological zones are named as follows, with reference to the pipeline chainages shown in Figure 1.1, and with the spatial extents agreed for this study shown in Figure 4.1:

- Offshore: the pipeline area beyond KP25, and generally all areas north of a boundary line containing Rosemary Island, Legendre Island and Delambre Island.

- Zone B: the pipeline area between KP8 and KP25, adjacent coral and macroalgae habitats within Mermaid Sound, and generally all coral, macroalgae and mixed community habitats between Dolphin Island and Bezout Island.

- Zone A: the pipeline area between the shoreline and KP8, adjacent macroalgae and mangrove habitats within Mermaid Sound, and generally all mangrove, marsh and seagrass habitats between Nickol Bay and Point Samson.

Thresholds for coral habitats within Zone B were developed with the aid of data collected during a previous dredging campaign at Barrow Island, which is considered a similar habitat. Water quality within Zone A is more turbid, and coral communities are comprised of more sediment-tolerant or resilient species. Offshore habitats are not likely to contain corals.

In developing the thresholds, it was assumed that benthic communities around Spoil Ground 2B and Borrow Ground A (see Figure 1.1) will be sparse and made up largely of sponges and filter feeders without corals.

4.2 Baseline Water Quality

Water quality data collected during the LNG Foundation Project over the period of 2007 to 2010 (MScience, 2010) demonstrated that turbidity at sites within the Zone A and Zone B management areas was raised by 0.7 NTU and 0.3 NTU, respectively, as a result of dredging activities. Subtraction of these dredge-induced values across the 2007-2010 data set yielded a set of baseline turbidity measurements.

Table 4.1 presents the mean and 80th-percentile SSC values calculated from the background turbidity measurements in each zone. For the purposes of threshold assessment, it has been assumed that the summer season comprises the period of November to March and the winter season contains the months of April to October.
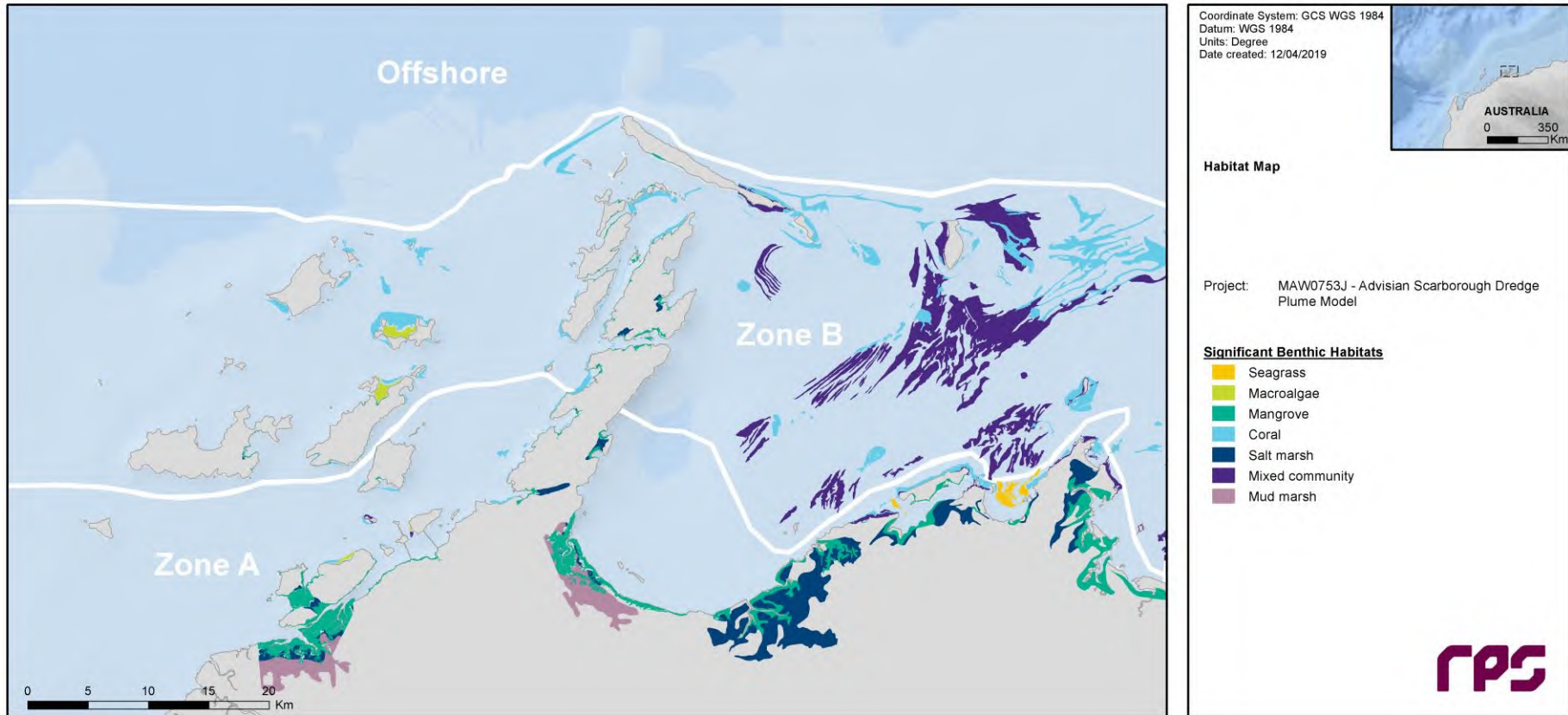
Figure 4.1 Delineation of the proposed ecological zones (Zone A, Zone B and Offshore) in the context of known habitat areas and types. Thresholds used to define the management zones will vary in magnitude between the ecological zones.

Table 4.1 Baseline mean and 80th percentile SSC values calculated from measurements undertaken during the LNG Foundation Project (2007-2010), categorised into summer and winter seasons for each of the three ecological zones.

Ecological Zone	Season	Mean SSC (mg/L)	80th Percentile SSC (mg/L)
A	Summer	4.1	5.0
	Winter	1.8	2.3
B	Summer	2.5	2.7
	Winter	1.2	1.6
Offshore	Summer	1.8	1.8
	Winter	0.6	0.9

4.3 Zone of Influence (ZoI)

The ZoI is defined as "*a zone where impacts to water quality will be detectable but below a level causing detectable impacts to biota*" (MScience, 2019). This is generally considered equivalent to the area around dredging activities where a plume may be visible to the naked eye.

The ZoI threshold will be exceeded at any point within the model domain where dredging is forecast to increase the depth-averaged concentration of SSC (specifically the contribution attributable to dredging activities) by a level greater than the seasonal 80th percentile baseline SSC over a 24-hour average period.

Table 4.2 presents the threshold SSC values used to define the extents of the ZoI. A background SSC value appropriate for each ecological zone and month of the year was added to the dredge-induced SSC predictions from the sediment fate model prior to evaluation of the thresholds.

Potential exceedances of the threshold were evaluated over the duration of each dredge scenario by calculating a rolling 24-hour average of SSC concentrations in each model grid cell and checking for breaches as this time-window progressed through the data set at hourly increments (the temporal resolution of the data set). If the 24-hour average SSC concentration exceeds the threshold value at any time, even if only on one occasion, the model grid cell is included in the ZoI area. With each scenario spanning a period of ten months, ZoI threshold checks were undertaken for more than 7,000 time steps. This approach allowed an increased opportunity to detect threshold exceedance events, compared with that afforded by the alternative method of simply analysing each unique 24-hour sequence in turn (i.e. with no temporal overlap) from the start to the end of the data set.

Typically, averaging discrete data points over an arbitrary time period will serve to reduce the influence of transient spikes in concentration, thereby reducing the possibility of spurious exceedances. More rarely, a transient concentration spike of sufficient magnitude to skew the rolling average to an above-threshold state may result in exceedances being recorded for a longer period than will be the case in reality. Generally, applying a time-average to a data set for the purposes of threshold analysis will result in a smaller zone of effect than if instantaneous data is evaluated. This methodology also has a strong connection to critical exposure times for benthic habitats or species of concern in the project area.

Table 4.2   Background, dredge-excess and threshold SSC values used as the criteria to define the ZoI outer boundary within each ecological zone.

Ecological Zone	Season	Time-Averaged Period (hours)	Background SSC (mg/L) [a]	Dredge-Excess SSC (mg/L) [b]	Threshold SSC (mg/L) [c]
A	Summer	24	4.1	5.0	9.1
	Winter	24	1.8	2.3	4.1
B	Summer	24	2.5	2.7	5.2
	Winter	24	1.2	1.6	2.8
Offshore	Summer	24	1.8	1.8	3.6
	Winter	24	0.6	0.9	1.5

[a] Background values are equivalent to 'Mean SSC' values in Table 4.1.

[b] Dredge-excess values are equivalent to '80th Percentile SSC' values in Table 4.1.

[c] Threshold values are the sum of background and dredge-excess values.

4.4   Zone of Moderate Impact (ZoMI)

The ZoMI is defined as "*a zone where impacts are sub-lethal or lethal but recoverable (in terms of the community) within a five-year period*" (MScience, 2019).

The ZoMI threshold will be exceeded at any point within the model domain where dredging is forecast to increase the depth-averaged concentration of SSC to a level sufficient to trigger impacts to EC_{10} (10% Effect Concentration or 10% Inhibition) or to cause bleaching through loss of light or sedimentation.

Thresholds chosen to indicate a transition between the ZoI and ZoMI areas are largely based on the 'possible mortality' thresholds of Fisher *et al.* (2019). These thresholds are based on analysis of water quality and coral monitoring data collected during a previous dredging project at Barrow Island, where coral communities exist in clear, near-oceanic conditions. Distinctions must be made between the thresholds most appropriate for each ecological zone.

Within the offshore zone, only thresholds of relevance to sponges and filter feeders are appropriate because corals, seagrasses and macroalgae are not known to form significant communities. A threshold relating to an LC_{10} (10% Lethal Concentration) effect on filter feeder-sponge habitats over a 28-day exposure period was selected (Pineda *et al.*, 2017).

For Zone B, coral communities experience similar conditions to those monitored at Barrow Island and the moderate-impact thresholds of Fisher *et al.* (2019) for coral/mixed benthos communities were deemed to be appropriate (MScience, 2019).

For Zone A, coral communities experience more turbid conditions and are more tolerant of elevated SSC levels and lowered light levels than their neighbours in Zone B due to adaptation and a different mix of species. To account for this greater tolerance, the moderate-impact thresholds in Zone A were defined as those of Zone B multiplied by a factor of 1.5, which is believed to be a conservative multiplier (MScience, 2019). Within both Zones A and B, spongers and filter feeders will occur among the corals, and the mixed community is best evaluated using coral-focused thresholds.

The taxa-specific thresholds and appropriate time-averaging periods (related to exposure times from experimental data) used to define the extents of the ZoMI are detailed in Table 4.3. A background SSC value appropriate for each ecological zone and month of the year was added to the dredge-induced SSC predictions from the sediment fate model prior to evaluation of the thresholds.

Potential exceedances of the thresholds were evaluated over the duration of each dredge scenario by calculating rolling 3-day, 7-day, 10-day, 14-day and 28-day averages (as appropriate in each ecological zone) of SSC concentrations in each model grid cell and checking for breaches as this time-window progressed through the data set at hourly increments (the temporal resolution of the data set). If any time-average SSC concentration exceeds the corresponding threshold value at any time, even if only on one occasion, the model grid cell is included in the appropriate ZoMI area.

Table 4.3   Threshold SSC values used as the criteria to define the ZoMI outer boundary within each ecological zone.

Ecological Zone	Time-Averaged Period (days)	Threshold SSC (mg/L)
A	3	29.1
	7	22.5
	10	19.6
	14	17.6
B	3	19.4
	7	14.7
	10	13.1
	14	11.7
Offshore	28	22.5

4.5   Zone of High Impact (ZoHI)

Thresholds chosen to indicate a transition between the ZoMI and ZoHI areas are largely based on the 'probable mortality' thresholds of Fisher *et al.* (2019).

Within the offshore zone, a threshold relating to an LC_{50} (50% Lethal Concentration) effect on filter feeder-sponge habitats over a 28-day exposure period was selected (Pineda *et al.*, 2017).

For Zone B, the high-impact thresholds of Fisher *et al.* (2019) for coral/mixed benthos communities were deemed to be appropriate (MScience, 2019).

For Zone A, the high-impact thresholds were defined as those of Zone B multiplied by a factor of 1.5, which is believed to be a conservative multiplier (MScience, 2019).

The taxa-specific thresholds and appropriate time-averaging periods (related to exposure times from experimental data) used to define the extents of the ZoHI are detailed in Table 4.4. A background SSC value appropriate for each ecological zone and month of the year was added to the dredge-induced SSC predictions from the sediment fate model prior to evaluation of the thresholds.

Potential exceedances of the thresholds were evaluated over the duration of each dredge scenario by calculating rolling 3-day, 7-day, 10-day, 14-day and 28-day averages (as appropriate in each ecological zone) of SSC concentrations in each model grid cell and checking for breaches as this time-window progressed through the data set at hourly increments (the temporal resolution of the data set). If any time-average SSC concentration exceeds the corresponding threshold value at any time, even if only on one occasion, the model grid cell is included in the appropriate ZoHI area.

Table 4.4   Threshold SSC values used as the criteria to define the ZoHI outer boundary within each ecological zone.

Ecological Zone	Time-Averaged Period (days)	Threshold SSC (mg/L)
A	3	53.6
	7	36.8
	10	31.4
	14	27.0
B	3	35.7
	7	24.5
	10	20.9
	14	18.0
Offshore	28	47.0

5 RESULTS OF SEDIMENT FATE MODELLING

5.1 Spatial Distributions of SSC

5.1.1 Summary

Simulations indicated that there may be significant spatial patchiness in the distribution of SSC at any point in time during the dredging, disposal and backfill operations because of variability in the number of sediment suspension sources, variability in the flux from each of these sources, and the varying dynamics of the transport, settlement and resuspension processes affecting the sediments.

The most pronounced differences in the predicted concentrations at any point in time are found in the vertical distributions, with a distinct increase in concentration towards the seabed. Most material will initially be suspended low in the water column, and material suspended higher in the water column will sink as it moves away from the source. Frequent resuspension of material will also mostly affect the lower reaches. Thus, the spatial area affected above a given concentration is typically greater in the near-seabed layer than in the near-surface layer. It should be noted, however, that there are instances throughout the simulations where elevated concentrations will occur in the near-surface layers – during TSHD overflow or split hopper barge dewatering operations, or during strong resuspension events affecting sediments that have migrated to shallow areas – but these will typically not be sustained for extended periods of time.

Although many of the activities related to dredging and backfilling of the pipeline will take place within Mermaid Sound, which is dominated by tidal currents year-round and is relatively sheltered from the variations in large-scale circulation observed beyond approximately KP30, reasonably distinct seasonal trends are evident in the modelling outcomes of each scenario.

The results observed on any given day will not always be representative of the given season's prevailing transport patterns, and plume concentrations and distributions are forecast to vary markedly. To explore this variability, statistical distributions for each scenario are examined. Percentile distributions will summarise the outcomes over the entire scenario and do not represent an instantaneous plume footprint at any point in time.

In the scenarios where the inshore borrow ground is utilised, forecasts of median depth-averaged SSC concentrations (values exceeded 50% of the time) for project works commencing in summer (Scenario 2B) were in the range 0.1-1 mg/L over an area stretching from the south-western end of Angel Island to the waters between Enderby Island and West Intercourse Island. For project works commencing in winter (Scenario 1B), the equivalent area is restricted to the waters between the inshore borrow ground and spoil ground AB. At the 95th percentile (values exceeded only 5% of the time), forecasts of depth-averaged SSC concentrations 5 mg/L or greater in both seasons are found between Intercourse Island and the waters between the Malus Islands and Gidley Island (Scenario 1B, Figure 5.4; Scenario 2B, Figure 5.8).

In the scenarios where the offshore borrow ground is utilised, forecasts of 50th percentile (median) depth-averaged SSC concentrations do not exceed 0.1 mg/L for works commencing in either season. At the 95th percentile, forecasts of depth-averaged SSC concentrations 5 mg/L or greater are found in nearshore areas between Intercourse Island and King Bay for project works commencing in summer (Scenario 2A, Figure 5.6), and also near Angel Island and Conzinc Island for project works commencing in winter (Scenario 1A, Figure 5.2).

When examined over the course of an entire scenario, the sediment distributions reveal areas that broadly straddle the dredging and disposal zones where recurrent elevations of near-seabed SSC are expected as a consequence of dredging operations. The forecast in each scenario is that the greatest concentrations will typically be found in the inshore waters of Mermaid Sound along the pipeline between the KP5 and KP25

points. This zone contains a significant volume of the overall in situ volume to be dredged, and there are many shallow locales where strong tidal flows both inhibit settlement of fine suspended sediments and stimulate significant levels of resuspension of sediments deposited after initial release in the water column. For Scenarios 1A and 2A, where the offshore borrow ground is dredged for backfill material, an additional plume signature results from recurrent elevations of near-seabed SSC north of Legendre Island and subsequent resuspension of this material as it is transported towards Nickol Bay.

Concentrations of suspended sediment in the key activity areas will represent the combined influence of new discharges and resuspension of fine sediments from earlier discharges. Temporal variations in intensity of the dredging operations, including overlap of multiple operations in time or downtime periods, will also influence turbidity peaks and troughs. At progressively more distant areas, the importance of resuspension as a contributor to the distribution of SSC concentrations in general, and near-seabed concentrations in particular, becomes a greater factor. The areas forecast to receive elevated concentrations are substantially larger than would be affected by plumes only from the initial sources. The plume extents tend to expand over periods of several weeks in the direction of net drift, indicating the progressive transport of fine sediments through continuous patterns of settlement and resuspension.

With the duration of each scenario (ten months) spanning almost the entire range of seasonal conditions, the direction of net drift will shift from summertime trends (generally longshore in a north-easterly direction) to wintertime trends (generally longshore in a south-westerly direction), or vice versa, depending on commencement times (winter for Scenarios 1A/1B and summer for Scenarios 2A/2B). A progressive shift in the available source of resuspendable fine sediments is also indicated. Periodic high wave-energy events will be a major contributor to estimates of high SSC in the near-seabed layer, particularly in shallow exposed areas. While these processes are forecast to extend the influence of dredging activities over a wider area, the longshore dispersal of finer sediments is indicated to be an important mechanism for limiting the trapping and build-up of fine sediments in the local region around the key activity areas. The build-up of resuspendable fine sediments in areas remote from dredging activities indicates that the supply of fines to these areas will be greater than their removal due to ongoing resuspension and longshore transport, for as long as sediment input from dredging activities continues.

5.1.2   Pipeline Dredging Activities

For pipeline dredging activities during winter conditions (Scenarios 1A and 1B), sediment plumes at low concentrations are forecast to drift generally towards the south-west. The plumes tend to follow the bathymetric contours between East Intercourse Island and East Lewis Island, and also between West Lewis Island and Rosemary Island.

In contrast, the net drift direction forecast for sediment plumes from pipeline dredging activities during summer conditions (Scenarios 2A and 2B) is towards the north-east, with the plumes following the bathymetric contours as they turn around Legendre Island towards Delambre Island. This drift is imposed by the prevailing south-westerly winds over the summer season. In general, the majority of the dispersing suspended material is forecast to migrate offshore rather than through Flying Foam Passage and Searipple Passage, which is attributable to the local bathymetric features. Much of the dredging occurs in water depths greater than that found within each passage, but strong tidal currents will drive significant sediment concentrations in and out of the passages on a regular basis.

5.1.3   Pipeline Backfill Activities

For the scenarios in which backfilling of the pipeline is facilitated by dredging of the inshore borrow ground (Scenarios 1B and 2B), the net drift direction of sediment plumes tends to be in opposition to that observed for the plumes attributable to pipeline dredging activities. This is because a gap of several months has been

assumed between pipeline dredging and backfilling operations (see Section 3.5.5), meaning that the seasonal trend has reversed over time. Because similar loss rates are applied during both the pipeline dredging and backfilling phases, the contribution of sediment suspended by dredging at the inshore borrow ground to the overall plume footprint will be significant; the volume of backfill material to be dredged (~1.6 Mm^3) is comparable to that required to be dredged over the entire pipeline length (~1.9 Mm^3), but is confined to a relatively small area. Suspended sediments resulting from placement of the backfill material along the pipeline will be concentrated near the seabed and will quickly settle due to the relative coarseness of the material.

For the scenarios in which backfilling of the pipeline is facilitated by dredging of the offshore borrow ground (Scenarios 1A and 2A), the bulk of the sediment suspended by dredging is forecast to be dispersed in the offshore area between the borrow ground and Legendre Island in both seasons. Strong tidal flows between Hauy Island and Delambre Island will aid movement of sediment towards the shallow waters of Nickol Bay, with this effect being greater during summer (Scenario 1A, following pipeline dredging activities in winter) due to predominant net drift towards the east imposed by prevailing south-westerly winds. In contrast, the net drift direction forecast during winter conditions (Scenario 2A) is towards the south-west, mostly following the bathymetric contours to the north of Rosemary Island. The sediment plume from operations in this area is forecast to migrate to the offshore pipeline and spoil ground areas, most noticeably in Scenario 2A when borrow ground dredging occurs in winter (following pipeline dredging activities in summer) but at lower concentrations than will have already occurred during pipeline dredging activities.

5.1.4   Spatial Outcomes

5.1.4.1   Scenario 1A: Dredging Operations Commencing during Winter, with Backfill Material Sourced from Borrow Ground A (Offshore)
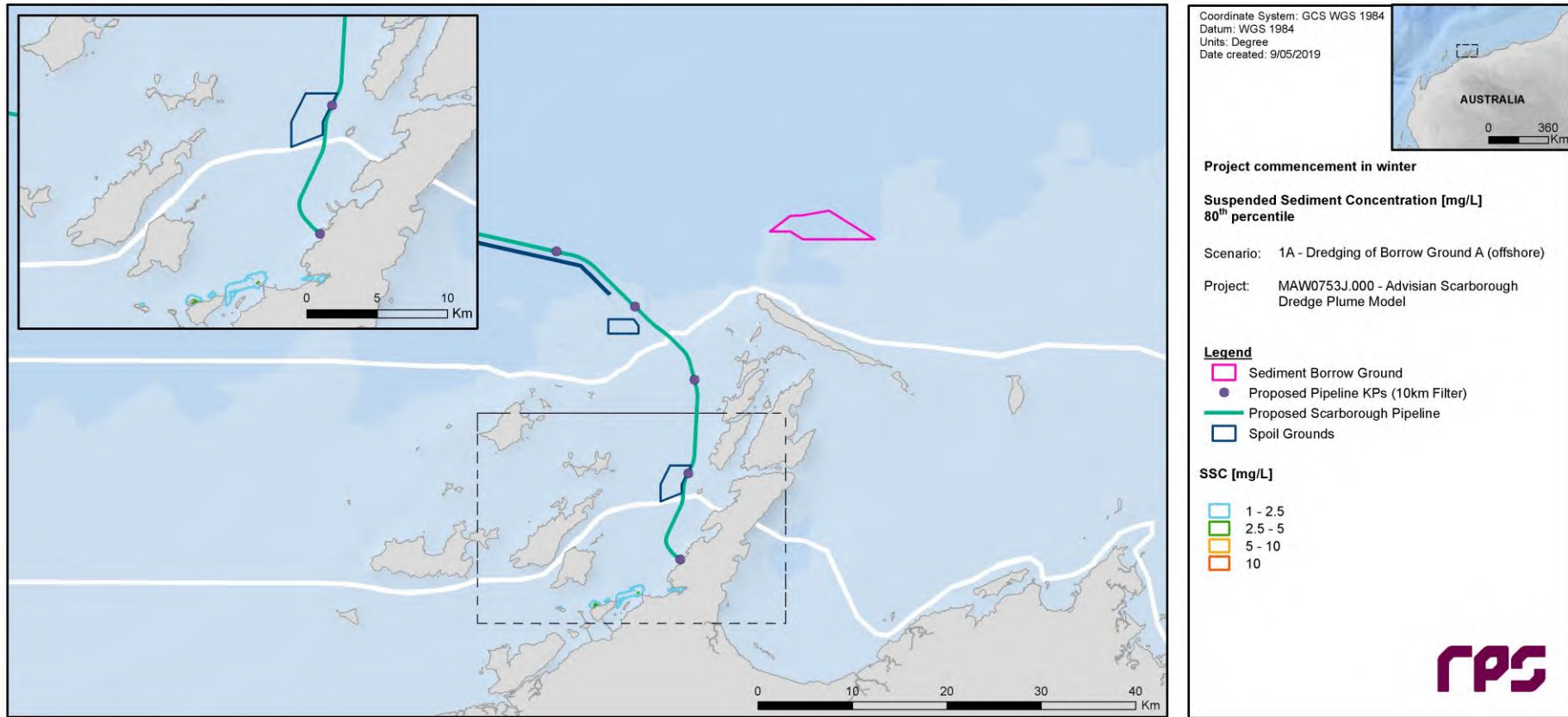
Figure 5.1   Predicted 80th percentile dredge-excess SSC throughout the entire scenario duration (1st July 2016 to 30th April 2017).
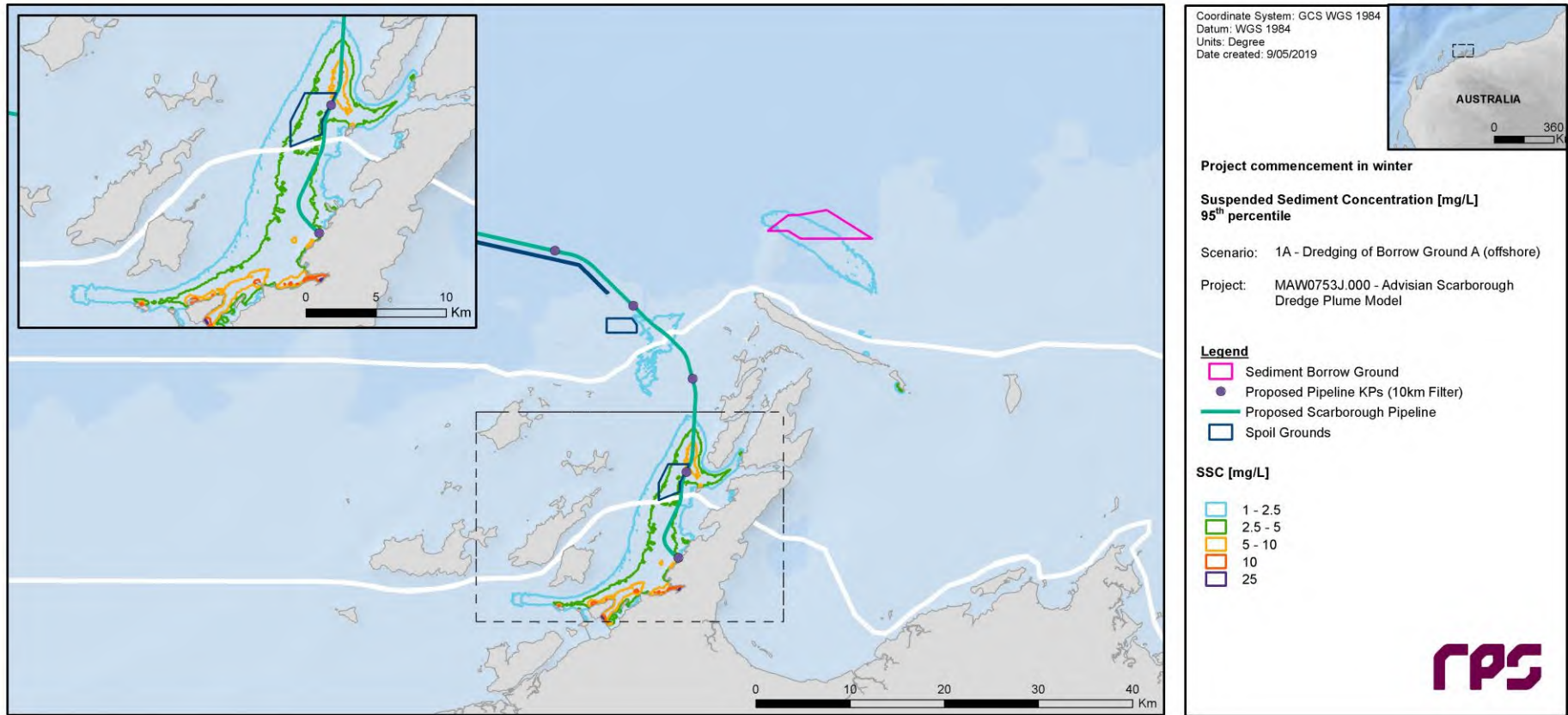
Figure 5.2   Predicted 95th percentile dredge-excess SSC throughout the entire scenario duration (1st July 2016 to 30th April 2017).

5.1.4.2 Scenario 1B: Dredging Operations Commencing during Winter, with Backfill Material Sourced from Borrow Ground B (Inshore)
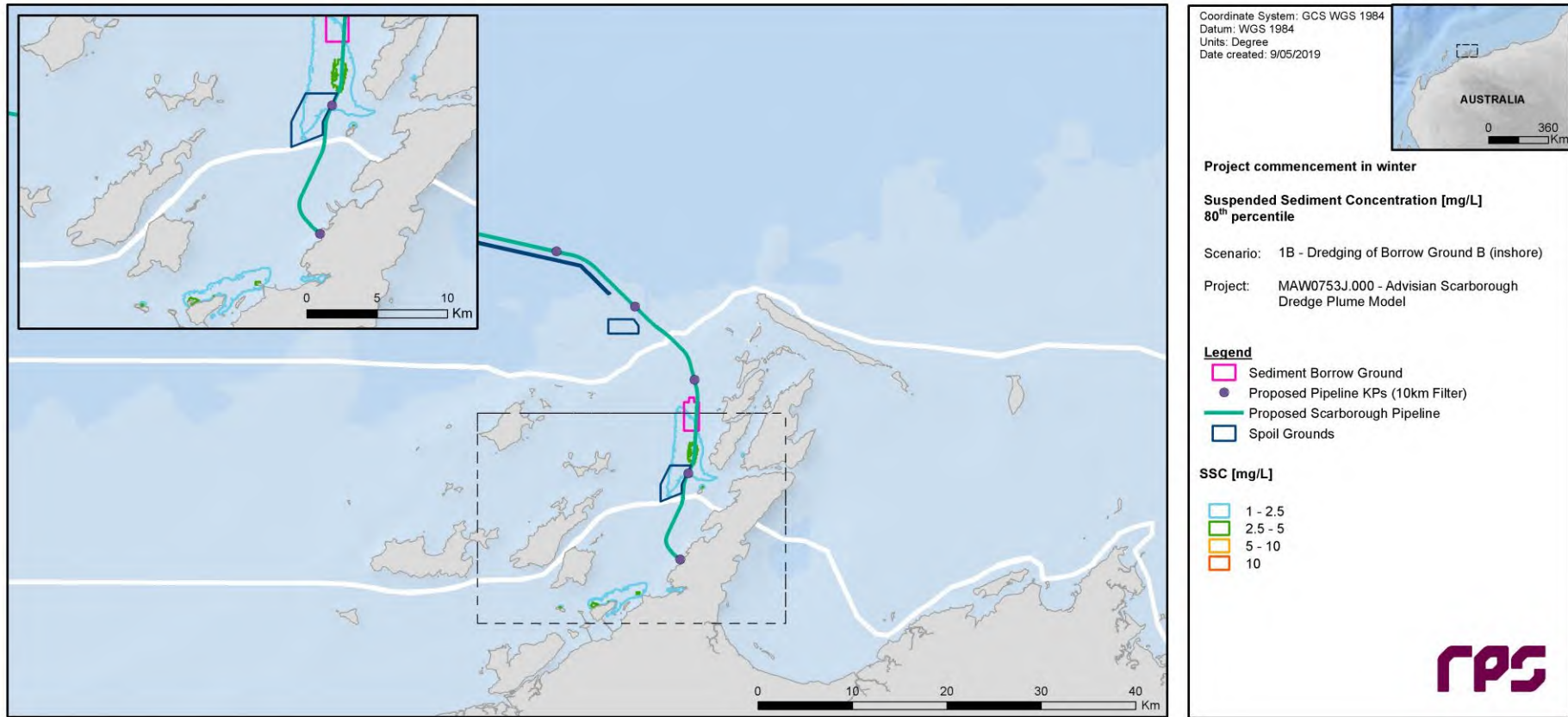
Figure 5.3   Predicted 80th percentile dredge-excess SSC throughout the entire scenario duration (1st July 2016 to 30th April 2017).
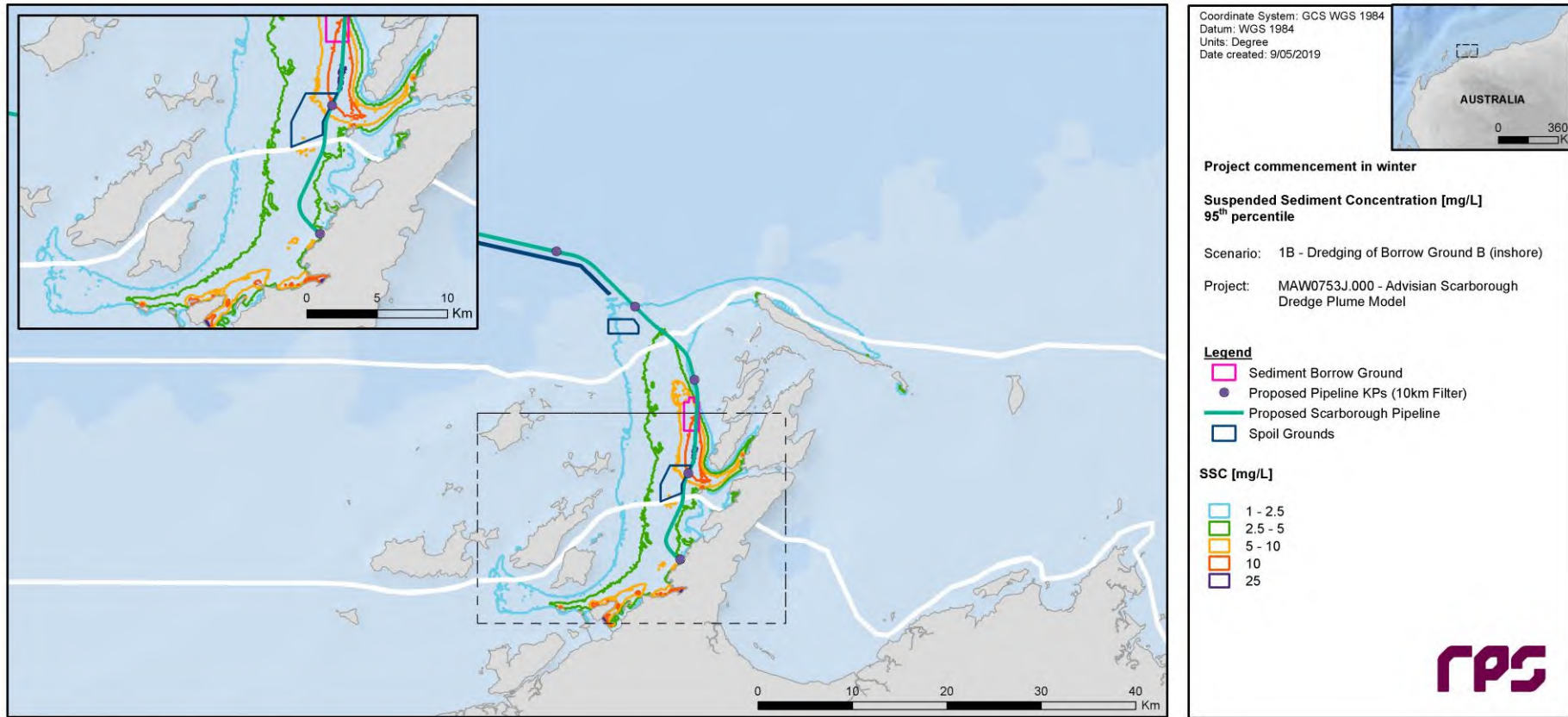
Figure 5.4   Predicted 95th percentile dredge-excess SSC throughout the entire scenario duration (1st July 2016 to 30th April 2017).

5.1.4.3 Scenario 2A: Dredging Operations Commencing during Summer, with Backfill Material Sourced from Borrow Ground A (Offshore)
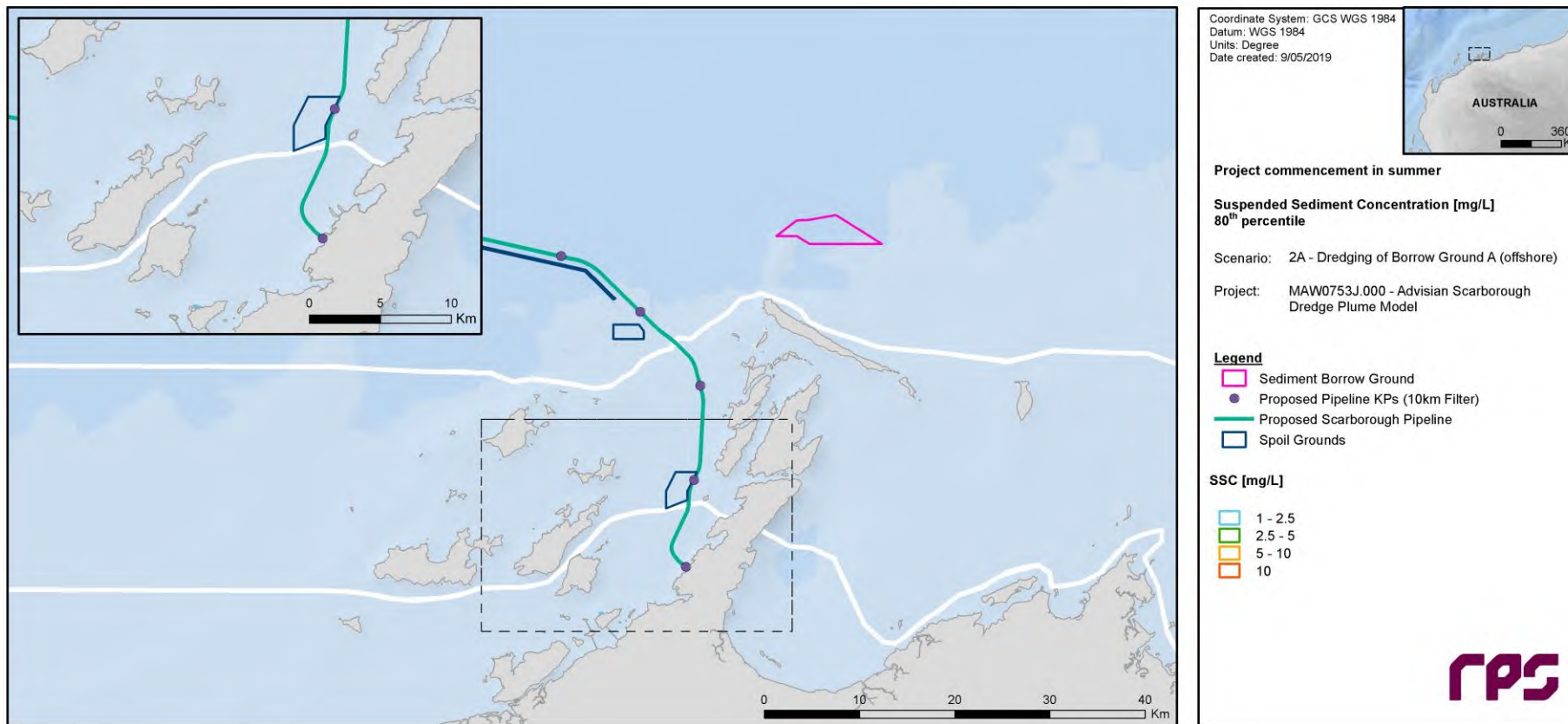
Figure 5.5 Predicted 80th percentile dredge-excess SSC throughout the entire scenario duration (1st January 2017 to 31st October 2017).
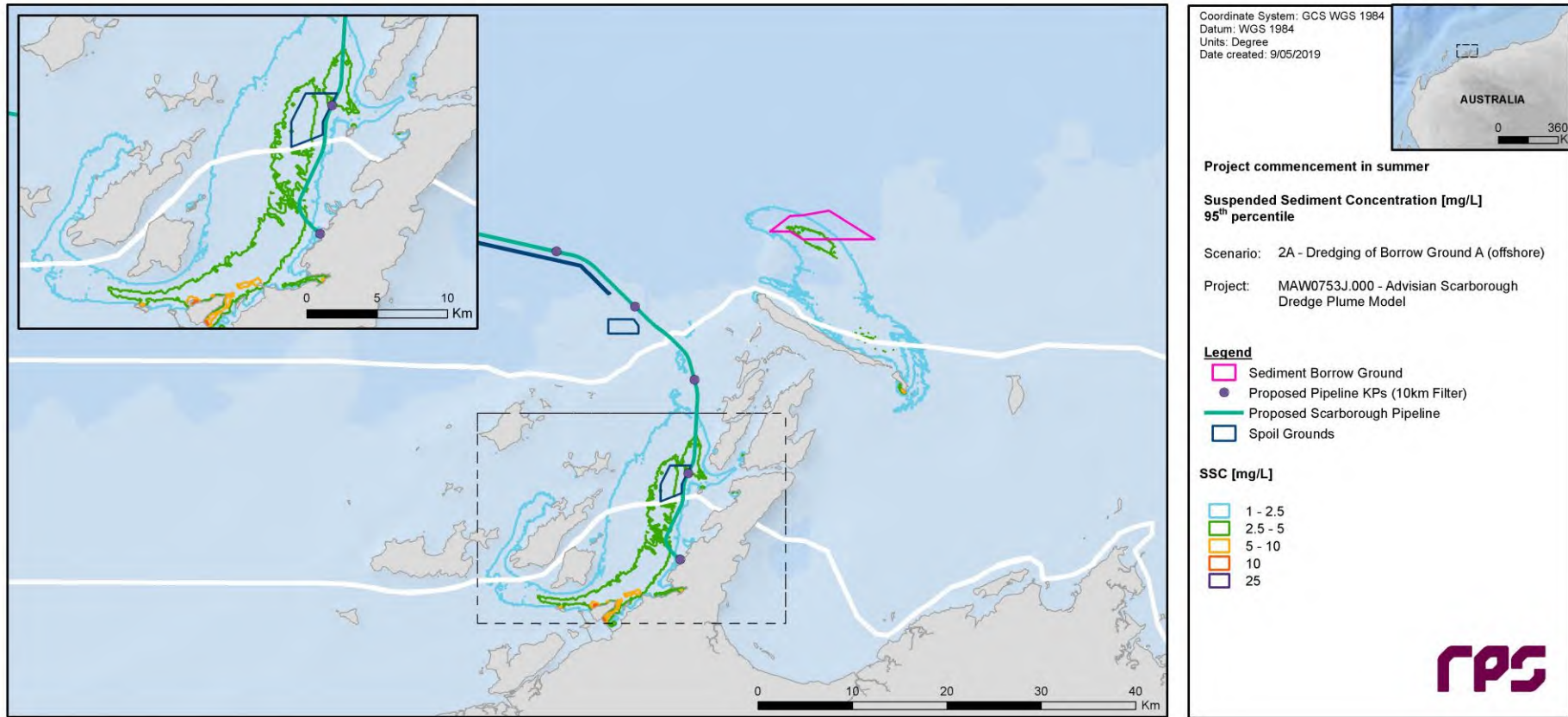
Figure 5.6   Predicted 95th percentile dredge-excess SSC throughout the entire scenario duration (1st January 2017 to 31st October 2017).

5.1.4.4 Scenario 2B: Dredging Operations Commencing during Summer, with Backfill Material Sourced from Borrow Ground B (Inshore)
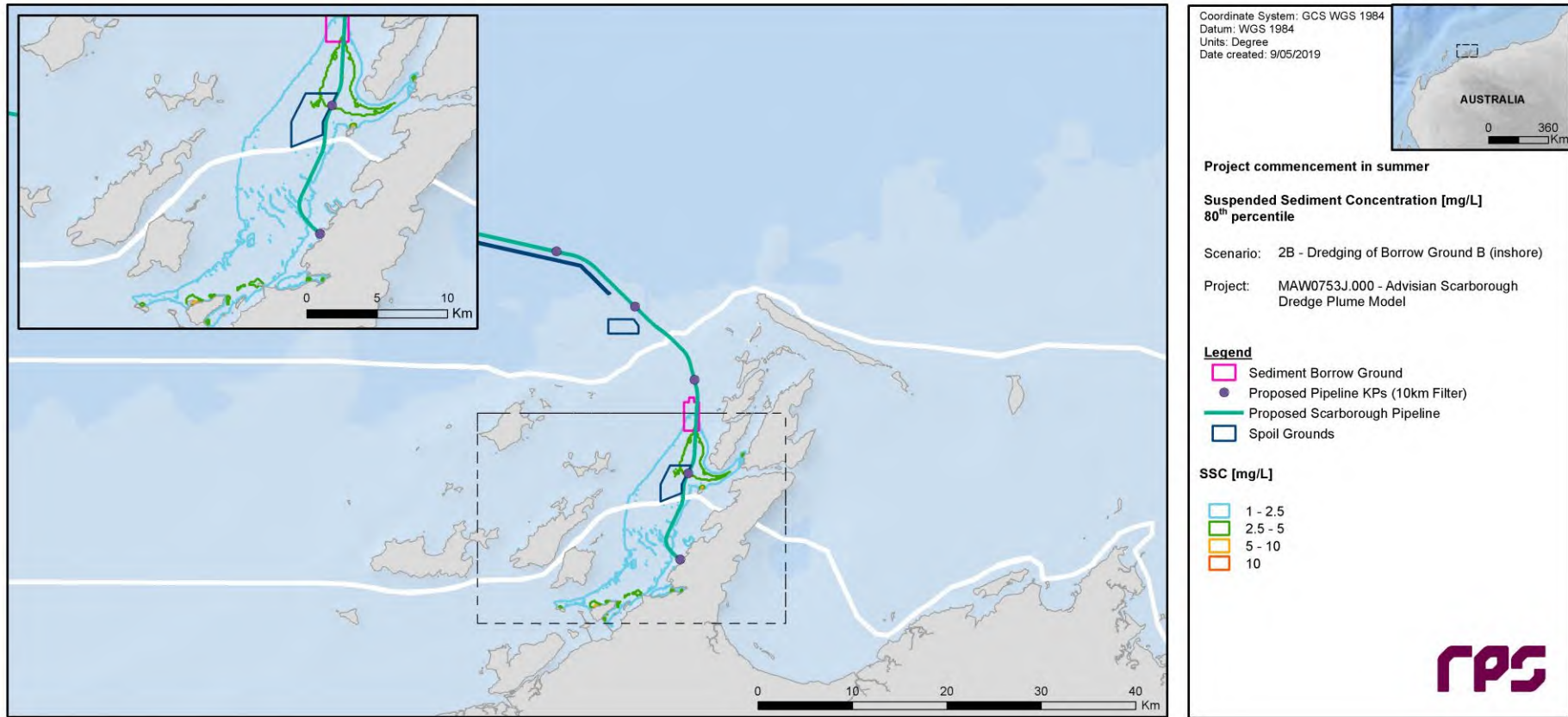
Figure 5.7   Predicted 80th percentile dredge-excess SSC throughout the entire scenario duration (1st January 2017 to 31st October 2017).
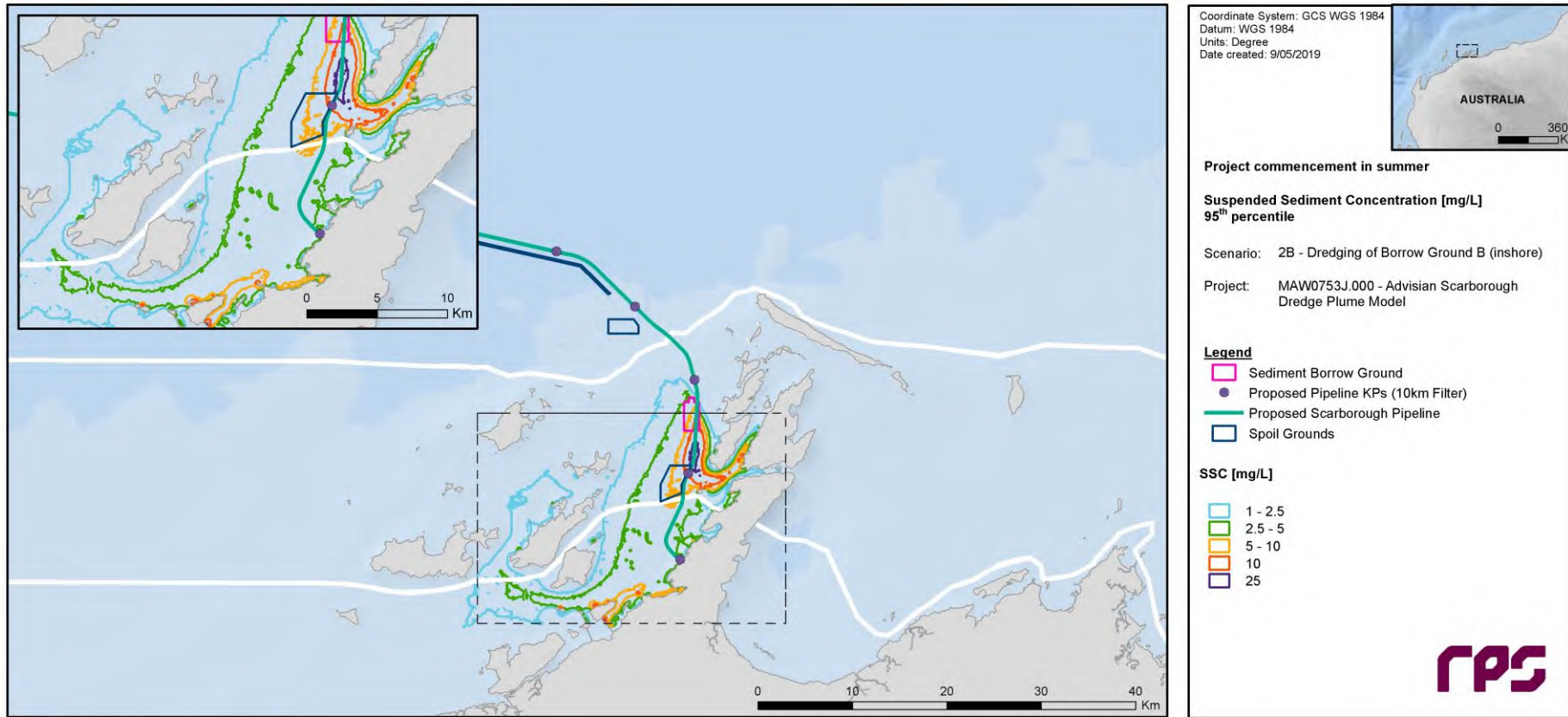
Figure 5.8   Predicted 95th percentile dredge-excess SSC throughout the entire scenario duration (1st January 2017 to 31st October 2017).

5.2 Predictions of Management Zone Extents

5.2.1 Summary

Figures showing the calculated extents of the defined management zones – ZoI, ZoMI and ZoHI – over the entire program of dredging, disposal and backfill operations are listed in Table 5.1 for each scenario.

Presentation of the ZoI areas is done on the basis of 95th percentile threshold exceedances for the 24-hour rolling average data.

It should be noted that the indicated management zone extents in each case represent a cumulative measure of exceedances of the relevant thresholds over a ten-month period, following the threshold criteria described in Section 4. They do not represent an instantaneous plume footprint at any point in time.

The indicated areas of threshold exceedances are largely a reflection of the areas of sediment confluence due to the proximity to key activity areas, where there is a sustained input of suspended sediments over periods of several months, and the influence of local metocean conditions acting to inhibit rates of settling and increase rates of resuspension.

The ZoI extents in ecological Zones A and B are broadly similar in all scenarios. In the Offshore ecological zone, a significantly larger ZoI is forecast along the pipeline in the vicinity of spoil grounds 2B and 5A for Scenarios 1A and 1B (where pipeline dredging operations will occur during winter) than for Scenarios 2A and 2B (where these operations will occur during summer). This is largely a consequence of the lower thresholds applicable during the winter period, and consequently the lower levels of dredge-excess SSC required to cause exceedances. In a similar manner, the larger ZoI predicted at the offshore borrow ground for Scenario 2A (where, following project commencement in summer, pipeline backfill operations will occur during winter) than for Scenario 1A (where these operations will occur during summer) is attributable to the lower winter thresholds.

The ZoMI/ZoHI threshold exceedances in isolated pockets of King Bay and around the Intercourse Islands may be attributable to the combined effects of model bathymetry and hydrodynamics, representing sediments that are transported into the shallowest-possible grid cells and then "trapped" upon reversal of the tide. While it is clear that there is a potential for dredged sediments to be found in the indicated areas, the persistently high concentrations at the water-land boundaries may be overstated – particularly in light of the long durations required to trigger the ZoMI/ZoHI thresholds.

Table 5.1   Index of the ZoI, ZoMI and ZoHI figures for each scenario.

Management Zone	Scenario 1A	Scenario 1B	Scenario 2A	Scenario 2B
Zone of Influence (95th percentile): 24-hour rolling average of total SSC	Figure 5.9	Figure 5.18	Figure 5.27	Figure 5.36
Zone of Moderate Impact: 3-day (Zones A and B) and 28-day (Offshore) rolling average of total SSC	Figure 5.10	Figure 5.19	Figure 5.28	Figure 5.37
Zone of Moderate Impact: 7-day (Zones A and B) and 28-day (Offshore) rolling average of total SSC	Figure 5.11	Figure 5.20	Figure 5.29	Figure 5.38
Zone of Moderate Impact: 10-day (Zones A and B) and 28-day (Offshore) rolling average of total SSC	Figure 5.12	Figure 5.21	Figure 5.30	Figure 5.39
Zone of Moderate Impact: 14-day (Zones A and B) and 28-day (Offshore) rolling average of total SSC	Figure 5.13	Figure 5.22	Figure 5.31	Figure 5.40
Zone of High Impact: 3-day (Zones A and B) and 28-day (Offshore) rolling average of total SSC	Figure 5.14	Figure 5.23	Figure 5.32	Figure 5.41
Zone of High Impact: 7-day (Zones A and B) and 28-day (Offshore) rolling average of total SSC	Figure 5.15	Figure 5.24	Figure 5.33	Figure 5.42
Zone of High Impact: 10-day (Zones A and B) and 28-day (Offshore) rolling average of total SSC	Figure 5.16	Figure 5.25	Figure 5.34	Figure 5.43
Zone of High Impact: 14-day (Zones A and B) and 28-day (Offshore) rolling average of total SSC	Figure 5.17	Figure 5.26	Figure 5.35	Figure 5.44

5.2.2   Spatial Outcomes

5.2.2.1   Scenario 1A: Dredging Operations Commencing during Winter, with Backfill Material Sourced from Borrow Ground A (Offshore)
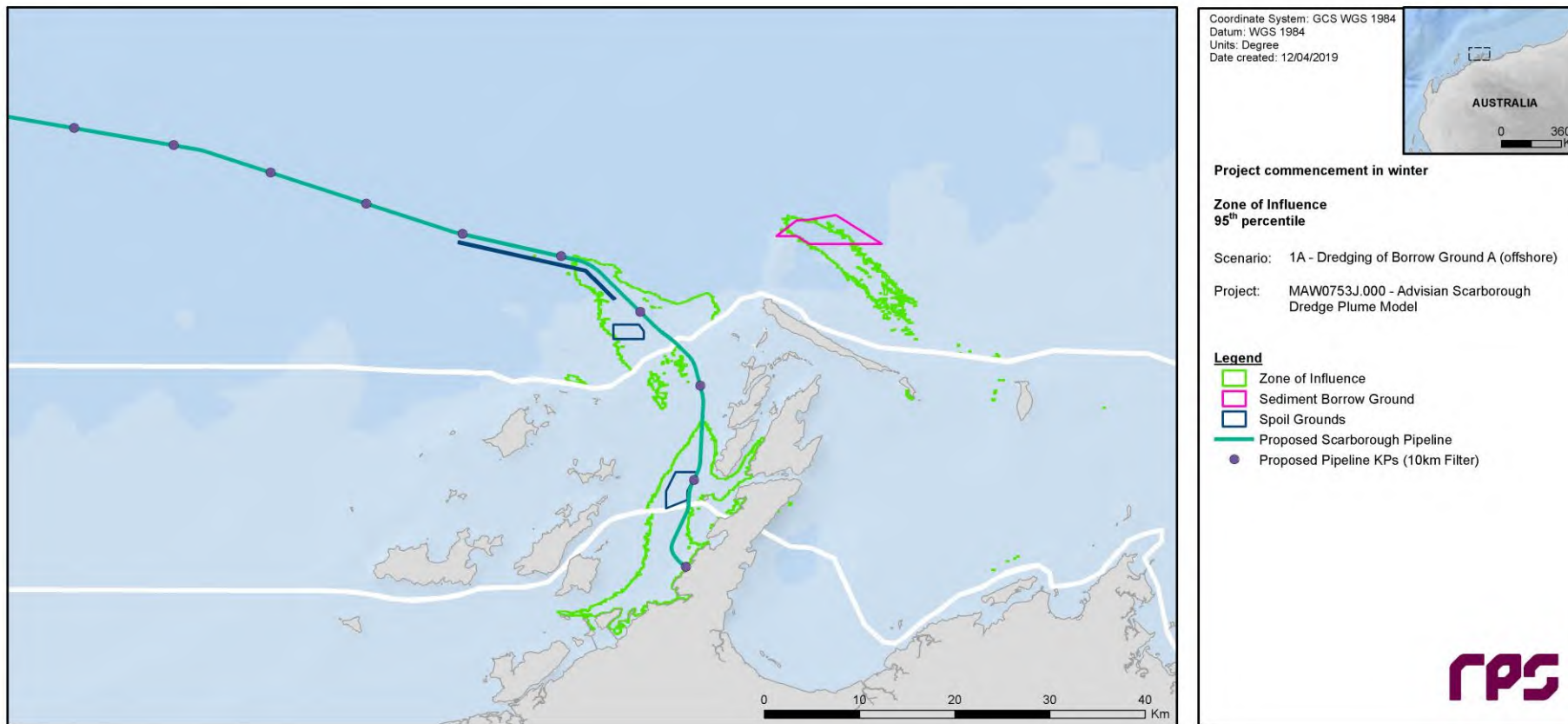
Figure 5.9 Predicted 95th percentile Zone of Influence following application of the appropriate spatial thresholds in Table 4.2 to a 24-hour rolling average of total (dredge and background) SSC throughout the entire scenario duration (1st July 2016 to 30th April 2017).
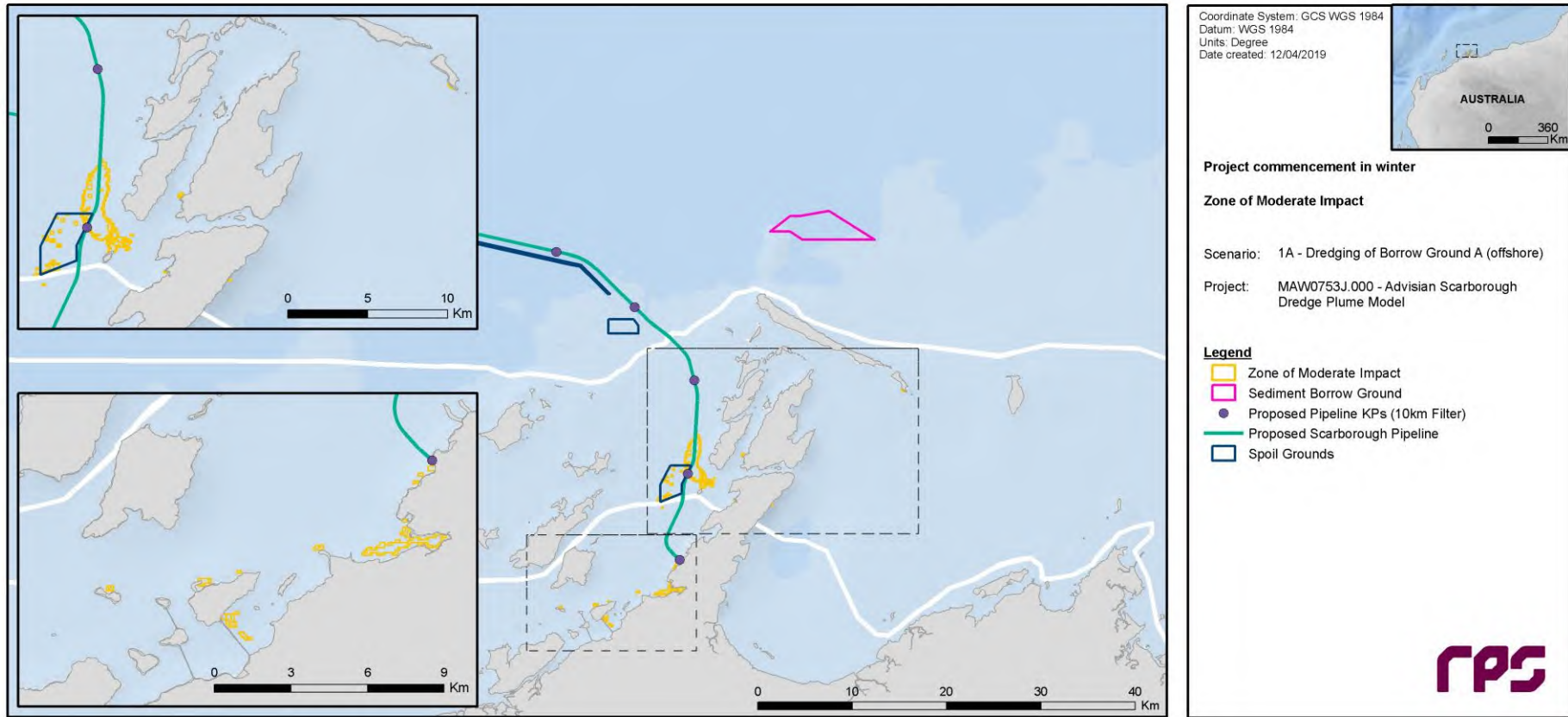
Figure 5.10 **Predicted Zone of Moderate Impact following application of the appropriate spatial thresholds in Table 4.3 to 3-day (Zones A and B) and 28-day (Offshore) rolling averages of total (dredge and background) SSC throughout the entire scenario duration (1st July 2016 to 30th April 2017).**
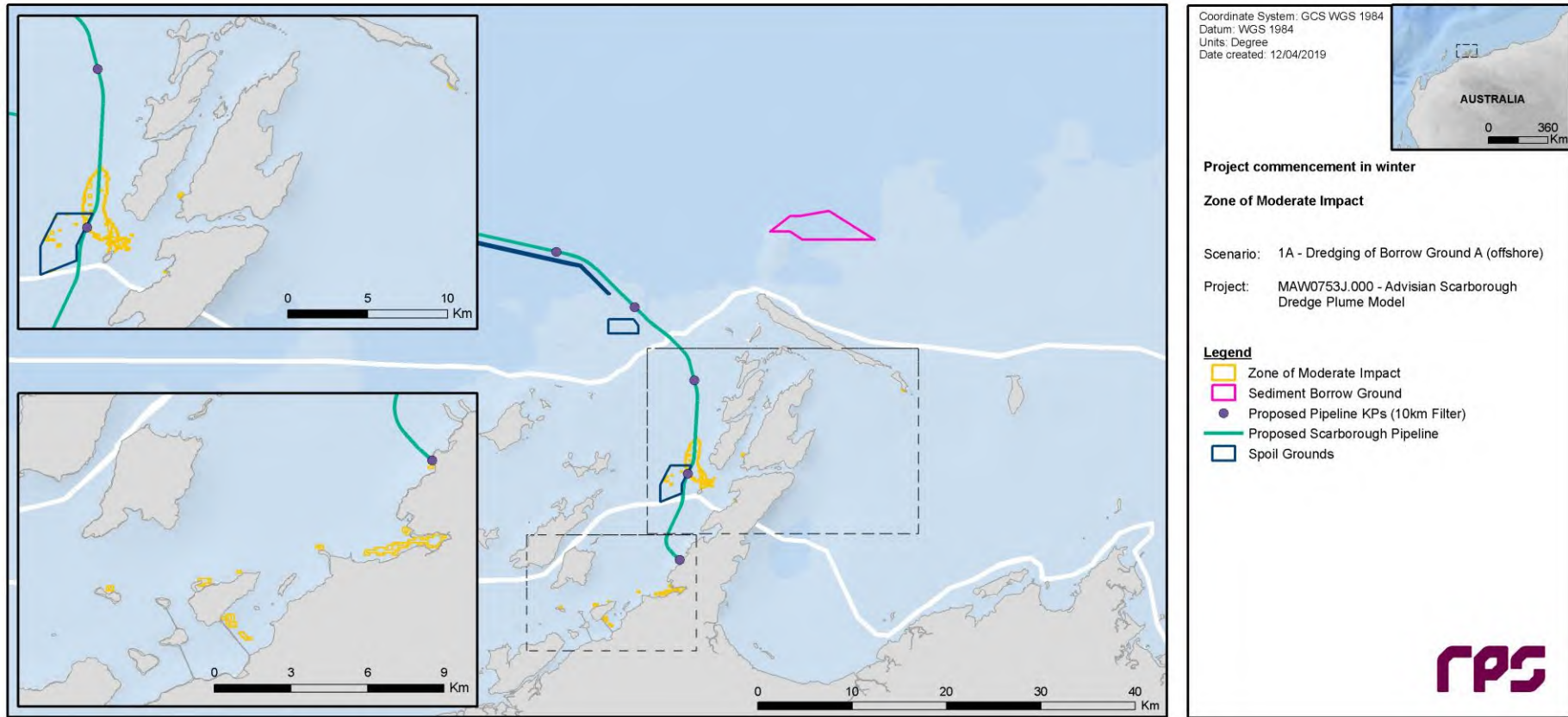
Figure 5.11 Predicted Zone of Moderate Impact following application of the appropriate spatial thresholds in Table 4.3 to 7-day (Zones A and B) and 28-day (Offshore) rolling averages of total (dredge and background) SSC throughout the entire scenario duration (1st July 2016 to 30th April 2017).
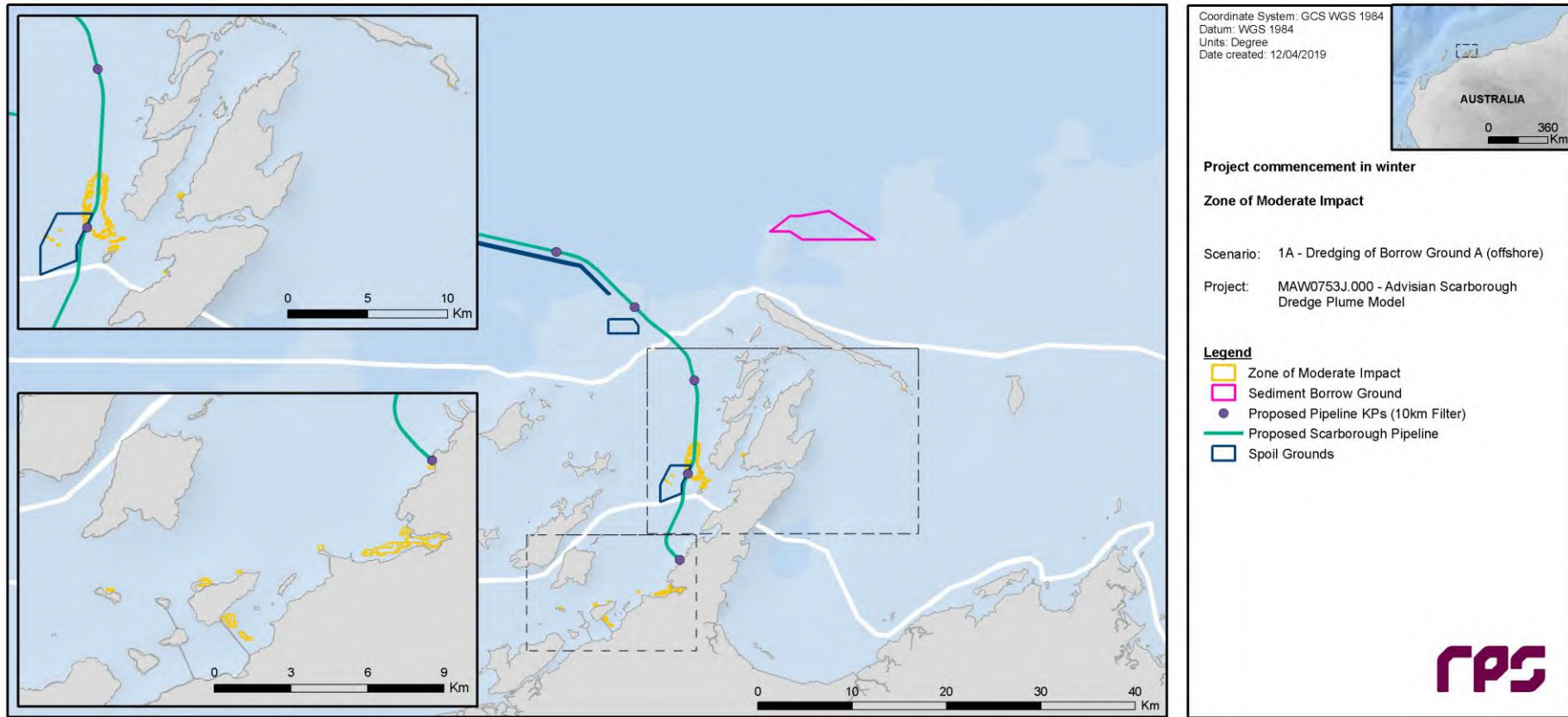
Figure 5.12 **Predicted Zone of Moderate Impact following application of the appropriate spatial thresholds in Table 4.3 to 10-day (Zones A and B) and 28-day (Offshore) rolling averages of total (dredge and background) SSC throughout the entire scenario duration (1st July 2016 to 30th April 2017).**
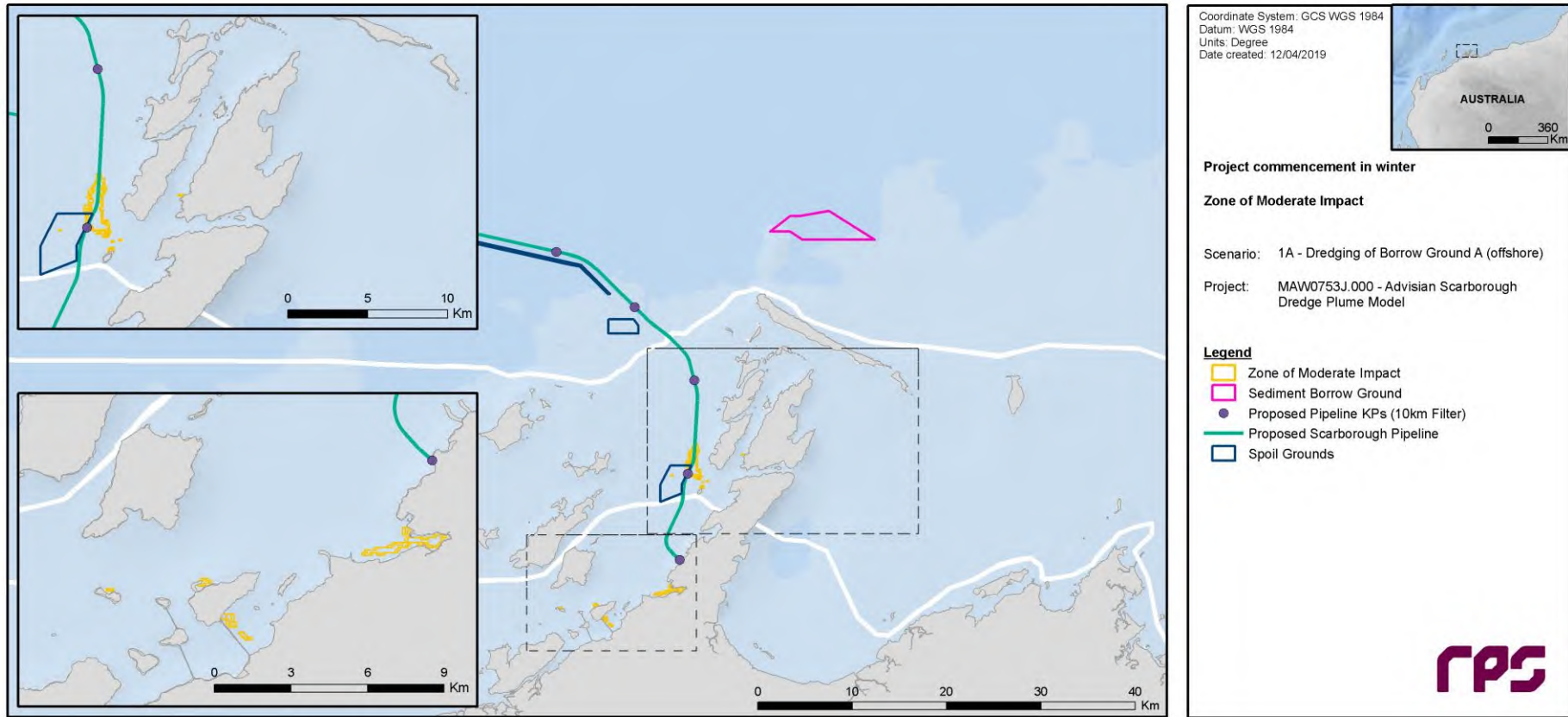
Figure 5.13 Predicted Zone of Moderate Impact following application of the appropriate spatial thresholds in Table 4.3 to 14-day (Zones A and B) and 28-day (Offshore) rolling averages of total (dredge and background) SSC throughout the entire scenario duration (1st July 2016 to 30th April 2017).
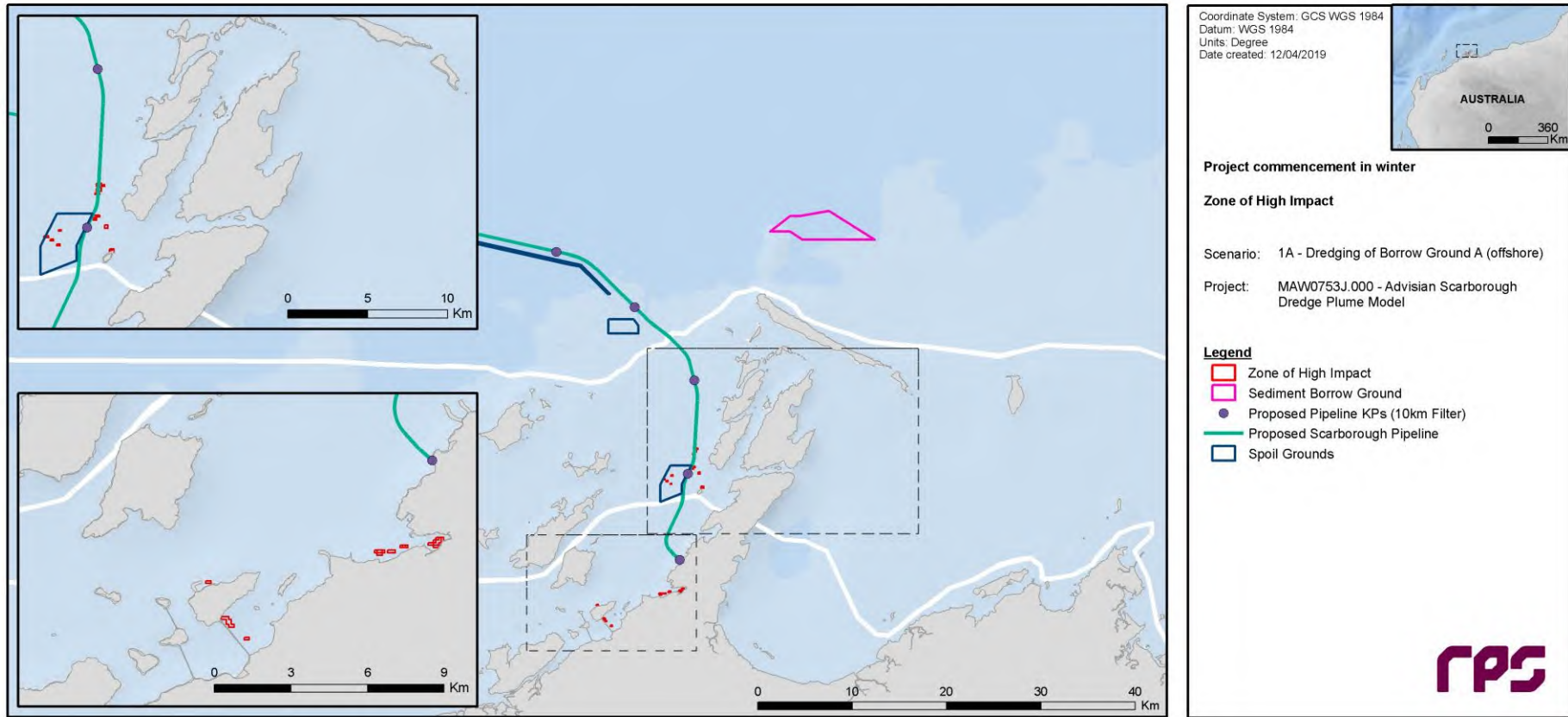
Figure 5.14 Predicted Zone of High Impact following application of the appropriate spatial thresholds in Table 4.4 to 3-day (Zones A and B) and 28-day (Offshore) rolling averages of total (dredge and background) SSC throughout the entire scenario duration (1st July 2016 to 30th April 2017).
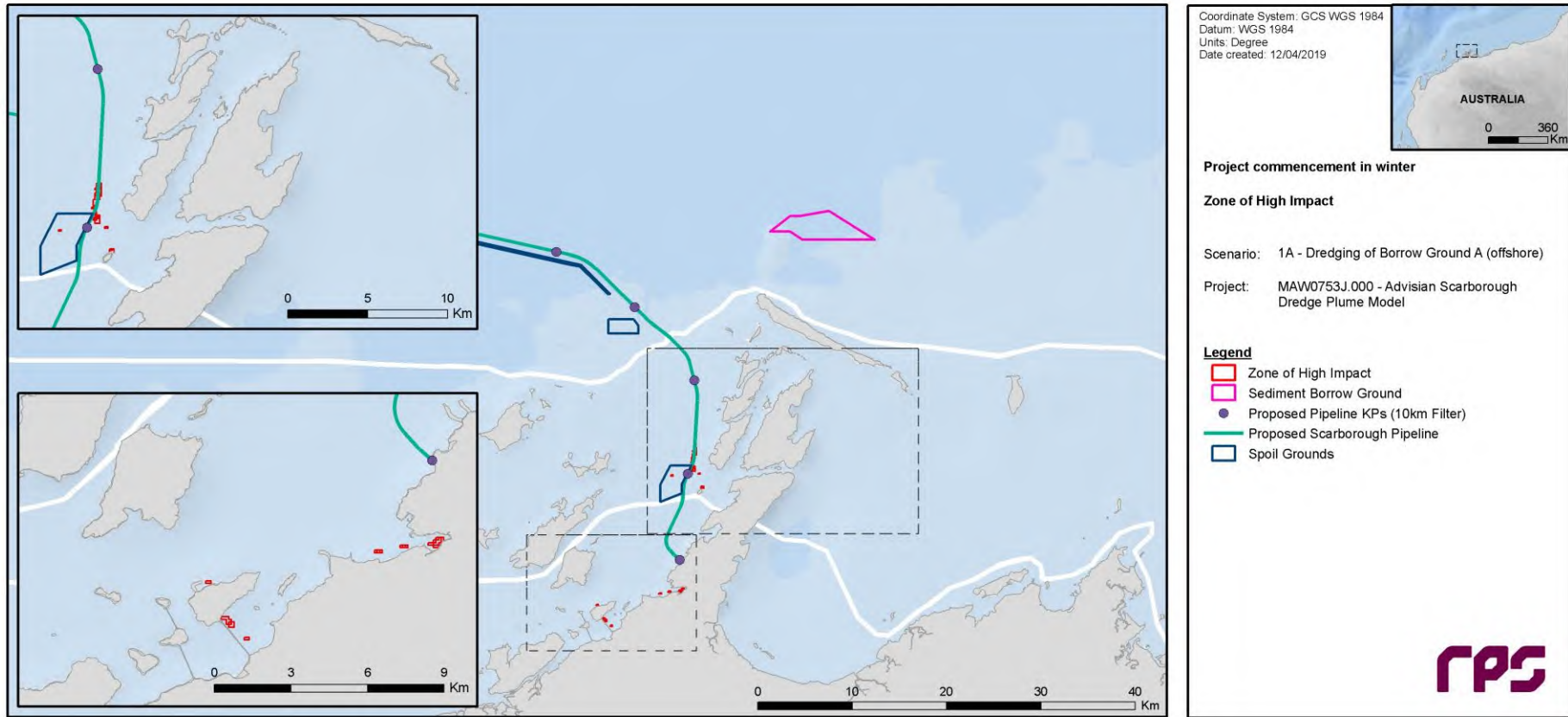
Figure 5.15 Predicted Zone of High Impact following application of the appropriate spatial thresholds in Table 4.4 to 7-day (Zones A and B) and 28-day (Offshore) rolling averages of total (dredge and background) SSC throughout the entire scenario duration (1st July 2016 to 30th April 2017).
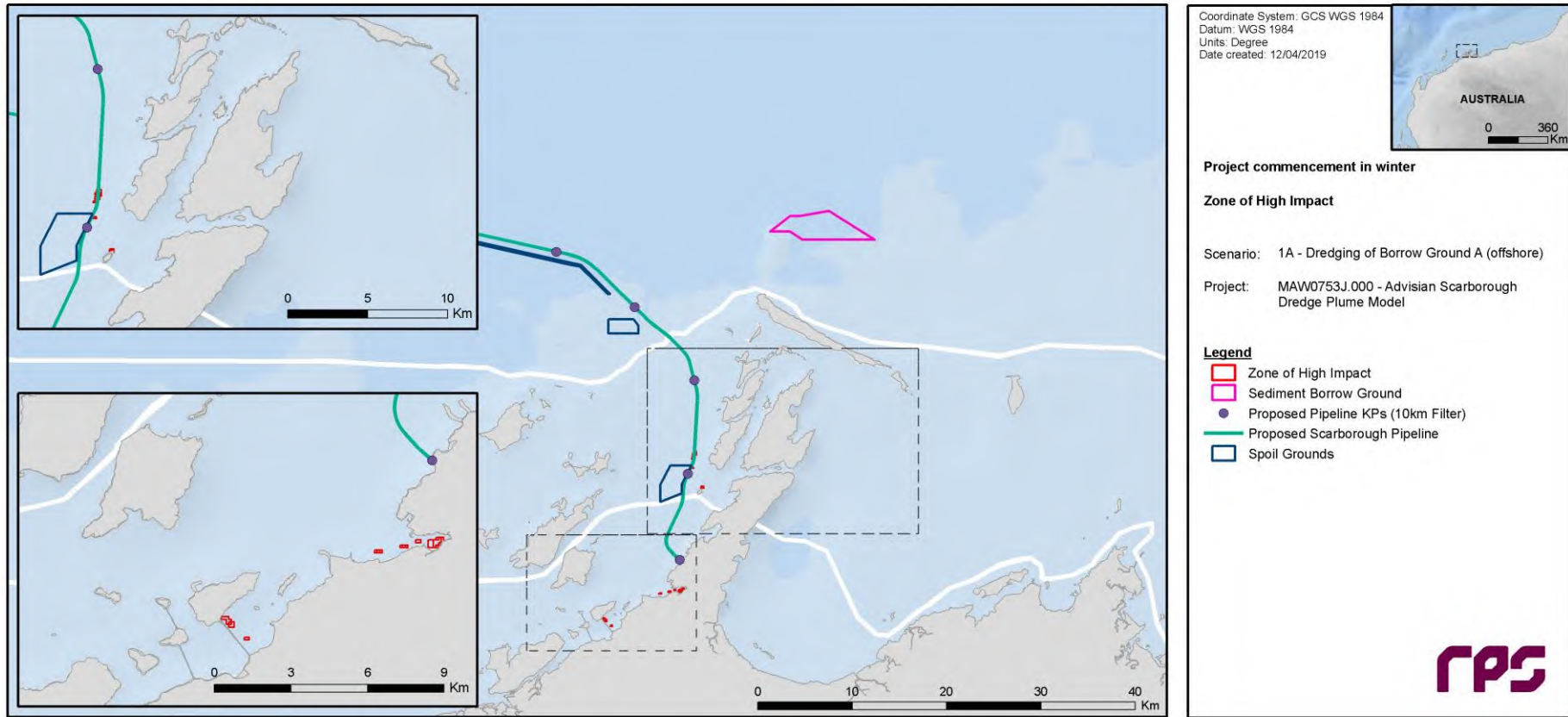
Figure 5.16 **Predicted Zone of High Impact following application of the appropriate spatial thresholds in Table 4.4 to 10-day (Zones A and B) and 28-day (Offshore) rolling averages of total (dredge and background) SSC throughout the entire scenario duration (1st July 2016 to 30th April 2017).**
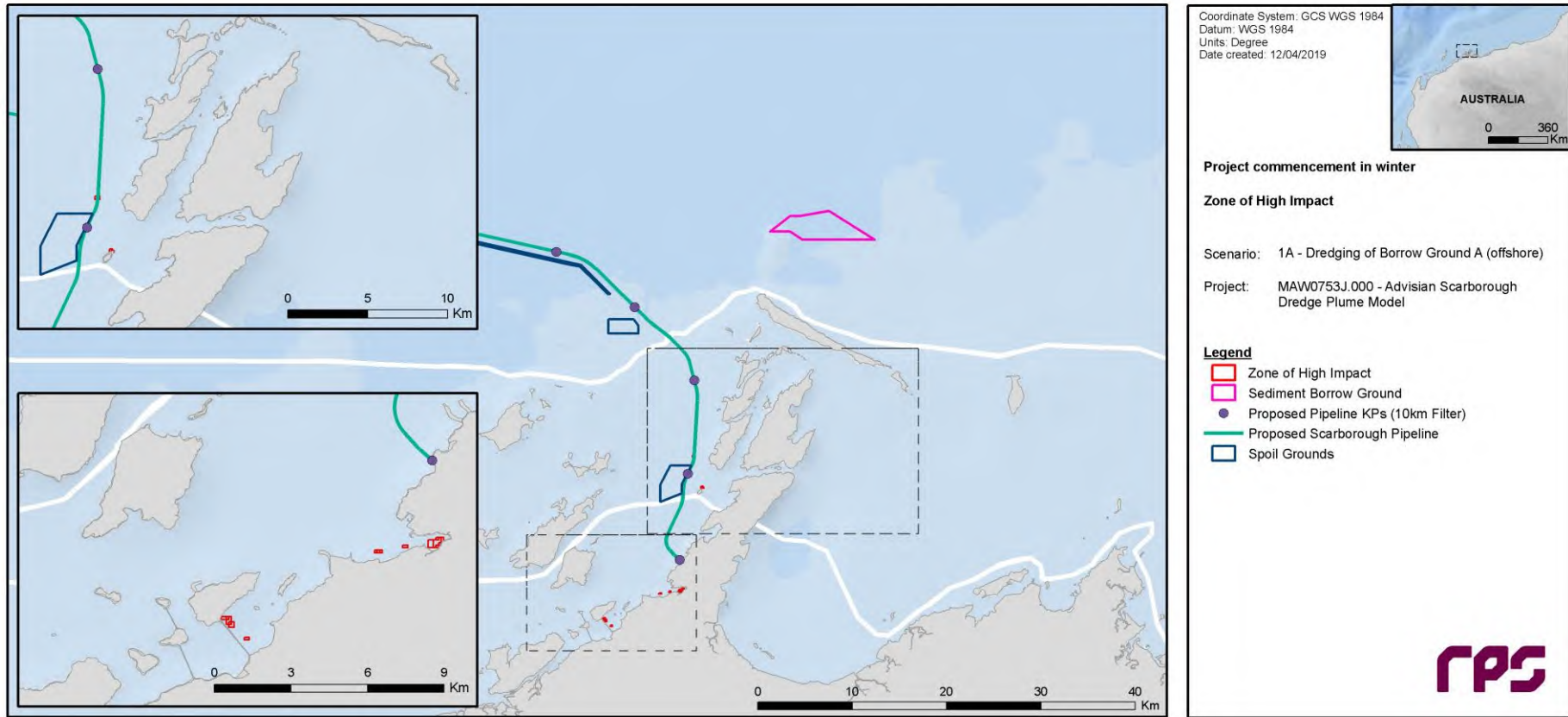
Figure 5.17 **Predicted Zone of High Impact following application of the appropriate spatial thresholds in Table 4.4 to 14-day (Zones A and B) and 28-day (Offshore) rolling averages of total (dredge and background) SSC throughout the entire scenario duration (1st July 2016 to 30th April 2017).**

5.2.2.2 Scenario 1B: Dredging Operations Commencing during Winter, with Backfill Material Sourced from Borrow Ground B (Inshore)
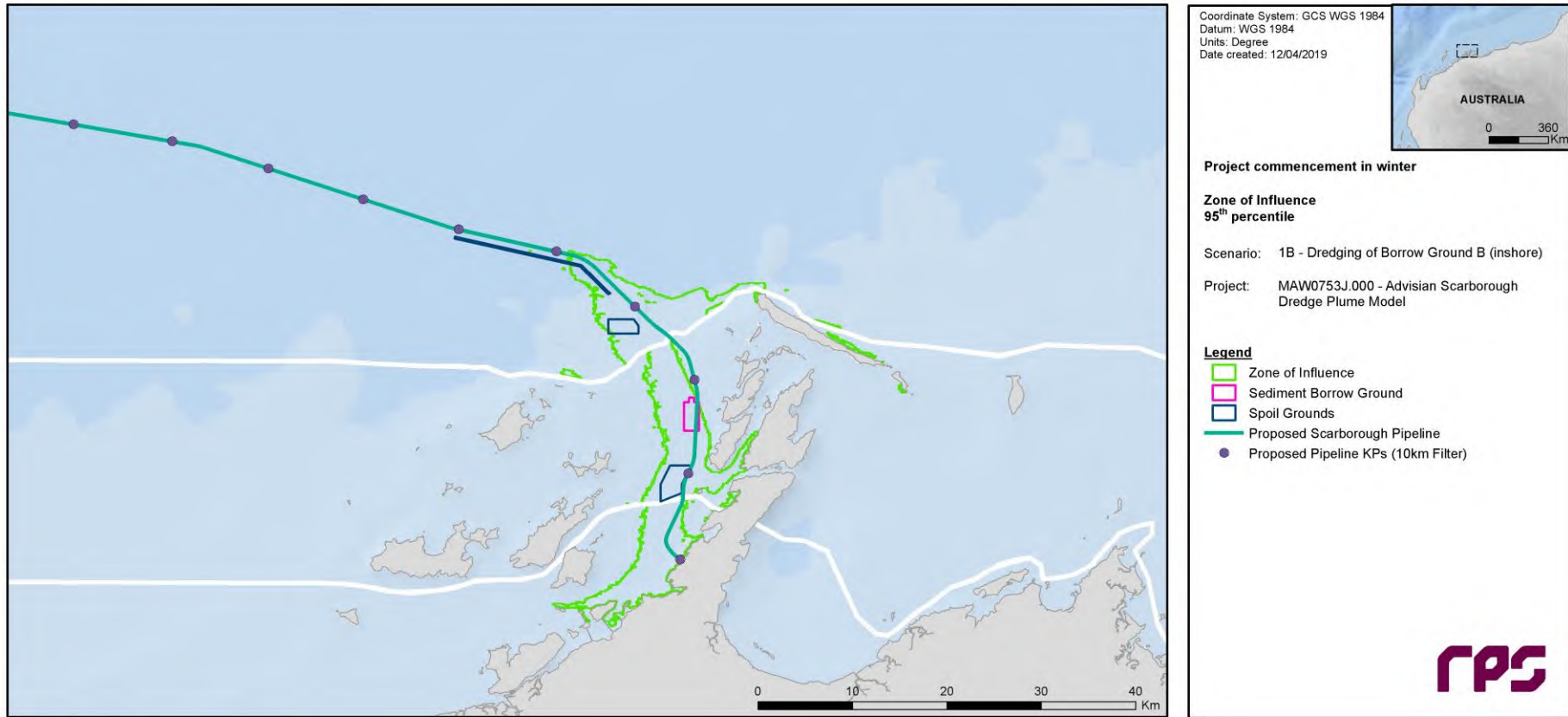
Figure 5.18 Predicted 95th percentile Zone of Influence following application of the appropriate spatial thresholds in Table 4.2 to a 24-hour rolling average of total (dredge and background) SSC throughout the entire scenario duration (1st July 2016 to 30th April 2017).
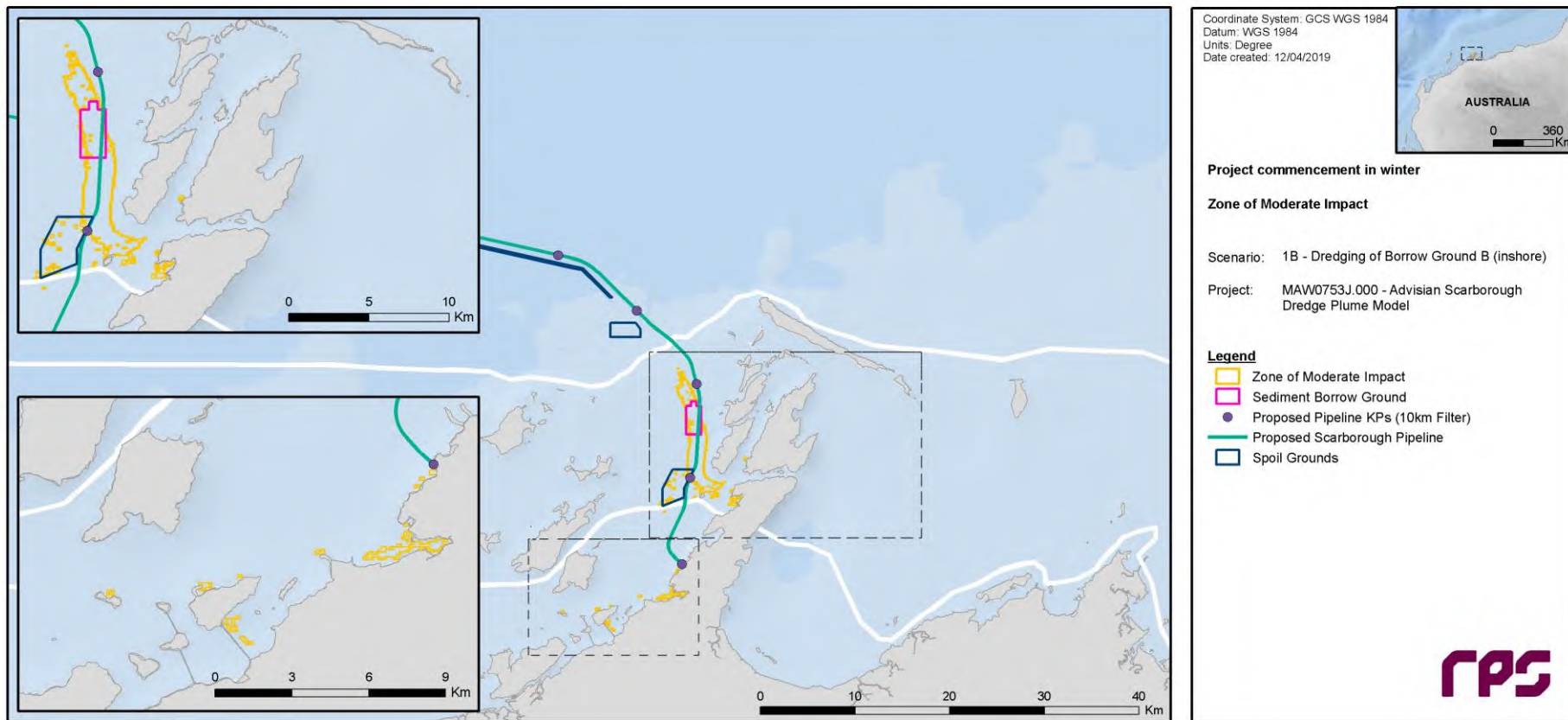
Figure 5.19 **Predicted Zone of Moderate Impact following application of the appropriate spatial thresholds in Table 4.3 to 3-day (Zones A and B) and 28-day (Offshore) rolling averages of total (dredge and background) SSC throughout the entire scenario duration (1st July 2016 to 30th April 2017).**
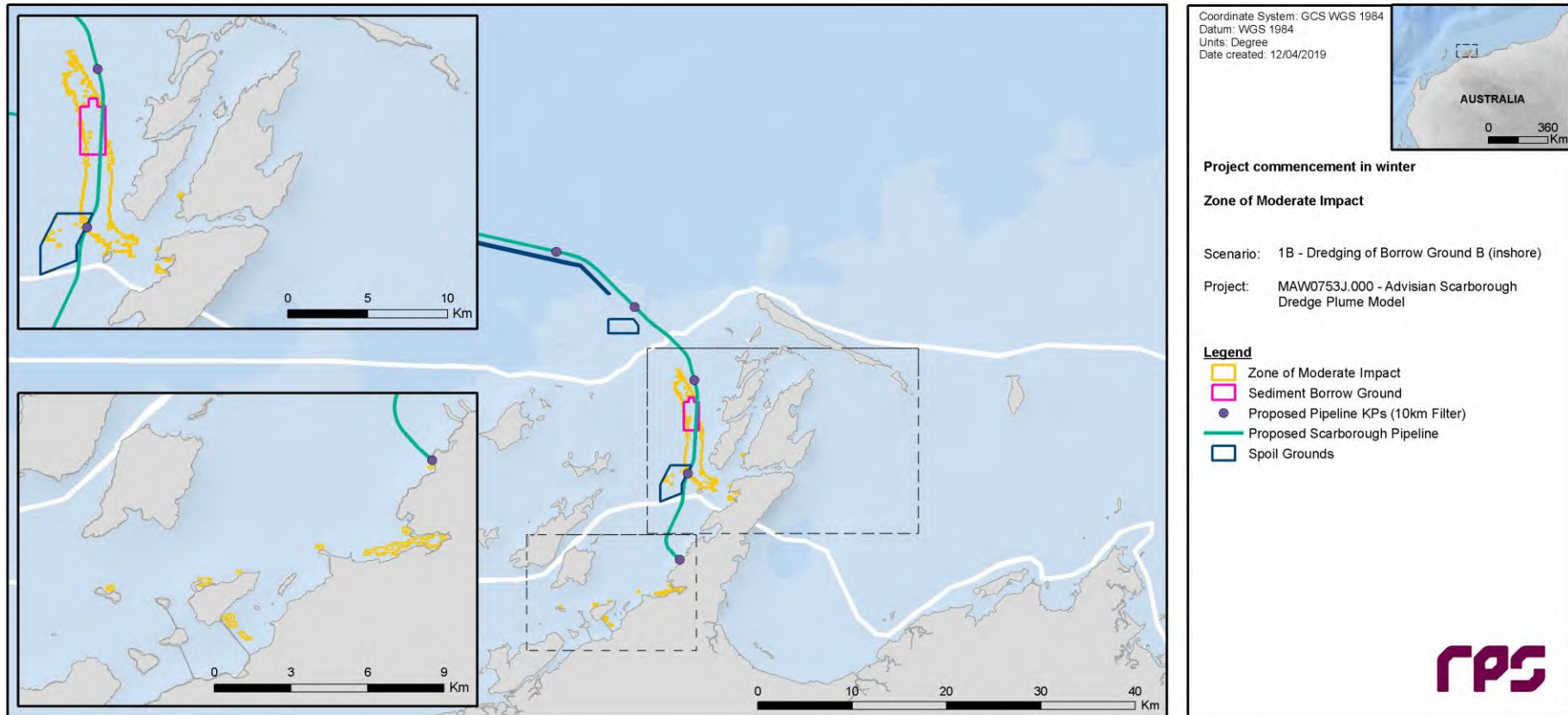
Figure 5.20 Predicted Zone of Moderate Impact following application of the appropriate spatial thresholds in Table 4.3 to 7-day (Zones A and B) and 28-day (Offshore) rolling averages of total (dredge and background) SSC throughout the entire scenario duration (1st July 2016 to 30th April 2017).
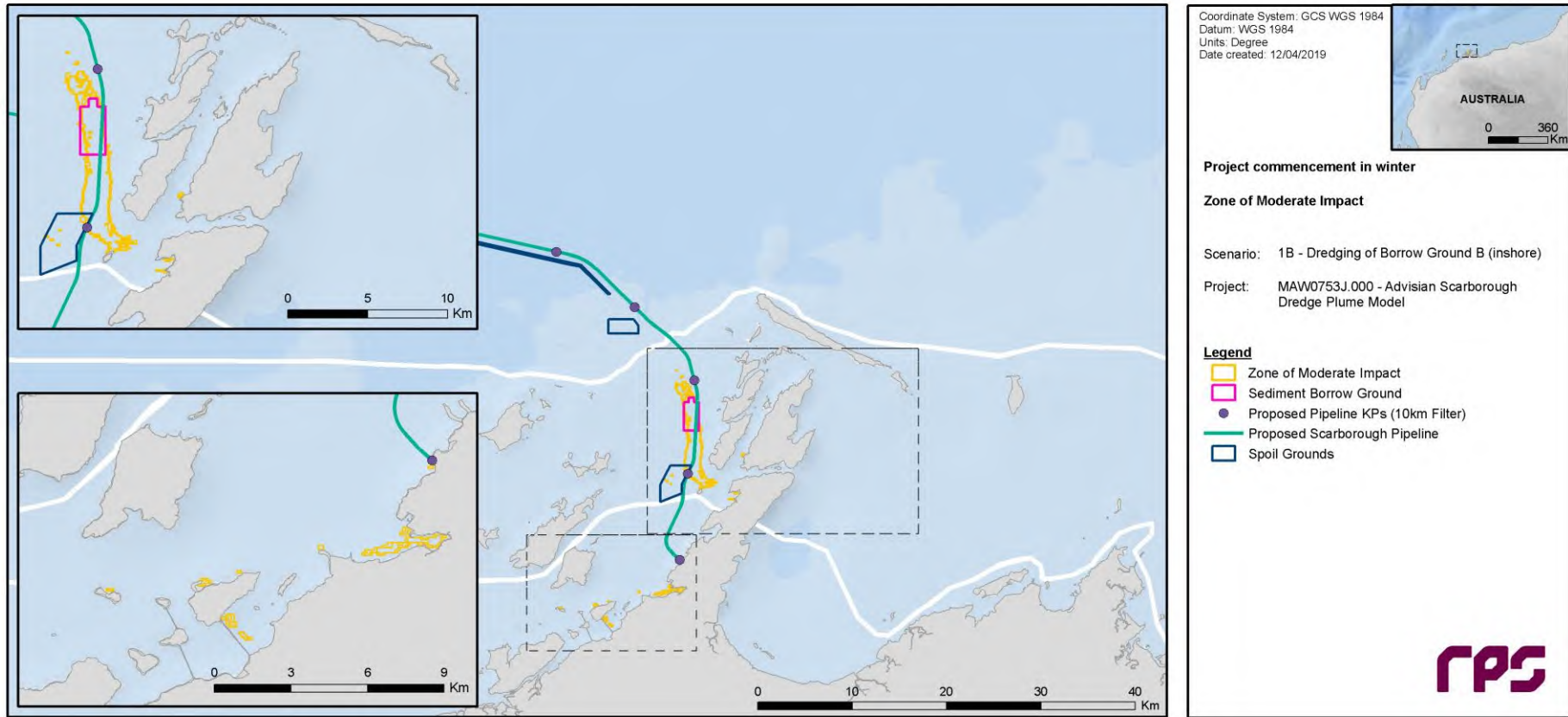
Figure 5.21 Predicted Zone of Moderate Impact following application of the appropriate spatial thresholds in Table 4.3 to 10-day (Zones A and B) and 28-day (Offshore) rolling averages of total (dredge and background) SSC throughout the entire scenario duration (1st July 2016 to 30th April 2017).
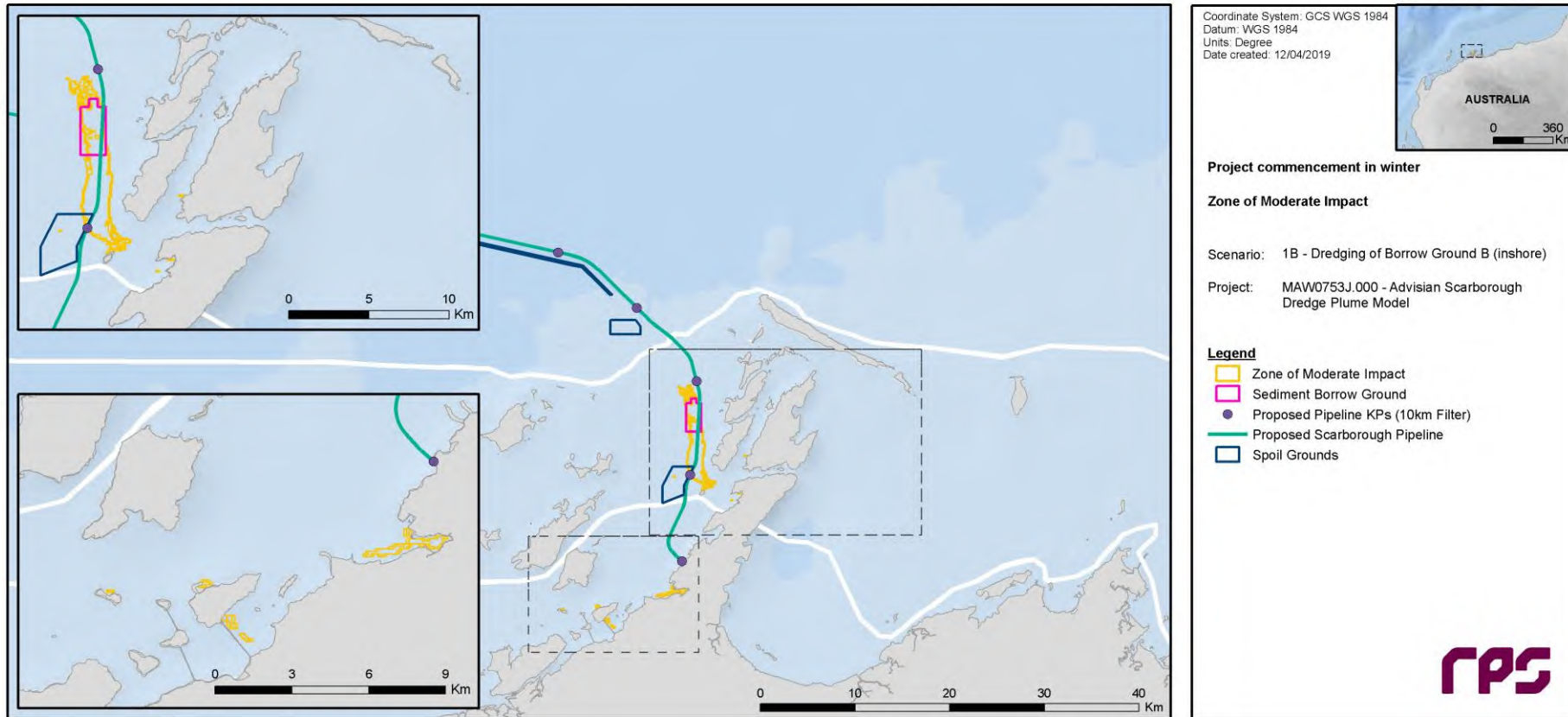
Figure 5.22 Predicted Zone of Moderate Impact following application of the appropriate spatial thresholds in Table 4.3 to 14-day (Zones A and B) and 28-day (Offshore) rolling averages of total (dredge and background) SSC throughout the entire scenario duration (1st July 2016 to 30th April 2017).
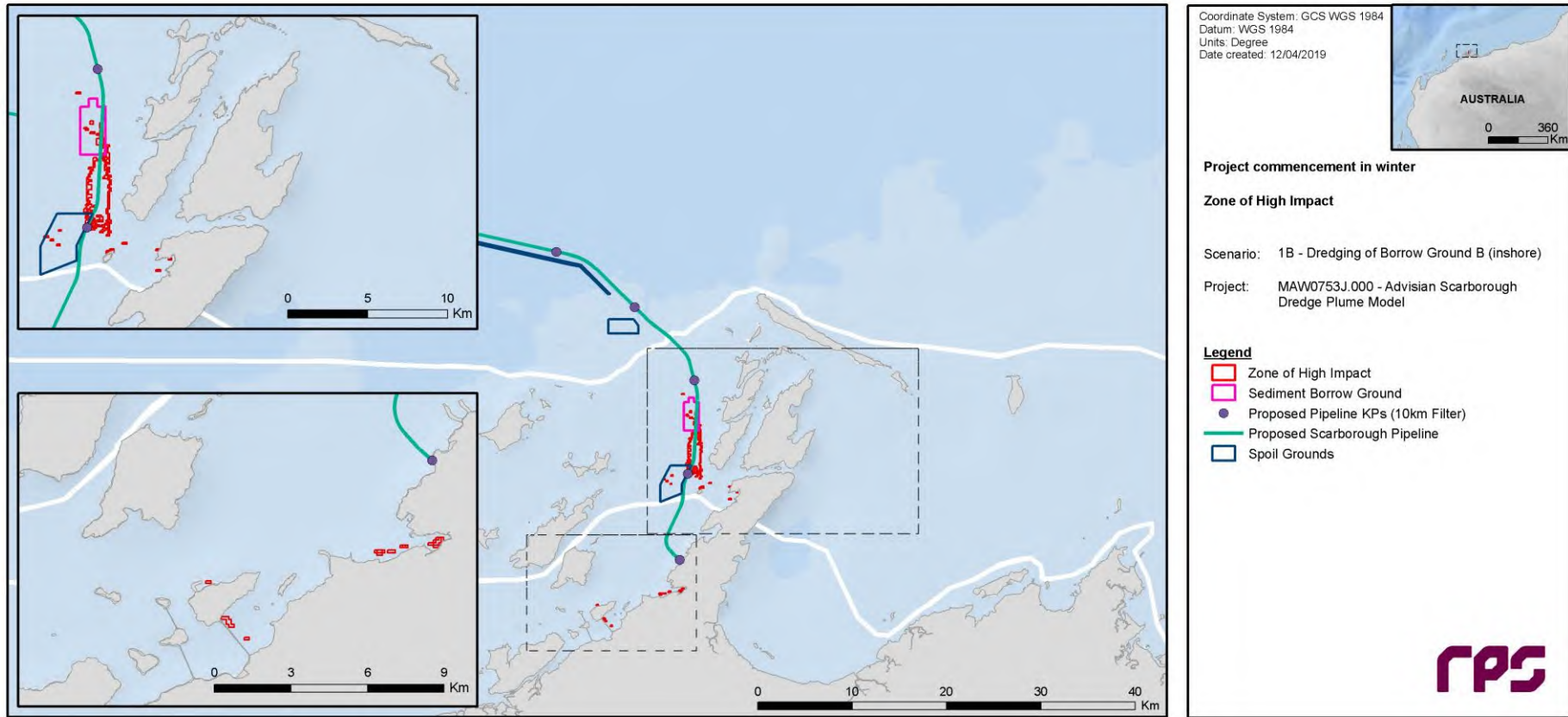
Figure 5.23 Predicted Zone of High Impact following application of the appropriate spatial thresholds in Table 4.4 to 3-day (Zones A and B) and 28-day (Offshore) rolling averages of total (dredge and background) SSC throughout the entire scenario duration (1st July 2016 to 30th April 2017).
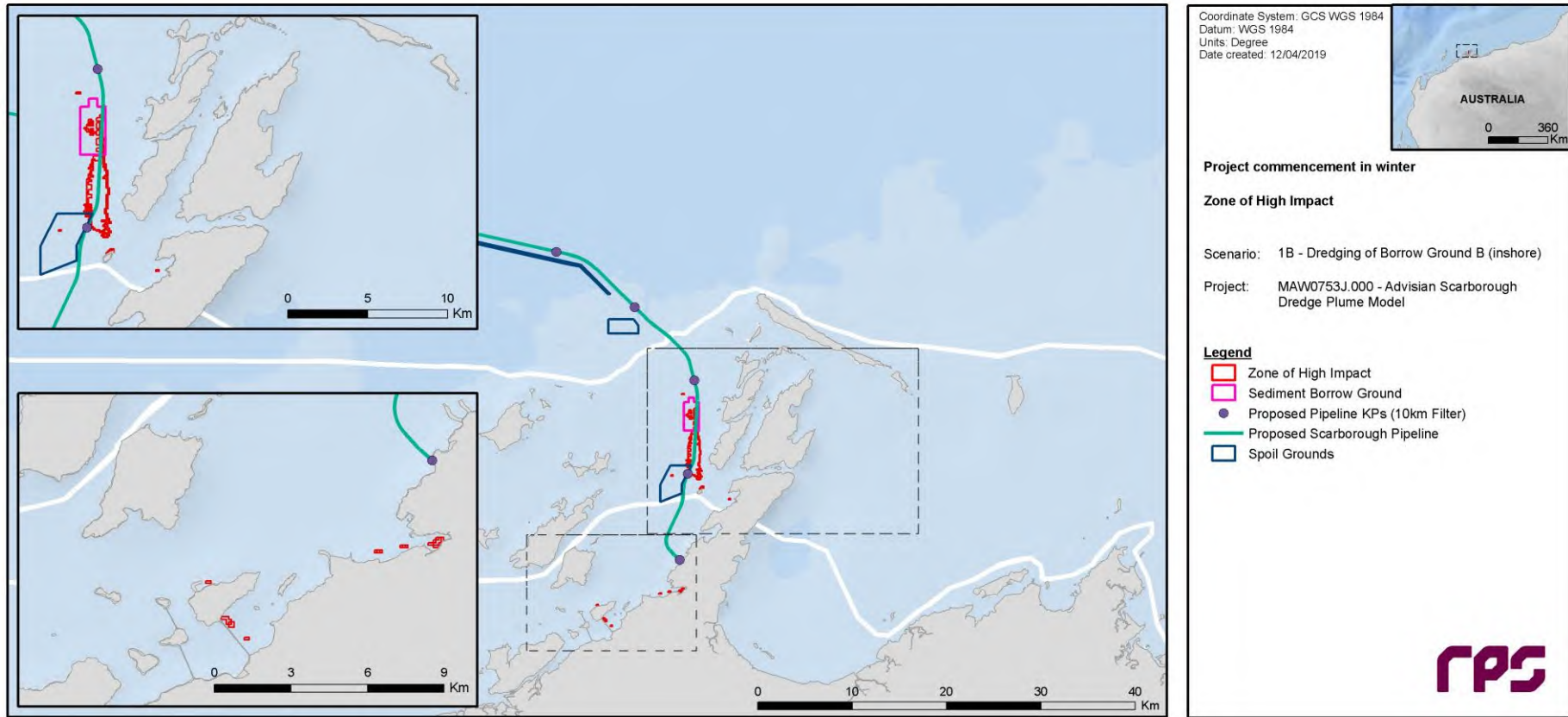
Figure 5.24 Predicted Zone of High Impact following application of the appropriate spatial thresholds in Table 4.4 to 7-day (Zones A and B) and 28-day (Offshore) rolling averages of total (dredge and background) SSC throughout the entire scenario duration (1st July 2016 to 30th April 2017).
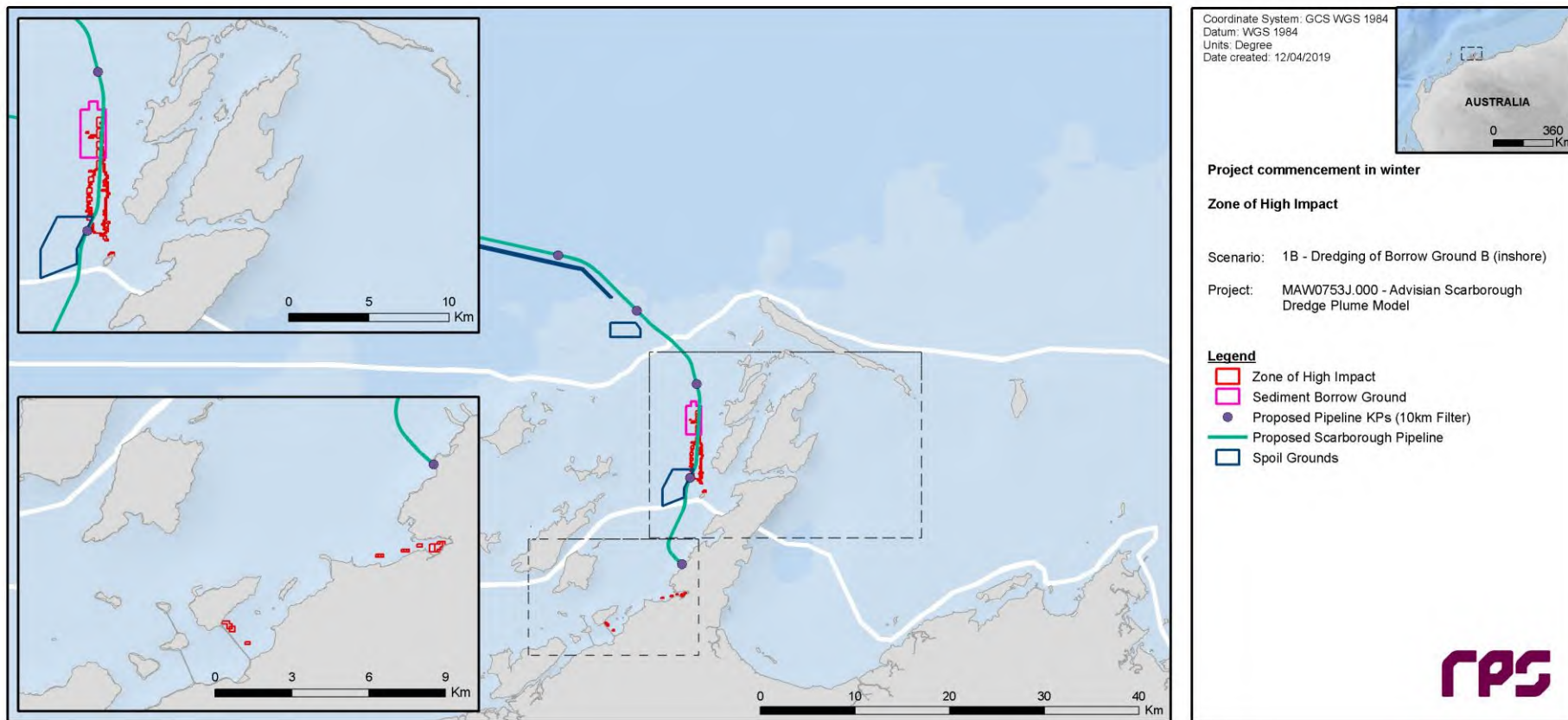
Figure 5.25 Predicted Zone of High Impact following application of the appropriate spatial thresholds in Table 4.4 to 10-day (Zones A and B) and 28-day (Offshore) rolling averages of total (dredge and background) SSC throughout the entire scenario duration (1st July 2016 to 30th April 2017).
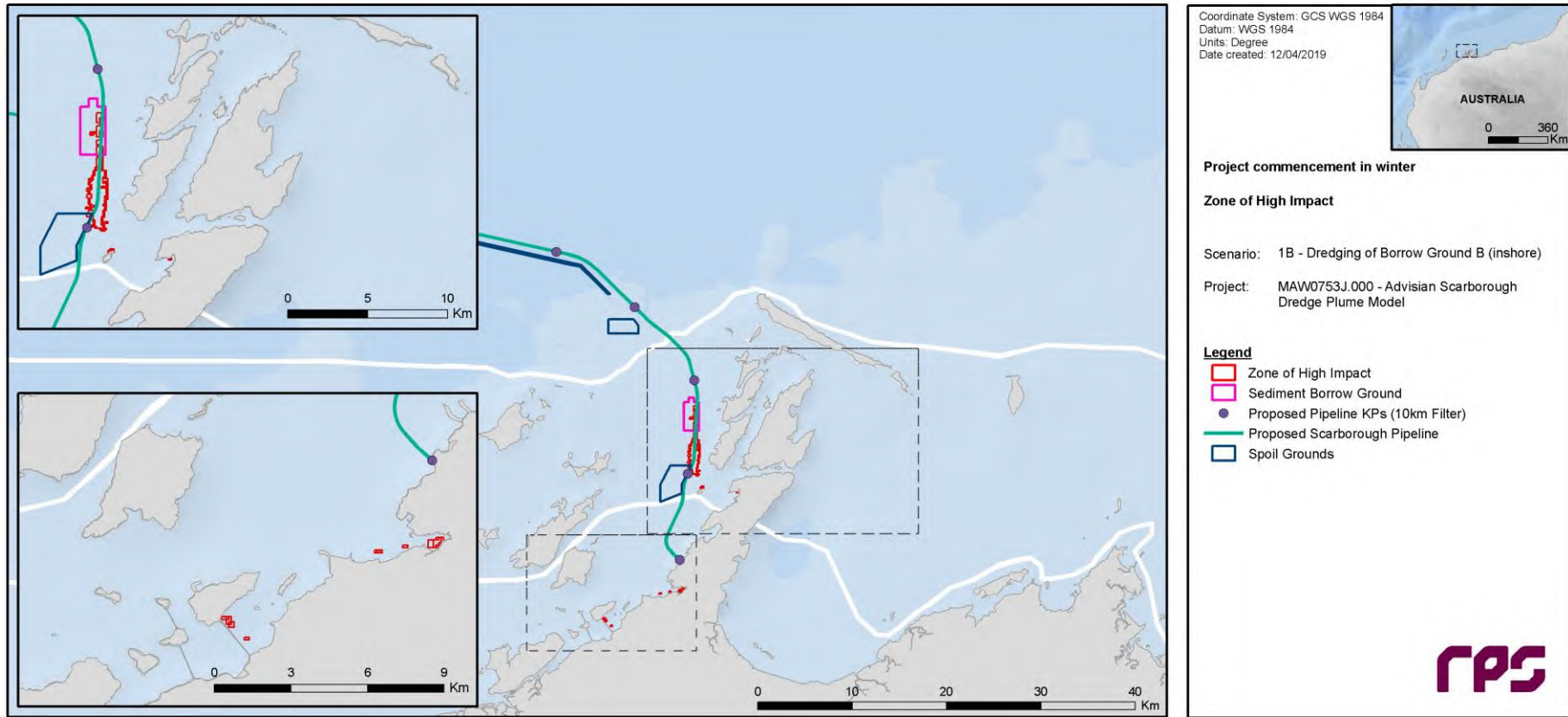
Figure 5.26 Predicted Zone of High Impact following application of the appropriate spatial thresholds in Table 4.4 to 14-day (Zones A and B) and 28-day (Offshore) rolling averages of total (dredge and background) SSC throughout the entire scenario duration (1st July 2016 to 30th April 2017).

5.2.2.3 Scenario 2A: Dredging Operations Commencing during Summer, with Backfill Material Sourced from Borrow Ground A (Offshore)
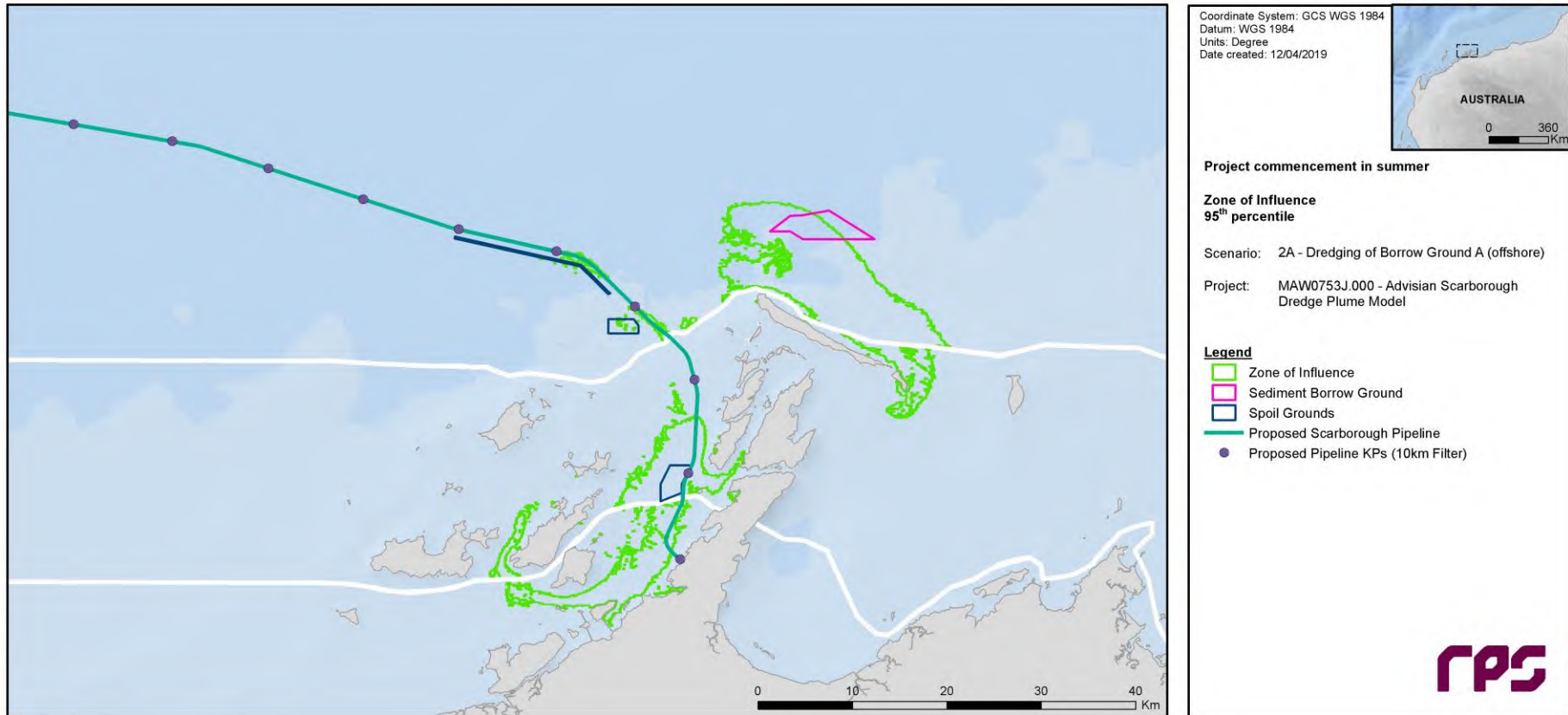
Figure 5.27 **Predicted 95th percentile Zone of Influence following application of the appropriate spatial thresholds in Table 4.2 to a 24-hour rolling average of total (dredge and background) SSC throughout the entire scenario duration (1st January 2017 to 31st October 2017).**
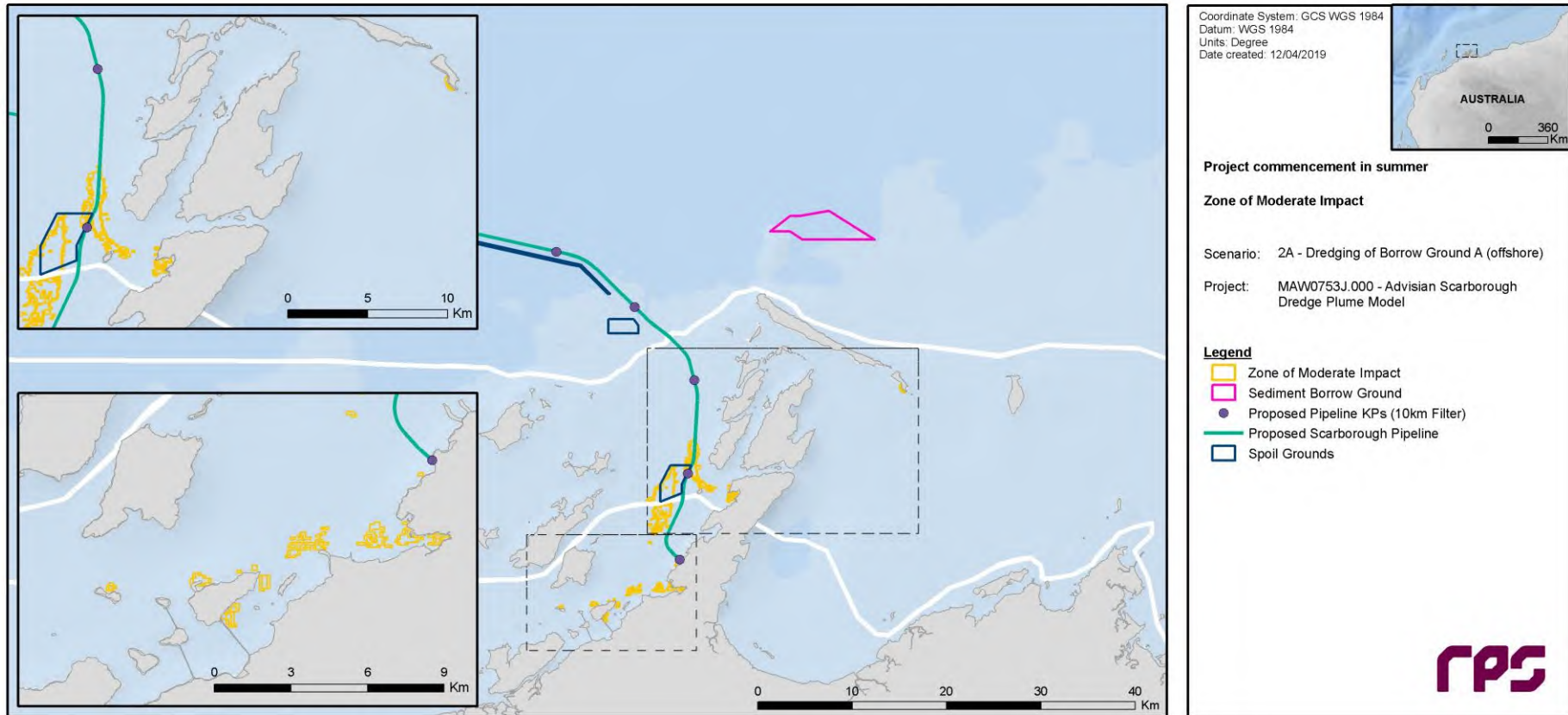
Figure 5.28 Predicted Zone of Moderate Impact following application of the appropriate spatial thresholds in Table 4.3 to 3-day (Zones A and B) and 28-day (Offshore) rolling averages of total (dredge and background) SSC throughout the entire scenario duration (1st January 2017 to 31st October 2017).
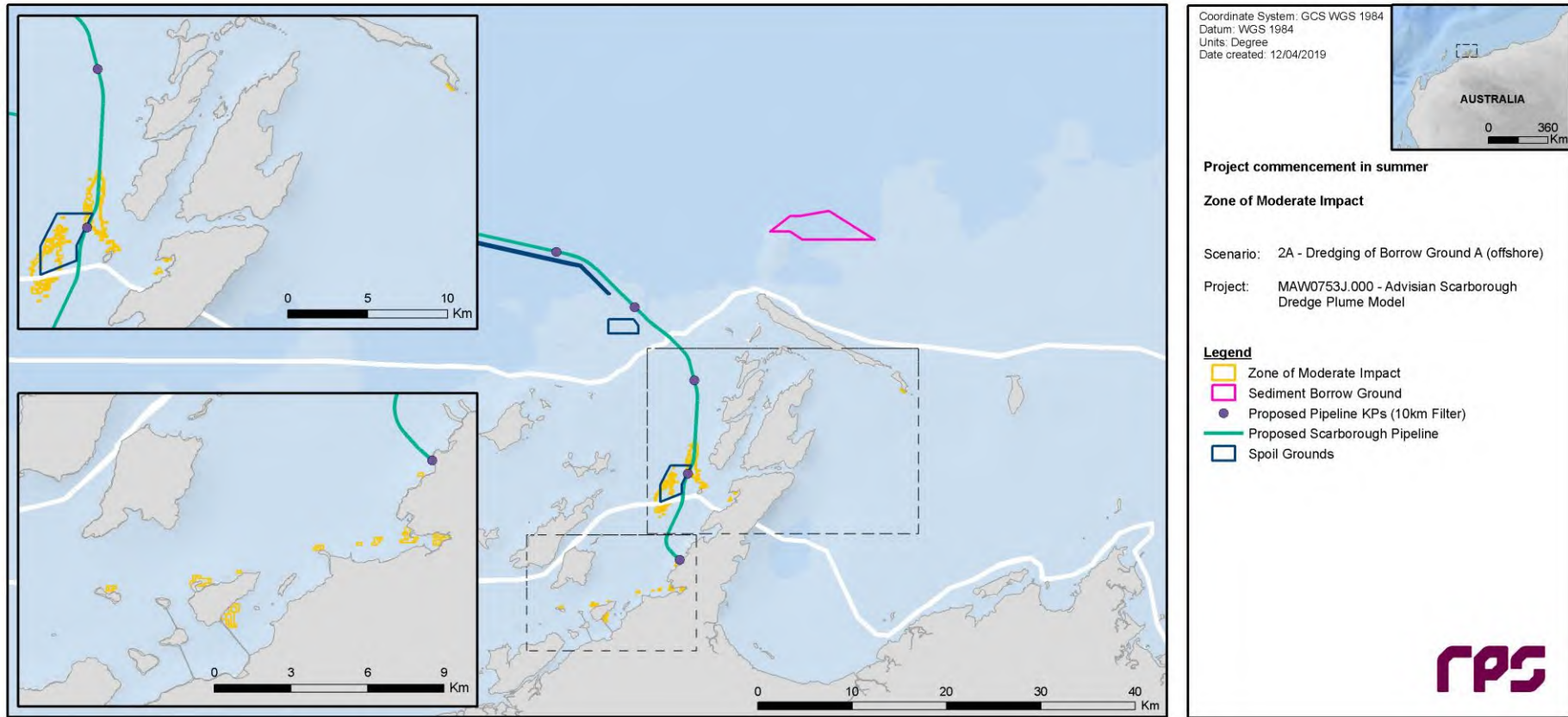
Figure 5.29 **Predicted Zone of Moderate Impact following application of the appropriate spatial thresholds in Table 4.3 to 7-day (Zones A and B) and 28-day (Offshore) rolling averages of total (dredge and background) SSC throughout the entire scenario duration (1st January 2017 to 31st October 2017).**
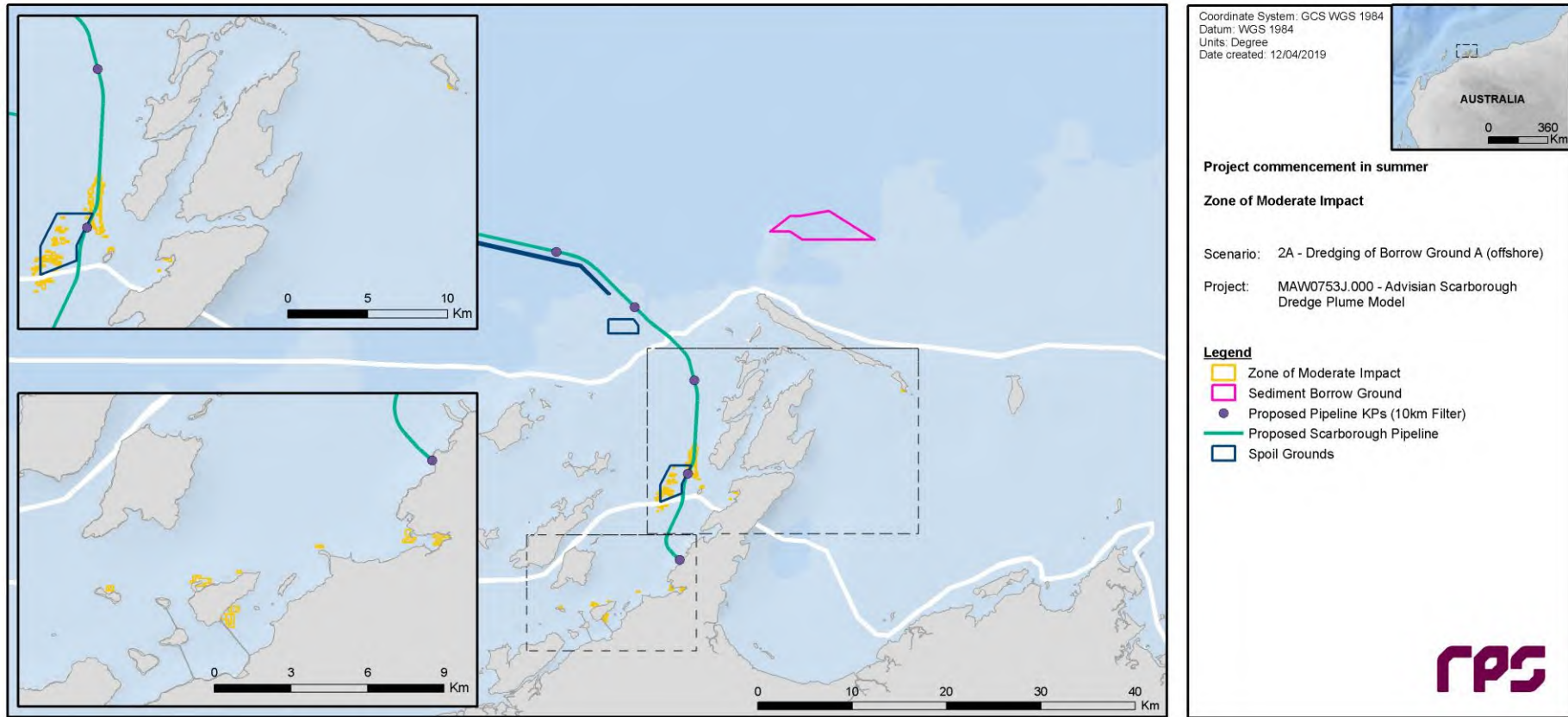
Figure 5.30 Predicted Zone of Moderate Impact following application of the appropriate spatial thresholds in Table 4.3 to 10-day (Zones A and B) and 28-day (Offshore) rolling averages of total (dredge and background) SSC throughout the entire scenario duration (1st January 2017 to 31st October 2017).
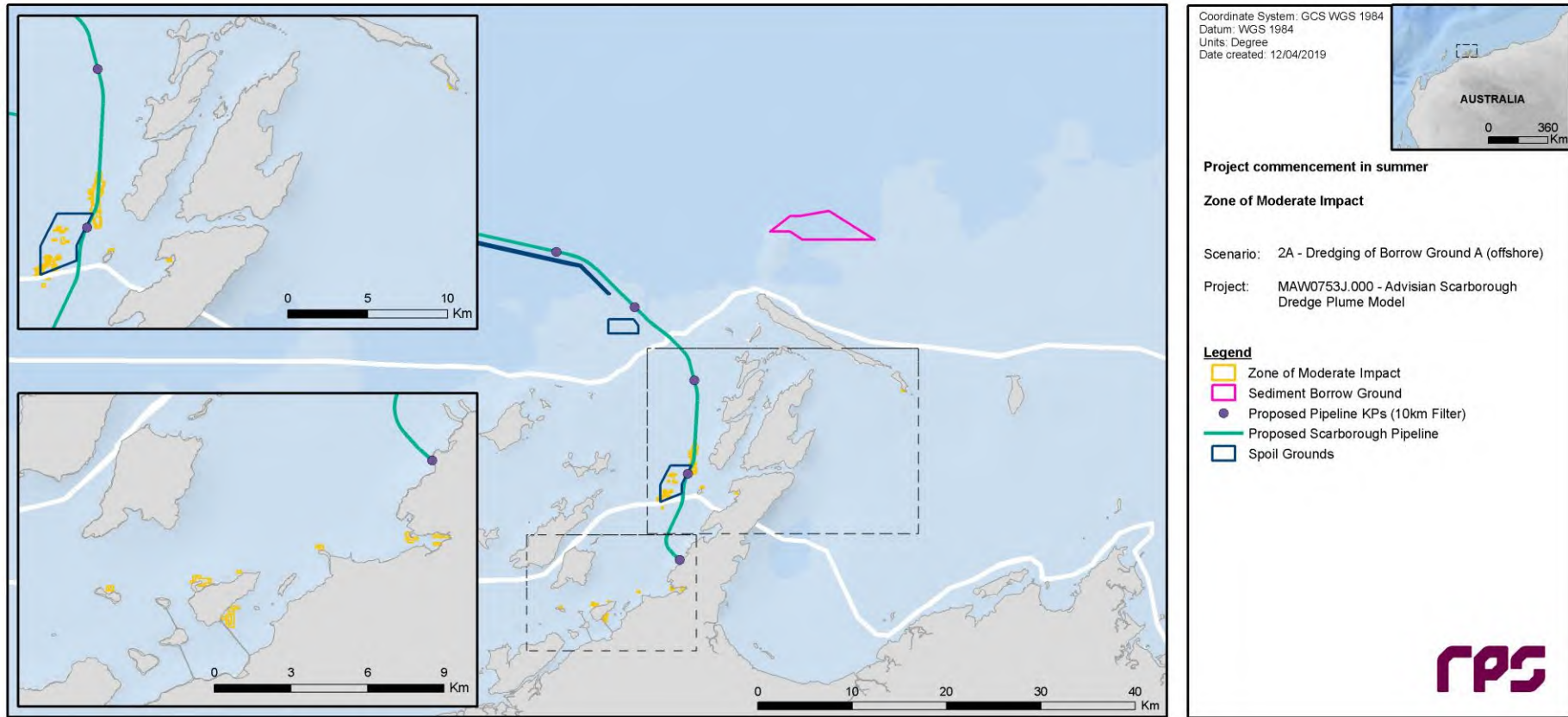
Figure 5.31 Predicted Zone of Moderate Impact following application of the appropriate spatial thresholds in Table 4.3 to 14-day (Zones A and B) and 28-day (Offshore) rolling averages of total (dredge and background) SSC throughout the entire scenario duration (1st January 2017 to 31st October 2017).
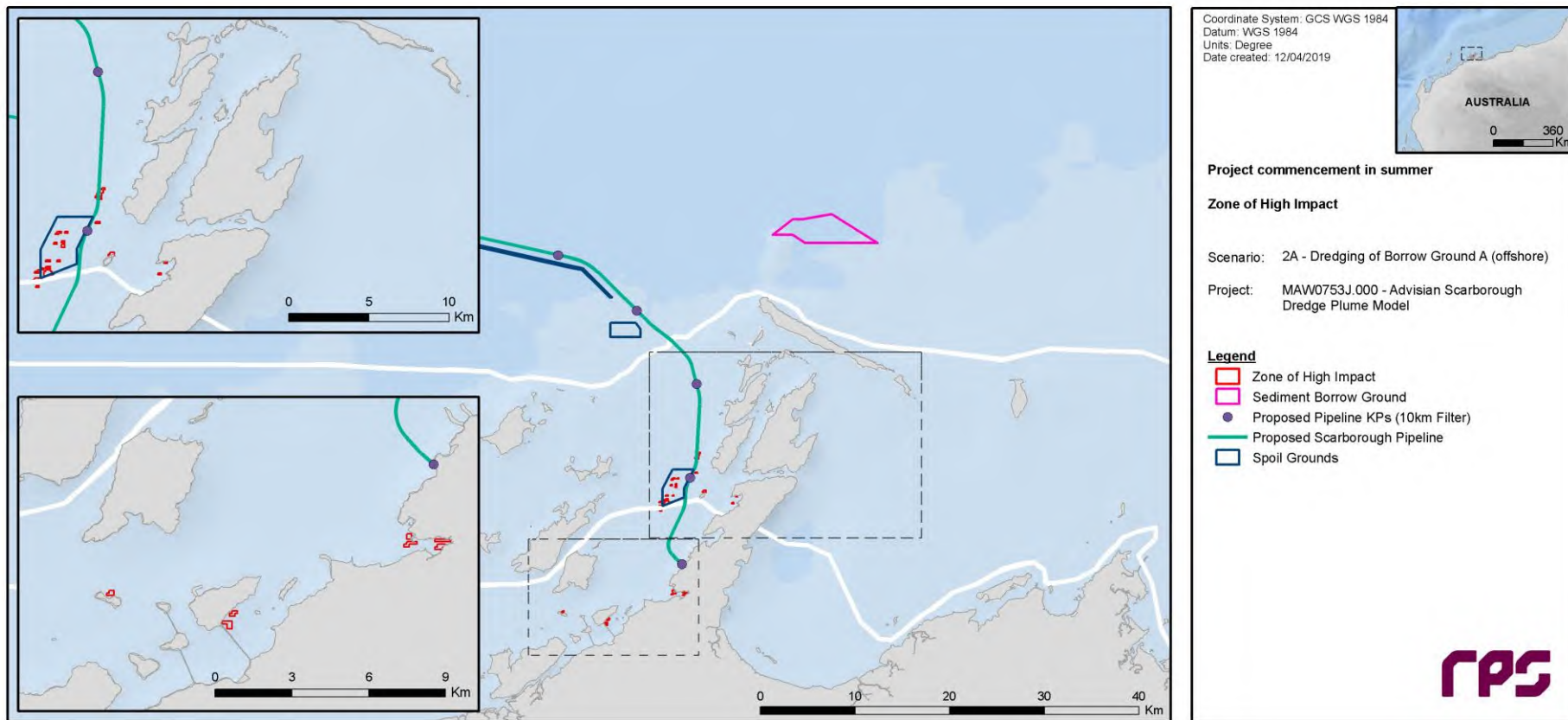
Figure 5.32 **Predicted Zone of High Impact following application of the appropriate spatial thresholds in Table 4.4 to 3-day (Zones A and B) and 28-day (Offshore) rolling averages of total (dredge and background) SSC throughout the entire scenario duration (1st January 2017 to 31st October 2017).**
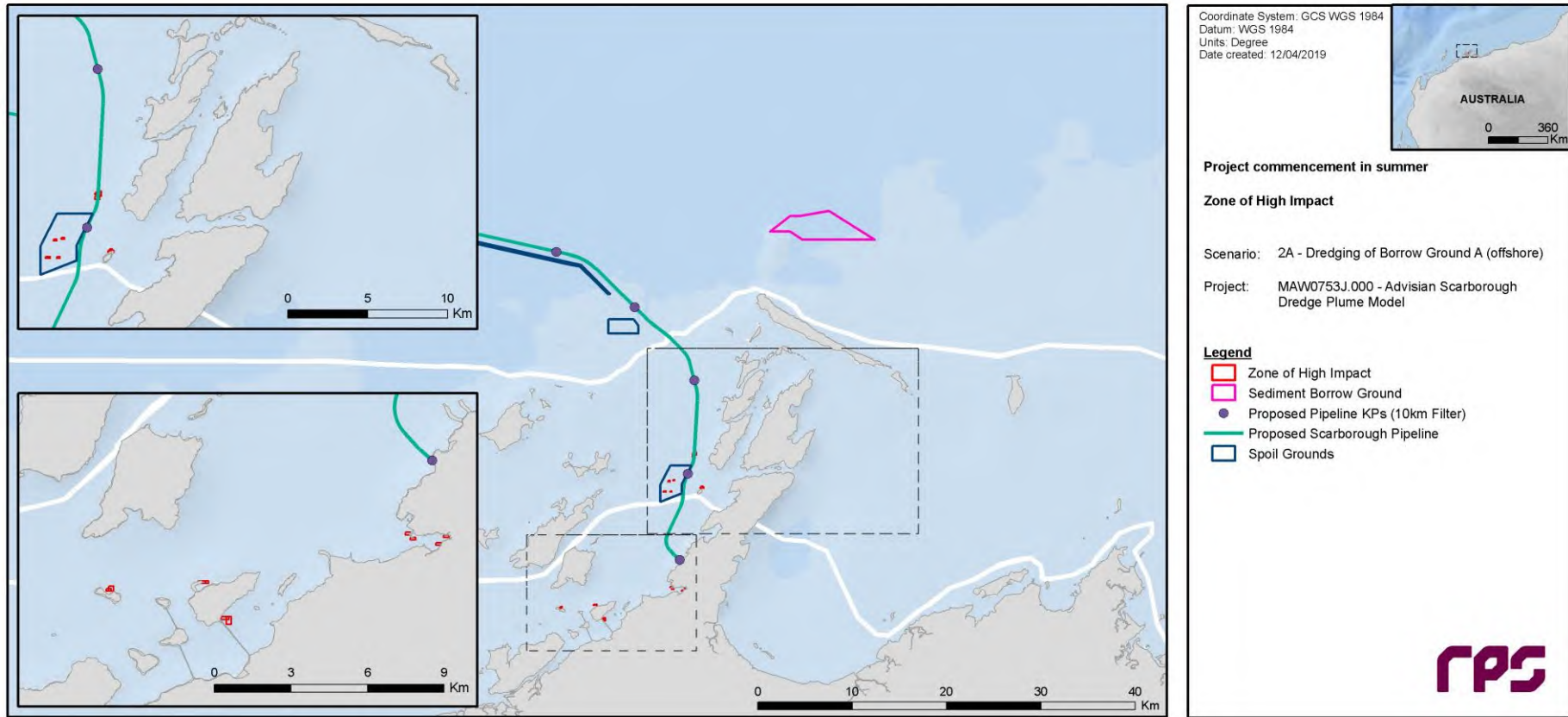
Figure 5.33 **Predicted Zone of High Impact following application of the appropriate spatial thresholds in Table 4.4 to 7-day (Zones A and B) and 28-day (Offshore) rolling averages of total (dredge and background) SSC throughout the entire scenario duration (1st January 2017 to 31st October 2017).**
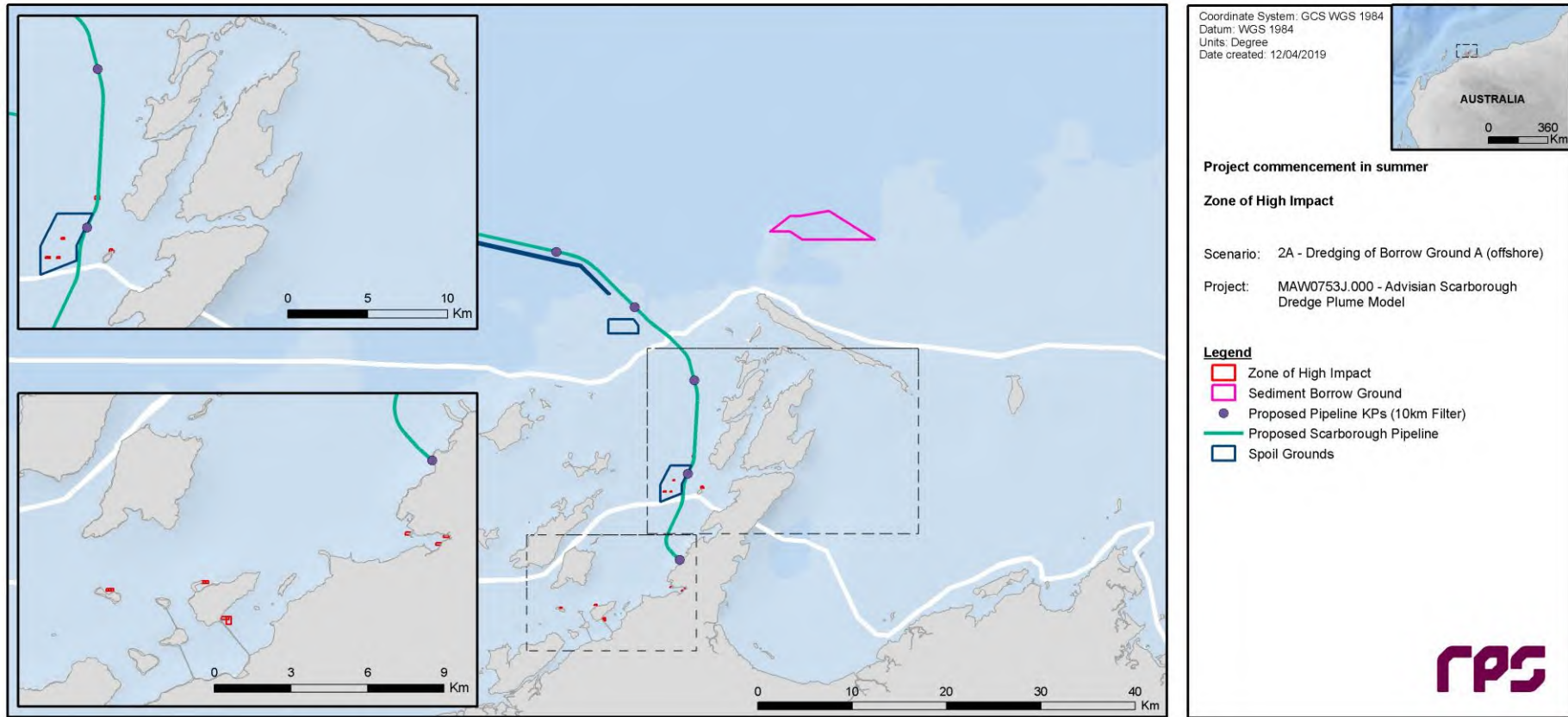
Figure 5.34 Predicted Zone of High Impact following application of the appropriate spatial thresholds in Table 4.4 to 10-day (Zones A and B) and 28-day (Offshore) rolling averages of total (dredge and background) SSC throughout the entire scenario duration (1st January 2017 to 31st October 2017).
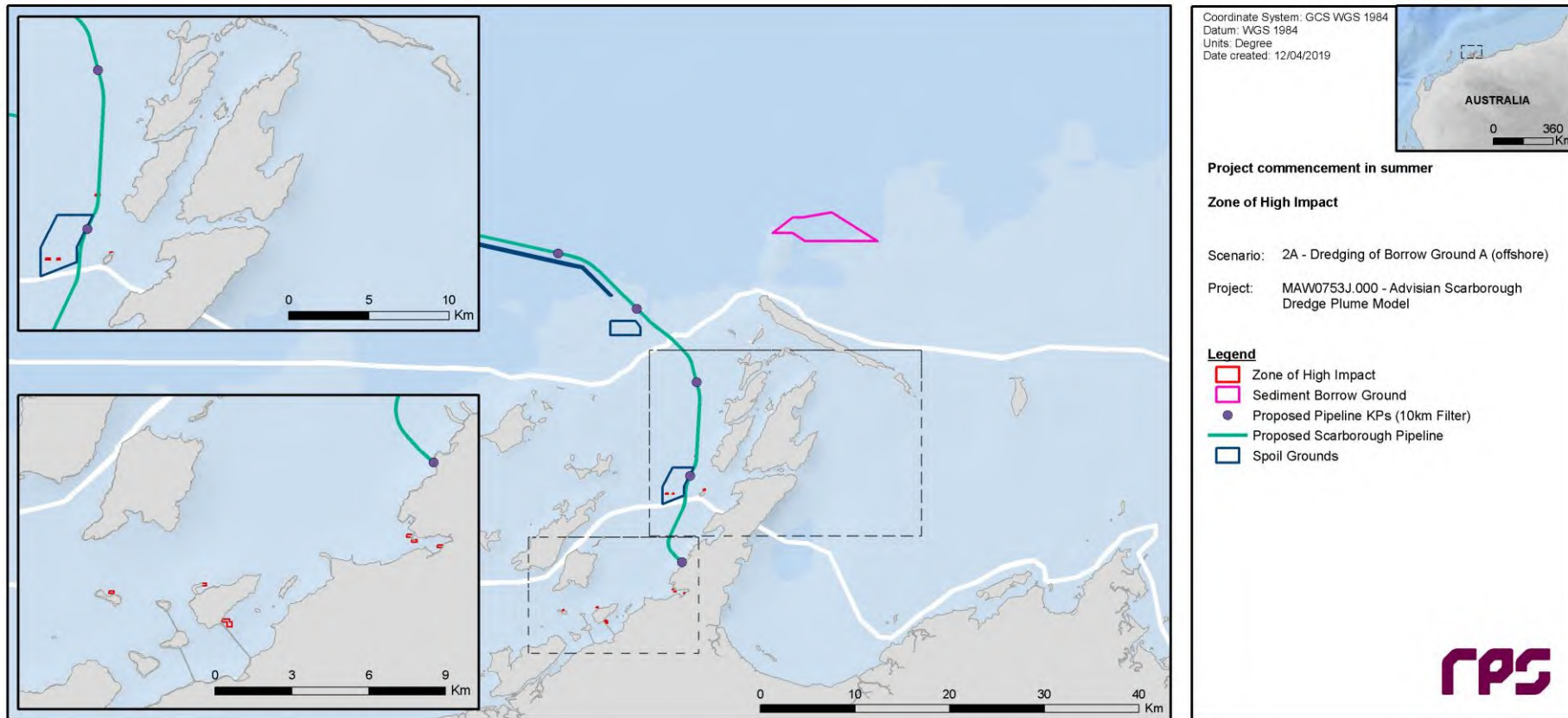
Figure 5.35 **Predicted Zone of High Impact following application of the appropriate spatial thresholds in Table 4.4 to 14-day (Zones A and B) and 28-day (Offshore) rolling averages of total (dredge and background) SSC throughout the entire scenario duration (1st January 2017 to 31st October 2017).**

5.2.2.4 Scenario 2B: Dredging Operations Commencing during Summer, with Backfill Material Sourced from Borrow Ground B (Inshore)
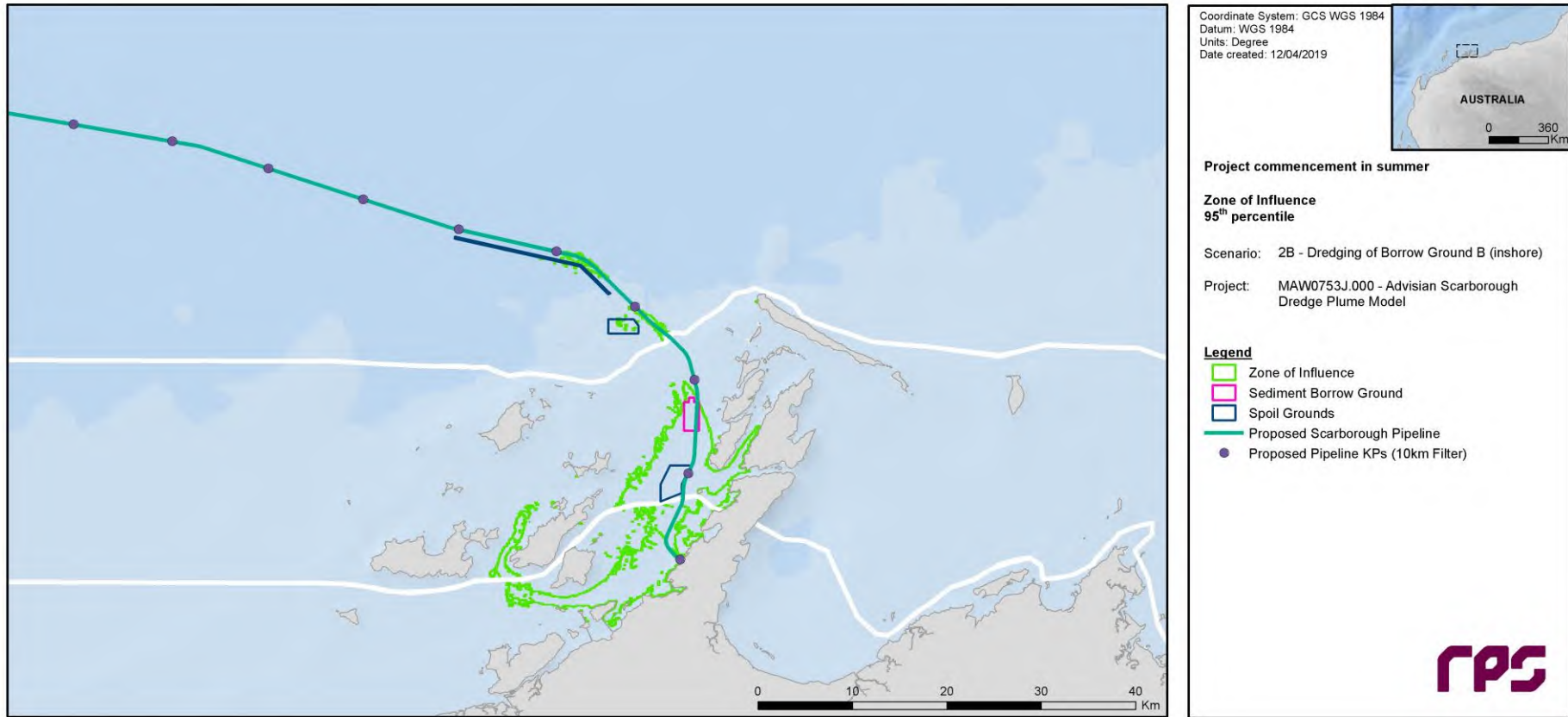
Figure 5.36 **Predicted 95th percentile Zone of Influence following application of the appropriate spatial thresholds in Table 4.2 to a 24-hour rolling average of total (dredge and background) SSC throughout the entire scenario duration (1st January 2017 to 31st October 2017).**
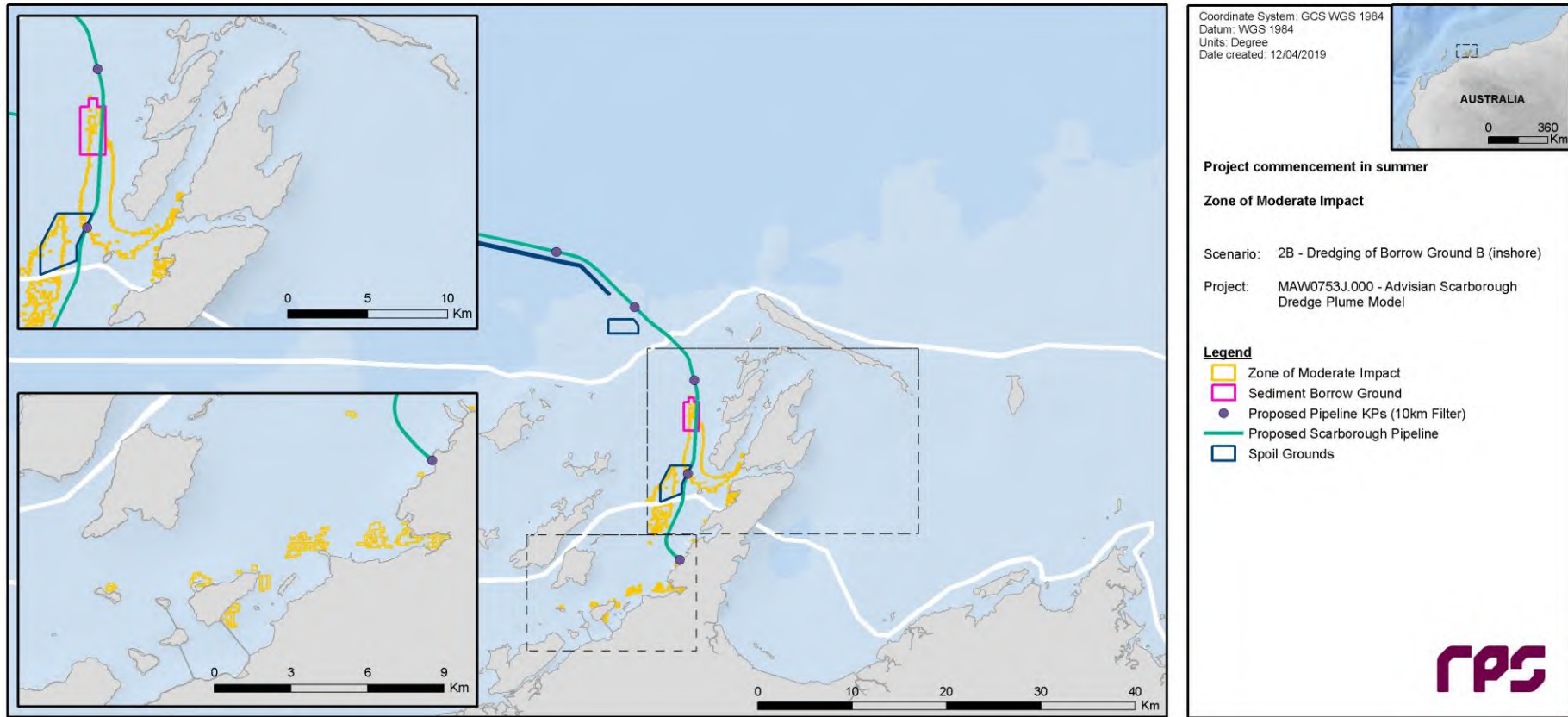
Figure 5.37 Predicted Zone of Moderate Impact following application of the appropriate spatial thresholds in Table 4.3 to 3-day (Zones A and B) and 28-day (Offshore) rolling averages of total (dredge and background) SSC throughout the entire scenario duration (1st January 2017 to 31st October 2017).
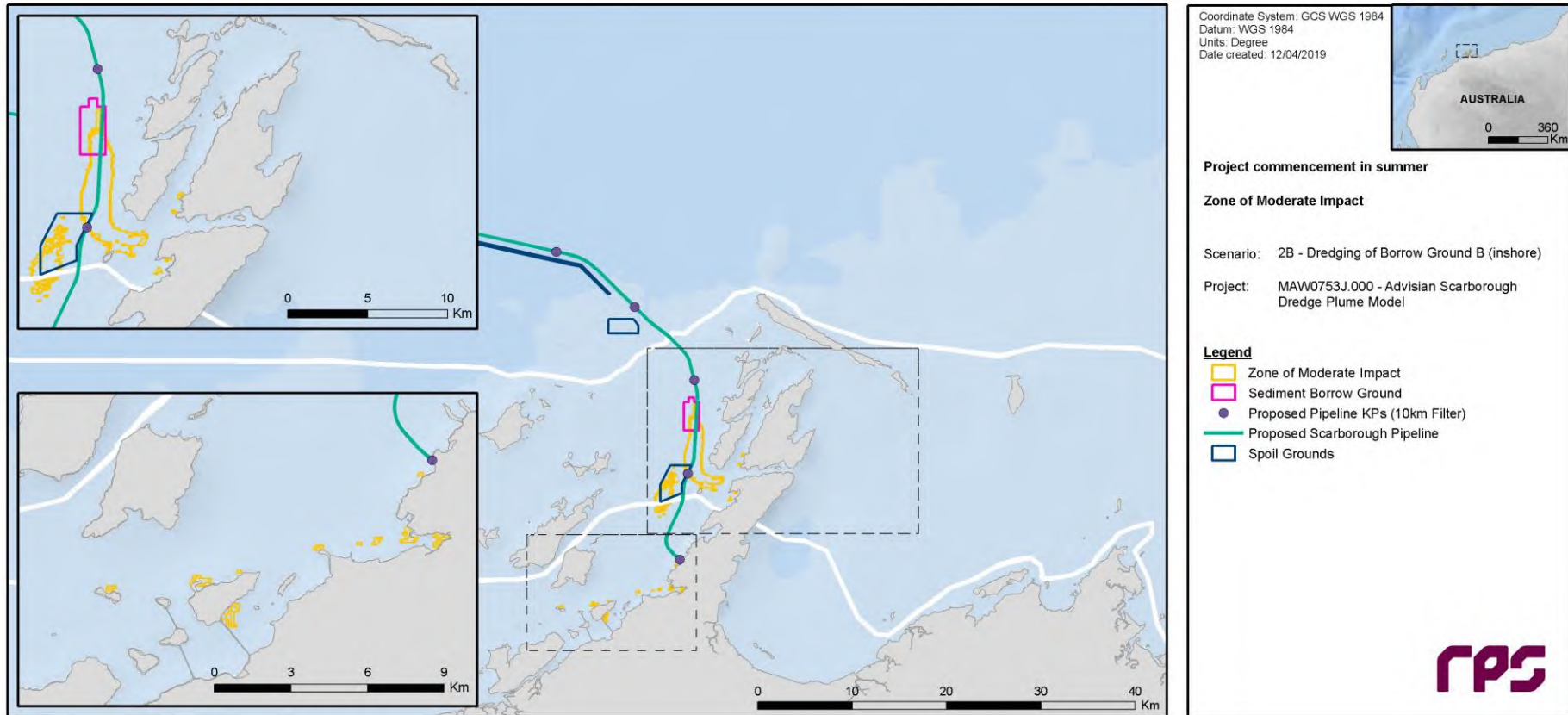
Figure 5.38 Predicted Zone of Moderate Impact following application of the appropriate spatial thresholds in Table 4.3 to 7-day (Zones A and B) and 28-day (Offshore) rolling averages of total (dredge and background) SSC throughout the entire scenario duration (1st January 2017 to 31st October 2017).
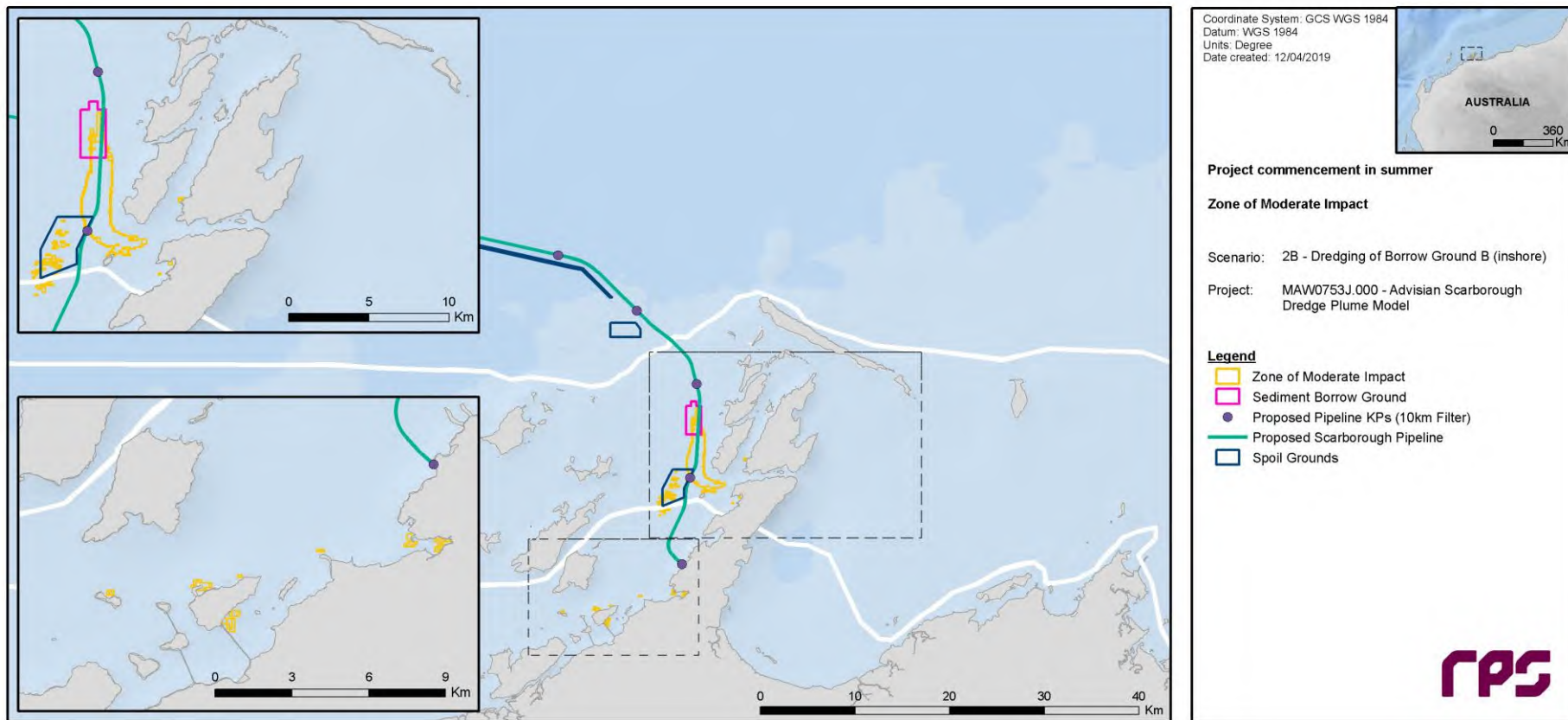
Figure 5.39 **Predicted Zone of Moderate Impact following application of the appropriate spatial thresholds in Table 4.3 to 10-day (Zones A and B) and 28-day (Offshore) rolling averages of total (dredge and background) SSC throughout the entire scenario duration (1st January 2017 to 31st October 2017).**
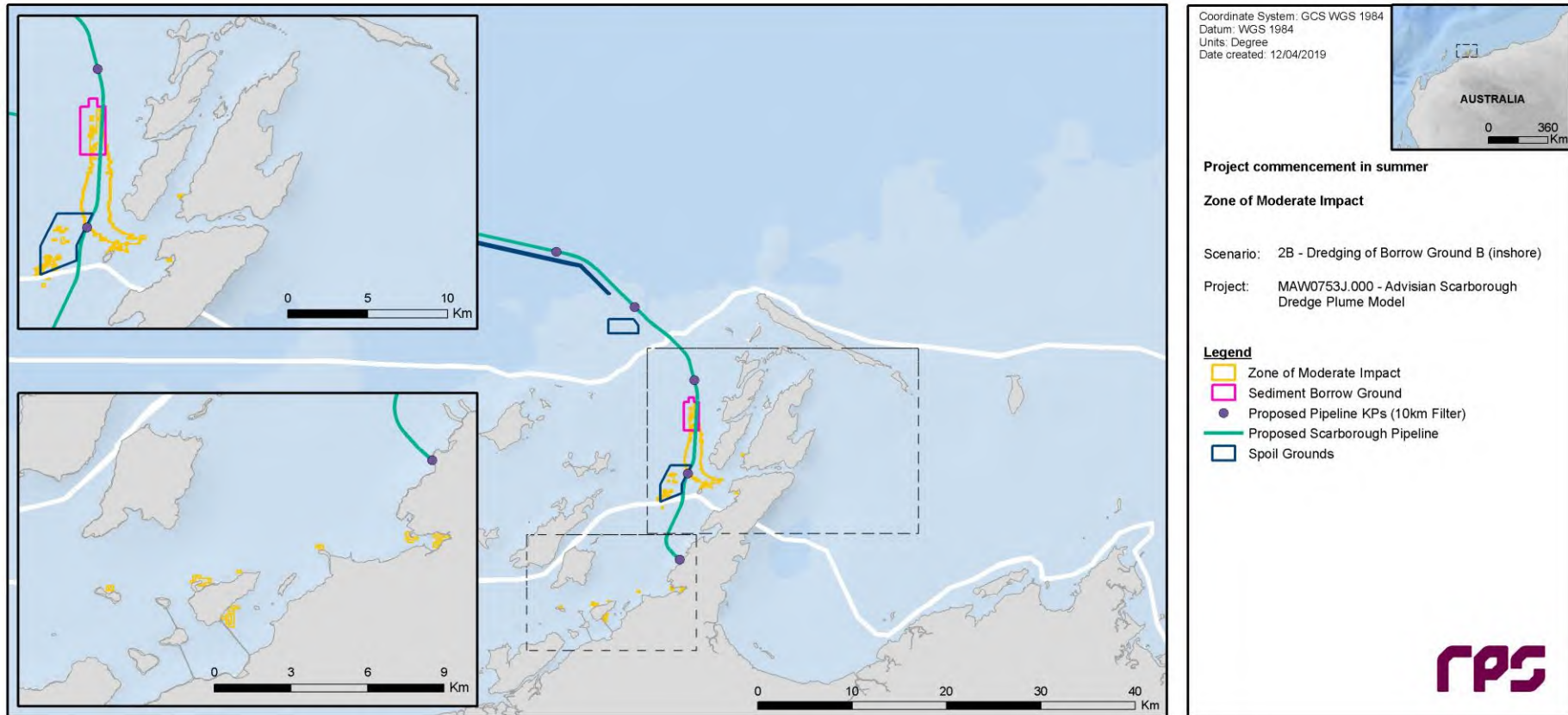
Figure 5.40 **Predicted Zone of Moderate Impact following application of the appropriate spatial thresholds in Table 4.3 to 14-day (Zones A and B) and 28-day (Offshore) rolling averages of total (dredge and background) SSC throughout the entire scenario duration (1st January 2017 to 31st October 2017).**
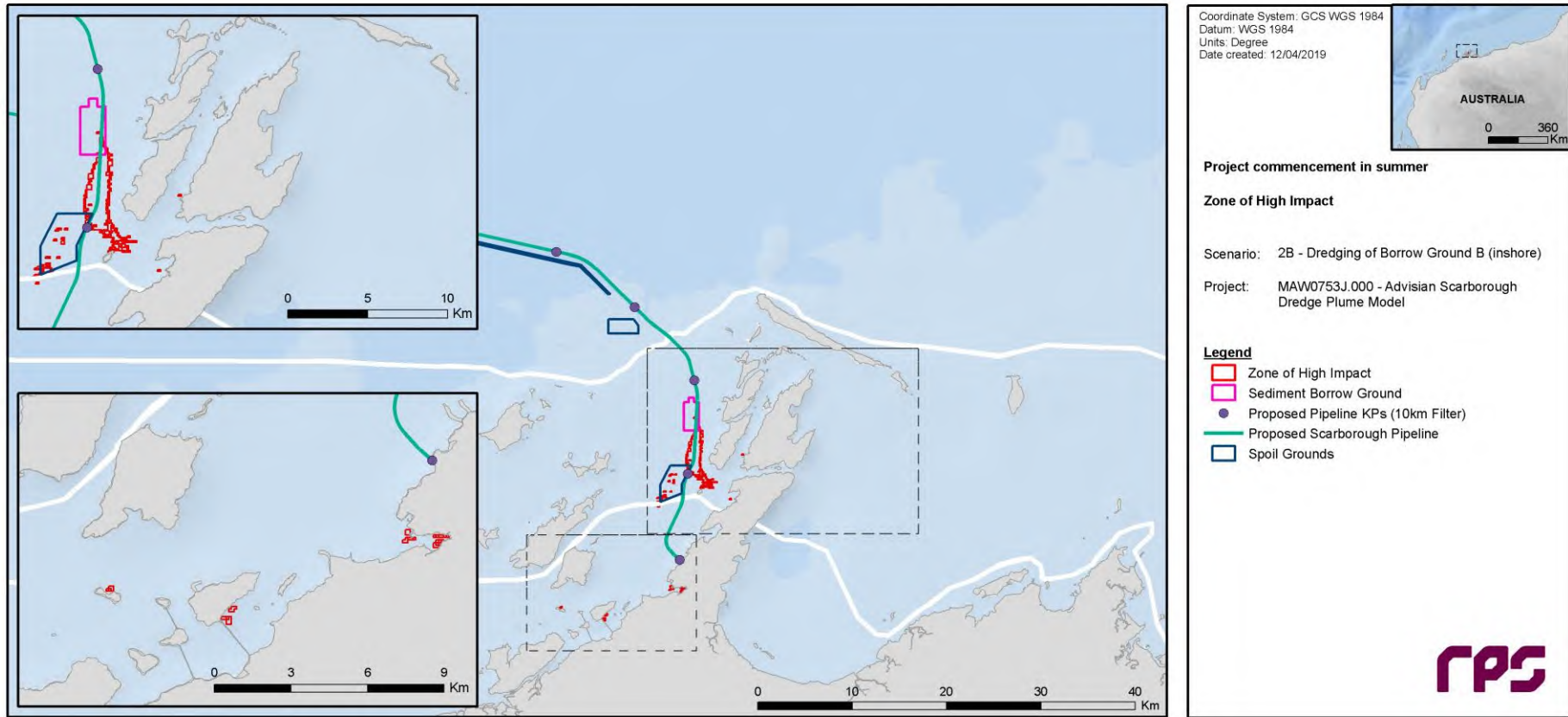
Figure 5.41 Predicted Zone of High Impact following application of the appropriate spatial thresholds in Table 4.4 to 3-day (Zones A and B) and 28-day (Offshore) rolling averages of total (dredge and background) SSC throughout the entire scenario duration (1st January 2017 to 31st October 2017).

Coordinate System: GCS WGS 1984
Datum: WGS 1984
Units: Degree
Date created: 12/04/2019

AUSTRALIA

0   360
Km

Project commencement in summer

Zone of High Impact

Scenario: 2B - Dredging of Borrow Ground B (inshore)

Project: MAW0753J.000 - Advisian Scarborough
             Dredge Plume Model

Legend
▢ Zone of High Impact
▢ Sediment Borrow Ground
● Proposed Pipeline KPs (10km Filter)
— Proposed Scarborough Pipeline
▢ Spoil Grounds
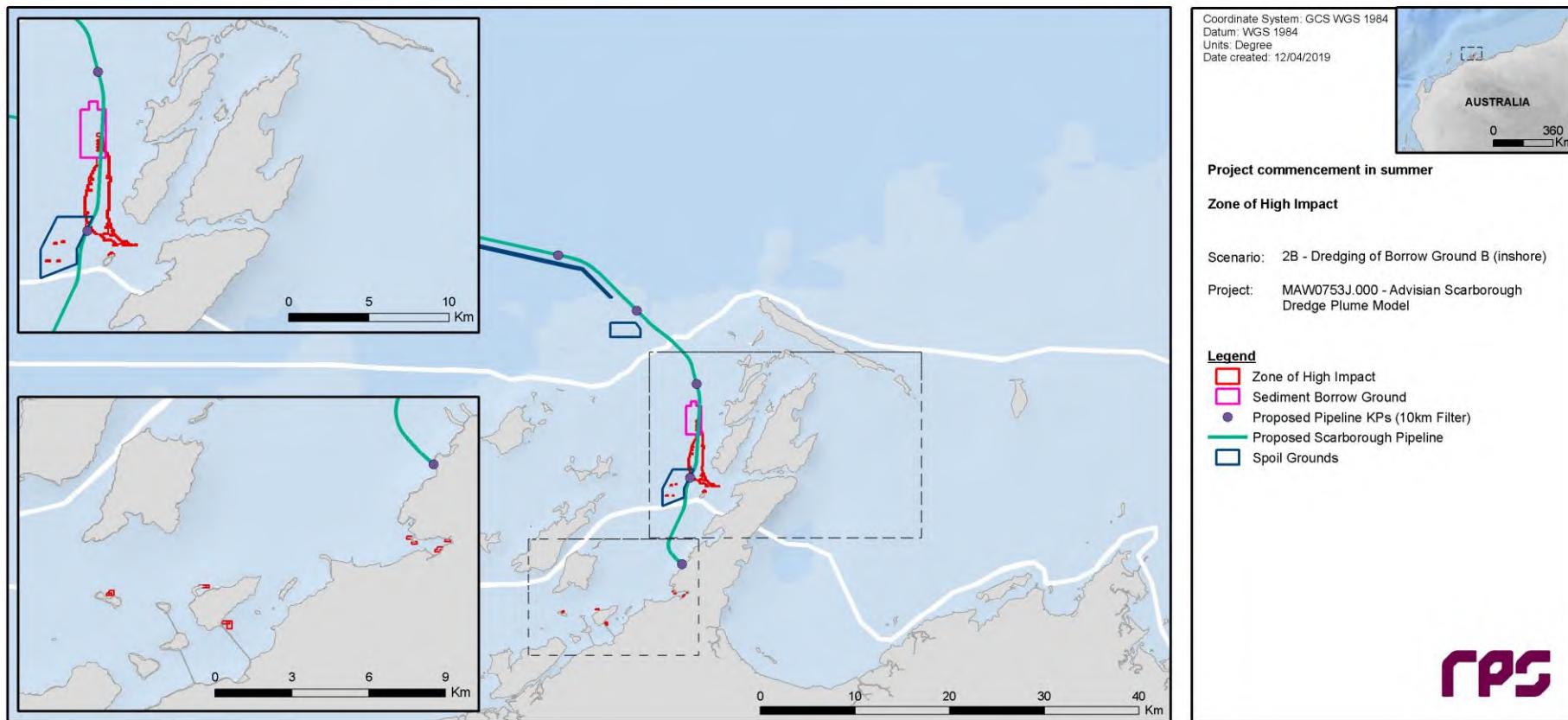
Figure 5.42 Predicted Zone of High Impact following application of the appropriate spatial thresholds in Table 4.4 to 7-day (Zones A and B) and 28-day (Offshore) rolling averages of total (dredge and background) SSC throughout the entire scenario duration (1st January 2017 to 31st October 2017).
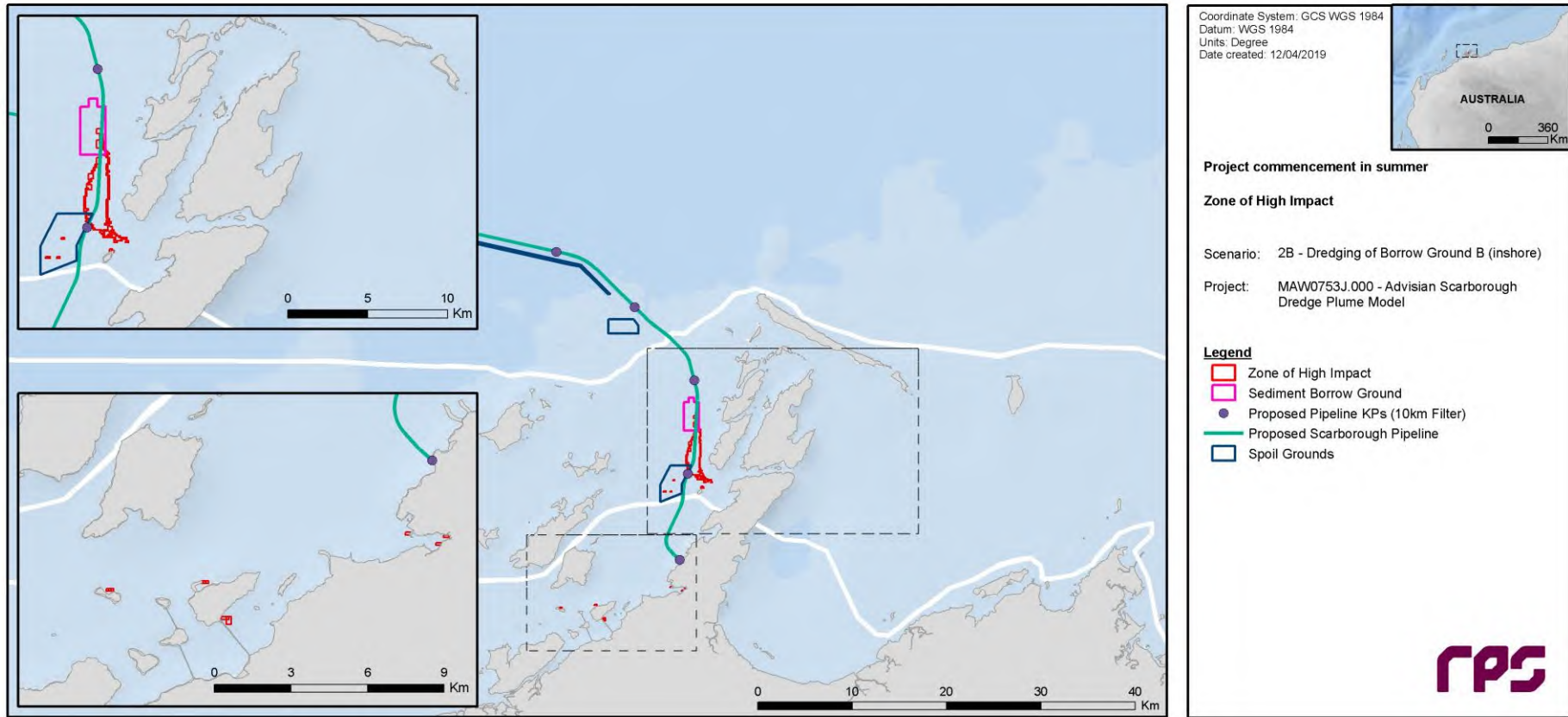
Figure 5.43 Predicted Zone of High Impact following application of the appropriate spatial thresholds in Table 4.4 to 10-day (Zones A and B) and 28-day (Offshore) rolling averages of total (dredge and background) SSC throughout the entire scenario duration (1st January 2017 to 31st October 2017).
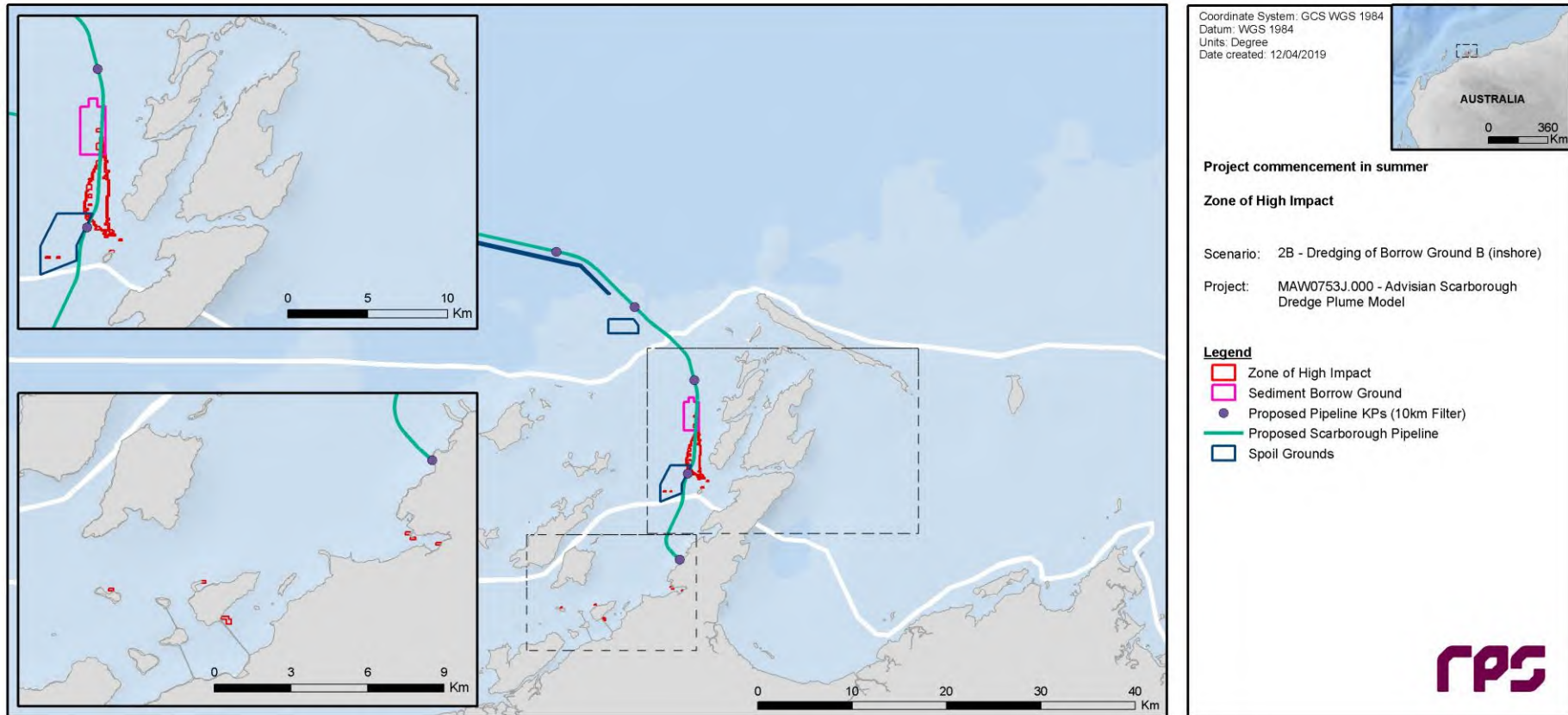
Figure 5.44 Predicted Zone of High Impact following application of the appropriate spatial thresholds in Table 4.4 to 14-day (Zones A and B) and 28-day (Offshore) rolling averages of total (dredge and background) SSC throughout the entire scenario duration (1st January 2017 to 31st October 2017).

6 REFERENCES

Advisian 2018, *Scope of work: Scarborough dredge plume modelling*, provided to RPS by Advisian Pty Ltd, West Perth, WA, Australia.

Anchor Environmental 2003, *Literature review of effects of resuspended sediments due to dredging operations*, prepared for Los Angeles Contaminated Sediments Task Force. Los Angeles, CA, USA by Anchor Environmental CA LP, Irvine, CA, USA.

Andersen, E, Johnson, B, Isaji, T & Howlett, E 2001, 'SSFATE (Suspended Sediment FATE), a model of sediment movement from dredging operations', presented at WODCON XVI, World Dredging Congress and Exposition, Kuala Lumpur, Malaysia.

Applied Science Associates (ASA) 2004, *SSFATE user manual*, Applied Science Associates (now RPS), Narragansett, RI, USA.

Blaauw, HG & van de Kaa, EJ 1978, 'Erosion of bottom and sloping banks caused by the screw race of manoeuvring ships', publication 202, Waterloopkundig Laboratorium Delft (Hydraulics Laboratory), Delft, Netherlands, 12pp.

Bleck, R 2002, 'An oceanic general circulation model framed in hybrid isopycnic-Cartesian coordinates', Ocean Modelling, vol. 4, no. 1, pp. 55-88.

Chassignet, EP, Smith, LT, Halliwell, GR & Bleck, R 2003, 'North Atlantic simulations with the Hybrid Coordinate Ocean Model (HYCOM): impact of the vertical coordinate choice, reference pressure, and thermobaricity', *Journal of Physical Oceanography*, vol. 33, pp. 2504-2526.

Coastline Surveys Limited (CSL) 1999, *Marine aggregate mining benthic & surface plume study final report*, report prepared for United States Department of the Interior Minerals Management Service, Washington, DC, USA by Coastline Surveys Ltd, Falmouth, UK.

Coastal Sediment Management Workgroup (CSMW) 2005, *Results from CSMW task 2 (natural and anthropogenic turbidity)*, prepared by the Coastal Sediment Management Workgroup, Government of California, CA, USA.

Fisher, R, Jones, R & Bessell-Browne, P 2019, *Effects of dredging and dredging related activities on water quality: Impacts on coral mortality and threshold development*, report of Theme 4 – Project 4.9, prepared for the Dredging Science Node, Western Australian Marine Science Institution, Perth, WA, Australia, 94 pp.

Flater, D 1998, *XTide: harmonic tide clock and tide predictor* (www.flaterco.com/xtide/).

Halliwell, GR 2004, 'Evaluation of vertical coordinate and vertical mixing algorithms in the HYbrid-Coordinate Ocean Model (HYCOM)', *Ocean Modelling*, vol. 7, no. 3-4, pp. 285-322.

Hayes, D & Wu, PY 2001, 'Simple approach to TSS source strength estimates', in *Proceedings of the WEDA XXI Conference*, Western Dredging Association, Houston, TX, USA.

Hitchcock, DR & Bell, S 2004, 'Physical impacts of marine aggregate dredging on seabed resources in coastal deposits, *Journal of Coastal Research*, vol. 20, no. 1, pp. 101-114.

HR Wallingford 2003, *Protocol for the field measurement of sediment release from dredgers: a practical guide to measuring sediment release from dredging plant for calibration and verification of numerical models*, produced for VBKO TASS Project by HR Wallingford Ltd & Dredging Research Ltd, Wallingford, UK.

Johnson, BH, Andersen, E, Isaji, T, Teeter, AM & Clarke, DG 2000, 'Description of the SSFATE numerical modeling system', *DOER Technical Notes Collection* (ERDC TN-DOER-E10), US Army Engineer Research and Development Center, Vicksburg, MS, USA.

Kemps, H & Masini, R 2017, *Estimating dredge source terms – a review of contemporary practice in the context of Environmental Impact Assessment in Western Australia*, report of Theme 2 – Project 2.2 prepared for the Dredging Science Node, Western Australian Marine Science Institution, Perth, WA, Australia, 29 pp.

Mills & Kemps 2016, *Generation and release of sediments by hydraulic dredging: a review*, report of Theme 2 – Project 2.1 prepared for the Dredging Science Node, Western Australian Marine Science Institution, Perth, WA, Australia, 97 pp.

MScience 2010, *Pluto LNG Development: Final report on coral and water quality monitoring*, report MSA93R160, prepared for Woodside Burrup Pty Ltd by MScience Pty Ltd, Highgate, WA, Australia.

MScience 2019, *Woodside Scarborough dredging threshold levels for model interrogation*, provided to RPS by Advisian Pty Ltd, West Perth, WA, Australia.

National Centers for Environmental Prediction (NCEP) 2016, *The Global Forecast System (GFS) - Global Spectral Model (GSM)* (www.emc.ncep.noaa.gov/GFS/doc.php), National Centers for Environmental Prediction, College Park, MD, USA.

National Environment & Planning Agency (NEPA) 2001, *Port Bustamante Container Terminal: Environmental Impact Assessment*, National Environment & Planning Agency, Kingston, Jamaica.

National Oceanic and Atmospheric Administration (NOAA) 2018, *WAVEWATCH III* (polar.ncep.noaa.gov/waves/index.shtml), National Oceanic and Atmospheric Administration, College Park, MD, USA.

Oakajee Port and Rail (OPR) 2010, *Oakajee Deepwater Port: Dredging, Breakwater Construction and Land Reclamation Management Plan* [301012-01054-1000-EN-PLN-0003 rev. 0], prepared for Oakajee Port and Rail Pty Ltd, Perth, WA, Australia by Oceanica Consulting Pty Ltd, Nedlands, WA, Australia.

Pineda, MC, Strehlow, B, Duckworth, A, Webster, NS 2017, *Effects of dredging-related stressors on sponges: laboratory experiments*, report of Theme 6 – Project 6.4, prepared for the Dredging Science Node, Western Australian Marine Science Institution, Perth, WA, Australia, 157 pp.

RPS 2016, *Rio Tinto Pilbara Ports: Dredge spoil placement stability study*, provided to Rio Tinto Iron Ore and Woodside Energy Ltd, Perth, WA, Australia.

Sun, C, Shimizu, K & Symonds, G 2016, *Numerical modelling of dredge plumes: a review*, report of Theme 3 – Project 3.1.3 prepared for the Dredging Science Node, Western Australian Marine Science Institution, Perth, WA, Australia, 55 pp.

Swanson, JC, Isaji, T, Ward, M, Johnson, BH, Teeter, A & Clarke, DG 2000, 'Demonstration of the SSFATE numerical modelling system', *DOER Technical Notes Collection* (ERDC TN-DOER-E12), US Army Engineer Research and Development Center, Vicksburg, MS, USA.

Swanson, JC, Isaji, T, Clarke, D & Dickerson, C 2004, 'Simulations of dredging and dredged material disposal operations in Chesapeake Bay, Maryland and Saint Andrew Bay, Florida', in *Proceedings of the WEDA XXIV Conference/36th TAMU Dredging Seminar*, Western Dredging Association, Orlando, FL, USA.

Swanson, JC, Isaji, T & Galagan, C 2007, 'Modeling the ultimate transport and fate of dredge-induced suspended sediment transport and deposition', presented at WODCON XVIII, World Dredging Congress and Exposition, Orlando, FL, USA.

Teeter, AM 2000, 'Clay-silt sediment modeling using multiple grain classes: Part I: settling and deposition', in WH McAnally & AJ Mehta (Eds.), *Proceedings in Marine Science: Coastal and Estuarine Fine Sediment Processes*, pp. 157-171, Elsevier BV, Amsterdam, Netherlands.

US Army Corps of Engineers (USACE) 2008, *The four Rs of environmental dredging: Resuspension, release, residual, and risk* (ERDC/EL TR-08-4), Dredging Operations and Environmental Research Program, US Army Corps of Engineers, Washington, DC, USA.

van Rijn, LC 1989, *Sediment transport by currents and waves*, report H461, Delft Hydraulics Laboratory, Delft, Netherlands.

Woodside 2018a, *20181210 - Estimated cycle times required for plume modeling*, extract of dredge contractor input data provided to RPS by Woodside Energy Ltd, Perth, WA, Australia.

Woodside 2018b, *Pluto trunkline PSDs*, extract of geotechnical survey field report provided to RPS by Woodside Energy Ltd, Perth, WA, Australia.

Appendix K

Scarborough Desktop Light Assessment

ADVISAN

SCARBOROUGH DESKTOP LIGHT ASSESSMENT

Prepared by

Pendoley Environmental Pty Ltd

For

Advisian

21 February 2020

DOCUMENT CONTROL INFORMATION

TITLE: Scarborough Desktop Lighting Impact Assessment

Disclaimer and Limitation

This report has been prepared on behalf of and for the use of Advisian. Pendoley Environmental Pty Ltd. takes no responsibility for the completeness or form of any subsequent copies of this Document. Copying of this Document without the permission of Advisian is not permitted.

Document History

Revision	Description	Date issued	Date received	Personnel
Draft	Report Draft	11/02/2020		Dr A Knipe
Rev AI	Internal Review	13/02/2020	11/02/2020	Dr K Pendoley
Rev A	Client review	13/02/2020	14/02/2020	WEL
Rev B	Address Client comments	17/02/2020	14/02/2020	Dr A Knipe
Rev 0	Final version	21/02/2020		Dr A Knipe

Printed:	21 February 2020
Last saved:	21 February 2020 01:10 PM
File name:	P:\06 Projects\J56 Advisian\J56004 Scarborough Desktop Lighting Assessment\Report\Rev C\J56004 Scarborough Desktop Lighting Assessment_Rev C.docx
Author:	Annabel Knipe
Project manager:	Annabel Knipe
Name of organisation:	Pendoley Environmental Pty Ltd
Name of project:	Scarborough Desktop Lighting Impact Assessment
Client	Advisian
Client representative:	Paul Nichols
Report number:	J56004
Cover photo:	Hatchling turtle © iStock

TABLE OF CONTENTS

LIST OF TABLES

LIST OF FIGURES

Acronyms

ALARP	As low as reasonably practicable
BIA	Biologically Important Areas
E	East
EPBC	Environment Protection and Biodiversity Conservation
F-Pil	Flatback turtle Pilbara breeding stock
G-NWS	Green turtle north west shelf breeding stock
H-WA	Hawksbill Western Australia breeding stock
KP	Kilometre point
m/s^{-1}	Meters per second
MODU	Mobile Offshore Drilling Unity
N	North
NE	Northeast
NNW	North-northwest
NW	Northwest
NWS	North West Shelf
S	South
SW	Southwest
TSHD	Trailing suction hopper dredger
W	West

1   INTRODUCTION

Woodside Energy Limited (Woodside), is proposing to develop the Scarborough gas resource through new offshore facilities. These facilities are proposed to be connected to the mainland through an approximately 430 km trunkline to an onshore facility.

Installation of the trunkline will involve pre-lay dredging and pipelay, followed by post-lay backfill within a Trunkline Project Area. Backfill material will be dredged from a separate area, the Borrow Grounds Project Area. Specialised vessels will be utilized for specific activities.

The Trunkline and Borrow Grounds Project Areas overlap, and are in proximity to, areas designated as Biologically Important Areas (BIAs) and habitat critical for the survival of a species ('habitat critical') for marine turtles. The Recovery Plan for Marine Turtles in Australia 2017-2027 (the 'Recovery Plan') (Commonwealth of Australia, 2017) identifies light pollution as high risk threat to marine turtles in the North West Shelf (NWS) region.

Advisian have engaged Pendoley Environmental on behalf of Woodside to conduct a desktop lighting impact assessment to support demonstration that the received levels of light within BIAs and habitat critical (including nesting beaches) associated with trunkline installation and borrow ground activities will be of an acceptable level and managed consistently with the Recovery Plan.

1.1   Exclusions

- This report assesses the potential impacts of activities undertaken in Commonwealth waters only.

- This report assesses the impacts of artificial light on marine turtles only, no other receptors are considered.

2 BACKGROUND

2.1 Project Description

Activities associated with the trunkline installation within 20 km of land are summarised in Table 2-1. The main activities of trunkline trenching, pipelay and backfill are required to be completed sequentially and will not occur concurrently. Of the vessels described in Table 2-1, the TSHD and pipelay vessels have the greatest potential for light emissions based on their size. Although an approximate schedule for activities is available, start dates are estimates only and are subject to change. Therefore, for the purpose of this report it is assumed that the activities below could occur at any time of year.

All activities will be undertaken in the Trunkline Project Area with the exception of dredging activities in the Borrow Grounds Project Area. The dredging will involve removal of sand from the borrow grounds to be transported to the trunkline for backfill.

Table 2-1: Details of activities to be undertaken in the Trunkline and Borrow Grounds Project Areas within 20 km of land

Activity	Estimated duration	Location	Vessels
Hydrographic, geophysical and geotechnical surveys	2 months Vessel continuously present within project areas and constantly moving	Trunkline and Borrow Grounds Project Areas	Survey vessels
Pre-lay trenching and spoil disposal	8 weeks Vessel continuously present within project areas and constantly moving	Trunkline Project Area	Trailing suction hopper dredger (TSHD)
Pipelay	3.5 weeks Vessel continuously present within project areas and constantly moving	Trunkline Project Area	Pipelay vessel (largest vessel), plus: • B-type bulk carrier OR • 1 - 2 primary support vessels • General Supply Vessels
Pre- and post-lay span rectification	2 weeks Intermittent activity: Activities at individual location ~48 hours	Trunkline Project Area	Construction Vessel
Post-lay dredging and backfill	8 weeks Intermittent cyclical activity: 2 hours dredging ion borrow grounds, material transported to trunkline for backfill. Material from borrow grounds placed in trench (5 hours), return to borrow grounds	Trunkline and Borrow Grounds Project Area s	TSHD

2.2   Light Sources and Area of Impact

Light may appear as a direct light source from an unshielded lamp with direct line of sight to the observer or through sky glow. Where direct light falls upon a surface, be it land or ocean, this area of light is referred to as light spill. Sky glow is the diffuse glow caused by light that is screened from view but through reflection and refraction creates a glow in the atmosphere. Scattering of light by dust, salt and other atmospheric aerosols increases the visibility of light as sky glow, while the presence of clouds reflecting light back to earth can substantially illuminate the landscape (Kyba *et al.,* 2011). White/blue light scatters more easily and further in the atmosphere compared to yellow-orange light (Kyba *et al.,* 2011). Therefore, the distance at which direct light and sky glow may be visible from the source is dependent on the number, intensity and types of lights, and how such lights are orientated or shielded, in addition to environmental conditions.

Existing light sources at the eastern end of the Trunkline Project Area (within 20 km of land) include heavy vessel traffic within the Pilbara Port Authority Management area and 26 designated anchorages for bulk carriers, petroleum and gas tankers, drilling rigs, offshore platforms, and pipelay vessels located offshore of Rosemary Island. These anchorages are located between Rosemary Island and the Trunkline Project Area (Figure 2-1). Although light monitoring within the Dampier Archipelago has not been undertaken, existing light pollution in this area is expected.

As described in Section 2.1, the TSHD and pipelay vessels have the greatest potential for light emissions based on size. In absence of representative light monitoring or modelling, or the required level of detail to allow meaningful comparison to existing information, it is assumed for this assessment that received light intensity within 20 km of the Project Areas may result in impacts to marine turtle behaviour. A 20 km buffer was selected based on recommendations proposed in the National Light Pollution Guidelines for Wildlife (Commonwealth of Australia, 2020; and references therein).

2.3   Relevant Marine Turtle Species

Five species of marine turtle may occur in the Trunkline and Borrow Grounds Project Areas: flatback (*Natator depressus*), green (*Chelonia mydas*), hawksbill (*Eretmochelys imbricata*), loggerhead (*Caretta caretta*) and leatherback (*Dermochelys coriacea*) turtles.

Although CALM (1990) reports loggerhead turtle nesting activity on Cohen Island, Pendoley *et al*. (2016) did not find any evidence of loggerhead nesting activity in over 20 years of track data. The northernmost key loggerhead nesting areas include the North West Cape and Muiron Islands and any nesting activity by loggerhead turtles in the Dampier Archipelago will not represent significant rookeries for this species. No major leatherback turtle rookeries are known to occur in Australia, with scattered nesting reported in Queensland (Limpus & MacLachlan, 1979, 1994; Limpus *et al.,* 1984) and the Northern Territory (Hamann *et al.,* 2006; Limpus & MacLachlan, 1994) only. As such, loggerhead and leatherback turtles are not considered further.

Marine turtles in Australia belong to discrete genetic stocks, within each species, that are defined by the presence of regional breeding aggregations. Marine turtles breeding in the vicinity of the activities belong to the Green North West Shelf (G-NWS), Flatback – Pilbara (F-Pil) and Hawksbill – Western

Australia (H-WA) genetic stocks. The Recovery Plan provides information for each stock which is summarised below:

- Green turtles: The trend for the G-NWS stock is reported as stable. Important nesting areas include the Montebello Islands (major), and Rosemary Island, Legendre Island and Delambre Island (minor).

- Flatback turtles: The trend of the F-Pil genetic stock is currently unknown. Important nesting areas include Delambre Island (major), and the Montebello Islands and Dampier Archipelago (minor).

- Hawksbill turtles: The trend for the H-WA stock is also unknown. Rosemary Island, Delambre Island and the Dampier Archipelago are all listed as major important nesting areas for this hawksbill stock.

- Light pollution was assessed as a high-risk threat to all three genetic stocks (green, G-NWS; flatback, F-Pil; hawksbill, H-WA).

2.3.1   Life Cycle

In general, marine turtle species share a very similar life cycle pattern. During non-breeding, adults of both sexes, and sexually immature juveniles, inhabit open ocean foraging habitat. Breeding adults then undergo a breeding migration from foraging areas to mating areas, which may or may not be close to the nesting beach (Miller, 1996). After mating, the males return to the foraging areas while the females will spend several months in internesting habitat in proximity to nesting beaches. Females typically demonstrate strong site fidelity, laying each of their clutches on the same group of beaches or island. As capital breeders, marine turtles are understood to show inactive behaviour during the internesting period (the period between a successful clutch and the next nesting attempt) (Hays *et al.,* 1999, Fossette *et al.,* 2012), presumably to conserve energy for successive reproductive events (see Hays *et al.,* 1999). Once the last clutch of eggs is laid, females will return to the foraging areas, building up their fat reserves before the next breeding migration. Most females will not nest in consecutive years (Miller, 1996).

Hatchlings emerge from the nest and orient towards the sea using the low elevation light horizon (Witherington & Bjorndal, 1991). After entering the water, hatchlings use a combination of cues (wave direction and currents) to orient and travel into deeper offshore waters (Lohmann & Lohmann, 1992; Wilson *et al.*, 2018; Wilson *et al.,* submitted). Crossing and swimming away from the beach is thought to imprint the hatchlings with the cues that allow individuals to return to their natal region to breed as adults (Lohmann *et al.,* 1997). Hatchlings do not feed for the first few days of life, relying on the remains of internalised yolk resources (Witherington, 1991). In general, hatchlings disperse into oceanic currents and gyres where they will stay in these pelagic environments (the pelagic juvenile stage) until large enough to settle in coastal feeding habitats (Boyle *et al.,* 2009; Car, 1987; Witherington, 1991). Flatback turtles have a slightly different life cycle to this generalised life cycle, as they do not have a pelagic phase. Juveniles grow to maturity in shallow coastal waters, thought to be close to their natal beaches (Musick & Limpus, 1996).

2.3.2   Habitat use

The Recovery Plan identifies BIAs and habitat critical for flatback, hawksbill and green turtles. Areas overlapping the Trunkline and Borrow Grounds Project Areas include:

- Flatback turtle internesting BIA (80 km) around the Montebello Islands and Dampier Archipelago.

- Green turtle internesting BIA (20 km) around the Dampier Archipelago.

- Hawksbill turtle internesting BIA (20 km) around the Dampier Archipelago.

- Flatback turtle internesting habitat critical (60 km) around the Montebello Islands and Dampier Archipelago.

Nesting areas identified as habitat critical for flatback, green and hawksbill turtles in the vicinity of the Project Areas include:

- Green turtle: Montebello Islands (all with sandy beaches) and Dampier Archipelago.

- Flatback turtle: Montebello Islands, Dampier Archipelago (including Delambre Island and Huay Island [adjacent to Legendre Island]).

- Hawksbill turtle: Dampier Archipelago (including Rosemary Island and Delambre Island) and Montebello Islands (including Ah Chong Island, South East Island and Trimouille Island).

Turtle nesting activity has been observed on a number of islands of the Dampier Archipelago, as summarised in Table 2-2 and shown in Figure 2-1 (CALM, 1990; Pendoley *et al.,* 2016). Islands that could occur within 20 km of the Project Areas are indicated in Table 2-2. The Montebello Islands also have important nesting beaches for flatback, green and hawksbill turtles (Pendoley *et al.,* 2016).

Within the Dampier Archipelago, Rosemary Island has the most significant nesting beaches, determined as mean number of hawksbill, green and flatback turtle tracks per day (Pendoley *et al*., 2016) and is recognised as an internationally significant rookery for hawksbill turtles (Limpus, 2009). On Rosemary Island, the majority of hawksbill nesting occurs on the north-western (NW) beaches (K. Pendoley, pers. comm.) with lower density flatback and green nesting occurring at beaches on the east of the island. An analysis of turtle track data from these beaches on Rosemary Island between 1990 and 2017 has been undertaken (Whiting, 2018), whichconcluded that nest counts were dominated by hawksbill turtles (9860 nesting events, or 92.1%), with lower flatback and green nests counts at 366 (3.4%) and 478 (4.5%), respectively. These results corroborate other conclusions that the nesting population of hawksbill turtles at Rosemary Island is one of the largest populations in Australia and globally (Limpus, 2009).

Other islands also with moderate nesting activity (11 – 100 tracks per day) for all three species, include Delambre Island, Enderby Island and Eaglehawk Island (Pendoley *et al*., 2016). Although track data confirmed presence of flatback turtles only at Legendre Island (Pendoley *et al.,* 2016), a tagging program conducted in 2008 demonstrated that flatbacks, hawksbill and green turtles nested in notable numbers at this island (Biota, 2009). Delambre Island has been recognised as the largest flatback turtle rookery in Australia with an estimated 3500 nesting females per year (Chaloupka,

2018). Track counts at Angel Island also demonstrate low nesting activity of hawksbill turtles and records of flatback turtle nesting. No additional published information regarding turtle nesting on Angel Island is available.

Seasonality of nesting differs between flatback, green and hawksbill turtles; Table 2-3 outlines the generalised seasonality across the NWS region. Whiting (2018) provides defined seasonality specific nesting data for Rosemary Island (indicated in Table 2-3 by *) and found that hawksbill turtles have a much earlier peak (October/November) compared to flatback turtles (December/January peak). Seasonality for green turtles was not well defined from the available data (Whiting, 2018). Given the discrete duration of surveys at Legendre Island (Biota, 2009), insufficient data is available to refine seasonality for this location.

Table 2-2: Records of nesting behaviour of green, flatback and hawksbill marine turtles on islands of the Dampier Archipelago (CALM, 1990; Pendoley *et al.,* 2016; Biota, 2009)

	Angel	Burrup Peninsula	Conzinc	Delambre	Dolphin	Eaglehawk	East Goodwyn	East Intercourse	Elphick Nob	Enderby	Hauy	Intercourse	Keast	Lady Nora	Legendre	Rosemary	West Intercourse	West Mid Intercourse
Trunkline Project Area distance (km)	17	22	22	38	17	41	25	32	14	27	27	34	13	12	12	14	36	35
Borrow ground Project Area distance (km)	21	26	28	20	16	57	41	42	32	43	14	45	10	28	6.6	40	48	46
Flatback	X	X	X	M	X	L	X	X	X	M	X	X	X	X	L	M	X	X
Green	-	X	-	L	X	L	-	X	-	L	X	-	-	-	X	M	X	-
Hawksbill	L	-	-	L	-	L	X	-	X	M	-	-	-	-	X	H	-	-

Key	
	Island is within 20 km of the Project Areas plus nesting at 'Low' or above
	Island is within 20 km of the Project Areas, but nesting is less than 'Low'
	Island is more than 20 km from Project Areas
-	Absent
X	Present
L	Low: 1 – 10 tracks per day
M	Moderate: 11 – 100 tracks per day
H	High: 101 – 500 tracks per day

Table 2-3: Peak activity of nesting females and emerging hatchlings of green, flatback and hawksbill turtles in the North West Shelf region.

Species	Activity	Jul	Aug	Sep	Oct	Nov	Dec	Jan	Feb	Mar	Apr	May	Jun
Green	Nesting				▓	▓	▓	▓	▓				
	Emergence						░	░	░	░	░		
Hawksbill	Nesting		▒	▒	* *	* *	▒	▒	▒				
	Emergence						* *	* *	░	░			
Flatback	Nesting						* *	* *					
	Emergence								* *	* *			

*Peak nesting reported for Rosemary Island (Whiting, 2018), peak hatchling emergence based on ~two month incubation (Commonwealth of Australia, 2017)

Although the body of literature describing marine turtle movement patterns during the breeding season is increasing, information specific to the Dampier Archipelago is more limited. Pendoley (2005) provides details of tracking data for green and hawksbill turtles nesting on Rosemary Island. Results suggested that nesting female hawksbill turtles remained within 1 km of nesting beaches on Rosemary Island (Pendoley, 2005). Female green turtles travelled greater distances, up to 5 km, but typically remained within shallow, nearshore waters between 0 and 10 m deep (Pendoley, 2005). Studies on the movements of internesting flatback turtles nesting within the Dampier Archipelago are lacking. However, an exhaustive analysis of a large dataset of satellite tracking data showed that flatback females remained in water depths of <44 m and favoured a mean depth of <10 m (Whittock *et al.,* 2016a). Flatback turtles generally demonstrate internesting displacement distances of 3.4 – 62 km from the nesting beach, typically confined to longshore movements in nearshore coastal waters or travelling between island rookeries and the adjacent mainland (Whittock *et al.,* 2014). There is no evidence to date to indicate that flatback turtles swim out into deep offshore waters during the internesting period. Incorporating tracking data, along with environmental variables, into a habitat suitability model, Whittock *et al.,* (2016) defined suitable internesting habitat as water 0 – 16 m deep and within 5 – 10 km of the coastline, while unsuitable internesting habitat was defined as water >25 m deep and >27 km from the coastline (Whittock *et al.,* 2016a).

Based on this understanding, it is considered unlikely that internesting turtles will occur in the Trunkline Project Area around the Montebello Islands where water depths range from 46 m to 214 m. At the shallowest point, which is in water adjacent to the Dampier Archipelago, water depths in the Trunkline Project Area are approximately 30 m. Water depths of the Borrow Grounds Project Area range between approximately '30 to 40 m. Internesting green and hawksbill turtles are unlikely to utilise habitat at these water depths. Flatback turtles nesting on beaches of the Dampier Archipelago may internest in the shallower waters of the Trunkline Project Area and Borrow Grounds Project Area, however, large numbers are not expected.

Following incubation, hatchlings emerge from the sand, crawl to the ocean and swim offshore, in a behaviour termed the "swim frenzy", under the influence of tides and currents before reaching deeper, less predator rich, waters. This offshore migration occurs in the top 30 cm of the ocean and this swimming behaviour is regularly interrupted by rest periods when hatchlings float on or near seaweed at the sea surface (Duran & Dunbar, 2015, Bell *et al.,* 2016). Current data for the Project Area at the closest point to the Montebello Islands and islands of the Dampier Archipelago are presented in RPS (2019). Estimates of the net currents were derived by combining predictions of the drift currents, available from mesoscale ocean models, with estimates of the tidal currents (RPS, 2019).

During peak hatchling season (November to April, inclusive of all species) currents at the Montebello Islands location flow in a westerly direction. Current speed ranged between <0.1 to 0.5 m/s^{-1} with the greatest proportion of records within the 0.1 – 0.2 m/s^{-1} range. At the Dampier Archipelago location, currents were predominantly in a northeast (NE) direction over the same time period. Current speed ranged from <0.04 to 0.16 m/s^{-1} (RPS, 2019). When modelled to include tidal influences incorporated, current speed at the Dampier Archipelago location increased to range between <0.1 – 0.5 m/s^{-1} and were predominantly in a west (W) or east (E) direction. Tidal influences had less of an effect on current speed at the Montebello Islands location, although the proportion of current speeds recorded in the 0.4 – 0.5 m/s^{-1} range increased. Currents in an easterly direction were also as dominant as those in a westerly direction (RPS, 2019).

Non-breeding habitat use may include migratory pathways (adults) or foraging areas (adults and pelagic juveniles) for loggerhead, green, hawksbill, leatherback and flatback turtles. During non-breeding, green turtles typically occupy nearshore, coastal bays, feeding on seagrasses and macroalgae (Bjorndal, 1997; Bolten, 2003). They are herbivorous for the majority of their life history; however, post-hatching green turtles are omnivorous in their pelagic stage, and recent findings point to an oceanic diet including sea jellies for some populations (Arthur *et al.,* 2008; Bolten, 2003). Flipper tagging data suggest WA waters are probable foraging grounds for green turtles that nest not only in WA, but also the Northern Territory and Indonesia (Prince, 1997). Flatback turtle foraging areas have been found to occur in waters shallower than 130 m and within 315 km of the shore, with many areas located in 50 m water depth and 66 km from shore (Whittock *et al.,* 2016b). Their main diet comprises algae, squid, invertebrates, and molluscs. Loggerheads feed on benthic invertebrates including molluscs and crustaceans (Shigenaka, 2003). Loggerhead turtles are a nearshore species who prefer warm, shallow continental shelves and coastal bays and estuaries (Shigenaka, 2003). Hawksbill turtles are the most tropical of all sea turtle species and are found within rock and reef habitats, coastal areas and lagoons. They are known to forage amongst vertical underwater cliffs, on coral reefs and on gorgonian (soft coral) flats, as well as seagrass or algae meadows (Bjorndal, 1996). Hawksbills feed primarily on sponges, but will also consume shrimp, squid, anemones, algae, seagrass, sea cucumber and soft corals (Bjorndal, 1996).

Benthic surveys of the trunkline route between the State waters boundary and approximately kilometre point (KP) 50, to determine the presence and extent of any sessile benthic assemblages adjacent to the proposed trunkline route, found that the seabed was characterised as fine to coarse sand with low species abundance and diversity with sparse sponges and soft corals typical of habitat on the NWS (Woodside, 2009). Benthic habitat surveys within the Borrow Grounds Project Area suggested that the benthic habitat is dominated by sandy bottom and with little to no biota (Advisian, 2019). Based on the key food sources of marine turtle species, and the relative abundance of epifauna and infauna found in the Trunkline and Borrow Grounds Project Areas, the trunkline and borrow grounds are unlikely to support foraging aggregations of marine turtles.

Tracking data has highlighted the importance of the Dampier Archipelago for both green and hawksbill turtles on migration, though tracks indicated individuals stayed outside the furthermost islands of the Archipelago, and the eastern side of the Burrup Peninsula (Pendoley, 2005). The tracking data from Pendoley (2005) did not identify any foraging grounds for greens and hawksbills within the Dampier Archipelago. However, foraging aggregations of unidentified marine turtles during a mid-winter aerial

marine fauna survey of the NWS region were concentrated in warm shallow waters off the offshore islands (Prince, 2001).

Figure 2-1: Islands of the Dampier Archipelago with turtle nesting beaches
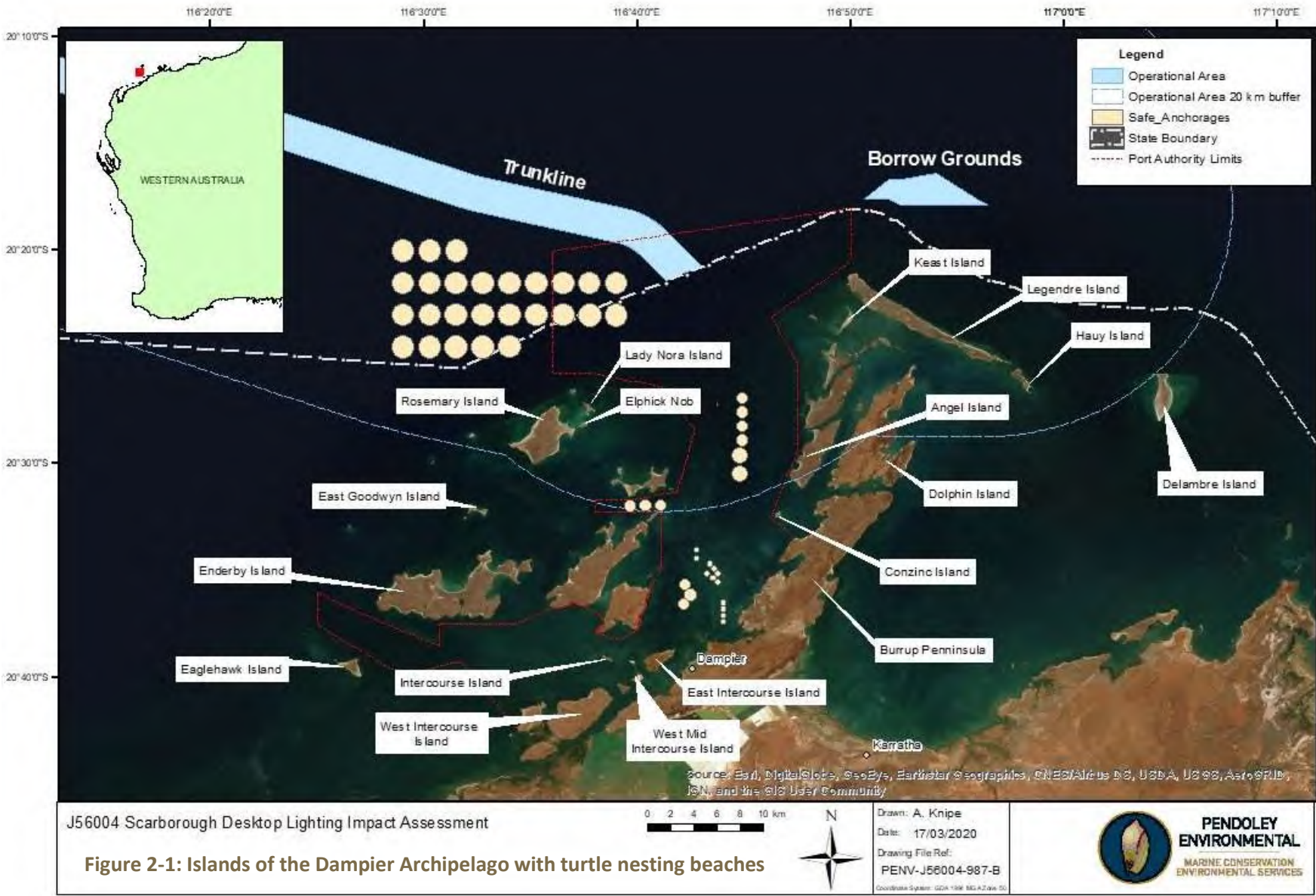
3   IMPACT ASSESSMENT

3.1   Rationale

As described in Section 2.2, this impact assessment assumes that received light intensity at nesting beaches within 20 km of the Project Area may result in impacts to marine turtle behaviour at these nesting beaches (Figure 2-1). The assessment is focused upon islands which have recorded at least 1 – 10 tracks per day (i.e low or above low activity) for either flatback, hawksbill or green turtles, as summarised in Table 2-2. These islands include Rosemary Island (14 km south (S) of the Trunkline Project Area), Legendre Island (12 km E of the Trunkline Project Area and 6.5 km S of the Borrow Grounds Project Area), and Angel Island (17 km southeast (SE) of the Trunkline Project Area). Although Delambre Island is located 20 km SE of the Borrow Grounds Project Area, the area within 20 km comprises rocky coastline unsuitable for turtle nesting. The sandy beaches where turtle nesting will occur at higher density are located more than 20 km from the Project Area. Therefore, potential impacts to nesting habitat of Delambre Island are not considered further.

Although the Project Areas are located in a general offshore direction from the islands listed above, variations in the coastline exist such that, at an individual beach level, the orientation of the vessels from individual nesting turtles may not always be in an offshore direction. Furthermore, as the vessels traverse through the Project Areas, the relative orientation to nesting beaches will change. Figure 3-1 presents the relative orientation of the Project Area from three nesting beaches on Rosemary Island, and one from Legendre Island. A generalised representation of unfavourable orientation of the Project Areas to these beaches was based on angles either less than 45°, or more than 135°, assuming that 90° was the most direct line to the ocean. The portions of the Project Areas that are considered to be at an unfavourable orientation to the nesting beaches are shown in red hatching. These hatched areas represent an area of increased vulnerability to behavioural impacts due to artificial light as a visualisation tool only; they do not constitute a definitive threshold at which an impact will or will not occur. Factors such as the aspect, including the location of individual nests/clutches on the beach, and surrounding topography, will all influence the vulnerability of individual turtles to behavioural impacts.

The majority of hawksbill nesting on Rosemary Island occurs on the west coast, while lower density nesting occurs on NE and E facing beaches (Whiting, 2018; K. Pendoley, pers. comm.). The portion of the Project Area that occurs within 20 km of Rosemary Island includes an area which ranges in orientation from north-northwest (NNW) to northeast (NE), resulting in potentially unfavourable orientations presented in Figure 3-1. Legendre Island runs on a northwest (NW) to SE axis; turtle nesting beaches are predominantly found on the NE and southwest (SW) coasts of the eastern half of the island (Biota, 2009; K. Pendoley, pers. comm.). The orientation of the Trunkline Project Area to Legendre Island ranges from E to NE and the orientation of the borrow grounds Project Area to Legendre Island range from NNW to north (N). Given the combination of distance and orientation, relatively small proportions of either the borrow grounds or Trunkline Project Areas overlap with areas of potentially unfavourable orientation (Figure 3-1). Nesting beaches on Angel Island face in a NW direction, with orientation of the Trunkline Project Area in a NNW direction.

Although the TSHD or pipelay vessels may be consistently present in the Trunkline Project Area for up to eight weeks, depending on the activity being undertaken, the continual movement of the vessel will prevent any one specific receptor (e.g. a particular nesting beach or an individual turtle) being

exposed for the duration of each activity and is most likely limited to less than eight weeks, depending on the nesting beach. Dredging activities in the Borrow Grounds, and backfill activities in the Trunkline Project Areas, will be undertaken intermittently; cycling between two hours in the borrow grounds followed by five hours in the Trunkline Project Area.
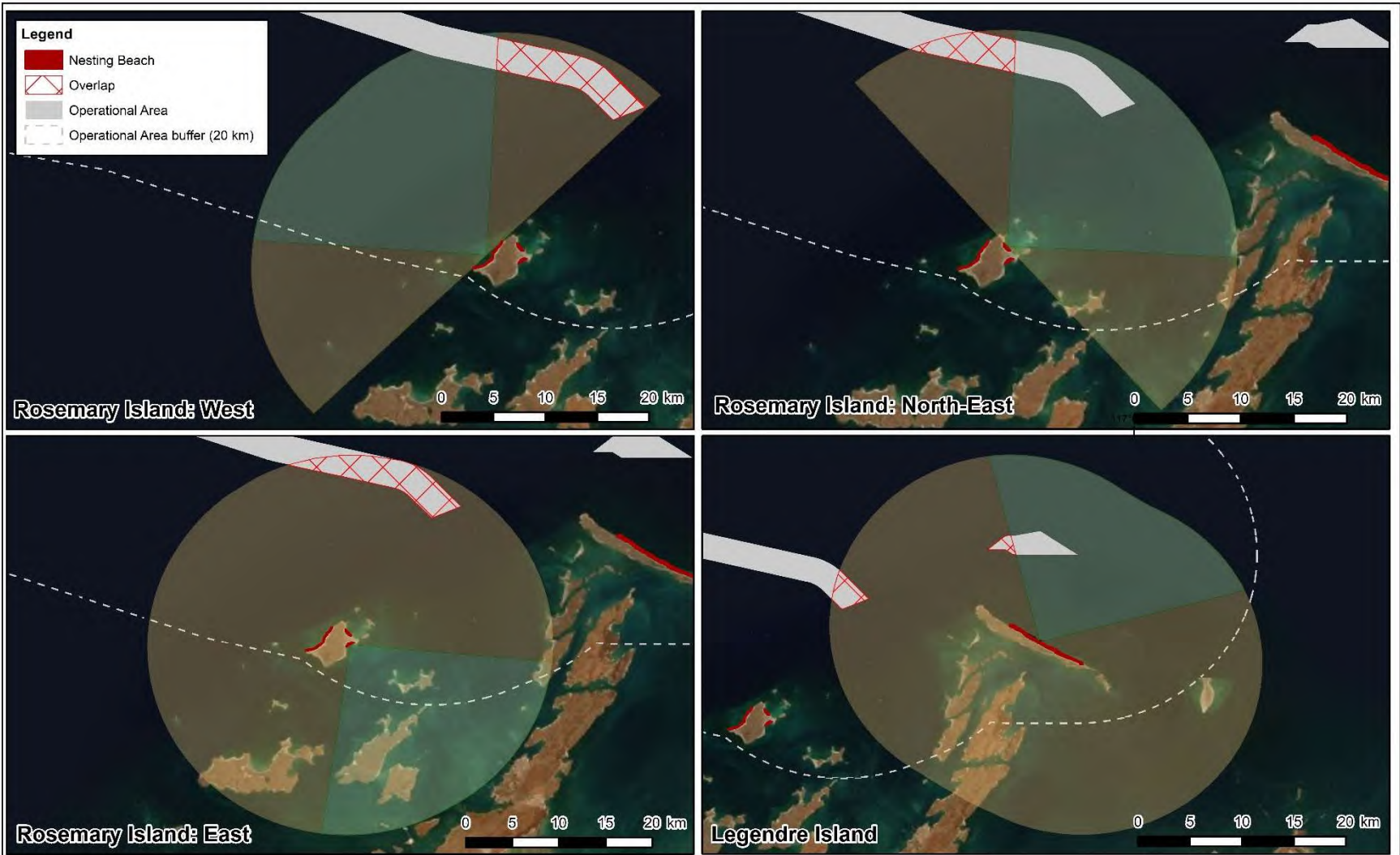
Figure 3-1: Orientation of the Project Areas to individual nesting beaches

J56004 Scarborough Desktop Light Assessment

Drawn: P. Whittock
Date: 13/02/2020
Drawing File Ref:
PENV-J56004-987-A
Coordinate System: GDA 1994 MGA Zone 50

3.1   Nesting

Adult female marine turtles return to land, predominantly at night, to nest on sandy beaches, relying on visual cues to select, and orient on, nesting beaches. That artificial lighting on or near beaches has been shown to disrupt nesting behaviour is relatively well documented (see Witherington & Martin, 2003 for review). Beaches with light spill, such as those located adjacent to urban developments, roadways and piers, often have lower densities of nesting females compared to beaches with less development (Salmon, 2003; Hu *et al.,* 2018). Further, on completion of laying, nesting females are thought to use light cues in order to return to open ocean, orientating towards the brightest light (Witherington & Martin, 2003). However, observations of nesting females and emerging hatchlings at the same beach showed that females were disorientated much less frequently than hatchlings (Witherington, 1992) indicating that nesting females are less vulnerable to impacts of artificial light on sea-finding.

Although it is assumed that artificial light emitted from project vessels may be visible at nesting beaches, given the distance between the light sources and the beaches (minimum of 6.5 km from Borrow ground and 12 km from Trunkline Project Area), direct light spill onto the beach is not considered credible. As such, the vessel light sources are not expected to discourage females from nesting, or effect nest site selection, and hence will not displace females from nesting habitat. There is a possibility that the orientation of light sources relative to individual nesting females returning to sea, may be in a longshore direction that could cause disruption to sea-finding behaviour. Although the maximum duration of a pipelay or TSHD vessel activity is eight weeks (Table 2-1), these vessels are either continually moving (within the Trunkline Project Area) or have intermittent presence (in the Borrow Ground Project Area), and, therefore, the relative orientation between the vessel and an individual beach will not occur for the duration of the activity. Intermittent activities are limited to a maximum of five hours in the Trunkline Project Area or two hours in the Borrow Grounds Project Area. The continuous movement, or intermittent presence, will unlikely result in the TSHD and pipelay vessel being located at an unfavourable orientation for the duration of the activity, limiting the number of females at risk to an insignificant proportion of the nesting population. Since females are not considered highly vulnerable to disorientation due to artificial light, the risk of artificial light preventing nesting behaviour at nesting beaches is considered low.

3.2   Mating, Internesting, Foraging and Migration

The Project Areas overlap habitat critical (internesting buffers) and BIAs for the flatback turtle around the Dampier Archipelago and Montebello Islands, and internesting BIAs for green and hawksbill turtles around the Dampier Archipelago (see Section 2.3). However, as described in Section 2.3.2, green and hawksbill internesting turtles showed preference for water depths less than 10 m and suitable flatback turtle internesting habitat is considered to be less than 25 m deep.

Minimum water depths within the Project Areas are 32 m suggesting that the majority of flatback, green and hawksbill turtles are not expected to use waters within the Project Areas for internesting, although some individual turtles may be encountered. Individuals may migrate through the Project Areas, and although foraging aggregations have not been identified, individuals may forage in low densities. No mating aggregations have been identified in the Project Areas.

Although individuals undertaking internesting, migration, mating (adults) or foraging (adults and pelagic juveniles) may occur within the Project Areas, marine turtles do not use light cues to guide these behaviours. Further, there is no evidence, published or anecdotal, to suggest that internesting, mating, foraging or migrating turtles are impacted by light from offshore vessels. As such, light emissions from the vessels are unlikely to result in displacement of, or behavioural changes to, individuals in these life stages.

3.3 Emerging hatchlings

Hatchling turtles emerge from the nest, typically at night (Mrosovsky & Shettleworth, 1968), and must rapidly reach the ocean to avoid predation (Salmon, 2003). Hatchlings locate the ocean using a combination of topographic and brightness cues, orienting towards the lower, brighter oceanic horizon, and away from elevated darkened silhouettes of dunes and/or vegetation behind the beach (Pendoley & Kamrowski, 2015; Lohmann *et al.,* 1997; Limpus & Kamrowski, 2013).

Artificial lights interfere with natural light levels and silhouettes, which disrupts hatchling sea-finding behaviour (Withington & Martin, 2003; Pendoley & Kamrowski, 2015; Kamrowski, *et al.,* 2014). Hatchlings may become disorientated - where hatchlings crawl on circuitous paths; or become misorientated - where they move in the wrong direction, possibly attracted to artificial lights (Withington & Martin, 2003; Lohmann *et al.,* 1997; Salmon, 2003). Hatchling orientation has been shown to be disrupted by light produced at distances of up to 18 km from the nesting beach (Hodge *et al.,* 2007, Kamrowski *et al.,* 2014), although the degree of impact will be influenced by a number of factors including light intensity, visibility (a function of lamp orientation and shielding), spectral power distribution (wavelength and colour), atmospheric scattering, cloud reflectance, spatial extent of sky glow, duration of exposure, horizon elevation and lunar phase. Hatchlings disoriented or misoriented by artificial lighting may take longer, or fail, to reach the sea. This may result in increased mortality through dehydration, predation or exhaustion (Salmon & Witherington, 1995).

Studies of hatchling sea-finding behaviour found that, on Curtis Island in Queensland, 20% of hatchling fans within proximity to artificial light associated with an onshore LNG plant had an offset bearing of >90°, indicating severe sea-finding disruption (Kamrowski *et al.,* 2014). However, the number of individual hatchlings that traversed the beach at bearings that indicated misorientation or disorientation are not reported. Although direct comparisons between light emissions of the proposed vessels and the LNG plant in this study are not possible (given the size of the LNG plant), it is considered credible that light emissions from the LNG plant will exceed those from the project vessels.

Disruption to orientation of emerging hatchlings has been found to occur most often during the new moon phase and least frequent during full moon phases (Salmon & Witherington, 1995). Experiments showed that background illumination from the moon (while in phases closer to full moon), restored normal seafinding behaviour in hatchlings but did not result in attraction in the direction of the moon. It was concluded that background illumination from the moon reduced light intensity gradients of artificial light, reducing, but not eliminating, its effect on hatchling orientation (Salmon & Witherington, 1995).

Although the Project Areas are located offshore, the orientation of vessels in relation to individual clutches at the local beach scale may occur in a longshore direction (as described above and presented

in Figure 3-1) providing the potential for emerging hatchlings to become mis- or disorientated. However, the proportion of hatchlings that may become mis or disorientated is unlikely to comprise a significant proportion of the total number of hatchlings emerging from nesting beaches for the following reasons:

- Since the TSHD and pipelay vessels will be continually moving within the Trunkline Project Area, and the TSHD will only be intermittently present in the Borrow Grounds Project Area, vessels will only be temporarily (i.e. days to weeks) located at an orientation that could result in hatchling mis- or disorientation.

- The potential impact of artificial light may be reduced during the full moon period (Salmon & Witherington, 1995), further reducing the overall timeframe within which an impact could occur.

- It is not credible that all nests on a given beach will hatch during the activity duration (less than eight weeks) given the length of the peak hatchling emergence season (Table 2-3), and considering the effects of moon phase (above), meaning that the number at risk of behavioural impact will be less than the total number of hatchlings hatching on any given beach.

- Even if it is assumed that sea-finding is disrupted for all hatchlings in a given clutch, which is highly unlikely (K. Pendoley, pers. comm.), the proportion of clutches that could demonstrate sea-finding disruption is expected to be less than 20% (assuming a lower probability of impact compared to that reported in Kamrowski *et al.,* (2014)).

Therefore, should light emissions from the project vessels result in sea-finding disruption, it would likely be limited to a small proportion of individual hatchlings, which is not expected to result in significant impacts to flatback, green or hawksbill turtles within important nesting areas in the Dampier Archipelago and Montebello Islands (as defined in the Recovery Plan) or at the level of the genetic stock. While disruption to the behaviour of a small number of hatchlings may occur, the temporary presence of the light sources allows hatchling sea-finding behaviour to continue, once the vessel has moved away. Since the vessel activities are not planned to occur in multiple breeding seasons, such behavioural response are highly unlikely to result in impacts at a population level or result in decreasing trends in nesting abundance.

3.4   Dispersing hatchlings

Once in nearshore waters, artificial lights on land can also interfere with the dispersal of hatchlings. Presence of artificial light can slow down their in-water dispersal (Witherington & Bjorndal, 1991; Wilson *et al.,* 2018) or increase their dispersion path, potentially depleting yolk reserves, or even attract hatchings back to shore (Truscott *et al.,* 2017). In addition to interfering with swimming, artificial light can influence predation rates, with increased predation of hatchlings in areas with significant sky glow (Gyuris, 1994; Pilcher *et al.,* 2000). Since the nearshore area tends to be predator-rich, hatchling survival may depend on them exiting this area rapidly (Gyuris, 1994). Should this be the case, aggregation of predatory fish occurring in artificially lit areas (e.g. Wilson *et al.,* 2019) may further increase predation of hatchlings.

An internal compass set while crawling down the beach, together with wave cues, are used to reliably guide hatchlings offshore (Lohmann & Lohmann, 1992, Stapput & Wiltschko, 2005; Wilson *et al.,* submitted). In the absence of wave cues, however, swimming hatchlings have been shown to orient towards light cues (Lorne & Salmon, 2007, Harewood & Horrocks, 2008) and in some cases, wave cues were overridden by light cues (Thums *et al.,* 2013, 2016; Wilson *et al.,* 2018).

The speed and direction of at-sea dispersal is substantially influenced by currents; the offshore trajectory of flatback hatchlings at Thevenard Island was displaced by tidal currents that ran parallel to the beach, an effect that increased as the hatchlings moved further offshore (Wilson *et al.,* 2018, 2019). However, when light was present this effect was diminished, showing that hatchlings actively swam against currents and towards the light source, which slowed their offshore dispersal from 0.5 m/s^{-1} when no light was present, to 0.35 - 0.44 m/s^{-1}, depending on the type of light (Wilson *et al.,* 2018). Wilson *et al.* (2018) demonstrated that when flatback hatchlings were within 150 m of the beach, they were able to swim against currents up to 0.3 m/s^{-1}.

These results suggest that hatchlings can move in any direction when their swimming speed is greater than the speed of the nearshore current, although the speed at which currents can no longer be overcome by hatchlings will be species specific and related to swimming speeds. The mean swimming of flatback hatchlings under natural light conditions (0.5 m/s^{-1}) were similar to speeds of green turtle hatchlings (0.49 m/s^{-1}) (Thums *et al.,* 2016), both of which are greater that hawksbill turtle hatchlings (0.21 m/s^{-1}) (Chung *et al.,* 2009). Given the similarities in swim speeds between flatback and green turtles, it is possible that green turtles will have the ability to swim against similar strength currents as reported for flatback turtles (0.3 m/s^{-1}). However, the slower swimming speeds recorded for hawksbill turtles suggest that current speeds at which hawksbill hatchlings could swim against would be weaker than 0.3 m/s^{-1}, though to what extent is currently unknown.

When tidal influences were considered, modelled currents around the Dampier Archipelago and Montebello Islands ranged from <0.1 to 0.5 m/s.$^{-1}$, with the greatest proportion of records within the 0.1 – 0.2 m/s^{-1} range (RPS, 2019). These modelling results suggest that flatback and green turtle hatchlings may be able to swim against currents, for at least a proportion of the activity, should they be attracted to artificial light. Hawksbill turtles may be able to swim against currents at the lowest end of the predicted range, which is less likely to comprise a significant proportion of the activity duration. In the event that hatchlings are able to swim against current speeds, there is a risk that they could become entrapped in areas of light spill. Wilson *et al.,* (2018) observed flatback hatchlings becoming entrapped in the light spill from a small survey vessel for up to one hour. Other reports of the duration of time in which hatchlings may be entrapped in direct light spill varies widely; while Thums *et al.* (2016) found that light trapping was very temporary (minutes), anecdotal observations of hatchlings entrapped by light spill from a pipelay vessel off Barrow Island found hatchlings remained within the light spill in the lee of the barge all night until dawn (K. Pendoley, pers. obs. 2003). It is possible that larger vessels, such as the pipelay vessel, provide shelter on the leeward side from tidal currents allowing hatchlings to remain trapped in the light spill longer (K. Pendoley, pers. obs. 2003).

Hatchlings emerging from nesting beaches of the Montebello Islands are expected to be carried E or W by the predominant current direction, and not in the direction of the Trunkline Project Area. Since the light sources are located more than 20 km from the nesting beaches, the risk of dispersing hatchlings becoming attracted to light sources in the Project Area is not considered credible.

The majority of hatchlings emerging from nesting beaches of Rosemary Island are hawksbill turtles, which, given their swimming speeds, are considered less likely to swim against the predominant currents for a significant proportion of the activity duration. Further, the predominant current direction (E or W) are unlikely to carry hatchlings (of any species) from Rosemary Island towards an artificial light source in the Trunkline Project Area. At Legendre Island, the predominant current direction (E or W) is unlikely to carry hatchlings in the direction of the Borrow Grounds Project Area. Should light emissions be at a level that results in attraction, green and flatback hatchlings may be able to swim against currents towards the TSHD light sources. However, given that the TSHD will only be present for two hours at a time within the Borrow Grounds Project Area, any attraction will be temporary, and once the TSHD has left the Project Area, dispersing behaviour under can continue under natural conditions. Since the Trunkline Project Area is W of Legendre Island, it is possible that hatchlings could be carried towards vessels within this area. However, while not tested empirically due to the logistical constraints of tracking large numbers of hatchlings concurrently, the density of hatchlings will decrease with distance from the nesting beach as individuals disperse in open ocean (see ambient treatment results in Thums *et al.,*2016, Wilson *et al.,* 2016, Wilson *et al.,*2019). Since the distance between Legendre Island and the Trunkline Project Area is 14 km, the number of hatchlings emerging from Legendre Island occurring within the Trunkline Project Area is likely be a small proportion of the total number emerging from the closest nesting beaches.

In the unlikely event that dispersing hatchlings from Rosemary Island or Legendre Island are carried by currents into the vicinity of the TSHD or pipelay vessel and become attracted to sources of artificial light, the impact will be temporary in that attraction will only occur during hours of darkness; following sunrise, the attraction will cease hatchling dispersal will return. Although attraction to light sources may have consequences at the individual level (e.g. energy depletion and increased predation risk), the numbers that could be impacted is unlikely to comprise a significant proportion of the annual number of hatchlings emerging from the nesting beaches.

4   SUMMARY

This impact assessment was conservatively based on the assumption that light emissions (in the form of either direct light or sky glow) from project vessels within the Trunkline and Borrow Ground Project Areas may be received at intensities that could result in behavioural disturbance at nesting beaches with 20 km of the light sources.

While conservative, the impact assessment concluded that the light emissions from vessel activities in the Trunkline and Borrow Grounds Project Areas would not have a significant impact on marine turtle species across the whole life cycle, when assessed against the EPBC Act Matters of National Environmental Significance Significant Impact Guidelines 1.1 (Commonwealth of Australia, 2013), as described in Table 4-1. Although behavioural impacts to marine turtles may occur, it is not expected that these impacts will be contrary to the priority actions or the measure of success criteria outlined in the Recovery Plan (Commonwealth of Australia, 2017) for the relevant marine turtle genetic stocks, or management of artificial light (Table 4-1).

Table 4-1: Alignment with the Recovery Plan and Significant Impact Criteria based on a conservative impact assessment

Consideration	Conclusion
Recovery Plan	
Marine turtles are not displaced from identified habitat critical to the survival	Vessel light sources are not expected to discourage females from nesting, or effect nest site selection, and hence will not displace females from nesting habitat. There is no evidence to suggest that internesting females are impacted by artificial light and, therefore, internesting females will not be displaced from internesting habitat.
That biologically important behaviour can continue in biologically important areas	Vessel light sources are not expected to discourage females from nesting, or affect nest site selection, meaning that impacts to nesting behaviour is not expected to occur. While there is a small potential for impact on post-nesting sea-finding behaviour of nesting females to occur, nesting females are not considered highly vulnerable to disorientation due to artificial light. Further, since vessels are either continually moving or intermittently present within the Project Areas, the number of adult females potentially impacted is further reduced. There is no evidence, published or anecdotal, to suggest that internesting turtles are impacted by light from offshore vessels and, therefore, changes to internesting behaviour are not expected to occur. While disruption to the behaviour of an insignificant proportion of the total annual number of emerging hatchlings may occur, the pipelay and TSHD vessels are continually moving within the Trunkline Project Area (at least 12 km away) meaning that specific beaches are not exposed to unfavourable orientation of light sources that could result in disruption of sea-finding behaviour for the duration of activities in this area. Once the vessels have moved out of an unfavourable orientation from individual beaches (which is likely to occur within days to weeks), hatchling sea-finding behaviour can continue. The Borrow Grounds Project Area is located 6.6 km from Legendre Island, the closest point to shore. However, activities within the borrow grounds are intermittent (approximately two-hour presence in the area and

Consideration	Conclusion
	absent for at least five hours) further reducing the timeframe in which behavioural impacts to emerging hatchlings could occur. While disruption to hatchling dispersal behaviour (e.g. attraction to or trapping by light at a vessel) of an insignificant proportion of the annual number of hatchlings emerging from a given beach is credible, following sunrise, any effect of the light sources on hatchlings will be eliminated allowing dispersal behaviour to resume. Further, the potential for hatchling dispersal behaviour to be affected decreases with distance to shore. The closest point between the Project Areas and turtle nesting beaches, where the potential of impacts to hatchling dispersal are more likely, is 6.6 km between the Borrow Ground Project Area and Legendre Island. However, TSHD activities within the borrow grounds are intermittent, as described above, further reducing the timeframe in which behavioural impacts could occur in the borrow grounds. While the above behavioural impacts are credible, under a conservative assessment, it is not expected these impacts will impede recovery of the relevant green (G-NWS), flatback (F-Pil) or hawksbill (H-WA) genetic stocks, or result in a decreasing trend in numbers/abundance and, therefore, the project will not impact the measure of success criteria of the Recovery Plan (Commonwealth of Australia, 2017).
Develop and implement best practice light management guidelines for existing and future developments adjacent to turtle nesting beaches	Additional controls outlined in Section 5 will ensure that the activity is conducted in a manner consistent with the National Light Pollution Guidelines for Wildlife (Commonwealth of Australia, 2020).
Identify the cumulative impact on turtles from multiple sources of onshore and offshore light pollution	The TSHD and pipelay vessels will not operate concurrently since activities are required to be undertaken sequentially. Although these vessels may be in the Project Areas for up to eight weeks, depending on the activity being undertaken, the continual movement of the vessels will prevent any one specific receptor (e.g. a particular nesting beach or an individual turtle) being exposed for the duration of each activity. Dredging activities in the borrow grounds Project Area, and backfill activities in the Trunkline Project Area, will also be undertaken intermittently, with periods of time in which the vessel will be absent.

Consideration	Conclusion
	Additional support vessels may be present during some activities (e.g. pipelay activities), however, given the size of the support vessels in comparison to the pipelay vessel, light emissions from the support vessels are unlikely to contribute significantly to overall light emissions. When considered in the context of existing industrial light sources in the region, light emissions from the activities are unlikely to significantly increase light pollution of the Dampier Archipelago. Specifically, at Rosemary Island, visibility of light emissions from the TSHD and pipelay vessels may be limited by existing light emissions from vessels at the designated anchorages.
Significant impact criteria	
Lead to a long-term decrease in the size of a population or important population	Behavioural impacts are limited to an insignificant proportion of the overall annual number of hatchlings emerging from nesting beaches when considered at the 'important nesting area'* level.
Reduce the area of occupancy of important population	The activity will not permanently displace marine turtles from habitats occupied during different life stages.
Fragment an existing important population into two or more populations	Given the temporary nature of the activity (as described in Section 3.1), fragmentation of important population is not credible.
Adversely affect habitat critical to the survival of a species	The activity is not expected to adversely affect nesting or internesting habitat due to the temporary nature of the activity (as described in Section 3.1), and that impacts at the individual level are unlikely.
Disrupt the breeding cycle of an important population	Behavioural impacts are limited to an insignificant proportion of the overall annual number of hatchlings emerging from nesting beaches when considered at the 'important nesting area' scale ('important nesting areas' as defined in the Recovery Plan). Disruption to mating, migration, internesting or nesting is not expected.

Consideration	Conclusion
Modify, destroy, remove, isolate or decrease the availability or quality of habitat to the extent that the species is likely to decline	Given the temporary nature of the activity (as described in Section 3.1), the availability or quality of the habitat will not be affected so that marine turtle species may decline.
Result in invasive species that are harmful to an endangered or vulnerable species becoming established in the species' habitat	Not applicable to light emissions.
Introduce disease that may cause the species to decline	Not applicable to light emissions.
Substantially interfere with the recovery of the species	Behavioural impacts are limited to an insignificant proportion of the overall annual number of hatchlings emerging from nesting beaches when considered at the 'important nesting area'* level. Such impacts will be temporary in nature (as described in Section 3.1) and will not interfere with the recovery at neither the species nor genetic stock level.

* Important nesting areas as defined in the Recovery Plan.

5   RECOMMENDATIONS

It is recommended that Woodside consider the application of a hierarchy or controls in accordance with the National Light Pollution Guidelines for Wildlife (Commonwealth of Australia, 2020) to reduce potential impacts to as low as reasonably practicable (ALARP) and acceptable levels. Controls for consideration are described below.

5.1   Control measures

These control measures are consistent with the National Light Pollution Guidelines for Wildlife (Commonwealth of Australia, 2020).

5.1.1   Avoid night work in sensitive windows

- Trunkline Project Area: peak hatchling emergence periods at Rosemary Island, Legendre Island.

- Activities in borrow grounds Project Area: peak hatchling emergence periods at Legendre Island.

- If night work cannot be avoided, limit non-routine activities at night. For example, heavy lift activities or crew transfers which may require additional or higher intensity of lighting, or orientation of lighting towards nesting beaches.

5.1.2   Activity-specific Lighting Management Plan

The Lighting Management Plan for specific activities should include details on:

Light modelling

Modelling can estimate light emissions from the worst-case scenario and identify:

- Specific nesting beaches that may receive light levels at an intensity that could result in behavioural impact.

- The distance from the vessel at which light radiance is considered ambient.

- Identify lights which contribute most to overall light emissions.

The modelling could therefore inform:

- The credibility of impacts at nesting beaches occurring (nesting females and emerging hatchlings).

- The distance at which hatchlings would need to swim offshore before encountering light sources that could result in disturbance to dispersal behaviour.

- The size of spatial buffers around important habitats within which additional or adaptive management may be required.

Light model accuracy can be increased by incorporating measurements of existing lighting levels within the region. This model could show that light from the pipelay vessel will not add significantly to light

intensity and sky glow at regional scale, when accounting for existing light sources (i.e. moorings and anchorages between Rosemary Island and the Trunkline Project Area).

Light type and positioning

If light modelling indicates impacts at beaches is credible, the following controls should be considered:

- Adjusting orientation of lights to minimise horizontal light spill (all lights)

- Apply additional shielding to a) all lights, or, if not practicable, b) the highest intensity lights, where practicable

- Change a) all lights, or, if not practicable, b) the highest intensity lights, to amber wavelength were safety standards allow.

Where orientation and additional shielding can be applied, the model can be rerun to indicate efficacy of these control measures.

Housekeeping

In all cases, additional housekeeping controls would reduce overall light emissions, including:

- Closing blinds during hours of darkness

- Switching off non-operational lights when not required

- Consider motion activated lights were safety standards allow

Vessel inspection

Prior to the vessel entering within 20 km of nesting beaches, or a spatial buffer informed by modelling, a vessel inspection would occur to:

- Ensure orientation of lights is such that only the intended object is illuminated

- Identify areas of direct light spill on the water and apply additional shielding

- Ensure compliance with housekeeping control measures

5.1.3 Adaptive management

If the activity is undertaken during peak hatchling season, and modelling predicts impacts are credible, adaptive management could be applied, such as:

- Dedicated observers will monitor the area of light spill for entrapped hatchlings. If a number of hatchlings, to be determined, are observed in an area of light spill, the lights will be switched off for half an hour (to allow dispersal behaviour to continue).

- If impacts at the nesting beach are credible, and activity is undertaken in hatchling season, hatchling orientation data will be collected when the vessel is operating within distances at which impacts may occur. If either the spread or offset angle is considered to deviate

significantly (to be determined) from a known baseline, restrictions in night operations will be considered.

6   REFERENCES

ADVISIAN (2019) Dampier Marine Park Benthic Habitat Survey. Prepared for Woodside Energy Ltd. Advisian WorleyParsons Group.

ARTHUR, K.E., BOYLE, M.C., & LIMPUS, C.J. (2008) Ontogenetic changes in diet and habitat use in green sea turtles (*Chelonia mydas*) life history. *Marine Ecology Progress Series*, 362: 303-311.

BELL, C. B., MORO, D. & PENDOLEY, K. (2016) Patterns and pathways: marine construction and patterns of dispersal in hatchling flatback turtles at Barrow Island. Proceedings of the 34th Annual Symposium on Sea Turtle Biology and Conservation: 2014 International Sea Turtle Symposium, New Orleans Louisiana 10 – 17 April 2014. NOAA Technical Memorandum NMFS-SEFSC ; 701

BIOTA (2009) Turtle Monitoring at Bell's Beach and Selected Rookeries of the Dampier Archipelago: 2008/09 Season. Report for Rio Tinto Iron Ore.

BJORNDAL, K.A. (1997) Foraging Ecology and Nutrition in Sea Turtles. In: The Biology of Sea Turtles (eds. P.L. Lutz & J.A. Musick), Vol. 1, pp. 199-231. CRC Press, Boca Raton.

BOLTEN, A.B. (2003) Variation in Sea Turtle Life History Patterns: Neritic vs Oceanic Developmental Stages. In: The Biology of Sea Turtles, Volume II (eds P.L. Lutz, J.A. Musick & J. Wyneken), Vol. 2, pp. 243-257. CRC Press, Boca Raton.

BOYLE, M. C., FITZSIMMONS, N. N., LIMPUS, C. J., KELEZ, S., VELEZ-ZUAZO, X., & WAYCOTT, M. (2009) Evidence for transoceanic migrations by loggerhead sea turtles in the southern Pacific Ocean. *Proceedings of the Royal Society B*, 276: 1993 – 1999 .

CALM (1990) Dampier Archipelago Nature Reserves Management Plan 1990 – 2000. Department of Conservation and Land Management.

CARR, A. (1987) Impact of non-degradable marine debris on the ecology and survival outlook of sea turtles. *Marine Pollution Bulletin*, 18: 352-356.

CHALOUPKA, M. (2018) presentation to DBCA / NWS committee 8/5/2018. https://rstudio-pubs-static.s3.amazonaws.com/448533_0eb04559be1c4df4934c9f69b22b9256.html

CHUNG, F.C., PILCHER, N.J., SALMON, M., & WYNEKEN, J. (2009) Offshore migratory activity of hawksbill turtle (*Eretmochelys 27ehaviour*) hatchlings, ii. Swimming gaits, swimming speed, and morphological comparisons. *Chelonian Conservation and Biology*, 8: 35-42

COMMONWEALTH OF AUSTRALIA (2013) EPBC Act Matters of National Environmental Significance Significant Impact Guidelines 1.1

COMMONWEALTH OF AUSTRALIA (2017) Recovery Plan for Marine Turtles in Australia (2017-2027).

COMMONWEALTH OF AUSTRALIA (2020) National Light Pollution Guidelines for Wildlife Including Marine Turtles, Seabirds and Migratory Shorebirds. January 2020.

DURAN, N. & DUNBAR, S.G. (2015) Differences in diurnal and nocturnal swimming patterns of olive ridley hatchlings in the Gulf of Fonseca, Honduras. *Journal of Experimental Marine Biology and Ecology*, 472: 63 – 71.

FOSSETTE, S., PUTMAN, N. F., LOHMANN, K. J., MARSH, R. & HAYS, G. C. (2012) A biologist's guide to assessing ocean currents: a review. *Marine Ecology Progress Series*, 457: 285e30

GYURIS., E. (1994) The rate of predation by fishes on hatchlings of the green turtle (*Chelonia mydas*). *Coral Reefs*, 13: 137-144.

HAMANN, M., LIMPUS, C.J., HUGHES, G., MORTIMER, J.A., & PILCHER N.J. (2006) Assessment of the Conservation Status of the Leatherback Turtle in the Indian Ocean and South-East Asia. Bangkok. IOSEA Marine Turtle MoU Secretariat. Pp 174.

HAREWOOD, A. & HORROCKS, J.A. (2008) Impacts of coastal development on hawksbill hatchling survival and swimming success during the initial offshore migration. *Biological Conservation*, 141, 394-401.

HAYS, G.C., LUSCHI, P., PAPI, F., SEPPIA, C. & MARSH, R. (1999) Changes in behaviour during the inter-nesting and post-nesting migration for Ascension Island green turtles. *Marine Ecology Progress Series*, 189, 263– 273.

HODGE, W., LIMPUS, C. J., & SMISSEN, P. (2007) Queensland turtle conservation project: Hummock Hill Island nesting turtle study December 2006 Conservation Technical and Data Report (pp. 1-10). Queensland, Australia: Environmental Protection Agency.

HU, Z., H. HU, & HUANG, Y. (2018) Association between nighttime artificial light pollution and sea turtle nest density along Florida coast: A geospatial study using VIIRS remote sensing data. *Environmental Pollutio*n, 239: 30-42.

KAMROWSKI R.L., LIMPUS C., PENDOLEY K. & HAMANN M. (2014) Influence of industrial light pollution on the sea-finding behaviour of flatback turtle hatchlings. *Wildlife Research* 41: 421-434.

KYBA, C.C.M., RUHTZ, T., FISCHER, J. & HÖLKER, F. (2011) Cloud coverage acts as an amplifier for ecological light pollution in urban ecosystems. *PloS ONE*, 6(3): e17307.

LIMPUS C.J. (2009) A Biological Review of Australian Marine Turtles. Brisbane, Queensland. Queensland Government Environmental Protection Agency. Pp 324.

LIMPUS, C.J. & N. MACLACHLIN (1979) Observations on the leatherback turtle, *Dermochelys coriacea* (L.), in Australia. *Australian Wildlife Research*, 6: 105-116.

LIMPUS, C.J. & N. MACLACHLIN (1994) The conservation status of the Leatherback Turtle, *Dermochelys coriacea*, in Australia. In: James, R, ed. Proceedings of the Australian Marine Turtle Conservation Workshop, Gold Coast 14-17 November 1990. Page(s) 63-67. Queensland Department of Environment and Heritage. Canberra: ANCA.

LIMPUS, C.J. & R.L. KAMROWSKI (2013) Ocean-finding in marine turtles: The importance of low horizon elevation as an orientation cue. *Behaviour*, 150: 863-893.

LIMPUS, C.J., A. FLEAY & M. GUINEA (1984). Sea turtles of the Capricornia section, Great Barrier Reef. Royal Society Queensland Symposium. Page(s) 61-78.

LOHMANN, C.M.F. & LOHMANN, K.J. (1992) Geomagnetic orientation by sea turtle hatchlings. In: Proceedings of the 12th International Symposium on Sea Turtle Biology and Conservation (eds. J.I. Richardson & T.H. Richardson), Jekyll Island.

LOHMANN, K.J., WITHERINGTON B.E., LOHMANN C.M.F. & SALMON M. (1997) Orientation, navigation, and natal beach homing in sea turtles. In: The Biology of Sea Turtles. Volume I, P.L. Lutz and J.A. Musick, Editors., CRC Press: Washington D.C. p. 107-135.

LORNE, J.K. & SALMON, M. (2007) Effects of Exposure to Artificial Lighting on Orientation of Hatchling Sea Turtles on the Beach and in the Ocean. *Endangered Species Research*, 3: 23-30.

MILLER, J.D. (1996) Reproduction in Sea Turtles. In: The Biology of Sea Turtles (eds P.L. Lutz & J.A. Musick), Vol. 1, pp. 51-81. CRC Press, Boca Raton.

MROSOVSKY, N. & S.J. SHETTLEWORTH (1968) Wavelength preferences and brightness cues in the water finding behaviour of sea turtles. *Behaviour*, 32: 211-257.

MUSICK, J.A. & LIMPUS, C.J. (1997) Habitat utilization and migration in juvenile sea turtles. *The Biology of Sea Turtles*, 1: 137 – 163.

PENDOLEY, K. & R.L. KAMROWSKI (2015) Influence of horizon elevation on the sea-finding behaviour of hatchling flatback turtles exposed to artificial light glow. *Marine Ecology Progress Series*, 529: 279-288.

PENDOLEY, K. (2005) Sea Turtles and Industrial Activity on the North West Shelf, Western Australia. PhD dissertation, Murdoch University, Perth, Australia.

PENDOLEY, K., WHITTOCK P.A., VITENBERGS A. & BELL, C. (2016) Twenty years of turtle tracks: marine turtle nesting activity at remote locations in the Pilbara, Western Australia. *Australian Journal of Zoology*, 64: 217–226.

PILCHER N., ENDERBY S., STRINGELL T. & BATEMAN L. (2000) Nearshore turtle hatchling distribution and predation. In: Sea turtles of the Indo-Pacific: research management and conservation. Proceedings of the Second ASEAN Symposium and Workshop on Sea Turtle Biology and Conservation, N. Pilcher and G. Ismail, Editors. ASEAN Academic Press: London.

PRINCE, R.I.T. (1997) Marine Turtle Conservation: The Links Between Populations in Western Australia and the Northern Australian Region. People and Turtles. In: Marine Turtle Conservation and Management in Northern Australia (eds. R. Kennett, A. Webb, G. Duff, M. Guinea & G. Hill). Centre for Indigenous Natural and Cultural Resource Management, Centre for Tropical Wetland Studies, Northern Territory University, Darwin.

PRINCE, R.I.T. (2001) Aerial survey of the distribution and abundance of dugongs and associated macrovertebrate fauna – Pilbara coastal and offshore region, WA. Environment Australia, Marine Species Protection Program and Department of Conservation and Land Management WA, May 2001.

RPS (2019) Woodside Scarborough Project – Quantitative Spill Risk Assessment. Rev 1, 17 April 2019.

SALMON, M., & WITHERINGTON, B. (1995) Artificial lighting and seafinding by loggerhead hatchlings: Evidence for lunar modulation. *Copeia,* 1995: 931 – 938.

SALMON, M., (2003) Artificial night lighting and sea turtles. *Biologist*, 50: 163-168.

SALMON, M., WYNEKEN, J., FRITZ, E. & LUCAS, M. (1992) Sea finding by hatchling sea turtles: role of brightness, silhouette and beach slope orientation cues. *Behaviour*, 122: 56-77.

SHIGENAKA, G. (2003) Oil and sea turtle. Biology, planning and response NOAA.

STAPPUT, K. & WILTSCHKO, W. (2005). The sea-finding 30ehaviour of hatchling olive ridley sea turtles, *Lepidochelys olivacea*, at the beach of San Miguel (Costa Rica). *Naturwissenschaften*, 92(5): 250-253.

THUMS, M., WAAYERS, D., HUANG, Z., PATTIARATCHI, C., BERNUS, J. & MEEKAN, M. (2017) Environmental predictors of foraging and transit behaviour in flatback turtles *Natator depressus*. *Endangered Species Research*, 32: 333 – 349.

THUMS, M., WHITING, S.D, REISSER, J.W., PENDOLEY, K.L., PATTIARATCHI C.B., HARCOURT, R.G., MCMAHON, C.R. & MEEKAN, M.G. (2013) Tracking sea turtle hatchlings—A pilot study using acoustic telemetry. *Journal of Experimental Marine Biology and Ecology,* 440: 156-163.

THUMS, M., WHITING, S.D, REISSER, J.W., PENDOLEY, K.L., PATTIARATCHI C.B., PROIETTI, M., HETZEL, Y., FISHER, R. & MEEKAN, M.G. (2016) Artificial light on water attracts turtle hatchlings during their near shore transit. *Royal Society Open Science 3*, doi: 10.1098/rsos.160142.

TRUSCOTT, Z., BOOTH, D.T. & LIMPUS C.J. (2017) The effect of on-shore light pollution on seaturtle hatchlings commencing their off-shore swim. *Wildlife Research*, 3(5): 127-134.

WHITING, A.U. (2018) Analyses of turtle track count data from Rosemary Island, Dampier Archipelago: 1990 to 2017. Unpublished report to the Parks and Wildlife Service, Department of Biodiversity, Conservation and Attractions, Pilbara Region.

WHITTOCK P.A, PENDOLEY K.L. & HAMANN, M. (2014) Internesting distribution of flatback turtles (*Natator depressus*) and industrial development in Western Australia. *Endangered Species Research*, 26: 25-38.

WHITTOCK, P.A., PENDOLEY, K.L. & HAMANN, M. (2016a) Using habitat suitability models in an industrial setting: the case for internesting flatback turtles. *Ecosphere*, 7(11): e01551. 10.1002/ecs2.1551.

WHITTOCK P.A, PENDOLEY K.L &, HAMANN, M. (2016b) Flexible foraging: post-nesting flatback turtles on the Australian continental shelf. *Journal of Experimental Marine Biology and Ecology*, 477: 112–119.

WILSON, P., THUMS, M., PATTIARATCHI, C., MEEKAN, M., PENDOLEY, K., FISHER, R. & WHITING, S. (2018) Artificial light disrupts the nearshore dispersal of neonate flatback turtles *Natator depressus*. *Marine Ecology Progress Series,* 600: 179-192. Doi: https://doi.org/10.3354/meps12649

WILSON, P., THUMS, M., PATTIARATCHI, C., WHITING, S., PENDOLEY, K., FERREIRA, L. C. & MEEKAN, M. (2019) High predation of marine turtle hatchlings near a coastal jetty. *Biological Conservation*, 236: 571-579.

WILSON, .P THUMS, M., PATTIARATCHIA, C., WHITING, S., MEEKAN, M., PENDOLEY, K. (submitted) Nearshore wave characteristics as cues for swimming orientation in flatback turtle hatchlings.

WITHERINGTON, B. & R.E. MARTIN (2003) Understanding, Assessing, and Resolving Light-Pollution Problems on Sea Turtle Nesting Beaches. Florida Fish and Wildlife Conservation Commission FMRI Technical Report TR-2: Jensen Beach, Florida. P. 84

WITHERINGTON, B.E. (1992). Behavioral responses of nesting sea turtles to artificial lighting. *Herpetologica*, 48: 31–39.

WITHERINGTON, B.E. & K.A. BJORNDAL (1991) Influences of artificial lighting on the seaward orientation of hatchling loggerhead turtles *Caretta caretta*. *Biological Conservation* 55(2): 139-149.

WOODSIDE (2009). Pluto LNG Project Spoil Ground 5A Survey Report.

Appendix L

Scarborough Light Modelling

Advisian

SCARBOROUGH LIGHT MODELLING

Prepared by

Pendoley Environmental Pty Ltd

For

Advisian

21 February 2020

DOCUMENT CONTROL INFORMATION

TITLE: SCARBOROUGH LIGHT MODELLING

Disclaimer and Limitation

This report has been prepared on behalf of and for the use of Advisian. Pendoley Environmental Pty Ltd. takes no responsibility for the completeness or form of any subsequent copies of this Document. Copying of this Document without the permission of Advisian is not permitted.

Document History

Revision	Description	Date issued	Date received	Personnel
Draft	Report Draft	19/02/202		Dr A Knipe
Rev AI	Internal Review	20/02/2020	19/02/2020	Dr K Pendoley
Rev A	Client review	20/02/2020	20/02/2020	WEL
Rev B	Address client comments	21/02/2020	21/02/2020	Dr A Knipe

Printed:	21 February 2020
Last saved:	21 February 2020 11:58 AM
File name:	P:\06 Projects\J56 Advisian\J56004 Scarborough Desktop Lighting Assessment\Modelling report\J56004 Scarborough Light Modelling_RevA.docx
Author:	Annabel Knipe, Adam Mitchell, Kellie Pendoley
Project manager:	Annabel Knipe
Name of organisation:	Pendoley Environmental Pty Ltd
Name of project:	Scarborough Light Modelling
Client	Advisian
Client representative:	Paul Nichols
Report number:	J56004
Cover photo:	Pipelay vessel (Saipem)

TABLE OF CONTENTS

LIST OF TABLES

LIST OF FIGURES

LIST OF ANNEXES

ACCRONYMS

ALAN	Artificial Light At Night
km	Kilometer
m	Meters
NWS	North West Shelf
SME	Subject Matter Expert
sr	steradian
TSHD	Trailing suction hopper dredger
W	Watts

1   INTRODUCTION

Woodside Energy Limited (Woodside), is proposing to develop the Scarborough gas resource, located on the North West Shelf (NWS), through new offshore facilities. These facilities are proposed to be connected to the mainland through an approximately 430 km trunkline to an onshore facility.

Installation of the trunkline will involve pre-lay dredging and pipelay, followed by post-lay backfill within a Trunkline Project Area. Backfill material will be dredged from a separate area, the Borrow Grounds Project Area. Specialised vessels will be utilized for specific activities. As described in the National Light Pollution Guidelines for Wildlife Including Marine Turtles, Seabirds and Migratory Shorebirds (Commonwealth of Australia, 2020), light emissions from project vessels have the potential to impact marine turtles at nesting beaches and in open ocean.

A conservative desktop assessment of potential impacts of ALAN on marine turtles was undertaken in absence of light modelling by assuming that potential impacts were credible within 20 km of the light sources (Pendoley Environmental, 2020). While this impact assessment is considered conservative, due to the uncertainties associated with predicting light emissions of the vessels without relevant information, Advisian engaged Pendoley Environmental on behalf of Woodside to undertake light modelling to aid assessment of light emissions from the proposed pipelay vessel and trailing suction hopper dredger (TSHD) vessel.

2   METHODOLOGY

Light modelling was undertaken for the proposed pipelay and TSHD vessels to predict the extent of biologically relevant light spill. Specifics of the respective vessel's lighting design and luminaire specifications were applied to the ILLUMINA Artificial Light At Night (ALAN) model (Aube *et al*. 2005). The ILLUMINA model is a three-dimensional model that accounts for both line of sight and atmospheric scattering, allowing the attenuation of light over distance and extent of light glow to be modelled. The reader is directed to Aube *et al*. (2005) for details of equations and model parameterisation.

Unlike a simple line of sight model based on the inverse square law formula, this is a more sophisticated model which allows individual light sources (i.e. individual luminaires) to be placed within the area of interest (as opposed to assuming a single large light point source for the entire vessel). The model input parameters also include project specific details about light type, spectral distribution, height and orientation of individual luminaires, including any shielding, which substantially increases the model precision and accuracy.

2.1   Model Inputs

Information regarding the light inventory was extracted from lighting layout drawings and light manufacturer data sheets provided to Pendoley Environmental by Woodside for both the *Casterone* pipelay vessel and *Gateway* TSHD, and included:

- number of each type of light

- spectral output of light type

- angular distribution of light (shielding)

- lumen output of each type of light

- height of each light

Details of individual lights are summarised in (Annex 1).

Because the atmospheric conditions over the NWS are typically clear, the model simulations presented here assumed no contribution of light from cloud reflectance.

Surface reflectance and elevation values are incorporated into the model from aerial imagery supplied by NASA (National Aeronautics and Space Administration) Earthdata and the NOAA (National Oceanic and Atmospheric Administration) (NASA, 2020; NOAA, 2020) as per the methodology outlined in Aube *et al*. (2005).

Model outputs are provided in radiance (W/m^2/sr, where W = watts, m^2 =meters squared and sr = steradian).

2.2   Scenarios

Four scenarios were modelled:

1. Pipelay vessel *Casterone* at the closest point of the Trunkline Project Area to Rosemary Island (point 1, 14.15 km)

2. Pipelay vessel *Casterone* at the closest point of the Trunkline Project Area to Legendre island (point 2, 12 km)

3. TSHD *Gateway* at the closest point of the Trunkline Project Area to Rosemary Island (point 1, 14.15 km)

4. TSHD *Gateway* at the closest point of the Borrow Grounds Project Area to Legendre island (point 3, 6.6 km)

Location and coordinates of these location points are provided in Figure 2-1.

J56004 Scarborough Desktop Light Assessment

Figure 2-1: Location and coordinates of light modelling source points
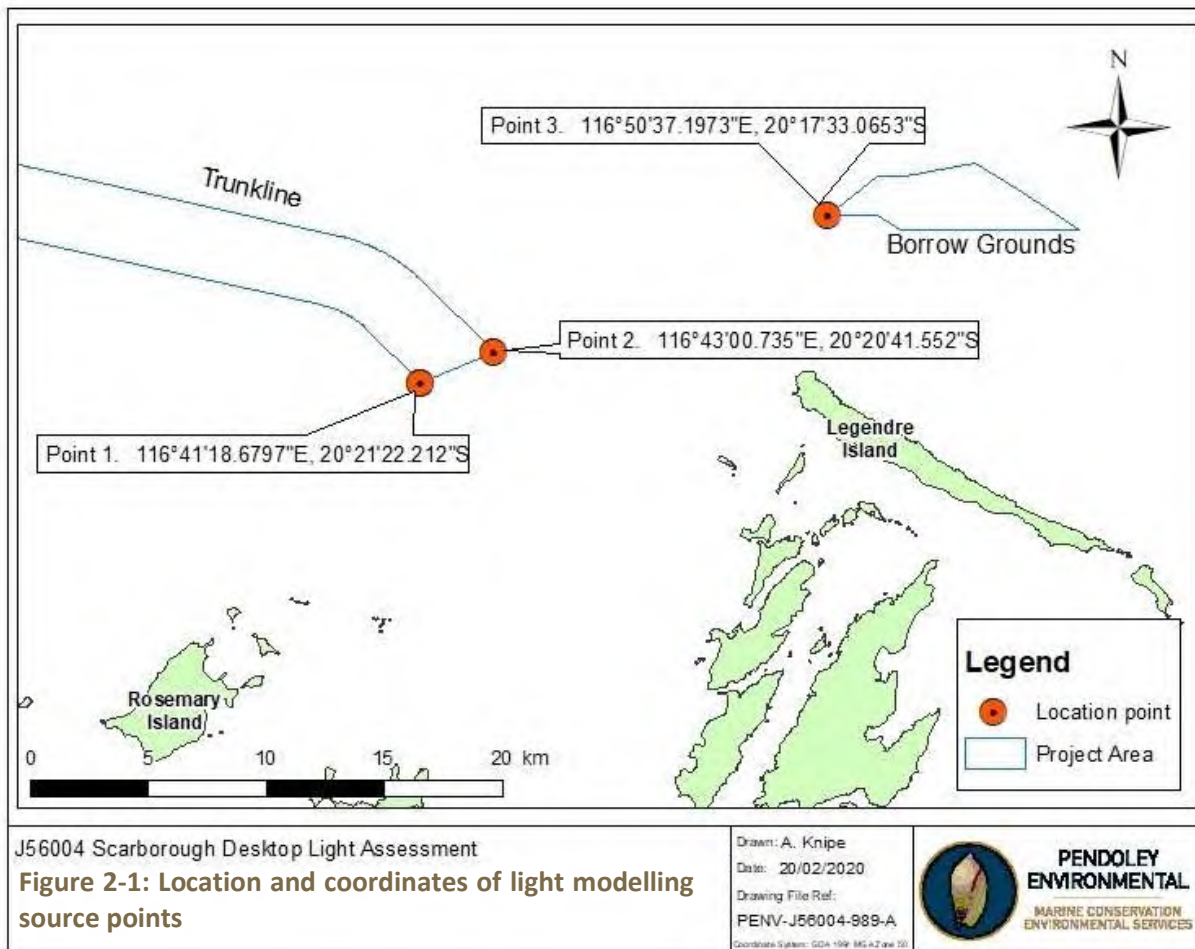
2.3   Interpretation and Limitations

In the absence of any published or generally accepted units of measurement, or scale, for measuring the impact of ALAN on marine turtles, moonlight was selected as a proxy and the light model output (radiance, units of Watts/m^2/sr) was converted to units of full moon equivalents in an attempt to give the radiance output some biological relevance and to aid interpretation in an environmental impact assessment context. The reasoning used was:

- the range of moon brightness across a whole lunar cycle is a realistic scale representative of the ambient light levels that turtle eyes are adapted to, at the lower end of the scale the radiant output is equivalent to no light in the sky while the upper limit is greater than the radiance from a single full moon and was selected to try to account for the increase in radiance levels that would occur if the light was reflected from clouds (recognizing that cloudy conditions are not the norm for this site). Extending the scale beyond this limit was deemed unnecessary.

- the scale for the units "the proportion of radiance of one full moon" was derived from the logarithmic nature of light decay with distance (a function of the inverse square law), e.g. the scale of <0.01, 0.01 – 0.1, 0.1 – 1, 1 – 10 represents a range of radiant brightness from a minimum of <0.01 full moon (so essentially a new moon) to a maximum radiant brightness of the equivalent to 10 full moons.

- While the behavioural response of marine turtles to light is relatively well understood (see Witherington and Martin (2003) for review), there is currently no agreed upon intensity limits for determining what the impact of a given light might be. A large range of factors influence the visibility and impact of light on hatchlings including light intensity, visibility (a function of lamp orientation and shielding), spectral power distribution (wavelength and colour), atmospheric scattering, cloud reflectance, spatial extent of sky glow, duration of exposure, horizon elevation, lunar phase, hatchling swimming speeds, tide and current speeds and flow direction etc. Using the scale of light radiance derived from the calculated decrease in light intensity with distance (proportion radiance of a full moon) and together with our extensive SME experience observing marine turtles and their response to both onshore and offshore construction light in field settings, we have proposed conservative, potential impact criteria for marine turtles based on radiance thresholds relative to moon radiance, as shown in Table 2-1.

Table 2-1: Artificial light impact potential criteria (marine turtles)

Proportion of radiance of a full moon*	Impact potential to marine turtles
1 - 10	Light or light glow visible and impact likely, represents a very bright light equivalence to up to 10 times the radiance of one moon. This light radiance will override the moderating influence of the ambient full moon at the time of exposure.
0.1 - 1	Light or light glow visible and behavioural impact possible, depending on ambient moon phase at the time of exposure, which will influence the visibility of the artificial light sources, equivalent to the light output. Artificial lights will be more visible to marine turtles under a first quarter moon than under a full moon.
0.01 - 0.1	Light or light glow visible but behavioural impact unlikely (i.e. not biologically relevant). Equivalent to the light output from the first quarter moon to new moon.
<0.01	Light or light glow is considered ambient and no impact expected, equivalent to a new moon

*Where 10 equals the radiance of ten full moons and 0.01 equals 100th the radiance of one full moon

3 RESULTS

3.1 Pipelay vessel

Results from the ILLUMINA model undertaken for the pipelay vessel at point 1 (closest point to Rosemary Island, 14.15) and point 2 (closest point to Legendre Island, 12 km) are summarised in Table 3-1 and presented in Figure 3-1 and Figure 3-3. At a given radiance (reported as proportion of radiance of a full moon) there is a small difference in distances reported for the same vessel at the two different points, with greater distances from source when modelled at point 2 compared to point 1 (Table 3-1). For example, radiance is equivalent to 0.01 of a full moon at 1,783.80 m when modelled at point 1, but 1,783.97 m when modelled at point 2 (Table 3-1). However, this difference is not detectable when the distance to source is reported in km to one decimal place. Since all other model inputs are identical (e.g. light inventory and cloud reflectance), site-specific differences in surface reflectance, as determined from the satellite imagery model inputs at each location, is the likely cause. Reflectance of the water surface can be influenced by oceanographic variables such as water turbidity, wave height and water depth.

When applying the potential impact criteria in Table 2-1 the results show that, at ~5.7 km from the source, radiance has reduced to ambient. At distances between ~ 1.8 km and ~5.7 km from the source, radiance is equivalent to between 0.1 and 0.01 radiance of a full moon and, therefore, light may be visible but unlikely to result in a behavioural impact (i.e. biologically relevant). Impacts may occur within ~1.8 km of the pipelay vessel, depending on moon phase, and are more likely within ~0.6 km of the vessel, when radiance is equivalent to that of one full moon.

At the closest point to Rosemary Island (14 km), radiance is equal to 0.002 (0.2%) that of a full moon. At the closest point to Legendre Island (12 km), radiance is equal to 0.003 (0.3%) that of a full moon.

Table 3-1: Distance of equivalent moon radiances for the pipelay vessel

Proportion of radiance of a full moon*	Distance from pipelay vessel at which equivalent moon radiance is reached (m)	
	Point 1 *(closest point from Trunkline Project Area to Rosemary Island)*	Point 2 *(closest point from Trunkline Project Area to Legendre Island)*
10	178.01	178.08
1	563.22	563.22
0.1	1783.80	1783.97
0.01	5730.33	5735.81

*Where 10 equals the radiance of ten full moons and 0.01 equals 100th the radiance of one full moon
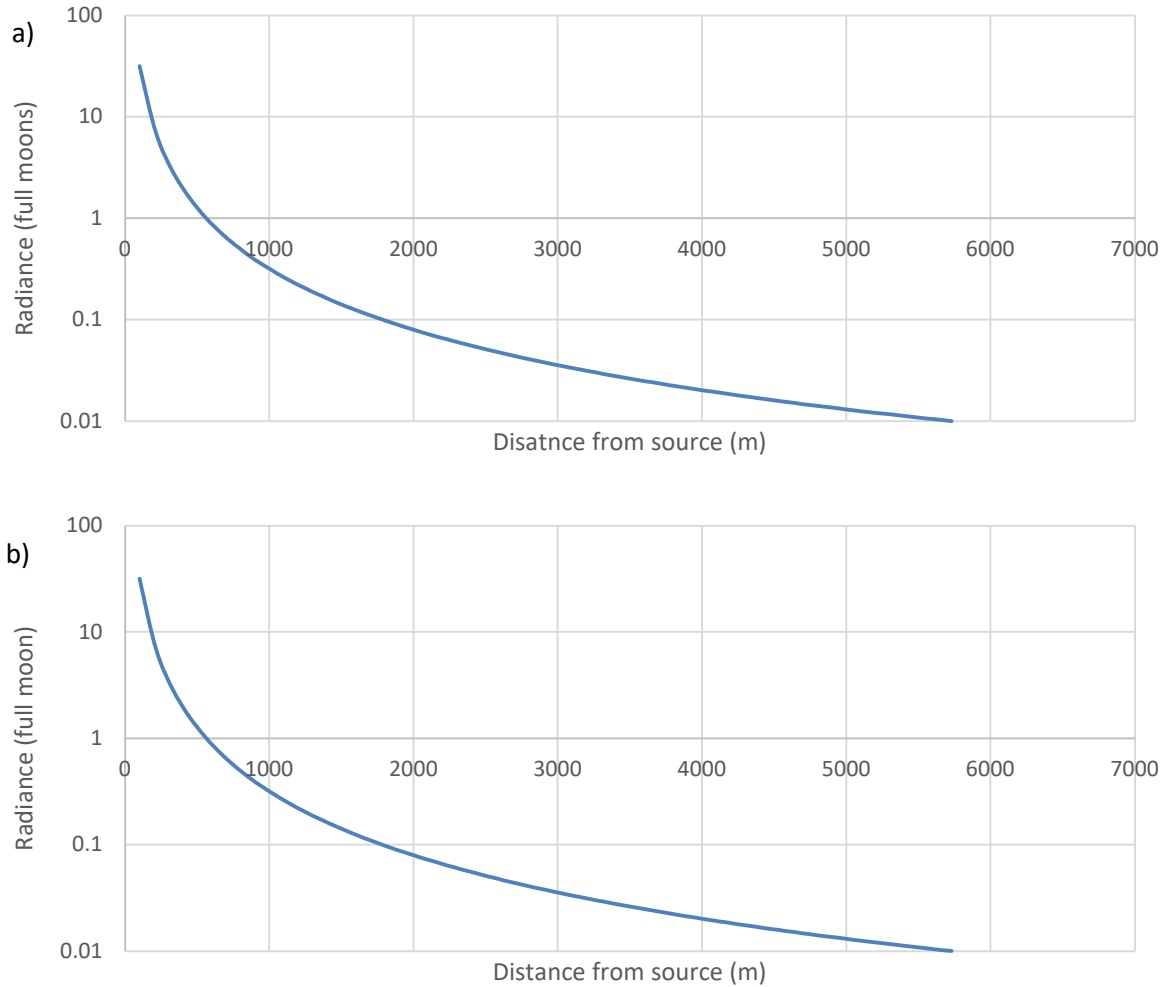
Figure 3-1: Radiance of light sources with distance from the pipelay vessel at a) point 1 (closest point to Rosemary Island) and b) point 2 (closest point to Legendre Island). Radiance (full moons) of 10 equals the radiance of ten full moons and 0.01 equals 100th the radiance of one full moon

3.2   TSHD

Results from the ILLUMINA model undertaken for the TSHD at point 1 (closest point to Rosemary Island, 14.15 km) and point 3 (closest point to Legendre Island, 6.6 km) are summarised in Table 3-2 and presented in Figure 3-2 and Figure 3-3. As with the pipelay vessel, there is a small difference in distances reported at the two different locations, with greater distances from source when modelled at point 3 compared to point 1 (Table 3-2). For example, radiance is equivalent to 0.01 of a full moon at 1,477.98 m when modelled at point 1, but 1,479.49 m when modelled at point 3 (Table 3-2). However, this difference is not detectable when the distance to source is reported in km to one decimal place. As described in Section 3.1 above, this difference is due to variation in surface reflectance at each location which is influenced by oceanographic variables.

Applying the potential impact criteria in Table 2-1, the results show that at ~4.7 km from the source light levels have reduced to ambient. At distances between ~ 1.5 km and 4.7 km from the

source, radiance is equivalent to between 0.1 and 0.01 radiance of a full moon and, therefore, light may be visible but unlikely to result in a behavioural impact. Impacts may occur within ~1.5 km of the TSHD, depending on moon phase, and are more likely within ~0.5 km of the TSHD, when radiance is equivalent to that of one full moon.

At the closest point to Rosemary Island (14 km), radiance is equal to 0.001 (0.1%) that of a full moon. At the closest point to Legendre Island (6.6 km), radiance is equal to 0.005 (0.5%) that of a full moon.

Table 3-2: Distance of equivalent moon radiances for the TSHD.

Proportion of radiance of a full moon*	Distance from TSHD at which equivalent moon radiance is reached (m)	
	Point 1 *(closest point from Trunkline Project Area to Rosemary Island)*	Point 3 *(closest point from Borrow Grounds Project Area to Legendre Island)*
10	147.80	147.80
1	467.38	467.43
0.1	1477.98	1479.49
0.01	4673.84	4722.37

*Where 10 equals the radiance of ten full moons and 0.01 equals 100th the radiance of one full moon
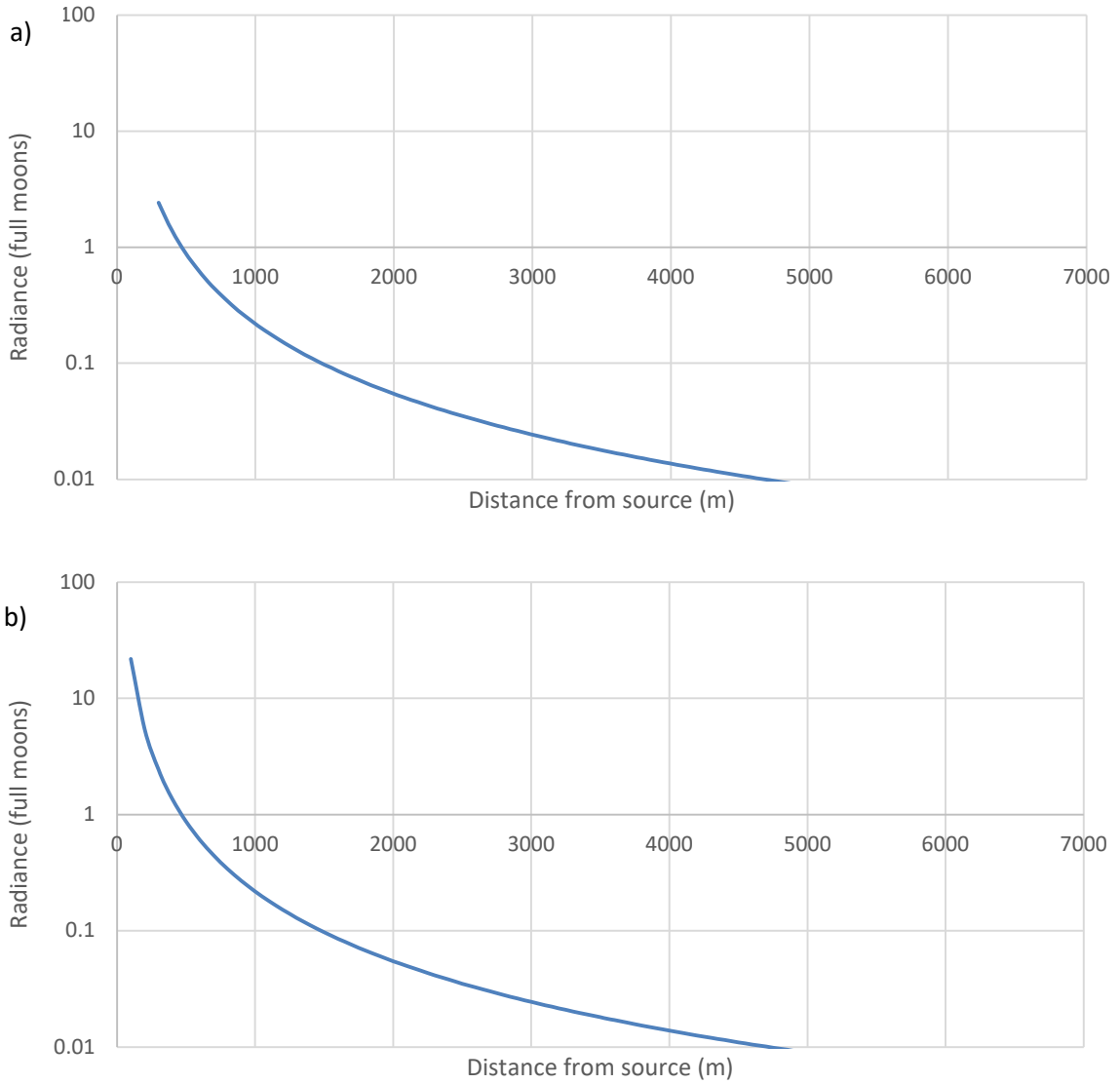
Figure 3-2: Radiance of light sources with distance from the TSHD at a) point 1 (closest point to Rosemary Island) and b) point 3 (closest point to Legendre Island).. Radiance (full moons) of 10 equals the radiance of ten full moons and 0.01 equals 100th the radiance of one full moon.
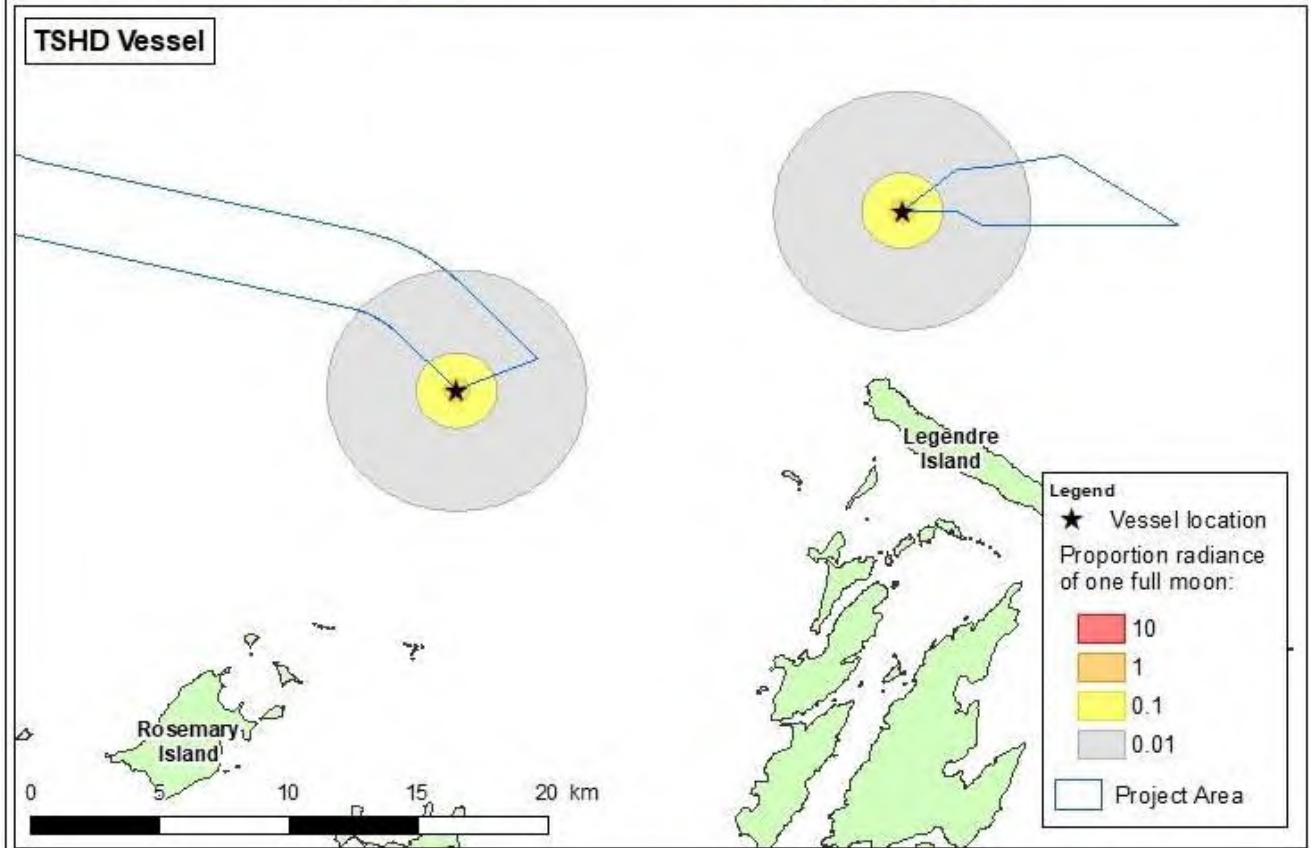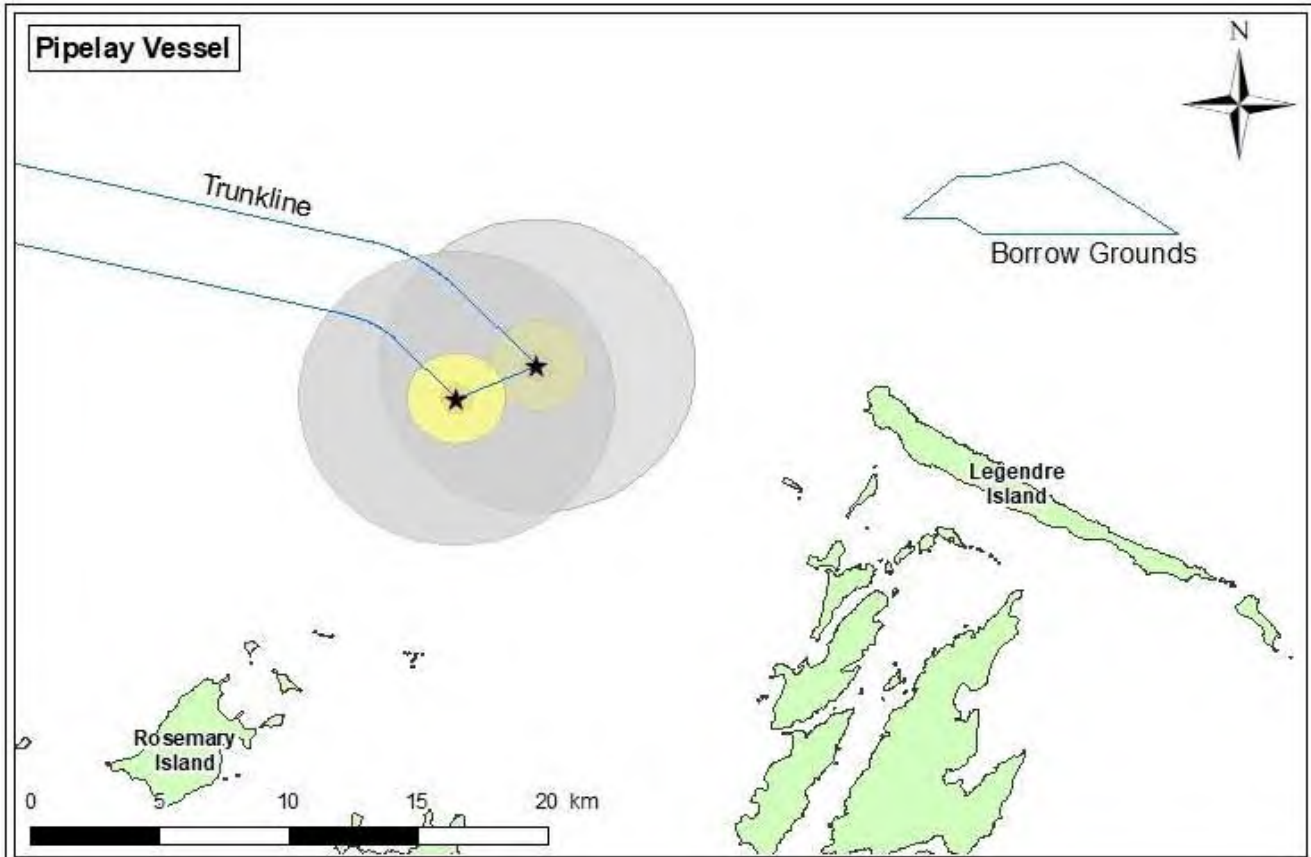
J56004 Scarborough Desktop Light Assessment

Figure 3-3: Light emissions from the pipelay vessel and TSHD, measured as the proportion radiance of one full moon. Radiance (full moons) of 10 equals the radiance of ten full moons and 0.01 equals 100th the radiance of one full moon.

Drawn: P. Whittock
Date: 19/02/2020
Drawing File Ref:
PENV-J56004-988-A
Coordinate System: GDA 1994 MGA Zone 50

PENDOLEY ENVIRONMENTAL
MARINE CONSERVATION ENVIRONMENTAL SERVICES

4   CONCLUSION

4.1   Model Results

ILLUMINA light modelling was undertaken using methodology presented in Aube *et al.*, (2005) for four scenarios associated with the Scarborough trunkline installation activities:

1. Pipelay vessel *Casterone* at the closest point of the Trunkline Project Area to Rosemary Island (point 1, 14.15 km)

2. Pipelay vessel *Casterone* at the closest point of the Trunkline Project Area to Legendre island (point 2, 12 km)

3. TSHD *Gateway* at the closest point of the Trunkline Project Area to Rosemary Island (point 1, 14.15 km)

4. TSHD *Gateway* at the closest point of the Borrow Grounds Project Area to Legendre island (point 3, 6.6 km)

Model outputs are in radiance ($W/m^2/sr$) and presented as a proportion of the radiance of a full moon as a realistic scale representative of the natural conditions experienced by a marine turtle in the field and to provide biological context.

The distance from source at which a given level of radiance was reached (reported as proportion of radiance of a full moon) was greater for the pipelay vessel compared to the TSHD, indicating that light emissions from the pipelay vessel are greater than the TSHD. Modelled light emissions of the same vessel differed between locations due to differences in the ocean reflectance values at each location. However, this difference is not detectable when the distance to source is reported in km to one decimal place.

Light emissions were predicted to reduce to ambient levels (0.01, or 1%, radiance of a full moon) at 5.7 km and 4.7 km from the pipelay vessel and TSHD, respectively. There is potential for behavioural impacts (more than 0.01, or 1%, radiance of a full moon) to occur within 1.8 km and 1.5 km from the pipelay vessel and TSHD, respectively. Behavioural impacts are more likely (≥ radiance of one full moon) within 0.6 km and 0.5 km of the pipelay vessel and TSHD, respectively.

At the closest point to Rosemary Island (14 km), radiance from the pipelay vessel is equal to 0.002 (0.2%), and from the TSHD 0.003 (0.3%), that of a full moon.

At the closest point to Legendre Island (12 km), radiance from the pipelay vessel is equal to 0.003 (0.3%) that of a full moon. From the TSHD (6.6 km), radiance is equal to 0.005 (0.5%) that of a full moon.

4.2   Impact Assessment

A conservative assessment of potential impacts of ALAN on marine turtles was undertaken in absence of light modelling by assuming that potential impacts were credible within 20 km of the light sources (Pendoley Environmental, 2020). The impact assessment concluded that the light emissions from vessel activities in the Trunkline and Borrow Grounds Project Areas would not have a significant impact

on marine turtle species across the whole life cycle, when assessed against the EPBC Act Matters of National Environmental Significance Significant Impact Guidelines 1.1 (Commonwealth of Australia, 2013). Although behavioural impacts to marine turtles were assessed as credible, it was concluded that these impacts would not be contrary to the priority actions or the measure of success criteria outlined in the Recovery Plan (Commonwealth of Australia, 2017) for the relevant marine turtle genetic stocks, or management of artificial light (Pendoley Environmental, 2020).

While this impact assessment is considered conservative, due to the uncertainties associated with predicting light emissions of the vessels without relevant information, light modelling was conducted, as detailed in this report.

Results of the light modelling suggest that, given the distance to Rosemary and Legendre Islands at the closest point (14 km and 6.6 km, respectively), light emissions from neither vessels are expected to be visible at nesting beaches of these islands and, therefore, impacts to nesting females and emerging hatchlings are not considered credible.

Dispersing hatchlings may be attracted to artificial light within 1.8 km and 1.5 km of the pipelay vessel and TSHD, respectively, but this potential for attraction is expected to be overridden by the radiance of the moon during full moon periods. Attraction of hatchlings to vessel lighting is more likely within 0.6 km and 0.5 km of the pipelay vessel and TSHD, respectively. Even assuming the greater distances of 1.8 km and 1.5 km, considering the predominant currents and distances to the nearest important nesting beaches, the proportion of hatchlings vulnerable to attraction is expected to be notably less than that assumed in the conservative impact assessment (Pendoley Environmental, 2020).

With consideration to the modelling results outlined in Section 3, the assessment of potential impacts against the Significance Significant Impact Guidelines 1.1 (Commonwealth of Australia, 2013), priority actions and measure of success criteria outlined in the Recovery Plan (Commonwealth of Australia, 2017) was reassessed, as summarised in Table 4-1.

It is recommended that Woodside consider the proposed control measures described in Section 5 of Pendoley Environmental (2020) in the context of these modelling results.

Table 4-1: Alignment with the Recovery Plan and Significant Impact Criteria based on a conservative impact assessment

Consideration	Conclusion
	Recovery Plan
Marine turtles are not displaced from identified habitat critical to the survival	Vessel light sources are not expected to be visible from nesting beaches and, therefore, displacement of females from nesting habitat will not occur.
	There is no evidence to suggest that internesting females are impacted by artificial light and, therefore, internesting females will not be displaced from internesting habitat (see Pendoley Environmental (2020) for further discussion).
That biologically important behaviour can continue in biologically important areas	Vessel light sources are not expected to be visible from nesting beaches and, therefore, disruption to female nesting behaviour, or hatchling emergence behaviour, is not expected to occur.
	There is no evidence, published or anecdotal, to suggest that internesting turtles are impacted by light from offshore vessels and, therefore, changes to internesting behaviour are not expected to occur (see Pendoley Environmental (2020) for further discussion).
	While disruption to hatchling dispersal behaviour (e.g. attraction to or trapping by light at a vessel) is credible, the number of hatchlings potentially impacted is expected to be an insignificant proportion of the annual number of hatchlings emerging from a given beach since the predominant currents are unlikely to transport hatchlings towards the Project Areas and that the distance from important nesting beaches to the point at which light emissions could elicit a behavioural response are:
	• 5.1 km from Legendre Island (when determined as the closest point to the Borrow Grounds Project Area (6.6 km) subtracted by the distance from the source at which impacts could occur – i.e. 1.5. km for the TSHD); or

Consideration	Conclusion
	• 12.2 km from Rosemary Island (when determined as the closest point to the Trunkline Project Area (14 km) subtracted by the distance from the source at which impacts could occur – i.e. 1.8. km for the pipelay vessel). In the unlikely event that hatchlings are attracted to vessel lighting, and become entrapped in light spill, following sunrise, any effect of the light sources on hatchlings will be eliminated allowing dispersal behaviour to resume. While behavioural impacts to dispersing turtle hatchlings are credible, it is not expected these impacts will impede recovery of the relevant green (G-NWS), flatback (F-Pil) or hawksbill (H-WA) genetic stocks, or result in a decreasing trend in numbers/abundance and, therefore, the project will not impact the measure of success criteria of the Recovery Plan (Commonwealth of Australia, 2017).
Develop and implement best practice light management guidelines for existing and future developments adjacent to turtle nesting beaches	Additional controls are outlined in Section 5 of Pendoley Environmental (2020) will ensure that the activity is conducted in a manner consistent with the National Light Pollution Guidelines for Wildlife (Commonwealth of Australia, 2020).
Identify the cumulative impact on turtles from multiple sources of onshore and offshore light pollution	The TSHD and pipelay vessels will not operate concurrently since activities are required to be undertaken sequentially. Although these vessels may be in the Project Areas for up to eight weeks, depending on the activity being undertaken, the continual movement of the vessels will prevent any one specific receptor (e.g. an individual turtle at sea) being exposed for the duration of each activity. Dredging activities in the Borrow Grounds Project Area, and backfill activities in the Trunkline Project Area, will also be undertaken intermittently, with periods of time in which the vessel will be absent (see Pendoley Environmental (2020) for further details on the activity). Additional support vessels may be present during some activities (e.g. pipelay activities), however, given the size of the support vessels in comparison to the pipelay vessel, light emissions from the support vessels are unlikely to contribute significantly to overall light emissions.

Consideration	Conclusion
	When considered in the context of existing industrial light sources in the region, light emissions from the activities are unlikely to significantly increase light pollution of the Dampier Archipelago. Specifically, at Rosemary Island, visibility of light emissions from the TSHD and pipelay vessels may be limited by existing light emissions from vessels at the designated anchorages (see Pendoley Environmental (2020) for further details on existing light sources).
Significant impact criteria	
Lead to a long-term decrease in the size of a population or important population	Behavioural impacts are limited to an insignificant proportion of the overall annual number of hatchlings dispersing from nesting beaches and is not considered likely to result in a long-term decrease in the size of a population or important population.
Reduce the area of occupancy of important population	The activity will not permanently displace marine turtles from habitats occupied during different life stages.
Fragment an existing important population into two or more populations	Given the temporary nature of the activity (in comparison to a permanent facility, for example), fragmentation of important population is not credible.
Adversely affect habitat critical to the survival of a species	The activity is not expected to adversely affect nesting or internesting habitat due to the limited spatial extent of potential impact, temporary nature of the activity, and that impacts at the individual level are unlikely.
Disrupt the breeding cycle of an important population	Behavioural impacts are limited to an insignificant proportion of the overall annual number of hatchlings dispersing from nesting beaches. Disruption to mating, migration, internesting or nesting is not expected.
Modify, destroy, remove, isolate or decrease the availability or quality of habitat to the extent that the species is likely to decline	Given the temporary nature of the activity, the availability or quality of the habitat will not be affected so that marine turtle species may decline.

Consideration	Conclusion
Result in invasive species that are harmful to an endangered or vulnerable species becoming established in the species' habitat	Not applicable to light emissions.
Introduce disease that may cause the species to decline	Not applicable to light emissions.
Substantially interfere with the recovery of the species	Behavioural impacts are limited to an insignificant proportion of the overall annual number of hatchlings dispersing from nesting beaches. Such impacts will be temporary in nature and will not interfere with the recovery at neither the species nor genetic stock level.

5   REFERENCES

AUBÉ, M.; FRANCHOMME-FOSSE, L.; ROBERT-STAEHLER, P.; HOULE, V. (2005) Light pollution modelling and detection in a heterogeneous environment: Toward a night-time aerosol optical depth retreival method. Proc. Spie, 5890, 248–256, DOI:10.1117/12.615405. Available at https://www.researchgate.net/publication/265746292_LIGHT_POLLUTION_MODELING_AND_DETECTION_IN_A_HETEROGENEOUS_ENVIRONMENT

COMMONWEALTH OF AUSTRALIA (2013) EPBC Act Matters of National Environmental Significance Significant Impact Guidelines 1.1

COMMONWEALTH OF AUSTRALIA (2017) Recovery Plan for Marine Turtles in Australia (2017-2027).

COMMONWEALTH OF AUSTRALIA (2020) National Light Pollution Guidelines for Wildlife Including Marine Turtles, Seabirds and Migratory Shorebirds. January 2020.

NASA (2020) https://earthdata.nasa.gov/ [Accessed 13th Feb 2020]

NOAA (2020) https://ngdc.noaa.gov/eog/viirs/download_dnb_composites.html [Accessed 13th Feb 2020]

PENDOLEY ENVIRONMENTAL (2020) Scarborough Desktop Lighting Impact Assessment. Prepared for Advisian. February 2020.

WITHERINGTON, B. AND R.E. MARTIN (2003) Understanding, Assessing, and Resolving Light-Pollution Problems on Sea Turtle Nesting Beaches. Florida Fish and Wildlife Conservation Commission FMRI Technical Report TR-2: Jensen Beach, Florida. p. 84

Annex 1: Vessel light inventory details: *Casterone* pipelay vessel

Summary of Vessel light inventory details: Casterone pipelay vessel

A summary of the Casterone pipelay vessel light inventory used as a basis for the light modelling is shown in the below table. A series of vessel lighting plans were also provided along with light elevations.

Light Type/Brand	Luminare Type	Wattage	Number of lights
Floodlight (Arran)	LED	122 W	12
Floodlight (Aquasignal)	High Pressure Sodium/Metal halide	400 W	34
Light tubing	Fluorescent (Cool white Phillips)	2 x 36 W 2 x 18 W	180
Floodlight (Aquasignal)	LED	1000W	42

Annex 2: Vessel light inventory details: *Gateway* TSHD

Summary of Vessel light inventory details: Gateway TSHD

A summary of the Gateway TSHD vessel light inventory used as a basis for the light modelling is shown in the below table. A vessel lighting plan was also provided.

Light Type/Brand	Luminare Type	Wattage	Number of lights
Light tubing	Phillips (yellow)	36 W	67
Light tubing	Phillips (yellow)	18 W	16
Floodlight (Aquasignal)	R7s Halogen	200 W	6
Floodlight (Aquasignal)	SON-t	250 W	20
Floodlight	LED	100 W x 2	3
Searchlight (Norselight)	Xenon	1000 W	2
Floodlight (Aquasignal)	LED	100W	6

Appendix M

Scarborough OPP Formal Consultation Report

Controlled Ref No: SA0006AF0000002   Revision: 5   DCP No: 1100144791

Uncontrolled when printed. Refer to electronic version for most up to date information.

	Name	Organisation	Email address	Key comment(s) on proposal (summarised where lengthy comment has been made) - including any objections or claims	Woodside assessment of merit of comment(s) and response to comment(s)	Changes made to the OPP in response to comment(s)
1		Murujuga Aboriginal Corporation (MAC)		*"The Murujuga Aboriginal Corporation (MAC) as the approved body corporate for the Burrup and Maitland Industrial Estates Agreement (BMIEA), respectfully requests a two-week extension to allow us time to prepare and finalise a submission on the Scarborough Offshore Project Proposal.* *MAC is typically reliant on pro bono support to review documents such as this proposal, so we are not able to always respond as quickly as we would like. I should add that we are broadly supportive of the proposed Burrup Hub project and do not seek to unnecessarily delay the process.* *If our request for an extension until the 13th of September 2019 can be granted, it would be most appreciated by MAC's members who are the cultural custodians of the land and waters which could potentially be impacted by this proposal."*	On the afternoon that the OPP public comment period closed on 30 August 2019, the Murujuga Aboriginal Corporation (MAC) lodged a request for a two-week extension to comment on the OPP. In response to this request, Woodside's Indigenous Affairs Manager met with MAC's CEO on 2 September 2019. Woodside explained the proposed Scarborough development area and asked whether there was a specific issue MAC had wished to raise. While MAC advised of its intention to make comment on the Dredging and Spoil Disposal Management Plan required by the Western Australian Environmental Protection Authority as part of its assessment of the proposed development, MAC responded that it did not have any particular concerns about the OPP. MAC further advised, the intention for requesting an extension was to reserve its right to comment, if necessary. Consequently, MAC was advised it would be unlikely Woodside would support an extension and MAC confirmed it would accept a decision not to extend the comment period. No further action was recorded. Woodside notes MAC's purpose is to administer the Burrup and Maitland Industrial Estate Agreement (BMIEA) on behalf of Traditional Owner "contracting parties". We further note that the organisation is the representative for joint management of the Murujuga National Park. MAC receives annual funding from Woodside under the BMIEA Agreement to carry out its specific cultural obligations and responsibilities including input on regulatory approvals. Annual payments in direct benefits are made under the BMIEA (annual lease payment) in addition to Conservation Agreement funds for MAC Rangers other direct financial support provided for related programs and activities. Woodside will continue to work with MAC and Traditional Owner representatives as the proposed Scarborough development is progressed.	Record of this engagement has been added to Table 10.5 ('Phase 2 stakeholder consultation activities').
2		Environmental Defenders Office (on behalf of CCWA)		Comments have been compiled by the EDO on behalf of CCWA. The key issues are summarised below according to the EDO submission section.	Subsections of the submission are addressed below.	Subsections of the submission are addressed below.
2.1		Environmental Defenders Office (on behalf of CCWA)		**Background** Contains statements about the proposal from the OPP.	The statements about the project reflect information in the OPP and do not require a response.	The statements about the project reflect information in the OPP and do not require amendment of the document.
2.2		Environmental Defenders Office (on behalf of CCWA)		**Impact of GHG Emissions (summary section)** (EDO submission sections 6-14) * It is submitted that: • the OPP fails to manage the impacts/risks of the Proposal's GHGe to a level that is acceptable in accordance with the established science of climate change, the EPBC Act or Australia's international obligations under the Paris Agreement • the OPP and the above controls are insufficient to manage the impacts and risks of the Proposal's GHGe to an acceptable level or as low as reasonably practicable (ALARP) • changes to the OPP are required to sufficiently manage impacts and risks of Greenhouse Gas emissions (GHGe); and	The themes raised in this summary section of the submission are covered in more detail in subsections of the submission. Responses to each subsection are provided below.	The themes raised in this summary section of the submission are covered in more detail in subsections of the submission. Changes to the OPP relevant to each subsection are described below.

Controlled Ref No: SA0006AF0000002   Revision: 5   DCP No: 1100144791

Uncontrolled when printed. Refer to electronic version for most up to date information.

	Name	Organisation	Email address	Key comment(s) on proposal (summarised where lengthy comment has been made) - including any objections or claims	Woodside assessment of merit of comment(s) and response to comment(s)	Changes made to the OPP in response to comment(s)
				• discussion of risk to Murujuga rock art and controls are included and changes to the OPP are required to sufficiently manage risk.		
2.3		Environmental Defenders Office (on behalf of CCWA)		**Insufficient Management and Regulation of Impacts of GHGE to Acceptable Level** (EDO submission sections 15-23) * It is submitted that: • national GHG regulation, Woodside's Climate Change Policy and WA EPA Public Environment Review (PER) documentation do not adequately regulate or manage GHG to acceptable levels. • The Pluto PER documentation is outdated and does not consider processing of Scarborough Gas at Pluto Train 2, and it is therefore inappropriate to rely on this to evaluate and manage scope 2 and 3 emissions. • a fresh Commonwealth assessment of risks and impacts associated with processing Scarborough gas through Pluto be undertaken; and • the OPP be amended to include details of additional GHG emitted from processing through the Pluto LNG and introduction of specific control measures that achieve net zero emissions.	The Paris Agreement represents global consensus on controls to limit anthropogenic climate change to an acceptable level. The Australian Government has ratified the Paris Agreement and implemented policy mechanisms as described in Section 3.4.1 (which has been added to provide further detail). Compliance with Australian legislation, as described in Sections 3.4.1 and 6.5 ensures that GHGe from the Project will be acceptable by keeping GHGe at or below the emissions baselines set by the Clean Energy Regulator or dealing with any excess emissions accordingly. As described in the OPP, raw product from the Scarborough Project will be processed at the onshore Pluto LNG facility. Existing environmental approvals for the Pluto LNG facility already include processing emissions for a second train and scope 3 emissions associated with sold product. Figure 7.6 has been added to section 7.1.3 of the OPP to better illustrate how related onshore processing emissions are considered in the existing approved Pluto PER. Pluto is required to have in place management plans including a Greenhouse Gas Abatement Program developed to address the requirements of Ministerial Statement 757, which ensures ongoing regulatory oversight. The Pluto approvals process is out of scope for the OPP.	Section 3.4.1 ('Greenhouse Gas Legislation') has been added, which describes Australian GHG legislation. A statement in the second paragraph of section 6.2.3 ('Risk Assessment – Environmental Legisation and other requirements') has been added about Australia's ratification of the Paris Agreement as a relevant international standard. Paragraph six has been added to Section 6.5 ('Environmental Perfomance Outcomes and Acceptable Levels') to link Australia's implementation of the Paris Agreement via legislation to the acceptability of the project. The part of section 7.1.3 (Planned Aspects – Routine Greenhouse Gas Emissions) describing related onshore processing emissions has been expanded, including incorporation of updated assumptions relating to scope 3 emissions. Discussion of risks and impacts associated with climate change, including change in habitats, fauna behaviour, injury/mortality to fauna, and social changes has been added in section 7.1.3.8
2.4		Environmental Defenders Office (on behalf of CCWA)		**Total Lifecycle GHGe Should be Considered and Managed** (EDO submission sections 24-30) * It is submitted that: • the Pluto PER process did not assess and approve Scope 3 emissions and proposes amendment of the OPP to include details and management of total lifecycle GHG, including risk and impact to the environment and rock art using the best available climate science.	As described in the OPP, raw product from the Scarborough project will be processed at the onshore Pluto LNG facility. Existing environmental approvals for the Pluto LNG facility already include processing emissions for a second train and scope 3 emissions associated with sold product. Figure 7.6 has been added to section 7.1.3 of the OPP to better illustrate how related onshore processing emissions are considered in the existing approved Pluto PER.	The part of section 7.1.3 (Routine Greenhouse Gas Emissions) describing indirect GHG emissions has been updated to include a reference to where in the Pluto PER lifecycle emissions are included and recalculation of scope 3 emissions attributed to Scarborough with updated assumptions. The new sections 7.1.3.3 (Lifecycle and Intensity) and 7.1.3.4 (Natural Gas in the Context of Global Emissions) have been added to more comprehensively explain how

Controlled Ref No: SA0006AF0000002   Revision: 5   DCP No: 1100144791

Uncontrolled when printed. Refer to electronic version for most up to date information.

	Name	Organisation	Email address	Key comment(s) on proposal (summarised where lengthy comment has been made) - including any objections or claims	Woodside assessment of merit of comment(s) and response to comment(s)	Changes made to the OPP in response to comment(s)
						Scarborough fits into a decarbonising global economy. Discussion of risks and impacts associated with climate change, including change in habitats, fauna behaviour, injury/mortality to fauna, and social changes has been added in section 7.1.3.8
2.5		Environmental Defenders Office (on behalf of CCWA)		**Cumulative Impacts Should be Considered and Managed** (EDO submission sections 31-44) * It is submitted that: • the OPP does not adequately consider the impacts of the broader Burrup Hub, including cumulative impacts. • given the decision to assess the Burrup Hub projects individually, the cumulative emissions from the proposal should be considered in context of the other projects and global GHG. • There are multiple cases which identify that small incremental increases to emissions as contribute to a broader global impact.	Burrup Hub is Woodside's vision to develop an integrated regional LNG production centre on the Burrup Peninsula. The Burrup Hub is not a proposal for a single activity for impact assessment; it describes Woodside's vision of several separate but related activities that, subject to respective joint venture approvals and relevant regulatory approvals, may be undertaken. The current allocation of approvals between jurisdictions has been established with all relevant regulatory bodies. As described in the OPP, the contribution of the Scarborough floating petroleum unit (FPU) to Australian and global GHGE is very low. Attempting to model the impact on global climate change is not feasible, and similarly it is not practical to describe associated risk to global receptors.	Woodside has determined that the approvals approach in place for the individual Burrup Hub activities are adequate and no changes were made to the document.
2.6		Environmental Defenders Office (on behalf of CCWA)		**Net Zero Emissions Outcome Should be Applied as Environmental Performance Outcome** (EDO submission sections 45-54) * It is submitted that: • the environmental performance outcomes described in the OPP are insufficient to achieve acceptability for GHG emissions, and that a "net zero" performance outcome should be adopted, stating that this should be the fundamental test for environmental acceptability. • by reference to the DOE Report for the Prelude FLNG Facility (2010), the project should result in no net increase in Australia's GHG emissions, and • the IPCC Special Report on Global Warming statement has established that global GHG must achieve net zero by 2050 to avoid global warming above 1.5°C is relevant. • a carbon budget approach is appropriate and proposes that internationally agreed science has established that the amount of emissions allowable to maintain a safe climate has already been exceeded and therefore all future developments should achieve net zero GHG emissions. • the project requires implementation of technologies such as renewables, all-electric design or carbon capture and storage, or offsets.	Achieving "net zero" GHGe abatement goes beyond the Climate Change Authority's recommendation to achieve that outcome by 2050. The Australian Government has established a 26-28% emissions reduction target by 2030 and the Paris Agreement encourages Australia to submit a new target by 2025. The State of Western Australian Government has also set an aspiration to achieve net zero emissions by 2050. Woodside's climate policy encourages government to set targets based on climate science. Acceptability for Scarborough project GHGe is achieved by actions taken to achieve compliance with Australian legislation which implements the Paris Agreement by keeping GHGe at or below the emissions baselines set by the Clean Energy Regulator or dealing with any excess emissions accordingly. Further details are provided within the response to 15-23 (Item 2.3).	Section 3.4.1 ('Greenhouse Gas Legislation') has been added, which describes Australian GHG legislation. A statement in the second paragraph of Section 6.2.3 ('Risk Assessment – Environmental Legisation and other requirements') has been added about Australia's ratification of the Paris Agreement as a relevant international standard. A new section 7.1.3.5 (Customer Commitments under the Paris Agreement) has been included to provide examples of how Scope 3 emissions from Scarborough will fit within the international agreement, Paragraph six has been added to section 6.5 ('Environmental Perfomance Outcomes and Acceptable Levels') to link Australia's implementation of the Paris Agreement via legislation to the acceptability of the project. The new sections 7.1.3.3 (Lifecycle and Intensity) and 7.1.3.4 (Natural Gas in the Context of Global Emissions) have been added to more

Controlled Ref No: SA0006AF0000002   Revision: 5   DCP No: 1100144791

Uncontrolled when printed. Refer to electronic version for most up to date information.

	Name	Organisation	Email address	Key comment(s) on proposal (summarised where lengthy comment has been made) - including any objections or claims	Woodside assessment of merit of comment(s) and response to comment(s)	Changes made to the OPP in response to comment(s)
						comprehensively explain how Scarborough fits into a decarbonising global economy.
2.7		Environmental Defenders Office (on behalf of CCWA)		**Energy Efficiency Measures Insufficient to Manage Impacts of GHGe to Acceptable Level** (EDO submission sections 55-58) * It is submitted that: • the energy efficiency measures listed in the OPP (allowance for battery energy storage system, waste heat recovery unit, gas-gas exchanger, flow coated trunkline, turbine and equipment selection) are not sufficient to achieve the current environmental performance outcome of reducing GHGe to ALARP and Acceptable Levels because there is no inclusion of control measures to avoid, reduce or offset the Proposal's GHG emissions.	The energy efficiency measures presented in section 4.5.4.1 reflect the design decisions taken to date based on ALARP principles. Demonstrations that greenhouse gas emissions have been reduced to ALARP levels in future design decisions will be submitted to NOPSEMA for approval as part of the regular Environment Plan process which will follow approval of this OPP.	A new section in the Assessment of Alternatives section (4.5.4.1 – Energy Efficiencies) has been added to describe measures implemented to date in design phase. A new section 7.1.3.6 (Greenhouse Gas Management and Mitigation) has been added to describe relevant controls in a hierarchy, including these design features but also how GHG emissions will be managed during operations.
2.8		Environmental Defenders Office (on behalf of CCWA)		**Specific Control Measures Required to Manage Impacts of GHGe to Acceptable Level** (EDO submission sections 59-64) * It is submitted that: • the OPP does not refer to any specific control measures to manage impacts or avoid, reduce or offset. DOE report on Prelude is cited in reference to required measures and offsets that result in no net increase to Australia's CO_2 emissions. • the OPP should consider LNG projects (Kitimat, Gorgon) that are employing renewable energy and carbon capture storage for management of GHG to an acceptable level.	The environmental performance outcomes in the OPP are designed to ensure that the risks and impacts associated with the project are acceptable. Compliance with the safeguarding mechanism will ensure that emission reductions implemented through the Emissions Reduction Fund (ERF) are not offset or exceeded by significant GHG emissions (above 'business-as-usual levels') emanating from other industrial or economic sectors. The safeguarding mechanism includes a framework to offset emissions if necessary for compliance.	Section 3.4.1 ('Greenhouse Gas Legislation') has been added, which describes Australian GHG legislation. A statement in the second paragraph of section 6.2.3 ('Risk Assessment – Environmental Legisation and other requirements') has been added about Australia's ratification of the Paris Agreement as a relevant international standard.
2.9		Environmental Defenders Office (on behalf of CCWA)		**Reporting Under NGER Act Insufficient to Manage Impacts of GHGe to Acceptable Level** (EDO submission sections 65-69) * Submits that voluntary public reporting should be implemented that includes facility level GHG data, including Scope 3, performance on managing GHG to acceptable and ALARP, publish through a government hosted portal and include data on offsets.	The NGER Act requires the Clean Energy Regulator to publish facility level emissions on an annual basis for facilities subject to the Safeguard Mechanism, including the use of Australian Carbon Credit Units. Additionally, Woodside also currently voluntarily participates in the Carbon Disclosure Project which includes publishing scope 3 emissions data at an equity, portfolio level.	Woodside considers that GHG emissions reporting is adequately described in the document and no changes were made. The new sections 7.1.3.3 (Lifecycle and Intensity) and 7.1.3.4 (Natural Gas in the Context of Global Emissions) have been added to more comprehensively explain how Scarborough fits into a decarbonising global economy. A new section in the Assessment of Alternatives section (4.5.4.1 – Energy Efficiencies) has been added to describe measures implemented to date in design phase. A new section 7.1.3.6 (Greenhouse Gas Management and Mitigation) has been added to describe relevant controls in a hierarchy, including these design features but also how GHG emissions will be

Controlled Ref No: SA0006AF0000002   Revision: 5   DCP No: 1100144791

Uncontrolled when printed. Refer to electronic version for most up to date information.

	Name	Organisation	Email address	Key comment(s) on proposal (summarised where lengthy comment has been made) - including any objections or claims	Woodside assessment of merit of comment(s) and response to comment(s)	Changes made to the OPP in response to comment(s)
						managed during operations and reporting.
2.10		Environmental Defenders Office (on behalf of CCWA)		**Argument that LNG Displaces Emission Intensive Fuels Not Substantiated** (EDO submission sections 70-79) * It is submitted that: • the statement that LNG is able to displace higher carbon intensity fossil fuels and complements renewables is not valid because it is not aligned with market mechanics and fails to consider policy trends and global market transition away from fossil fuels; and • the Proponent must produce proof that the claim is substantiated and backed with credible evidence, data from customer countries and robust reporting of Scope 3 GHG emissions.	Woodside acknowledges that the effect of LNG exports on global GHGe is complex and subject to market mechanisms. However, it does have the potential to play a role in displacing higher carbon intensity fossil fuels and complementing renewables. In 2019, the International Energy Agency concluded that gas use has resulted in over 500 MtCO2e emissions savings since 2010, where it had displaced coal power. Providing clean burning LNG as a power source can displace higher emissions energy sources in transport and power generation and provide firming capacity for renewable energy sources in a growing global economy.	The new sections 7.1.3.3 (Lifecycle and Intensity) and 7.1.3.4 (Natural Gas in the Context of Global Emissions) have been added to more comprehensively explain how Scarborough fits into a decarbonising global economy.
2.11		Environmental Defenders Office (on behalf of CCWA)		**Impact on Rock Art** (EDO submission sections 80-86) * It is submitted that: • the OPP does not contain details of risk and impact of the project and related Burrup Hub on Murujuga rock art, or any control measures. • includes reference to NOx and CO2 from the proposal over estimated 2070 life of field and refers to controls for French cave paintings which include mitigation of CO2 from tourists' breath.	The effective management of Aboriginal cultural heritage is critical to Woodside's continued operations and growth success. Woodside's preferred development concept is to transport gas from the Scarborough fields through a pipeline for processing at the Woodside operated onshore Pluto LNG Facility. Emissions from the Pluto LNG Facility will remain within the impact envelope of the existing approval for that facility. Woodside has contributed to air monitoring studies of the Burrup Peninsula since 2008 and our approach to emissions management practices has been informed by third-party studies including the work undertaken by the Burrup Rock Art Monitoring Management Committee. Woodside's approach to protection of rock art on the Burrup Peninsula is further informed by our relationship with the Murujuga Aboriginal Corporation and Traditional Owners and takes into account their vision for the protection and management of cultural heritage. Woodside is also playing an active and productive role in the Department of Water and Environmental Regulation's Burrup Rock Art Stakeholder Reference Group, established in 2018. Woodside will continue to focus on emissions reductions from all its operations and support appropriate scientific air emissions monitoring.	Woodside considers potential measures described in this comment to be outside the scope of the OPP. As indicated in the response to this comment, Woodside will continue to work with stakeholders on this issue through the appropriate mechanisms.
2.12		Environmental Defenders Office (on behalf of CCWA)		**Control Measures to Manage Impacts on Rock Art Required** (EDO submission sections 87-91) * It is submitted that: • the OPP must include control measures for managing the impacts/risks on rock art and proposes a precautionary approach in context of UNESCO World Heritage nomination for the Burrup Peninsula.	Woodside supports the decision of Traditional Owners and the State to pursue World Heritage listing for the Burrup Peninsula. This support reflects our commitment to the successful co-existence of heritage and industry. In this context, Woodside also supports the reinstatement of ambient air quality monitoring on the Burrup Peninsula and is working with stakeholders including Traditional Owners and the State on the preferred monitoring options and approach.	Woodside considers potential measures described in this comment to be outside the scope of the OPP. As indicated in response to a related comment above, Woodside will continue to work with stakeholders on this issue through the appropriate mechanisms.
3		Western Gas		It is suggested that in relation to Woodside's statement in the OPP that it is engaging other resource owners on future development opportunities (section 4.1) these opportunities should be included as alternate development options in the OPP.	The OPP currently identifies the Equus development as a future proposal in section 5.7.6. This section has been further updated to show the location of the Equus fields in Figure 5-57 and notes the proposed project in Table 5-11. As per Table 10.5 Woodside has held a series of consultations with Western Gas with regards to alternate development concepts. The merits of these concepts were subject to internal assessment processes and were considered unsuitable for the current development timeline. Details of this assessment process were communicated to	Updates have been made to section 5.7.6 ('Description of the Environment – Industry') and consultation has been added to the table in section 10.4.2 ('Formal OPP Consultation').

Controlled Ref No: SA0006AF0000002   Revision: 5   DCP No: 1100144791

Uncontrolled when printed. Refer to electronic version for most up to date information.

	Name	Organisation	Email address	Key comment(s) on proposal (summarised where lengthy comment has been made) - including any objections or claims	Woodside assessment of merit of comment(s) and response to comment(s)	Changes made to the OPP in response to comment(s)
					Western Gas along with a commitment to consider future opportunities for cooperation including tie-backs. This consultation has been added to the table in section 10.4.2.	
4	Anonymous			*"It is clear reviewing all combined impacts from the Scarborough project that offsetting residual impacts (e.g. on protected matters impacted including but not limited to pygmy blue whales, other whales/cetaceans, seabirds, whale sharks, turtles, commonwealth marine area) should occur because the project is not delivering net biodiversity benefit.* *In addition, cumulative impacts of the O&G industry operating on the NW shelf should be taken into account here i.e. considering what's there already and what is planned to come and what may reasonably be expected to come in future, the cumulative impacts on the MNES of the marine environment are nothing short of significant.* *EPBC policy and international impact assessment process (hierarchy of control) requires offsets to be considered in such circumstances which result in a net biodiversity benefit from the project.* *Note, I don't think like for like offsets are appropriate or required in the case of Scarborough, however there should be a strong case of indirect offsets which add value to the broader region from a biodiversity perspective.* *Implementing this will ensure the impact assessment follows EPBC policy (http://www.environment.gov.au/epbc/publications/epbc-act-environmental-offsets-policy) and is consistent with international practice for impact assessment (see bottom of page 16 https://www.unepfi.org/fileadmin/documents/biodiversity_offsets.pdf and principle 7 of https://www.iaia.org/uploads/pdf/SP3%20Biodiversity%20Ecosystem%20Services%2018%20Jan.pdf).* *These standards, and many more like them apply to setting the acceptable levels of impact of the project as a whole - no net loss of biodiversity."*	The Australian Government's *Environmental Protection and Biodiversity Conservation Act 1999 Environmental Offsets Policy, October 2012*, refers to 'environmental offsets' as measures that compensate for all residual adverse impacts of an action on the environment. The policy states that for assessments under the EPBC Act, offsets are only required if residual impacts are significant, with significance to be as defined in the *Matters of National Environmental Significance (MNES) – Significant impact guidelines 1.1.* The residual impacts of Scarborough to all MNES has been assessed to not be significant under the significant impact guidelines. In terms of cumulative impacts, in section 8.2.2 ('Receptor-based Culmulative Impacts'), the cumulative impacts from Pluto, Equus, Fisheries and Shipping were assessed, and it was identified that the aspects that were common to those activities related to vessel movements (i.e. physical presence – displacement, light emissions and vessel discharges). Cumulative assessment has been undertaken which indicates that residual impacts to species (including MNES) are low.	A seventh paragraph was added to section 6.2.3 ('Risk Assessment – Environmental Legislation and other requirements') which describes obligations under the *Environmental Protection and Biodiversity Conservation act 1999 Environmental Offsets Policy.*
5		Possible Spam	eupoqala@eerr.namnerbca.com	Spurious web link provided.	Comment appears to be spam. This comment is not relevant and has not been addressed further.	No changes made to the document.
6		Possible Spam	eupoqala@eerr.namnerbca.com	Spurious web link provided.	Comment appears to be spam. This comment is not relevant and has not been addressed further.	No changes made to the document.
7	▉▉▉▉	Private		*"Great to see another project in the planning. W/A and communities like Exmouth need these projects to go ahead to create secure long-term jobs."*	Woodside is pleased to note that independent economic modelling indicates its Burrup Hub proposals, of which Scarborough is a key component, will support the creation of an average 4,000 full-time equivalent jobs per annum nationally over a 40-year time-frame. Almost half of these will be located in northern Western Australia.	Woodside considers that no modification to the document is necessary.
8	Anonymous			*"It's great to see these projects going ahead and delivering much needed employment opportunities and opportunities for local businesses under the company's local content policy. In particular the Exmouth community has suffered from all this activity happening offshore for many years now yet very little economic benefit to the town or meaningful contracts for the town and its community. "*	Woodside welcomes community support for the proposed development of the Scarborough gas field and will work with communities to identify opportunities for local content and employment.	Woodside considers that no modification to the document is necessary.

Controlled Ref No: SA0006AF0000002   Revision: 5   DCP No: 1100144791

Uncontrolled when printed. Refer to electronic version for most up to date information.

	Name	Organisation	Email address	Key comment(s) on proposal (summarised where lengthy comment has been made) - including any objections or claims	Woodside assessment of merit of comment(s) and response to comment(s)	Changes made to the OPP in response to comment(s)
				"Get it going as soon as possible and push as much work through Exmouth as practicable. Don't let the loud voices of the minorities drown out the support of the silent majority. The Exmouth community wants it and it is in line with the shire council's strategic plans."		
9	▬	Private	▬▬▬ ▬	*"The Scarborough development proposal is an excellent opportunity for further expansion of Australia's gas resource potential.* *This development should be fully endorsed by all Australians for the benefit of all Australians."*	Woodside is pleased to note that independent economic modelling indicates its Burrup Hub proposals, of which Scarborough is a key component, will boost Australia's Gross Domestic Product by $414 billion between now and 2063 while tax and royalties payments are estimated to total $82 billion.	Woodside considers that no modification to the document is necessary.
10	▬	Private	▬▬▬	*"What capping plan is in place to meet highest risk i.e. a spill results from a leaking well?* *We know from Macondo failings majority of loss / risk resulted from spill.* *Why has little been done by operators / regulators to assure that a faster safer capping system is not in place for offshore projects, i.e. a system designed around a Xmas tree that can be kept on site in the field to be able to respond to cap and kill a well in hrs vs days or weeks of spillage that could result to meet worst case needs?* *There are systems available; e.g. Abel Engineering well control specialists etc. Why is such a safer better cheaper faster response system not to be used?"*	The OPP process, is in place to allow the regulator to make an assessment of the environmental acceptability of proposed offshore projects. Following OPP acceptance, activity specific Environment Plans (EPs) (and other permissioning documents such as Well Operations Management Plans (WOMPs) will be required to be prepared and accepted. Broadly, the purpose of EPs will be for the titleholder to confirm that the impacts and risks are within the scope of that accepted under the OPP, and to identify the control measures that will manage the impacts and risks ALARP. The EP will describe the level of performance for these control measures during activities and including emergency situations. An emergency response plan which identifies source control options including capping systems, will be developed and submitted as a part of the activity's EPs. At this stage of the approval process, there will be consideration of source control methods and technology in order to demonstrate that the impacts and risks will be managed to ALARP levels. Hydrocarbons of the Scarborough, Jupiter and Thebe reservoirs contain no measurable liquid condensate fraction. It is therefore expected that there would be no, or negligible, liquid component in a loss of containment scenario. In the event of a loss of well control, the response strategy detailed in the EP will be based on the risk, and the properties of the released hydrocarbons.	On review of the merit of this comment, Woodside considers that the concern raised is adequately addressed and no modification to the document is required.
11	▬	Private	▬▬▬ ▬	*"I think that this project should go ahead with the caveat that cheaper gas is made available for Western Australia.* *What would be even better is that the AU government develops the fields, undertake all production and distribution / sales of LNG. That way Australia would have a sustainable income for years to come. Not only that all future exploration and development of fields should be under the control of the Australian government not a foreign government or company.* *With this then could be the Australian engineering rig/ship building capability to ensure jobs and growth for Australia."*	Woodside is proposing to expand the Pluto LNG facility to process Scarborough gas and work is underway on the design of a domestic gas plant at Pluto to facilitate supply to Western Australia. As an Australian company, Woodside has a proud history of developing resources and delivering long term benefits to the country. Independent economic modelling indicates tax and royalties payments from the proposed Burrup Hub projects will add up to $82 billion. Woodside has also developed an Australian Industry Participation Plan for the proposed Scarborough development. This plan has been approved by the Australian Government and is designed to maximise opportunities for Australian businesses.	Woodside considers that no modification to the document is necessary.

*EDO's comments have been summarised and grouped in accordance with section headers provided in EDO's submission.

Controlled Ref No: SA0006AF0000002   Revision: 5   DCP No: 1100144791

Uncontrolled when printed. Refer to electronic version for most up to date information.

THIS PAGE HAS BEEN INTENTIONALLY LEFT BLANK